The role of the NFAT signalling pathway in Diffuse Large B-cell Lymphoma

Holly White

Doctor of Philosophy Thesis

September 2015

Supervisors: Dr Chris Bacon, Professor Neil Perkins & Dr Vikki Rand

Northern Institute for Cancer Research

Word count: 66,024

Abstract

Diffuse Large B-Cell Lymphomas (DLBCL) are common, aggressive malignancies of mature B-lymphocytes that represent ~40% of lymphomas. Despite the widespread use of combined immunochemotherapy, approximately 50% of patients with DLBCL die from their disease. The two main DLBCL subgroups resemble activated B cells (ABC) or germinal centre B cells (GCB), where patients with ABC-DLBCL have significantly worse outcome. There is urgent need for novel therapeutic strategies in the treatment of DLBCL, which requires a better understanding of the molecular pathways upon which tumours depend.

Accumulating evidence suggests that the signalling networks promoting and sustaining DLBCL derive from dysregulation of the normal pathways controlling B-lymphocyte activation and differentiation. There is increasing evidence indicating important roles for the NFAT family of transcription factors in DLBCL. Constitutively-active nuclear NFAT2 has been demonstrated in approximately 40% of primary DLBCL samples and NFAT has been shown to regulate a small number of genes associated with DLBCL growth/survival.

This project investigated the role of NFAT in DLBCL. Nuclear localisation and activation of NFAT family members were characterised in a panel of DLBCL cell lines and chemical inhibition of calcineurin/NFAT, using Cyclosporin A (CsA), indicated dependency on the calcineurin/NFAT pathway for survival. Gene expression microarray analysis performed in DLBCL cell lines treated with CsA revealed potential NFAT target genes involved in the tumour microenvironment and anergy.

These data revealed that the cytokine TNFα was downregulated by CsA in ABC, but not GCB cell lines. TNFα expression has recently been reported a significant prognostic factor for OS and PFS in DLBCL and evidence suggests dependency of some DLBCL on autocrine TNFα signalling for survival. Biologically active TNFα was produced by DLBCL cell lines, however inhibition of TNFα signalling using Infliximab and Etanercept had no effect on cell viability, suggesting that TNFα may be functionally important in DLBCL by other mechanisms.

Acknowledgements

It is a pleasure to thank those who have made this research project possible. Thank you to my supervisors Dr Chris Bacon, Professor Neil Perkins and Dr Vikki Rand for their support and guidance throughout my PhD. I am especially grateful to Chris, who during times when I doubted myself, gave me the confidence to push myself further and gain a great sense of achievement. I would also like to thank Cancer Research UK for giving me the opportunity to complete my PhD by funding this project.

I am also thankful to Dr Anja Krippner who kindly provided the anti-TNFα agents for the TNFα investigation.

I would also like to express my gratitude to my colleagues at the Northern Institute for Cancer Research, particularly within the lymphoma research group. I fully appreciate the technical support and advice given during the last three years. Many thanks also go to researchers in the Neil Perkins laboratory, especially to Dr Alex Sfikas for helping me with the NF-κB luciferase assays and to Dr Jill Hunter for her enthusiasm and guidance during my studies.

I am also very thankful for the friendships I have made during my PhD, especially with Laura Ogle, Sarah Wilkinson and Paul Gibson, who always brightened my days.

Finally, I would like to thank my boyfriend Iain for being my shoulder to cry on, and my family, who gave me emotional support through all the ups and downs during the past three years.

Table of Contents

List of Figures

List of Tables

List of Abbreviations

aa	Amino Acid
aaIPI	Age-Adjusted IPI

ABC DLBCL	Activated B-cell like Diffuse Large B-Cell Lymphoma
ADP	Adenosine Diphosphate
AICD	Activation Induced Cell Death
AID	Activation-Induced Cytidine Deaminase
AKAP79	A Kinase Anchor Protein 79
AP-1	Activator Protein 1
APS	Ammonium Persulphate
ATR	Ataxia Telengiectasia and Rad3-related
BCA	Bicinchoninic Acid
BCL-2	B-Cell Lymphoma 2
BCL-6	B-Cell Lymphoma 6
BCL-10	B-Cell Lymphoma 10
BCR	B-Cell Receptor
BL	Burkitt's lymphoma
BLNK	B-cell Linker Protein
BLyS	B-Lymphocyte Stimulator
BMP4	Bone-Morphogenetic Protein 4
B-NHL	B-cell Non Hodgkin Lymphoma
BTK	Bruton's Tyrosine Kinase
BSA	Bovine Serum Albumin
CABIN1	Calcineurin Binding Protein 1
CARD11	Caspase Recruitment Domain Family, Member 11
CBM	CARD11-BCL10-MALT1
CCC	Comprehensive Consensus Clustering
CLL	Chronic Lymphocytic Leukaemia
CCL4	Chemokine (C-C) motif Ligand 4
CCL4L	Chemokine (C-C) motif Ligand 4-like
CDK	Cyclin Dependent Kinase
cDNA	Complementary Deoxyribonucleic acid
CERI	Cytoplasmic Extraction Reagent I

CERII	Cytoplasmic Extraction Reagent II
c-FLIP	Cellular FLICE (FADD-Like IL-1β-Converting Enzyme)-Inhibitory Protein
ChIP-Seq	Chromatin Immunoprecipitation Sequencing
CI	Combination Index
CK-1	Casein Kinase 1
CML	Chronic Myeloid Leukaemia
COO	Cell of Origin
CRAC	Calcium Release-Activated Channels
CREBBP	CREB Binding Protein
CRISPR-Cas9	Clustered, Regularly Interspaced, Short Palindromic Repeat-Cas9
CRUK	Cancer Research United Kingdom
CsA	Cyclosporin A
CSF1	Colony Stimulating Factor 1
CSR	Class Switch Recombination
Ct	Cycle threshold
CXCL12	Chemokine (C-X-C) motif Ligand 12
CypA	Cyclophilin A
DAG	Diacylglycerol
DDI H_2O	Distilled De-ionised Water
DDIT3	DNA-Damage-Inducible Transcript 3
DEPC	Diethylpyrocarbonate
DLBCL	Diffuse Large B-cell Lymphoma
DLBCL NOS	Diffuse Large B-cell Lymphoma Not Otherwise Specified
DMSO	Dimethyl Sulfoxide
DNA	Deoxyribonucleic Acid
dNTP	Deoxynucleotide Triphosphates
DSCR1	Down's Syndrome Critical Region 1
ds-RNA	Double-stranded RNA
DYRK	Dual Specificity Tyrosine Phosphorylation-Regulated Kinase

EBV	Epstein - Barr virus
ECL	Enhanced Chemiluminescence
EDTA	Ethylenediaminetetraacetic Acid
EGF	Epidermal Growth Factor
EGFR	Epidermal Growth Factor Receptor
EGR	Early Growth Response
ELISA	Enzyme Linked Immunosorbent Assay
EMT	Epithelial Mesenchymal Transition
ENCODE	The Encyclopaedia of DNA Elements
EP300	E1A Binding Protein P300
ER	Endoplasmic Reticulum
ERK	Extracellular signal Regulated Kinase
ES	Enrichment Score
EZH2	Enhancer of Zeste 2 Polycomb Repressive Complex 2 Subunit
FACS	Fluorescence-Activated Cell Sorting
FADD	Fas-Associated protein with Death Domain
FBS	Foetal Bovine Serum
FC	Fold-Change
FCS	Foetal Calf Serum
FDR	False Discovery Rate
FILIP1L	Filamin A Interacting Protein 1-Like
FKBP12	FK506 Binding Protein 12
FL	Follicular Lymphoma
FOXC2	Forkhead Box protein C2
FOXP3	Forkhead Box P3
FST	Follistatin
GAPDH	Glyceraldehyde 3-Phosphate Dehydrogenase
GC	Germinal Centre
GCB DLBCL	Germinal Centre B-cell like Diffuse Large B-Cell Lymphoma
GCET1	Germinal Centre B-cell-Expressed Transcript 1

GM-CSF	Granulocyte-Macrophage Colony-Stimulating Factor
GOI	Gene of Interest
GPCR	G Protein-Coupled Receptor
GSEA	Gene Set Enrichment Analysis
GSK3β	Glycogen Synthase Kinase 3 Beta
HDAC	Histone Deacetylase
HRAS	Harvey Rat Sarcoma Viral Oncogene Homolog
huIgG	Human Immunoglobulin G
IC50	Half maximal Inhibitory Concentration
ID3	Inhibitor of DNA Binding 3, Dominant Negative Helix-Loop-Helix Protein
IFNγ	Interferon Gamma
IGHV	Immunoglobulin Heavy Chain Variable
IHC	Immunohistochemistry
IκBα	I kappa B Alpha
IκBε	I kappa B Epsilon
IκBζ	I kappa B Zeta
IKK	I kappa B Kinase
IL	Interleukin
INCA-6	Inhibitor of NFAT-Calcineurin Activation 6
$InsP_3$	Inositol 1,4,5-triphosphate
IPI	International non-Hodgkin's Lymphoma Prognostic factor
IRAK	Interleukin-1 Receptor-Associated Kinase
IRF4	Interferon Regulatory Factor 4
IRF7	Interferon Regulatory Factor 7
ITAM	Immunoreceptor Tyrosine-based Activation Motif
JAK	Janus Kinase
JNK	c-Jun N-terminal Kinase
LDH	Lactate Dehydrogenase
logFC	Log Fold-Change

LPS	Lipopolysaccharide
LTA	Lymphotoxin
LUBAC	Linear Ubiquitin Chain Assembly Complex
LZ	Leucine Zipper
MALT1	Mucosa-Associated Lymphoid Tissue Lymphoma Translocation protein 1
MAPK	Mitogen-Activated Protein Kinases
MAP3K7	Mitogen-Activated Protein Kinase Kinase Kinase 7
MCL	Mantle Cell Lymphoma
MCV-1	Maleimido-Conjugated VIVIT 1
MEF2	Myocyte Enhancer factor 2
MEK	MAPK/ERK Kinase
MLL2	Myeloid/Lymphoid or Mixed-Lineage Leukaemia 2
MMP	Matrix Metalloproteinase
MPA	Mycophenolic Acid
mRNA	messenger RNA
MRP2	Multidrug Resistance Protein 2
MT	Mutated
mTNFα	Membrane-bound Tumour Necrosis Factor Alpha
MUM1	Melanoma Associated Antigen (Mutated) 1
MYD88	Myeloid Differentiation primary response gene 88
MZB1	Marginal Zone B and B1 Cell-Specific Protein
NaCl	Sodium Chloride
NER	Nuclear Extraction Reagent
NES	Nuclear Export Sequence
NFAT	Nuclear Factor of Activated T cells
NF-κB	Nuclear Factor Kappa-light-chain-enhancer of activated B cells
NFKBIA	Nuclear Factor Kappa B Inhibitor Alpha
NFKBIE	Nuclear Factor Kappa B Inhibitor Epsilon
NFKBIZ	Nuclear Factor Kappa B Inhibitor Zeta

NHL	Non Hodgkin Lymphoma
NHR	NFAT Homology Region
NIK	NF-κB Inducing Kinase
NK	Natural Killer
NLS	Nuclear Localisation Sequence
NMDA	N-Methyl-D-Aspartate
NMZL	Nodal Marginal Zone Lymphoma
NS	Non-Specific/Silencing
OD	Optical Density
OS	Overall Survival
OxPhos	Oxidative Phosphorylation
PAGE	Polyacrylamide Gel Electrophoresis
PARP	Poly ADP Ribose Polymerase
PAX9	Paired Box Gene 9
PBS	Phosphate Buffered Saline
PCA	Principal Component Analysis
PCK2	Phosphopyruvate Carboxylase
PCR	Polymerase Chain Reaction
PDCD1	Programmed Cell Death Protein 1
PFS	Progression Free Survival
PGE_2	Prostaglandin E2
PHA	Phytohemagglutinin
PI	Propidium Iodide
P-IκBα	Phospho-I kappa B Alpha
PIP3	Phosphatidylinositol (3-5) -triphosphate
PI3K	Phosphatidylinositol 3-kinase
PLCγ	Protein Lipase C Gamma
PMA	Phorbol 12-Myristate 13-Acetate
PMBL	Primary Mediastinal B-cell Lymphoma
PPIase	Peptidyl Prolyl Isomerase

P-p65	Phospho-p65
PRC2	Polycomb Repressive Complex 2
PROX1	Prospero Homeobox 1
PtdIns(4,5)P_2	Phosphatidylinositol 4,5-bisphosphate
PTEN	Phosphatase and Tensin homolog
PVDF	Polyvinylidene Difluoride
QC	Quality Control
RAG	Recombination Activating Gene
qRT-PCR	Quantitative Real-Time Polymerase Chain Reaction
R-CHOP	Rituximab, Cyclophosphamide, Doxorubicin, Vincristine, Prednisolone
RFP	Red Fluorescent Protein
RHR	Rel Homology Region
RIPA	Radioimmunoprecipitation
r-IPI	Revised IPI
RLU	Relative Light Units
RNA	Ribonucleic Acid
RPMI	Roswell Park Memorial Institute Medium
RT	Room Temperature
RTK	Receptor Tyrosine Kinase
qRT-PCR	Quantitative Real-Time Polymerase Chain Reaction
SDS	Sodium Dodecyl Sulphate
SDS-PAGE	Sodium Dodecyl Sulphate-Polyacrylamide Gel Electrophoresis
SHIP1	SH2 Domain-Containing Inositol 5-Phosphatase 1
SHM	Somatic Hypermutation
shRNA	Short hairpin RNA
siRNA	Small Interfering RNA
SNORD96A	Small Nucleolar RNA, C/D Box 96A
SOCE	Store-Operated Calcium Entry
SOCS3	Suppressor of Cytokine Signalling 3

SODD	Silencer of Death Domains
SP	Serine-Proline
SR	Serine Rich
STAT3	Signal Transducer and Activator of Transcription 3
STIM	Stromal Interaction Protein
sTNFα	Soluble Tumour Necrosis Factor Alpha
SUMO1	Small Ubiquitin-related Modifier 1
SYK	Spleen Tyrosine Kinase
TACE	TNFα Converting Enzyme
TAD	Trans-Activating Domain
TAK	Transforming Growth Factor-Beta-Activated Kinase 1
T-ALL	T-cell Acute Lymphoblastic Leukaemia
TBP	TATA Box Binding Protein
TBS-Tween	Tris-Buffer Saline-Tween
TCR	T-Cell Receptor
TEMED	Tetramethylenediamine
TGFβ	Transforming Growth Factor Beta
TMA	Tissue Microarray Analysis
TNFα	Tumour Necrosis Factor Alpha
TNFβ	Tumour Necrosis Factor Beta
TNFR1	Tumour Necrosis Factor Receptor type 1
TNFR2	Tumour Necrosis Factor Receptor type 2
TPCA-1	IKK2 Inhibitor IV
TP53	Tumour Protein 53
TRADD	TNF Receptor type 1 Associated Death Domain
TRAF3	TNF Receptor-Associated Factor 3, E3 Ubiquitin Protein Ligase
TRAF6	TNF Receptor-Associated Factor 6, E3 Ubiquitin Protein Ligase
TRIM13	Tripartite Motif Containing 13
VEGF	Vasculature Endothelial Growth Factor
VEGF-C	Vasculature Endothelial Growth Factor C

WT	Wild-Type

Chapter 1.

Introduction

1. Introduction

1.1. Lymphoma

Cancer is a disease caused by the uncontrolled division and survival of abnormal cells, leading to the formation of malignant growths or tumours in specific parts of the body. There are over 200 different types of cancer, with over 300,000 new cases being diagnosed each year in the UK (CRUK, 2015). Most cancers develop as solid tumours at a primary site and may spread, or metastasise, to other tissues, such as through the blood or lymphatic system. Spread of cancer throughout the body is often life-threatening, sometimes preventing the function of vital organs.

For a cell to transform from a normal cell to a cancerous cell, it is believed that specific biological capabilities are required. These were summarised by Hanahan and Weinberg in 2000, who proposed six hallmarks of cancer, forming a framework for understanding the diverse characteristics of neoplastic disease (Hanahan *et al.*, 2000). The hallmarks included sustaining proliferative signals, evading growth suppressors, enabling replicative immortality, resisting cell death, inducing angiogenesis and activating invasion and metastasis (Hanahan *et al.*, 2000). More recently, an additional two traits have been added to the list of hallmarks: the ability to evade immune destruction and the ability to reprogram energy metabolism (Hanahan *et al.*, 2011). A better understanding of the common traits shared by various malignancies is key to deciphering the multistep process of tumour pathogenesis.

Lymphomas are cancers of lymphocytes and their immediate precursors which form solid masses within the lymphatic system, such as within lymph nodes or spleen, or in extranodal tissues throughout the body. Similar neoplasms based in blood and bone marrow are considered leukaemias, however this is a generalisation, with some myelomas also being located in the bone marrow and some lymphomas being present in the blood. There are two main types of lymphoma, the largest group being the non-Hodgkin lymphomas (NHL), which are the fifth most common cancer in the UK, with around 12,000 new cases being diagnosed each year (Macian, 2005; Cancer Research UK, 2012). Named after Dr Thomas Hodgkin, who first diagnosed the disease, a less common group are the Hodgkin lymphomas (Burkitt, 1958). The abnormal cells in classical Hodgkin

lymphomas are large, often multinucleate, Hodgkin/Reed-Sternberg cells (Küppers *et al.*, 2012).

1.2. B-Cell Non-Hodgkin Lymphoma

Since their first recognition, the classification of lymphomas has evolved considerably as our understanding of the underlying biology has increased. NHL can derive from B cells, T cells or natural killer-cells (NK-cells). Less common are the T/NK-cell lymphomas, which include peripheral T-cell lymphoma not otherwise specified, cutaneous T-cell lymphomas, anaplastic large cell lymphomas and T-cell lymphoblastic lymphoma. B-cell NHL (B-NHL) on the other hand are the most common NHL, representing a very diverse group of malignant diseases.

Briefly, mantle cell lymphomas (MCL) account for 5-10% of lymphoma cases and are derived from a naïve pre-germinal centre B-cell, localising to the mantle region of secondary follicles (Shaffer *et al.*, 2002b; Nogai *et al.*, 2011). MCL are typically aggressive lymphomas and patients with this disease have a median survival of only 3 to 4 years (Goy *et al.*, 2011; Vose, 2013). Follicular lymphomas (FL) are the most frequent indolent, low-grade B-NHL, accounting for roughly 20% of all lymphomas (Nogai *et al.*, 2011). FL are derived from germinal centre B cells (GCB) and localise principally to the germinal centres (GC) of follicles where they undergo somatic hypermutation (Nogai *et al.*, 2011). Also derived from the GC, Burkitt lymphoma (BL) is an aggressive type of B-NHL found in mainly children and young adults (Shaffer *et al.*, 2002b).

The B-NHL of interest in this study were the diffuse large B-Cell lymphomas (DLBCL), which are aggressive malignancies of mature B cells. DLBCL are the most common type of NHL, representing around 40% of lymphomas in adults in the UK (Staudt, 2010). Although cures are achieved in approximately 60% of patients, outcome is largely unpredictable due to substantial disease heterogeneity (Shipp, 2007). Over 30% of patients do not respond to conventional first-line therapies or relapse, highlighting the requirement for a better understanding of the biology underlying lymphoma (Pasqualucci, 2013).

Examples of other, less common B-cell lymphoid malignancies include extranodal marginal zone B-cell (MALT) lymphomas, primary mediastinal large B-cell lymphomas (PMBL) and nodal marginal zone lymphomas (NMZL).

1.3. Diagnosis, prognosis and treatment of DLBCL

Patients with DLBCL present with solid tumours, most commonly in the lymph nodes but also in extranodal sites. Following initial clinical consultation, DLBCL is typically diagnosed by a biopsy from an involved site, which is examined microscopically. Immunophenotyping by immunohistochemistry or flow cytometry is used to confirm B-cell lineage, exclude other diagnoses and determine their phenotypic subgroup. Genetic analysis for chromosomal translocations and mutations is now increasingly clinically important. Accordingly, DLBCL is currently sub-classified based on a combination of morphological, immunophenotypic, clinical and genetic features.

The prognosis of DLBCL depends upon both clinical and intrinsic biological and genetic features. The International Prognostic Index (IPI) has been the main method for predicting patient response to therapy for the past 20 years (Unknown, 1993; Zhou *et al.*, 2014). Based on analysis of more than 2000 patients with aggressive lymphomas, the IPI integrates five negative prognostic factors at diagnosis into a risk score (Unknown, 1993). These factors are age (>60 years), stage (extent) of disease, elevated lactate dehydrogenase (LDH) level, Eastern Cooperative Oncology Group (ECOG) performance status (≤2) and whether the lymphoma is present at more than one extranodal site (Unknown, 1993). Patients are then put into four separate outcome groups, identified initially as having a 5-year overall survival from 26%-73% (Unknown, 1993). Two modifications to the IPI have been introduced recently, in response to changes in therapy and outcome: an age-adjusted IPI (aaIPI) and a revised IPI (r-IPI) with only three risk factors (Sehn *et al.*, 2007).

Conventional methods of treatment for various cancers include local surgery, radiotherapy or chemotherapy. As a cancer frequently disseminated throughout the lymphoid system, DLBCL is treated principally with chemotherapy. In the UK, DLBCL is usually treated with moderately aggressive combined immunochemotherapy using the R-CHOP regimen. The chemotherapeutic agents that make up this drug combination include cyclophosphamide (an alkylating agent), doxorubicin (an anthracycline) and vincristine (an alkaloid). Prednisolone on the other hand, is a glucocorticoid drug, whereas rituximab is an anti-CD20 monoclonal antibody.

The addition of Rituximab to the standard CHOP regimen has been shown to be beneficial in many trials and has significantly improved the survival of patients with DLBCL

(Habermann *et al.*, 2006; Coiffier *et al.*, 2010; Pfreundschuh *et al.*, 2011). Nevertheless, clinical responses vary considerably depending on a patient's genetic profile and stage of disease, meaning that further improvements are required for patients who are poor-risk or chemo-refractory, or who relapse after treatment (Coiffier *et al.*, 2002; Zhang *et al.*, 2013b). Second-line chemotherapy regimes, haematopoietic stem cell transplantation and radiotherapy have important roles in certain clinical contexts, but when the diagnosis of DLBCL is known, surgery is rarely utilised.

1.4. Sub-classification of DLBCL by cell of origin (COO)

Genomic analysis has shown DLBCL to harbour a high degree of complexity when compared to other haematological malignancies (Pasqualucci, 2013). This is largely due to significant variability between patients, which is one of the main obstacles to therapeutic success in DLBCL (Pasqualucci, 2013). Studies investigating the molecular heterogeneity of DLBCL have enabled identification of three molecularly distinct subgroups of DLBCL, which arise from B cells at different stages of differentiation (Alizadeh *et al.*, 2000; Wright *et al.*, 2003). Genome-scale gene-expression microarrays have demonstrated unique gene-expression signatures for each disease subtype, where one expressed genes characteristic of germinal centre B cells (GCB type) including BCL6, CD10 and LMO2, and a second type expressed genes induced during the activated B-cell state (ABC type) such as IRF4/MUM1, FOXP1 and CCND2 (Alizadeh *et al.*, 2000). Interestingly, the gene expression subgroups were shown to differ by the expression of more than 1000 genes, proving how distinct these lymphomas really are (Alizadeh *et al.*, 2000; Rosenwald *et al.*, 2002).

GCB DLBCLs are thought to derive from germinal centre centroblasts, expressing high levels of genes characteristic of normal germinal centre B cells (Alizadeh *et al.*, 2000). In contrast, the gene expression profile of ABC DLBCLs suggests that these lymphomas are derived from B cells that are in the process of differentiating into plasma cells (Alizadeh *et al.*, 2000). Importantly, multiple genetic lesions of pathogenic significance are correlated with different subgroups of DLBCL (Shaffer *et al.*, 2012a). This suggests that these tumours depend on specific oncogenic pathways, which may be therapeutically targetable.

The third type of DLBCL, which also arose from gene expression profiling, is PMBL (Alizadeh *et al.*, 2000) . This disease mostly occurs in young females, with a median age

of only 30 to 35 years (Nogai *et al.*, 2011). It is thought that PMBL originates from a rare, post-germinal B-cell population that resides in the thymus, showing different characteristics to other types of DLBCL, but similarities to Hodgkin lymphomas by gene expression profiling (Rosenwald *et al.*, 2003; Yuan *et al.*, 2015).

Approximately 15% of DLBCLs cannot be assigned to a molecular subgroup as they exhibit gene expression profiles not typical of GCB DLBCL, ABC DLBCL or PMBL subtypes. These are referred to as 'unclassifiable' or 'Type 3' DLBCL, (Lenz *et al.*, 2008b).

Immunohistochemistry has been used in attempts to stratify DLBCL into COO subgroups in diagnostic practice as genome-scale expression profiling is not clinically practical. Various immunohistochemical algorithms have been used to try to reproduce the cell of origin subgroups found by gene expression profiling. The Hans classification system, for example, distinguishes GCB and non-GCB subgroups according to expression of CD10, BCL6 and IRF4/MUM1 (Hans *et al.*, 2004). CD10-positive and CD10-negative/BCL6-positive/MUM1-negative tumours are classed as GCB tumours, and the remainder as non-GCB (Hans *et al.*, 2004). Recently, additional antibodies (including FOXP1, LMO2, GCET1 and BCL2), have been incorporated into additional algorithms which has increased the accuracy of the approach (Choi *et al.*, 2009) (Meyer *et al.*, 2011). Nevertheless, immunostaining remains an imperfect substitute for gene expression profiling, fails to identify Type 3 DLBCLs, and suffers from poor inter-laboratory reproducibility. More recently, new platforms for molecular profiling of fixed diagnostic tissue such as NanoString have been used for COO classification with promising results (Scott *et al.*, 2015; Xue *et al.*, 2015). Importantly, when treated with current standard therapies, patients with GCB DLBCL have a significantly better overall survival than those with the ABC subtype. Patients with ABC DLBCL have a 5-year overall survival rate of only 35%, compared to 60% in patients with GCB DLBCL (Shaffer *et al.*, 2002b; Dunleavy *et al.*, 2009; Meyer *et al.*, 2011).

Despite recognition of two very different DLBCL phenotypes by gene expression analysis, at present, patients with either ABC or GCB DLBCL receive the same therapy. It is therefore not surprising that there are differences between response and cure rates between these disease subgroups. Future therapies would ideally target the disease in a subgroup-specific manor, which first requires a better understanding of the molecular

machinery to which they depend. Indeed, several agents targeting subgroup-selective pathogenic mechanisms, (as discussed below) are currently in clinical trials.

1.5. Pathogenesis of DLBCL

1.5.1. Genetic abnormalities in DLBCL

Similar to other types of cancer, B-cell lymphomas arise from the multistep accumulation of genetic abnormalities such as translocations, point mutations and deletions (Shaffer *et al.*, 2012a). Multiple genetic lesions in DLBCL are often associated with the genes and molecular pathways which affect behaviours in relation to the hallmarks of cancer.

B-cell development is initiated in the primary lymphoid organs and differentiation occurs in the secondary lymphoid tissues such as the spleen, lymph nodes or tonsils. During these stages of development a number of DNA modifications occur which can predispose to various genetic aberrations (figure 1) (Nogai *et al.*, 2011). Initiation of normal B-cell development occurs in the bone marrow whereby formation of the BCR occurs by the rearrangement of genes which encode the immunoglobulin heavy and light chains (Hozumi *et al.*, 1976). This process, called V(D)J recombination, involves double-stranded DNA breaks by the recombination activating genes 1 (RAG1) and 2 (RAG2), followed by end-joining repair processes (Hozumi *et al.*, 1976). Cells that do not acquire heavy and light chain variable regions correctly undergo apoptosis at this stage, whereas cells expressing the BCR become mature naïve B cells which leave the bone marrow and enter the periphery.

Until B cells encounter an antigen, they are considered naïve B cells, as shown in figure 1 (Bertoni *et al.*, 2007). Following contact with an antigen, the BCR becomes activated and naïve B cells are stimulated, resulting in their proliferation and migration to the secondary lymphoid tissues such as the lymph nodes, where they form the germinal centre (Steinhardt *et al.*, 2012). Here, B cells differentiate into germinal centre cells (centrocytes and centroblasts) and subsequently into plasma cells (MacLennan, 1994). Centrocytes and centroblasts cycle through the light and dark zones of the germinal centre, where they rapidly proliferate, differentiate, and revise their antigen receptors (Berek *et al.*, 1991; Jacob *et al.*, 1991). This occurs by somatic hypermutation (SHM) of the immunoglobulin heavy chain variable region (IGHV) genes, as well as by the process of class switch recombination (CSR) which involves DNA double strand breaks (Steinhardt *et al.*, 2012).

Both of these processes are mediated by activation-induced cytidine deaminase (AID), which deaminates cytosine to uracil (Muramatsu *et al.*, 1999; Muramatsu *et al.*, 2000).

Although highly controlled, V(D)J recombination, SHM and CSR each lead to an inevitable degree of collateral damage to other genes, resulting the accumulation of various somatic genetic changes which may promote lymphomagenesis (Nogai *et al.*, 2011). During SHM for example, activating or inactivating mutations and small insertions/deletions can occur in numerous key non-immunoglobulin genes involved in B-cell differentiation (Nogai *et al.*, 2011). In addition, chromosomal translocations can occur as a result of misrepair of DNA breaks that occur during V(D)J recombination in the bone marrow and class-switch recombination in the germinal centre (Nogai *et al.*, 2011). AID-induced DNA lesions during SHM also predispose to double strand DNA breaks and promote translocation formation. Unfortunate consequences of these initial recombination events are the development of select chromosomal aberrations, affecting specific oncogenes and tumour suppressors. In fact, up to 50% of DLBCLs have translocations involving immunoglobulin loci (Shipp, 2007).

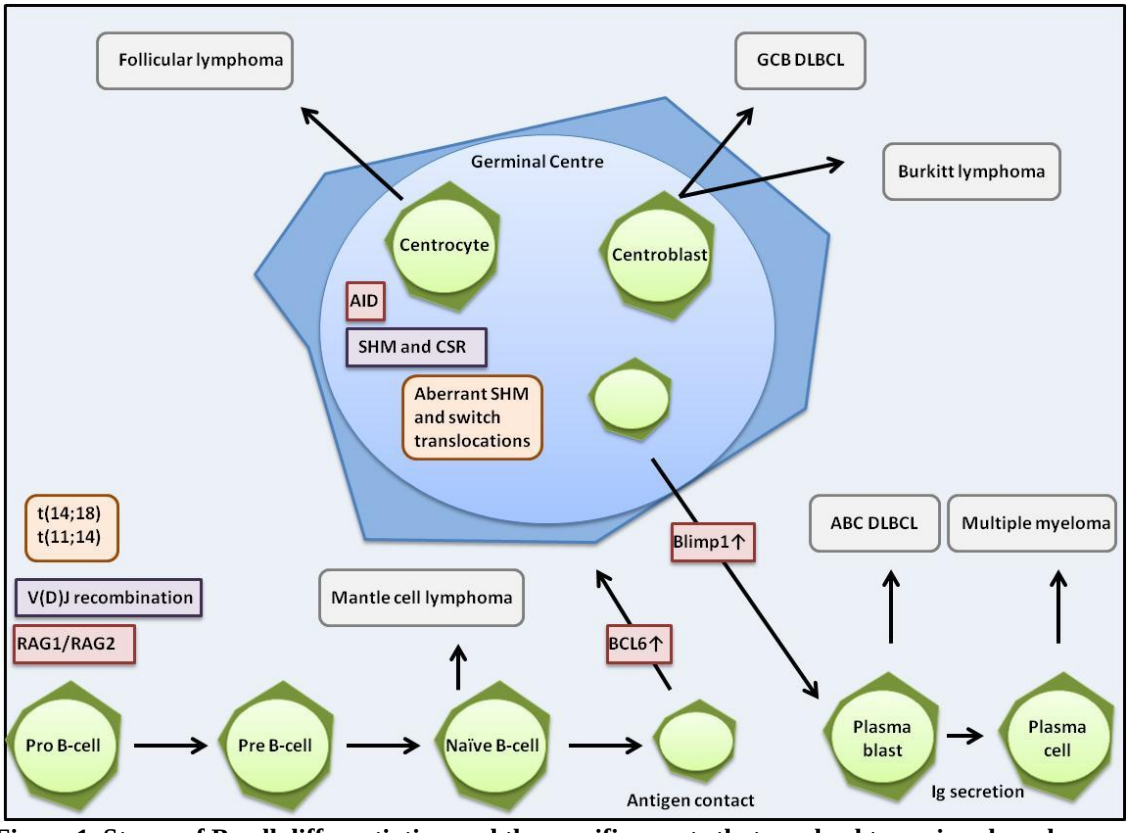

Figure 1. Stages of B-cell differentiation and the specific events that can lead to various lymphomas. Image adapted from (Nogai *et al.*, 2011)

1.5.2. Deregulation of BCL2 activity

B-cell lymphoma 2 (BCL2) is the founding member of a family of regulatory proteins which regulate apoptosis (Tsujimoto Y, 1984). First discovered for its role in t(14;18) translocations in follicular lymphoma, BCL2 is now regarded as a central anti-apoptotic, pro-survival protein of oncogenic nature (Aukema *et al.*, 2011). Recurrent t(14;18) (q32;q21): *BCL2-IGH* translocations lead to upregulation of BCL2, causing it to be aberrantly regulated and constitutively expressed (Willis *et al.*, 2000; Rui *et al.*, 2011) (Huang *et al.*, 2002; Kuppers, 2005). This translocation occurs in 20% of DLBCL, where it is more common in the GCB subtype (Willis *et al.*, 2000; Iqbal *et al.*, 2004). In fact, RNA-sequencing data has recently shown that *BCL2* is the most highly mutated gene in GCB DLBCL (Schuetz *et al.*, 2012). *BCL2* deregulation can also occur in ABC DLBCL; however this is usually by amplification of the *BCL2* gene or transcriptional upregulation through constitutive activation of NF-κB (Iqbal *et al.*, 2006).

1.5.3. Deregulation of BCL6 activity

Another recurrent translocation in DLBCL involves the transcription factor and master regulator of the germinal centre reaction, B-cell lymphoma 6 (*BCL6)*. BCL6 is a zinc finger transcriptional repressor which has essential roles in B cells and T cells in normal antibody responses and regulates genes involved in the cell cycle, differentiation and inflammation (Shaffer *et al.*, 2000). BCL6 principally functions to allow cells in the germinal centre to differentiate and sustain rapid proliferation, while tolerating DNA breaks (without initiating DNA damage responses) during SHM and class switch recombination (Rui *et al.*, 2011). BCL6 therefore prevents premature differentiation of B cells and their escape from the germinal centre before selection of clones producing high affinity antibodies (Basso *et al.*, 2012).

BCL6 in DLBCL is frequently deregulated by chromosomal rearrangements of the *BCL6* locus, which occurs in around 20% of DLBCL patients, where a higher frequency is observed in patients with the ABC subgroup of DLBCL (Iqbal *et al.*, 2007; Basso *et al.*, 2012; Shaffer *et al.*, 2012a). Often deregulated by t(3;14) (q27;q32) *BCL6-IGH* translocations, recombination events place the coding domain of *BCL6* downstream of heterologous regulatory regions from over 20 chromosomal partners (Ye *et al.*, 1993; Willis *et al.*, 2000; Pasqualucci, 2013). *BCL6* translocations therefore ultimately prevent the normal downregulation of BCL6 during differentiation of cells into post-GCB cells (Basso *et al.*, 2012).

Gene expression profiling experiments have been a useful tool for understanding the role of BCL6 in lymphomagenesis, where BCL6 has been demonstrated to block plasmacytic differentiation and promote progression of the cell cycle (Shaffer *et al.*, 2000). Moreover, BCL6 has also been shown to block the DNA-damage response by repressing ATR and TP53 (Phan *et al.*, 2004; Ranuncolo *et al.*, 2007). In addition, another important target of BCL6 is the previously described pro-survival factor BCL2, which is also frequently amplified on locus 18q24 in patients with the GCB subgroup of DLBCL (Iqbal *et al.*, 2004; Ci *et al.*, 2009; Saito *et al.*, 2009). The fundamental role of BCL6 in lymphomagenesis has been highlighted by the promotion of human-like lymphoma development in mouse models with deregulated BCL6 expression and BCL6 now represents an attractive therapeutic target in lymphoma (Cattoretti *et al.*, 2005).

1.5.4. Disruption of terminal differentiation

A significant role for BCL6 is in the control of differentiation to plasma cells via suppression of PR domain zinc finger protein 1 (PRDM1), which is also known as BLIMP1 (Shapiro-Shelef *et al.*, 2003). *BLIMP1* is a tumour suppressor gene that functions a transcriptional repressor by binding to DNA and acting as a scaffold to recruit multiple core-repressor proteins (Bikoff *et al.*, 2009). Its role is to promote terminal differentiation of B cells into plasma cells by repressing genes important in B-cell receptor signalling and proliferation (Lin *et al.*, 1997; Shaffer *et al.*, 2002a) . This was demonstrated by Shapiro-Shelef et al (2003), where conditional knockout of Blimp-1 in the B cells of mice failed to produce plasma cells and serum immunoglobulins (Shapiro-Shelef *et al.*, 2003).

In 25% of cases of DLBCL, aberrant loss of expression of BLIMP1 is due to constitutive repression by deregulated BCL6 (Pasqualucci *et al.*, 2006; Mandelbaum *et al.*, 2010). A consequence of these events is that ABC DLBCLs escape from terminal differentiation and cell cycle arrest (Pasqualucci, 2013). This pathogenic block in the differentiation pathway may also be due to inactivating mutations and deletions of the *BLIMP1* gene, which have also been detected in one quarter of ABC DLBCLs (Mandelbaum *et al.*, 2010). The importance of correctly functional BLIMP1 in ABC DLBCL has been demonstrated in mouse models with conditional deletion of *BLIMP1* in the germinal centre, where mice developed an ABC DLBCL-like disease (Mandelbaum *et al.*, 2010).

1.5.5. Alterations in epigenetic modifiers

In recent years there have been increasing studies reporting recurrent genetic lesions in histone/chromatin modifiers such as acetyltransferases and histone methyltransferases (Morin *et al.*, 2010; Béguelin *et al.*, 2013; Pasqualucci, 2013). Inactivating mutations and deletions of CREB Binding Protein *(CREBBP)* and less frequently, E1A Binding Protein P300 (*EP300)* have been detected in up to 35% of DLBCL, and found to occur more commonly in GCB DLBCLs (Morin *et al.*, 2011; Pasqualucci *et al.*, 2011b). These proteins modify lysine residues on both histone and non-histone nuclear proteins, functioning as transcriptional coactivators for many transcription factors (Pasqualucci *et al.*, 2011a). CREBBP and EP300 enhance transcription by mechanisms such as by acetylation of chromatin and transcriptional activators, such as p53, and acetylation-mediated inactivation of repressors of transcription such as BCL6 (Pasqualucci *et al.*, 2011a). Mutations of CREBBP and EP300 cause disruption of their ability to acetylate substrates such as p53 and BCL6, which consequently leads to constitutive active BCL6 and decreased tumour suppressor activity from p53 (Pasqualucci *et al.*, 2011a). There is no surprise that CREBBP and EP300 have become attractive therapeutic targets for DLBCL. Current attempts have targeted these proteins by histone deacetylase inhibitors (HDACs), which have had growth inhibitory effects in DLBCL cell lines and patients with chemotherapy-resistant DLBCL (Cai *et al.*, 2013; Xue, 2015).

Mixed-lineage leukaemia 2 (*MLL2*) is an example of a gene which encodes a highly conserved histone methyltransferase, its role being to control gene transcription by modification of lysine-4 on histone 3 (Shilatifard, 2012). Interestingly, *MLL2* is the most commonly mutated gene in B-NHL, representing over 30% of DLBCL and 89% of follicular lymphomas (Morin *et al.*, 2011; Pasqualucci *et al.*, 2011b). Inactivating mutations of MLL2 in DLBCL generate truncated proteins that lack the catalytic activity that is required for methyltransferase activity, suggesting that this gene acts as a tumour suppressor in both ABC and GCB DLBCL (Morin *et al.*, 2011; Pasqualucci *et al.*, 2011a).

Moreover, a particularly striking difference between ABC and GCB DLBCL is the presence of somatic gain-of-function mutations in the histone methyltransferase enhancer of zeste homolog 2 (*EZH2),* which occurs in approximately 22% of GCB DLBCL patient samples, but not in ABC DLBCL (Morin *et al.*, 2010). EZH2 is the catalytic subunit of the chromatin regulator polycomb repressive complex 2 (PRC2) and mediates

transcriptional repression using its methyltransferase activity (Velichutina *et al.*, 2010). EZH2 is critical for normal embryo development and important for V(D)J recombination in pre-B cells (Su *et al.*, 2003). Normally, after the pre-B-cell stage, EZH2 expression decreases as B cells exit the GC reaction, allowing expression of genes that control terminal differentiation (Velichutina *et al.*, 2010). However, when EZH2 is somatically mutated, suppression of GC exit genes and checkpoints continues, resulting in hyperplasia (Béguelin *et al.*, 2013). Several recent studies have investigated the effects of selective small molecule inhibitors of EZH2, which were shown to effectively induce cell cycle arrest and apoptosis in EZH2-mutated DLBCL cells (Knutson *et al.*, 2012; McCabe *et al.*, 2012).

Overall, these studies suggest a critical role for epigenetic remodelling in the malignant setting, highlighting new therapeutic opportunities for these lymphomas (Morin *et al.*, 2010; Pasqualucci *et al.*, 2011a; Lohr *et al.*, 2012).

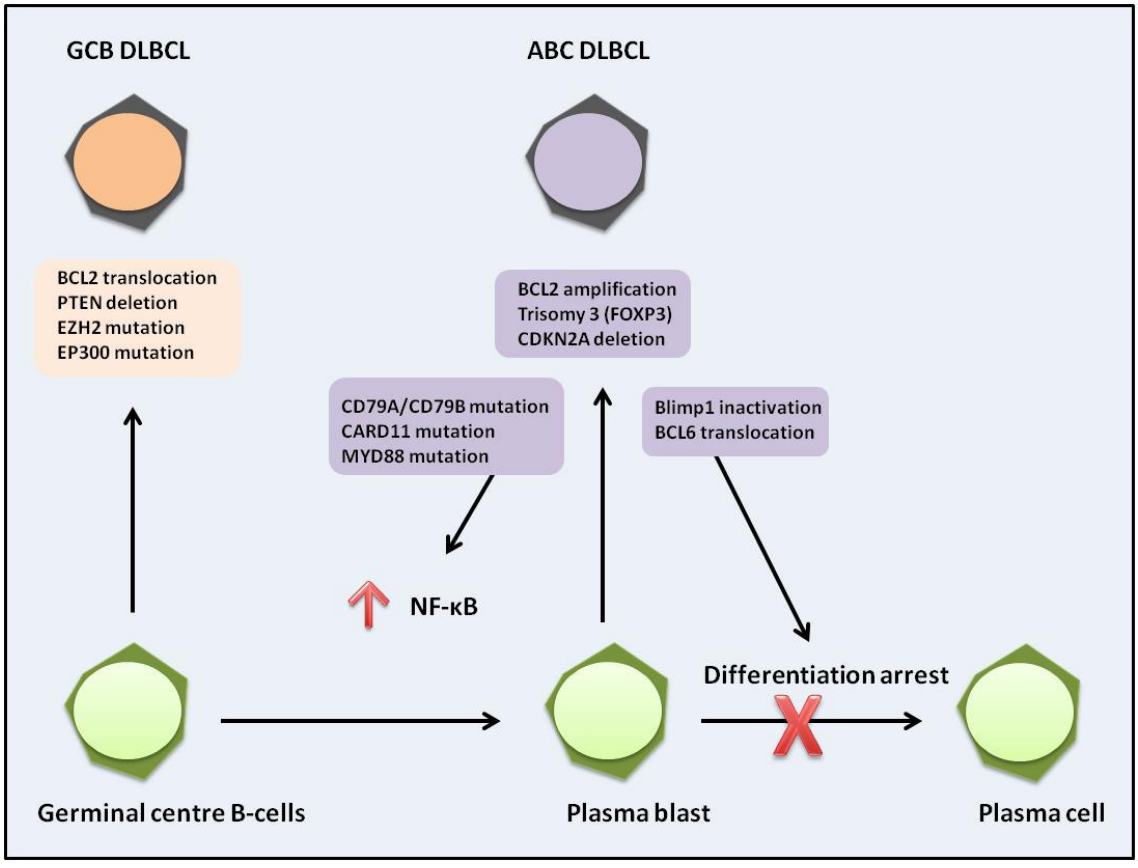

Figure 2. The origin of human lymphoid malignancies and the underlying genetic aberrations commonly associated with ABC and GCB DLBCL. Image adapted from (Rui *et al.*, 2011)

In summary, the pathogenesis of DLBCL is caused by a combination of chromosomal translocations, mutations and deletions that disrupt normal B-cell proliferation, survival and differentiation. While GCB DLBCLs are associated with translocations of BCL2,

mutations within the BCL6 autoregulatory domain and mutations of epigenetic regulators such as EZH2, patients with ABC DLBCL often harbor BCL6 translocations and amplifications of BCL2 (Ye *et al.*, 1993; Huang *et al.*, 2002; Iqbal *et al.*, 2004; Iqbal *et al.*, 2007; Morin *et al.*, 2010). In addition to the underlying genetic abnormalities previously described (and shown in figure 2), it is common for ABC DLBCLs to harbor mutations associated with BCR signalling, such as within the NF-κB pathway, as discussed in the following sections.

1.6. B-Cell Receptor signalling

1.6.1. Normal B-Cell receptor signalling

Signals propagated through the BCR are critical for the development of normal B cells and the survival of mature B cells (Kraus *et al.*, 2004). In summary, upon ligand stimulation, BCRs aggregate in microclusters, which recruit Src family tyrosine kinases, which phosphorylate tyrosine residues within the immunoreceptor tyrosine-based activation motif (ITAM) of the BCR components CD79A and CD79B (Rickert, 2013). This causes recruitment of the spleen tyrosine kinase (SYK), which phosphorylates the B-cell linked (BLNK) protein, engaging Bruton's tyrosine kinase (BTK) (Rickert, 2013). In turn, phosphatidylinositol -4, 5-bisphosphate 3-kinase (PI3K) activation allows recruitment of BTK to the plasma membrane by binding to phosphatidylinositol (3, 4, 5)-trisphosphate (PIP3) (Shaffer *et al.*, 2012a). This enables activation of phospholipase C gamma 2 (PLCγ2), which hydrolyses phosphatidylinositol (4,5)-bisphosphate (PIP2) into diacylglycerol (DAG) and inositol trisphosphate (IP3) (Shaffer *et al.*, 2012a). IP3 induces release of calcium stores via the IP3 receptor on the endoplasmic reticulum. Together, calcium and DAG activate protein kinase C beta (PKCβ), leading to activation of NF-κB via activation of the CARD11-BCL10-MALT1 (CBM) complex (Shaffer *et al.*, 2012a).

B cells use antigen-dependent BCR signalling to induce their differentiation and proliferation during an immune response. This occurs through the initiation of a set of signalling pathways (figure 3), including the NF-κB, NFAT, PI3K and MAPK pathways, as reviewed by Dar Porto et al (2004) (Dal Porto *et al.*, 2004). Upon activation, NF-κB and NFAT bind to the promoters, enhancers and other regulatory regions of copious genes and regulate their expression. As a result, these transcription factors are responsible for controlling the growth, proliferation and function of peripheral lymphocytes.

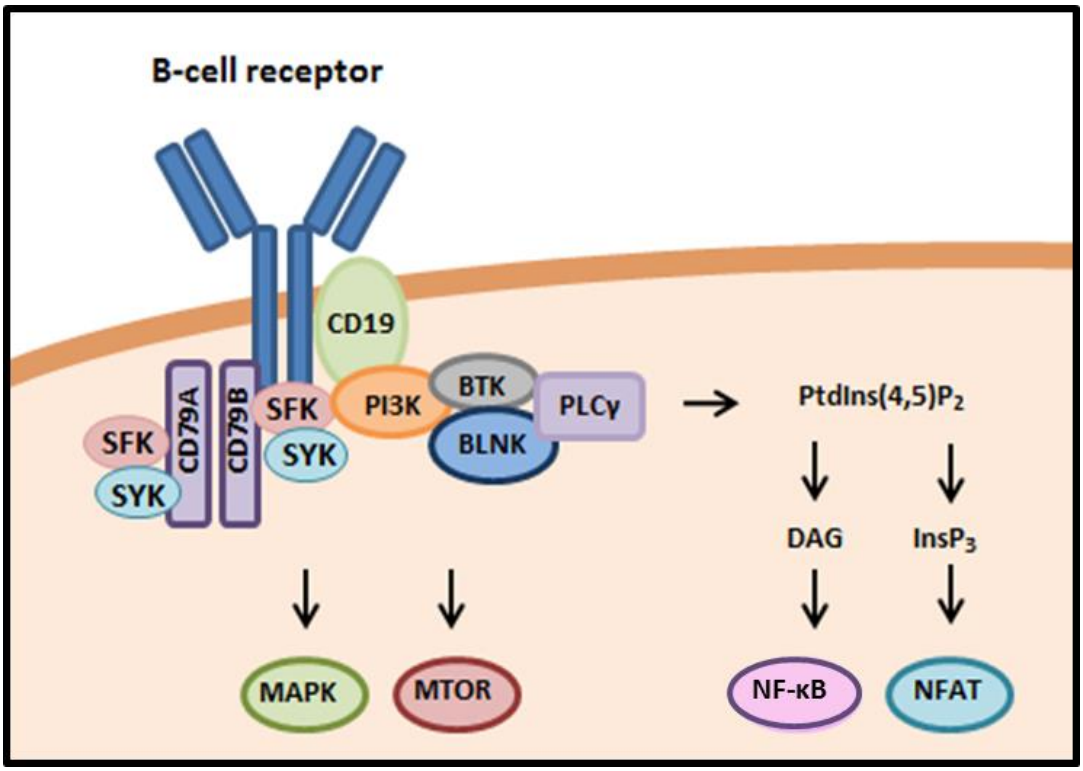

Figure 3. The B-cell receptor and the key signalling pathways initiated by BCR stimulation.

1.6.2. B-Cell receptor signalling in DLBCL

Despite the numerous somatic hypermutation events and *IG* translocations that occur during lymphomagenesis, there is rarely loss of the BCR in the malignant setting, indicating that continued BCR signalling is important for B-cell lymphoma maintenance (Kuppers, 2005). Indeed, signals from the BCR are known to be critical promoters of lymphoma cell proliferation and survival (Shaffer *et al.*, 2012b). Interestingly, prominent BCR clusters, resembling those on normal B cells following stimulation by an antigen, were identified on cell lines and patient samples of ABC DLBCL, suggesting that this subtype resembles normal, activated B cells (Davis *et al.*, 2010). In contrast, BCRs in GCB cell lines were likened to those of a normal resting B-cell, where BCRs were evenly distributed across the plasma membrane (Davis *et al.*, 2010).

1.6.3. Chronic active BCR signalling

There is accumulating evidence that ABC DLBCL are sustained by dysregulation of normal BCR signalling pathways that regulate B-cell activation and survival (Lenz *et al.*, 2010). This may be a consequence of ligand-independent BCR signalling due to

mutations in components of the B-cell receptor, such as somatic mutations of the Igα or Igβ subunits (Davis *et al.*, 2010). This altered BCR surface expression is described as 'chronic-active BCR signalling', which can lead to constitutive activation of downstream signalling events, as described in the sections below.

1.7. The NF-κB signalling pathway

Constitutive activation of NF-κB is a hallmark of numerous malignancies, where the functional consequences of its activation have a striking correlation with the hallmarks of cancer (Hanahan *et al.*, 2000; Perkins, 2012). NF-κB can drive the malignant phenotype in a number of ways, such as by inhibiting apoptosis, driving cell proliferation and promoting migration and invasion (Kumar *et al.*, 2004; Karin, 2006; Kim *et al.*, 2006). The oncogenic nature of the NF-κB pathway and its many roles have now been extensively reviewed (Baldwin, 2001; Karin *et al.*, 2002).

Deregulation of NF-κB in cancer, leading to nuclear NF-κB-localisation and aberrant NF-κB target gene expression, may be due to oncogenes such as Harvey Rat Sarcoma Viral Oncogene Homolog (HRAS), or by positive regulation from upstream components such as mutated Caspase Recruitment Domain Family Member 11 (CARD11) (Lenz *et al.*, 2008a; Staudt, 2010; Perkins, 2012). Alternatively, constitutively active NF-κB may be a consequence of the inability of negative regulators of NF-κB, such as the intracellular ubiquitin-editing protein A20 (also known as TNFAIP3) to switch off NF-κB (Compagno *et al.*, 2009; Kato *et al.*, 2009; Perkins, 2012)

Many types of B-cell lymphoma harbour constitutive activation of NF-κB, such as DLBCL and multiple myeloma, which is likely to stem from the fact that NF-κB signalling has a major role in the differentiation, proliferation and maturation of normal B cells (Gerondakis *et al.*, 2010; Staudt, 2010).

1.7.1. Biology of NF-κB/primary structure of NF-κB

NF-κB was first identified as a transcription factor that binds to the enhancer of the kappa immunoglobulin light chain gene in B cells (Sen *et al.*, 1986). Soon after, NF-κB was recognised as a major regulator of immune function and the inflammatory response (Karin, 2009; Vallabhapurapu *et al.*, 2009). The NF-κB transcriptional pathway has since been associated with the regulation of hundreds of genes involved in a vast array of

cellular processes such as apoptosis, the cell cycle, inflammation and immunoregulation (Jost *et al.*, 2007).

NF-κB belongs to the evolutionarily conserved Rel family of proteins (figure 4), which includes c-Rel, RelA (p65), RelB, NF-κB1 (p50) and NF-κB2 (p52). NF-κB1 and NF-κB2 encode longer precursor proteins that can be processed to active p50 and p52 respectively (Hayden *et al.*, 2008). In resting cells, NF-κB proteins are sequestered in the cytoplasm in association with inhibitory IκB proteins including IκBα, IκBβ and IκBε. Ankyrin repeats found in IκB proteins are also present in p100 and p105, allowing them to also function as IκB proteins (Vallabhapurapu *et al.*, 2009).

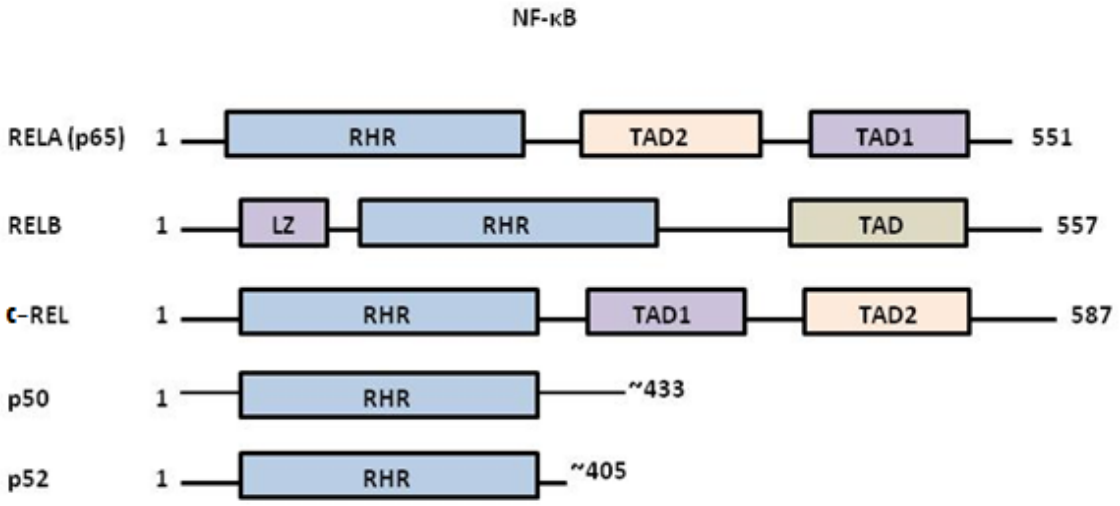

Figure 4. The primary structure of the NF-κB subunits. The NF-κB subunits share a DNA binding domain and dimerization domain called the REL homology region (RHR). RelA, RelB and c-Rel contain transactivation domains whereas RelB has an amino-terminal leucine zipper-like (LZ) motif. Image adapted from (Perkins, 2012)

1.7.2. Activation of the NF-κB signalling pathway

NF-κB is activated by many different stimuli, including antigen-binding to immune receptors and by binding of inflammatory cytokines, such as TNFα, to toll-like receptors (TLR) and the TNFα receptor. Many stimuli activate the canonical NF-κB pathway, which specifically requires the catalytic IKKα and IKKβ and the regulatory IKKγ (NEMO) subunits, (which comprise the heterotrimeric IKK complex) (Perkins, 2007). Phosphorylation of IκBα on serine 32 or serine 36 causes IκBα to be targeted for polyubiquitination and degradation by the 26S proteasome, allowing release of NF-κB subunits (Karin *et al.*, 2000; Karin, 2009), as shown in figure 5. There is the potential for the formation of 15 different NF-κB dimers, which for the canonical pathway are typically

p50/p65 and p50/c-Rel heterodimers, (Staudt, 2010; Vincent Feng-Sheng Shih, 2011). Following release of NF-κB subunits from inhibitory IκB proteins, dimers translocate to the nucleus and bind to κB sites on DNA, leading to transcriptional activation of genes with a broad spectrum of roles.

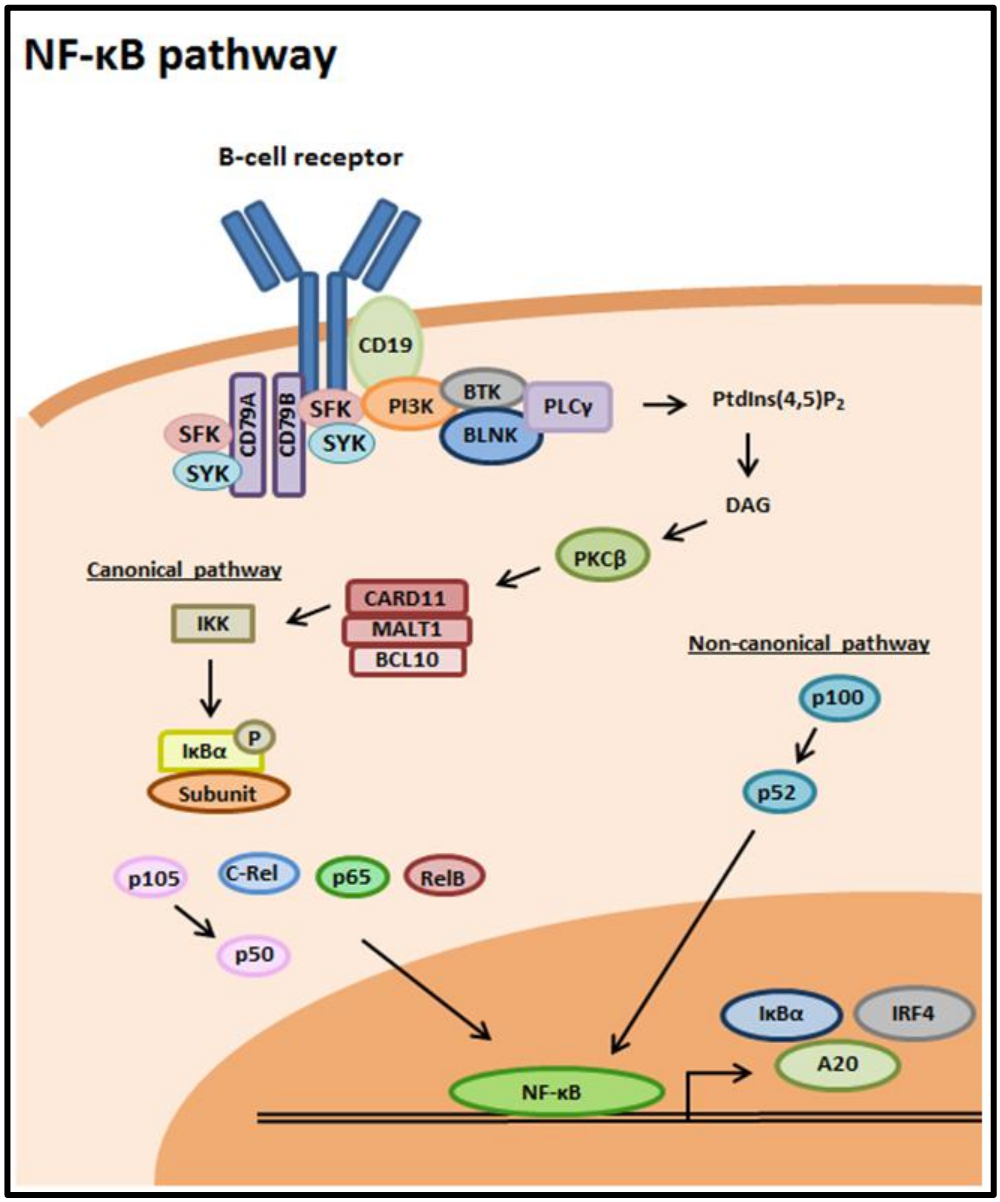

Figure 5. The NF-κB signalling pathway. NF-κB signalling can be initiated by activation of the B-cell receptor, leading to activation of the CBM complex via recruitment of TRAF6 (not shown) and subsequent activation of IKK subunits and the NF-κB signalling cascade.

The non-canonical pathway on the other hand, is initiated by other stimuli and is engaged specifically by TNF-family receptors such as CD40, BAFF receptor and the lymphotoxin β receptor (Bonizzi *et al.*, 2004). The pathway is dependent on phosphorylation of homodimers of IKKα by activation of the upstream kinase NIK. In non-stimulated cells NIK is subject to rapid turnover, however stimulation of the pathway causes stabilisation of NIK and IKKα activation, which in turn regulates the processing of the p100 precursor

protein to p52, leading to nuclear translocation of the p52-RelB heterodimer (Liao *et al.*, 2004).

1.7.3. NF-κB signalling in DLBCL

Mutations in several upstream components of the NF-κB pathway have been identified in ABC DLBCL tumours, leading to sustained activation of the NF-κB pathway, which is now a well-known hallmark of this subgroup of DLBCL (Lam *et al.*, 2005). This was first recognised by Davis et al (2001) where small molecule inhibitors of IκB Kinase were found to be toxic for ABC DLBCL cell lines (Lam *et al.*, 2005). Their data indicated that specifically DLBCLs of the ABC subgroup were addicted to constitutive NF-κB signalling and require it for their survival (Davis *et al.*, 2001; Lam *et al.*, 2005). Moreover, as described previously, gene expression profiling has shown that many genes upregulated in ABC DLBCL are known NF-κB target genes, such as BCL2 and IL6, suggesting that these lymphomas utilise the transcriptional activity of NF-κB to express genes detrimental for patient survival (Davis *et al.*, 2001; Lenz *et al.*, 2008c).

1.7.4. CD79A/B mutations

Constitutive NF-κB activation in approximately 20% of ABC DLBCLs appears to be due to somatic mutations in the *CD79A* and *CD79B* genes which encode components of the B-cell receptor (Davis *et al.*, 2010). Mutations are usually non-synonymous missense substitutions that affect the N-terminal tyrosine of *CD79B*. Therefore ABC DLBCL mutated cases retain an intact ITAM region of either *CD79A* or *CD79B*, so that at least one docking site for SYK signalling is functional (Davis *et al.*, 2010). Mutations ultimately lead to ligand-independent chronic active BCR signalling, enhancing BCR signalling in two ways; first by enhancing the surface expression of the BCR, therefore enhancing the duration of BCR-dependent signalling and second by making the BCR resistant to negative regulation by the tyrosine-protein kinase LYN (Davis *et al.*, 2010; Rossi *et al.*, 2013). Mutations in *CD79A* and *CD79B* are rare or absent in other types of lymphoma and have been described as being the genetic 'smoking gun' that links the pathogenesis of ABC DLBCLs with chronic active BCR signalling (Rui *et al.*, 2011; Shaffer *et al.*, 2012b).

1.7.5. Alterations in positive regulators of NF-κB

In an attempt to identify novel oncogenes, Ngo et al (2006) used RNA interference techniques in a loss-of-function 'Achilles heel' screen of DLBCL cell lines (Ngo *et al.*, 2006). They identified components of the antigen receptor – NF-κB signalling pathway such as CARD11, BCL10 and MALT1 (components of the CBM complex) as essential for the survival of ABC DLBCL cell lines, a dependency which was not shared by other DLBCL types (Ngo *et al.*, 2006). The CBM complex is formed following antigenic stimulation of the BCR and acts as a signalling scaffold, responsible for the recruitment of TRAF6, TAK1 and the IKK complex to activate the canonical NF-κB pathway (Nogai *et al.*, 2011). In normal lymphocyte activation, CBM complex formation is transient, whereas in ABC DLBCL the complex is constitutively active, which is likely due to mutations in the complex that function oncogenically (Nogai *et al.*, 2011).

The pro-tumour function of the CARD11 scaffold protein was first confirmed by the observation of constitutive NF-κB activation in lymphoma cell lines into which CARD11 mutants had been introduced (Lenz *et al.*, 2008a). It is now established that mutations in CARD11 are present in approximately 10% of ABC DLBCL cases, causing a conformational change in CARD11 (Lenz *et al.*, 2008a). CARD11 encodes a multidomain signalling scaffold protein consisting of an N-terminal CARD motif, an inhibitory domain, a coiled-coil domain and a C-terminal MAGUK domain (Thome *et al.*, 2010). In resting B cells, CARD11 exists in a latent closed conformation, but upon engagement of the BCR the inhibitory domain of CARD11 is phosphorylated by PKCβ (Thome *et al.*, 2010). In turn, this effectively results in the spontaneous opening of CARD11, which subsequently relocalises to the plasma membrane to recruit MALT1 and BCL10 into the CBM complex, activating the IKK2 kinase and initiating NF-κB activity (Lenz *et al.*, 2008a; Thome *et al.*, 2010). Interestingly, the active conformation of the CBM complex has been identified in ABC DLBCLs with wild-type CARD11, where this is due to mutations of components of the BCR itself, for example in CD79A or CD79B, as described previously in section 1.8.4 (Davis *et al.*, 2010).

Although the CBM complex represents a key area of study in the field of DLBCL research, a recent study screened for additional components of the CBM complex in lymphocytes, where the linear ubiquitin chain assembly complex (LUBAC) was found to bind to and preassemble the CBM complex following engagement of the BCR, governing NF-κB activation (Dubois *et al.*, 2014). Knockdown of LUBAC hampered NF-κB activity

and was lethal to ABC DLBCL cell lines, suggesting that targeting LUBAC may also be important for the treatment of ABC DLBCL (Dubois *et al.*, 2014).

1.7.6. Alterations in negative regulators of NF-κB

Interestingly, an alternative mechanism of constitutive active NF-κB in ABC DLBCL was detected by several research groups investigating genetic lesions in the genes encoding NF-κB regulatory proteins. 30% of cases of ABC DLBCL have inactivating mutations of A20, which negatively regulates NF-κB (Compagno *et al.*, 2009; Kato *et al.*, 2009). Biallelic inactivation of TNFAIP3 (which encodes A20), further enhances NF-κB signalling in ABC DLBCL, inhibiting apoptosis and promoting cell proliferation (Compagno *et al.*, 2009).

1.7.7. Targeting NF-κB in DLBCL

Although there is now vast information supporting the role of NF-κB signalling in DLBCL, inhibition of this pathway for the treatment of DLBCL has been a difficult task. Due to the requirement of NF-κB for the function of normal, non-cancerous cells, and the ability of this signalling cascade to crosstalk with many other pathways, inhibition of NF-κB can cause many unwanted side effects.

Some success has been achieved in the clinic using the proteasome inhibitor Bortezomib (Velcade®) for the treatment of various NHLs such as multiple myeloma (Palumbo *et al.*, 2011; Bose *et al.*, 2014). Bortezomib inhibits NF-κB activation by blocking proteasomal degradation of IκBα (therefore preventing the release of NF-κB subunits to the nucleus) (Bose *et al.*, 2014). Although known to have many other effects in the cell, Bortezomib has been shown to have efficacy in relapsed/refractory DLBCL when combined with chemotherapy (Dunleavy *et al.*, 2009; Chen *et al.*, 2011a; Bose *et al.*, 2014). A significantly higher response and median overall survival was observed in ABC DLBCL compared to GCB DLBCL, which was expected due to their dependency on NF-κB (Dunleavy *et al.*, 2009).

In recent years, the immuno-modulatory agent Lenalidomide (Revlimid®) has shown potential for treatment of patients with haematological malignancies, including DLBCL (Rajkumar, 2014; Abou Zahr *et al.*, 2015; Ghosh *et al.*, 2015). Patients with relapsed/refractory ABC DLBCL have shown a 52% response rate to lenalidomide

monotherapy, compared to 8.7% in patients with GCB DLBCL (Hernandez-Ilizaliturri *et al.*, 2011). The molecular mechanism through which lenalidomide is active in ABC DLBCL was found to be by downregulating the transcription factors IRF4 and SPIB, which together repress IRF7, thereby preventing production of IFN-β, which in turn reduces amplification of NF-κB signalling (Yang *et al.*, 2012). The selectivity of *in vitro* activity of lenalidomide against ABC DLBCL cell lines has led to phase I and II clinical trials using lenalidomide as a monotherapy (Hernandez-Ilizaliturri *et al.*, 2011). Moreover, subsequent trials have now been conducted using R-CHOP + lenalidomide (R2CHOP), which has been shown to be safe for both ABC and GCB patients in two phase I trials (Nowakowski *et al.*, 2011; Chiappella *et al.*, 2013).

Chronic active BCR signalling in DLBCL also provides an opportunity for therapeutic targeting upstream of IKK (Davis *et al.*, 2010). Inhibition of Bruton's tyrosine kinase (BTK) using Ibrutinib, has been shown to kill ABC DLBCL with chronic active BCR signalling, but not other types of lymphomas (Pan *et al.*, 2007; Davis *et al.*, 2010). This potent, covalent inhibitor has been well-tolerated and shown significant anti-tumour activity in CLL and MCL and combination therapies are currently being tested in DLBCL (Herman *et al.*, 2011; Wang *et al.*, 2015). Interestingly, a recent study investigated the effects of combined treatment of ABC DLBCLs using the BTK inhibitor ibrutinib and lenalidomide (Yang *et al.*, 2012). These therapies were reported to synergise in killing ABC DLBCLs and were described as being a synthetically lethal drug combination by also blocking IRF4 induction by oncogenic NF-κB signalling. Finally, peptide inhibition of the MALT1 paracaspase of the CBM complex has demonstrated selective toxicity for ABC DLBCL, which may represent a future therapy for these lymphomas (Ferch *et al.*, 2009; Hailfinger *et al.*, 2009; Fontan *et al.*, 2012).

Despite progress being made in these fields, future targeting of NF-κB is likely to benefit from a better understanding of the contribution of individual NF-κB subunits to the pathogenesis of DLBCL and the genes they target, which is currently unclear. c-Rel has been shown to have oncogenic potential in a number of B-cell cancers and some evidence suggests a role for c-Rel in the pathogenesis of DLBCL, where *REL* is amplified in approximately 25% of GCB DLBCL (Gilmore, 1999; Gilmore *et al.*, 2004). Moreover, knockdown of c-Rel expression was shown to impair cell survival in a GCB DLBCL cell line (Pham *et al.*, 2005; Lenz *et al.*, 2008c).

Constitutive NF-κB signalling may not be restricted to the ABC subtype. For example, engagement of both the classical and alternative NF-κB pathways in DLBCL patient tumour samples were observed in 61% of ABC DLBCL tumour samples and a smaller fraction (30%) of GCB DLBCL (Compagno *et al.*, 2009). *In vitro* studies are in agreement with these findings, whereby heterogeneous expression of p52 (as a marker for noncanonical NF-κB activity) was detected in DLBCL cell lines of both ABC and GCB subgroups (Compagno *et al.*, 2009). Oncogenic lesions that specifically activate the alternative NF-κB pathway in DLBCL have not been reported until recently, whereby mutations of the TRAF3 negative regulator of the NF-κB pathway was found in ~15% of DLBCL, often coexisting with *BCL6* translocations (Zhang *et al.*, 2015).

1.8. Tonic BCR signalling and the PI3K/AKT signalling pathway

While some lymphomas remain antigen-dependent throughout their history, some DLBCL have been identified by gene expression profiling as depending on "low level" BCR survival signals in the absence of antigen engagement (Kraus *et al.*, 2004; Monroe, 2004; Srinivasan *et al.*, 2009). Continuous signals delivered by the BCR in an antigen-independent manor is a mechanism termed ‘tonic signalling’ and has been shown to enable long term B-cell survival throughout their lifespan (Gauld *et al.*, 2002; Monroe, 2004). Tonic BCR signalling was first identified in murine models where ablation of the BCR or mutation of Igα caused apoptosis of normal mature B cells (Lam *et al.*, 1997; Kraus *et al.*, 2004). Unlike chronic active BCR signalling, which is reminiscent of antigen-stimulated B cells, tonic BCR signalling is typical of a resting B-cell and is CARD11-independent (Rossi *et al.*, 2013).

In a study investigating the BCR-mediated survival signals upon which mature B cells depend, constitutively active PI3K/AKT signalling was found to rescue the survival of mature BCR-deficient B cells (Srinivasan *et al.*, 2009). Interestingly, this was not the case for the NF-κB or MAPK pathways, highlighting differences between tonic BCR signalling pathways and pathways downstream of an activated BCR (Srinivasan *et al.*, 2009).

Activation of PI3K/AKT signalling is a hallmark of many cancer types, targeting a number of cellular processes linked to tumourigenesis including the promotion of cell survival, proliferation and cell growth (Song *et al.*, 2012; Pfeifer *et al.*, 2013b). Although some BCR-dependent ABC DLBCLs with chronic active BCR signalling exhibit

constitutive PI3K activation, their main mechanism for survival is through the NF-κB pathway (Kloo *et al.*, 2011). In contrast, in BCR-dependent GCB DLBCL, tonic BCR signalling promotes survival predominantly by utilising the phosphatidylinositol-4,5-bisphosphate 3-kinase/protein kinase B (PI3K/AKT) pathway (Gauld *et al.*, 2002; Davis *et al.*, 2010). This group of DLBCL utilise tonic BCR signalling by retaining normal expression of the BCR, but with higher relative expression of BCR signalling components, such as the spleen tyrosine kinase SYK, leading to activation of the PI3K/AKT pathway (Srinivasan *et al.*, 2009; Kenkre *et al.*, 2012; Chen *et al.*, 2013).

Of note, BCR dependent DLBCLs had, in fact, already been predicted by Monti et al (2005), using a different classification system for detecting disease subtype to the COO system described in section 1.4 (Monti *et al.*, 2005). Using multiple, comprehensive consensus clustering (CCC-defined) algorithms, Monti et al (2005) identified three separate subgroups defined by the expression of genes involved in oxidative phosphorylation (OxPhos subgroup), genes involved in proliferation (BCR subgroup) and genes involved in the tumour microenvironment/host inflammatory response (Monti *et al.*, 2005). The BCR subtype was shown to have higher expression of BCR signalling components such as CD19, IgH, CD79a, BLK, SYK, PLCγ2 and genes associated with tumourigenesis such as c-Myc and BCL6 (Monti *et al.*, 2005). Although comprehensive consensus clustering classification of DLBCL is highly reproducible, the subgroups derived from COO-defined and CCC-defined methods of analysis do not overlap and the BCR-type thus includes both ABC and GCB DLBCL (Pasqualucci, 2013). Clearly the complexity of DLBCL must not be underestimated, where the success of future therapies likely lies in a targeted, patient-specific approach.

Chemical inhibition of SYK, using the ATP-competitive inhibitor R406, has been shown to decrease aberrant BCR signalling and induce apoptosis in BCR-type DLBCL cell lines regardless of COO type (Chen *et al.*, 2008). Follow-up studies investigating the role of SYK in DLBCL led to the discovery of *SYK* amplifications in BCR-type DLBCLs (Chen *et al.*, 2013). Clinical trials using the oral SYK inhibitor fostamatinib (R788) have since showed a 22% response rate in patients with DLBCL, and clinical efficacy has been demonstrated *in vivo* using lymphoma mouse models (Young *et al.*, 2009; Friedberg *et al.*, 2010).

A characteristic feature specifically found in GCB DLBCL is deregulation of the phosphatase and tensin homolog (PTEN) pathway (Pfeifer *et al.*, 2013a). Normally,

PTEN is an antagonist of the oncogenic PI3K/AKT pathway, therefore playing an important tumour suppressive role (Song *et al.*, 2012). In a screen for the expression of PTEN in primary DLBCL patient samples, loss of PTEN was identified in approximately 50% of GCB DLBCL but only approximately 15% of ABC DLBCL (Pfeifer *et al.*, 2013a). Loss of PTEN in GCB DLBCL was correlated with constitutive activation of the PI3K/AKT pathway, which was not apparent in PTEN positive samples (Pfeifer *et al.*, 2013a) while ABC DLBCL showed PI3K/AKT pathway activation independent of PTEN status. Functional analysis demonstrated a dependency of PTEN negative cells on this pathway for their survival, therefore suggesting their addiction to PI3K/AKT (Pfeifer *et al.*, 2013a).

The underlying genetic abnormalities behind PTEN loss in some GCB DLBCL are mostly unknown; however deletions of the PTEN locus on chromosome 10q23 have been reported, including somatically acquired PTEN mutations and downregulation of PTEN by various microRNA (Lenz *et al.*, 2008c; Song *et al.*, 2012; Chen *et al.*, 2013; Pfeifer *et al.*, 2013a). For example, amplifications of the PTEN suppressor miR-17-92 have also been found in roughly 15% of GCB DLBCL (Xiao *et al.*, 2008).

Importantly, the studies described suggest that only patients with abnormal expression of PTEN may respond to inhibition of the PI3K pathway, which interestingly, was found evident in an *in vitro* setting, using DLBCL cell lines (Pfeifer *et al.*, 2013a). From a clinical perspective this is of key importance, where stratification of treatment may benefit many patients with GCB DLBCL.

Although not fully comprehensive, figure 6 summarises some of the genes and pathways disrupted in ABC and GCB DLBCL.

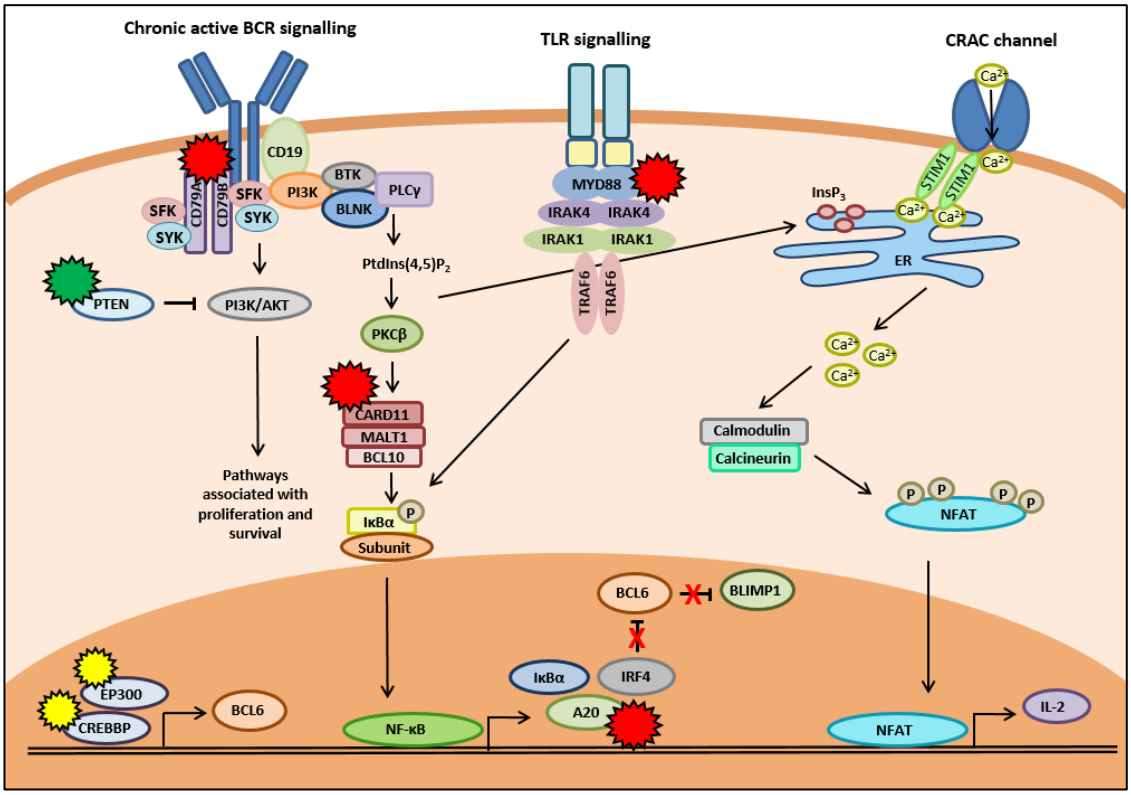

Figure 6. The genes and pathways disrupted in ABC and GCB DLBCL. The stars indicate genetic aberrations in common DLBCL signalling pathways where red = ABC DLBCL, green = GCB DLBCL and yellow = aberrations affecting both subgroups (but more common in GCB DLBCLs). Mutations of the BCR components CD79A/B cause chronic active signalling of downstream pathways, such as the NF-κB pathway and potentially other pathways downstream of the BCR, such as the NFAT pathway. Mutations in the coiled-coil domain of CARD11 also causes constitutive activation of the NF-κB pathway, which is a hallmark of ABC DLBCLs. Mutations in the negative regulator of NF-κB, A20 leads to further promotion of the NF-κB pathway and cell survival in these lymphomas. Activation of NF-κB leads to the transcriptional activation of IRF4, which in turn downregulates BCL6 expression, allowing the release of the plasma cell master regulatory PRMD1. In a normal cell, this leads to the development of the cell into a differentiated plasma cell, however this circuit is disrupted in DLBCL, blocking terminal B-cell differentiation. Some DLBCLs rely on survival signals independent of antigen engagement of the BCR. Some of these lymphomas depend on the PI3K/AKT pathway for survival, which has been shown to be constitutively activated in GCB DLBCLs with loss of the negative regulator of the PI3K/AKT pathway, PTEN. TLR signalling is also another pathway which is aberrantly expressed in ABC DLBCL cells due to mutations in the MYD88 adaptor, leading to activation of NF-κB. Finally, dysregulation of epigenetic modifiers are frequent in DLBCL, particularly in the GCB DLBCL. Mutations of EP300 and CREBBP, for example, have been shown to cause constitutive activation of BCL6 and TP53.

1.9. Pathway lesions downstream of TLR signalling

TLRs are key receptors in the BCR-independent response to infectious organisms which sense a plethora of molecules from pathogens including lipoproteins, double stranded RNA/DNA and many other foreign components, collectively termed pathogen-associated molecular patterns (Rawlings *et al.*, 2012). Ligand binding to TLRs leads to engagement of various cytoplasmic adaptor molecules such as myeloid differentiation primary response gene 88 (MYD88). Upon stimulation of the TLR, MYD88 triggers the activation

of NF-κB via assembly of the interleukin-1 receptor-associated (IRAK) kinases IRAK4, IRAK1, and IRAK2, followed by activation of TRAF6 and polyubiquitination of the MAP3K7 kinase, which in turn phosphorylates IKK2 (Lin *et al.*, 2010; Rawlings *et al.*, 2012).

Dysregulation of BCR-independent immune signalling pathways, such those triggered by the TLRs have been demonstrated in the pathogenesis of DLBCL. For example, components of the TLR – NF-κB signalling pathway (such as MyD88 and IRAKs) are essential for NF-κB activation in various ABC DLBCL cell lines (Ngo *et al.*, 2006; Ngo *et al.*, 2011). Moreover, recurrent somatic mutations of MYD88 occur in 39% of ABC DLBCLs, where 29% have a specific single nucleotide substitution of L265P (Ngo *et al.*, 2011). Located in the C-terminal TIR domain of the MYD88 protein, L265P mutations allow spontaneous and activation-independent interaction with IRAK4 and IRAK1 (Lin *et al.*, 2010; Rossi *et al.*, 2013). Targeting MYD88 is a potential therapeutic strategy for DLBCL and other B-cell NHL with MYD88 mutations. MYD88 knockdown for example, has been shown to induce death in ABC cell lines, which was rescued by a MYD88 mutant, but not by wild-type MYD88 (Ngo *et al.*, 2011). Moreover recent studies have successfully targeted mediators of MYD88, such as TAK-1, effectively decreasing cell proliferation (Ansell *et al.*, 2014).

1.10. Lymphoma summary

The recognition of comprehensive molecular signatures for ABC and GCB DLBCL has enabled the identification of genetic aberrations associated with each subgroup (Alizadeh *et al.*, 2000). Many genetic aberrations lead to dysregulated activity of specific signalling pathways that drive tumour formation and progression. It is important that these pathways and the cellular dependencies that result from them are identified so that new therapeutic strategies, based on specific drugs which effectively and specifically target cancer cells and spare normal cells, can be developed.

The BCR and pathways downstream of the BCR are proving to be central for DLBCL cell survival, thus representing excellent novel targets for therapy. Although considerable progress has been made in understanding the involvement of pathways such as the NF-κB and PI3K/AKT signalling pathways in DLBCL, there remains potential for other pathways downstream of the BCR to play an important role. For example, increasing evidence supports a role for the Nuclear Factor of Activated T cells (NFAT) transcription

pathway in many cancers, including DLBCL (Pham *et al.*, 2005; Fu *et al.*, 2006; Pham *et al.*, 2010; Qin *et al.*, 2014). Moreover, recent studies have indicated that the NF-κB and NFAT pathways may functionally intersect in DLBCL, together regulating the expression of combined target genes important for lymphoma growth and survival (Pham *et al.*, 2005; Pham *et al.*, 2010).

1.11. Nuclear factor of activated T-cell (NFAT) family of proteins

Nuclear Factor of activated T cells (NFAT) was discovered over two decades ago as an inducible nuclear protein binding to the antigen receptor response element-2 (ARRE-2) of the interleukin-2 (IL-2) promoter in activated human T cells (Shaw, 1988). The role of NFAT in the immune system has now been extensively reviewed (Macian, 2005; Müller *et al.*, 2010; Fric *et al.*, 2012) although novel roles for NFAT continue to emerge in the literature, particularly in the field of T-cell tolerance, the mechanisms underlying T-cell anergy and in the function of regulatory T cells (T_{Reg}) (Serfling *et al.*, 2006b; Noemi Soto-Nieves, 2009).

Following its initial discovery, a plethora of studies established that NFAT family members are not only important for T-cell activation and differentiation, but are ubiquitously expressed in many mammalian tissues, implying a broader role for NFAT isoforms than was originally thought (Müller *et al.*, 2010). In addition to regulating the function of cells of the immune systems, such as B cells, dendritic cells and megakaryocytes, the NFAT signalling axis has a key role in vertebrate-specific development of the heart, bones, skin, blood vessels, skeletal muscle and pancreas (Yaseen *et al.*, 1993; Hogan *et al.*, 2003; Heit *et al.*, 2006; Winslow *et al.*, 2006; Crist *et al.*, 2008; Oro, 2008; Negishi-Koga *et al.*, 2009; Shukla *et al.*, 2009; Zanoni *et al.*, 2009).

Dysregulation of NFAT signalling is now know to be associated with a broad range of diseases including autoimmune and inflammatory disorders such as Alzheimer's disease and pathological cardiac hypertrophy (Ferraccioli *et al.*, 2005; Heineke *et al.*, 2006). It has long been suspected that NFAT signalling may also be dysregulated in cancer, but this has only been reported recently (Jauliac *et al.*, 2002). Aberrant NFAT signalling has now been associated with malignant transformation and tumour progression in a number of cancers, including solid tumours such as breast, pancreatic, lung, and colon cancers (Jauliac *et al.*, 2002; Holzmann *et al.*, 2004; Duque *et al.*, 2005; Maxeiner *et al.*, 2009). NFAT has also demonstrated a role in cancers of the haematopoietic system, for example in Chronic Lymphocytic Leukaemia (CLL), DLBCL, Burkitt's lymphoma and some T-cell lymphomas (Marafioti *et al.*, 2005; Pei *et al.*, 2012). However, the respective contribution of specific NFAT family members and their function in various cancer phenotypes is not known. Further research on the role of NFAT in tumourigenesis would

allow us to evaluate potential targeting of NFAT for therapy but also to gain a greater understanding for the molecular machinery driving cancer types.

1.12. Biology of NFAT/primary structure of NFAT

The human NFAT family consists of five members (table 1) including NFAT1 (NFATc2/NFATp), NFAT2 (NFATc1/NFATc), NFAT3 (NFATc4), NFAT4 (NFATc3/NFATx) and NFAT5 (TonEBP/OREBP). When compared to other transcription factors, a unique feature of NFAT members 1-4 is their dependency on an influx of Ca^{2+} by the PLC-γ pathway or via store-operated Ca^{2+} entry. This distinguishing factor requires Ca^{2+} binding sites present on NFAT1-NFAT4, but not NFAT5, which is insensitive to Ca^{2+} stimulation. Exclusively important for cellular responses to osmotic stress, NFAT5 is expressed in almost all cells and is known as the primordial NFAT family member, emerging as early as *Drosophila spp*. (López-Rodríguez *et al.*, 1999; Miyakawa *et al.*, 1999; López-Rodríguez *et al.*, 2001; Mancini *et al.*, 2009). Table 1 summarises the alternative names for NFAT family members, their mechanisms of regulation and whether they are expressed in immune and cancer cells.

NFAT family member	Alternative names	Regulation	Expressed in immune cells	References	Expressed in tumour cells
NFAT1	NFATc2/NFATp	Calcium-calcineurin	Yes	(McCaffrey PG, 1993)	Yes
NFAT2	NFATc1/NFATc	Calcium-calcineurin	Yes	(Northrop *et al.*, 1994)	Yes
NFAT3	NFATc4	Calcium-calcineurin	No	(Hoey T, 1995)	Yes
NFAT4	NFATc3/NFATx	Calcium-calcineurin	Yes	(Ho *et al.*, 1995; Hoey T, 1995; Masuda *et al.*, 1995)	Yes
NFAT5	TonEBP/OREBP	Osmotic stress	Yes	(Miyakawa *et al.*, 1999)	Yes

Table 1. The NFAT family of transcription factors are expressed in cells of the immune system and in tumour cells.

Structurally, NFAT members contain three main tandem domains; a regulatory domain known as the NFAT homology region (NHR), a highly conserved Rel-homology region (RHR) (which binds DNA) and a carboxy-terminal domain, as illustrated in figure 7. The NHR is moderately conserved between NFAT family members and contains an amino-

terminal transactivation domain (TAD) which initiates gene transcription by binding gene promoter elements. The NHR contains docking sites for both calcineurin and NFAT kinases which control NFAT activation by regulating its phosphorylation status. In resting cells, the NHR is heavily phosphorylated at multiple serine residues within several conserved serine-rich sequence motifs. The RHD is a unifying characteristic of NFAT family members which is structurally related to the DNA binding domain of NF-κB REL-family of transcription factors, classifying NFATs as extended members of the NF-κB family. Characterised by a set of 300 evolutionary conserved amino acid residues, the RHR confers the DNA binding specificity of NFAT transcription factors and is a well characterised mode of DNA binding (Ghosh *et al.*, 1995; Muller *et al.*, 1995). Of the five NFATs, NFAT5 has the highest structural similarity to NF-κB, however NFAT5 lacks a calcineurin binding site, making it insensitive to calcium-calcineurin activation (López-Rodríguez *et al.*, 1999).

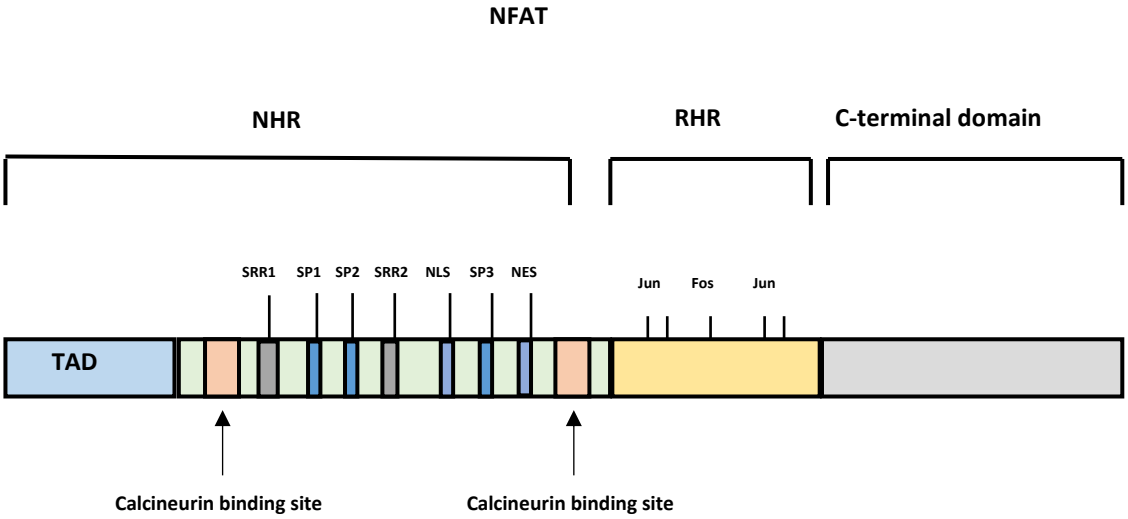

Figure 7. General structure of NFAT family members. The primary structure of a typical NFAT family member consists of the NFAT homology region (NHR), Rel-homology region (RHR) and a C-terminal domain. The NHR contains a transactivation domain (TAD), two calcineurin binding sites, a nuclear localisation sequence (NLS) and a nuclear export sequence (NES). Also contained in the NHR are multiple serine-rich motifs including SRR1, SRR2, SP1, SP2 and SP3. The RHR consists of a DNA binding domain and areas for recognition with other transcription factor partners, such as the Jun and Fos members of the AP-1 transcriptional family. The structure of NFAT family members are highly comparable, however NFAT5 does not possess a NHR, making it calcium insensitive. Image adapted from (Qin *et al.*, 2014).

1.13. NFAT isoforms

NFAT complexity is also increased since the subunits are comprised of several isoforms generated by alternative splicing or by use of individual promoters. Table 2 shows the various NFAT transcription factor genes and their isoform variants. For most NFATs, each protein has two or more alternatively spliced forms, which result in variations at the amino (N) and carboxyl (C) termini. However, the core region, containing the regulatory domain, NHR and RHR remains conserved (Park *et al.*, 1996; Imamura *et al.*, 1998; Chuvpilo *et al.*, 1999a).

Among the three NFAT proteins expressed in immune cells (NFAT1, NFAT2 and NFAT4), NFAT1 and NFAT2 are most prominently expressed in peripheral T cells (Chuvpilo *et al.*, 1999b). These two family members differ in their mode of expression in peripheral effector lymphocytes. The three NFAT1 variants and five of the six NFAT variants are constitutively expressed, whereas the transcription of the NFAT2 isoform NFAT2/αA is strongly induced following stimulation of T or B-lymphocytes (Chuvpilo *et al.*, 1999b; Serfling *et al.*, 2006a; Rudolf *et al.*, 2014).

NFAT isoform	Protein variant	Chromosomal loci	Proteins (amino acids)
NFAT1	A	20q13	1064
	B	20q13	921
	C	20q13	925
NFAT2	αA	18q23	716
	βA	18q23	703
	αB	18q23	825
	βB	18q23	812
	αC	18q23	943
	βC	18q23	930
NFAT3		14q11	902
NFAT4		16q22	1075
		16q22	1068
		16q22	1065
NFAT5		16q22	1531
		16q22	1455

Table 2. The protein variant forms of the NFAT family of transcription factors, their chromosomal loci and length in amino acids.

In peripheral lymphocytes, the synthesis of six NFAT2 proteins is directed by the existence of two promoters (P1 and P2), coupled with two poly A sites and alternative splicing events (figure 8) (Park *et al.*, 1996; Sherman *et al.*, 1999). P1 transcripts begin at exon 1 and encode NFAT2 proteins with an N-terminal α-peptide whereas P2 transcripts start at exon 2 and encode β-peptide proteins (Park *et al.*, 1996; Sherman *et al.*, 1999). The C-termini of individual proteins defines the A, B or C isoforms which differ in amino acid length, where a short stretch of 19aa comprises the A isoform, 128aa in the B isoform or 126aa in the C isoform (Chuvpilo *et al.*, 1999b). Alternative splicing and poly A addition at the distal site pA2 gives rise to the B and C isoforms, whereas formation of the short isoform A uniquely results from polyadenylation at the proximal poly A site pA1 (Chuvpilo *et al.*, 1999b).

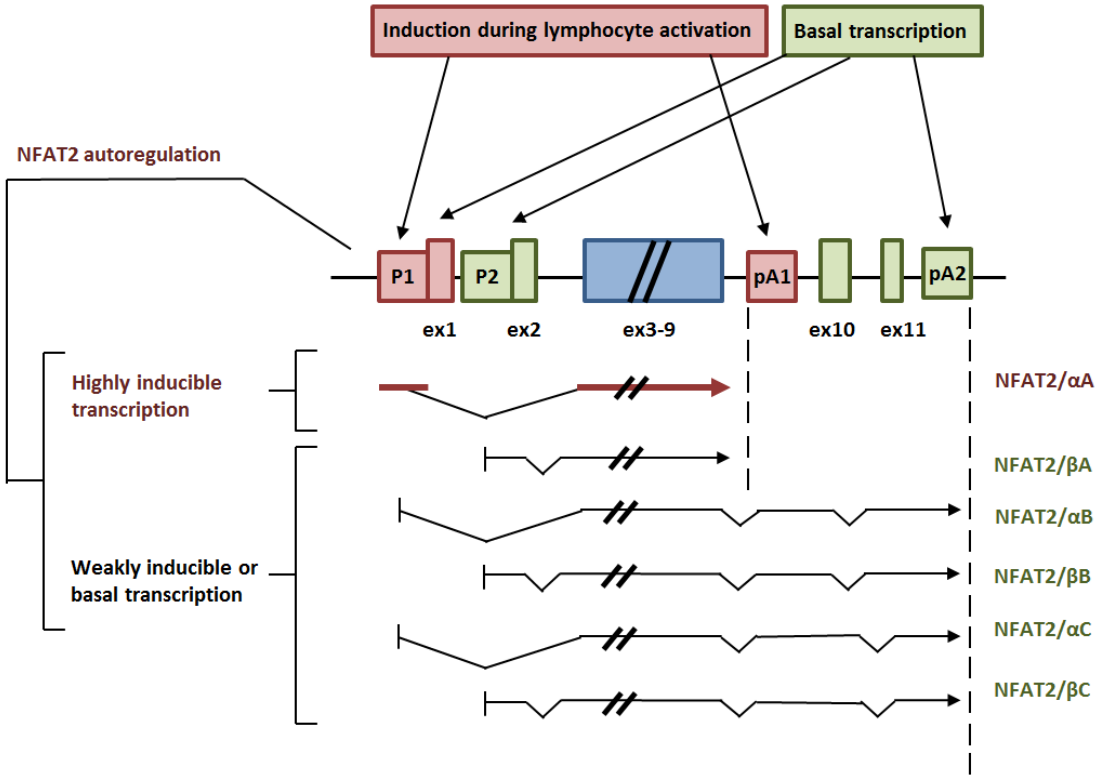

Figure 8. Expression of the NFAT2 gene. Alternative splicing events and use of different promoters allows the expression of six NFAT2 RNAs. The two promoters (P1 and P2) and two poly A addition sites (pA1 and pA2) are shown. Exons are indicated by number below the gene model. Red blocks indicate sequences specific for NFAT2/αA, green are sequences occurring in β isoforms and blue are sequences common to all isoforms. In resting T cells, transcription of exon 2 is achieved by activation of promoter P2, followed by splicing to exon 3 to generate three β isoforms. During T-cell activation, a promoter switch from P2 to P1 results in the transcription of exon 1, followed by splicing to exon 3, therefore synthesising three α isoforms. NFAT2/αA is the predominant isoform generated, by the use of the proximal poly A site pA1. Image adapted from (Serfling *et al.*, 2006a)

In resting T and B cells, the P2 promoter is primarily active (resulting in the generation of three β isoforms), however during T-cell activation a promoter switch from P2 to P1 allows the generation of the α isoforms, in particular a strong induction of the predominant shorter isoform (Chuvpilo *et al.*, 1999b). In fact, a 15-20 fold induction of NFAT2/αA RNA was detected in primary effector T cells and human T-cell lines upon T-cell activation, compared to a 2.5 fold increase for the NFAT2/αB and NFAT2/αC isoform RNAs (Chuvpilo *et al.*, 1999b). Induction results in the predominant synthesis of NFAT2/αA, which differs in length, compared to other isoforms, lacking a 250aa residue long C-terminal and a second transactivation domain that is present in other NFAT isoforms. Absence of this domain prevents sumoylation of NFAT2/αA, which has been reported to inhibit induction of IL-2 by NFAT2/C (Nayak *et al.*, 2009). Moreover, NFAT2/αA also differs from other family members in that its half-life is 2-4 hours (compared to around 8 hours for other isoforms), suggesting it to be less stable (Hock *et al.*, 2013).

1.14. NFAT2 autoregulation

Of the five NFAT family members, NFAT2 is uniquely regulated by a positive autoregulatory feedback loop (Zhou *et al.*, 2002a). In a study characterising the structure of the murine NFAT2 gene and its 5'-flanking region, a CsA-sensitive consensus NFAT-binding site was located and identified in the promoter region of the inducible NFAT2 short isoform (NFAT2A) (Zhou *et al.*, 2002a). Promoter activity was increased when NFAT1 was overexpressed, indicating that NFAT2/αA expression is under the control of a distinct inducible promoter (Chuvpilo *et al.*, 2002). As mentioned previously, NFAT1 is found abundantly in the cytoplasm of resting T cells, whereas NFAT2 expression is induced during T or B-cell activation (Chuvpilo *et al.*, 1999a). The auto-regulatory feedback circuit described is therefore beneficial to T and B-lymphocytes during an immune response, allowing high levels of NFAT2/αA synthesis to be kept constant during lymphocyte induction (Serfling *et al.*, 2006a). Despite original research findings reporting that NFAT2 autoregulation was due to heightened NFAT1 expression, other studies have revealed that NFAT2 induction may not depend on just NFAT1 (Zhou *et al.*, 2002a). This has come to light since reports showing that NFAT2/αA remains strongly induced in T cells deficient in both NFAT1 and NFAT3 (Hock *et al.*, 2013).

Interestingly, positive auto-regulation of NFAT2 is likely a common strategy during cell linage commitment, ensuring accumulation of an isoform of particular biological importance (Serfling *et al.*, 2006a). Moreover, this regulatory mechanism explains why deletion of NFAT2 during development is more lethal than other NFAT isoforms (Qin *et al.*, 2014). The architecture and expression of the NFAT2 gene in lymphocytes is clearly a complex system that is highly researched. NFAT2/αA induction, however, is not limited to immune cells. In fact, studies have shown that induction is a crucial step in determining the fate of the cell in many systems, including osteoclastogenesis and cardiac valve development (Asagiri *et al.*, 2005; Zhou *et al.*, 2005). Recent reports have highlighted dysregulation of NFAT2/αA in immune cells that are suggestive of its contribution to lymphoid disorders, including lymphomagenesis (Asagiri *et al.*, 2005). However, these will be discussed in a later section.

1.15. The NFAT signalling pathway

The activation of NFAT by calcium signalling is a well-studied mechanism. Upon ligand binding to immunoreceptors (such as the BCR), receptor tyrosine kinases (RTK) or G-protein-coupled receptors (GPCR) activate phospholipase C gamma (PLCγ), as shown in figure 9, which leads to the hydrolyse of phosphatidyl-4,5-bisphosphate (PtdIns(4,5)P_2) to diacylglycerol (DAG) and ionositol-1,4,5-trisphosphate ($InsP_3$) (Pan *et al.*, 2013). In turn, $InsP_3$ binds to the $InsP_3$ receptor ($InsP_3R$) on the ER membrane and initiates calcium release from endoplasmic reticulum Ca^{2+} stores. In many cell types, this initial release of calcium is not sufficient to activate NFAT target genes (Müller *et al.*, 2010). Store-operated Ca^{2+} entry (SOCE) is activated by detection of calcium by STIM1 and STIM2, which communicate with the CRAC channel ORAI1 at the plasma membrane and trigger its conformational change (Müller *et al.*, 2010). Essential for lymphocyte activation and NFAT activation, this process is termed "inside-out" signalling and leads to the opening of CRAC channels and an influx of extracellular calcium (Putney Jr *et al.*, 1993). A sustained calcium signal is required for NFAT activation, where binding of calcium to calmodulin leads to activation of the serine/threonine phosphatase calcineurin.

In the basal state, the calcium-responsive NFAT isoforms exist in a hyperphosphorylated inactive conformation in the cytoplasm. NFAT1 for example, demonstrates a high level of complexity, harbouring more than 20 phosphorylation sites, 18 of which are located in the regulatory region (Okamura *et al.*, 2000). Dephosphorylation by activated calcineurin

occurs on multiple serine-proline rich (SP) motifs, serine rich regions (SSR1) and the SPXX (X represents any amino acid) (figure 7) (C R Beals, 1997; Okamura *et al.*, 2000). Dephosphorylation of SP motifs (SP1, SP2 or SP3) reveal a nuclear localisation sequence and also leads to masking of the nuclear export sequence, allowing NFAT isoforms to translocate to the nucleus and bind either as monomers, homodimers or heterodimers to DNA elements (Zhu *et al.*, 1998; de Lumley *et al.*, 2004). In the nucleus, NFAT transcriptionally regulates an array of genes in a cell-type and context-dependent manor. Transcriptional activity is terminated by the rephosphorylation of NFAT and exposure of a nuclear export sequence.

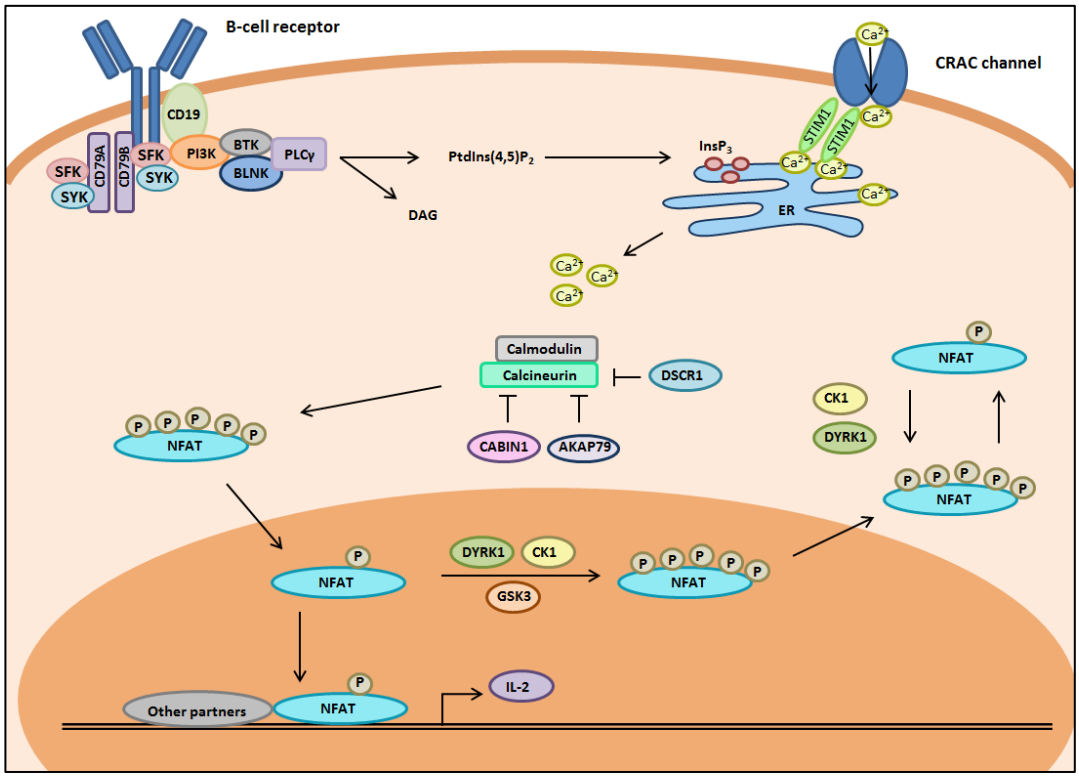

Figure 9. The NFAT signalling pathway and its regulatory factors. Immunoreceptors, receptor tyrosine kinases (RTK) and G-protein-couple receptors (GPCR) activate PLCγ which hydrolyses phophatidylinositol-4-5-bisphosphate (PIP2) into diacylglycerol (DAG) and inositol trisphosphate (IP3). IP3 binds to Ca^{2+}-permeable receptors on the endoplasmic reticulum (ER) and stimulates the release of calcium into the cytosol. ER store depletion is detected by STIM receptors, resulting in the opening of calcium release-activated channels (CRAC) at the plasma, allowing entry of additional calcium. An influx of calcium allows activation of calmodulin, which induces the phosphatase calcineurin to dephosphorylate NFAT proteins, causing them to translocate to the nucleas bind to DNA as monomers, dimers or with other transcription factors to initiate gene trascription such as IL-2 in T cells. NFAT is regulated by multiple levels of control. The NFAT kinase glycogen synthase kinase 3 beta (GSK3β) acts as an export kinase by rephosphorylating NFAT, leading to its nuclear exit. Dual specificity tyrosine phosphorylation-regulated kinases (DYRK) and casein kinase 1 (CK1) are multi-functional, behaving as both export kinases and maintainance kinases which retain fully phosphorylated NFAT in the cytoplasm. Another level of NFAT pathway regulation is by endogenous inhibition of calcineurin by the calcineurin-binding protein 1 (CABIN1), Down's syndrome critical region 1 (DSCR1) and A-kinase anchor protein 79 (AKAP79).

1.16. Regulation of NFAT

1.16.1. Kinase regulation of NFAT

In addition to control of NFAT activation by their unique sensitivity to intracellular calcium and by autoregulation of the short NFAT2 isoform, the complexity of NFAT signalling is further increased by additional levels of regulation. Serine/threonine kinases, for example are fundamental in controlling the precise subcellular location of NFAT isoforms and their transcriptional activity. Subdivided into maintenance and export kinases, these key regulators effectively retain NFAT in the cytoplasm, or promote NFAT nuclear export. The export kinase glycogen synthase kinase 3 beta (GSK3β) phosphorylates the SP2 and SP3 motifs of NFAT2, terminating transcriptional activity and promoting nuclear exit (Beals *et al.*, 1997; Neal *et al.*, 2003). In contrast, kinases such as casein kinase 1 (CK1) and the dual specificity tyrosine phosphorylation-regulated kinases (DYRKs) are multi-functional, behaving as either export kinases or as maintenance kinases by retaining fully phosphorylated NFAT in the cytoplasm, preventing nuclear translocation (Okamura H, 2004; Arron *et al.*, 2006; Gwack *et al.*, 2006). It is likely that additional kinases are yet to be discovered, highlighting a key area of unexplored research. Kinase activity may explain the differential activation or deregulation of specific NFAT isoforms in various cellular and pathological contexts.

1.16.2. Regulation of NFAT by calcineurin

The use of the pharmacological immune-suppressant drugs CsA and FK506 to antagonise calcineurin activity have been a useful resource to aid our understanding of the endogenous role of calcineurin and NFAT signalling. In addition to its role as an activator of NFAT in the cytoplasm, calcineurin has been identified as a regulatory protein in the nucleus of stimulated cells, maintaining the dephosphorylated state of NFAT and consequently sustaining active transcription (Zhu *et al.*, 1999). Moreover, direct control of calcineurin activity by endogenous calcineurin inhibitors has become evident, such as by calcineurin-binding protein 1 (CABIN1), Down's syndrome critical region 1 (DSCR1) and A-kinase anchor protein 79 (AKAP79) (Lai *et al.*, 1998; Lin *et al.*, 1999; Fuentes *et al.*, 2000; Jurado *et al.*, 2010).

1.16.3. Post-translational modifications

In addition to regulation by phosphorylation, other post-translational modifications have been identified for NFAT proteins. For example, nuclear retention of NFAT1 and NFAT2 can be regulated by sumoylation (Terui *et al.*, 2004; Nayak *et al.*, 2009). Distinct isoform specific effects have been reported (Terui *et al.*, 2004; Nayak *et al.*, 2009). The long NFAT2/C isoform (but not the NFAT2/A short inducible isoform) is modified by Small ubiquitin-like modifier 1 (SUMO1), causing its nuclear translocation and transformation from a transcriptional activator to a transcriptional repressor by recruitment of histone deacetylases (HDACs) and induction of transcriptionally inactive chromatin (Nayak *et al.*, 2009). Other examples of post-translational modifications include the ubiquitination of NFAT1 by the E3 ubiquitin ligase MDM2 in breast cancer cells and the binding of Poly-ADP-ribose polymerase (PARP) to NFAT, inducing adenosine di-phosphate (ADP) –ribosylation, hence increasing NFAT binding activity (Wyszomierski *et al.*, 2005; Yoeli-Lerner *et al.*, 2005; Olabisi *et al.*, 2008; Yoeli-Lerner *et al.*, 2009).

1.17. NFAT transcriptional partners

Although calcium is one of the broadest signalling molecules, having a wide range of cellular effects, very few gene targets are activated by a calcium signal alone (Crabtree *et al.*, 2002). It is likely that NFAT binds DNA with the assistance of other proteins. Summarised nicely by Crabtree et al (2002) 'NFAT genes are probably not "master" genes that wear camouflage clothes and live in caves, but rather that they function within the community of proteins in a cell when a calcium signal is given' (Crabtree *et al.*, 2002). Studies investigating the mechanism of NFAT contact with DNA have revealed significant NFAT conformational flexibility. NFAT isoforms 1-4, for example, can bind DNA as monomers to specific (GGAA) sites or bind as dimers at kappa B-like (κB-like) sites; however this is with fairly weak affinity (Chen *et al.*, 1998; Hogan *et al.*, 2003). Cooperation with partner transcription factors to form heterodimeric complexes enhances DNA contact and is the mechanism by which NFATs regulate most of their target genes (Chen *et al.*, 1998). The Activator Protein 1 (AP-1) transcription factors (comprised of Fos-Jun complexes) represent the most well established NFAT binding partner (Jain *et al.*, 1992; Macian, 2001). AP-1 and NFAT cooperatively bind a composite DNA binding site to synergistically activate the expression of genes involved in an immune response,

where formation of a quaternary DNA complex achieves high affinity binding (Jain *et al.*, 1992; Chen *et al.*, 1998).

The biological implications of NFAT activity are further enhanced by interaction with many other transcription factor proteins, for example, zinc finger proteins such as GATA (globin transcription factor 1), helix-turn-helix domain proteins such as Oct and other transcription factors including FOXP3 (forkhead box P3), EGR (early growth response) proteins and MEF2 (myocyte enhancer factor 2) (Decker *et al.*, 1998; Bert *et al.*, 2000; Nemer *et al.*, 2002; Rengarajan *et al.*, 2002; Wada *et al.*, 2002; Decker *et al.*, 2003; Tone *et al.*, 2008; Li *et al.*, 2012). Although the interaction between NFAT and IRF4 (interferon regulatory factor 4) is not well characterised, an IRF4/NFAT complex modelled on a putative composite binding site from the IL-4 promoter suggested that IRF4 and NFAT2 may potentially bind to DNA simultaneously, with their DNA binding interacting (Hu *et al.*, 2002). NFAT transcription factors form stable nuclear complexes with a plethora of partners to perform an array of biological functions (Qin *et al.*, 2014). These may range from immunotolerance (FOXP3), to proliferation (GATA) and even the malignant transformation. For example, shRNA depletion of the NFAT binding partner STAT3 (signal transducer and activator of transcription 3), decreased the transforming ability of NFAT2 in 3T3-L1 fibroblasts (Tone *et al.*, 2008; Lagunas *et al.*, 2009; Li *et al.*, 2012).

1.18. Role of NFAT in Cancer

NFAT proteins transactivate downstream targets that support the development of cancer and tumour progression, as reviewed in (Mancini *et al.*, 2009; Müller *et al.*, 2010; Pan *et al.*, 2013; Qin *et al.*, 2014; Shou *et al.*, 2015). Consequently, constitutive activation and overexpression of NFAT has been reported in an increasing number of both solid tumours and haematological malignancies, as highlighted in table 3. NFAT family members have been shown to regulate key cellular processes involved in malignant transformation, including cell survival, differentiation, migration, angiogenesis and the tumour microenvironment, which will be discussed in the subsequent sections (Mancini *et al.*, 2009; Pan *et al.*, 2013; Qin *et al.*, 2014).

The first implication that NFAT had oncogenic potential came from a study showing the involvement of NFAT in promoting carcinoma invasion downstream of the α6β4 integrin, resulting in enhanced cell migration (Jauliac *et al.*, 2002). Soon after, another study demonstrated a proliferative role for NFAT in cancer, where the expression of a

constitutively active NFAT2 mutant in murine fibroblasts caused cells to adopt a transformed cell phenotype (Neal *et al.*, 2003). Since these discoveries, activated and/or overexpressed NFAT has identified in several types of cancer, including pancreatic cancer, breast cancer, Burkitt's lymphoma and aggressive T-cell lymphomas (Marafioti *et al.*, 2005; Pham *et al.*, 2005; Yoeli-Lerner *et al.*, 2005; Buchholz *et al.*, 2006; Yoeli-Lerner *et al.*, 2009; Pham *et al.*, 2010).

Although NFATs often perform redundant functions, distinct isoform-specific roles are also emerging with cell-type and context dependent effects being observed in cancer (Hogan *et al.*, 2003; Robbs *et al.*, 2008). Despite the highly conserved sequence similarities between NFAT isoforms (and assumed functional redundancy), specific oncogenic or tumour suppressive functions have been correlated with particular NFAT family members. These distinct roles have particularly been identified between NFAT1 and NFAT2, which although share 72% sequence similarity in their C-terminal DNA binding domains, appear to have strikingly opposing roles (Robbs *et al.*, 2008). It is likely that NFAT1 and NFAT2 induce a non-overlapping selection of gene targets, which either suppress or promote cell growth (Mancini *et al.*, 2009). However, Rudolf et al (2014) suggest that functional differences between NFATs may be due to the synthesis of the NFAT2/αA short isoform of NFAT2 (Rudolf *et al.*, 2014). Aberrant expression of this isoform may be influenced by the autoregulatory mechanisms of NFAT2 and this may explain its oncogenic nature (Chuvpilo *et al.*, 2002).

Mutations of NFAT proteins have not been associated with human cancers, in fact, recent cancer genome sequencing suggests that mutations and amplifications in NFAT genes may only occur at very low frequencies (Macian, 2005). Aberrant NFAT signalling in cancer is reportedly by overexpression and/or hyperactivity, which is likely due to drivers of NFAT activity or retention of NFAT in the nucleus (Müller *et al.*, 2010). Differential regulation of NFATs in specific cell types may be due to the selective activation of export kinases such as GSK3β, which in cancer may become dysregulated; however these areas remained largely unexplored.

Cancer type	NFAT isoform	Proposed mechanism	Clinical/biological outcomes	Reference
T-cell leukaemia	NFAT1-4	Activation of calcineurin and NFAT nuclear translocation	Chemoresistance	(Glud *et al.*, 2005; Pham *et al.*, 2005; Medyouf *et al.*, 2007)
Chronic lymphocytic leukaemia	NFAT2	Overexpressed and constitutively active	Increased cancer progression	(Le Roy *et al.*, 2012; Pei *et al.*, 2012)
Chronic myelogenous leukaemia	NFAT2	Constitutively activated	Chemoresistance to TKI treatment	(Gregory *et al.*, 2010)
Diffuse Large B-cell lymphoma	NFAT2	Constitutively activated. Interacts with NF-κB to synergistically activate CD54 gene transcription	Increased tumour growth. Maintaining cell survival and counteracting apoptosis by induction of CD40 and BLYS survival factors	(Pham *et al.*, 2005; Fu *et al.*, 2006; Pham *et al.*, 2010)
Breast cancer	NFAT1, NFAT5	Overexpressed	Increased migration and invasion by induction of COX2	(Yoeli-Lerner *et al.*, 2005; Yoeli-Lerner *et al.*, 2009)
Pancreatic cancer	NFAT2	Overexpressed	Increased tumour growth by induction of MYC expression	(Buchholz *et al.*, 2006)
Prostate cancer	NFAT	Activated NFAT promoter by TRPV6-mediated Ca^{2+} influx	Increased cancer cell proliferation	(Lehen'Kyi *et al.*, 2007)
Colon cancer	NFAT1	Constitutively activated	Induces tumour progression	(Gerlach *et al.*, 2012)
Melanoma	NFAT	Increased NFAT activity via BRAF-MEK-ERK pathway and a TGF-β dependent pathway	Increased migration and invasion by induction of COX2	(Flockhart *et al.*, 2009; Werneck *et al.*, 2011)
Angiosarcoma	NFAT4	Activated by SFRP2	Increased angiogenesis	(Courtwright *et al.*, 2009)
Ewing sarcoma	NFAT1	Amplified chimera due to chromosomal translocation	Not known	(Szuhai *et al.*, 2009; Sankar *et al.*, 2011; Arbajian *et al.*, 2013)
Endometrial cancer	NFAT	Regulation of IL11 and CXCL8 expression	Increased migration	(Sales *et al.*, 2009; Cook *et al.*, 2010)
Glioblastoma	NFAT1	Overexpressed	Increased invasiveness	(Wu, 2010; Tie *et al.*, 2013)
Non-small cell lung cancer	NFAT	Overexpressed	Decreased post-operative survival	(Zhang, 2007; Chen *et al.*, 2011c)

Table 3. Evidence linking NFAT isoforms with different malignancies, including biological and clinical outcomes. Image adapted from (Qin *et al.*, 2014)

It is becoming clear that therapeutic targeting of the NFAT pathway is a desirable approach for cancer treatment; however with the increasingly level of complexity of NFAT regulation and function, it is essential that we gain a greater level of understanding of the molecular mechanisms involved.

1.18.1. Study of NFAT using mouse models

Mice with single NFAT isoform knockouts show mild phenotypes, which may be due to a high degree of redundancy (Mancini *et al.*, 2009). However, a few effects have been observed, including defective cardiac valve formation with embryonic lethality in mice with a NFAT2 deletion and reduced mast cell cytokine production in mice with a NFAT1 deletion (de la Pompa *et al.*, 1998; Ranger *et al.*, 1998). Importantly, until at least two NFAT proteins are absent no distinct physiological effects are seen (Macian, 2005). Deletion of multiple NFAT family members can result in abolished cytokine production in T cells (NFAT1 and NFAT2 deletion), lethal defects in formation of the vasculature system (NFAT3 and NFAT4 deletion) and impairment of nervous system growth (NFAT1, NFAT3 and NFAT4 deletion). The deleterious effects of double knockout mice substantiate the pivotal role of NFAT proteins in the immune system and vertebrate development and have been reviewed comprehensively (Macian, 2005; Müller *et al.*, 2010; Fric *et al.*, 2012; Pan *et al.*, 2013)

Using NFAT knockout in mouse knockout models of cancer would allow a better understanding of the individual roles of NFAT isoforms; however research on NFAT in cancer has largely been restricted to *in vitro* studies. This is mostly due to the fact that the use of *in vivo* mouse models are hampered by the extreme immunological disorders that occur in NFAT double knockout mice, as described above. Despite a lack of *in vivo* evidence, several recent studies have been of particular value. NFAT1 null mice, for example, were shown to be susceptible to chemically induced carcinogenesis when compared to wild-type mice, supporting the tumour suppressive role for NFAT1 demonstrated in *in vitro* studies (Robbs *et al.*, 2008; Werneck *et al.*, 2011). Moreover, mice deficient in NFAT1 and NFAT4 show decreased activation-induced cell death (AICD), increased proliferation and impaired induction of Fas ligand, adding to its potential anti-tumour effects (Oukka *et al.*, 1998; Ranger *et al.*, 1998). Importantly, the research findings of *in vivo* studies overall have largely complemented *in vitro* studies.

Further examples of NFAT mouse model studies will be described throughout the rest of the chapter.

1.18.2. Roles of NFAT in cancer development and progression

As described in the sections below, increasing evidence supports a role for NFAT in the underlying principles of Hanahan and Weinberg's hallmarks of cancer, providing cancer cells with characteristic traits such as the ability to sustain angiogenesis, invade surrounding tissues and metastasise (Hanahan *et al.*, 2000).

1.18.3. Role of NFAT in the malignant transformation and cell proliferation

Following Neil and Clipstone's discovery that NFAT2 proteins induce malignant transformation and increase cell proliferation in fibroblasts (Neal *et al.*, 2003), other research groups have revealed contrasting effects of NFAT1. In 2008 for example, Robbs et al reported that induction of constitutively active NFAT1 mutants in fibroblasts induced cell cycle arrest and apoptosis, whereas NFAT2 increased proliferation and transformation (Robbs *et al.*, 2008). This apoptotic role for NFAT1 is likely due to the inhibition of cyclin dependent kinase 4 (CDK4) and cyclin A2 expression, which are previously documented roles for this NFAT family member (Baksh *et al.*, 2002; Carvalho *et al.*, 2007; Robbs *et al.*, 2008). Interestingly, NFAT1 was recently shown to cooperate with the oncogenic Ras/Raf/MEK/ERK pathway (but not with JNK, p38 or NF-κB) (Robbs *et al.*, 2013). Its role was found to shift signalling from an oncogenic to a tumour suppressive pathway by the induction of TNFα (Robbs *et al.*, 2013).

However, in other studies, the expression of NFAT1 is correlated with aggressive and invasive behaviour in various malignancies, suggesting that the predominant role for NFAT1 is the promotion of cell migration (Yoeli-Lerner *et al.*, 2005; Yoeli-Lerner *et al.*, 2009; Tie *et al.*, 2013; Zhang *et al.*, 2013a; Qin *et al.*, 2014). In breast cancer cells for example, NFAT1 has been shown to induce MDM2 transcription, increasing p53 inactivation and therefore functioning in a pro-proliferation manner (Qin, 2012). Moreover, induction of NFAT1 has been reported in advanced stages of pancreatic cancer, a malignancy where NFAT1 was shown to aid silencing of the p15(INK4b) tumour suppressive pathway, promoting pancreatic cancer cell growth (Baumgart *et al.*, 2012). NFAT1 has also demonstrated oncogenic behaviours in colon and breast cancer (Zheng *et al.*, 2011; Gerlach *et al.*, 2012).

A number of studies have found oncogenic functions for NFAT2. For example, NFAT2 has been shown to work cooperatively with TGF-β to promote breast cancer cell proliferation (Sengupta *et al.*, 2013; Sengupta *et al.*, 2014). Moreover, overexpression of NFAT2 was identified in 70% of pancreatic carcinomas where the c-*myc* oncogene was found to be a direct target gene of NFAT2 (Buchholz *et al.*, 2006). Binding of active NFAT2 to a specific element in the c-*myc* promoter caused upregulation of c-*myc* transcription, increasing cell proliferation and growth in a calcium/calcineurin dependent manor (Buchholz *et al.*, 2006). Interestingly, activated MYC subsequently interacted with NFAT complexes to transactivate genes involved in cell cycle progression such as cyclinD1/D3 (Buchholz *et al.*, 2006). Of further significance is the ability of NFAT2 to regulate the switch between dormancy of stem cells to a proliferative state (Horsley *et al.*, 2008; Oro, 2008). NFAT2 maintains a state of quiescence in the stem cell population by inhibiting the CDK4 checkpoint kinase downstream of bone morphogenetic protein 4 (BMP4) signalling (Horsley *et al.*, 2008). By promoting a tumour cell population that possesses stem cell characteristics, NFAT2 can provide tumour cells (which are potentially metastasising) with a capacity for self-renewal (Horsley *et al.*, 2008; Mani *et al.*, 2008; Oro, 2008; Qin *et al.*, 2014).

1.18.4. Role of NFAT in cell invasion and metastasis

The ability of tumour cells to acquire migratory and invasive characteristics during the epithelial-mesenchymal transition is fundamental to metastatic progression. NFAT family members have been shown to play important roles in this process, particularly in breast cancer (Thiery, 2002). Isoform specific roles have been identified, for example, the migration and invasion of breast cancer cells through matrigel *in vitro* is promoted by expression of active NFAT1, whereas NFAT5 promotes migration but not invasion (Jauliac *et al.*, 2002). As mentioned previously, a significant positive correlation between NFAT1/NFAT5 and expression of the integrin α6β4 was observed in patients with invasive breast cancer and ductal breast carcinoma cell lines (Jauliac *et al.*, 2002). The α6β4 integrin is released from hemi-desmosomes in cancer cells, associating with the actin cytoskeleton to activate transcription of NFAT5, which in turn activates metastasis-associated target genes such as COX-2 (Rabinovitz *et al.*, 1997; Yiu *et al.*, 2006; Vázquez-Cedeira *et al.*, 2012). COX-2 is required for NFAT proteins to promote invasive migration, by catalysing the synthesis of prostaglandin E2 (PGE_2), a mitogen known to promote invasion though the extra-cellular matrix (Yiu *et al.*, 2006; Greenhough *et al.*,

2009). In addition to COX-2, NFAT family members also target other genes that promote invasive properties. In breast epithelial cells NFAT induces the expression of autotoxin, a protein involved in synthesis of the potent mitogen and motogen lysophosphatidic acid (Chen *et al.*, 2005)

Due to their pro-invasive properties, it is reasonable to predict that NFATs are involved with the transcription or secretion of matrix metalloproteinases (MMPS) which regulate proteolytic degradation of the basement membrane during tumour invasion (Mott *et al.*, 2004). Although this has been highlighted in a number of NFAT review papers, only recently has a study reported an oncogenic association between NFAT and MMPs in lung cancer (Mancini *et al.*, 2009; Minami *et al.*, 2013; Qin *et al.*, 2014).

1.18.5. Role of NFAT in angiogenesis and lymphangiogenesis

Establishment of a tumour vasculature allows solid malignancies to be provided with the oxygen and nutrients essential for cancer cells to thrive and proliferate. Angiogenesis is a key hallmark of cancer, since it also provides tumour cells with a pathway for dissemination to other bodily organs. The importance of NFAT in formation of the vasculature was first recognised in mice lacking both NFAT3 and NFAT4, which was lethal for mouse development during stage E11 (Graef *et al.*, 2001). Mechanistically, NFAT is known to control the expression of vascular endothelial growth factor (VEGF), by regulating the expression of the VEGF receptor (VEGFR) (Jinnin *et al.*, 2008). VEGF is an important molecule that induces angiogenesis by stimulating endothelial cell proliferation (Dvorak, 2006). In a positive feedback loop, NFAT induction of VEGF also enables VEGF to increase calcium signalling via PLCγ, hence activating NFAT and promoting transcription of downstream pro-angiogenic targets such as COX2, PGE_2 and granulocyte-macrophage colony-stimulating factor (GM-CSF) (Cockerill *et al.*, 1995; Schulz *et al.*, 2004; Ferrara, 2005; Yiu *et al.*, 2006; Jinnin *et al.*, 2008; Vázquez-Cedeira *et al.*, 2012).

Isoform-specific roles for NFAT family members have also emerged in the field of lymphangiogenesis where NFAT2 has been shown to modulate the formation of lymphatic vessels, which some cancers (such as breast, lung and gastrointestinal) utilise for effective metastasis (Graef *et al.*, 2001; Karpanen *et al.*, 2001; Skobe *et al.*, 2001; Kulkarni *et al.*, 2009). NFAT2 functions downstream of vascular endothelial growth factor C (VEGFC) by interacting with other lymphangiogenesis factors such as forkhead

box C2 (FOXC2) and prospero-homeobox 1 (PROX1), a mechanism that Qin et al 2014 suggest may contribute to the tumourigenic activity of NFAT2 in haematological cancers (Kulkarni *et al.*, 2009; Norrmén *et al.*, 2009; Qin *et al.*, 2014). In summary, NFAT family members regulate both angiogenesis and lymphangiogenesis, further supporting their role in the malignant setting.

1.18.6. Role of NFAT in the tumour microenvironment

Stephen Paget proposed the 'seed and soil' hypothesis in 1889 to explain the behaviour of tumour cells when they metastasise (Paget, 1889; Mathot *et al.*, 2012). Paget described the cancer cells as 'seeds' which metastasise to areas that are biochemically and physiologically favourable (the 'soil') for implantation and further growth (Paget, 1889). Considering that metastasis is a leading cause of death in cancer patients, over a century later, this phenomenon has become one of the main focuses of cancer research (Mathot *et al.*, 2012).

The tumour microenvironment is an intricate system of many cell types, including immune cells, fibroblasts, endothelial cells and the extracellular matrix. A close relationship between cancer cells and the cells of the microenvironment can potentiate tumourigenesis by providing optimal conditions for cancer cells (the seeds) to thrive. Tumour cells themselves for example, release extracellular signals to the microenvironment to promote angiogenesis and induce peripheral immune tolerance. Furthermore, infiltrating immune cells in the microenvironment can also benefit cancer cell survival by the release of factors which promote cell growth. The molecular mechanisms involved in these processes are yet to be fully understood, however it is becoming increasingly apparent that future strategies for cancer treatment will be to target both the seed and the soil.

In the past, the study of lymphoma involved analysis of isolated malignant lymphocytes, however recent studies suggests that the tumour microenvironment should also be considered. Research, for example, has shown that the tumour microenvironment in B cell malignancies is crucial for promotion of survival and proliferation signals, contributing to disease progression and relapse (Burger *et al*., 2014). Intercellular stromal and immune cell crosstalk in the tissue microenvironment has been demonstrated to allow some malignant B cells to escape from the host anti-tumour response by switching on immune evasion mechanisms. Examples of such include altered expression of surface molecules that are involved in immune cell recognition (allowing escape from immune surveillance) and hijacking of the immune checkpoint network by the tissue microenvironment (Nicholas *et al*., 2016).

Compared to other malignancies, such as CLL, the precise contributions of the cells associated with the tumour microenvironment in DLBCL are less well defined. Generally speaking, malignant B cells have been shown to dampen down the T cell mediated response and suppress the anti-tumour effects of cytotoxic T lymphocytes (Nicholas *et al*., 2016).

The tumour microenvironment in DLBCL has been shown to involve a plethora of cells, including tumour-associated macrophages, T cells, endothelial stromal cells, dendritic cells and mesenchymal stem cells (Burger *et al.,* 2014, Nicholas *et al*., 2016). Of those characterised, there is evidence suggesting that some may have an anti-tumour effect, which contrasts the functions identified in other haematological cancers such as CLL. An influx of CD4+ T cells in CLL for example, has been shown to promote tumour proliferation, whereas immunohistochemical analysis of DLBCL diagnostic tissue biopsies showed a correlation between CD4+ T-cell infiltration and response to therapy, increasing overall survival (Nicholas *et al*., 2016). Moreover, in CLL, tumour-associated macrophages have been shown to inhibit apoptosis and attract other immune cells, such as T cells (Burger *et al.,* 2009, Zucchetto *et al.,* 2010). The effect of tumour-associated macrophages on the prognosis of DLBCL is not well understood and requires a better understanding of their phenotype and precise function (Kridel *et al*., 2015).

Aside from the cell specific effects on prognosis, histopathological analysis of the degree of microvessel density surrounding the tumours of DLBCL patients has been shown to correlate with significantly worse overall survival (Cardesa-Salzmann *et al.,* 2011). Moreover, analysis of the molecular signatures associated with the tumour

microenvironment in DLBCL has revealed specific genes in the microenvironment which are associated with a poorer outcome (Puvvada *et al.,* 2013). Gene expression profiling of 787 DLBCL patients for example, showed that the tumour necrosis factor receptor superfamily member 9 (TNFRSF9) was associated with the DLBCL microenvironment and correlated with adverse outcomes in GCB DLBCL (Alizadeh *et al.,* 2011). Overall, it is becoming clearer that the clinically exploitable immune sensitivity of haematological malignancies makes their tumour microenvironment a sensible target for immunotherapy and should be considered a primary target for research in this field.

Recently, several studies have shown that NFAT signalling has an important role in the microenvironment, particularly by enhancing inflammatory chemokine production (Gwack *et al.*, 2007). Chemokines function as chemo-attractants for leukocytes, enabling recruitment of cells (such as monocytes and neutrophils) to the site of tissue damage or in the context of cancer towards the tumour (Allavena *et al.*, 2008). Often highly expressed in advanced stages of cancer, chemokines promote chemotaxis and migration of epithelial cells, which can also promote cancer cell dissemination (Allavena *et al.*, 2008). In advanced breast cancer, chemokines such as CXCL12 (chemokine (C-X-C) motif) and CCL21 (chemokine (C-C) motif ligand 21) are highly upregulated by NFAT, mediating metastasis by promoting chemotaxis of epithelial cells and therefore cancer cell invasion (Muller *et al.,* 2001). In turn, infiltration of macrophages to the tumour microenvironment facilitates tumour proliferation and migration by macrophage secretion of epidermal growth factor (EGF) and colony-stimulating factor 1 (CSF1) (Wyckoff *et al.*, 2004). Tumour cells expressing epidermal growth factor receptors (EGFR) respond to EGF secretion, which consequently activates store-operated calcium entry into cells, stimulating NFAT signalling (Wang *et al.*, 2012). NFAT further integrates into this feedforward paracrine loop between inflammation, immune activation and cancer progression by inducing CSF1 in both immune and tumour cells (Cockerill *et al.*, 1993; Masuda *et al.*, 1993). Functioning alongside infiltrating macrophages, which often localise adjacent to tumour vasculature, NFAT is likely to promote epithelial cell migration and tumour progression (Wyckoff *et al.*, 2004; Shou *et al.*, 2015).

Until recently, evidence showing that NFAT activation initiates primary tumour formation was lacking. Tripathi et al (2013) recently reported, for the first time, direct evidence of primary tumour induction by NFAT2 *in vivo*, through establishment of the tumour microenvironment (Tripathi *et al.*, 2013). Using inducible transgenic mouse

systems, in which NFAT2 activation could be controlled by the administration of doxycycline, they showed that constitutively active NFAT2 caused tumours to form in specific sites and tissues, including the ovaries and the skin (Tripathi *et al.*, 2013). Their data indicated that NFAT functions oncogenically in a cell-type and tissue-dependent manner, where NFAT2 induction was found to promote production of cytokines to produce an inflammatory microenvironment (Tripathi *et al.*, 2013). Interestingly, they found that cells expressing constitutively active NFAT2, as well as wild-type neighbouring the tumour cells, had upregulated expression of tumour-promoting STAT3 and c-Myc (Tripathi *et al.*, 2013).

In summary, NFAT is likely to have a complex role in the tumour microenvironment, demonstrating both cell autonomous and non-autonomous mechanisms. Further studies are required regarding the disease-specific roles for NFAT in the microenvironment, including a greater understanding of the molecular mechanisms behind its recently reported role in tumour-associated anergy (Serfling *et al.*, 2006b; Abe *et al.*, 2012).

1.19. Targeting the NFAT pathway in cancer therapy

NFATs have long been considered good targets for the treatment of immune related disorders. However, with an increasing number of studies also reporting of a role for NFAT in cancer, therapeutic intervention in this pathway may also prove useful for anti-tumour therapy. Research on NFAT activity in immune function largely stemmed from recognition that NFAT induction was inhibited by the potent immunosuppressants cyclosporin A (CsA) and FK506. Derived from fungal metabolites, these drugs have revolutionised the field of transplant medicines. CsA and FK506 are widely used in the clinic to prevent organ transplant rejections but also serve as a useful research tool for understanding the role of NFAT in various systems (Kiani *et al.*, 2000).

Mechanistically, CsA and FK506 both prevent the nuclear translocation of NFATs by preventing calcineurin activation (Liu *et al.*, 1991; Matsuda *et al.*, 2000). Lacking structural similarity, CsA binds to the immunophillin protein cyclophilin A (CyPA) whereas FK506 bindings to FKBP12 respectively. Used in this PhD study, CsA binds to cyclophilin A (CyPA) (an immunophillin peptidyl-prolyl cis-trans isomerase (PPIase)), effectively preventing its PPIase activity which usually enables calcineurin activation. CsA-CyPA complexes bind between the catalytic and regulatory regions of calcineurin, forming a stable ternary complex (Barik, 2006; Sieber, 2009). Formation of respective

CsA or FK506 complexes with calcineurin effectively inhibits its phosphatase activity (Liu *et al.*, 1991; Matsuda *et al.*, 2000). This prevents the dephosphorylation of substrates downstream of calcineurin, including NFAT, therefore preventing the transcription of multiple genes, such as a cytokines and chemokines. (Liu *et al.*, 1991; Matsuda *et al.*, 2000).

Inhibition of calcineurin activity blocks the dephosphorylation of many other substrates (in addition to NFAT), which is likely to explain the neurotoxicity and nephrotoxicity experienced by patients administered these drugs (Kiani *et al.*, 2000; Rezzani, 2004). Although valuable agents for transplant therapy, patients on long term treatment have a significant increase in the incidence of cancer due to suppression of tumour immunosurveillance mechanisms (Dantal *et al.*, 2005). Despite this observation, short term CsA treatment of mouse models with human T-cell leukaemia results in anti-leukaemic effects (Medyouf review 2008). CsA in combination with other agents has also been used successfully in the treatment of some T-cell lymphomas (Advani *et al.*, 2007; Chen *et al.*, 2011b).

For NFAT therapy to be effective for the treatment of cancer, a targeted approach is essential. Selective inhibitors of NFAT have also been developed in the form of peptide sequences that interfere with the interaction between calcineurin and NFAT, blocking NFAT dephosphorylation and nuclear translocation. The VIVIT peptide for example, with a Pro-Val-Ile-Val-Ile-Thr sequence, has a high affinity for NFAT's docking site on calcineurin (Aramburu *et al.*, 1998; Aramburu *et al.*, 1999). Developed in 1998, VIVIT was valued for its enhanced selectivity when compared to CsA (Aramburu *et al.*, 1998; Aramburu *et al.*, 1999). VIVIT was shown to attenuate breast cancer cell invasion *in vitro* (Jauliac *et al.*, 2002), however the efficacy of VIVIT in mouse models of cancer progression remain to be evaluated. Furthermore, the use of peptides in the clinic introduces issues of delivery and stability, whereas development of effective small molecule inhibitors is likely a more promising strategy. Analogues of CsA and FK506 (L-732531 and ISATX47 respectively), have shown less side effects than CsA and FK506 themselves, however their efficacy in mouse models of cancer have not yet been performed (Karanam *et al.*, 1998; Aspeslet *et al.*, 2001).

1.20. Role of NFAT in haematological malignancies

NFAT1, 2 and 4 are the NFAT family members expressed in lymphoid tissues. Increasing evidence suggests a role for NFAT1 and NFAT2 in haematological malignancies, although less is known about the role of NFAT4. First implicated in blood malignancies by Marafioti et al (2004), a comprehensive analysis of 300 biopsies of human lymphomas showed the overexpression and nuclear activation of NFAT2 in a range of disease types, including DLBCL, Burkitt's lymphoma, aggressive T-cell lymphoma and chronic lymphocytic leukaemia (Marafioti *et al.*, 2005; Pei *et al.*, 2012). In this study, active nuclear NFAT2 was observed in 70% of Burkitt lymphomas and 30% of DLBCL (Marafioti *et al.*, 2005). Nuclear localisation of NFAT2 or dephosphorylation of both NFAT2 and NFAT1 has also been observed in sample material from patients with DLBCL and aggressive T-ALL (T-cell acute lymphoblastic leukaemia) (Fu *et al.*, 2006; Medyouf *et al.*, 2007). It is possible that overexpression of NFAT may be due to genomic amplification, owing to the fact that approximately 5% of ABC DLBCL have amplification of a 1.9Mb region of chromosome 18q containing NFAT2, suggesting an effect of gene dosage in these cells (Lenz *et al.*, 2008c; Müller *et al.*, 2010).

NFAT activation was also demonstrated to be calcineurin-dependent in cell lines derived from DLBCL and T-ALL, where treatment with CsA or FK506 suppressed NFAT activation (Pham *et al.*, 2005; Medyouf *et al.*, 2007). Moreover, from an *in vivo* standpoint, sustained activation of calcineurin/NFAT signalling, in leukaemia cells of mouse models of human T-ALL, could also be inhibited using CsA or FK506 and this resulted in leukaemia regression and induction of apoptosis (Medyouf *et al.*, 2007). Leukaemic progression was also enhanced by transduction of cells with a constitutively active calcineurin mutant, further demonstrating the oncogenic nature of activating this pathway (Medyouf *et al.*, 2007). Furthermore, it was recently reported that activation of the NFAT signalling pathway has an important role in the development of resistance to tyrosine kinase inhibitors in CML, providing further evidence that NFAT may be of key functional relevance in haematological malignancies (Gregory *et al.*, 2010).

1.21. Evidence for cooperative roles of NFAT and NF-κB in DLBCL

Because NFAT-dependent transcription commonly requires assistance from other DNA binding proteins, this suggests a transcription factor that functions amongst a community of proteins that together promote tumourigenesis. Indeed, there is increasing evidence for

a cooperative role of the NF-κB and NFAT transcriptional pathways in the pathogenesis of DLBCL.

A number of key studies have shown a small number of genes that may enhance tumour growth and survival are regulated co-ordinately by NF-κB and NFAT in lymphocytes (Fu *et al.*, 2006). Pham et al (2005) investigated mechanisms that explain the abnormal expression of CD40 ligand (CD40L) in B-cell lymphomas (Pham *et al.*, 2005). They demonstrated constitutive activation of NFAT2, which directly interacted with the NF-κB subunit c-Rel, resulting in both cooperatively binding to the CD40L promoter, activating CD40L gene transcription and enhancing cell survival (Pham *et al.*, 2005). NF-κB and NFAT bound to two sites, including the distal CD40 ligand promoter kB sites -1180 and the proximal NFAT site -250, where cooperation between these two key transcription factors was compared to the formation of an enhanceosome –like complex (Pham *et al.*, 2005).

Another study investigated regulation of the cell-survival factor BLyS in B-cell non-Hodgkin lymphomas and found that constitutive NF-κB and NFAT regulated its expression through at least one NF-κB and two NFAT binding sites in the BLyS promoter (Fu *et al.*, 2006).

1.22. Importance of the BCR and NFAT signalling

As described previously, signalling pathways downstream of the BCR are fundamental for the survival of many lymphomas, including ABC and some GCB DLBCLs. Chronic-active BCR signalling leads to activation of the NF-κB pathway, for example, which is a well-established, critical pathway used for the survival of ABC DLBCL. Interestingly, in a recently study, clinical outcomes were predicted based on the degree of BCR and NFAT activation in Chronic Lymphocytic Leukaemia (CLL) (Le Roy *et al.*, 2012). Although resistant to cell death *in vivo*, most CLL cells quickly become apoptotic when cultured *in vitro* (Le Roy *et al.*, 2012). Remarkably, some CLL cells avoid apoptosis *in vitro* by survival responses that result from BCR stimulation. Le Roy et al (2012) show that B cells isolated from patients with unfavourable prognostic forms of CLL, had a survival advantage *in vitro* due to the degree of BCR and NFAT activation (Le Roy *et al.*, 2012). In cells with an activated BCR, phosphorylation of SYK, activation of phospholipase Cγ2 and intracellular calcium mobilisation demonstrated upregulation and constitutively active NFAT2 (Le Roy *et al.*, 2012). Interestingly, when induced with IgM, responding

cells were converted to an unresponsive state when also treated with the VIVIT peptide NFAT inhibitor, whereas Ionomycin-induced NFAT activation caused non-responding cells to survive (Le Roy *et al.*, 2012). The degree to which NFAT activation correlates with engagement of the BCR has not been studied in DLBCL. However, given the importance of the previously described forms of chronic and tonic BCR signalling for survival of DLBCL, this is an interesting and unexplored area of research.

1.23. NFAT summary

These studies collectively provide compelling evidence for the pathogenicity of the calcineurin-NFAT signalling pathway in haematological malignancies such as DLBCL. The presence of nuclear, active NFAT in DLBCL patients suggests that NFAT is transcriptionally active in these cells; however its function in this disease setting has not been fully investigated.

At present, we have little understanding of the mechanisms that drive constitutive activation of NFATs, such as regulation by the BCR. It is possible that similar to NF-κB, NFAT signalling is critical for the survival of a specific subgroup of DLBCL, a hypothesis that if proven true could allow more targeted treatments for DLBCL.

NFAT may exert its function in DLBCL by direct regulation of specific target genes, however these have surprisingly not yet been defined. Given the diverse roles of NFAT isoforms highlighted previously in other forms of cancer, is it possible that specific NFAT family members function differently, perhaps as oncogenes or tumour suppressors. Moreover, NFAT may not be a master regulator of DLBCL, but rather work in synergy with other transcription factors such as NF-κB to co-ordinately regulate genes encoding survival factors.

1.24. Aims

Accumulating evidence suggests that the signalling networks promoting and sustaining DLBCL derive from dysregulation of the normal pathways controlling B-lymphocyte activation and differentiation. There are increasing studies supporting a role for the NFAT

family of transcription factors in the malignant setting, where NFAT family members have demonstrated characteristics which represent many of the hallmarks of cancer (Macian, 2001; Qin *et al.*, 2014). Constitutively-active nuclear NFAT2 has been demonstrated in approximately 40% of primary DLBCL samples, however a fully comprehensive analysis of its expression and activation in different subgroups of DLBCL has not yet been investigated (Marafioti *et al.*, 2005). Moreover, although NFAT has been shown to regulate a small number of genes associated with DLBCL growth/survival, a broader analysis of the genes to which NFAT targets in DLBCL has not been explored (Pham *et al.*, 2005; Fu *et al.*, 2006; Pham *et al.*, 2010).

In addition to the NFAT family of transcription factors, the NF-κB pathway is also individually important for the pathogenesis of DLBCL. A small number of genes in lymphocytes have been shown to be regulated by NFAT and NF-κB in combination, suggesting that these pathways functionally intersect to drive lymphomagenesis (Pham *et al.*, 2005; Fu *et al.*, 2006).

Together, there is convincing evidence supporting a role for NFAT in DLBCL. Therefore, the central hypothesis tested in this PhD study was if 'the NFAT family of transcription factors play an important role in the survival and maintenance of DLBCL'.

This hypothesis will be investigated as follows:

- Aim 1: To investigate the expression and activation of NFAT in DLBCL
- Aim 2: To determine novel NFAT target genes in DLBCL
- Aim 3: To investigate cooperativity between the NFAT and NF-κB signalling pathways in DLBCL

Chapter 2.

Materials and Methods

2. Materials and Methods

2.1. Culture of mammalian cell lines

The human DLBCL cell lines U2932, SUDHL-4, Farage, WSU-NHL, SUDHL-6, OCI-LY18, OCI-LY19, Pfeiffer, Toledo and Karpas-422 were purchased from DSMZ or ATCC. The ABC DLBCL cell lines HLY-1, RIVA and OCI-Ly3 were generously provided by Dr Alison Banham, Nuffield Department of Clinical Laboratory Sciences (University of Oxford). The specific molecular subgroups of the panel of human DLBCL cells are indicated in table 4. HLY-1 cells (not commercially available) were validated as an ABC subtype DLBCL cell line with expression of BCR components by a combination of flow cytometric and immunohistochemical immunotyping performed by the Department of Pathology, Newcastle Upon Tyne NHS Foundation Trust. Cells were cultured in plastic 75cm^2 flasks and maintained in Gibco Roswell Park Memorial Institute (RPMI) 1640 medium with either 10% or 20% (as indicated in table 4) Gibco foetal calf serum (FCS). They were sustained in a humidified atmosphere at 37ºC with 5% CO_2. Cultures were split every 2-3 days at a ratio of 1:3-1:6 in order to maintain a cell density of less than 1x10^{6}cells/ml.

U2OS cells were kindly cultured by Dr Alex Sfikas and were maintained at 37ºC, 5% CO2 in DMEM medium (Lonza), supplemented with 10% FCS and 1% penicillin, streptomycin and L-Glutamine. Cells were grown to a maximum confluency of 90% and were split every 2-3 days.

Disease	Cell line	Culture medium
ABC DLBCL	RIVA	Gibco RPMI 1640, 10% FCS
ABC DLBCL	HLY-1	Gibco RPMI 1640, 10% FCS
ABC DLBCL	U2932	Gibco RPMI 1640, 10% FCS
ABC DLBCL	OCI-Ly3	Gibco RPMI 1640, 10% FCS
GCB BCR DLBCL	SUDHL-4	Gibco RPMI 1640, 20% FCS
GCB BCR DLBCL	Farage	Gibco RPMI 1640, 10% FCS
GCB BCR DLBCL	WSU-NHL	Gibco RPMI 1640, 10% FCS
GCB BCR DLBCL	SUDHL-6	Gibco RPMI 1640, 10% FCS
GCB BCR DLBCL	OCI-Ly18	Gibco RPMI 1640, 10% FCS
GCB non-BCR DLBCL	OCI-Ly19	Gibco RPMI 1640, 10% FCS
GCB non-BCR DLBCL	Pfeiffer	Gibco RPMI 1640, 10% FCS
GCB non-BCR DLBCL	Toledo	Gibco RPMI 1640, 10% FCS
GCB non-BCR DLBCL	Karpas-422	Gibco RPMI 1640, 20% FCS
Osteosarcoma	U2OS	Lonza DMEM, 10% FCS, 1% antibiotics

Table 4. Cell lines and culture medium. Mammalian cell lines used throughout the study are listed above, indicating cancer type and appropriate culture medium. ABC (Activated B-Cell), GCB (Germinal Centre B-Cell), DLBCL (Diffuse Large B-Cell Lymphoma).

2.1.1. Thawing of cryopreserved cell lines

Cells frozen in freezing medium (section 2.1.3) were removed from liquid nitrogen stores and were thawed at 37ºC before being combined with 5ml warm cell culture medium. To remove Dimethyl Sulfoxide (DMSO) (contained in the freezing media), cells were centrifuged (300g, 5mins) before the media was removed and replaced with an appropriate volume of fresh media and incubated at 37ºC, 5% CO_2.

2.1.2. Counting of cells using a haemocytometer

Equal volumes of 0.4% Trypan Blue stain (Sigma) and cell suspension were mixed and pipetted under the cover slip of the haemocytometer e.g. 20µl Trypan Blue and 20µl cell suspension. Under the microscope, live cells (colourless and bright) were counted from all four large corner grids ($1mm^2$). To calculate the cell concentration per/ml the following calculation was made;

$$\frac{\text{Total cell count}}{\text{Number of } 1mm^2 \text{ grids counted}} \text{ x dilution factor } (2) = \text{cells/ml x } 10^4$$

2.1.3. Freezing of cryopreserved cell lines

Cells growing in the exponential phase were counted using 0.4% Trypan Blue and a haemocytometer (as described in section 2.1.2). A total of 10^7 cells were collected and centrifuged (300g, 5mins) before the supernatant was removed and the remaining pellet dissolved in freezing medium (1ml cell culture medium, 10% DMSO). Cells were transferred to cryovial tubes and stored at -80ºC for 24 hours before transportation into liquid nitrogen tanks (-195ºC).

2.1.4. Mycoplasma testing

Mycoplasma is a genus of bacteria that lack a cell wall around their cell membrane, meaning that they are often unaffected by many common antibiotics. Known to alter the DNA, RNA and protein synthesis of infected host cells, mycoplasma are difficult microorganisms to detect. The MycoAlert® (Lonza) test for mycoplasma infection used in this project exploits the activity of mycoplasmal enzymes. Enzymes are found in all

six of the main mycoplasmal cell culture contaminants and the majority of 180 species of mycoplasma, but are not present in eukaryotic cells. Viable mycoplasma are first lysed, before addition of the MycoAlert® substrate, which reacts with mycoplasmal enzymes, converting ADP to ATP. The level of ATP in a sample is measure before and after addition of the substrate, providing a ratio which is indicative of the presence or absence of mycoplasma.

2.2. Protein Methods

2.2.1. Preparation of whole cell extracts

Untreated or treated cells were pelleted by centrifugation and washed twice in 1ml cold PBS. Lysis buffer was prepared by addition of 10µl of EDTA-free Halt™ Protease and Phosphatase Inhibitor (100x) (1mM Aminoethyl benzenesulfonyl hydrochloride, 800nM Aprotinin, 50µM Bestatin, 15µM E-64, 5uM EDTA, 20µM Leupeptin, 10µM Pepstatin A) single-use cocktail (Thermo-Scientific) to 1ml radioimmunoprecipitation (RIPA) Lysis and Extraction Buffer (Thermo-Scientific). 40µl lysis buffer per 1 million cells was added to samples and mixed by pipetting up and down until a clump of cellular material was formed. Samples were then incubated on ice for 30 minutes to ensure total lysis of cells. Samples were subsequently centrifuged (15mins, 16,000g at 4^{o}C) and the supernatant removed and decanted into eppendorfs. Samples were stored at -20^{o}C.

2.2.2. Preparation of nuclear and cytoplasmic extracts

The NE-PER™ Nuclear and Cytoplasmic Extraction Kit (Thermo-Scientific, catalogue number 78833) was used to perform nuclear and cytoplasmic extractions as per the manufacturer's protocol. Addition of two cytoplasmic extraction reagents (CERI and CERII) to cell pellets causes disruption of cell membranes and the release of cytoplasmic components. The nuclei remain intact and are removed from the cytoplasmic extract by centrifugation. Addition of the nuclear extraction reagent (NER) lyses the nuclei, yielding a nuclear extract with less than 10% contamination between fractions. For experiments analysing the subcellular localisation of proteins and NFAT2 binding (ELISA), 10^7 untreated or treated cells were harvested for each sample and (following centrifugation) the volumes of kit reagents used were based upon an approximate packed cell volume of 20µl. For experiments using nuclear extracts to investigate NF-κB DNA binding

(ELISA), $5x10^6$ cells were harvested and kit reagent volumes were based on a packed cell volume of 10µl.

Optimisation experiments for this assay indicated that an additional wash step was beneficial to remove cytoplasmic contamination of the nuclear fraction. Following removal of the cytoplasmic extract, the nuclear pellet was washed in 1ml PBS, followed by centrifugation (5mins, 16,000g at 4°C) and removal of the PBS wash before the addition of the NER. This adjustment to the protocol was included throughout the study.

2.2.3. Protein quantification

2.2.3.1. Pierce™ BCA Protein Assay

The Pierce™ BCA Protein Assay Kit (Thermo-Scientific, catalogue number 23225) was used to determine the concentration of protein in cell lysates. This method makes use of the biuret reaction (Cu^{+2} cations are reduced to Cu^{+1} cations by the presence of protein peptide bonds in an alkaline medium) and is quantified colourimetrically by using a reagent containing bicinchoninic acid (BCA). Chelation of two molecules of BCA with one cuprous Cu^{1+} cation produces a purple-coloured reaction product which exhibits strong absorbance at 562nm. The degree of colour change reflects the relative concentration of protein in a sample.

Protein lysate samples were diluted 1:5 in 10µl RIPA buffer and added to a 96-well plate in triplicate alongside a series of dilutions of bovine serum albumin (BSA) protein standards (ranging from 0.125-2mg/ml) and a column of RIPA buffer blanks. Working reagent was prepared by mixing BCA Reagent A with BCA reagent B in the ratio 50:1. In turn, 200µl of working reagent was added to all wells and the plate incubated for 30mins at 37°C, 5% CO_2. Absorbance readings were recorded using the FLUOstar Omega plate reader (BMG Labtech) at a wavelength of 562nm. The protein concentration of samples was subsequently determined, based on a standard curve produced by protein standards.

2.2.3.2. BioRad protein assay (Bradford Assay)

The BioRad Protein Assay (catalogue number 500-0006) is based on the method of the Bradford assay, which is a colourimetric assay used for the determination of solubilised protein. The assay is based on an absorbance shift of Coomassie® Brilliant Blue G-250 dye. The dye binds primarily to basic and aromatic amino acid residues and under acidic conditions is red in colour, occurring as a doubly protonated cationic form (A_{max} = 470nm). When the dye binds to protein it is converted to a stable, unprotonated form which is blue in colour (A_{max} = 595nm) and can be detected using a spectrophotometer at this wavelength.

For experiments investigating NF-κB activity using the NF-κB luciferase reporter assay (as described in section 2.8), the Bradford assay was performed in order for Relative Light Units (RLU) to be normalised to the respective protein concentrations of samples. First, the dye reagent was prepared by diluting 1 part dye with 4 parts distilled, de-ionised water (DDI H_2O). To a 96-well plate, 10µl of supernatant from cell lysates or BSA protein standard was pipetted in duplicate and 200µl of diluted dye reagent was mixed into wells. The plate was incubated at room temperature for 5 minutes before absorbance measurements were taken using the POLARstar Omega spectrophotometer (BMG, Labtech) at 596nm. The protein concentration of samples was determined based on a standard curve of protein concentrations produced by protein standards (ranging from 0.05-0.5mg/ml).

2.2.4. Western blotting

Western blotting is a technique used for the detection of specific proteins in a cell extract or tissue homogenate. Proteins are first denatured by heating to 100^{o}C in a solution of SDS sample loading buffer. The 2-β-Mercaptoethanol contained in the sample buffer aids the denaturing process by breaking disulphide bonds, whereas the SDS adds a negative charge to proteins so that proteins will migrate through the acrylamide gel to the positive charged electrode during SDS-PAGE electrophoresis. Proteins are separated according to their molecular weight, for example, smaller, lower molecular weight proteins migrate further down the gel. Following electrophoresis, the separated protein bands on the gel are transferred to a nitrocellulose or polyvinylidene difluoride (PDVF) membrane by using an electric current to pull proteins from the gel onto the membrane. To avoid non-specific binding of antibodies, the membrane is then blocked using a solution of diluted protein from either 5% BSA in PBS or 5% milk in TBS-Tween. In turn, the membrane is

probed with antibodies specific to a protein of interest, followed by exposure to a secondary antibody specific to the species of the primary antibody. Attached to the secondary antibody is usually a reporter enzyme such as alkaline phosphatase or horseradish peroxidase which cleaves a chemoluminescent agent to produce luminescence which is relative to the amount of protein present. The protein bands are visualised by placing photographic film on top of the membrane, exposing the light emitted from the chemoluminescent reaction in the areas of antibody binding.

2.2.4.1. Sodium Dodecyl Sulphate Polyacrylamide Gel Electrophoresis (SDS-PAGE)

Electrophoresis gels were poured in-house, using the recipes in table 5. To achieve optimal resolution of NFAT transcription factors, an 8% acrylamide concentration was used for NFAT detection, due to NFAT isoforms being of high molecular weight (90-160kDa). In contrast, 10% resolving gels were poured for all other proteins which were smaller in size, such as for NF-κB subunits. A 6% stacking gel was used for all gels.

	Ingredients	**Volume for x1 gel (10ml)**

8% Resolving Gel	Protogel: 30% acrylamide, 0.8% bisacrylamide (National Diagnostics)	2.7ml
	4x Resolving Gel Buffer: 1.5M Tris-HCL, 0.4% SDS, pH8.8 (National Diagnostics)	2.6ml
	Tetramethylenediamine (TEMED) (Sigma)	10µl
	Ammonium Persulphate (APS) (Sigma))	30µl
	DiH_2O (Gibco)	4.7ml
10% Resolving Gel	Protogel: 30% acrylamide, 0.8% bisacrylamide (National Diagnostics)	3.3ml
	4x Resolving Gel Buffer: 1.5M Tris-HCL, 0.4% SDS, pH8.8 (National Diagnostics)	2.6ml
	TEMED (Sigma)	10µl
	APS (Sigma)	30µl
	DiH_2O (Gibco)	4.1ml
6% Stacking Gel	Protogel: 30% acrylamide, 0.8% bisacrylamide (National Diagnostics)	1ml
	Protogel Stacking Buffer: 0.5M Tris-HCL, 0.4% SDS, pH6.8 (National Diagnostics)	1.25ml
	TEMED (Sigma)	5µl
	APS (Sigma)	50µl
	DiH_2O (Gibco)	2.75ml

Table 5. Material information and recipe for pouring SDS-PAGE gels.

While gels were setting, cell lysates were diluted in RIPA buffer and 4x SDS sample buffer so that the final amount of protein added to individual wells was 12-20µg. Protein lysates were then denatured by heating samples to 100^{o}C in a heat block for 5 minutes and then centrifuged at full speed for one minute (to collect condensation) and then pipetted into wells. 10µl Spectra™ Multicolour Broad Range Protein Ladder standards (Thermo-Scientific) were run alongside samples. Once loaded, Mini-PROTEAN® 3 system tanks (BioRad) were filled with 500ml running buffer (table 6) and electrophoresis was performed at 120V for approximately 90 minutes.

	Ingredients to make stock	**Preparation of 1x solution**

4x SDS Sample Buffer (50ml)	250mM Tris pH 6.8 (12.5ml)	Dilute 1:4 with sample lysate and RIPA buffer
	40% Glycerol (20ml)	
	8% SDS (4g)	
	Sterile diH_2O to 40ml, pH to 6.8, then make up to 50ml. with diH_2O	
	2.86M 2-β-Mercaptoethanol (2ME) (200µl/ml)	
	0.04% saturated aqueous Bromophenol Blue solution (40µl/ml)	
10x Running Buffer (2L)	25mM Tris (60g)	For 500ml: Dilute 100ml 10x running buffer with 900ml sterile diH_2O
	192mM Glycine (288g)	
	0.1% SDS (20g)	
	Sterile diH_2O to 2L	
5x Transfer Buffer (2L)	25mM Tris (30g)	For 1L: 200ml 5x transfer buffer, 200ml Methanol, 600ml sterile diH_2O
	192mM Glycine (144g)	
	0.0075% SDS (7.5g)	
	Sterile diH_2O to 2L	
10x TBS pH 7.6 (2L)	20mM Tris (175.32g)	For 1L 1xTBS 0.1% Tween: Dilute 100ml 10x TBS with 900ml sterile diH_2O plus 1ml Tween® 20 (Sigma)
	150mM NaCl (87.66g)	
	Sterile DiH_2O to 1.8L, pH to 7.6, then make up to 2L with diH_2O	

Table 6. Material information and recipes for preparing Western blotting buffers and washing agents.

2.2.4.2. Transfer and Immunoblotting

Proteins were transferred to an Immobilon-P PDVF transfer membrane (Millipore) using the BioRad Mini Trans-Blot system. The gel and methanol-activated membrane were

placed between two sponges and two pieces of filter paper that had been soaked in transfer buffer (table 6). The transfer was run at 100V for 1 hour with a block of ice inserted in the tank, which was replaced with another block of ice halfway through the transfer process. Following protein transfer, the membrane was blocked with TBS-Tween 5% milk solution for 1 hour to prevent non-specific binding. The membrane was then washed (2x10mins) in TBS-Tween 5% milk before being incubated for 1 hour or overnight in the specified concentration of primary antibody, as indicated in table 7. A further 2x10min washes with TBS-Tween 5% milk were made followed by incubation of the membrane in the specified concentration of secondary antibody for 1 hour. The membrane was then washed for 4x10mins in TBS-Tween 5% milk.

2.2.4.3. Protein detection

Proteins were detected using the Amersham enhanced chemiluminescence (ECL) Western Blotting Detection Reagents (GE Healthcare) by adding 1ml of ECL per membrane for 1 minute. The membrane was wrapped in Saran wrap and fastened into an X-Ray film cassette. Autoradiography film (Amersham Hyperfilm) was exposed to the membrane and developed using a D3300 X-Ray system (Gulmay Medical Ltd, Surrey, UK).

2.2.4.4. Stripping membranes

When required, membranes were stripped to remove bound antibodies by incubation in 20mls stripping buffer solution (6.25ml 0.5M Tris pH 6.8, 5ml 20% SDS, 350µl 2-β-mercaptoethanol (Sigma) and 38.5ml sterile H_2O) in a shaking water bath at 70ºC for 30 minutes. Membranes were washed for 4x10min in TBS-Tween and subsequently blocked in TBS-Tween 5% milk for 1 hour before re-probing with the primary antibody of interest.

	Target protein	Species	Manufacturer	Catalogue number	Dilution	Diluent	Incubation period	Molecular weight
Primary Antibodies	NFAT1 (4G6-G5)	Mouse monoclonal	Santa Cruz Biotechnology	SC-7296	1:1000	TBS-Tween 5% milk	1 hour RT or Overnight 4°C	135kDa
	NFAT2 (7A6)	Mouse monoclonal	Santa Cruz Biotechnology	SC-7294	1:1000	TBS-Tween 5% milk	1 hour RT or Overnight 4°C	Isoforms 1/2/3: 90/110/140kDa
	NFAT3 (H-74)	Rabbit polyclonal	Santa Cruz Biotechnology	SC-13036	1:1000	TBS-Tween 5% milk	Overnight 4°C	Dephosphorylated 140kDa, hyperphosphorylated 160kDa
	NFAT4 (F-1)	Mouse monoclonal	Santa Cruz Biotechnology	SC-8405	1:1000	TBS-Tween 5% milk	1 hour RT or Overnight 4°C	115kDa
	NFAT5 (H-300)	Rabbit polyclonal	Santa Cruz Biotechnology	SC-13035	1:1000	TBS-Tween 5% milk	Overnight 4°C	170kDa
	NF-κB p65 (C-20)	Rabbit polyclonal	Santa Cruz Biotechnology	SC-372	1:1000	TBS-Tween 5% milk	1 hour RT or Overnight 4°C	65kDa
	Phospho-NF-κB p65 (Ser536) (93H1)	Rabbit polyclonal	Cell Signalling Technology	3033	1:1000	TBS-Tween 5% milk	1 hour RT or Overnight 4°C	65kDa
	NF-κB c-Rel (C)	Rabbit polyclonal	Santa Cruz Biotechnology	SC-71	1:1000	TBS-Tween 5% milk	Overnight 4°C	75kDa
	NF-κB RelB	Rabbit polyclonal	Cell Signalling Technology	4954	1:1000	TBS-Tween 5% milk	Overnight 4°C	70kDa
	NF-κB p50/p105	Rabbit polyclonal	Upstate Millipore	06-886	1:1000	TBS-Tween 5% milk	Overnight 4°C	p50 50kDa and precursor p105 105kDa
	NF-κB p52/p100	Mouse monoclonal	Upstate Millipore	05-361	1:1000	TBS-Tween 5% milk	Overnight 4°C	p52 52kDa and precursor p100 100kDa
	NF-κB IκBα	Rabbit polyclonal	Cell Signalling Technology	9242	1:1000	TBS-Tween 5% milk	Overnight 4°C	39kDa
	Phospho-IκBα (Ser32) (14D4)	Rabbit monoclonal	Cell Signalling Technology	2859	1:1000	TBS-Tween 5% milk	Overnight 4°C	40kDa
	Alpha-Tubulin (clone DM1A)	Mouse monoclonal	Sigma Aldrich	T6199	1:10,000	TBS-Tween 5% milk	1 hour RT or Overnight 4°C	50kDa
	PARP C2-10	Mouse monoclonal	Trevigen	4338-MC-50	1:3000	TBS-Tween 5% milk	Overnight 4°C	114kDa holoenzyme, 85kDa (apoptosis), 50kDa, 62kDa and 74kDa (necrosis)
	PARP	Rabbit polyclonal	Cell Signalling	9542	1:1000	PBS 5% BSA	Overnight 4°C	116kDa holoenzyme, 89kDa (apoptosis)
Secondary Antibodies	Anti-Mouse	Goat polyclonal	Dako	P044701	1:5000	TBS-Tween 5% milk	1 hour RT	N/A
	Anti-Rabbit	Goat polyclonal	Dako	P0048	1:5000	TBS-Tween 5% milk	1 hour RT	N/A

Table 7. Antibodies used for Western blot analysis. The target protein, molecular weight and species in which the antibody was raised are indicated in the table. The manufacturer, catalogue number are stated and the conditions used for probing are described.

2.3. Cell viability/proliferation methods

2.3.1. Trypan blue exclusion

The Trypan Blue exclusion assay was used to determine the number of viable cells in a cell suspension. Dead cells are visually identified as blue in colour, where their disrupted cell membranes have allowed the dye to be taken up into the cytoplasm of cells. Live cells with intact membranes will not absorb the dye and appear visually as having a clear cytoplasm. Cell suspensions were mixed in a 1:1 ratio with 0.4% Trypan Blue (Sigma) solution (e.g. 20µl cells: 20µl Trypan Blue) and pipetted onto a haemocytometer before counting (as described in section 2.1.2). The following calculation was made to determine cell viability in samples;

$$\frac{\text{No. of viable cells counted}}{\text{Total cells counted (viable and dead)}} \text{ x } 100 = \% \text{ viable cells}$$

2.3.2. Growth curves

To obtain optimal cell seeding densities for subsequent cell viability assays, the growth of cell lines was analysed over 4 days and recorded using the resazurin assay, as described in section 1.6.3. Cells were first counted using trypan blue staining and seeded out at a range of densities ($0.05x10^6$/ml to $1x10^6$/ml) in 100µl volumes. Samples were assayed in triplicate and for each cell line 4x96-well plates were filled, one to be assayed each day. To avoid evaporation of cells, the outer wells were filled with 100µl PBS. Cells were incubated (37ºC, 5% CO_2) for 24, 48, 72 and 96 hours before 11µl resazurin agent was added to each well and the plates incubated for 2 hours. Viable cells were quantified using the FLUOstar Omega plate reader (BMG Labtech) at an excitation wavelength of 560nm and emission wavelength of 590nm and growth curves were plotted using Microsoft Excel.

2.3.3. Resazurin cell viability assay

To analyse the effects of specified chemical inhibitors, peptides and anti-TNFα agents on cell viability, the resazurin assay (Sigma, catalogue number R7017) was used. The assay estimates the number of viable cells present in multi-well plates by using the indicator dye resazurin to measure the metabolic activity of cells. Resazurin is readily reduced into

the fluorescent compound resorufin in viable cells, shifting the colour from a dark blue to a pink, fluorescent colour ($579_{Ex}/584_{Em}$), which can be measured using a spectrophotometer. The fluorescent signal is directly proportional to the number of viable cells. In contrast, non-viable cells without the capacity to metabolise, are unable to reduce the resazurin dye and so do not generate a fluorescent signal.

Upon arrival, the resazurin sodium salt was reconstituted in sterile H_2O (Gibco) to a concentration of 100µg/µl and stored in 1ml aliquots at -20ºC. Immediately prior to performing the assay (after the desired time point), the resazurin was thawed in the absence of light. For the assay setup, cells were first counted and seeded out into 96-well plates at a cell-specific density, as indicated in chapter 3, figure 16k. A volume of 50µl of cells was added to wells in triplicate, including triplicates of control wells (cells with or without DMSO/agent diluents) and triplicates of blank media control wells. To avoid evaporation of outer wells, these were loaded with 100µl PBS. Specific concentrations of chemical inhibitor, peptide or anti-TNFα agent were prepared at double the final desired concentration and 50µl of each added to wells accordingly (1:2 dilution to achieve final concentration). Plates were incubated at 37ºC, 5% CO_2 for the specified time point, followed by addition of 11ul of resazurin reagent (final concentration in wells 100µg/ml) and incubated at 37ºC, 5% CO_2 for 2 hours. Fluorescence readings were recorded using the FLUOstar Omega plate reader (BMG Labtech) at an excitation wavelength of 560nm and emission wavelength of 590nm. The percentage cell viability was determined by comparing fluorescence values to the untreated control and IC50 values (when reached) were established using cell viability curves on GraphPad Prism 6 software.

2.3.4. Propidium Iodide (PI) assay for cell cycle analysis

Flow cytometry is a useful technique used for many research applications including cell counting, sorting and for the detection of biomarkers of interest. The physical and chemical properties of cells (such as their granularity, size and fluorescence intensity) can be characterised. Cells are typically resuspended in a stream of fluid and passed through at least one laser, exciting fluorescently labelled components of cells, therefore emitting light at various wavelengths. An electronic detection apparatus is used to record fluorescence and how the light is scattered from the laser.

During the phases of the cell cycle, levels of DNA change, which can be detected using a DNA-staining dye such as propidium iodide (PI). PI binds to DNA by intercalating

between bases and is stoichiometric, binding in direct proportion to the amount of DNA present in the cell. The binding property of the dye therefore allows the different stages of the cell cycle to be identified. Cells in S-phase for example, will have more DNA than cells in G1 and fluorescence intensity will further increase when cells are in the G2 growth phase.

For the experimental assay, following the appropriate treatment, cells were counted using a haemocytometer and centrifuged (300g, 5mins) and washed in 1ml PBS. Cells were spun down again (300g, 5mins) and fixed in 1ml of cold 70% ethanol (prevents lysis and degradation of cells). To ensure fixation of all cells, the ethanol was added to eppendorfs drop-wise while vortexing at a low speed. Samples were placed on ice for 30 minutes (or at this stage stored at 4^{o}C for several days) before being washed in 1ml PBS (300g, 5mins). To prevent the binding of PI to RNA, RNA was degraded by resuspending pellets in 50µl of 100µg/ml RNaseA. To stain the DNA, 200µl of propidium iodide (Sigma) was added to the pellet to a final concentration of 50µg/ml. Samples were subsequently protected from light by tin foil and taken for flow cytometry analysis using the FACSCalibur (BD Biosciences). A total of 10,000 events were analysed using the CellQuest Pro software (BD Biosciences). For data analysis, cell cycle phase distribution was determined using Cyflogic flow cytometry software (version 1.2.1), as described in Appendix Figure 22.

2.3.5. Preparation of calcineurin/NFAT chemical inhibitors and peptides

Cyclosporin A (CsA), *Tolypocladium Inflatum*	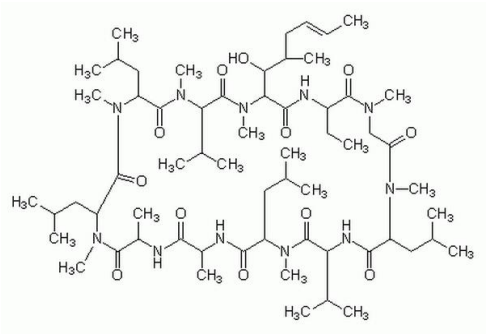
Calcineurin inhibitor Cyclosporin A (molecular weight 1202.6) was purchased from Merck Chemical Ltd. (Calbiochem, catalogue number 239835) in a powder form and was dissolved in DMSO (Sigma) to a concentration of 100mg/ml and stored at 4ºC.	Source: www.merckmillipore.com

Figure 10. Molecular structure and preparation of calcineurin inhibitor CsA.

FK506, *Tacrolimus*	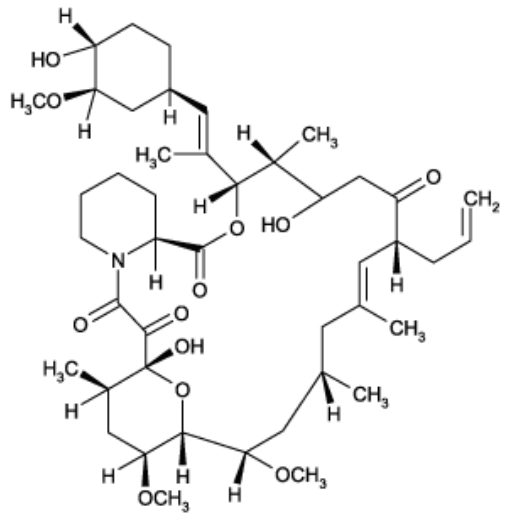
Calcineurin inhibitor FK506 (molecular weight 804.03) was purchased from Cell Signalling (catalogue number 9974) in a powder form and was dissolved in DMSO (Sigma) to a concentration of 12.4µM and stored at -20ºC.	Source: www.enzolifesciences.com

Figure 11. Molecular structure and preparation of calcineurin inhibitor FK506.

11R-VIVIT Peptide

Cell permeable NFAT inhibitor 11R-VIVIT peptide (molecular weight 3573.1) was purchased from Merck Chemicals Ltd (Calbiochem, catalogue number 480401). It was obtained in a lyophilised solid, salt form and was dissolved in sterile distilled water to a concentration of 250µM and stored at -20ºC. Peptide sequence; H-Arg-Arg-Arg-Arg-Arg-Arg-Arg-Arg-Arg-Arg-Arg-Gly-Gly-Gly-Met-Ala-Gly-Pro-His-Pro-Val-Ile-Thr-Gly-Pro-His-Glu-Glu-OH.

Maleimido-conjugated VIVIT 1 (MCV-1)

Cell permeable NFAT inhibitor MCV-1 (HP-VIVIT) peptide (molecular weight 1020.2) was purchased from Merck Chemicals Ltd (Calbiochem, catalogue number 480404) in a salt form and was dissolved in DMSO (Sigma) to a concentration of 40mM and stored at -20ºC.

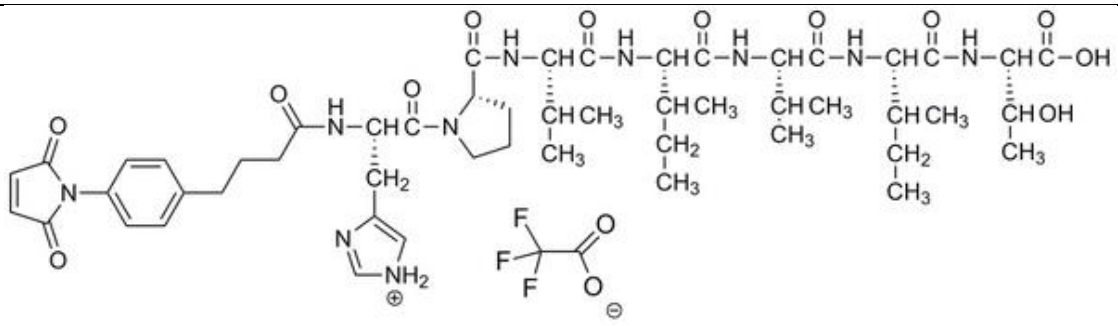

Source: www.merckmillipore.com

Figure 12. Molecular structure and preparation of MCV-1 VIVIT peptide.

Inhibitor of NFAT-Calcineurin Activation 6 (INCA-6)	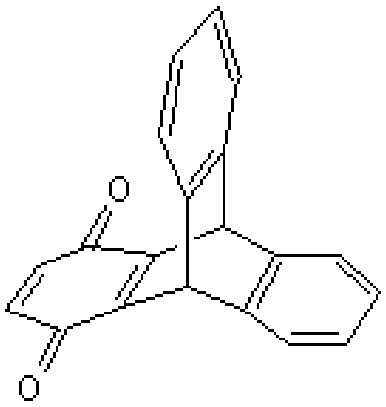 Source: www.tocris.com
The NFAT inhibitor INCA-6 (molecular weight 284.31) was purchased from Tocris Biosciences (catalogue number 2162) in a powder form and was dissolved in DMSO (Sigma) to a concentration of 18mM and stored at room temperature.	

Figure 13. Molecular structure and preparation of the NFAT inhibitor INCA-6.

2.3.6. Preparation of NF-κB chemical inhibitors

IKK2 inhibitor IV (TPCA-1)	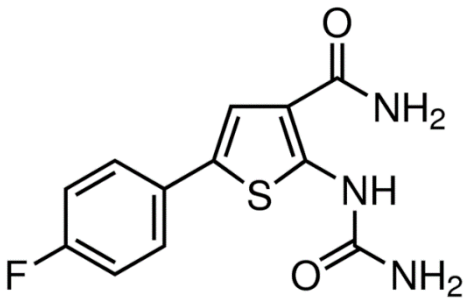 Source: ww.sigmaaldrich.com
The IKK2 (NF-κB) inhibitor 2-[amino carbonyl) amino]-5-(4-fluorophenyl)-3-thiophenecarboxamide (TPCA-1) (molecular weight 279.29) was purchased from Selleckchem (catalogue number S2824 and was dissolved in DMSO (Sigma) to a concentration of 35mM and stored at -80ºC.	

Figure 14. Molecular structure and preparation of the IKK2 inhibitor TPCA-1.

2.3.7. Preparation of anti-TNF-α agents

Etanercept (Enbrel®)
The TNF-α fusion protein Etanercept was a kind gift from Dr Anja Krippner (University of Newcastle, UK) and was diluted in PBS with 5% FCS to a concentration of 10mg/ml and stored at 4^{o}C.

Infliximab (Remicade®)
The TNF-α neutralising antibody Infliximab was a kind gift from Dr Anja Krippner (University of Newcastle, UK) and was diluted in PBS with 5% FCS to a concentration of 10mg/ml and stored at 4^{o}C.

Human Immunoglobulin G (IgG)
The human IgG was a kind gift from Dr Anja Krippner (University of Newcastle, UK) and was diluted in PBS with 5% FCS to a concentration of 10mg/ml and stored at 4^{o}C.

2.4. RNA Methods

2.4.1. GeneFlow EZ-RNA total RNA isolation

RNA extraction was performed by using the EZ-RNA Total RNA Isolation Kit (GeneFlow, catalogue number 20-400-100) which uses a denaturing solution comprised of guanidine thiocyanate to disrupt cells, followed by a phenol-based organic extraction and isopropanol-based precipitation of RNA. The assay procedure was followed according to the manufacturer's protocol. RNA pellets were dissolved in 20µl sterile, RNAse/DNase free H_2O (Gibco) and stored at -80^oC.

2.4.2. Qiagen RNeasy RNA extraction

RNA extraction of samples used for gene expression microarray analysis was performed using the RNeasy Mini Kit (Qiagen, catalogue number 74106). The assay procedure was followed according to the manufacturer's protocol, where samples are first lysed with guanidine-isothiocyanate and washed in ethanol. A series of steps to remove contaminants are subsequently followed by loading samples into silica membrane spin columns. Samples were eluted in 30µl RNase-free H_2O (Gibco) and were stored at -80^oC before further use.

2.4.3. Reverse Transcription of RNA to cDNA

The NanoDrop ND1000 spectrophotometer (LabTech International) was used to determine the quantity of RNA in each sample. Samples were diluted in sterile DNase/RNase free water (Gibco) to a concentration of approximately 500ng/µl. The 260:230 and 260:280 ratios were recorded as an indication of contaminant absorption e.g. phenol. The RevertAid H Minus First Strand cDNA Synthesis Kit (Fermentas) was used for the reverse transcription of RNA to cDNA. First, 500ng RNA was added to Fisherbrand PCR tubes (Fisher Scientific) and the volume made up to 11µl with RNase free water (Gibco). 1µl of random hexamer primers was then added to the cDNA followed by denaturing of the samples at 65^oC using the GeneAmp PCR system 2700 (Applied Biosystems). 8µl of master mix (4µl reaction buffer, 2µl 10nM dNTP mix, 1µl Ribolock RNase Inhibitor and 1µl RevertAid H Minus M-MulV Reverse Transcriptase per sample) was added to each of the cDNA samples which were then incubated in the GeneAmp

PCR system 2700 (Applied Biosystems) for 10mins at 25^{o}C, 60mins at 42^{o}C and 75^{o}C for 10mins. Samples were then stored at -20^{o}C until further use.

2.4.4. Quantitative Real-Time PCR (qRT-PCR)

qRT-PCR is a quantitative method used for the determination of a relative expression of a gene. In this study the SYBR green dye based-method was used, whereby SYBR green acts as a reporter dye by binding to newly synthesised double-stranded DNA causing a green fluorescent signal to be emitted. For signals to be detectable the PCR reaction is repeated 40 times, amplifying the DNA each time and increasingly fluorescence intensity, which can be detected at 520nm. The absolute and relative DNA quantities can therefore be measured and compared between samples.

First, a master mix for each Sigma primer set was prepared using 0.3µl of forward and reverse primers (final concentration of primer 100nM), 5µl 2X SYBR-Green master mix (Invitrogen) and 3.2µl RNase/DNase free H_2O (Gibco). For Qiagen primers, 1µl of 10x primer was used per reaction, 5µl 2X SYBR-Green master mix and 3µl H_2O. The master mix was mixed by vortexing and 8µl was added into wells of a 384-well plate respectively. 1µl of cDNA was added (using a multistep electronic pipette) to wells accordingly and a row of non-template controls (Gibco sterile distilled H_2O) were run alongside samples. Samples were run in triplicate so that a mean cycle threshold (Ct) value could be calculated after the qRT-PCR step. The plate was then sealed and centrifuged at 300g for 1 minute. Quantitative Real-time PCR was subsequently performed using the ABI Prism 7900HT sequence detections system (Applied Biosystems).

The PCR reaction was run for 90mins and used specific conditions to allow the amplification of specific genes as follows. First, samples were heated to 95^{o}C for 10mins causing denaturation of DNA and separation of strands. The reaction temperature was then reduced to the annealing temperature (60^{o}C) for 1min and increased to 95^{o}C for 15 seconds for 40 cycles to allow forward and reverse primers to anneal to complementary regions of single-stranded DNA and begin synthesising DNA for genes of interest.

2.4.5. Primers used for qRT-PCR

SYBR green-based Quantitect primers were purchased from Qiagen, as indicated in table 8a and 8b. Each primer set was supplied as a lyophilised mix of forward and reverse primers and had been bioinformatically validated to ensure high specificity and sensitivity. Primers were reconstituted to make a 10x stock solution by adding 1.1ml TE, pH 8.0 to individual vials of primers. Primers were stored at -20^{o}C in small aliquots to avoid repeated freezing and thawing.

Gene	Gene name	Qiagen Catalogue number	Primer set ID	Ensembl Transcript ID	Transcripts targeted (NCBI reference sequence)	Transcript name (NCBI reference)
NFATC1 (NFAT2)	Nuclear Factor of Activated T Cells C1	QT00094157	Hs_NFATC1_1_SG QuantiTect Primer Assay	ENST00000253506	NM_006162	Transcript variant 2 NFATC1/αβ
				ENST00000329101	NM_172387	Transcript variant 3 NFATC1/Cβ
				ENST00000397790	NM_172388	Transcript variant 4
				ENST00000318065	NM_172389	Transcript variant 5 NFATC1/ββ
				ENST00000591814	NM_172390	Transcript variant 1 NFATC1/αA
				ENST00000427363	NM_001278669	Transcript variant 6 NFATC1/αC
				ENST00000542384	NM_001278670	Transcript variant 7
				ENST00000586434	NM_001278672	Transcript variant 8
				ENST00000545796	NM_001278673	Transcript variant 10
				ENST00000592223	NM_001278675	Transcript variant 9 NFATC1/βA
NFATC2 (NFAT1)	Nuclear Factor of Activated T Cells C2	QT00053599	Hs_NFATC2_1_SG QuantiTect Primer Assay	ENST00000371564	NM_012340	Transcript variant 1
				ENST00000396009	NM_173091	Transcript variant 2
PDCD1	Programmed Cell Death 1	QT01005746	Hs_PDCD1_1_SG QuantiTect Primer Assay	ENST00000334409	NM_005018	PDCD1
CCL4L2	Chemokine (C-C motif) Ligand 4-Like 2	QT01679209	Hs_CCL4L2_1_SG QuantiTect Primer Assay	ENST00000620250	NM_001001435	Reference removed
				ENST00000620732	NM_001291469	CCL4L2b1
				ENST00000620250	NM_001291468	CCL4L2
				ENST00000617416	NM_001291470	CCL4L2b2
				ENST00000620098	NM_001291471	CCL4L2c
				Not identified	NM_001291472	Not identified
				ENST00000610565	NM_001291473	CCL4L2e
				ENST00000617405	NM_001291475	CCL4L2f

Table 8a. Qiagen Quantitect primers for qRT-PCR, indicating order information and reference to Ensembl and NCBI transcript ID

Gene	Gene name	Qiagen Catalogue number	Primer set ID	Ensembl Transcript ID	Transcripts targeted (NCBI reference sequence)	Transcript name (NCBI reference)
NFKBIE	Nuclear Factor of Kappa Light Polypeptide Gene Enhancer in B-cells Inhibitor Epsilon	QT00075082	Hs_NFKBIE_1_SG QuantiTect Primer Assay	ENST00000275015	NM_004556	NFKBIE
TNF-α	Tumour Necrosis Factor Alpha	QT00029162	Hs_TNF_1_SG QuantiTect Primer Assay	ENST00000449264	NM_000594	TNF
EGR2	Early Growth Response 2	QT00000924	Hs_EGR2_1_SG QuantiTect Primer Assay	ENST00000242480	NM_000399	Transcript variant 1
				ENST00000242480	NM_001136177	Transcript variant 2
				ENST00000439032	NM_001136178	Transcript variant 3
				ENST00000411732	NM_001136179	Transcript variant 4
EGR3	Early Growth Response 3	QT00246498	Hs_EGR3_1_SG QuantiTect Primer Assay	ENST00000522910	NM_001199880	Transcript variant 2
				Not identified	NM_001199881	Not identified
				ENST00000	NM_004430	Transcript variant 1

Table 8b. Qiagen Quantitect primers for qRT-PCR, indicating order information and reference to Ensembl and NCBI transcript ID

Gene	Gene name	Company	Forward sequence 5' - 3'	Reverse sequence 5'- 3'
GAPDH	Glyceraldehyde 3-Phosphate Dehydrogenase	Sigma	GAAGGTGAAGGTCGGAGTC	GAAGATGGTGATGGGATTTC
TBP	TATA Box Binding Protein	Sigma	TGCACAGGAGCCAAGAGTG	CACATCACAGCTCCCCACCA
BCL-6	B-Cell Lymphoma 6	Sigma	CAAGACCGTCCATACCGGTG	GCCCCACAGATGTTGCAAC
MYC	Avian Myelocytomatosis Viral Oncogene Homolog	Sigma	GTCTCCACAGATCAGCACA	GTTCGCCTCTTGACATTCTC

Table 8c. Custom-designed primers for qRT-PCR, indicating order information and sequences

Sequences for the SYBR green-based primers for the house-keeping gene GAPDH and reference genes TBP, BCL-6 and MYC (Sigma) are shown in table 8c. Sequences were designed using the Ensembl Genome Browser and PrimerQuest (Integrated DNA Technologies). The criteria for primer design were for sequences to span at least 2 exons and contain no intronic sequence, PCR amplicon length 75-150bp, Primer length 19-25bp, percentage GC content 45-55%, melting temperature 60-65^{o}C. The specificity of primers was checked using the online PrimerBlast tool (NCBI). 100µM stock concentrations were made for all Sigma primers by reconstitution in sterile DNase/RNase free diH_2O (Gibco) and were stored at -20^{o}C. Before use in qRT-PCR experiments, primers were diluted into 2.5µM aliquots in RNase/DNase H_2O (Gibco). The quality of all primers was checked by analysis of their dissociation curves where the presence of one single peak indicated that primers did not form dimers and non-specific products had not been amplified.

Using the ABI SDS 2.3 system software, amplification plots and dissociation curves were constructed (SYBR selected as the reporter gene and ROX as the reporter dye) in order for Ct values to be calculated. The Ct value indicates the intersection between the amplification plot and the threshold line and represents the relative concentration of the target gene. The relative level of gene expression was calculated using the $2^{-\Delta\Delta Ct}$ method. Accordingly, the mean Ct value of the gene of interest (GOI) was normalised to the mean Ct value of the endogenous control gene GAPDH or for each sample to give a ΔCt value (Ct (GOI) – Ct (GAPDH) = ΔCt). The ΔCt values of the treated samples were then further normalised to the ΔCt values of the control samples such as the untreated DMSO sample (ΔCt treated sample – ΔCt control sample = ΔΔCt). As every Ct unit represents a 2-fold change (=log2), the ΔΔCt values were subsequently linearised to give the relative RNA expression / fold difference ($2^{-\Delta\Delta Ct}$ = relative RNA expression). Although not shown throughout this thesis, the human TATA-box binding protein (TBP) was also used as an additional control gene. Following these calculations, data was input into Microsoft Excel for graph interpretation.

2.5. Illumina gene expression microarray

Gene expression arrays for expression analysis are a powerful approach for comparing gene activity in biological samples. Providing genome-wide transcriptional coverage of well-established genes (including splice variants), arrays can be used for a wide range of

experimental purposes, such as to compare treated versus untreated cell culture experiments or to profile tissue samples.

Typically, RNA is isolated from samples, followed by conversion to fluorescently labelled cDNA via reverse transcription. The cDNA is subsequently hybridised to the array and any unhybridised cDNA is removed. The cDNA that has hybridised to the complementary DNA on the array is detected by the excitation of molecules in the fluorescent dye using a laser. Photons emitted from the array are measured by scanning a digital image of the dye which is then analysed to locate probes on the array and to record the intensity of their fluorescence.

To investigate changes in gene expression induced by CsA treatment, three cell lines (U2932, HLY-1 and WSU-NHL) were treated with their respective IC50 concentration for 2 timepoints (2 hours and 6 hours) in 4 independent biological repeat experiments. Following treatment, RNA was isolated from all 48 samples using the RNeasy Mini Kit (Qiagen), as described in section 2.4.2. Samples were then randomised and reassigned a numerical sample ID before being shipped to The Welcome Trust Centre for Human Genetics (Oxford Genomics Centre, UK) on dry ice.

Samples were subsequently hybridised to Illumina Human HT-12v4 Expression BeadChip arrays, which deliver high-throughput processing of 12 samples per BeadChip, therefore using a total of 4 BeadChips in this particular study. Arrays on the expression BeadChip target approximately 47,231 probes derived from the National Centre for Biotechnology Information Reference Sequence (NCBI) RefSeq Release 38 (November 7th, 2009) and other sources.

2.5.1. Data analysis

Paired and unpaired data analysis was analysed by Dr Simon Cockell (Bioinformatic Support Unit, University of Newcastle, UK), using R Software (version 3.1.2).

2.6. Gene Set Enrichment Analysis (GSEA)

GSEA is a useful analytical method for extracting meaning from genome-wide expression arrays, which often yield an extremely large amount of data. Classes of genes that are over-represented in the dataset (such as by being significantly enriched or depleted) are identified and compared to existing prior biological knowledge from previously published

gene sets. Gene sets, for example, may be groups of genes that share similar biological function, biochemical pathways or regulation. The ultimate aim of this powerful computational technique is to determine whether a set of genes show statistically significant differences between phenotypes, however this will be described in greater detail in the results section.

Parameter	**Settings used in study**
Number of permutations	1000
Phenotype labels	Vehicle_versus_treatment
Collapse dataset to gene values	True
Permutation type	Gene_set
Chip platform	Ilmn_HumanHT_12_V4_0_R1_15002873_B.chip
Enrichment statistic	Weighted
Metric for ranking genes	Log2_Ratio_of_Classes
Gene list sorting mode	Real
Gene list ordering mode	Descending
Max size: exclude large sets	500
Min size: exclude smaller sets	15
Collapsing mode for probe sets => 1 gene	Max_probe
Normalisation mode	Meandiv
Randomisation mode	No_balance
Omit features with no symbol match	True
Make detailed gene set report	True
Median for class metrics	False
Number of markers	100
Plot graphs for the top sets of each phenotype	50
Seed for mutation	Timestamp

Table 9. Parameters used for GSEA.

GSEA was performed using the Broad Institute of Harvard and MIT GSEA software (http://www.broadinstitute.org/gsea/index.jsp) and the Molecular Signatures Database

v5.0 (MSigDB) (Subramanian, Tamayo 2005), which was used to provide a collection of annotated gene sets. Data from the Illumina gene expression microarray was uploaded into the GSEA software to investigate expression profiles between CsA-treated and untreated samples using the parameters indicated in table 9.

2.7. Enzyme-Linked Immunosorbent Assay (ELISA)

An ELISA is a technique used to measure the concentration of an analyte or hormone in solution, relying on the basic principle of an interaction between an antigen and an antibody with a complimentary binding site. Samples are first immobilised onto a solid surface (such as a 96-well plate) either directly by adsorption or indirectly using a capture antibody already bound to the plate. Addition of a specific detection antibody forms an analyte-antibody complex, where the antibody may be covalently linked to an enzyme, or detected itself by a secondary antibody linked to an enzyme. Between binding steps, the plates are washed with a detergent to remove non-specific binding. Following the final wash, an enzymatic substrate solution is added to produce a detectable signal, commonly a change in colour. The end product colour is relative to the amount of analyte being investigated and can be measured using spectrophotometry.

2.7.1 TransAM® DNA-binding ELISA

The TransAM® NFAT2 (Active Motif, catalogue number 40296) and TransAM® NF-κB family assays (Active Motif, catalogue number 43296) are ELISA-based kits specifically designed to quantify NFAT2 and NF-κB subunit transcriptional activity.

The TransAM® kit contained 96-well plates to which a specific double-stranded oligonucleotide containing the NFAT2 consensus binding site (5'-AGGAAA-3') or NF-κB consensus binding site (5'-GGGACTTTCC-3') had been immobilised. NFAT2 or NF-κB contained in nuclear extracts bound specifically to the oligonucleotide, which was detected upon DNA binding by an antibody directed against an accessible epitope on the NFAT2, p65, p50, p52, c-Rel or RelB protein that is accessible only when NFAT or NF-κB are active and bound to their DNA target. Addition of a secondary antibody (conjugated to horseradish peroxidase) produced colourimetric readouts which were quantified by spectrophotometry. Inclusion of competitive binding experiments allowed the specificity of the assay to be monitored. The wild-type consensus oligonucleotide should prevent NFAT2 or NF-κB from binding to the immobilised probe by acting as a

competitor for their binding, whereas the mutated oligonucleotide should have no effect on NFAT2 or NF-κB binding.

For experiments measuring the relative NFAT2 transcription factor activation in a panel of cell lines, cells were collected one day after being split and nuclear extracts were prepared, as described in section 2.2.2. For experiments measuring the effect of a chemical inhibitor on NFAT2 binding activity, treated and untreated DLBCL cells were incubated at 37ºC, 5% CO_2 for the specified duration before being harvested and nuclear extracts prepared. The experimental procedure for the NFAT2 ELISA was followed according to the TransAM protocol in the Active Motif manual. Samples were assayed in duplicate at a concentration of 5µg per well, including the PHA-treated Jurkat nuclear extract (provided by kit). Samples were incubated in developing solution for 12 minutes before addition of stop solution, as advised for the particular kit lot number. The experimental procedure for the NF-κB ELISA was also followed according to the TransAM protocol in the Active Motif manual. Samples were assayed in duplicate at a concentration of 4µg per well, including the Raji nuclear extract (provided by kit). Samples were incubated in developing solution for 5 minutes before addition of stop solution, as advised for the particular kit lot number. Absorbance for both assays was recorded using the FLUOstar Omega plate reader (BMG Labtech) at 450nm with a reference wavelength of 655nm. Data was analysed using GraphPad Prism 6 software.

2.7.2. Quantikine® TNFα Colourimetric Sandwich ELISA

The human TNF-alpha (TNFα) Quantikine® HS ELISA SixPak kit (R&D Systems, catalogue number STA00C) was used to measure human TNFα in cell culture supernatants. Employing a sandwich enzyme immunoassay technique, Quantikine® solid-phase ELISA plates contained pre-coated monoclonal antibody specific for human TNFα. *E.coli*-derived recombinant human TNFα standards and samples were pipetted into wells and any TNFα present was immobilised by the antibody. Following a series of wash steps to remove unbound substances, an enzyme-linked polyclonal antibody specific for human TNFα was added to wells, followed by addition of a substrate solution to initiate colour development in proportion to the amount of TNFα. The measurement of TNFα in the kit detected the total amount of TNFα in samples (the total amount of free TNFα plus the amount of TNFα bound to soluble receptors).

For experiments measuring the relative mass values of human TNFα produced in a cell line panel, cells were split as normal and cultured for 2 days without addition of fresh medium. This incubation period enabled sufficient time for cells to produce TNFα adequate for detection within the linear range of standards used in the ELISA. Following incubation, samples were centrifuged (5mins, 300g) and the supernatant transferred into fresh eppendorf tubes. Samples were stored on ice temporarily before addition to the TNFα ELISA 96-well plate accordingly.

For experiments measuring the effect of a chemical inhibitor on TNFα production, DLBCL cells were counted and washed in 1ml PBS before 2mls of cells (per sample) were seeded into 6-well plates at a density of $1x10^6$/ml. The PBS wash was included to sufficiently remove the cell culture medium in which TNFα may have built-up as a result of normal TNFα production. In turn, cells were treated with the appropriate concentrations of small molecule inhibitors and an untreated DMSO control sample was included into each experiment. Cells were incubated for 2 hours before centrifugation (5mins, 300g) and the supernatant transferred into fresh eppendorf tubes. Samples were stored on ice temporarily before addition to the TNFα ELISA 96-well plate accordingly. The assay procedure for the Quantikine TNFα ELISA was followed according to the manufacturer's protocol. Optimal density readings were taken using the FLUOstar Omega plate reader (BMG Labtech) at 450nm and wavelength correction set at 570nm. The concentration of TNFα produced by samples was calculated based on a standard curve produced by TNFα Standards. Data was analysed using GraphPad Prism 6 software.

For the TNFα ELISA experiment shown in chapter 6, figure 65c, a new Quantikine kit (R&D Systems, catalogue number DTA00C) was purchased. The assay procedure was followed according to the manufacturer's protocol, however some reagents differed and the protocol in this kit had been updated. This kit did not contain an amplifier solution step and washes were reduced from six to four repetitions.

2.8. NF-κB luciferase reporter assay

Luciferase reporter assays are a useful tool for measuring gene expression and cellular events associated with gene expression. A typical reporter assay involves cloning the regulatory region of the gene of interest upstream of the firefly luciferase gene in an expression vector. The vector is then transfected into the DNA of cells (such as U2OS cells); followed by an incubation period where cells are selected to ensure the whole cell

line population expresses the vector. Following an experimental procedure/treatment, cells are lysed and luciferase is added, initiating the following reaction process;

$$\text{Luciferin} + O_2 + \text{ATP} \xrightarrow[\text{Luciferase}]{} \text{Oxyluciferin} + CO_2 + \text{AMP} + \text{PPi} + \text{Light}$$

The Luciferase enzyme is expressed under the control of the promoter of interest and is therefore directly proportional to the transcriptional activity of the gene being studied, such as NF-κB. Enzymatic activity is subsequently measured in the form of light emission using a luminometer.

The U2OS cell reporter system was generated previously in Sonia Rocha's laboratory (Dundee) by using a pGL4.32 [luc2P/NF-κB-RE/Hygro] vector (Promega, catalogue number E849A) containing five copies of an NF-κB response element, which drives transcription of the luciferase reporter gene *luc2P (Photinus pyralis)*. To allow selection, the vector contains a mammalian selectable marker for hygromycin resistance. Cells were cultured for 2-3 months in selection media to ensure formation of stable cell lines expressing the NF-κB response element.

For experiments confirming the function of the TNFα neutralising antibody Infliximab and the TNFα antagonist Etanercept, U2OS cells were split 1 day before the assay procedure to a confluency of 70-80% and were seeded into 6-well plates. The next day, media from U2OS cells was replaced with fresh media and cells were treated with 10ng/ml human TNFα (to positive control wells), followed by immediate addition of 10µg/ml Etanercept or Infliximab to wells accordingly. Following 2 hours incubation (37ºC, 5% CO_2), media from U2OS cells was aspirated and cells washed with ice cold PBS. Cells were subsequently lysed using 200µl 1x lysis buffer (Promega) and lysates collected. Samples were then transferred into eppendorfs and stored overnight at -80ºC to achieve optimal lysis. The following day, samples were thawed, vortexed and centrifuged at maximum speed for 1 minute. 20µl supernatant was then assayed using the Luciferase Assay System (Promega) in a Lumat LB9507 Luminometer (Bethold Technologies). Due to the short half-life of the luciferase reagent, 100µl luciferase reagent (Promega) was added to tubes one at a time, immediately before each sample reading. Relative light units were recorded and results were normalized to the respective protein concentrations of samples (quantified by the Bradford assay), as described in section 2.2.3.1.

For experiments investigating TNFα production and the effects of TNFα production by DLBCL cells on NF-κB transcriptional activity, DLBCL cells were incubated (37ºC, 5% CO_2) for 2 days (following splitting as normal) before the assay procedure commenced. This period of growth enabled sufficient time for the production of TNFα by DLBCL cells and secretion into the surrounding media. U2OS cells were split 1 day before the assay procedure to a confluency of 70-80% and were seeded into 6-well plates. On the day of the assay, DLBCL cells were centrifuged (5mins, 300g) and the supernatant (containing TNFα media) decanted into fresh tubes. Media from U2OS cells was removed by aspiration and replaced with 2mls of DLBCL cell media or 2mls RPMI 1640, 10% FCS for untreated control wells. U2OS cells were treated accordingly with Etanercept and Infliximab to a concentration of 10µg/ml, followed by immediate addition of 10ng/ml human TNFα to appropriate positive control wells. Cells were incubated for either 2 or 6 hours (37ºC, 5% CO_2) before the remainder of the assay performed as described previously.

2.9. Statistical analysis

Paired and unpaired statistical analysis for the gene expression microarray was performed by Dr Simon Cockell (Bioinformatic Support Unit, Newcastle University, UK). For other all other data analysis, P-values were calculated for respective experiments using the Minitab 16 statistical software using paired t-test analysis.

Chapter 3.

Investigation of NFAT expression, activation and dependency in DLBCL cell lines

3. Investigation of NFAT expression, activation and dependency in DLBCL cell lines

3.1.Introduction

One of the initial aims of this study was to confirm the findings of other groups reporting constitutive expression and activation of NFAT family members in DLBCL. Constitutively active nuclear NFAT2 had previously been reported in 30% of DLBCL patient samples and in a small selection of DLBCL cell lines (Marafioti *et al.*, 2005; Pham *et al.*, 2005; Fu *et al.*, 2006; Pham *et al.*, 2010). Although these reports demonstrated clear correlations between DLBCL and NFAT expression, they were not fully comprehensive. Due to a lack of effective antibodies for immunohistochemistry, Marafioti et al (2005) were only able to detect NFAT2 in patient samples, however the expression of other isoforms such as NFAT1 were not recorded (Marafioti *et al.*, 2005). Additionally, studies illustrating a role for NFAT-mediated regulation of lymphocyte survival factors in DLBCL were mostly restricted to cell lines established in-house and were not commercially available (Pham *et al.*, 2005; Fu *et al.*, 2006; Pham *et al.*, 2010). Therefore, although the scientific evidence for a role of NFAT in DLBCL was clear, the relative expression of individual NFAT family members in a comprehensive panel of representative ABC and GCB DLBCL cell lines had not been explored.

In addition, although it is well known that NFAT activation is a result of events preceding engagement of the BCR, the distinct nature of NFAT regulation in DLBCL has not been investigated. Signalling pathways downstream of the BCR represent promising treatment targets for the treatment of DLBCL and other B-cell malignancies, some of which have been studied in great detail (Kuppers, 2005; Gupta *et al.*, 2007; Chen *et al.*, 2008). As described previously, ABC DLBCLs exhibit constitutive activation of NF-κB and NF-κB pathway components (Davis *et al.*, 2001; Rosenwald *et al.*, 2002; Compagno *et al.*, 2009). DLBCLs in this subgroup also harbour increased BCR surface expression and frequent somatic mutations of components of the BCR itself, including the Igα or Igβ subunits (Davis *et al.*, 2001; Davis *et al.*, 2010). The BCR is critical for the survival of ABC DLBCLs, which are described as having ‘chronic active’ BCR signalling, whereby the BCR and downstream pathways (such as NF-κB) are constitutively activated (Davis *et al.*, 2001; Davis *et al.*, 2010). Whether NFAT signalling is also a pathway upregulated as a result of increased BCR expression currently remains unexplored and was a question I aimed to address in this study.

GCB DLBCL, on the other hand, are known to utilise their BCR more akin to normal B cells, which rely on low level antigen dependent 'tonic' BCR-dependent survival signals (Kraus *et al.*, 2004; Monroe, 2004; Srinivasan *et al.*, 2009). BCR ablation in murine models has been shown to cause apoptosis of normal mature B cells (Lam *et al.*, 1997; Kraus *et al.*, 2004). Interestingly, when the PI3K/AKT signalling cascade was activated, the survival of BCR-deficient B cells was rescued, although this was not apparent for activation of the NF-κB or MAPK pathways (Srinivasan *et al.*, 2009). These studies suggest that there are dissimilarities between tonic BCR survival signals and signals propagated from pathways downstream of the BCR, such as NF-κB (Chen *et al.*, 2013). Moreover, in consensus clustering methods to define DLBCL transcriptional profiles, Shipp et al (2013) defined two GCB DLBCL tumour groups which were defined as 'BCR' or 'non BCR' (Chen *et al.*, 2008; Chen *et al.*, 2013). Unlike non-BCR DLBCLs, BCR DLBCL had increased expression of multiple components of the BCR, such as high expression of SYK and were responsive to blockade of SYK in BCR-dependent DLBCLs (Chen *et al.*, 2008; Friedberg *et al.*, 2010).

Analysis of DLBCL expression and dependency on the NFAT signalling axis may define NFAT as an additional, targetable pathway in GCB DLBCL, but could also reveal interesting insights into the upstream regulation of NFAT. Hypothetically, NFAT expression would likely be highest in ABC cell lines with chronic active BCR signalling and GCB BCR cell lines with increased expression of BCR components. Alternatively, NFAT expression and activation in GCB non-BCR cell lines is suggestive of BCR-independent activation of NFAT, which could be an interesting avenue to explore.

Although targeting BCR signalling pathways is a rational therapeutic approach for treatment of DLBCL, the subtype-specific pathways and their core genetic mechanisms are not fully understood. Identification of a potential role for NFAT in a particular subgroup of DLBCL would enhance our knowledge of the molecular mechanisms of this aggressive disease while allowing opportunity for future therapies to be more targeted.

Lastly, based on expression, activation and chemical sensitivity data, one of the key goals of this chapter was to strategically select a small number of DLBCL cell lines for use in gene expression array analysis. In brief, the purpose of the microarray was to investigate potential NFAT target genes by comparing differentially expressed genes upon treatment with/without a suitable inhibitor of NFAT. It was therefore necessary that model cell lines

expressed detectable levels of active NFAT and were shown to respond to inhibition of the NFAT pathway.

3.2.Results

3.2.1. NFAT transcription factors are heterogeneously expressed in DLBCL cell lines

To gain a general understanding of the expression and activation of NFAT family members in DLBCL and to help determine appropriate cell lines models for future experiments, NFAT isoforms and their respective activation status were analysed by Western blot in a comprehensive panel of ABC and GCB DLBCL cell lines with defined BCR status. The total expression of individual NFAT family members from samples prepared as whole cell extracts was heterogeneous across the panel (figure 15), where some cell lines had markedly high or low expression of specific isoforms. Due to the multiple serine residues on NFAT that can be phosphorylated or dephosphorylated, detection of active NFAT is best analysed by SDS-PAGE, where phosphorylated NFAT proteins are slower migrating and dephosphorylated NFAT proteins are faster migrating. For NFAT1, these principally represent differentially phosphorylated species, for example the lower band in the Toledo cell line indicates that NFAT1 is in the dephosphorylated, active form. However, in some cell lines however (such as HLY-1 and U2932) both the inactive and active forms of NFAT1 were expressed at high levels, indicating that only a certain degree of NFAT1 activation is important in these cell lines. OCI-Ly19 did not appear to express either the hyperphosphorylated or dephosphorylated form of NFAT1, suggesting this isoform is of little functional importance in this cell line.

For NFAT2, the three broad groupings of bands seen represent different protein products, resulting from alternative mRNA splicing, while the closely spaced bands within each cluster represent different phospho-isoforms. Given the predicted sizes of the A, B and C isoforms of NFAT2, the lower band represents the NFAT2/A α and β isoforms, the middle band the NFAT2/B α and β variants, while the upper band represents the NFAT2/C α and β isoforms (www.ensembl.org, NFAT2). HLY-1 cells, for example showed striking expression of all splice products, whereas SUDHL-4 lacked expression of the upper and lower proteins (NFAT2/C α and β and NFAT2/Aα and β). NFAT2 expression across the panel of cells was highly variable; with some cell lines (particularly those in the GCB non-BCR subgroup) expressing little to no NFAT2. NFAT4 was also differentially

expressed between cell lines, however the identity of the two NFAT4 species observed is not known.

Although the NFAT1, NFAT2 and NFAT4 family members are known to be the three main isoforms expressed in lymphocytes, the expression of the NFAT3 isoform was also analysed (Rudolf *et al.*, 2014) (figure 15). Unexpectedly, all DLBCL cell lines expressed moderate levels of NFAT3 with the upper band representing the hyperphosphorylated form and the lower band being in its dephosphorylated, active form (www.ensembl.org, NFAT3). NFAT3 was activated in a small number of cell lines including RIVA, U2932, SUDHL-4, SUDHL-6, OCI-Ly18 and Toledo.

The expression of NFAT isoforms generally did not correlate with any particular subgroup of DLBCL. This was especially apparent for NFAT1, NFAT3 and NFAT4; however the expression of NFAT2 in the GCB non-BCR group was noticeably lower than the ABC and GCB-BCR subgroups. Pfeiffer and Toledo appeared to express NFAT2 at very low levels while expression was non-existent in OCI-Ly19 and Toledo cell lines.

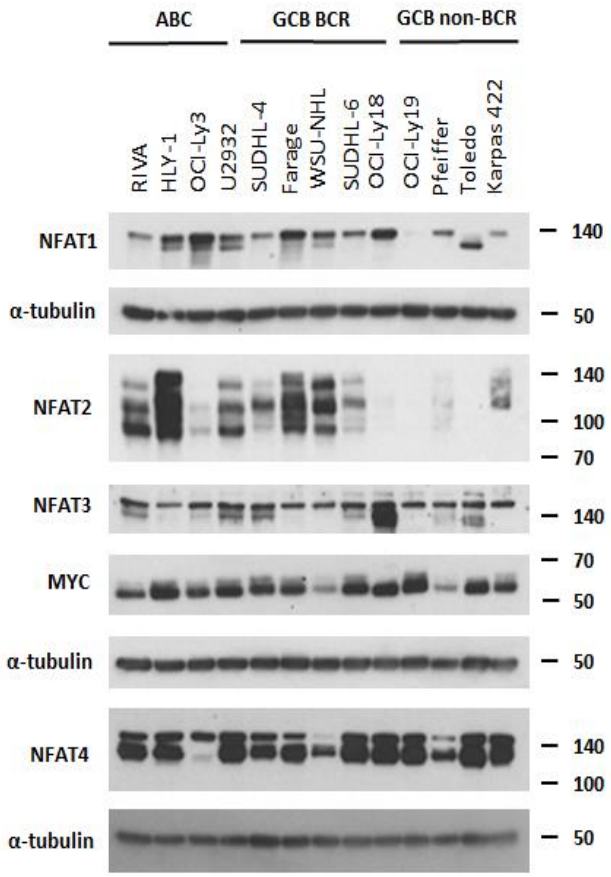

Figure 15. NFAT transcription factors are heterogeneously expressed in DLBCL cell lines. Whole cell extracts were taken from a panel of ABC and GCB DLBCL cell lines and the expression of NFAT family members analysed by Western blot. Cell lines are categorised into their respective DLBCL subgroups where ABC = activated B-cell, GCB = germinal centre B-cell, BCR = B cell receptor. Molecular weight marker lines to the right of the Western blot indicate the approximate size of detected bands (KDa). α-tubulin was included as a loading control. Data is representative of three biological repeat experiments apart from NFAT3, NFAT4 and MYC which were analysed in two repeat experiments.

Deregulated MYC expression due to MYC translocations, amplifications or mutations is a negative prognostic indicator in DLBCL (Klapper *et al.*, 2008). Moreover, the c-Myc oncoprotein was recently reported to be an NFAT target gene in DLBCL cell lines, with its expression correlating with the nuclear levels of NFAT2 (Pham *et al.*, 2010). Interestingly, c-Myc is known to regulate the NFAT pathway in B-lymphocytes by amplifying calcium signalling, therefore maintaining NFAT nuclear translocation (Habib *et al.*, 2007). c-Myc and NFAT are therefore proposed to function in DLBCL by providing a positive regulatory feedback loop where NFAT2 and c-Myc reinforce each other's expression, including the expression of their respective target genes (Pham *et al.*, 2010). To assess whether this mutual regulatory relationship was reflected in my DLBCL cell lines, the relative expression of c-Myc protein was evaluated. c-Myc expression was

heterogeneous between cell lines but did not correlate with the expression of NFAT2 or with any other NFAT isoform (figure 15).

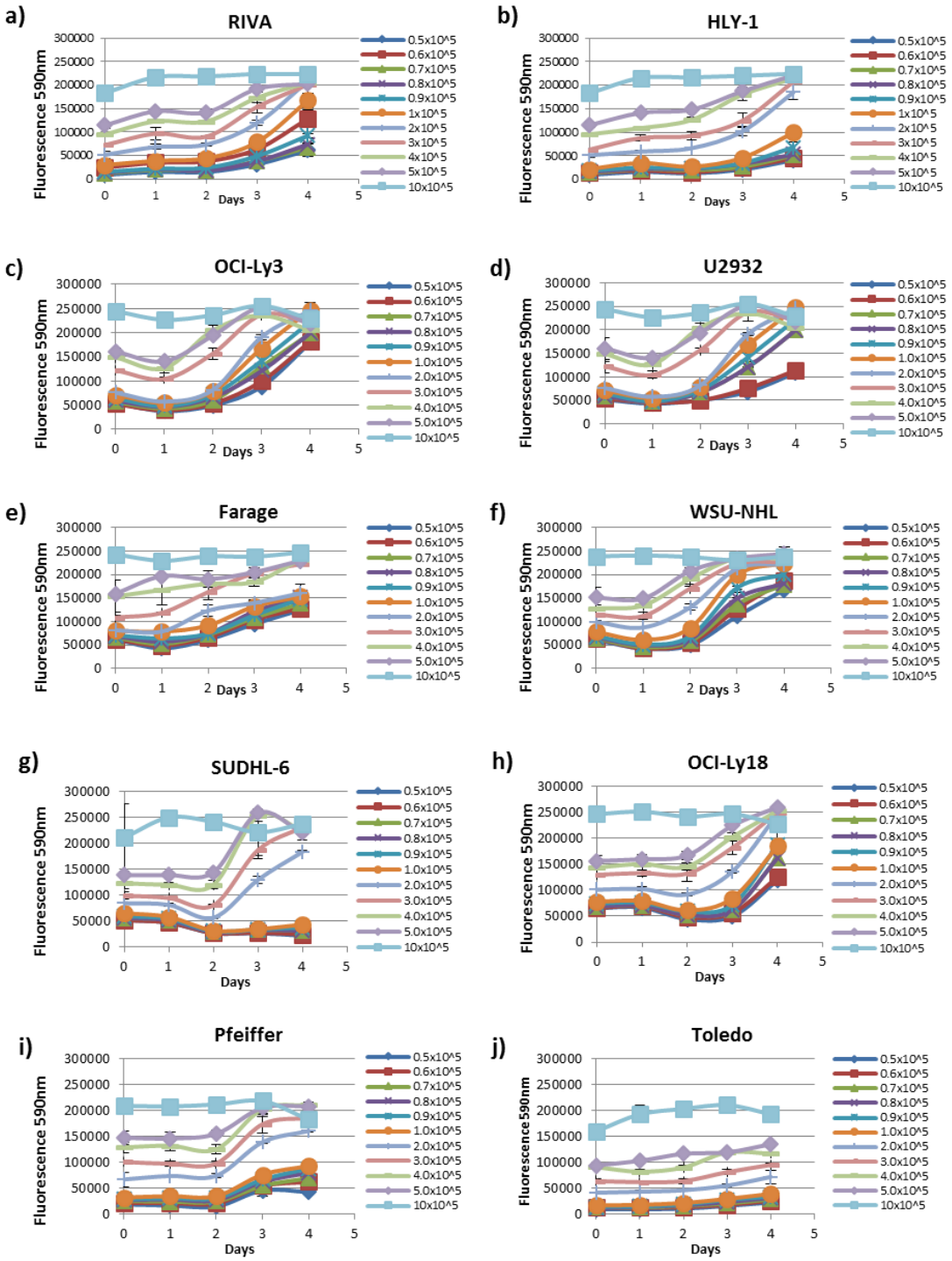

k)

DLBCL subtype	Cell line	Optimal cell seeding density for resazurin assay experiments
ABC	RIVA	3×10^5/ml
ABC	HLY-1	3×10^5/ml
ABC	U2932	2×10^5/ml
ABC	OCI-Ly3	2×10^5/ml
GCB BCR	SUDHL-4	2×10^5/ml
GCB BCR	Farage	3×10^5/ml
GCB BCR	WSU-NHL	2×10^5/ml
GCB BCR	SUDHL-6	3×10^5/ml
GCB BCR	OCI-Ly18	2×10^5/ml
GCB non-BCR	OCI-Ly19	3×10^5/ml
GCB non-BCR	Pfeiffer	2×10^5/ml
GCB non-BCR	Toledo	3×10^5/ml
GCB non-BCR	Karpas-422	3×10^5/ml

Figure 16 (Continued from previous page). Growth curves for DLBCL cell lines. a-j) To find the optimal cell seeding density of cells for resazurin proliferation assays, the growth of DLBCL cell lines was analysed over 4 days and recorded using the resazurin assay. Cells were seeded out at a range of densities ($0.05x10^6$/ml to $1x10^6$/ml) and incubated for 24, 48, 72 or 96 hours before viable cells were quantified. k) Table showing the optimal cell seeding densities chosen for resazurin proliferation assays. Data is representative of one experiment. Error bars indicate standard deviation between triplicate wells of cells.

3.2.2. Growth curves for DLBCL cell lines

To analyse the growth of cell lines in subsequent resazurin proliferation assays, it was essential that optimal seeding densities were obtained, to take account of the growth behaviour of individual cell lines. The growth of cells plated out at a range of seeding densities was analysed over a period of 24, 48, 72 and 96 hours before data analysed in the form of growth curves (figure 16). The shape of the growth curves for some cell lines indicated their particularly slow growth rates, such as Toledo (figure 16j), whereas most other cell lines began multiplying after 2 days (48 hours) of culture. Keeping in mind that future experiments aimed to use the resazurin assay to investigate the effects of chemical inhibitors on cell viability over a 72 hour period of incubation, the growth of cells at this timepoint were carefully considered. To accurately capture the physiological effects of inhibitors at this timepoint it is important that cells are growing in their exponential phase. For most cell lines, a seeding density less than $0.9\text{-}1x10^5$/ml did not allow cells to form an exponential growth curve over 96 hours, with some cells unable to multiply at all in these conditions. On the other hand, seeding densities above $3x10^5$/ml were generally too high for most cell lines, where cells reached their stationary and death phases of growth

at early stages of incubation. The table in figure 16k indicates the seeding densities chosen for subsequent resazurin assay experiments, based on their exponential growth at 72 hours incubation. Optimal seeding densities were considerably similar between cell lines, indicating similar growth behaviours between these DLBCL cells.

3.2.3. DLBCL cell lines have heterogeneous expression and activation of NFAT family members

To further investigate the expression and activation of NFAT family members in DLBCL cell lines, Western blot analysis of nuclear protein extracts (figure 17a) allowed a comparative analysis of subcellular location and hence activation status of NFAT between cell lines. Most cell lines expressed moderate to high levels of nuclear NFAT and expression typically reflected whole cell extract expression (figure 15). For example, (as indicated previously) Toledo cells demonstrated striking expression of active NFAT1 compared to OCI-Ly19, while HLY-1 cells were the highest expressers of NFAT2. The Western blot in figure 17b shows that nuclear samples in figure 17a were absent of cytoplasmic contamination, as demonstrated by detection of α-tubulin.

Interestingly, in U2932 cells, the expression of the lower molecular weight band in NFAT1 in nuclear extract is considerably lower than the whole cell lysate. An explanation for this may be due to the fact that two stable tumour clones have been identified in this cell line. This was identified by Quentmeier et al (2013), whereby they found that one subclone overexpressed genes such as *BCL6*, whereas the other subclone overexpressed *MYC* (Quentmeier *et al.,* 2013). In fact, microarray analysis showed that around 200 genes were differentially expressed between the clones, including transcriptional targets of the aberrantly expressed oncogenes (Quentmeier *et al.,* 2013). The variability between experiments discussed above may therefore be due to differences in the ratios of these two U2932 clones.

Although cells lines of the GCB non-BCR subgroup appeared to express very little NFAT in whole cell extracts (figure 15), expression is visibly higher in nuclear extracts, perhaps due to the preparation of concentrated/enriched NFAT2 in nuclear samples. However, overall there is no distinctive correlation between ABC and GCB subgroups, indicating that NFAT may be of importance in all subtypes of DLBCL.

To further compare NFAT activity in DLBCL cell lines, the DNA-binding activity of NFAT2 was analysed using an ELISA assay (figure 17c). Despite differential activity of

NFAT1 in figure 17a, only NFAT2 was assayed for activity because TransAM assay kits were not available for the other NFATs. The nuclear samples used in figure 17a were run alongside a PHA-stimulated Jurkat positive control extract and to monitor assay specificity, a mutated (MT) consensus oligonucleotide and wild-type (WT) consensus oligonucleotide were included as competitors for NFAT2 DNA-binding. The Jurkat control performed as expected, showing a high level of NFAT2 activity. Also as expected, the MT oligo had little effect on NFAT2 activity, whereas the WT oligo effectively competed with NFAT2 for binding. A clear trend was observed between NFAT2 DNA binding activity and protein expression, demonstrating consistency between two different experimental techniques. The NFAT2 ELISA, for example, highlighted the elevated activity of NFAT2 in cell lines such as HLY-1 and WSU-NHL but was also sensitive enough to measure low levels of NFAT2 activity in cell lines with very little protein expression, such as OCI-Ly3, OCI-Ly18 and Toledo.

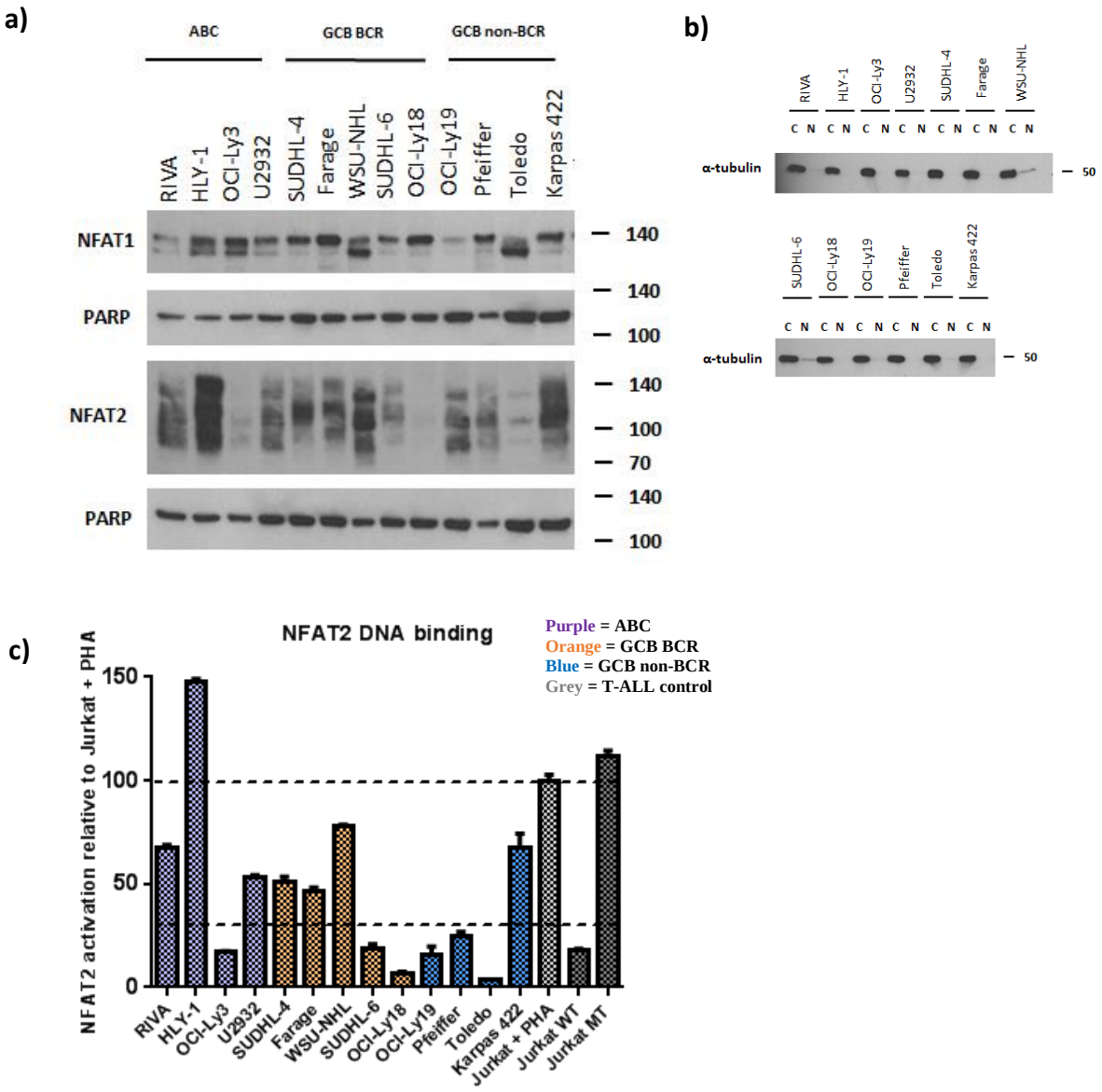

Figure 17. DLBCL cell lines have heterogeneous expression and activation of NFAT family members and are sensitive to chemical inhibition of the calcineurin-NFAT pathway by CsA a) nuclear extracts were taken from a panel of ABC and GCB DLBCL cell lines and the expression of NFAT family members analysed by Western blot. Nuclear-cytoplasmic preparations illustrate the comparative subcellular localisation and activation of family members. Cell lines are categorised into their respective DLBCL subgroups where ABC = activated B-cell, GCB = germinal centre B-cell, BCR = B cell receptor. PARP was included as a nuclear loading control. b) To check for cytoplasmic contamination in nuclear extracts, samples in (a) were probed for the cytoplasmic loading control α-tubulin. Molecular weight marker lines to the right of Western blots indicate the approximate location of antibody binding, therefore confirming antibody specificity for proteins of a particular size (KDa). Data is representative of two individual experiments apart from NFAT2 expression in GCB non-BCR extracts which was performed in a single experiment. c) The DNA binding activity of NFAT2 was analysed by ELISA using nuclear extract samples in (a). PHA-treated Jurkat nuclear extracts were included as a positive control for NFAT2 activation. To monitor the specificity of the assay, samples were run alongside a mutated (MT) consensus oligonucleotide and a wild-type (WT) consensus oligonucleotide (as a competitor for NFAT2 binding). ELISA data is representative of two biological experiments apart from the panel of GCB non-BCR cell lines which were run in a single experiment. Error bars indicate the standard deviation of duplicate wells.

3.2.4. DLBCL cell lines sensitive to chemical inhibition of the calcineurin-NFAT pathway by CsA

After confirming the expression, activation and DNA-binding of NFAT in most DLBCL cell lines, their relative dependency on the calcineurin-NFAT pathway for survival was assessed using the chemical inhibitor CsA. DLBCL cell lines were treated with a range of concentrations of CsA (0µg/ml-30µg/ml) for 72 hours before cell viability was determined using the resazurin assay. Figure 18 shows the growth inhibitory effects of CsA in a panel of cell lines, where a dose-dependent reduction in cell viability was observed. Differences between the shapes of the kill curves indicate how individual cell lines responded to the inhibitory effects of CsA. In most cell lines the curve is sigmoidal, where lower doses had little effect on cell viability but higher doses caused the viability to reduce to zero. In RIVA cells however (figure 18a), higher doses did not entirely kill cells. In other cell lines the response to CsA was marginal at low concentrations, cells remaining viable until a specific dose of CsA which drastically initiated cell death, as shown in Farage, Toledo and Karpas 422 cells (figure 18f, l and m).

Figure 19 shows the average IC50 values obtained from cell lines treated with a range of concentrations of CsA (0µg/ml-30µg/ml) for 72 hours. An IC50 value is the half maximal inhibitory concentration, indicating the concentration needed to inhibit a biological or chemical function by half, which in this study is cell viability. The viability of all cell lines was reduced in a dose-dependent manner (figure 18), indicating the requirement of the calcineurin-NFAT pathway for lymphoma cell survival. However, there was no apparent relationship between IC50 concentrations and particular DLBCL subgroups or BCR status. IC50 values varied between cell lines and when compared to NFAT protein expression and DNA binding assays, there was no correlation with inhibitor sensitivity. Cell line IC50 values are also shown in table 10, where cell line-specific CsA sensitivity is also classified according to respective IC50 values, where high sensitivity = <8µg/ml, medium sensitivity = 8µg/ml-13µg/ml and low sensitivity = >13µg/ml.

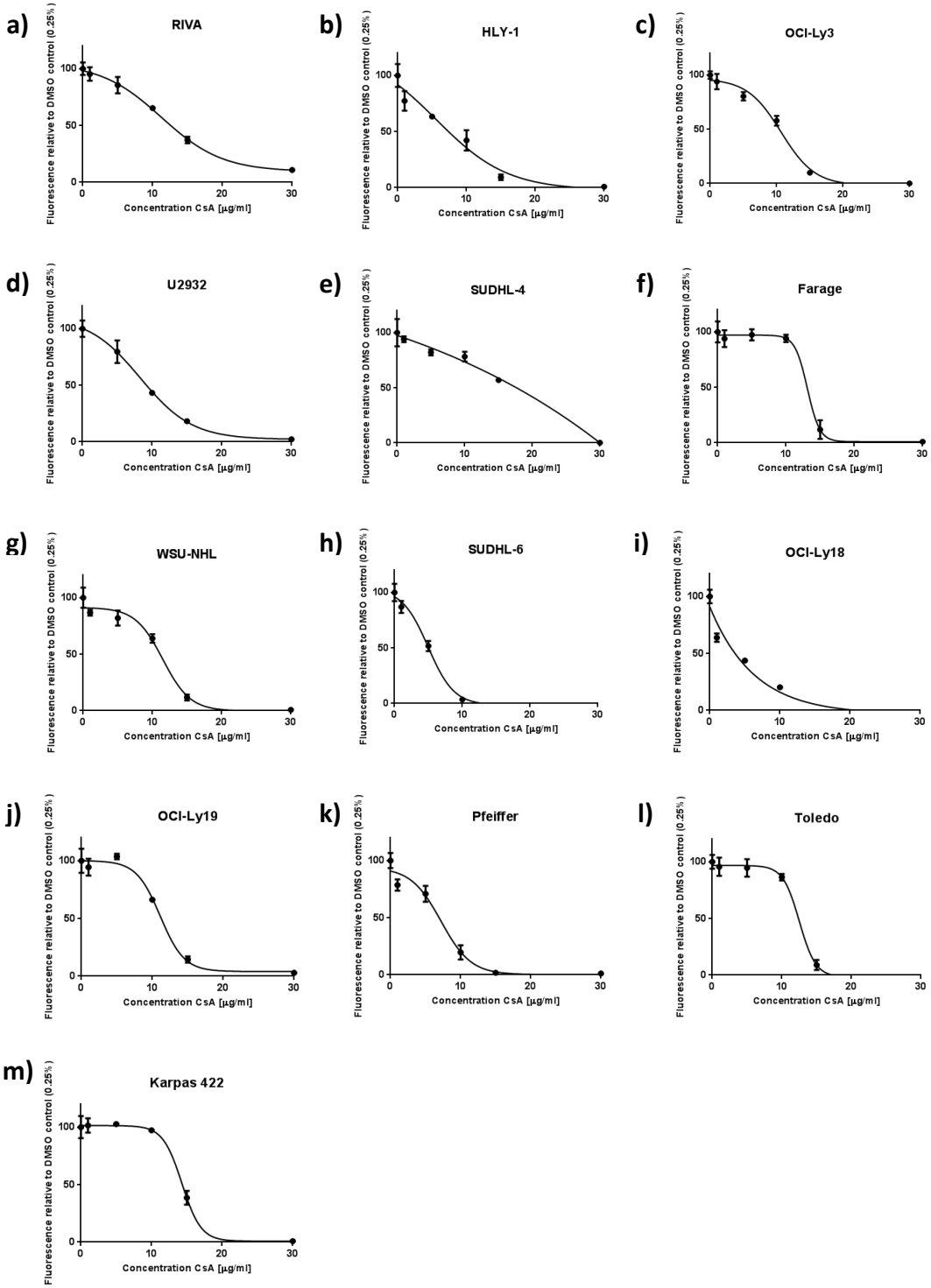

Figure 18. CsA causes a dose-dependent reduction in cell viability in DLBCL cell lines. A panel of ABC (a-d), GCB BCR (e-i) and GCB non-BCR (j-m) DLBCL cell lines were treated with a range of concentrations of CsA (0µg/ml-30µg/ml), including a vehicle control (0.25% DMSO). Cells were incubated for 72 hours before cell viability was recorded using the resazurin assay. Data is representative of one experiment from three biological repeat experiments where error bars indicate the standard deviation of triplicate wells.

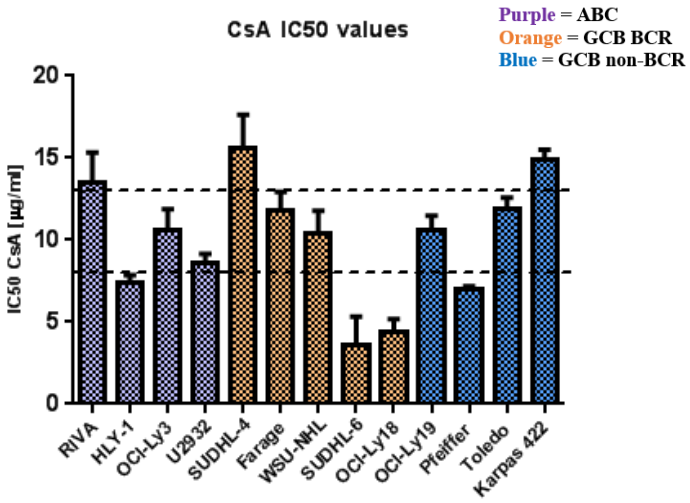

Figure 19. DLBCL cell lines sensitive to chemical inhibition of the calcineurin-NFAT pathway by CsA The panel of DLBCL cell lines were treated with a range of concentrations of CsA (0µg/ml-30µg/ml, including a vehicle control (0.25% DMSO) and were incubated for 72 hours before viable cells were measured using the resazurin assay. Dose-response curves were plotted for each cell line and the IC50 concentration recorded. The average IC50 concentration across three independent experiments was determined and plotted. Data is representative of three biological repeat experiments, error bars indicate the standard error of the mean.

Table 10 summarises NFAT2 activity based on ELISA data (figure 17c) and corresponding Western blots (figure 17a), where high activity = NFAT2 activation >100%, medium activity = 30-100% and low activity = <30% of the Jurkat + PHA positive control. The classification of NFAT1 activation is based on the presence of the lower band in figure 17a, which indicates the dephosphorylated active form of NFAT1.

Cell line	DLBCL subgroup	NFAT2 activity	NFAT1 activity	CsA sensitivity	CsA IC50 [µg/ml]
RIVA	ABC	Medium	-	Low	13.5
HLY-1	ABC	High	+	High	7.4
OCI-Ly3	ABC	Low	+	Medium	10.6
U2932	ABC	Medium	-	Medium	8.6
SUDHL-4	GCB BCR	Medium	-	Low	15.6
Farage	GCB BCR	Medium	-	Medium	11.8
WSU-NHL	GCB BCR	Medium	+	Medium	10.4
SUDHL-6	GCB BCR	Low	-	High	3.6
OCI-Ly18	GCB BCR	Low	-	High	4.4
OCI-Ly19	GCB non-BCR	Low	-	Medium	10.6
Pfeiffer	GCB non-BCR	Low	-	High	7.0
Toledo	GCB non-BCR	Low	+	Medium	11.9
Karpas 422	GCB non-BCR	Medium	-	Low	14.9

Table 10. Summary of NFAT expression, activation and sensitivity to CsA. Table classifying DLBCL cell lines into categories of NFAT1 and NFAT2 activity, including sensitivity to CsA. The degree of NFAT2 activity is based on ELISA data and corresponding Western blots, where high activity = NFAT2 activation >100%, medium activity = 30-100% and low activity = <30% of Jurkat + PHA positive control. The degree of NFAT1 activation is based on the presence of the lower band, which indicates the dephosphorylated active form of NFAT1. CsA sensitivity is classified according to respective IC50 values, where high sensitivity = <8µg/ml, medium sensitivity = 8µg/ml-13µg/ml and low sensitivity = >13µg/ml.

3.2.5. Cyclosporin A (CsA) inhibits nuclear translocation and activation of NFAT2

NFAT activation has been shown to be calcineurin-dependent in cell lines derived from DLBCL and T-ALL, where treatment with CsA or FK506 suppressed NFAT activation (Pham *et al.*, 2005; Medyouf *et al.*, 2007). Confirmation of CsA-induced NFAT inhibition can be demonstrated effectively by determining its effect on the subcellular localisation and phosphorylation status of NFAT. The ABC DLBCL cell lines U2932 and HLY-1 and the GCB cell line WSU-NHL were chosen for analysis due to previous data confirming their medium-high sensitivity to CsA treatment and their medium-high expression of NFAT family members when compared to other DLBCL cell lines. Of note, these three cell lines were used for many subsequent experiments, including the gene expression microarray, as described in chapter 5.

Cells were treated with CsA using their respective IC50 concentrations for 2 and 6 hours before nuclear-cytoplasmic extracts were made and Western blot analysis performed. Timepoints were selected based on previous experiments performed by past-members of the Bacon laboratory. As shown in figure 20, in the DMSO controls, NFAT1 and NFAT2 were at higher levels in the nucleus compared to the cytoplasm and detection of the lower band in these samples indicates they were in their dephosphorylated (activated) state. When treated with CsA, a shift from the nucleus to the cytoplasm is observed, occurring in a time-dependent manner. CsA also caused an increase in the intensity of upper bands within each cluster and a slight decrease in the dephosphorylated splice variants which is indicative of the rephosphorylation of the remaining NFAT proteins in the nucleus.

To confirm the inhibitory effects of CsA using a different assay technique, nuclear samples from figure 20b were used for analysis in an NFAT2 DNA binding ELISA (figure 20c). The relative NFAT activity between U2932, HLY-1 and WSU-NHL cell lines was similar to previous experimental findings (figure 17a and c) and DNA binding activity was substantially reduced upon CsA treatment in all three cell lines. These data confirm that at these doses CsA effectively inhibits NFAT from translocating to the nucleus and binding to DNA, and therefore would be expected to prevent the induction of NFAT-specific target genes.

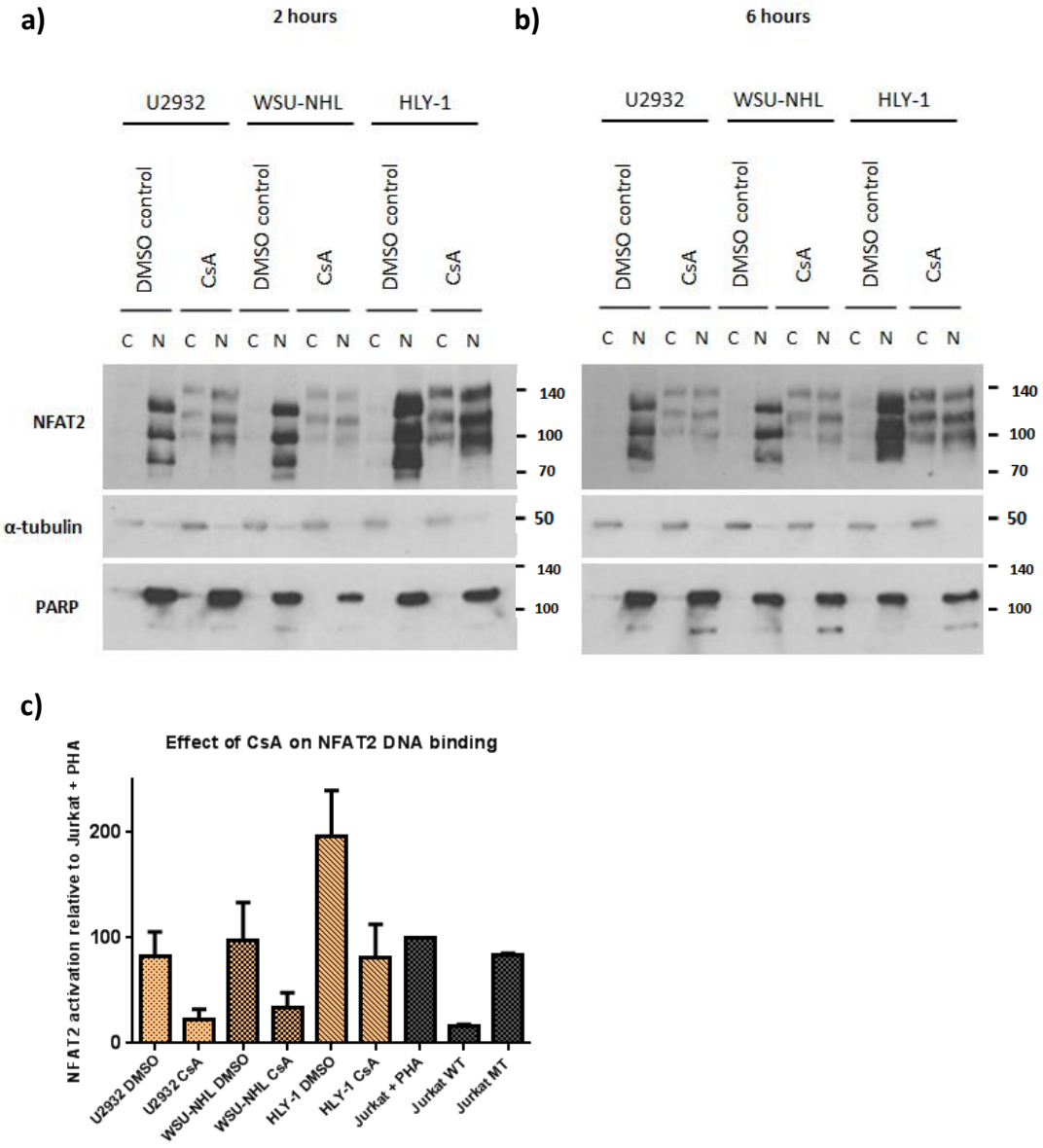

Figure 20. The calcineurin inhibitor CsA inhibits NFAT2 activation and DNA binding a) Two ABC DLBCL cell lines (U2932 and HLY-1) and one GCB DLBCL cell line (WSU-NHL) were treated with their IC50 concentration of CsA (8.6μg/ml, 7.4μg/ml and 10.4μg/ml respectively for 2 hours and 6 hours before preparation of nuclear and cytoplasmic extracts. A vehicle control sample (0.01% DMSO) was also included. The effect of CsA on NFAT2 activity was analysed by Western blot analysis, including α-tubulin as a cytoplasmic loading control and PARP as a nuclear loading control. Data is representative of four individual experiments b) the effect of CsA on NFAT2 DNA binding activity was measured by an NFAT2 ELISA using nuclear extract samples from the 6 hour CsA timepoint (b). PHA-treated Jurkat nuclear extract was included as a positive control for NFAT2 activation. To monitor the specificity of the assay, samples were run alongside a mutated (MT) consensus oligonucleotide and a wild-type (WT) consensus oligonucleotide (as a competitor for NFAT2 binding). ELISA data is representative of one experiment, where error bars indicate the standard deviation between duplicate wells.

3.2.6. Cells treated with CsA undergo cell cycle arrest and apoptosis

To explore the mechanisms behind the reduction in cell viability observed upon treatment of DLBCL cells with CsA, the Propidium Iodide (PI) assay for cell cycle analysis was performed. WSU-NHL, U2932 and HLY-1 cells were treated with their respective IC50 concentration and double their IC50 concentration of CsA for 24 hours before PI staining and analysis of cell cycle phase distribution by FACs. Previous proliferation assays (appendix figure 1) confirmed that a 24 hour incubation of cells with CsA was an ideal timepoint for PI experimental analysis. Treatment with CsA IC50 and 2xIC50 concentrations killed approximately 20-40% of cells after 24 hours, allowing enough time for CsA to exert its cytostatic or cytotoxic effects while leaving sufficient remaining live cells for PI analysis (appendix figure 1).

Figure 21a and b shows the percentage of cells in the G1/G0, S, G2/M and Sub-G1 stages of the cell cycle following CsA treatment. An increase of cells in the G1/G0 growth phase was observed in both WSU-NHL and U2932 cell lines upon CsA treatment (although slightly more so in U2932). This indicates a cytostatic effect of CsA, where cells are prevented from progressing further through the cell cycle. CsA also caused a dose-dependent reduction in S phase and the G2/M phase. Moreover, CsA also had a cytotoxic effect on cells, as indicated by the accumulation of cells in the sub-G1 phase, which was particularly prevalent in WSU-NHL cells treated with 2x their IC50 concentration. Although HLY-1 cells were included in this experiment, unfortunately the nature of the PBS washes required for this assay repeatedly caused loss of the HLY-1 pellet, which is frequently very loose and scattered in this particular cell line and therefore PI analysis for this cell line was not possible.

To assess whether cells undergo CsA-induced apoptosis, the effects of CsA on the cleavage of PARP was analysed by Western blot (figure 21c and d). PARP is a nuclear 116KDa stress response protein involved in the detection and repair of DNA damage. Proteolytic cleavage of PARP into 85KDa and 24KDa fragments by caspases is an early indicator of apoptosis and can be detected by Western blot using an antibody directed against the PARP holoenzyme (114KDa) and its cleaved forms. Figure 21c and d show a dose-dependent induction of cleaved PARP (lower 85KDa band) in all three cell lines when compared to the DMSO control, which only expressed very low levels of uncleaved PARP protein. By 48 hours incubation with CsA (figure 21d), the apoptotic effect is

particularly apparent in WSU-NHL cells treated with 2xIC50 CsA, demonstrating strong expression of cleaved PARP, in addition to near complete loss of expression of the PARP holoenzyme itself. Moreover, expression of the cytoplasmic control protein α-tubulin is also lost in this sample, indicating that the apoptotic effects of CsA are also beginning to cause degradation of key cellular proteins.

In summary, the data in figure 21 indicates that CsA uses a combination of cytostatic and cytotoxic mechanisms to reduce the viability of DLBCL cell lines.

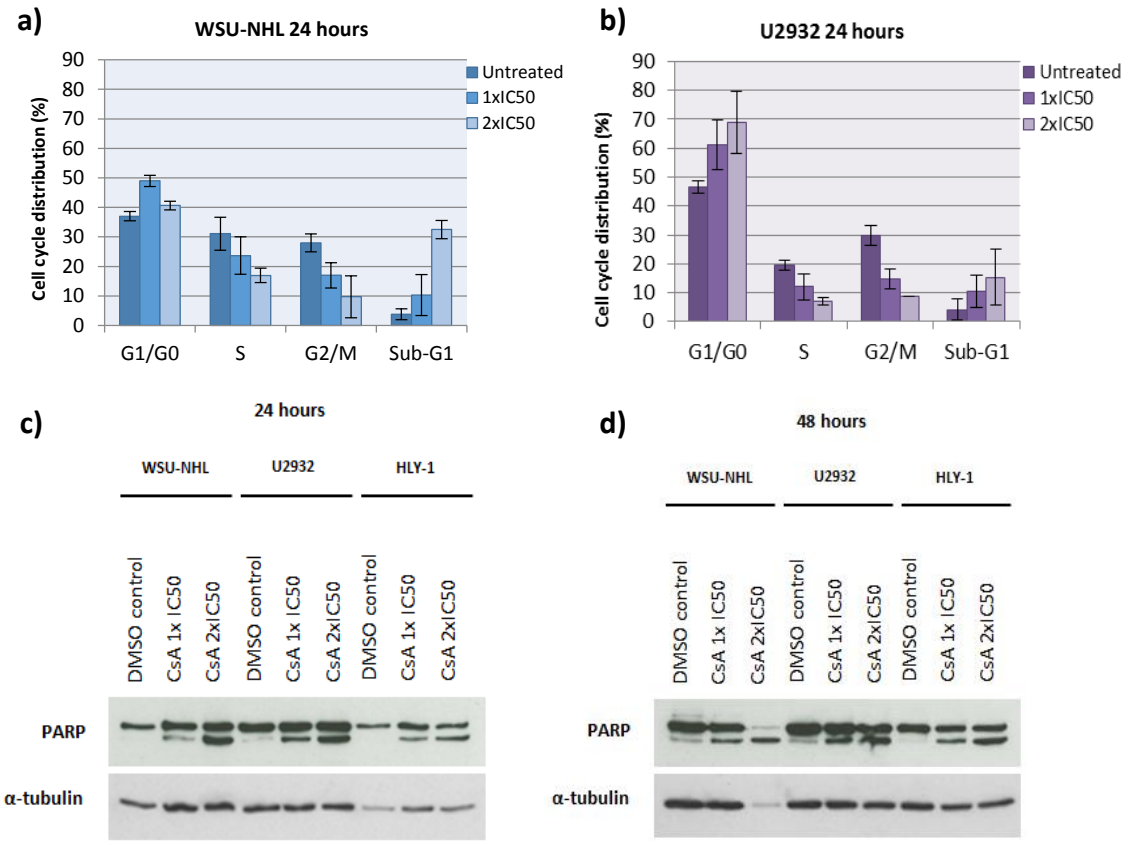

Figure 21. Cells treated with CsA undergo cell cycle arrest and apoptosis. DLBCL cell lines were treated with their respective CsA IC50 concentration and double their IC50 concentration alongside a vehicle control (0.02% DMSO). For WSU-NHL (a); 1xIC50 = 20.8μg/ml and 2xIC50 = 41.6μg/ml. For U2932 (b); 1xIC50 = 8.6μg/ml and 2xIC50 = 17.2μg/ml. Cells were incubated for 24 or 48 hours before being stained with PI and the cell cycle phase distribution recorded by FACs analysis. The x-axis represents the G1/G0, S, G2/M and Sub-G1 stages of the cell cycle, while the y-axis indicates the percentage of cells in each phase. Data is representative of two independently performed experiments, where error bars indicate the standard error of the mean. c-d) Whole cell extracts of cells treated with CsA (as described above, including HLY-1 1xIC50 = 11.5μg/ml and 2xIC50 = 23μg/ml) were probed for PARP and analysed using Western blot analysis. Cleavage of PARP (lower band) was used as an indicator for CsA-induced apoptosis and α-tubulin was used as a loading control. Western blot data is representative of a single experiment.

3.2.7. The calcineurin inhibitor FK506 kills DLBCL cell lines in a dose-dependent manor by inhibiting NFAT activation

To further support this data indicating that DLBCL cell lines rely on the calcineurin-NFAT signalling pathway for survival, it was important to test this model using another inhibitor of the pathway. FK506 (*tacrolimus*) is another highly effective immunosuppressant drug which also targets calcineurin activity. Originally sourced from the soil bacterium *Streptomyces tsukubaensis*, FK506 is a chemically distinct microbial product to CsA, exerting its effect by binding to the immunophillin FKBP12 (FK506 binding protein 12) to form a complex which binds to calcineurin and prevents its phosphatase activity (Barik, 2006; Sieber, 2009).

As shown in figure 22a and b, HLY-1 and RIVA cells were treated with increasing concentrations of FK506 (0-100µM) before the survival of cells was assessed by the resazurin assay. FK506 exerted a dose-dependent effect on the viability both cell lines, completely killing cells at the maximal dose, therefore allowing calculation of IC50 concentrations. HLY-1 cells were more sensitive to FK506 compared to RIVA cells, with an IC50 of 25.3µM compared to 48.3µM in RIVA cells. These data confirmed that DLBCL cell lines are also sensitive to inhibition of the NFAT-calcineurin pathway using FK506.

The effects of inhibiting the calcineurin NFAT pathway on NFAT protein expression were subsequently determined using nuclear extracts of HLY-1 cells treated with 30µg/ml of FK506 or 10µg/ml CsA for 1 hour or 4 hours (figure 22c). The effect of FK506 on the subcellular localisation and phosphorylation status of NFAT was identical to that of CsA treatment, shifting predominantly nuclear NFAT2 (in untreated samples) to the cytoplasm. FK506 also caused an increase in the intensity of upper bands within each cluster and a slight decrease in the dephosphorylated splice variants which demonstrates rephosphorylation of remaining NFATs in the nucleus. Both FK506 and CsA had a small effect on NFAT4, causing less to be expressed in the nucleus. This was most noticeable after 4 hours of CsA treatment.

To confirm specificity, the effects of FK506 and CsA treatment on expression of members of the NF-κB pathway were analysed by Western blot (figure 22d). FK506 and CsA had no effect on the expression of most canonical members of the NF-κB pathway, including p65, phospho S536 p65 (P-p65) or p50 (including its precursor p105). These inhibitors

did however seem to cause slight elevation of c-Rel levels after 4 hours treatment, suggesting that they may have some secondary effects on pathways other than the calcineurin-NFAT pathway. Despite this, CsA and FK506 had no effect on the non-canonical markers of the NF-κB pathway, including RelB and p52 (including its precursor p100).

These data confirmed the calcineurin-NFAT pathway to be of key importance for the survival of DLBCL cell lines and validated FK506 as an alternative mechanism for effectively inhibiting the expression and activation of NFAT in DLBCL cell lines.

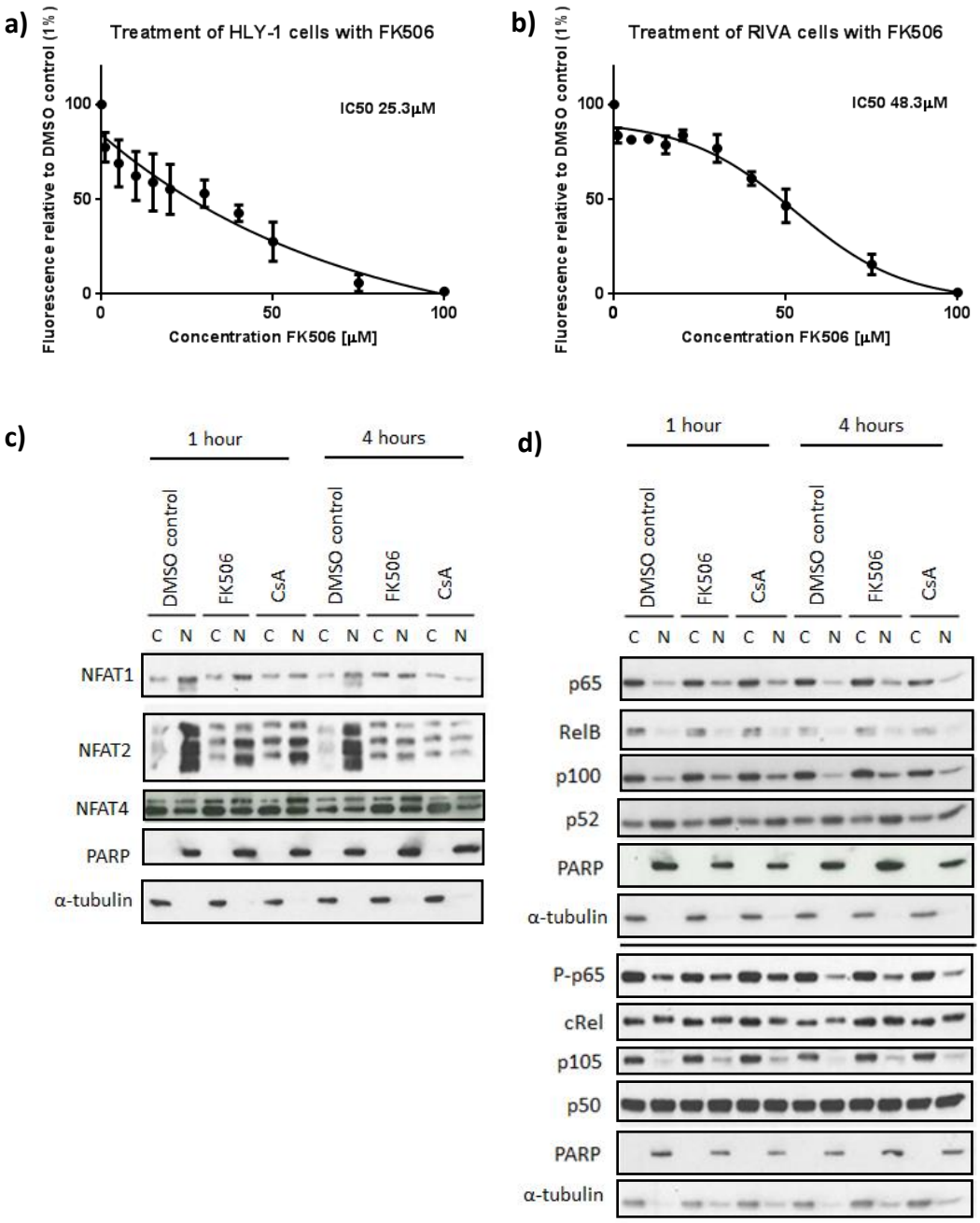

Figure 22. The calcineurin inhibitor FK506 kills DLBCL cell lines in a dose dependent manor by inhibiting NFAT activation a-b) The ABC DLBCL cell lines HLY-1 and RIVA were treated with a range of concentrations of FK506 (0µM-100µM) for 72 hours before recording cell viability using the resazurin assay. Data is representative of three biological replicates where error bars indicate the standard error of the mean. c-d) HLY-1 cells were treated with 10µg/ml CsA or 30µM FK506 for 1 hour and 4 hours before preparation of nuclear and cytoplasmic extracts. A vehicle control sample (1% DMSO) was also included. The effect of CsA and FK506 on NFAT family members (c) and NF-κB (d) was analysed by Western blot analysis. Simple indicators of NF-κB pathway activation were used to assess the mode of NF-κB activation, where activation of the non-canonical NF-κB pathway is indicated by the presence of p100 cleavage to the active p52 subunit and the presence of the RelB unit. α-tubulin was used as a cytoplasmic loading control and PARP as a nuclear loading control. Data is representative of a single experiment.

3.2.8. DLBCL cell lines have variable sensitivity to the NFAT pathway inhibitor INCA-6, which was found to be non-specific

Targeting calcineurin as a means of deciphering DLBCL dependency on NFAT is not ideal because calcineurin itself regulates signalling proteins other than NFAT (Macian, 2005). As an alternative compound therefore, the inhibitor of NFAT-Calcineurin Association-6 (INCA-1) was investigated. INCA-6 is a highly selective compound that interferes with the interaction between calcineurin and NFAT by binding to calcineurin's discrete binding site on NFAT, rather than inhibiting the enzymatic activity of calcineurin like other NFAT inhibitors (Roehrl *et al.*, 2004). Importantly, INCA-6 provides a potential practical advantage over CsA and FK506 by inhibiting NFAT dephosphorylation without altering calcineurin phosphatase activity, preventing dephosphorylation of other substrates (Roehrl *et al.*, 2004; Kang *et al.*, 2005)

To investigate the dependency of cell lines on the NFAT pathway for survival, a large panel of DLBCL cell lines were treated with a range of concentrations of INCA-6 (0μM-40μM) before average IC50 values for each cell line were calculated and plotted in figure 23a. INCA-6 sensitivity was variable among the panel, with no apparent relationship between average IC50 concentration and NFAT protein expression, activation or DNA binding seen earlier (figure 17a and c). There was also no correlation between DLBCL subgroups or their respective BCR status. Despite this, all cell lines were killed in a dose-dependent manor (data not shown), further supporting previous data illustrating the requirement for NFAT signalling in lymphoma cell survival.

Cell line IC50 values for INCA-6 are shown in figure 23b, where cell line-specific INCA-6 sensitivity is also classified according to respective IC50 values, where high sensitivity = <15μM, medium sensitivity = 15-20μM and low sensitivity = >20μM. Reassuringly, the relative sensitivity of cell lines to INCA-6 broadly matched CsA data (figure 19 and table 10), which can be compared in figure 23b. SUDHL-6 and OCI-Ly18 cells for example, were highly sensitive to both INCA-6 and CsA, whereas Karpas-422 and SUDHL-4 were among the least sensitive. These data initially provided confidence that both inhibitors were targeting the same pathway.

When considering INCA-6 as a potential inhibitor for use in gene expression microarray analysis, it was important to confirm its effect on NFAT protein expression. WSU-NHL cells were treated with 12μM INCA-6 or 10μg/ml CsA for 2 hours or 6 hours before the

effects on NFAT expression were determined by Western blot analysis (figure 23c). While CsA worked as predicted, the INCA-6 compound had an unusual effect on NFAT and other cellular proteins. After 2 hours treatment, both NFAT1 and NFAT2 were completely absent from the nucleus, however by 6 hours cytoplasmic NFAT was also undetectable. Additionally, INCA-6 treatment affected PARP cleavage, where detection of the lower 85KDa band indicated cells were undergoing rapid apoptosis. Loss of the 114KDa holoenzyme after 6 hours treatment also suggested INCA-6-induced degradation of PARP. The fact that INCA-6 induced rapid cleavage of PARP by just 2 hours suggested that INCA-6 may be having broader effects in the cell, perhaps targeting the proteasomal degradation of proteins by activating caspases.

These observations suggested that INCA-6 was not functioning as desired and was likely having off-target effects. To test this hypothesis, the effects of INCA-6 on NF-κB subunits were assessed (figure 23d and e). Similar to NFAT, the NF-κB pathway members IκBα, p100/p52, c-Rel, RelB and P-p65 all seemed to become degraded upon incubation for 6 hours with INCA-6. Of note, in these experiments there is also some effect of CsA treatment on NF-κB. After 6 hours treatment for example, CsA appears to cause a reduction in p100 and P-p65, including a very slight reduction in c-Rel expression. A potential explanation for this is included in section 3.3.2. Overall, however, these analyses confirmed that INCA-6 was targeting signalling pathways other than NFAT and was not suitable for further use in this study.

a)

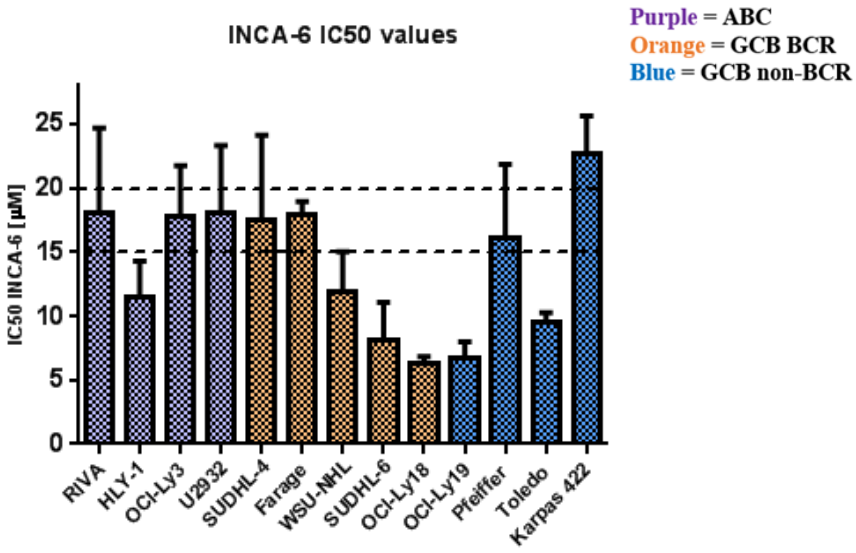

b)

Cell line	DLBCL subgroup	INCA-6 sensitivity	INCA-6 IC50 [µM]	CsA sensitivity
RIVA	ABC	Medium	18.0	Low
HLY-1	ABC	High	11.5	High
OCI-Ly3	ABC	Medium	17.8	Medium
U2932	ABC	Medium	18.0	Medium
SUDHL-4	GCB BCR	Medium	17.5	Low
Farage	GCB BCR	Medium	17.9	Medium
WSU-NHL	GCB BCR	High	11.8	Medium
SUDHL-6	GCB BCR	High	8.1	High
OCI-Ly18	GCB BCR	High	6.3	High
OCI-Ly19	GCB non-BCR	High	6.7	Medium
Pfeiffer	GCB non-BCR	Medium	16.1	High
Toledo	GCB non-BCR	High	9.6	Medium
Karpas 422	GCB non-BCR	Low	22.7	Low

c)

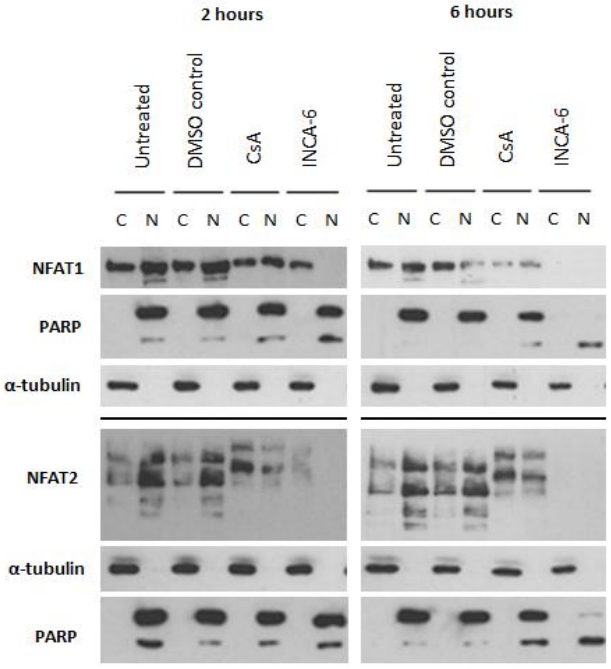

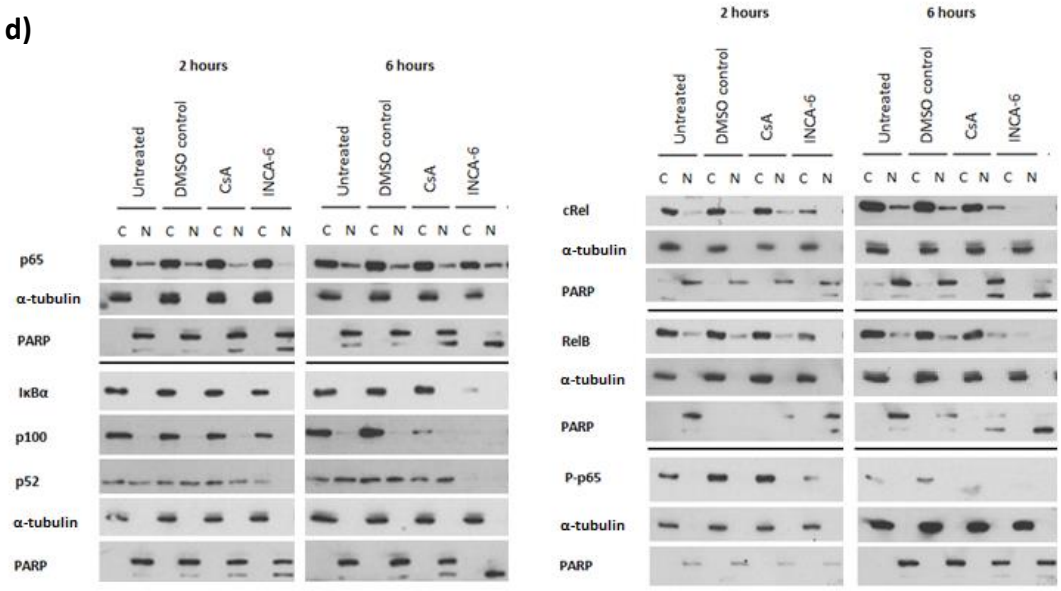

Figure 23 (Continued from previous page). DLBCL cell lines have variable sensitivity to the NFAT pathway inhibitor INCA-6, which was found to be non-specific. a) A panel of DLBCL cell lines were treated with a range of concentrations of INCA-6 (0μM-40μM), including an untreated vehicle control sample (0.25% DMSO) and were incubated for 72 hours before viable cells were measured using the resazurin assay. DLBCL subgroups are colour coded, where purple = ABC DLBCL, orange = GCB BCR DLBCL and blue = GCB non-BCR DLBCL. Dose-response curves were plotted for each cell line and the IC50 concentration recorded. The average IC50 concentration across three independent experiments was determined and plotted in (a). Data is representative of three biological repeat experiments, where error bars indicate the standard error of the mean b) Table showing respective INCA-6 IC50 concentrations for DLBCL cell lines and their relative sensitivity to INCA-6 (high sensitivity = <15μM, medium sensitivity = 15-20μM and low sensitivity = >20μM. The relative sensitivities of cells to CsA are provided as a comparison. c) WSU-NHL cells were treated with 10μg/ml calcineurin inhibitor CsA or 12μM NFAT inhibitor INCA-6 , including a vehicle control sample (0.1% DMSO) for 2 hours or 6 hours before nuclear and cytoplasmic extracts were prepared. The effect of CsA and INCA-6 on NFAT family members (c) and NF-κB (d-e) was analysed by Western blot analysis. Simple indicators of NF-κB pathway activation were used to assess the mode of NF-κB activation, where activation of the non-canonical NF-κB pathway is indicated by the presence of p100 cleavage to the active p52 subunit and the presence of the RelB unit. α-tubulin was used as a cytoplasmic loading control and PARP as a nuclear loading control. Data is representative of a single experiment in this cell line, however the experiment was also performed in the U2932 cell line, where the same effect was observed (data not shown).

3.2.9. 11R-VIVIT and MCV-1 peptides have no effect on DLBCL cell viability

Although CsA and FK506 have revolutionised transplant therapy, their use is associated with a number of side effects, which are likely due to off target effects (Kiani *et al.*, 2000; Rezzani, 2004). An alternative to small molecule inhibition of targets is the development of peptide sequences which are designed to selectively bind to complementary sites on

protein targets. As described previously, the VIVIT peptide has a high affinity Pro-Val-Ile-Val-Ile-Thr motif and has been valued for its enhanced selectivity when compared to CsA (Aramburu *et al.,* 1998; Aramburu *et al.,* 1999). VIVIT interferes with the interaction between calcineurin and NFAT, by binding to NFAT's docking site on calcineurin, blocking NFAT dephosphorylation and nuclear translocation (Aramburu *et al.*, 1999). By effectively competing with NFAT proteins for calcineurin binding, VIVIT prevents all downstream NFAT signalling.

In 2004, Noguchi and colleagues synthesised a cell-permeable version of the VIVIT peptide which was used successfully in prolonging graft survival after islet cell transplantation in mice (Noguchi, 2004). Cell permeable VIVIT also proved to be a less toxic drug than calcineurin inhibitors, such as FK506 (Noguchi, 2004). As an alternative approach to inhibition of NFAT activity, the effects of the VIVIT peptide on cell viability were analysed using the resazurin assay. As shown in figure 24a-b, RIVA and HLY-1 cells were unresponsive to treatment with a range of concentrations of VIVIT (0μM-20μM), even at high doses. VIVIT peptide was subsequently tested using a range of conditions, including changing the medium type (from Gibco RPMI to Sigma RPMI), the percentage foetal calf serum and by testing concentrations of VIVIT up to 100μM (data not shown). However cells remained insensitive.

In recent years a second generation VIVIT peptide has become commercially available for use in research laboratories. MCV-1 is a bipartite NFAT inhibitor that targets two separate calcineurin docking motifs, making it more potent than the 11R-VIVIT (Yu *et al.*, 2012). Moreover. MCV-1 is reported to prevent NFAT activation at nanomolar potencies, independent of calcineurin activity and without impairing NF-κB activity (Yu *et al.*, 2012). Following the lack of effect of VIVIT on DLBCL proliferation, the sensitivity of a large panel of cell lines to MCV-1 was analysed using concentrations ranging from 0μM-50μM (figure 24c-h), however cell viability was unaffected in all six cell lines. These data indicated that peptide-based inhibition of NFAT did not have the same growth inhibitory effect as small molecule inhibition. However, in these experiments I lacked a positive control and was not able to tell if the peptide was getting into cells.

The experiments described in figure 24 were performed very early on in the PhD, before biochemical experiments showing the effects of other NFAT inhibitors on NFAT subcellular localisation (such as those in figure 23) were performed. By this stage, a

suitable inhibitor of NFAT (CsA) had already been chosen for use in a gene expression microarray. Although it would have been interested to confirm the effects of the VIVIT peptides on NFAT biochemically, I decided not revisit the peptides at this later stage of my studies, but to instead make the best use of my time using CsA.

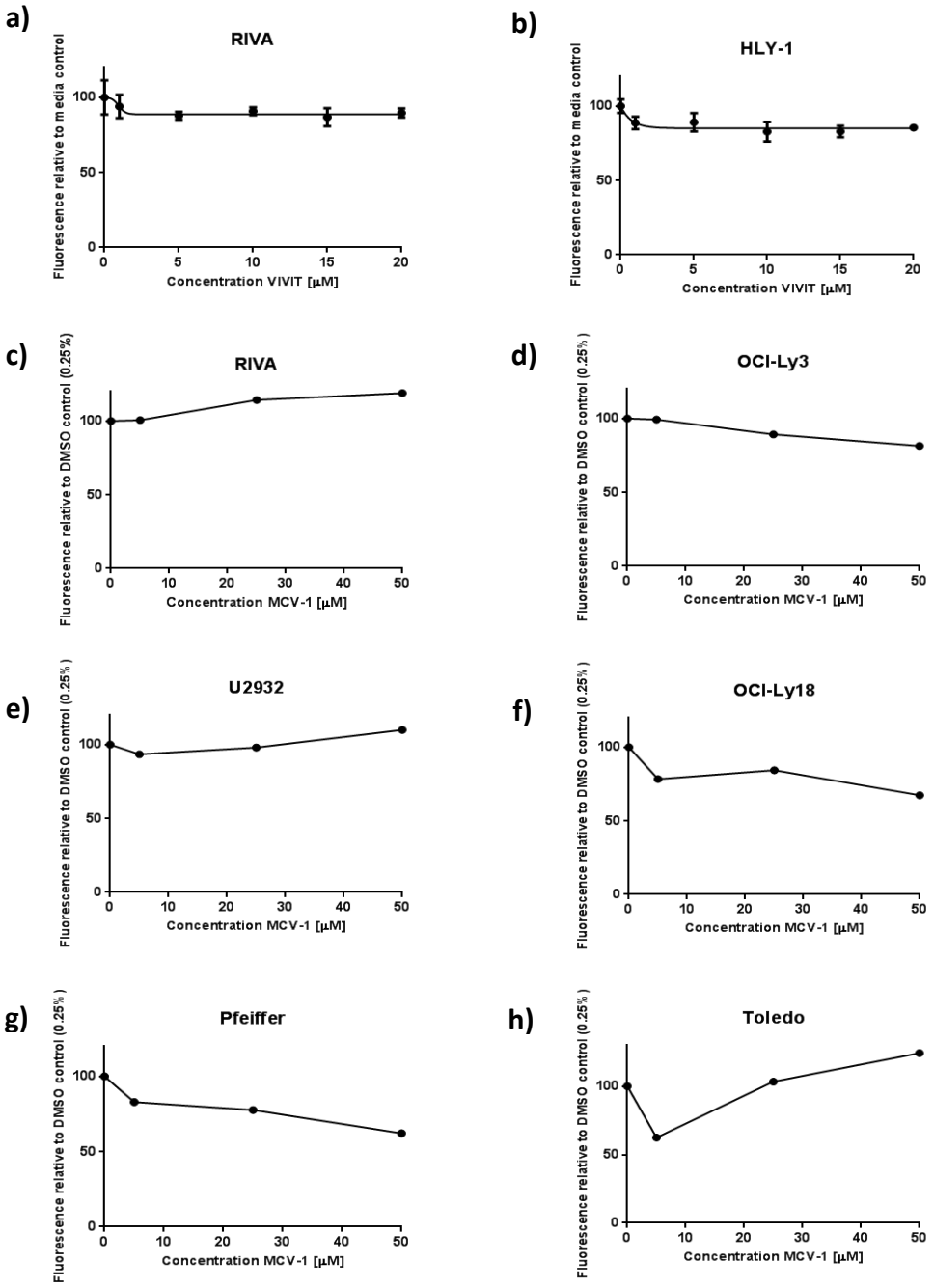

Figure 24. 11R-VIVIT and MCV-1 peptides have no effect on DLBCL cell viability. a-b) DLBCL cell lines RIVA and HLY-1 were treated with increasing concentrations of the VIVIT-11R peptide (0-20μM), including a vehicle (water) control sample. Cells were incubated for 72 hours before cell viability was measured using the resazurin assay. Data is representative of three biological repeat experiments where error bars indicate the standard error of the mean. c-h) A panel of DLBCL cell lines were treated with a range of concentrations of the VIVIT MCV-1 peptide (0-50μM), including a vehicle control sample (0.25% DMSO). Cells were incubated for 72 hours before cell viability was measured using the resazurin assay. Data is representative of one experiment, where each concentration was plated out in a single well.

3.3.Discussion

3.3.1. Expression and activation of NFAT in DLBCL cell lines

A significant part of this chapter involved a comprehensive analysis of the expression and activation of NFAT family members in a large panel of DLBCL cell lines. As expected, the lymphocyte-specific NFAT family members NFAT1, NFAT2 and NFAT4 were expressed at high levels in some cell lines. Analysis showed that expression of particular family members were fairly heterogeneous across the panel, with some cell lines demonstrating strikingly higher levels of expression than others, suggesting that NFAT plays an important role in these cell lines. Analysis of NFAT activation was also investigated with the presence of the lower dephosphorylated bands indicating that NFAT was in its activated state, combined with the expression of NFAT in the nucleus of DLBCL cells. Moreover, NFAT2 DNA-binding ELISA data correlated well with protein expression analysis, providing further evidence that NFAT2 is transcriptionally active in most DLBCL cell lines.

These data supported the findings of Marafioti et al (2005), where NFAT2 was detected in the nucleus of routine DLBCL biopsy samples, suggesting ongoing activation of the NFAT pathway (Marafioti *et al.*, 2005). Results were also consistent with the constitutively active NFAT2 identified in the nucleus of DLBCL cell lines in studies demonstrating a role for NFAT in maintaining lymphoma cell survival (Pham *et al.*, 2005; Pham *et al.*, 2010).

It was interesting to observe expression of active and inactive NFAT3 in DLBCL cells. NFAT3 is known to have roles in the neuronal system and has recently been implicated in PTEN-regulated intestinal differentiation and non-small cell lung cancer (Zhao X, 2010; Wang *et al.*, 2011; Ulrich *et al.*, 2012). However, a role for NFAT3 in immune cells has not been reported and could be an interesting area to explore in the future

When considering the positive feedback loop between NFAT2 and MYC described by Pham et al (2005), the expression of MYC relative to its transcriptional regulator NFAT2 and other NFAT family members was analysed (Pham *et al.*, 2010). Expression was heterogeneous between cell lines but did not correlate with NFAT expression. Moreover, despite the cell lines SUDHL-6 and OCI-Ly18 having MYC translocations, their expression of MYC was not significantly different to other cell lines. Although researchers at the MD Anderson Cancer Centre USA have shown convincing data correlating NFAT2 expression with MYC in SUDHL-4 and OCI-Ly10 cells, much of their research utilises DLBCL cells established in-house (Pham *et al.*, 2010). Given the heterogeneity of the disease and representative cell lines, the use of alternative cell lines may be the reason that we do not see similar correlations in our system. Moreover, differences in the culture technique and culture medium over time can lead to changes in the underlying genetics of validated cell lines (such as in SUDHL-4), which can results in variation in cell behaviour.

Given that NFAT is a key signalling pathway downstream of the BCR, it was hypothesised that cell lines with chronic active BCR signalling (ABC DLBCLs) and GCB BCR DLBCLs would harbour high expression of NFAT when compared to other cell lines. NFAT2 expression was generally higher in ABC and GCB BCR cell lines, suggesting that the NFAT pathway was of importance in these subgroups. Interestingly, it has been reported that BCR signals only increase the transcription of the *NFAT2* gene, but not that of the *NFAT1* and *NFAT4* genes (Muhammad *et al.*, 2014; Rudolf *et al.*, 2014). Indeed, the degree of NFAT1 and NFAT4 expression were similar between ABC, GCB BCR and GCB non-BCR cell lines, however NFAT2 expression and transcriptional activity in GCB non-BCR cell lines compared to BCR-dependent cell lines was noticeably lower. Conversely, some cell lines, such as OCI-Ly19, Pfeiffer and Karpas 422, demonstrated low-medium expression and DNA binding of NFAT2, suggesting that NFAT in these lymphomas could be regulated by mechanisms other than the BCR.

There is little information available regarding the upstream events that control NFAT activation in cancer cells. In addition to the BCR or TCR, NFAT is positioned downstream of a number of receptor initiated pathways, including RTK and GPCR receptors, which may explain the NFAT expression observed in GCB non-BCR cell lines (Pan *et al.*, 2013). An interesting experiment, which would underpin more precisely the interaction between the BCR and NFAT in DLBCL cell lines, would be to treat cells with

inhibitors of various components of the BCR, such as the SYK inhibitor R406 or Ibrutinib which targets Bruton's tyrosine kinase (BTK) to assess the effects on NFAT expression.

Another consideration for future studies is whether calcineurin-modulation of NFAT is the only mechanism for NFAT activation in DLBCL. Upregulation of the expression of NFAT1 and NFAT5, for example, has been demonstrated in a calcineurin-independent manner in mammary tumour cells and was associated with the assembly of the α6β4 integrin and promotion of carcinoma invasion (Jauliac *et al.*, 2002). Additionally, NFAT activation *in vivo* has been proposed to occur via phosphorylation-induced protein stabilisation in the absence of Ca^{2+} activity (Kuroda *et al.*, 2008). Mikishiba et al (2008) found that Ca2+ oscillation-independent osteoclastogenesis was insensitive to inhibition of calcineurin with FK506, with NFAT2 activity being unaffected (Kuroda *et al.*, 2008). Cot, a serine threonine kinase was reported to phosphorylate NFAT2 in osteoblast cells, increasing its protein stability and resistance to degradation, thereby upregulating its total levels while also inducing calcineurin-independent activation of NFAT2 (Kuroda *et al.*, 2008; Kuroda *et al.*, 2012). These reports provide evidence that NFAT expression is mediated by mechanisms other than calcium or calcineurin modulation in some systems, highlighting potential areas of future research.

3.3.2. Inhibition of the calcineurin/NFAT pathway

Another key aim at the beginning of the study was to investigate the effects of NFAT inhibition on DLBCL cell viability and to find a suitable, reliable inhibitor for use in gene expression microarray analysis. In addition to their huge success in the field of transplant therapy, CsA and FK506 are also practical tools for investigating the NFAT signalling pathway *in vitro*. CsA treatment caused a dose-dependent reduction in cell viability, confirming that the calcineurin-NFAT pathway is critical for lymphoma cell survival. It was hypothesised that CsA treatment may prevent the transcription and translation of survival/growth factors regulated by NFAT, BLyS, CD40 and MYC (Pham *et al.*, 2005; Fu *et al.*, 2006; Pham *et al.*, 2010). To date, very few NFAT target genes have been reported in the context of B-cell lymphoma, highlighting a key area of unexplored investigation.

The sensitivities of DLBCL cells to CsA were fairly similar, as indicated by their IC50 concentrations which ranged from 3.6-15.6µg/ml. These were very comparable to concentrations reported in the literature. For example, in a study investigating the

sensitivity of 37 melanoma cell lines to CsA, the IC50 concentrations ranged from 3-13µg/ml (Perotti *et al.*, 2012). Moreover, the differences between the shapes of CsA kill curves also showed that the effect of CsA was different between cell lines, perhaps due to differences in the mechanisms of regulation by NFAT. However, as discussed previously, no relationship between IC50 value and NFAT protein expression was identified. HLY-1 cells for example, expressed the highest levels of active NFAT1 and NFAT2 (including NFAT2 transcriptional activity) and were one of the most sensitive cell lines to CsA. In comparison, OCI-Ly18 was also highly sensitive to CsA; however this cell line demonstrated virtually undetectable NFAT2 protein expression and DNA binding. Although this suggests that CsA sensitivity is independent of NFAT protein expression, it is important to consider that even small quantities of NFAT expressed in cells could be critical for their survival. Moreover, cell lines with low level expression of NFAT2 may in fact have a greater dependency on the expression of other NFAT isoforms. OCI-Ly18, for example, may depend on NFAT3, which was expressed at very high levels in this cell line. Considering that CsA targets multiple NFAT family members, the relative dependencies of cell lines on specific NFAT isoforms cannot be determined by this approach, which was recognised early on in the study to be a potential limitation.

Mouse studies have demonstrated that FK506 and CsA are highly specific inhibitors of NFAT-mediated signalling (Graef *et al.*, 2001). Furthermore, the phenotype of NFAT3 and NFAT4 double knockout mice is almost identical to that of the embryos of mothers treated with CsA during embryonic development (Graef *et al.*, 2001). However, inhibiting the activation of calcineurin also prevents the dephosphorylation of target proteins other than NFAT. Calcineurin, for example, also modulates other signalling pathways, such as the RAS-MAP kinase cascade and the TGF-β/Smad pathway (Manninen *et al.*, 2000; Gooch *et al.*, 2004). Other targets include the pro-inflammatory molecules NF-κB, Elk-1 and AP-1, the InsP3R, ryanodine and NMDA receptors, as well as enzymes such as PKA, NO synthase and the MEF2C and MEF2D transcription factors (Blumenthal *et al.*, 1986; Liu *et al.*, 1991; Dawson *et al.*, 1993; Cameron *et al.*, 1995; Tong G, 1995; Wu *et al.*, 2001; Lynch *et al.*, 2005; Medyouf *et al.*, 2007; Vafadari *et al.*, 2013).

Of particular relevance to DLBCL is the reported off-target effects of CsA on the NF-κB pathway, whereby CsA has been shown to inhibit NF-κB activation by approximately 50% in three specific positions of the NF-κB cascade in peripheral human T cells (González-Guerrero *et al.*, 2013; Vafadari *et al.*, 2013). Mechanistically, calcineurin has

been demonstrated to bind to and inactivate the cytoplasmic inhibitor of κB (IκB) (which usually keeps NF-κB proteins inactive in the cytoplasm), leading to activation and nuclear translocation of NF-κB (Biswas *et al.*, 2003). Moreover, an interesting mechanism of CsA-induced activation of NF-κB was proposed by Palkowitsch et al (2011) where calcineurin was found to dephosphorylate BCL10 downstream of TCR-CD28 engagement (Palkowitsch *et al.*, 2011). BCL10 dephosphorylation is a central step for the formation of the CBM complex which in turn causes the activation of NF-κB (Frischbutter *et al.*, 2011). To date, CsA-mediated NF-κB activation has only been demonstrated in T cells, but given that the CBM complex is essential for the survival of ABC DLBCL cell lines downstream of BCR signalling, it would be interesting to investigate whether CsA has a similar effect (Ngo *et al.*, 2006).

To investigate as these reported alternate effects in our system, the effects of FK506 and CsA on the activity of the NF-κB pathway were analysed. As described previously, the NF-κB pathway is a key pathway critical for lymphoma cell survival and is known to cross-talk with many other signalling pathways. The levels of some markers of NF-κB activation remained constant with FK506 and CsA treatment, however CsA caused some reduction of expression of other markers, such as p100, P-p65 and c-Rel after 6 hours treatment. These particular effects support data in the literature which show CsA to have an effect on NF-κB. It cannot therefore be confirmed that CsA is a specific inhibitor of NFAT in DLBCL. Moreover, the timescales of treatment used in this study were very short. Indirect effects on NF-κB and other pathways may become more apparent at the same timescale as the viability phenotype. It cannot therefore be guaranteed that there aren't any effects on NFAT that in turn affect NF-κB at later timepoints, such as 24 and 48 hours.

During these early stages of the study, one of the principle aims was to choose appropriate model cells for use in a gene expression microarray with the aim of discovering novel NFAT target genes important for lymphoma cell survival. The key criteria for this were to find cell lines which expressed detectable levels of active NFAT and were dependent on the calcineurin-NFAT pathway for their survival based on their sensitivity to CsA. With the gene expression microarray in mind, two cell lines from the ABC DLBCL subgroup were chosen, which would be compared to gene expression changes in one GCB DLBCL cell line. HLY-1, U2932 (ABC) and WSU-NHL (GCB) cells were found to meet the above criteria and so were used for further experimental analysis.

The off-target effects seen with INCA-6 have not yet been reported in the literature. Presently, INCA-6 has only been used in a handful of studies in the literature, most of which have investigated the effects of NFAT inhibition on various proteins and mRNAs of interest (Shiratori *et al.,* 2010; Prasad *et al.,* 2011; Bretz *et al.,* 2013; Faralli *et al.,* 2015; Savage *et al.,* 2015). These studies did not investigate the direct effects of INCA-6 on the expression of NFAT family members themselves. Biochemical experiments in these publications used similar concentrations of INCA-6 (5-20μM) to those in this study (12μM) but off-target effects were not reported. Deciphering the precise mechanism of action of INCA-6 would have been an interesting area to explore. However, my goal was to investigate the role of NFAT in DLBCL, for which it was decided that the use of CsA was suitable.

In summary, this chapter confirmed the differential expression, activation and transcriptional activity of NFAT family members in a comprehensive panel of DLBCL cell lines. The use of chemical inhibition of calcineurin-NFAT signalling demonstrated this pathway to be critical for lymphoma cell survival, where analysis of IC50 concentrations further demonstrated heterogeneity between cell lines. Although CsA and FK506 some specificity, attempts were made to inhibit NFAT more directly by use of the INCA-6 compound and two potent VIVIT peptides. Inhibition using these agents was ineffective due to off-target effects by INCA-6 and possibly issues of peptide cell permeability. After testing the majority of small molecule and peptide inhibitors commercially available, CsA was chosen for further experimental analysis. For example, its effects on cell viability were investigated in greater detail, where it was found to exert both cytostatic and cytotoxic effects on DLBCL cell lines. The decision to use CsA for the remainder of this study introduced a number of potential limitations. As described previously, NFAT is not the only calcineurin target and CsA has reported off-target effects. To specifically understand the role of NFAT in DLBCL, these factors would require consideration in future experiments, as described in chapter 5. Furthermore, CsA is a pan inhibitor of all calcineurin-regulated NFAT isoforms, therefore the function of specific NFAT family members cannot be determined using CsA, but rather would require siRNA or shRNA-mediated knockdown of individual proteins.

Overall, these data provided a useful insight into *in vitro* models of NFAT in DLBCL, allowing me to strategically decide on the ABC DLBCL cell lines HLY-1 and U2932 and

the GCB DLBCL cell line WSU-NHL as appropriate cell lines for use in a gene expression array.

Chapter 4.

Exploration of cooperativity between the NFAT and NF-κB signalling pathways

4. Exploration of cooperativity between the NFAT and NF-κB signalling pathways

4.1. Introduction

4.1.1. Evidence for cooperativity between NFAT and NF-κB

The structural similarities between NFAT and NF-κB suggest they are evolutionarily derived from common ancestors, sharing similar modes of induction and structure of their DNA binding domain (de Lumley *et al.*, 2004). Recent evidence demonstrates the coordinate regulation of lymphocyte survival factors by NFAT and NF-κB, suggesting that the pathways may function together to promote lymphomagenesis (Pham *et al.*, 2005; Fu *et al.*, 2006; Pham *et al.*, 2010).

Evidence for the cooperative interaction of NFAT and NF-κB was first identified in activated T cells, where transcriptional induction of the IFN-γ promoter was enhanced by the simultaneous binding of NFAT proteins with the p50 and p65 NF-κB subunits (Sica *et al.*, 1997). Moreover, Li-Weber et al (2004) showed synergistic activation of interleukin-4 gene transcription by NFAT and NF-κB in T cells via two overlapping binding sequences for NF-κB and NFAT (Li-Weber *et al.*, 2004). Studies prior to this had proposed that NF-κB and NFAT competed for binding to specific DNA sites, where NF-κB could antagonise NFAT and inhibit NFAT-mediated transcriptional at this site (Casolaro *et al.*, 1995). However, Li-Weber et al (2004) demonstrated that combined p65 and NFAT signalling actually enhanced the expression of IL-4, suggesting that NFAT and NF-κB function in a cooperative manner (Li-Weber *et al.*, 2004).

The precise NF-κB subunits and NFAT family members that can function cooperatively in different systems are still in early stages of investigation. It is well known that the NF-κB subunits p65 and c-Rel are highly involved in the activation of T cells following TCR-engagement. However, the mechanisms through which TCR engagement drives p65 and c-Rel activation are not fully understood (Köntgen *et al.*, 1995; Grumont *et al.*, 2004; Hatchi *et al.*, 2014). While p65 rapidly translocates to the nucleus, c-Rel activation requires calcineurin and NFAT amplification (Tan *et al.*, 1992; Grumont *et al.*, 2004). A recent study found that the ubiquitin E3-ligase TRIM13 is a key enhancer of NF-κB activation in T cells, where diminished expression of TRIM13 reduced activation of p65,

c-Rel and NFAT (Hatchi *et al.*, 2014). Furthermore, another study in CD4+ T cells confirmed cooperative functions of NFAT1 and p65 (Jash *et al.*, 2012). In the study, NFAT1 induced an active chromatin configuration for the assembly of transcriptional coactivators at the IL-9 promoter, whereas binding of the p65 NF-κB subunit caused transactivation of the promoter (Jash *et al.*, 2012). Finally, in a study investigating signalling defects in NF-κB $p50^{-/-}$ $c\text{-}Rel^{-/-}$ CD8+ T cells an unexpected role for these NF-κB subunits were identified, where the expression p50 and c-Rel was crucial for proximal TCR signalling and for the activation of NFAT (Bronk *et al.*, 2014).

It appears that the interaction between NFAT and NF-κB may differ between various cellular contexts. For example, the molecular mechanisms underlying the marked differences in regulation of the transcriptional co-activator BOB.1/OBF.1 between B cells and T cells was recently investigated (Mueller *et al.*, 2013). Unlike B cells, where BOB.1/OBF.1 is constitutively expressed throughout B-cell development, BOB.1/OBF.1 expression is inducible in T cells by PMA/Ionomycin or antigen receptor engagement (Schubart *et al.*, 1996; Zwilling *et al.*, 1997; Sauter P, 1997). In addition to an array of genetic and biochemical analysis, Mueller et al (2003) found that *in silico* analysis of the BOB.1/OBF.1 promoter identified previously unknown combined NF-κB and NFAT target sites in T cells (Mueller *et al.*, 2013). Deletion of NFAT or NF-κB impaired expression of BOB.1/OBF.1 and its transcriptional recruiter Oct2 and was predicted to participate in T-cell mediated immunodeficiency (Mueller *et al.*, 2013).

Cooperative roles of NFAT and NF-κB are not limited to cells of the immune system. For example, the p65 subunit of NF-κB coimmunoprecipitates with NFAT in cardiomyocytes and this interaction maps to the RHD of p65 (Liu *et al.*, 2012). Moreover, parallel activation of NFAT and NF-κB was found to be required for expression of COX-2 in bronchial epithelial cell lines exposed to carcinogenic nickel compounds (Cai, 2011). Overall, these studies provide compelling evidence for combined NFAT and NF-κB signalling in various cellular contexts.

As described previously, both the NFAT and NF-κB pathways are individually important for the pathogenesis of DLBCL and a small number of genes in lymphocytes have been shown to be regulated by NFAT and NF-κB in combination (figure 25) (Pham *et al.*, 2005; Fu *et al.*, 2006; Pham *et al.*, 2010). We hypothesised that the NFAT and NF-κB pathways functionally intersect to co-ordinately promote lymphoma development and maintenance. To address whether the NFAT and NF-κB pathways co-ordinately promote

lymphoma development and maintenance, I aimed to investigate whether simultaneous depletion of the NFAT and NF-κB pathways caused additive or synergistic effects on the viability of DLBCL cell lines. Moreover, I aimed to better understand the expression, activation and dependency of DLBCL cells on NF-κB with the intention of picking model cell lines for use in a gene expression microarray analysis.

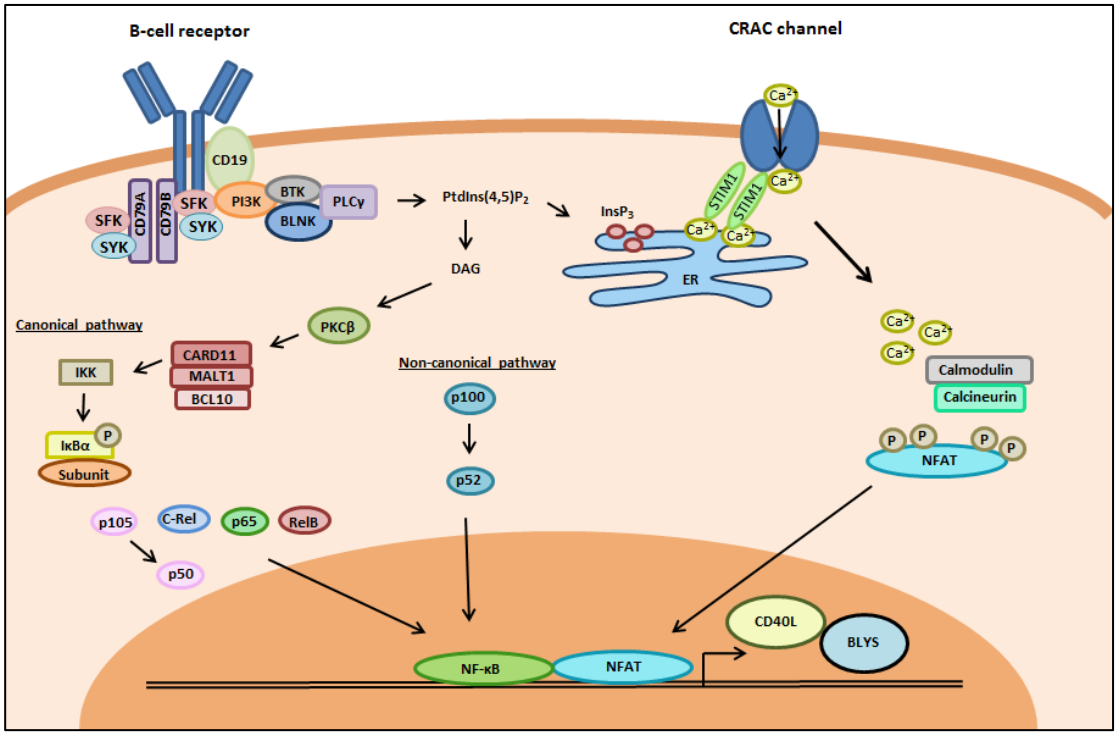

Figure 25. The NF-κB and NFAT signalling pathways may function in synergy to coordinate the regulation of genes known to promote B-cell survival.

4.2. Results

4.2.1. DLBCL cell lines have heterogeneous expression and activation of NF-κB family members and are sensitive to chemical inhibition of the NF-κB pathway by TPCA-1

To gain a general understanding of the expression and activation of NF-κB family members in DLBCL and to help determine appropriate cell lines models for use in gene expression array analysis, NF-κB family members and their respective activation status were analysed by Western blot in a comprehensive panel of ABC and GCB DLBCL cell lines. The total expression of individual NF-κB family members from samples prepared as whole cell extracts was heterogeneous across the panel (figure 26). DLBCL lines of both the ABC and GCB subgroup expressed almost all NF-κB subunits at relatively high

comparative levels; however some cell lines had markedly high or low expression of specific subunits. Some NF-κB family members, such as p65 and c-Rel for example, were expressed at relatively high levels by all cell lines, whereas the expression of p50 and p52 (and their inactive precursors) were extremely heterogeneous.

Indicators of NF-κB pathway activation were used to assess the mode of NF-κB activation in DLBCL cell lines. Activation of the NF-κB pathway occurs via phosphorylation of IκBα at serine 32 and serine 36 followed by proteasome-mediated degradation that results in the release of subunits and their translocation to the nucleus (Finco *et al.*, 1994; Brockman *et al.*, 1995; Traenckner *et al.*, 1995; Chen *et al.*, 1996). While expression of the inhibitor of NF-κB subunits (IκBα) was at similar levels in all cell lines, the expression of P-IκBα was highly variable, indicating that the general activation of NF-κB family members was heterogeneous between cell lines. Although an indicator of NF-κB activation, the absolute levels of P-IκBα expression are hard to measure due to its rapid turnover by proteasomal degradation.

Activation of the canonical NF-κB pathway, represented by phosphorylation of p65 (P-p65) at serine 536 was observed at strikingly high levels in HLY-1 cells. The canonical pathway was also active in other DLBCL cells, such as OCI-Ly3 and Farage; however their apparent faint P-p65 expression is likely due to the low exposure of this particular Western blot. Activation of the non-canonical NF-κB pathway is indicated by the presence of p100 cleavage to the active p52 subunit and the expression of the RelB subunit. There was generally no significant correlation between the expression of either the canonical or noncanonical pathways in cell lines, indicating that both pathways could be important for most lymphoma cells. Interestingly however, Farage cells expressed non-canonical pathway components at high levels, whereas OCI-Ly18, OCI-Ly19 and Karpas 422 cells had very low expression of p52, p100 and RelB. Finally, the inactive precursor p105 and its active cleavage product p50 were expressed in almost all cell lines, but were not expressed at all by Karpas 422 cells.

To further investigate the expression and activation of NF-κB family members in DLBCL cell lines, Western blot analysis of cytoplasmic and nuclear protein extracts allowed a comparative analysis of subcellular location and activation status of NF-κB between cell lines (figure 27a). This analysis correlated well with the whole cell extracts, with for example, SUDHL-4, OCI-Ly18, OCI-Ly19 and Karpas-422 cells lacking expression of the non-canonical pathway subunit p52. Apart from SUDHL-4, these particular cell lines

also expressed low levels of RelB, indicating inactivity of the non-canonical signalling pathway. Similar to the whole cell extracts, p65 was expressed in the cytoplasm of most cell lines, although detection of nuclear p65 was significantly more varied. Again, despite NF-κB being a hallmark of ABC DLBCL, the expression and nuclear activation of family members in GCB cell lines was comparable to ABC cell lines, suggesting that NF-κB signalling could be important for all subgroups of DLBCL.

Overall these data gave a general insight into the relative expression and activation of NF-κB in a large panel of cell lines. Although expression was heterogeneous between cell lines, these data allowed cell lines to be identified as being particularly high or low in NF-κB which could have been useful for selection of cell lines for microarray analysis using an NF-κB inhibitor. Farage cells for example demonstrated high expression of almost all family members, whereas Karpas 422 had distinctly low expression of most NF-κB subunits.

The IKK2 inhibitor IV (TPCA-1) is a potent small molecule inhibitor of IKK2 and therefore inhibits the canonical NF-κB pathway (Podolin *et al.*, 2005). When compared to other commonly used NF-κB inhibitors such as BAY 11-7082, TPCA-1 has shown to be potent and very selective in inhibiting the canonical NF-κB pathway (Rauert-Wunderlich *et al.*, 2013). Figure 27b shows the average IC50 values obtained from cell lines treated with a range of concentrations of TPCA-1 (0μM-40μM) for 72 hours. All cell lines were killed in a dose-dependent manor, indicating the requirement of the NF-κB pathway for lymphoma cell survival. However, there was no apparent relationship between IC50 concentrations and particular DLBCL subgroups. IC50 values were highly varied between cell lines and when compared to NF-κB protein expression, there was no correlation with inhibitor sensitivity. Cell line IC50 values are shown in the table in figure 27c, where cell line-specific TPCA-1 sensitivity is also classified according to respective IC50 values, where high sensitivity = <3μM, medium sensitivity = 3μM-6μM and low sensitivity = >6μM.

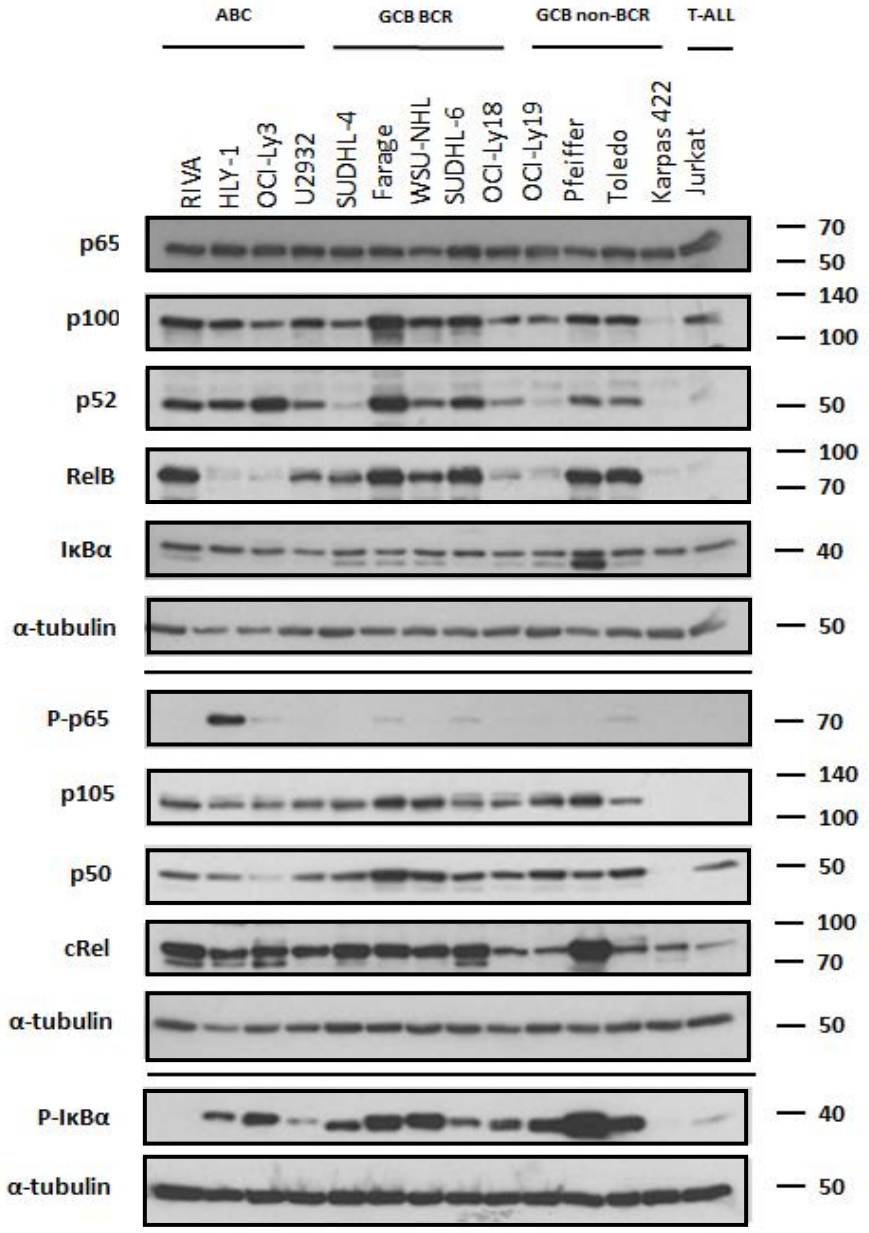

Figure 26. DLBCL cell lines have heterogeneous expression and activation of NF-κB family members. Whole cell extracts were taken from a panel of ABC and GCB DLBCL cell lines, including one T-ALL cell line and the expression of NF-κB family members were analysed by Western blot. Indicators of NF-κB pathway activation were used to assess the mode of NF-κB activation, where activation of the non-canonical NF-κB pathway is indicated by the presence of p100 cleavage to the active p52 subunit and the presence of RelB expression. Cell lines are categorised into their respective DLBCL subgroups where ABC = activated B-cell, GCB = germinal centre B-cell, BCR = B cell receptor. α-tubulin was included as a loading control. Data is from one experiment.

b)

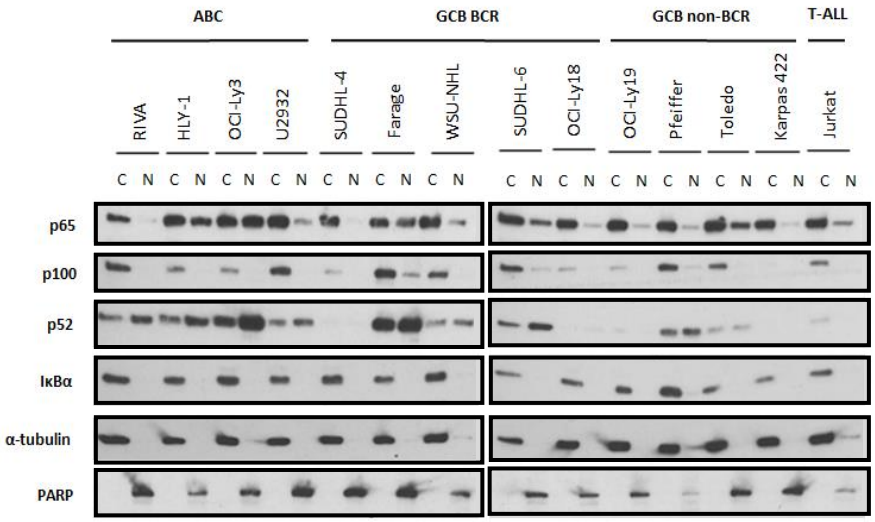

c)

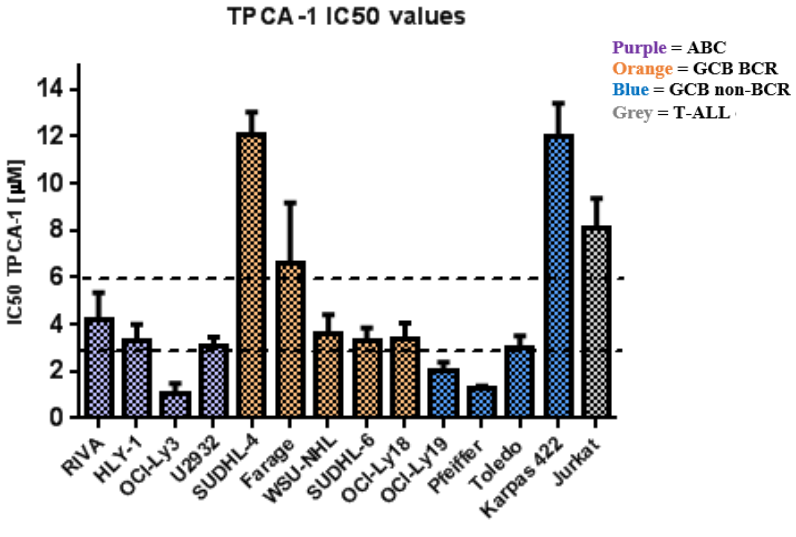

d)

Cell line	NF-κB activity	TPCA-1 sensitivity	TPCA-1 IC50 [μM]
RIVA	Low	Medium	4.2
HLY-1	Medium	Medium	3.3
OCI-Ly3	High	High	1.1
U2932	Medium	Medium	3.1
SUDHL-4	Low	Low	12.1
Farage	High	Low	6.6
WSU-NHL	Medium	Medium	3.6
SUDHL-6	Medium	Medium	3.3
OCI-Ly18	Low	Medium	3.4
OCI-Ly19	Low	High	2.0
Pfeiffer	Medium	High	1.3
Toledo	Medium	Medium	3.0
Karpas 422	Low	Low	12.0
Jurkat	Low	Low	8.1

Figure 27 (Continued from previous page). DLBCL cell lines have heterogeneous expression and activation of NF-κB family members and are sensitive to chemical inhibition of the NF-κB pathway by TPCA-1 a) Nuclear-cytoplasmic preparations were used to analyse comparative subcellular localisation and activation of NF-κB family members in a panel of ABC and GCB DLBCL cell lines by Western blot. α-tubulin was included as a cytoplasmic loading control and PARP was included as a nuclear loading control. Data is from one experiment. b) The panel of DLBCL cell lines were treated with a range of concentrations of TPCA-1 (0μM-40μM), including an untreated vehicle control sample (0.25% DMSO) and were incubated for 72 hours before viable cells were measured using the resazurin assay. Dose-response curves were plotted for each cell line and the IC50 concentration recorded. The average IC50 concentration across three independent experiments was determined and plotted in (b). Data is representative of three biological repeat experiments, where error bars indicate the standard error of the mean. c) Table showing the degree of NF-κB activity based on nuclear protein levels, respective IC50 concentrations for DLBCL cell lines and their relative sensitivity to TPCA-1 (high sensitivity = IC50 <3μM, medium sensitivity = 3-6μM, low sensitivity >6μM. DLBCL subgroups are colour coded, where purple = ABC DLBCL, orange = GCB BCR DLBCL and blue = GCB non-BCR DLBCL.

4.2.2. Combined inhibition of the NFAT and NF-κB pathways using CsA and TPCA-1 has variable effects in DLBCL cell lines

The effects of simultaneous inhibition of NFAT and NF-κB signalling on cell viability was tested using increasing concentrations of CsA and the IKK2 inhibitor TPCA-1 (figure 28). In these experiments I aimed to assess whether the drug combination was synergistic, where the addition of two drugs have a greater effect than one drug alone. Combined inhibition of both pathways had variable effects across the panel of cell lines, as shown in figure 29. Cell lines such as U2932 (figure 29e) exhibited very little additional effect of dual treatment when compared to inhibition of a single pathway alone, whereas the viability of RIVA cells (figure 29b) was reduced with both inhibitors, perhaps indicating a slight additive effect of the two drugs. In some cell lines, combined treatment merely reflected the sensitivity of inhibition of one pathway alone, for example addition of the drug combination to OCI-Ly3 (figure 29d) did not alter the dose-response curves of cells treated with TPCA-1 alone. Similarly, OCI-Ly18 treatment with both drugs had no effect on cell viability compared to single agent CsA treatment (figure 29j). Interestingly, the GCB DLBCL cell lines WSU-NHL (figure 29h) and SUDHL-4 (figure 29f) displayed dramatic cell death when treated with specific concentrations of both drugs compared to single agent treatments.

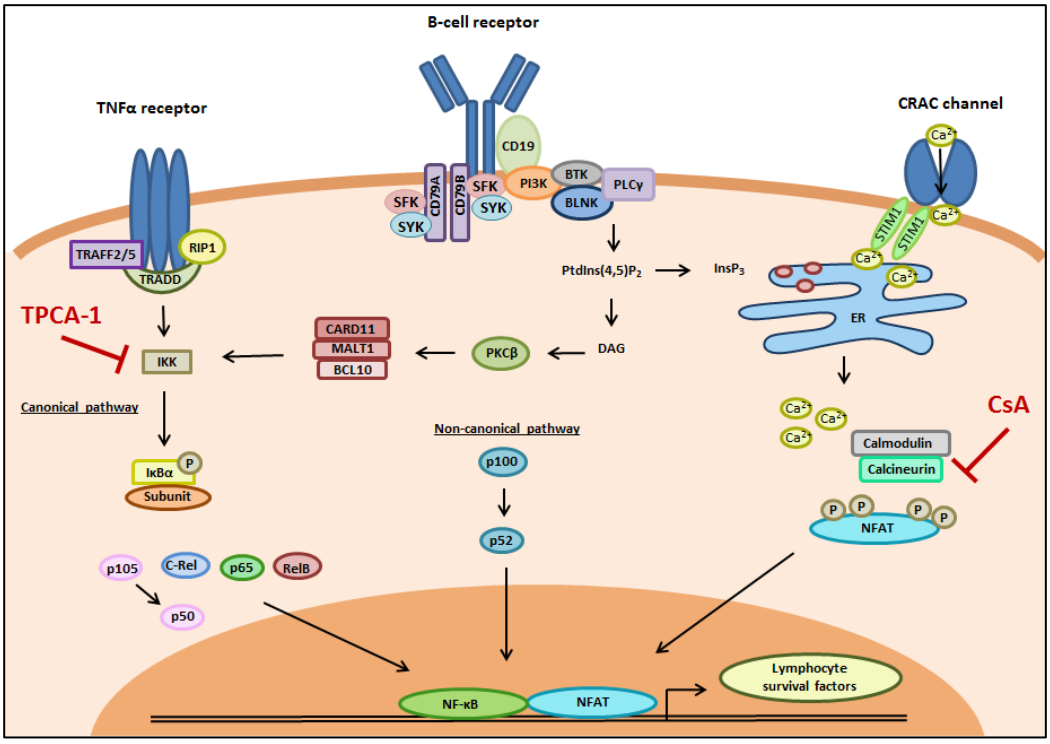

Figure 28. Combined chemical inhibition of the NFAT and NF-κB signalling pathways. The calcineurin/NFAT inhibitor CsA prevents the nuclear translocation of NFATs by inhibiting calcineurin activation. Inhibition of calcineurin's phosphatase activity prevents the dephosphorylation of substrates downstream of calcineurin, including NFAT, therefore preventing the transcription of multiple genes. The IKK2 inhibitor TPCA-1 inhibits canonical NF-κB signalling by inhibiting IKK2 activity. Image adapted from figure 25.

This effect was most apparent in the Jurkat T-cell line (figure 29o), which was included in the study due to previous reports showing calcineurin/NFAT and NF-κB dependencies in T-ALL (Medyouf *et al.*, 2007; dos Santos *et al.*, 2010). This was an interesting observation given that sustained calcineurin activation and highly active NF-κB signalling (via constitutively active NOTCH1) are known features of T-ALL (Medyouf *et al.*, 2007; Vilimas *et al.*, 2007; Gachet *et al.*, 2013). To test for similar effects in another T-ALL cell line, the experiment was also performed in MOLT-4 cells, (figure 29p); however CsA/TPCA-1 cooperativity was not observed.

Overall, these data suggest that although there may be some cooperative effects of combined inhibition of the NFAT and NF-κB pathways in some cell lines, these effects were not striking in most cell lines. To validate the effects observed, it was decided to quantify results by calculation of the combination index using the CalcuSyn analysis software, as described below.

a)

Concentration	TPCA-1	CsA
1	0.5µM	1µg/ml
2	1µM	5µg/ml
3	3µM	10µg/ml
4	10µM	15µg/ml
5	40µM	30µg/ml

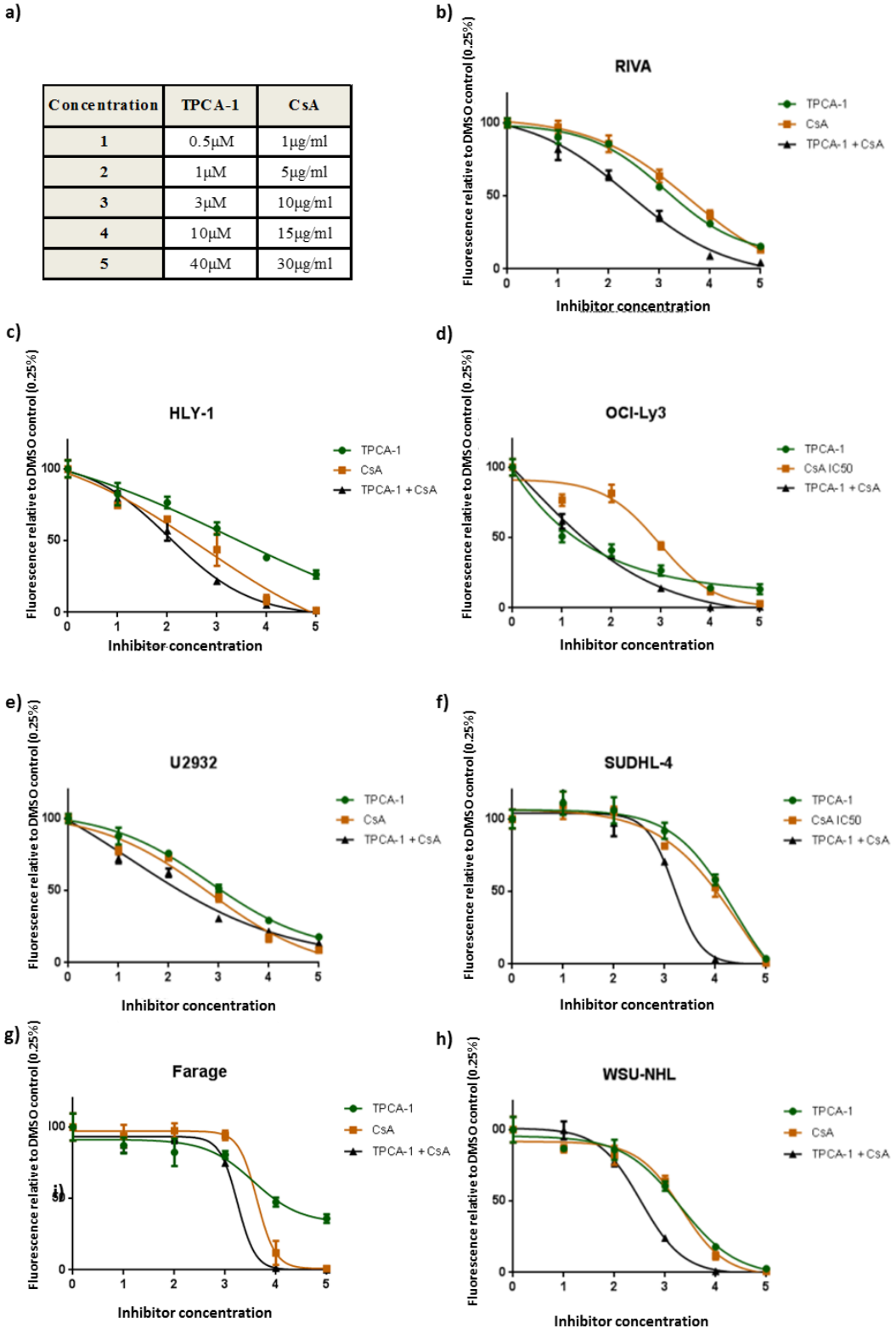

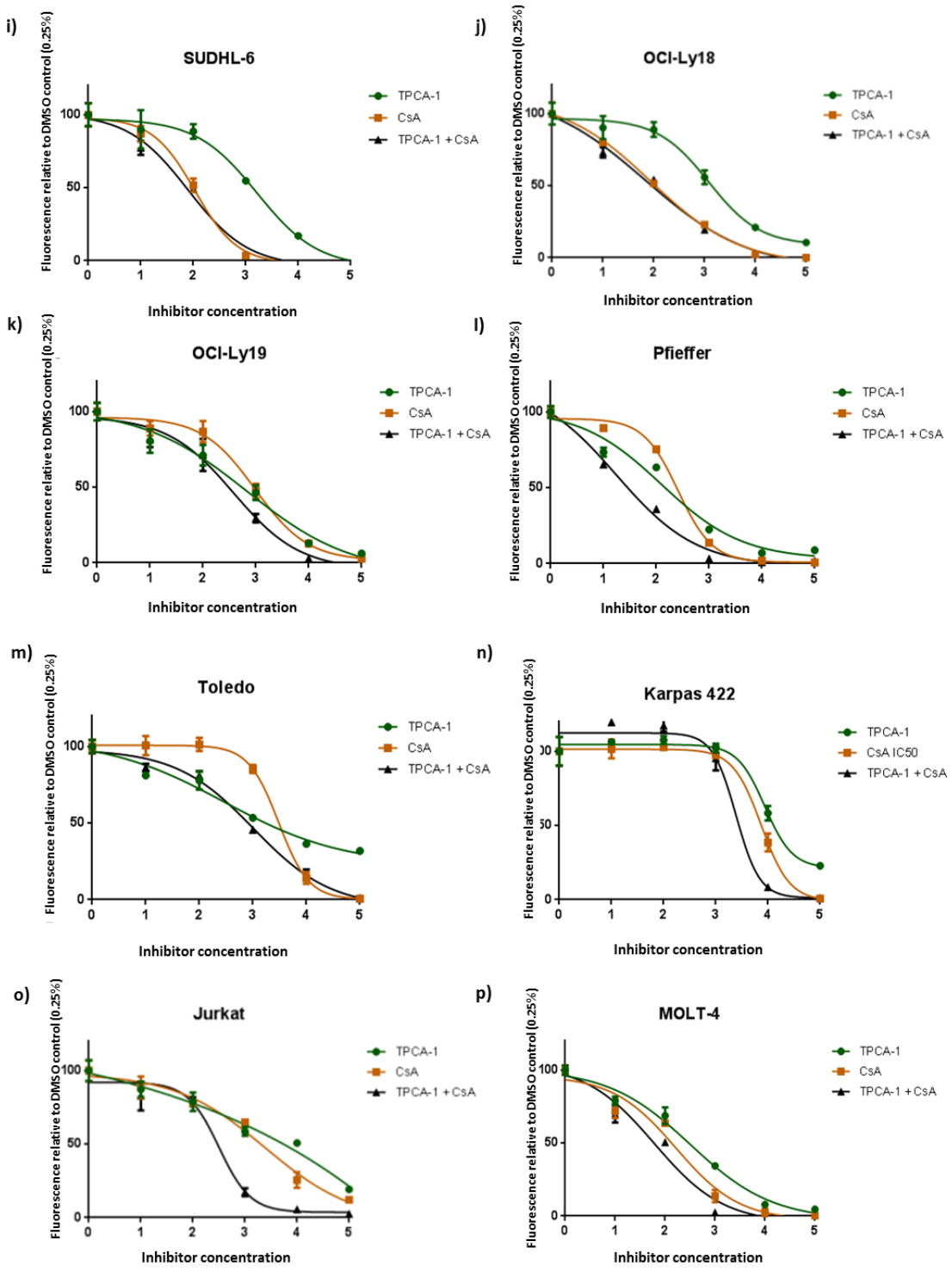

Figure 29 (Continued from previous two pages). Combined inhibition of the NFAT and NF-κB pathways using CsA and TPCA-1 has variable effects in DLBCL cell lines. a) A panel of DLBCL cell lines were treated with five concentrations of the calcineurin inhibitor CsA and the IKK2 inhibitor TPCA-1 (a), both alone and in combination and incubated for 72 hours before addition of resazurin and the viability of cells recorded. Cell lines represent four ABC DLBCL (b-d), nine GCB DLBCL (f-m) and two T-ALL cell lines (o-p). Data shown are representative of 3 separate experiments where error bars indicate the standard error of the mean.

4.2.3. CalcuSyn analysis of combined inhibition of the NFAT and NF-κB pathways suggests some synergistic effects between CsA and TPCA-1

To more rigorously investigate the potential synergistic effects seen in WSU-NHL cells treated with CsA and TPCA-1, the calcineurin/NFAT and NF-κB inhibitors were used alone at 0.25x, 0.5x, 1x, 2x and 4x their respective IC50 concentration and at equipotent concentrations at the ratios in combination, as shown in figure 30a. Figure 30b shows the dose-response curve for WSU-NHL cells, which is of similar shape to previous experiments using non-fixed ratios, where at least two pairs of inhibitor combinations were more growth inhibitory than either compound alone (figure 29h).

The most noticeable effect on cell viability was observed at an IC50 fraction of 1 (1x the IC50 concentration for each drug). To assess whether this effect was statistically significant the CalcuSyn software for dose-effect analysis was used. CalcuSyn provides the software for calculating the median-drug effect analysis for quantifying synergism or antagonism, as originally described by Chou and Talalay (Chou TC, 1984). The median-effect equation for dose-effect relationship was designed by Chou-Talalay in 1983 and is based on a mathematical analysis of hundreds of enzyme kinetic models, where it correlates the drug dose with the effect (Chou, 1974; Chou TC, 1984). Following calculation of the median effect, Chou's method for analysis uses a combination index (CI) equation which calculates whether a drug combination has an additive effect (Chou TC, 1984). Chou and Talalay proposed the designation of an additive effect being based on a CI greater than 1, where synergism is defined as more than an expected additive effect (CI less than 0.9) and antagonism as a less than expected additive effect, as shown in the table in figure 30c (Chou TC, 1984).

a)

Fraction of IC50 value	CsA	TPCA-1	Combination Index
0.25	2.6µg/ml	0.9µM	1.31
0.5	5.2µg/ml	1.8µM	1.24
1	10.4µg/ml	3.6µM	0.67
2	20.8µg/ml	7.2µM	0.91
4	41.6µg/ml	14.4µM	1.86

b)

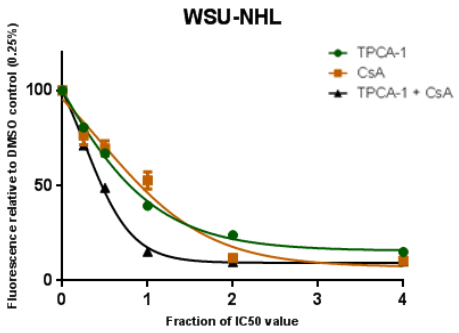

c)

Range of CI	Symbol	Description
<0.1	+++++	Very strong synergism
0.1-0.3	++++	Strong synergism
0.3-0.7	+++	Synergism
0.7-0.85	++	Moderate synergism
0.85-0.90	+	Slight synergism
0.90-1.10	±	Nearly additive
1.10-1.20	–	Slight antagonism
1.20-1.45	– –	Moderate antagonism
1.45-3.3	– – –	Antagonism
3.3-10	– – – –	Strong antagonism
>10	– – – – –	Very strong antagonism

Figure 30. CalcuSyn analysis of combined inhibition of the NFAT and NF-κB pathways suggests some synergistic effects between CsA and TPCA-1. The DLBCL cell line WSU-NHL was treated with five fixed-ratio concentrations of the calcineurin inhibitor CsA and the IKK2 inhibitor TPCA-1, both alone and in combination (a). Fixed ratio concentrations are based on cell-line specific fractions of CsA or TPCA-1 IC50 values (as determined previously), where a fraction of 0.25=0.25xIC50, 0.5 =0.5xIC50, 1=1xIC50 concentration, 2=2xIC50 and 4=4xIC50. Cells were incubated for 72 hours before addition of resazurin and the viability of cells recorded. The effects of chemical inhibition are shown in (b). CalcuSyn software was used to determine combination index scores for each fixed ratio concentration (a) which were compared CalcuSyn combination index scores indicative of drug synergy (c). Data shown is representative of one individual experiment where error bars indicate the standard deviation between triplicate wells.

Viability data for WSU-NHL data was analysed by median effect analysis to investigate whether the growth inhibitory actions of drug combinations represented a synergistic effect. With a combination index of 0.67 (figure 30a and c), only one drug combination (1xIC50) was classified as being synergistic when combined at the IC50 concentration compared with CsA and TPCA-1 treatment alone. The remaining drug combination doses were classified as either nearly additive or antagonistic.

4.3.4. Biochemical experiments suggest TPCA-1 is an ineffective inhibitor of NF-κB activation

Despite a lack of synergistic effects on cell viability, I considered it possible that NFAT and NF-κB may still co-ordinately regulate joint target genes that are important in lymphoma. Using RNA from cells depleted with NFAT and NF-κB components I aimed to use gene expression microarray analysis to investigate genes whose expression patterns

indicate coordinate regulation. NFAT and NF-κB may for example, separately regulate genes whose coinciding depletion creates a synthetic lethal phenotype resulting from loss of in-built redundancy. To confirm the inhibitory effects of TPCA-1, WSU-NHL cells were treated with their respective IC50 concentration (3.5μM) of TPCA1 for 2 hours or 6 hours (figure 31).

As shown in figure 31a, simple indicators of NF-κB pathway activation were used to assess the effects of TPCA-1. Figure 31a shows that activation of the canonical pathway (determined by the nuclear expression of subunits such as p65 and c-Rel) was somewhat reduced at 2 hours and 6 hours. P-p65 (serine 536) was also inhibited upon treatment with TPCA-1. Effective inhibition of IKK2 may also cause an accumulation of IκBα; however this was not observed and may be due to its rapid turnover. The reduction in p52 expression by TPCA-1 (observed at both timepoints and in both cytoplasmic and nuclear extracts) may be due to off target or secondary effects of the treatment.

Promisingly, TPCA-1 did not have major off target effects on NFAT activation (figure 31b), although there does seem to be a small effect on NFAT1 at 6 hours. Interestingly, despite a mild effect on NF-κB, TPCA-1 clearly induced apoptosis, represented by expression of the cleaved form of PARP. This experiment was also performed in an additional cell line (U2932), where TPCA-1 also had no effect on NF-κB activity (data not shown).

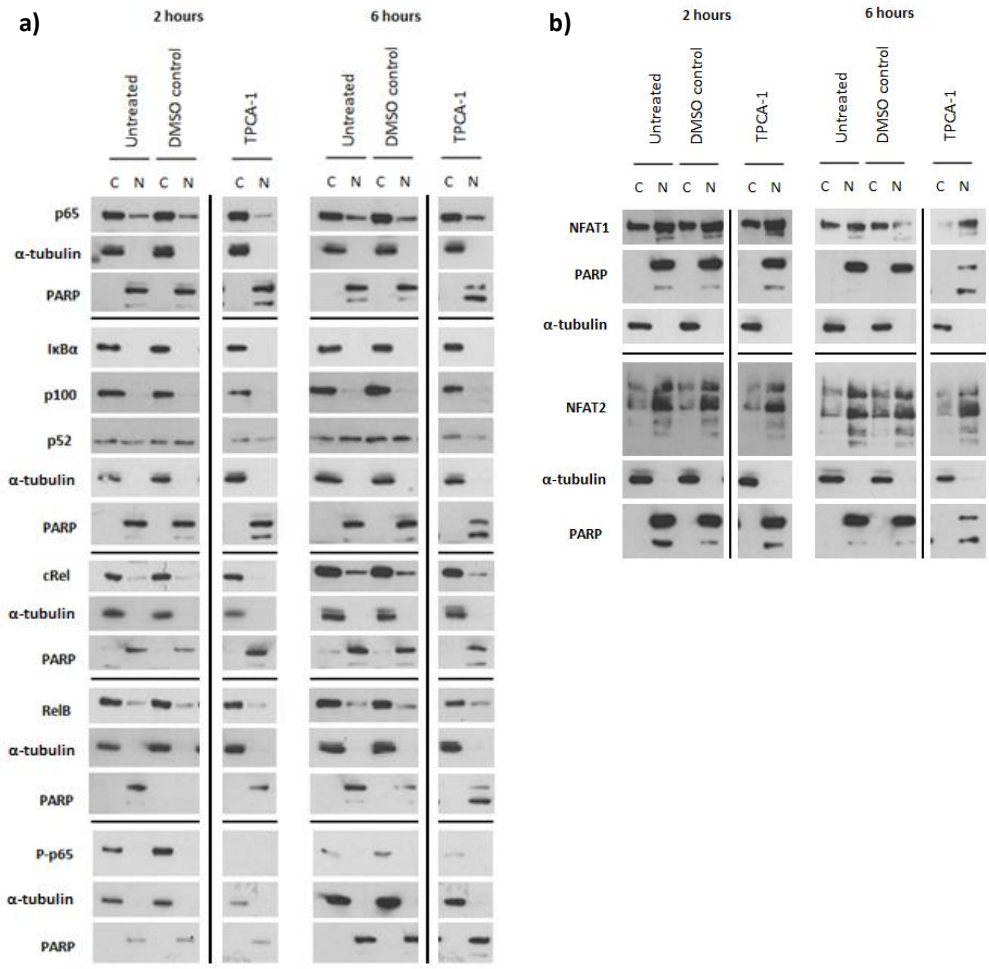

Figure 31. Biochemical experiments suggest TPCA-1 is an ineffective inhibitor of NF-κB activation. WSU-NHL cells were treated with 3.5μM IKK2 inhibitor TPCA-1, including a vehicle control (0.01% DMSO) for 2 hours or 6 hours before nuclear and cytoplasmic extracts were prepared. The untreated and DMSO controls used in this data were the same as those presented in a previous chapter (chapter 3, figure 23d). The effect of TPCA-1 on NF-κB (a) and NFAT (b) were analysed by Western blot analysis. Simple indicators of NF-κB pathway activation were used to assess the mode of NF-κB activation, where activation of the non-canonical NF-κB pathway is indicated by the presence of p100 cleavage to the active p52 subunit and the presence of the RelB unit. α-tubulin was used as a cytoplasmic loading control and PARP as a nuclear loading control. Data is representative of a single experiment in this cell line, however the experiment was also performed in the U2932 cell line, where the same effect was observed (data not shown).

3.1.1. TPCA-1 inhibits DNA binding activity of the NF-κB subunit p65

Here, I used a more sensitive assay to investigate whether TPCA-1 did indeed target NF-κB. U2932 cells were treated with TPCA-1 and the effects on the two main canonical NF-κB subunits p65 and c-Rel were analysed by ELISA. Reassuringly, p65 DNA binding activity was reduced upon treatment with TPCA-1, showing that this inhibitor was indeed exerting its desired effect by targeting NF-κB (figure 32). An interesting result here was the differential effects of TPCA-1 on p65 and c-Rel activity. Unlike p65, IKK2 inhibition by TPCA-1 had insignificant effects on c-Rel activity, suggesting that the effects of TPCA-1 may be subunit-specific. Of note, the effect of CsA treatment on p65 and c-Rel DNA binding activity was also investigated using this assay, however the data was inconclusive. It can therefore not be ruled out that CsA functions through the use of the NF-κB pathway in DLBCL cells.

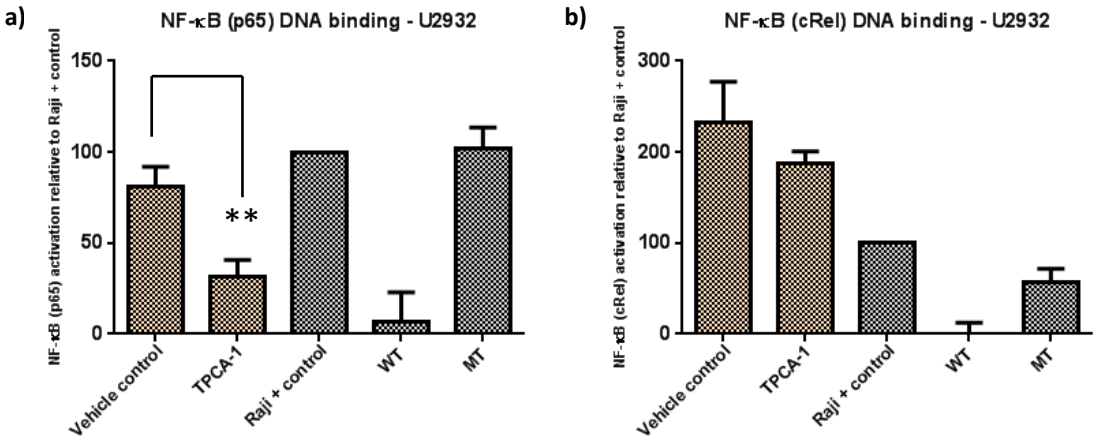

Figure 32. TPCA-1 inhibits DNA binding activity of the NF-κB subunit p65. The DLBCL cell line U2932 was treated with its IC50 concentration of TPCA-1 (3.1μM) for 2 hours before extraction of nuclear protein. The DNA binding activities of the NF-κB subunits p65 and c-Rel were analysed using an NF-κB ELISA. Raji cell nuclear extracts were included as a positive control for NF-κB activation. To monitor the specificity of the assay, samples were run alongside a mutated (MT) consensus oligonucleotide and a wild-type (WT) consensus oligonucleotide (as a competitor for NF-κB binding). p65 ELISA data is representative of four biological experiments (a). c-Rel data represents three biological experiments, however the WT and MT samples represent one experiment (b). Error bars indicate the standard deviation of duplicate wells. P-values: p65 = 0.005, cRel = 0.20 (insignificant).

3.2.Discussion

One of the main aims of the study was to investigate the contribution of different pathway components and transcription factor subunits to lymphoma cell growth and survival. During the MRes portion of this study I attempted to use siRNA knockdown of individual

NFAT and NF-κB subunits to help understand the relative contribution and combinatorial interactions of these different transcription factors to disease. Unfortunately, due to difficulties achieving effective knockdown of proteins in DLBCL cells this approach was not considered feasible.

3.2.1. Combined inhibition of the NFAT and NF-κB pathways

Instead, I investigated whether simultaneous depletion of the pathways caused additive or synergistic effects on DLBCL cells by combined treatment with the calcineurin/NFAT inhibitor CsA and the IKK2 inhibitor TPCA-1. In hindsight the experimental design of these experiments was slightly flawed with respect to the choice of drug doses. The ranges of concentrations chosen were based on the sensitivity of a small selection of cell lines (RIVA and HLY-1) treated with these agents in preliminary experiments. The middle dose (concentration 3) was established by the average IC50 concentration from cells used in early experiments, whereas the upper and lower concentrations chosen aimed to cover as best possible the broad effects on different cell lines. Using non-fixed doses were a major limitation to these experiments, making it difficult to make comparisons between cell line sensitivities and cooperative effects. Although I was not able to extrapolate statistical interpretation of these results, the data was still useful since it showed no striking inhibition of cell viability when the NF-κB and calcineurin/NFAT pathways were simultaneously inhibited.

To investigate cooperativity in a more rigorous way, the experiment was performed using fixed ratio drug doses. CalcuSyn software was used to calculate the combination index as a measure of synergism between respective doses of CsA and TPCA-1. Based on Chou and Talalay's statistical measure for drug interactions, CsA and TPCA-1 showed maximum synergy when cells were dosed with 1x their IC50 value, effectively having a lethal effect on the viability of WSU-NHL cells at these concentrations. Although a fraction of 0.5xIC50 concentration was suggestive of having a 'nearly additive' effect of combining the chemical inhibitors, most other drug doses did not indicate significant cooperative effects. Some dose combinations were classified as being antagonistic, however the reasons for this are not understood.

Although synergistic effects were observed in the WSU-NHL cell line tested, for a drug combination to be considered exciting and of potential use in the clinic the combination index values are usually required to be strongly synergistic. An example of this was

demonstrated by Haagensen et al (2012) where the combined treatment of colorectal cell lines with specific MEK and PI3K inhibitors resulted in marked synergy at all fixed IC50 ratio concentrations, where combination index values were almost all less than 0.6 (Haagensen *et al.*, 2012). Nonetheless, reports of synergy between pathways to a lesser degree are also important biological findings and can aid our understanding of interactions between signalling pathways. For example, a study reporting cooperative signalling through STAT3 and NF-κB used CalcuSyn analysis to shown cooperative effects between a Janus Kinase (JAK) inhibitor and the IKK2 inhibitor MLN120B (Lam *et al.*, 2008). The combination index values for some cell lines were in the same category for synergy as those in this study, where synergy was also only observed at specific doses (Lam *et al.*, 2008). Ideally, the CalcuSyn method of experimental setup and data analysis would have been repeated in all cell lines, however it was clear from the previous data that there were no strikingly obvious cooperative effects between CsA and TPCA-1. Moreover, these experiments were not intended to assess the precise drug interaction mechanisms or clinical relevance of these inhibitors. It was therefore decided that the generation of repeat negative data was not time well spent and it would be best to focus on other aspects of the project.

Although we did not observe significant additive or synergistic effects in cells treated with CsA and TPCA-1, it was possible that NFAT and NF-κB may still coordinate joint target genes which are important in lymphoma and so I considered using CsA and TPCA-1 together in a gene expression microarray. This could determine the key genes which function as nodes of integration between these pathways and which are required for lymphoma growth and survival. Ultimately I hoped to evaluate the potential of the proteins encoded by these gene targets to be exploited as future drug targets.

3.2.2. Inhibition of NF-κB

One of the major challenges for this part of the study was finding a selective and reliable NF-κB inhibitor. Previously, I observed no effect on cell viability or NF-κB activity by the selective IKK2 inhibitor PS-1145 which was likely due to its extremely poor solubility (http://www.kinase-screen.mrc.ac.uk/kinase-inhibitors, 2015). Additionally, the biochemical effects of the IKK inhibitor BAY 11-7082 were investigated (data not shown), however no biochemical effects on NF-κB were observed. Interestingly, studies on multiple myeloma cells have comparatively tested NF-κB inhibition using the IKK2

inhibitor TPCA-1 and BAY 11-7082, where BAY 11-7082 was found to induce cell death independently from inhibition of activation of NF-κB (Rauert-Wunderlich *et al.*, 2013). In fact, BAY 11-7082 was recently reported to not inhibit the IKKs at all, but rather targets upstream components of the ubiquitin system by inactivating the E2-conjugating enzymes Ubc (ubiquitin conjugating) 13 and UbcH7 and the E3 ligase LUBAC (linear ubiquitin assembly complex), therefore preventing formation of polyubiquitin chains (Strickson *et al.*, 2013). Due to the poorly selective and off-target effects of BAY 11-7082, this compound was disregarded from the study (Rauert-Wunderlich *et al.*, 2013; Strickson *et al.*, 2013).

Biochemical analysis of NF-κB activation in cells treated with TPCA-1 showed inhibitory effects on NF-κB and the inhibitor also clearly affected the apoptotic machinery of the cell, as indicated by the expression of cleaved PARP. An effect on NF-κB activity would be expected during the period of incubation tested and the concentrations used were similar to published studies (Rauert-Wunderlich *et al.*, 2013). Treatment of multiple myeloma cells with 5μM TPCA-1 for 1 hour for example, has been shown to largely block TNFα-induced phosphorylation and degradation of IκBα, while having no effect on expression of non-canonical markers such as p52 (Rauert-Wunderlich *et al.*, 2013).

Importantly, during this period of the study a report emerged in the literature demonstrating TPCA-1 to be a dual inhibitor of the NF-κB and STAT3 pathways (Nan *et al.*, 2014). STAT3 has been reported to be constitutively activated in ABC DLBCL, where inactivation of STAT3 inhibited proliferation and initiated apoptosis (Ding *et al.*, 2008). In fact, biological interplay between the NF-κB and STAT3 pathways was also established by the Staudt laboratory, where a gene expression signature of IL-6 and IL-10 signalling through STAT3 was found in ABC DLBCLs, reflecting NF-κB activity (Lam *et al.*, 2008). Moreover, inhibition of STAT3 using a JAK inhibitor synergised with an inhibitor of NF-κB signalling (Lam *et al.*, 2008). These studies suggest that the STAT3 and NF-κB pathways may be exploited for the treatments of ABC DLBCL. However, not only does inhibition of STAT3 increase the off target effects of TPCA-1, it also makes it very difficult to compare the response between DLBCL subgroups with different degrees of STAT3 dependency.

With this in mind it was decided that microarray analysis with this inhibitor would no longer be pursued. In fact, during this stage of the study it became apparent that without a reliable and specific inhibitor of NF-κB, the output of a gene expression microarray

may be composed of many off-target effects. It was decided that further investment and time spent validating an effective NF-κB inhibitor was not the primary focus of the project and consequently the strategy and experimental approach for the microarray was reformed. Instead, I aimed to use single agent treatment with CsA to discover novel NFAT target genes which could then be cross-referenced with known, already documented NF-κB target genes, as described in chapter 5. Please note that this decision was also made before the data in figure 32 (which confirmed that TPCA-1 was having an effect in a more sensitive assay than Western Blots) was obtained.

Regardless of this decision, the comprehensive analysis of NF-κB expression and activation in DLBCL cells produced some interesting data. Despite constitutively active NF-κB being associated with the ABC subgroup, high levels of NF-κB expression were also observed in GCB cell lines indicating that NF-κB activity and function may not be restricted to the ABC group. These results were in keeping with studies in the literature, where engagement of both the classical and alternative NF-κB pathways in DLBCL tumour samples were observed in 61% of ABC DLBCL tumour samples and a smaller fraction (30%) of GCB DLBCL (Compagno *et al.*, 2009). Moreover, heterogeneous expression of p52 (as a marker for noncanonical NF-κB activity) was detected in DLBCL cell lines of both ABC and GCB subgroups by Compagno et al (2009) (Compagno *et al.*, 2009). Overall, the heterogeneity of NF-κB expression and activation observed between DLBCL cell lines probably reflects the different mechanisms of pathway activation used by these cells. Future studies would benefit from comprehensively analysing the expression, activation and sensitivity of cell lines to NF-κB inhibition with the underlying genetic abnormalities of cell lines. For example, it would be interesting to correlate cell line NF-κB activity or sensitivity to TPCA-1 with presence of CARD11, CD79B or MYD88 mutations.

3.2.3. Cooperative effects between NFAT and NF-κB

There are a number of explanations as to why we did not see cooperative effects when inhibiting the NFAT and NF-κB pathways. First, it is possible that both transcription factors bind to the same gene promoters, co-regulating their expression. Chemical depletion of a gene which has already been depleted by either CsA or TPCA-1 treatment alone may not cause additional effects on cell viability. There is evidence for a group of κB-like DNA binding motifs of which both transcription factors bind, such as the CD28-

responsive element of the *IL2* promoter (Maggirwar *et al.*, 1997; Zhou *et al.*, 2002b). However, the structural basis of synergy of NFATs with other transcription factors remains an area that is largely unexplored.

Although there is currently no experimental evidence for the formation of NFAT/NF-κB heterodimers, cooperative binding of NFAT with other transcription factors is frequently observed in various systems (Chen *et al.*, 1998). In 2005, Pham et al were the first researchers to demonstrate a cooperative interaction between NF-κB and NFAT family members in B-cell lymphoma (Pham *et al.*, 2005). They demonstrated that NFAT2 and c-Rel proteins interact with each other at the CD154 (CD40 ligand) promoter by binding simultaneously to two sites; the distal CD154 κB site and the proximal NFAT site (Pham *et al.*, 2005). Pham et al further suggested that the promoter DNA may 'loop or bend to form an enhanceosome-like complex that synergistically regulates CD154 gene expression' (Pham *et al.*, 2005). This phenomenon has been reported at the promoter of IFN-β, where an ordered recruitment of chromatin modifying and transcription factors generated an enhanceosome complex (Agalioti *et al.*, 2000).

In contrast to these findings, a recent study argued that NFAT and NF-κB do not interact or collaborate when they bind to DNA (Muhammad *et al.*, 2014). Muhammad et al (2014) showed that the NF-κB subunits p50 and c-Rel controlled the induction of the NFAT2/αA short isoform in BCR-induced splenic B cells (Muhammad *et al.*, 2014). Ablation of c-Rel or p50 led to a suppressive effect on NFAT2, which consequently (due to inhibition of the positive autoregulatory loop) caused the loss of induction of the short NFAT2/αA isoform (Muhammad *et al.*, 2014). Researchers identified two NFAT/NF-κB binding sites in the P1 region of the inducible NFATC1 promoter which results in a persistent induction of NFAT2/αA by BCR signals (Serfling *et al.*, 2004; Muhammad *et al.*, 2014).

Since NFAT2/αA is known to play a key role in the proliferation and survival of lymphocytes, it is possible that this isoform is a potential novel target in malignancies with dysregulated NF-κB or NFAT signalling. Although the study by Muhammad et al (2014) does not fit with the reported evidence for synergy by means of coordinate regulation of NF-κB and NFAT target genes, these data provided further evidence for a close connection between NFAT2 and NF-κB induction in peripheral B-lymphocytes.

In their publication, Muhammad et al (2014) are critical of the study showing coordinate regulation of CD154 by NFAT and NF-κB by Pham et al (2005). They argue that their

use of conventional EMSAs and co-precipitation of NFAT2 by an antibody specific for c-Rel only suggest interplay between NFAT2 and NF-κB (Muhammad *et al.*, 2014). Muhammad *et al* highlight that use of overexpression of NFAT and NF-κB by Pham et al does not allow consideration of possible interactions in normal physiological conditions (Muhammad *et al.*, 2014). Also to be questioned is whether the protein-protein interactions described by Pham et al (2005) actually affect their DNA binding activity and subsequent regulation of genes (Pham *et al.*, 2005; Muhammad *et al.*, 2014).

In summary, the results in this chapter suggest that simultaneous depletion of the NFAT and NF-κB pathways using CsA and TPCA-1 does not have substantial additive or synergistic effects on cell viability. Additionally, I experienced difficulty finding an effective, specific NF-κB inhibitor for gene expression microarray analysis. These data consequently prompted me to investigate cooperativity and combined target genes by alternative methods. Finally, analysis of NF-κB expression and activation in a comprehensive panel of DLBCL cell lines produced interesting data, some of which may be useful sources of reference for the lab in the future. Based on the data described in this chapter, it was decided that I would proceed with a gene expression microarray using CsA alone.

Chapter 5.

Gene expression microarray analysis to investigate calcineurin/NFAT target genes

4. Gene expression microarray analysis to investigate calcineurin/NFAT target genes

4.1. Introduction

The role of the NFAT transcription factor family is well studied in T cells and in immune activation, however, less is known about NFAT function in B cells, especially in the malignant setting. Activation and overexpression of NFAT has been implicated in an array of cancers, including haematopoietic malignancies such as DLBCL (Marafioti *et al.*, 2005; Pham *et al.*, 2005; Fu *et al.*, 2006; Pham *et al.*, 2010). Of the few NFAT target genes reported in lymphoma, most are involved in lymphocyte survival (such as CD40L and BLyS) and proliferation (such as c-Myc), indicating that some NFAT family members are oncogenic and could be targets for therapeutic intervention (Pham *et al.*, 2005; Fu *et al.*, 2006; Pham *et al.*, 2010).

Prior to this study, a comprehensive analysis of the transcriptional targets of NFAT in DLBCL had not been investigated, highlighting an area of unexplored research. In this study, I aimed to identify primary NFAT target genes by gene expression microarray analysis using the Illumina Human HT-12v4 Expression BeadChip array, as described in chapter 2, section 2.5. Two ABC DLBCL cell lines (HLY-1 and U2932) and one GCB DLBCL cell line (WSU-NHL) were chosen as appropriate cell lines based on data in chapter 3. To investigate changes in gene expression affected by calcineurin/NFAT inhibition, cells were treated with their respective IC50 concentration of CsA for two timepoints (2 and 6 hours) in 4 independent biological repeat experiments. These samples, used for the microarray were those showing effective drug treatment from previous experiments (figure 20). In addition to identifying potential NFAT gene targets, I aimed to analyse potential differences between NFAT-mediated gene regulation between ABC and GCB DLBCL cell lines.

4.2. Results

4.2.1. Normalisation and Quality Control

Data from the gene expression microarray was analysed by Dr Simon Cockell from the Bioinformatics Support Unit, Newcastle University. Firstly, of the 47,231 probes on the microarray, 24,493 probes passed the detection P-value threshold (0.01) on at least one array, allowing 51.9% of the total number of probes to be taken forward for analysis.

Next, to achieve sample- and probe-level filtering, analysis included a series of quality control steps. The data from all 48 samples in the array were first transformed to log2 space via a variance stabilising transformation, as described by Lin et al (2008) (Lin *et al.*, 2008). Using the robust spline normalisation algorithm that was designed for Bead-array data, the data was normalised, as shown in the box plot in appendix figure 2 (Du *et al.*, 2008).

Subsequently, samples underwent principal component analysis (PCA), which is a dimension reduction technique that allows the multivariate data to be projected and visualised on a two-dimensional plot (figure 33). This statistical procedure converts a set of observations that are possibly correlated, into a set of values of linearly uncorrelated variables called principal components. The first principal component accounts for as much variability in the data as possible (x-axis), whereas the second component (y-axis) has the highest possible variance that is statistically independent of the first component (Rencher, 2003).

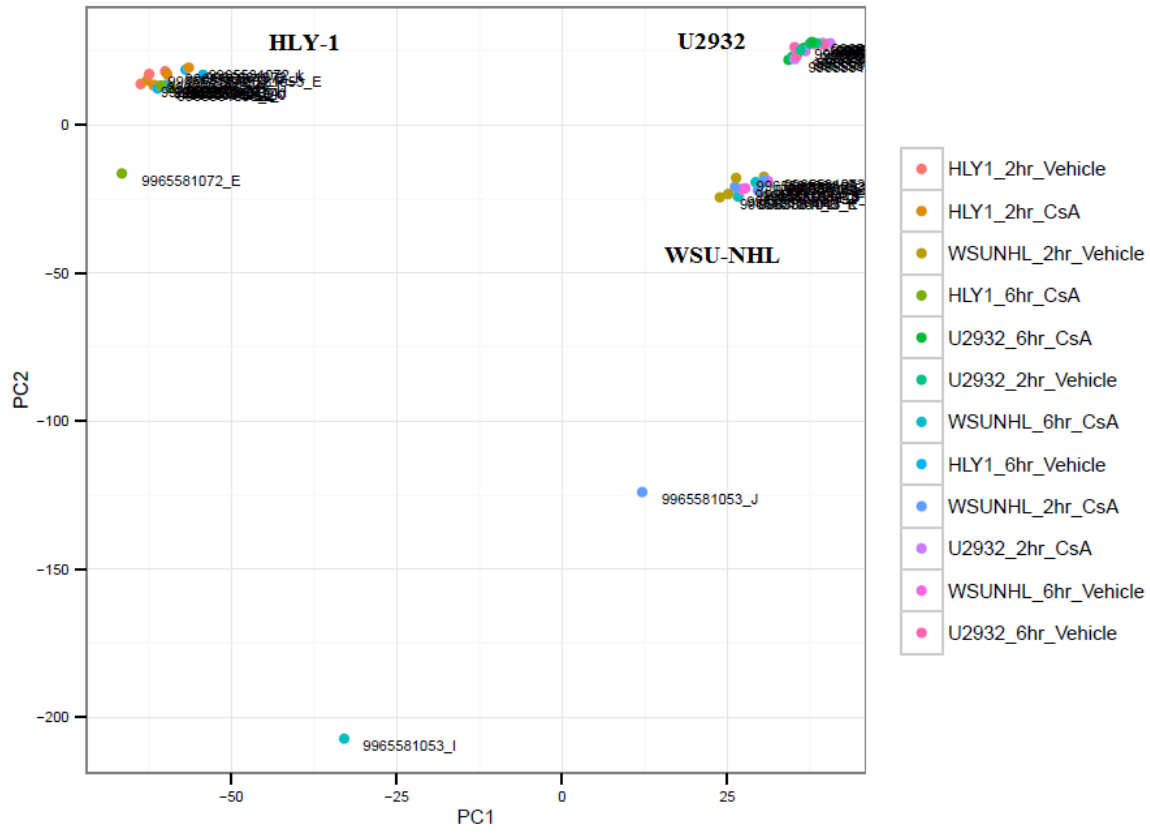

Figure 33. Principle component analysis for gene expression microarray data. A scatterplot of the microarray data along the two first two principle components. Clusters of samples represent samples which responded similarly to others in the cohort and are labelled as either HLY-1, U2932 or WSU-NHL cells. Three outlier samples were identified. The colour-coded key to the right of the figure indicates individual samples and their respective treatment conditions.

Here, the spacial arrangement of the samples reflects their overall similarities or dissimilarities in the array. Samples were colour coded by the experimental groups they fell into, allowing identification of samples that responded similarly to others in their cohort as well as samples that were outliers. Using the first two principal components (PC1 and PC2), the PCA scatterplot in figure 33 shows three clusters of samples, which individually represent each of the three cell lines used in the array. Three samples were noticeably separate from the three groupings in the dataset and were recorded as outliers. Although the presence of outliers implies underlying experimental or biological problems, their occurrence in datasets this large are expected. Sample outliers included a sample from HLY-1 cells (6hr CsA, experimental repeat 3/4, chip 3/4), WSU-NHL cells (6hr CsA, experimental repeat 3/4, chip 1/4) and WSU-NHL cells (2hr CsA, experimental repeat 4/4, chip 1/4). Although all three outliers were treated with CsA, there was no uniform association with a particular experimental repeat or microarray chip. However,

to remove erroneous data, these samples and their partners were excluded from further analysis of the microarray.

4.2.2. Overview of statistically significant genes differentially expressed in DLBCL cells treated with CsA

Table 11 shows an overview of the number of genes with statistical significance (adjusted P-value <0.05), after multiple testing correction (using Benjamini-Hochberg FDR correction), that were either upregulated or downregulated by treatment with CsA (Benjamini, 1995). A 1.3 fold-change (FC) cut-off was used here and throughout the rest of the study.

The number of differentially expressed genes listed overall is surprisingly low, especially in the GCB DLBCL cell line WSU-NHL. In fact, initial analysis of the data set as a whole, revealed a high number of genes which were differentially expressed with a fold-change greater than 1.3, but with insignificant adjusted P-values (data not shown). There are a number of possible reasons for this, such as the short duration of calcineurin/NFAT inhibition or a lack of sensitivity of the array when detecting changes to low abundance mRNA. Increasing the incubation period of cells treated with CsA would likely have revealed more differentially expressed genes. However, my aim was to identify primary NFAT target genes, rather than genes which may have been up- or downregulated as a secondary response to calcineurin/NFAT inhibition.

Table 11 shows a time-dependent increase in genes differentially expressed in U2932 and HLY-1 cell lines. Generally, after two hours, there were more genes downregulated by CsA compared to upregulated. However, by 6 hours of calcineurin/NFAT inhibition, there were generally more genes upregulated by CsA treatment, indicating that these genes (which NFAT may normally downregulate) were slower to respond to chemical inhibition of this pathway.

a)

U2932		Unpaired		Paired	
Timepoint	**Expression**	**Genes**	**Total**	**Genes**	**Total**
2hr	Downregulated	7	9	2	2
	Upregulated	2		0	
6hr	Downregulated	25	123	133	347
	Upregulated	98		214	

b)

HLY-1		Unpaired		Paired	
Timepoint	**Expression**	**Genes**	**Total**	**Genes**	**Total**
2hr	Downregulated	12	14	28	36
	Upregulated	2		8	
6hr	Downregulated	17	29	52	153
	Upregulated	12		101	

c)

WSU-NHL		Unpaired		Paired	
Timepoint	**Expression**	**Genes**	**Total**	**Genes**	**Total**
2hr	Downregulated	0	0	0	0
	Upregulated	0		0	
6hr	Downregulated	1	4	0	0
	Upregulated	3		0	

Table 11. Overview of statistically significant genes differentially expressed in DLBCL cells treated with CsA. Data indicates the number of statistically significant gene probes (adjusted P-value <0.05) differentially expressed upon treatment with CsA for 2hrs and 6hrs in the ABC DLBCL cell lines U2932 (a), HLY-1 (b) and the GCB DLBCL cell line WSU-NHL (c). Data includes genes identified from both unpaired and paired data analysis. Orange indicates genes downregulated by CsA, whereas blue indicates genes upregulated by CsA. Data includes occasional probes marked as N/A.

Surprisingly, there were no statistically significant genes identified in WSU-NHL cells at the 2 hour timepoint and only 4 genes were revealed by unpaired analysis after 6 hours CsA treatment (table 11, c). It is possible that WSU-NHL cells may have a slower acting response to inhibition of calcineurin/NFAT signalling. It would be of interest in the future to perform microarray analysis on these cells with a longer incubation of CsA. On the other hand, it is possible that calcineurin/NFAT signalling regulates fewer target genes in

this GCB cell line compared to the two ABC cell lines. This hypothesis is explored in subsequent sections of this chapter.

4.2.3. Differences between unpaired and paired data analysis

During initial analysis of the array, both unpaired and paired methods of analysis were used. In summary, unpaired data analysis is applied to two independent groups e.g. vehicle control samples versus CsA-treated samples. It compares the mean of the entire set of vehicle control samples to the mean of the entire set of CsA-treated samples. This type of analysis assumes that the data is from a normal distribution and that the standard deviation is approximately the same in both groups. Paired data analysis on the other hand, is derived from study subjects, or samples, which have been subjected to two separate measurements. In this case, pairs were based on samples prepared in each of the four repeat experiments, where paired data analysis compared individual vehicle control samples with their specific CsA-treated partner.

Interestingly, the number of genes identified was highly dependent on the way in which the data was analysed. For example, one of the most striking differences between paired and unpaired analysis was in the HLY-1 6 hour timepoint, where paired analysis produced 153 differentially expressed genes compared to only 29 genes by unpaired analysis (table 11, b).

As described in the methods section (chapter 2, section 2.5), the 48 RNA samples sent for microarray analysis were randomised prior to shipping. Samples were then hybridised across four chips, containing twelve samples per chip. Although each of the four experimental repeats could have fitted nicely on one chip, it was decided that randomisation of samples was a more suitable method. The aim was to avoid chip-to-chip variability, which could ultimately skew an entire experimental repeat. Should one repeat experiment be different from the rest, the mean of an entire set of vehicle controls, for example, could be skewed, having a negative impact on unpaired data analysis. Randomisation of samples, however, meant that it was very unlikely that sample pairs, from specific experimental repeats, were on the same chip.

After analysing the data using unpaired analysis, and obtaining a very low number of differentially expressed genes, it seemed possible that paired analysis may be more useful. Although this was true for all samples in some cell lines, such as HLY-1 (table 11b), this

did not appear true for other cell lines. This may be due to the fact that randomisation of samples may still be affected by differences between the readings of particular chips, upon which a particular sample partner may be hybridised.

To gain a better insight into which type of analysis was best for this study, genes from the two methods of analysis were compared between treatment time points for U2932 and HLY-1 cells. Due to the absence of genes identified in the analysis of WSU-NHL, this cell line was not included. As shown by the Venn diagrams in figure 34 and figure 35, in HLY-1 cells, paired analysis produced many more genes of interest when compared to unpaired analysis. This was apparent at both time points, where only a fairly small number of genes were shared between the two methods of analysis.

In contrast, in U2932 cells, at the 2 hour timepoint, unpaired data analysis produced more statistically significant genes than paired analysis, as shown in figure 36. In fact, after two hours CsA, only one gene (CCL4L2) was significant by paired analysis (figure 37). CCL4L2 was also identified by unpaired analysis, which included 6 additional genes. By 6 hours CsA treatment however, far more genes were produced by paired analysis in U2932 compared to unpaired analysis. Although 99 genes at the 6 hour timepoint were common between the two methods of analysis, considerably more genes (186) were generated by paired analysis alone (figure 37).

Overall, there were clear differences in the genes generated by paired versus unpaired analysis, where analysis in some cell lines and samples produced a much larger dataset of significantly up- or downregulated genes. Due to the overall lack of overlapping genes, it was not clear which analysis type was best. It was therefore decided that the data generated from both methods of analysis would be considered for experimental confirmation and validation of the array.

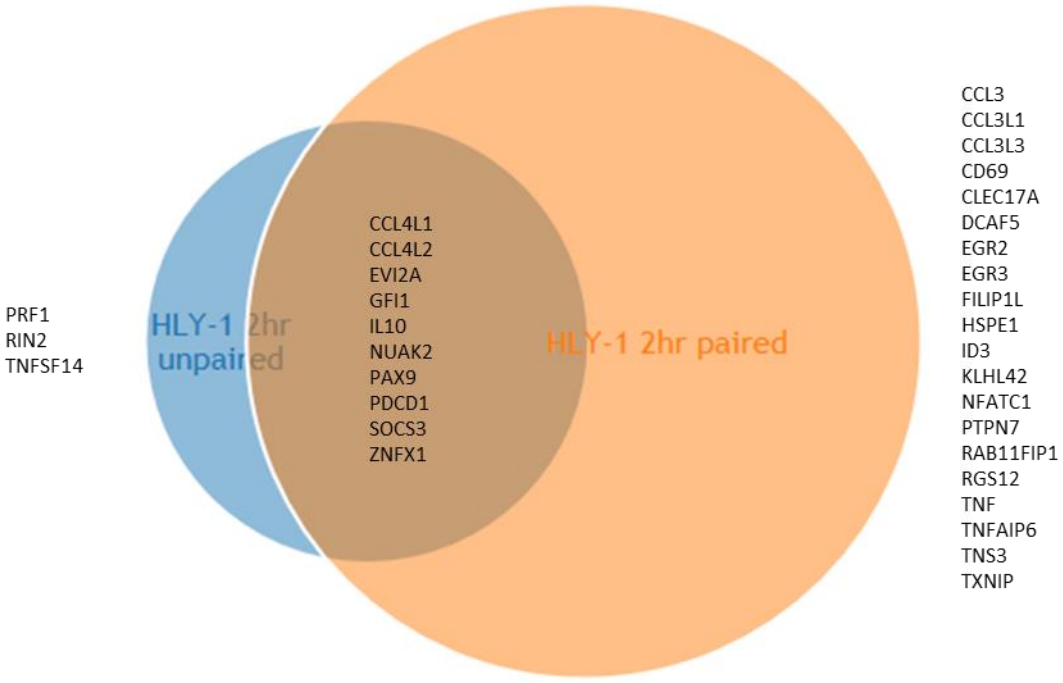

Figure 34. Paired data analysis produced more statistically significant genes that unpaired analysis in HLY-1 cells treated with CsA for 2hrs. The Venn diagram compares statistically significant, differentially expressed genes (adjusted P-value <0.05) analysed by unpaired (blue) or paired (orange) in HLY-1 cells treated with CsA for 2hrs. Data excludes gene probes marked as N/A.

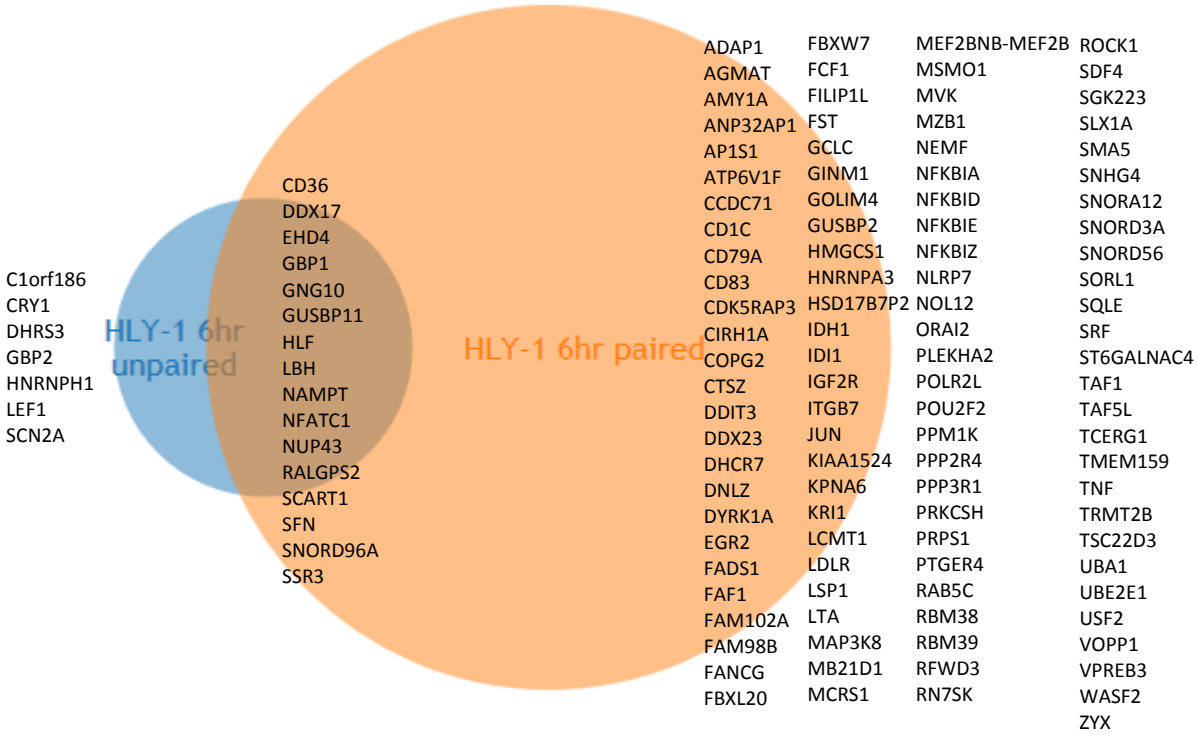

Figure 35. Paired data analysis produced more statistically significant genes that unpaired analysis in HLY-1 cells treated with CsA for 6hrs. The Venn diagram compares statistically significant, differentially expressed genes (adjusted P-value <0.05) analysed by unpaired (blue) or paired (orange) in HLY-1 cells treated with CsA for 6hrs. Data excludes gene probes marked as N/A.

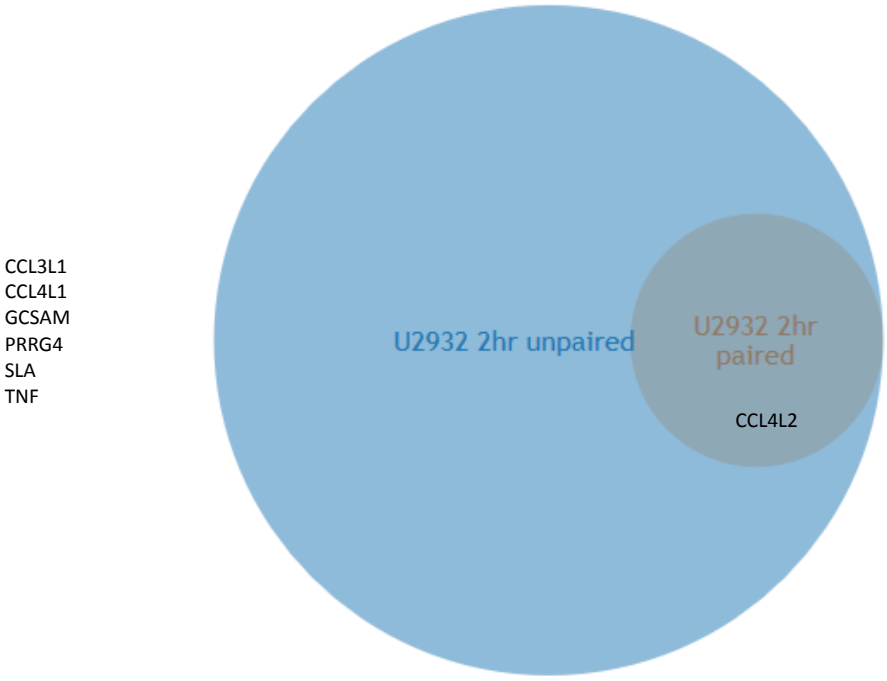

Figure 36. Unpaired data analysis produced more statistically significant genes that unpaired analysis in U2932 cells treated with CsA for 2hrs. The Venn diagram compares statistically significant, differentially expressed genes (adjusted P-value <0.05) analysed by unpaired (blue) or paired (orange) in U2932 cells treated with CsA for 2hrs. Data excludes gene probes marked as N/A.

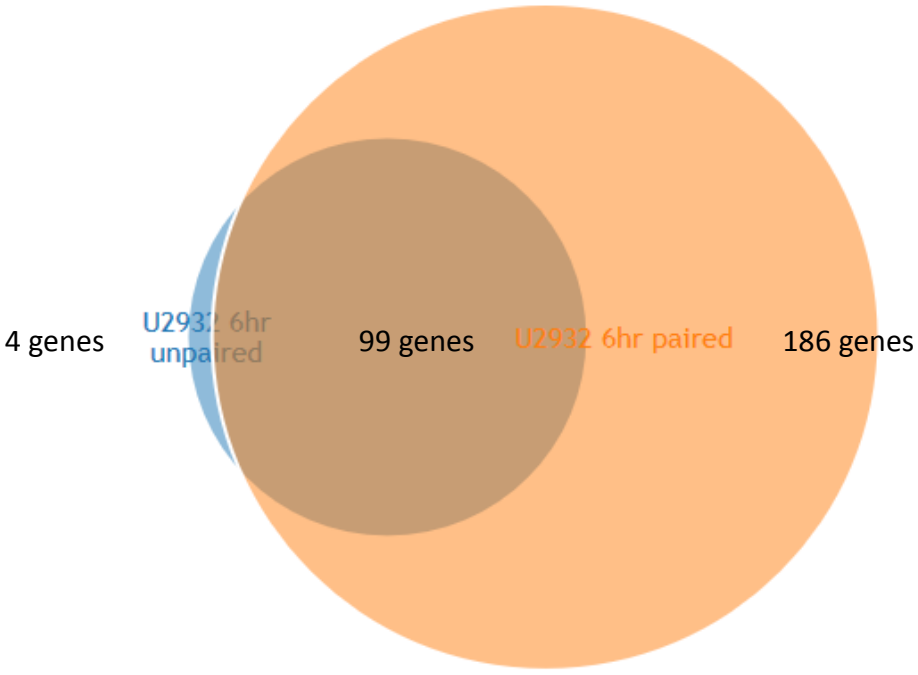

Figure 37. Paired data analysis produced more statistically significant genes that unpaired analysis in U2932 cells treated with CsA for 6hrs. The Venn diagram compares statistically significant, differentially expressed genes (adjusted P-value <0.05) analysed by unpaired (blue) or paired (orange) in U2932 cells treated with CsA for 6hrs. Data excludes gene probes marked as N/A.

4.2.4. Heat-map analysis of genes differentially expressed in HLY-1 and U2932 cells treated with CsA

As discussed previously, analysis of the array produced far more significantly relevant genes in the two ABC DLBCL cell lines U2932 and HLY-1, compared to the GCB cell line WSU-NHL. The heat-map in figure 38 shows the relative differential expression of these genes in the two ABC cell lines at both time points by paired analysis. Although there were some similarities between cell lines, this data indicates many differences between calcineurin/NFAT-regulated expression of certain genes. The Filamin A Interacting Protein 1-like gene (FILIP1L), for example, was significantly downregulated in HLY-1 cells after both 2 and 6 hours treatment with CsA, but not in U2932 cells. For many other genes, such as IL-10 and PCK2, expression was up- or downregulated at just one timepoint, indicating that NFAT may regulate these genes very transiently.

Figure 39, on the other hand, shows the relative differential expression of genes in ABC cell lines analysed by unpaired data analysis. Some genes, such as PKC2, demonstrated similar differential expression to paired analysis. However, other genes, such as EGR2 and EGR3 (which were significantly downregulated by CsA in some samples analysed by paired analysis) were not identified as significant by unpaired analysis. Similar to paired analysis however, most genes were significantly upregulated or downregulated at just one timepoint for each cell line. Exceptions to this however, were demonstrated in U2932 cells, were CCL3L1, CCL4L1, CCL4L2 and SLA were downregulated at both timepoints in U2932 cells.

Moreover, both heat maps highlight the striking number of genes upregulated by CsA in U2932 cells, suggesting that NFAT may have a key role in suppressing the expression of these genes.

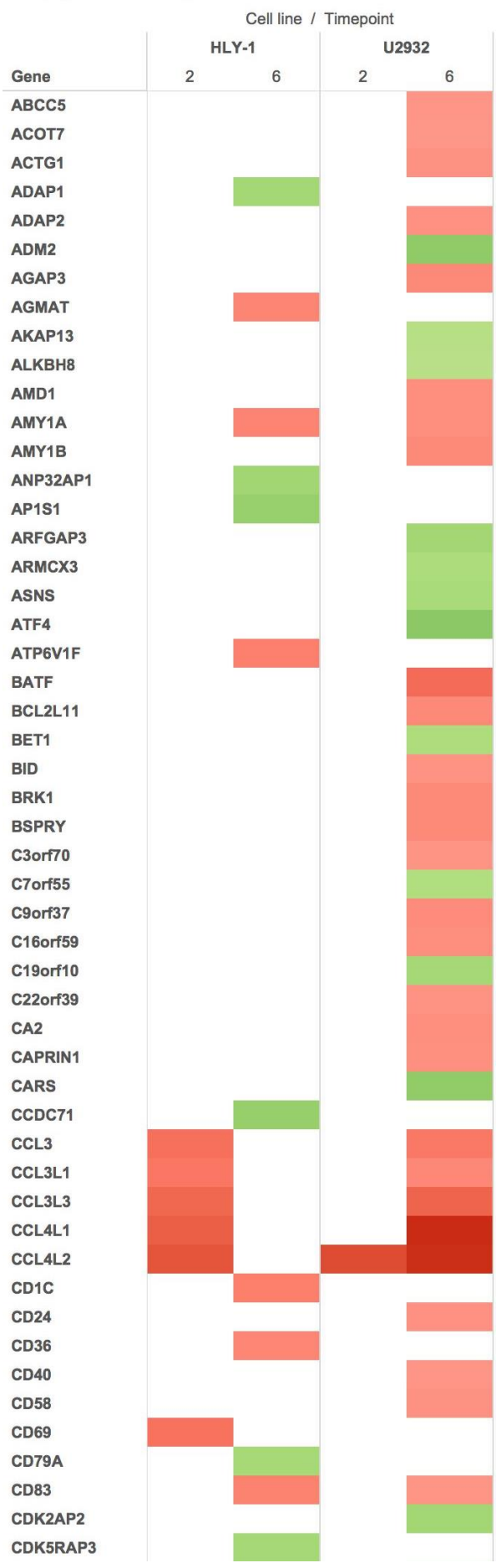
Cell line / Timepoint
HLY-1
U2932
Gene
2
6
2
6
ABCC5
ACOT7
ACTG1
ADAP1
ADAP2
ADM2
AGAP3
AGMAT
AKAP13
ALKBH8
AMD1
AMY1A
AMY1B
ANP32AP1
AP1S1
ARFGAP3
ARMCX3
ASNS
ATF4
ATP6V1F
BATF
BCL2L11
BET1
BID
BRK1
BSPRY
C3orf70
C7orf55
C9orf37
C16orf59
C19orf10
C22orf39
CA2
CAPRIN1
CARS
CCDC71
CCL3
CCL3L1
CCL3L3
CCL4L1
CCL4L2
CD1C
CD24
CD36
CD40
CD58
CD69
CD79A
CD83
CDK2AP2
CDK5RAP3

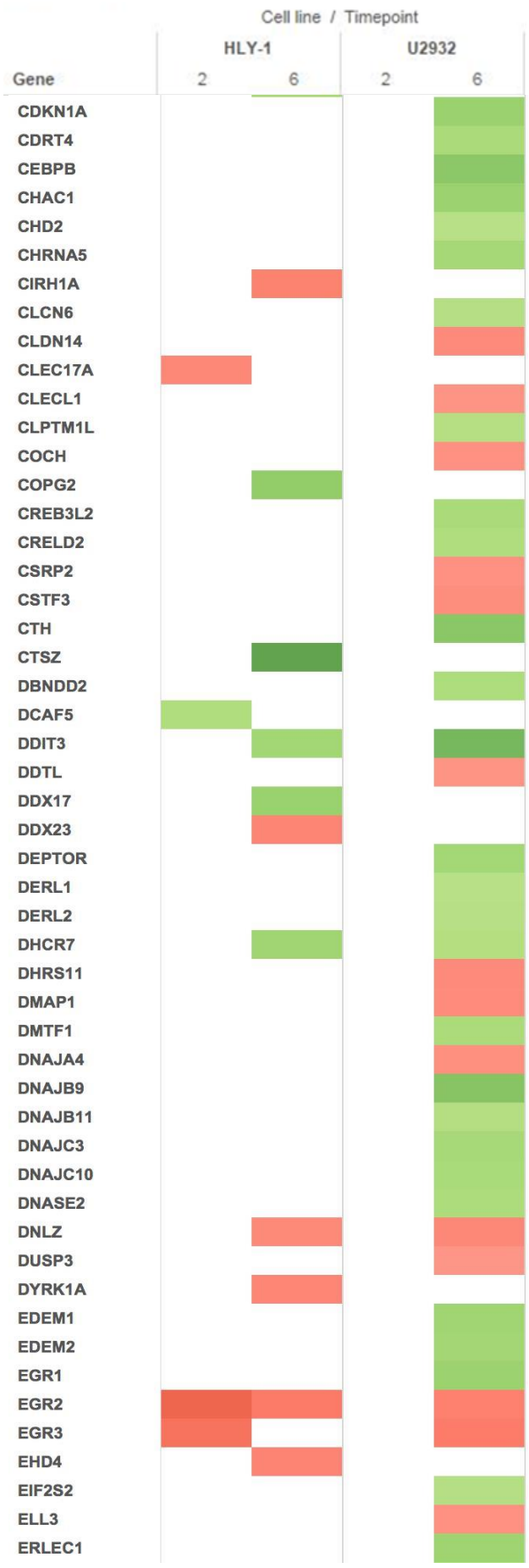
Cell line / Timepoint
HLY-1
U2932
Gene
2
6
2
6
CDKN1A
CDRT4
CEBPB
CHAC1
CHD2
CHRNA5
CIRH1A
CLCN6
CLDN14
CLEC17A
CLECL1
CLPTM1L
COCH
COPG2
CREB3L2
CRELD2
CSRP2
CSTF3
CTH
CTSZ
DBNDD2
DCAF5
DDIT3
DDTL
DDX17
DDX23
DEPTOR
DERL1
DERL2
DHCR7
DHRS11
DMAP1
DMTF1
DNAJA4
DNAJB9
DNAJB11
DNAJC3
DNAJC10
DNASE2
DNLZ
DUSP3
DYRK1A
EDEM1
EDEM2
EGR1
EGR2
EGR3
EHD4
EIF2S2
ELL3
ERLEC1

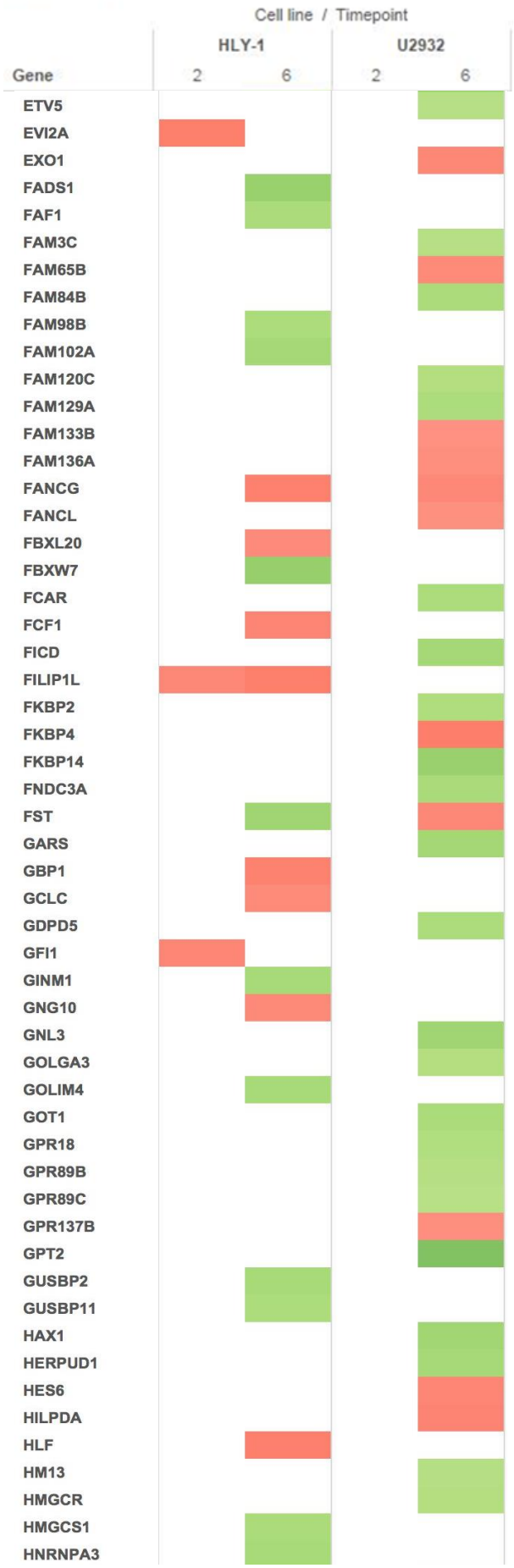
Cell line / Timepoint
HLY-1
U2932
Gene
2
6
2
6
ETV5
EVI2A
EXO1
FADS1
FAF1
FAM3C
FAM65B
FAM84B
FAM98B
FAM102A
FAM120C
FAM129A
FAM133B
FAM136A
FANCG
FANCL
FBXL20
FBXW7
FCAR
FCF1
FICD
FILIP1L
FKBP2
FKBP4
FKBP14
FNDC3A
FST
GARS
GBP1
GCLC
GDPD5
GFI1
GINM1
GNG10
GNL3
GOLGA3
GOLIM4
GOT1
GPR18
GPR89B
GPR89C
GPR137B
GPT2
GUSBP2
GUSBP11
HAX1
HERPUD1
HES6
HILPDA
HLF
HM13
HMGCR
HMGCS1
HNRNPA3

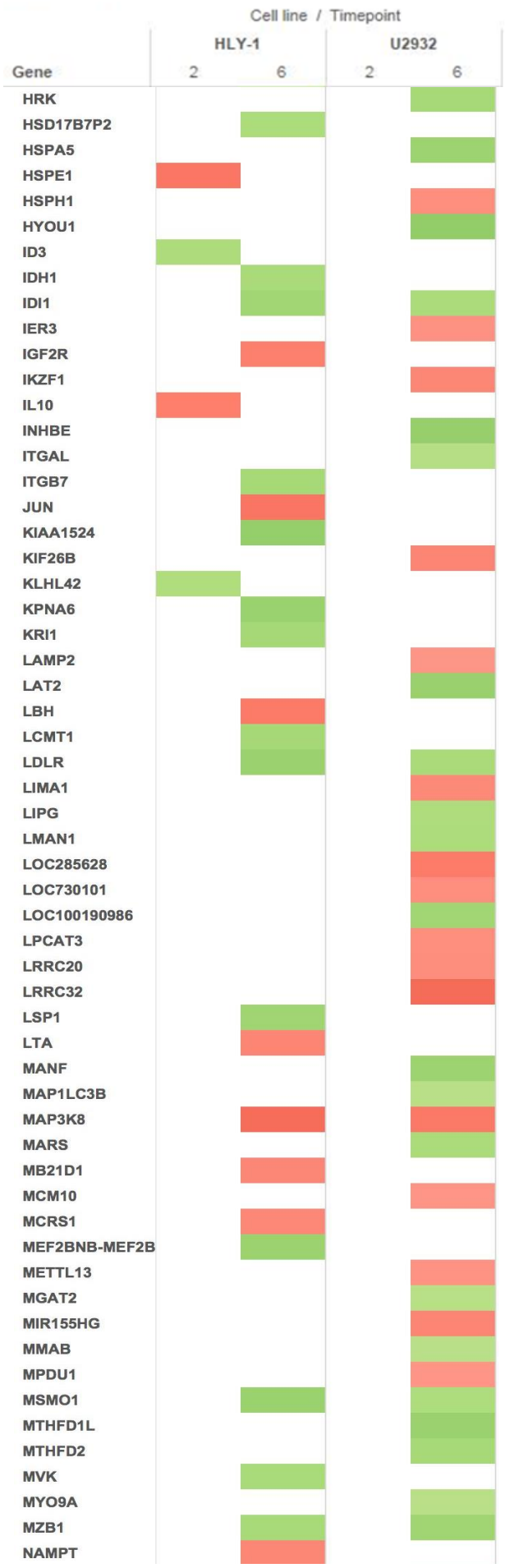
Cell line / Timepoint
HLY-1
U2932
Gene
2
6
2
6
HRK
HSD17B7P2
HSPA5
HSPE1
HSPH1
HYOU1
ID3
IDH1
IDI1
IER3
IGF2R
IKZF1
IL10
INHBE
ITGAL
ITGB7
JUN
KIAA1524
KIF26B
KLHL42
KPNA6
KRI1
LAMP2
LAT2
LBH
LCMT1
LDLR
LIMA1
LIPG
LMAN1
LOC285628
LOC730101
LOC100190986
LPCAT3
LRRC20
LRRC32
LSP1
LTA
MANF
MAP1LC3B
MAP3K8
MARS
MB21D1
MCM10
MCRS1
MEF2BNB-MEF2B
METTL13
MGAT2
MIR155HG
MMAB
MPDU1
MSMO1
MTHFD1L
MTHFD2
MVK
MYO9A
MZB1
NAMPT

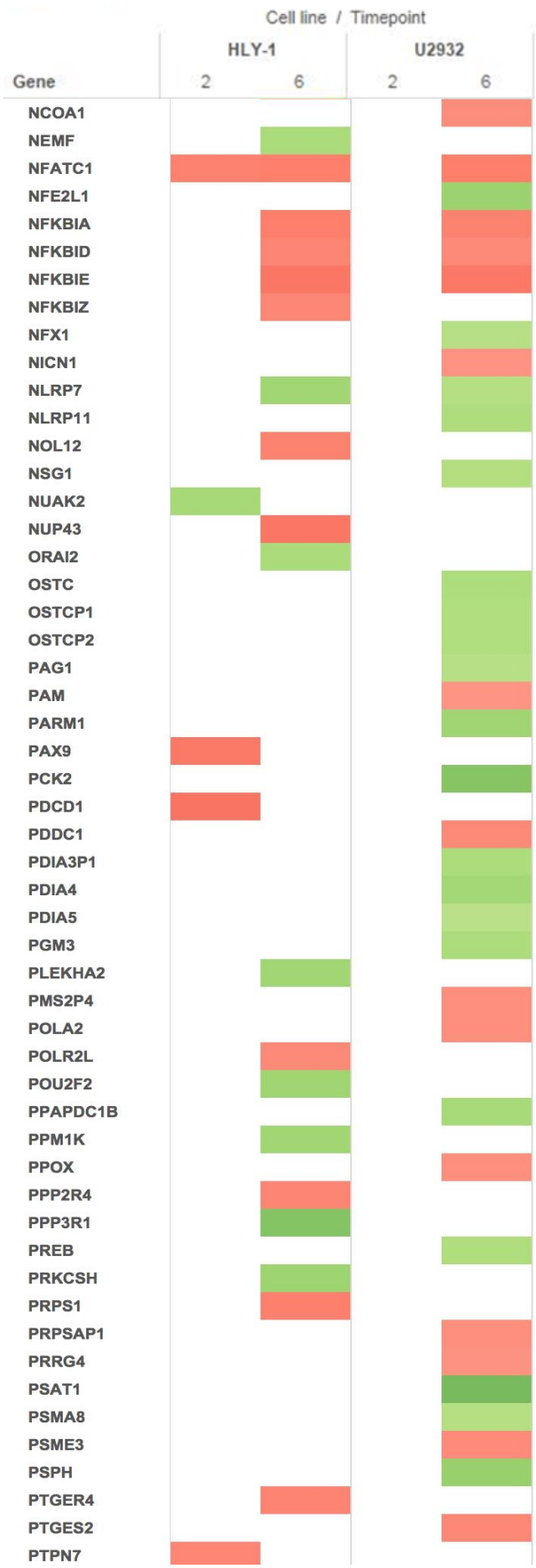
Cell line / Timepoint
HLY-1
U2932
Gene
2
6
2
6
NCOA1
NEMF
NFATC1
NFE2L1
NFKBIA
NFKBID
NFKBIE
NFKBIZ
NFX1
NICN1
NLRP7
NLRP11
NOL12
NSG1
NUAK2
NUP43
ORAI2
OSTC
OSTCP1
OSTCP2
PAG1
PAM
PARM1
PAX9
PCK2
PDCD1
PDDC1
PDIA3P1
PDIA4
PDIA5
PGM3
PLEKHA2
PMS2P4
POLA2
POLR2L
POU2F2
PPAPDC1B
PPM1K
PPOX
PPP2R4
PPP3R1
PREB
PRKCSH
PRPS1
PRPSAP1
PRRG4
PSAT1
PSMA8
PSME3
PSPH
PTGER4
PTGES2
PTPN7

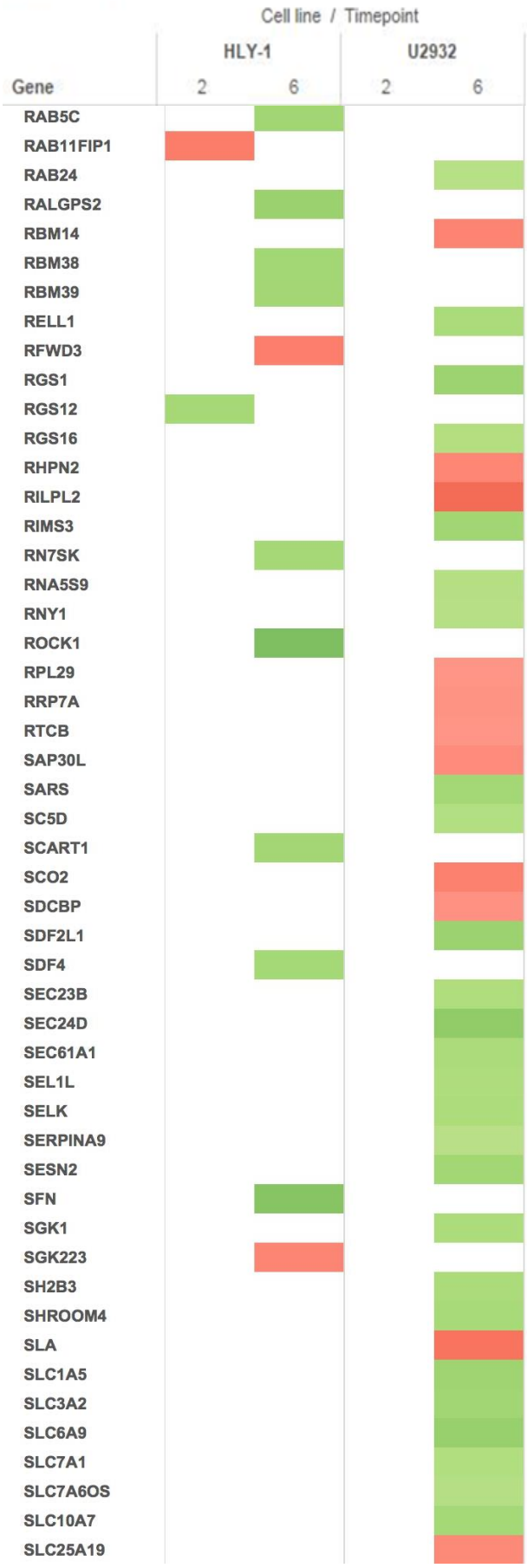
Cell line / Timepoint
HLY-1
U2932
Gene
2
6
2
6
RAB5C
RAB11FIP1
RAB24
RALGPS2
RBM14
RBM38
RBM39
RELL1
RFWD3
RGS1
RGS12
RGS16
RHPN2
RILPL2
RIMS3
RN7SK
RNA5S9
RNY1
ROCK1
RPL29
RRP7A
RTCB
SAP30L
SARS
SC5D
SCART1
SCO2
SDCBP
SDF2L1
SDF4
SEC23B
SEC24D
SEC61A1
SEL1L
SELK
SERPINA9
SESN2
SFN
SGK1
SGK223
SH2B3
SHROOM4
SLA
SLC1A5
SLC3A2
SLC6A9
SLC7A1
SLC7A6OS
SLC10A7
SLC25A19

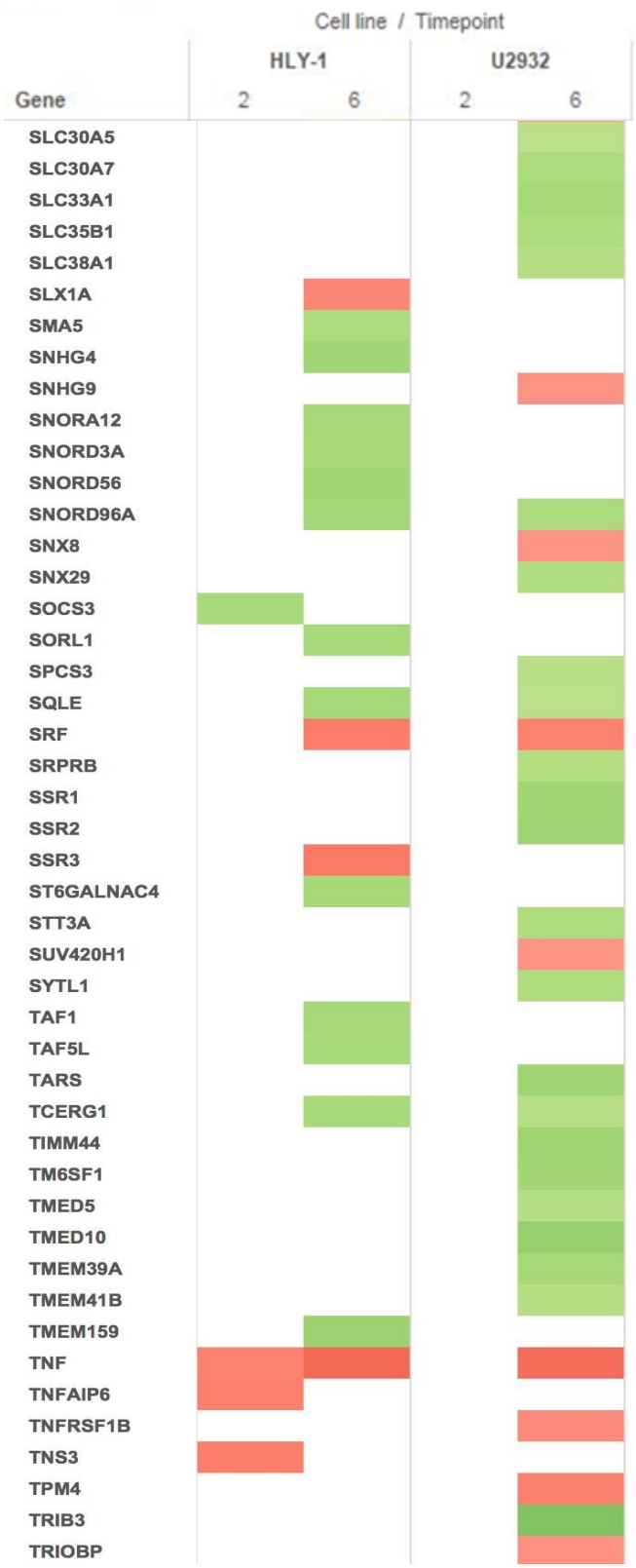
Cell line / Timepoint
HLY-1
U2932
Gene
2
6
2
6
SLC30A5
SLC30A7
SLC33A1
SLC35B1
SLC38A1
SLX1A
SMA5
SNHG4
SNHG9
SNORA12
SNORD3A
SNORD56
SNORD96A
SNX8
SNX29
SOCS3
SORL1
SPCS3
SQLE
SRF
SRPRB
SSR1
SSR2
SSR3
ST6GALNAC4
STT3A
SUV420H1
SYTL1
TAF1
TAF5L
TARS
TCERG1
TIMM44
TM6SF1
TMED5
TMED10
TMEM39A
TMEM41B
TMEM159
TNF
TNFAIP6
TNFRSF1B
TNS3
TPM4
TRIB3
TRIOBP

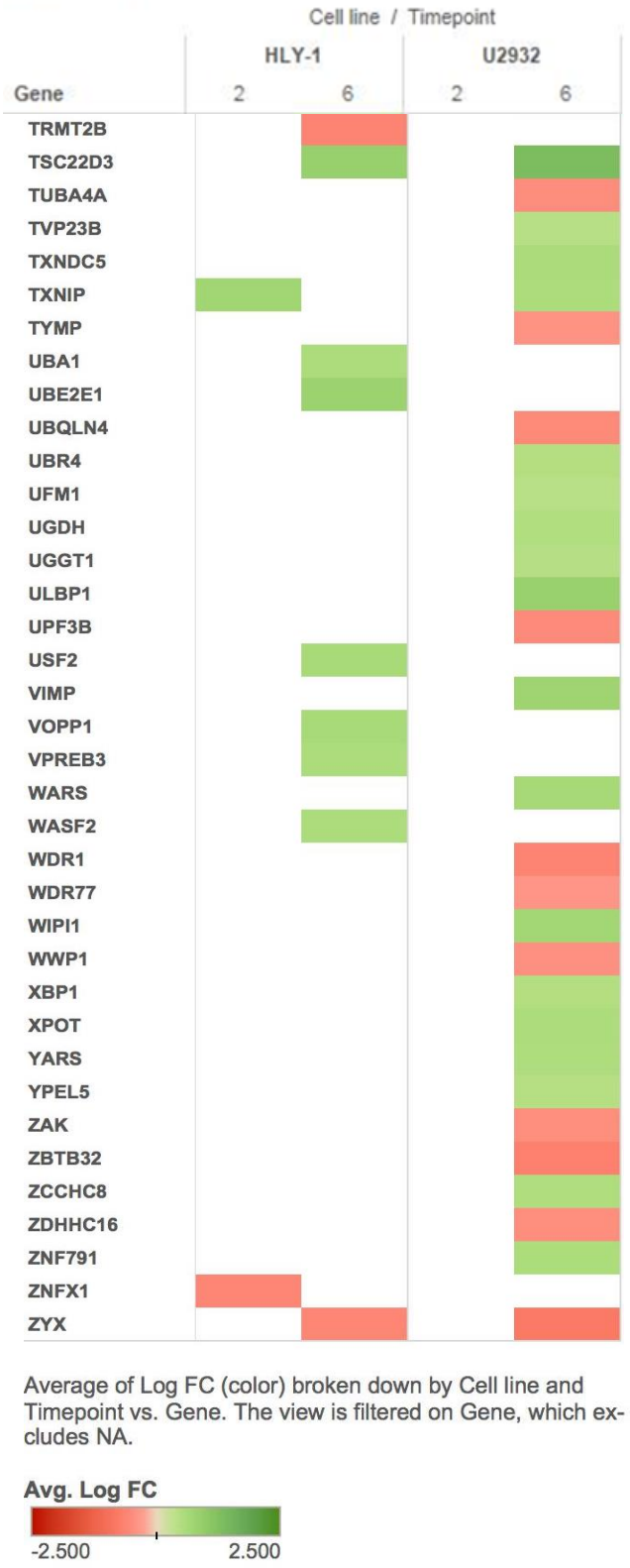

Figure 38 (Continued from previous 7 pages). Heat-map analysis of genes differentially expressed in HLY-1 and U2932 cells treated with CsA (paired analysis). The heat-map compares the statistically significant genes (adjusted P-value <0.05) which were differentially expressed in HLY-1 and U2932 cells treated with CsA for 2 and 6 hours. Red indicates genes which were downregulated by CsA, whereas green indicates genes that were upregulated by CsA. The intensity of the colour signifies the degree to which genes were differentially expressed where a deeper colour represents a greater extent of differential expression. Genes are listed in alphabetical order. Data excludes gene probes marked as N/A. For genes where there were more than one probe, the average FC was used.

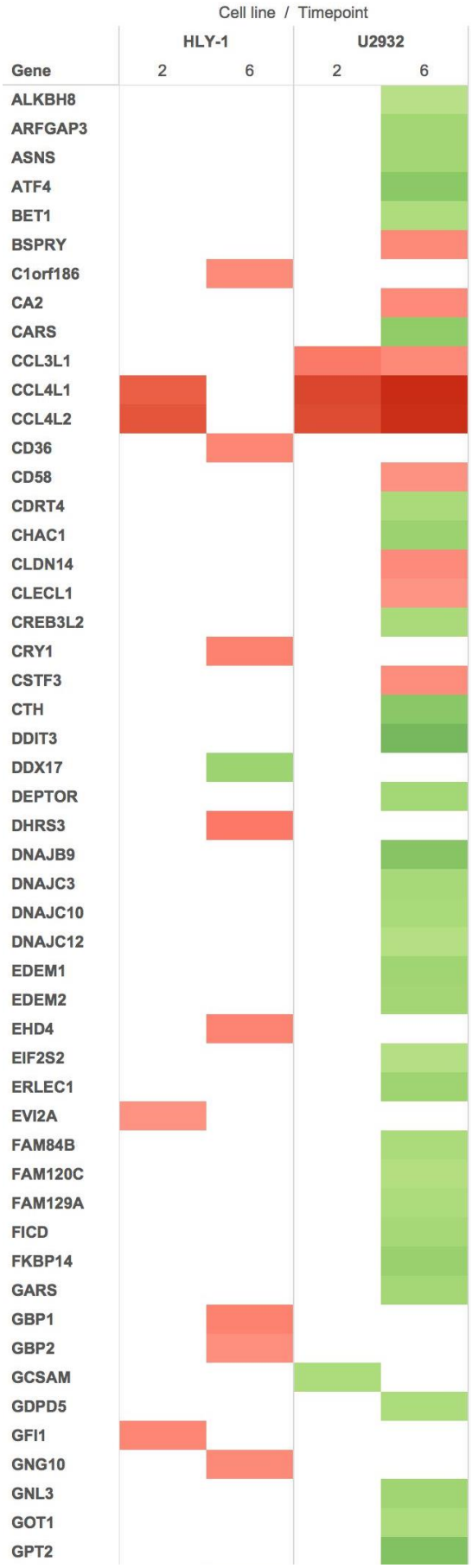
Cell line / Timepoint
HLY-1
U2932
Gene
2
6
2
6
ALKBH8
ARFGAP3
ASNS
ATF4
BET1
BSPRY
C1orf186
CA2
CARS
CCL3L1
CCL4L1
CCL4L2
CD36
CD58
CDRT4
CHAC1
CLDN14
CLECL1
CREB3L2
CRY1
CSTF3
CTH
DDIT3
DDX17
DEPTOR
DHRS3
DNAJB9
DNAJC3
DNAJC10
DNAJC12
EDEM1
EDEM2
EHD4
EIF2S2
ERLEC1
EVI2A
FAM84B
FAM120C
FAM129A
FICD
FKBP14
GARS
GBP1
GBP2
GCSAM
GDPD5
GFI1
GNG10
GNL3
GOT1
GPT2

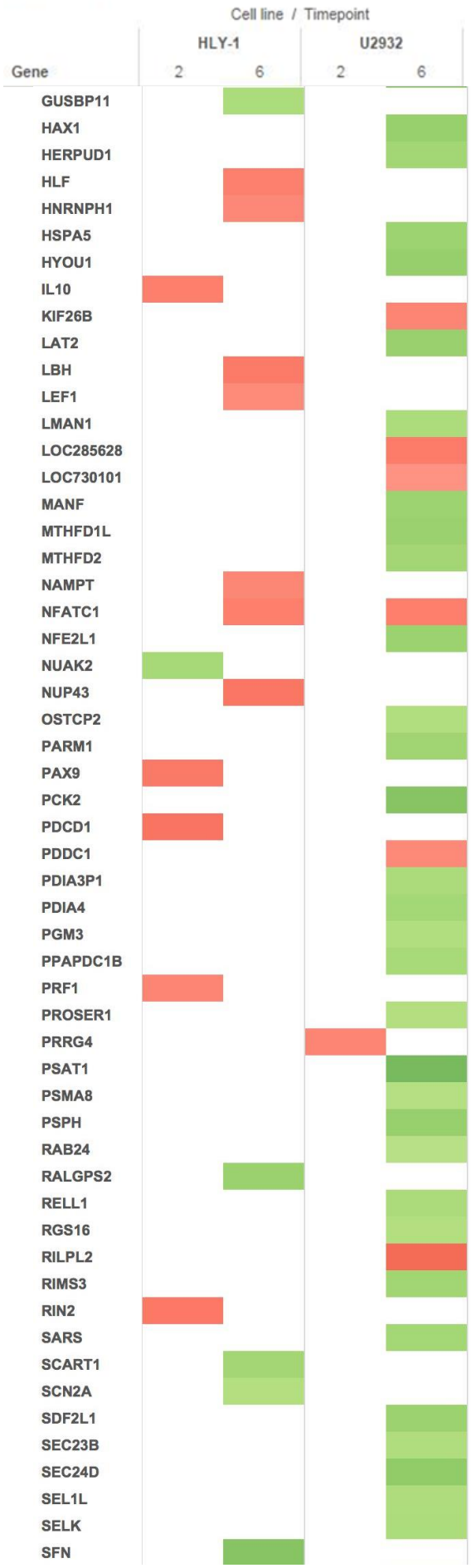
Cell line / Timepoint
HLY-1
U2932
Gene
2
6
2
6
GUSBP11
HAX1
HERPUD1
HLF
HNRNPH1
HSPA5
HYOU1
IL10
KIF26B
LAT2
LBH
LEF1
LMAN1
LOC285628
LOC730101
MANF
MTHFD1L
MTHFD2
NAMPT
NFATC1
NFE2L1
NUAK2
NUP43
OSTCP2
PARM1
PAX9
PCK2
PDCD1
PDDC1
PDIA3P1
PDIA4
PGM3
PPAPDC1B
PRF1
PROSER1
PRRG4
PSAT1
PSMA8
PSPH
RAB24
RALGPS2
RELL1
RGS16
RILPL2
RIMS3
RIN2
SARS
SCART1
SCN2A
SDF2L1
SEC23B
SEC24D
SEL1L
SELK
SFN

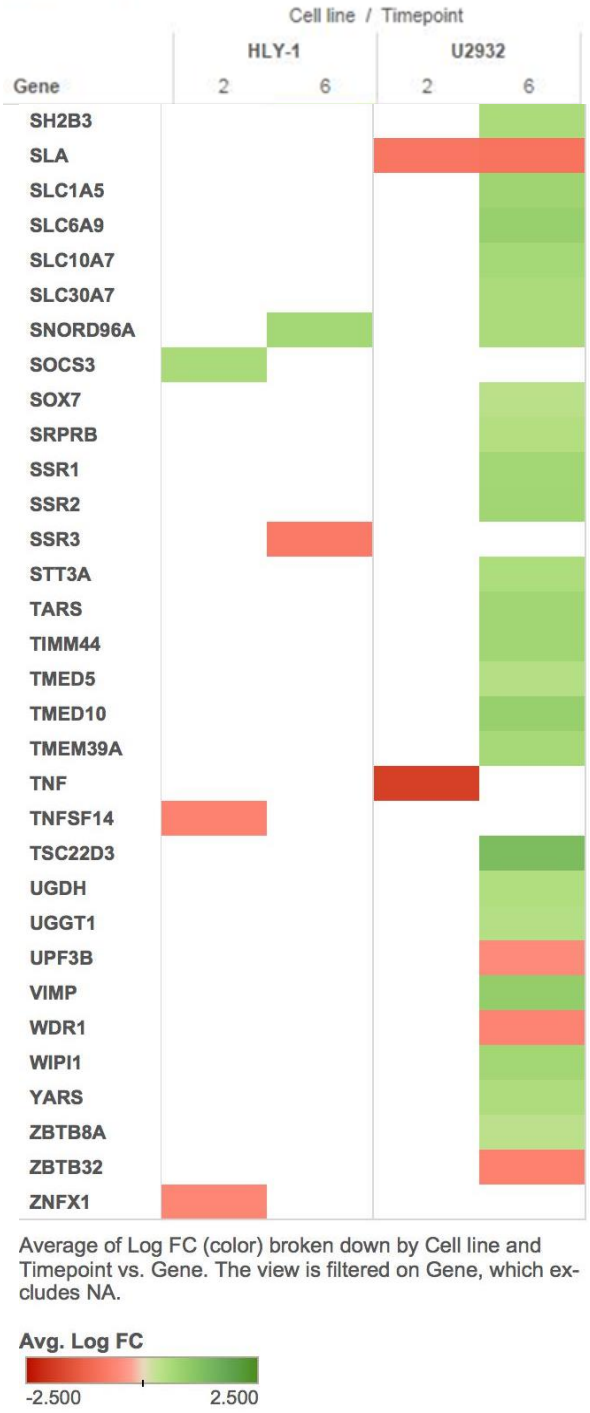

Figure 39 (Continued from previous 2 pages). Heat-map analysis of genes differentially expressed in HLY-1 and U2932 cells treated with CsA (unpaired analysis). The heat-map compares the statistically significant genes (adjusted P-value <0.05) which were differentially expressed in HLY-1 and U2932 cells treated with CsA for 2 and 6 hours. Red indicates genes which were downregulated by CsA, whereas green indicates genes that were upregulated by CsA. The intensity of the colour signifies the degree to which genes were differentially expressed where a deeper colour represents a greater extent of differential expression. Genes are listed in alphabetical order. Data excludes gene probes marked as N/A. For genes where there were more than one probe, the average FC was used.

4.2.5. Inhibition of calcineurin/NFAT signalling in ABC and GCB DLBCL cell lines results in upregulation or downregulation of common target genes

The heat-map in figure 40 shows the differential expression of genes commonly up- or downregulated by CsA in more than one DLBCL cell line. Genes in the heat-map were included based on their shared differential expression in at least two cell lines, regardless of their timepoint. The data as a whole gives a good representation of the broad shared directionality of response to CsA treatment of genes across cell lines. Of the 21 genes downregulated by CsA in U2932 cells, all but one of these genes were also downregulated by HLY-1 cells. Interestingly, the gene encoding follistatin (FST) was upregulated in HLY-1 cells, suggesting that NFAT may occasionally regulate the same genes differently between cell lines. For some genes, such as CCL4L2 and CCL4L1, the deep red colour in HLY-1 (2hr) and U2932 (2hr and 6hr) samples indicates a high level of downregulation upon CsA treatment, which is common in both HLY-1 and U2932 cell lines. In addition, EGR2 and NFAT2 (NFATC1) are downregulated in HLY-1 (2hr and 6hr) and U2932 (6hr). In contrast, some genes, such as DDIT3 and TSC22D3 were commonly upregulated by both ABC DLBCL cell lines, but only at later timepoints.

Interestingly, inhibition of the calcineurin/NFAT pathway caused significant downregulation of TNFα in all four ABC conditions, when both paired and unpaired data analysis was considered. The fact that TNFα also represents the fourth most downregulated gene overall suggests that this cytokine may be an important gene regulated by calcineurin/NFAT in these ABC DLBCL cell lines. Furthermore, of the very few significant genes differentially expressed in WSU-NHL cells, three out of four of these were shared with a least one ABC DLBCL cell line, particularly U2932 cells. Again, the regulation of gene expression induced by CsA treatment was comparable between all cell lines, suggesting similar modes of regulation by calcineurin/NFAT signalling between all three cell lines.

The Venn diagrams in figures 41-44 indicate the overlapping genes affected by CsA in DLBCL cell lines. While unpaired analysis highlights the chemokines CCL4L1 and CCL4L2 as overlapping target genes (figure 41), only CCL4L2 was shared by paired analysis (figure 42). After 6 hours treatment, statistically significant genes were identified in all three cell lines by unpaired analysis, including WSU-NHL cells (figure 43). While

genes such as NFAT2 (NFATC1) were common between U2932 and HLY-1 cells, the only overlapping gene between all three cell lines was the gene encoding the small nucleolar RNA SNORD96A. Paired analysis of the 6 hour timepoint did not reveal any genes of significance in WSU-NHL (figure 44), however, U2932 and HLY-1 cells demonstrated 25 overlapping genes, including NFAT2 (NFATC1), early growth response 2 (EGR2), the nuclear factor of kappa light polypeptide gene enhancer in B cells inhibitors epsilon (NFKBIE) and alpha (NFKBIA) and tumour necrosis factor alpha (TNFα).

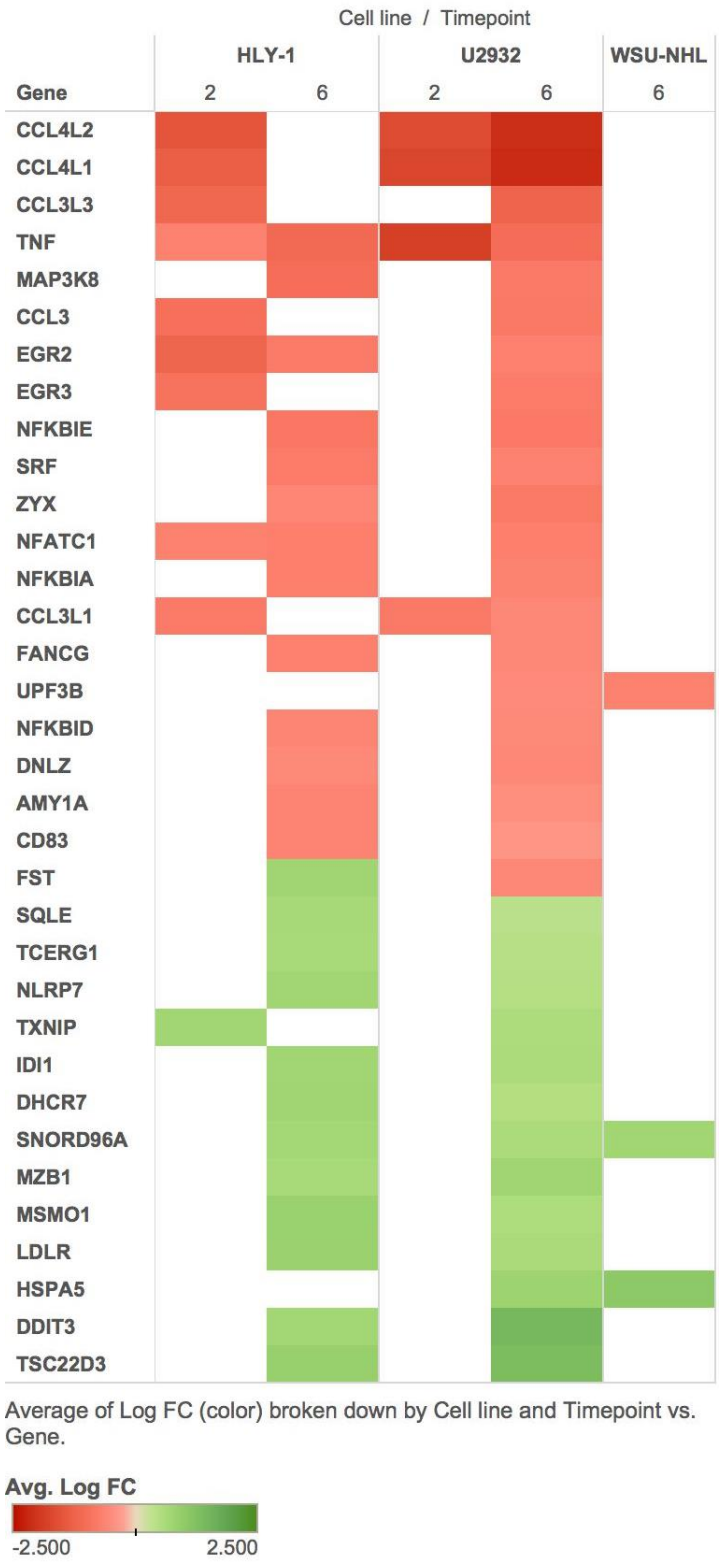

Figure 40. Heat-map analysis of genes differentially expressed in HLY-1, U2932 and WSU-NHL cells treated with CsA (combined paired and unpaired analysis). The heat-map compares the statistically significant genes (adjusted P-value <0.05) which were differentially expressed in HLY-1, U2932 and WSU-NHL cells treated with CsA for 2 and 6 hours. Genes in the heat-map were included based on their shared differential expression between at least two cell lines, regardless of timepoint. Red indicates genes which were downregulated by CsA, whereas green indicates genes that were upregulated by CsA. The intensity of the colour signifies the degree to which genes were differentially expressed where a deeper colour represents a greater extent of differential expression. Genes are ordered by their average logFC across all timepoints. Data excludes gene probes marked as N/A.

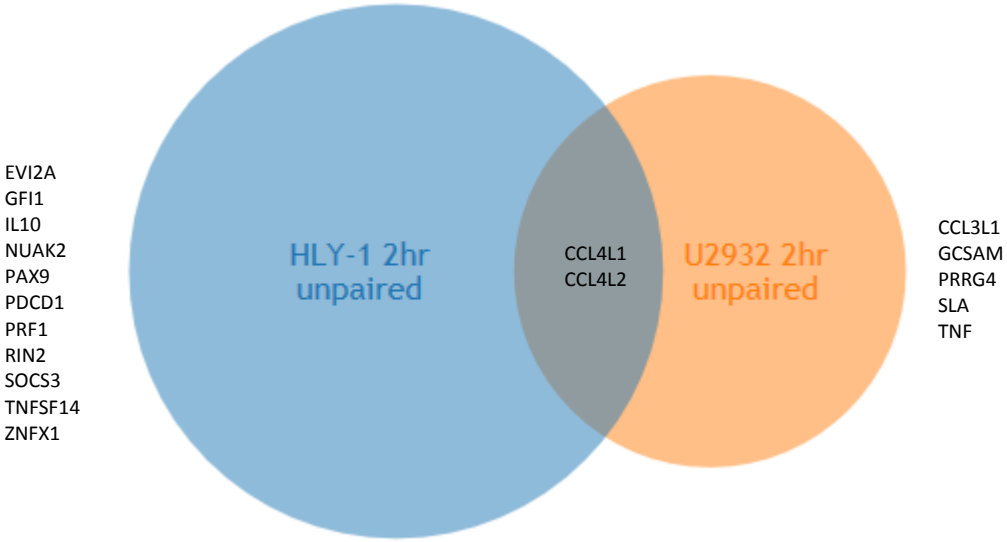

Figure 41. HLY-1 and U2932 cells share two genes that were significantly upregulated or downregulated when treated with CsA for 2hrs. The Venn diagram compares statistically significant, differentially expressed genes (adjusted P-value <0.05) between HLY-1 (blue) and U2932 (orange) cells treated with CsA for 2hrs (unpaired analysis). Data excludes gene probes marked as N/A.

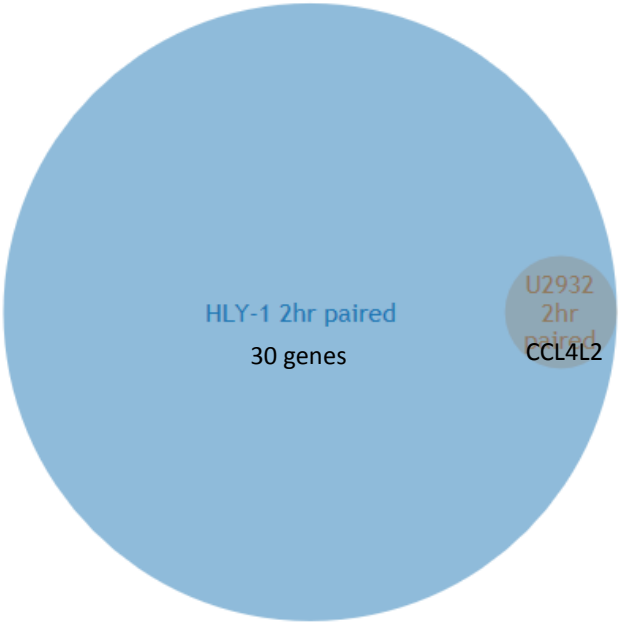

Figure 42. HLY-1 and U2932 cells share one gene that was significantly upregulated or downregulated when treated with CsA for 2hrs. The Venn diagram compares statistically significant, differentially expressed genes (adjusted P-value <0.05) between HLY-1 (blue) and U2932 (orange) cells treated with CsA for 2hrs (paired analysis). Data excludes gene probes marked as N/A.

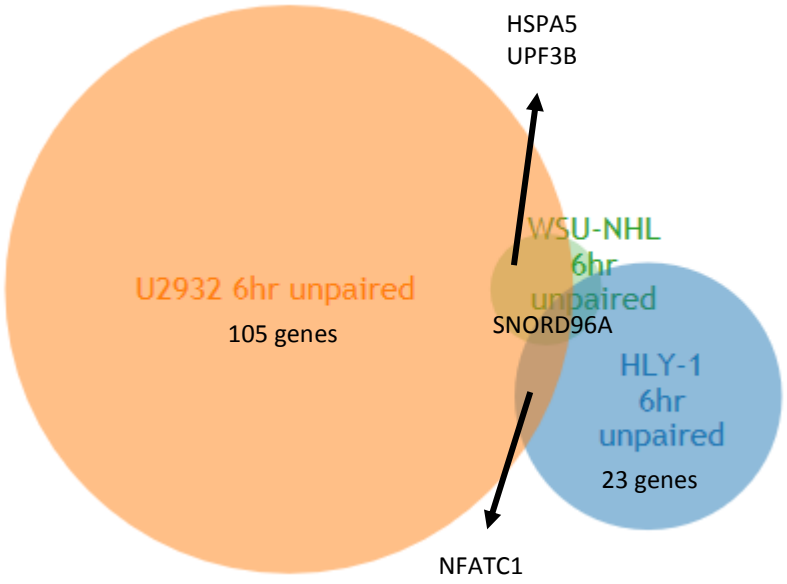

Figure 43. HLY-1, U2932 and WSU-NHL cells share one gene that was significantly upregulated or downregulated when treated with CsA for 6hrs. The Venn diagram compares statistically significant, differentially expressed genes (adjusted P-value <0.05) between HLY-1 (blue), U2932 (orange) and WSU-NHL (green) cells treated with CsA for 6hrs (unpaired analysis). Data excludes gene probes marked as N/A.

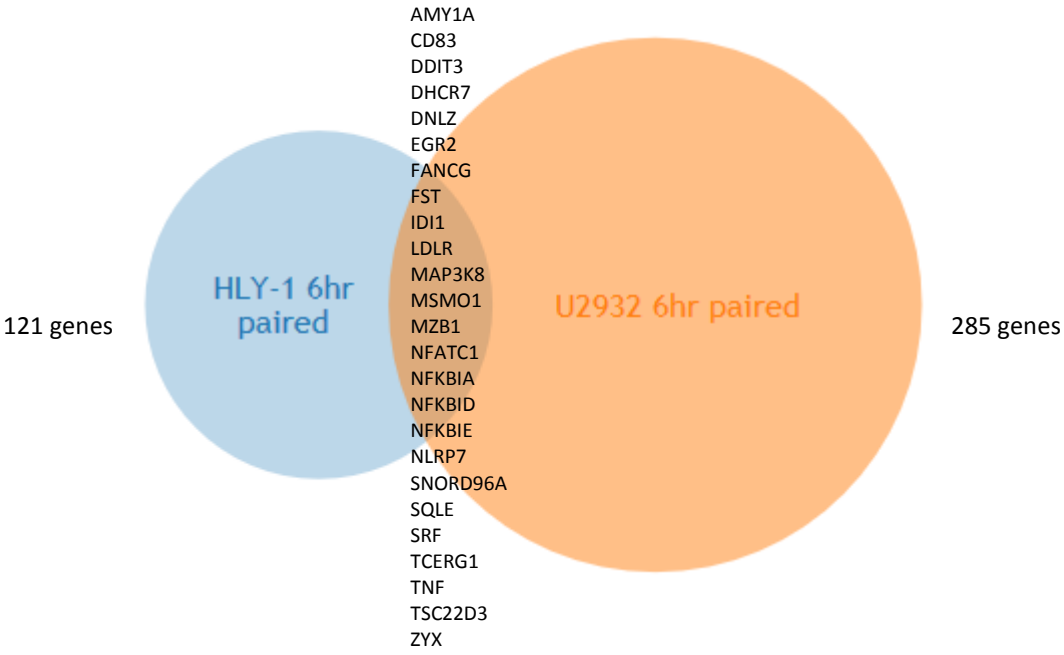

Figure 44. HLY-1 and U2932 cells share 25 genes that were significantly upregulated or downregulated when treated with CsA for 6hrs. The Venn diagram compares statistically significant, differentially expressed genes (adjusted P-value <0.05) between HLY-1 (blue) and U2932 (orange) cells treated with CsA for 6hrs (paired analysis). Data excludes gene probes marked as N/A.

4.2.6. Statistically significant genes differentially expressed in DLBCL cell lines treated with CsA

The following tables (tables 12-20) provide the details of all the statistically significant genes (adjusted P-value <0.05) differentially expressed in each cell line and timepoint. Genes are ranked by logFC, where genes highlighted in orange indicate genes downregulated by CsA whereas data in blue represents genes upregulated by CsA. Adjusted P-values are also included. For a more comprehensive description of the top 150 differentially expressed genes for each treatment condition, please refer to appendix tables 1-9. For bubble diagrams ranking genes by adjusted P-value, please locate appendix figures 3-19.

U2932 2hr (unpaired data analysis)

Number	symbol	name	logFC	adjusted P value
1	TNF	tumor necrosis factor	-1.894	0.004706188
2	NA	NA	-1.843	3.07E-05
3	CCL4L1	chemokine (C-C motif) ligand 4-like 1	-1.778	1.59E-05
4	CCL4L2	chemokine (C-C motif) ligand 4-like 2	-1.690	6.47E-05
5	SLA	Src-like-adaptor	-0.879	4.14E-05
6	CCL3L1	chemokine (C-C motif) ligand 3-like 1	-0.804	0.004706188
7	PRRG4	proline rich Gla (G-carboxyglutamic acid) 4 (transmembrane)	-0.626	0.022147325
2	GCSAM	germinal center-associated, signaling and motility	0.564	0.027467991
1	NA	NA	0.578	0.022147325

Table 12. Statistically significant genes differentially expressed in U2932 cells treated with CsA for 2hrs (unpaired data analysis). Columns indicate the gene symbols, names, log fold-change (logFC) and P values for statistically significant genes (adjusted P-value <0.05) differentially expressed upon treatment with CsA. Data in orange indicates genes downregulated by CsA and data in blue indicates genes upregulated by CsA. Gene numbers represent genes ordered by logFC, where 1 indicates the gene with the greatest logFC. Data includes gene probes marked as N/A.

U2932 2hr (paired data analysis)

Number	symbol	name	logFC	adjusted p value
2	CCL4L2	chemokine (C-C motif) ligand 4-like 2	-1.690	0.009380052
1	NA	NA	-1.843	0.021429372

Table 13. Statistically significant genes differentially expressed in U2932 cells treated with CsA for 2hrs (paired data analysis). Columns indicate the gene symbols, names, log fold-change (logFC) and P values for statistically significant genes (adjusted P-value <0.05) differentially expressed upon treatment with CsA. Data in orange indicates genes downregulated by CsA. Gene numbers represent genes ordered by logFC, where 1 indicates the gene with the greatest logFC. Data includes gene probes marked as N/A.

U2932 6hr (unpaired data

Number	symbol	name	logFC	adjusted P value
1	NA	NA	-2.460	3.22E-08
2	CCL4L1	chemokine (C-C motif) ligand 4-like 1	-2.209	3.22E-08
3	CCL4L2	chemokine (C-C motif) ligand 4-like 2	-2.147	2.96E-07
4	RILPL2	Rab interacting lysosomal protein-like 2	-1.072	0.00261022
5	NA	NA	-1.048	0.000295978
6	SLA	Src-like-adaptor	-0.928	7.22E-06
7	SLA	Src-like-adaptor	-0.922	0.000917712
8	NA	NA	-0.853	0.014970312
9	LOC285628	uncharacterized LOC285628	-0.780	0.008035991
10	NFATC1	nuclear factor of activated T-cells, cytoplasmic, calcineurin-dependent 1	-0.728	0.001868128
11	ZBTB32	zinc finger and BTB domain containing 32	-0.698	0.029049451
12	WDR1	WD repeat domain 1	-0.650	0.02630768
13	KIF26B	kinesin family member 26B	-0.638	0.029049451
14	CCL3L1	chemokine (C-C motif) ligand 3-like 1	-0.570	0.041515298
15	PDDC1	Parkinson disease 7 domain containing 1	-0.557	0.029049451
16	BSPRY	B-box and SPRY domain containing	-0.554	0.007613104
17	NA	NA	-0.551	0.02407641
18	UPF3B	UPF3 regulator of nonsense transcripts homolog B (yeast)	-0.550	0.003270619
19	CLDN14	claudin 14	-0.549	0.021746963
20	CA2	carbonic anhydrase II	-0.547	0.002162172
21	UPF3B	UPF3 regulator of nonsense transcripts homolog B (yeast)	-0.516	0.003673103
22	CSTF3	cleavage stimulation factor, 3' pre-RNA, subunit 3, 77kDa	-0.501	0.02630768
23	CD58	CD58 molecule	-0.445	0.00532788
24	LOC730101	uncharacterized LOC730101	-0.431	0.017416102
25	CLECL1	C-type lectin-like 1	-0.424	0.021963104
98	ZBTB8A	zinc finger and BTB domain containing 8A	0.382	0.02146968
97	SOX7	SRY (sex determining region Y)-box 7	0.391	0.013375629
96	NA	NA	0.402	0.030102889
95	ALKBH8	alkB, alkylation repair homolog 8 (E. coli)	0.420	0.031423395
94	RAB24	RAB24, member RAS oncogene family	0.423	0.016228488
93	NA	NA	0.446	0.020574108
92	TMED5	transmembrane emp24 protein transport domain containing 5	0.455	0.02972874
91	EIF2S2	eukaryotic translation initiation factor 2, subunit 2 beta, 38kDa	0.458	0.019950904
90	UGGT1	UDP-glucose glycoprotein glucosyltransferase 1	0.458	0.017416102
89	UGGT1	UDP-glucose glycoprotein glucosyltransferase 1	0.459	0.038104893
88	DNAJC12	DnaJ (Hsp40) homolog, subfamily C, member 12	0.463	0.042674281
87	PSMA8	proteasome (prosome, macropain) subunit, alpha type, 8	0.476	0.039280693
86	SRPRB	signal recognition particle receptor, B subunit	0.481	0.028675312
85	RGS16	regulator of G-protein signaling 16	0.482	0.012504995
84	FAM120C	family with sequence similarity 120C	0.482	0.02018112
83	PROSER1	proline and serine rich 1	0.484	0.02630768
82	OSTCP2	oligosaccharyltransferase complex subunit pseudogene 2	0.502	0.005774258
81	PGM3	phosphoglucomutase 3	0.509	0.042674281
80	UGDH	UDP-glucose 6-dehydrogenase	0.510	0.008748128
79	SEC23B	Sec23 homolog B (S. cerevisiae)	0.515	0.01915417
78	SEL1L	sel-1 suppressor of lin-12-like (C. elegans)	0.532	0.008748128
77	YARS	tyrosyl-tRNA synthetase	0.535	0.014009867
76	BET1	Bet1 golgi vesicular membrane trafficking protein	0.539	0.042522949
75	STT3A	STT3A, subunit of the oligosaccharyltransferase complex (catalytic)	0.547	0.000830742
74	LMAN1	lectin, mannose-binding, 1	0.568	0.044160822
73	DEPTOR	DEP domain containing MTOR-interacting protein	0.569	0.002814085
72	SELK	selenoprotein K	0.572	0.00532788
71	FAM129A	family with sequence similarity 129, member A	0.579	0.014777277
70	GDPD5	glycerophosphodiester phosphodiesterase domain containing 5	0.582	0.012479994
69	NA	NA	0.588	0.016283125
68	PDIA3P1	protein disulfide isomerase family A, member 3 pseudogene 1	0.591	0.048405193
67	SH2B3	SH2B adaptor protein 3	0.591	0.009016194
66	RELL1	RELT-like 1	0.594	0.019470183
65	SLC30A7	solute carrier family 30 (zinc transporter), member 7	0.596	0.042687224
64	SNORD96A	small nucleolar RNA, C/D box 96A	0.598	0.002250795
63	GOT1	glutamic-oxaloacetic transaminase 1, soluble	0.601	0.027193809

U2932 6hr (unpaired data analysis) continued.

62	FAM84B	family with sequence similarity 84, member B	0.602	0.005567665
61	DNAJC10	DnaJ (Hsp40) homolog, subfamily C, member 10	0.607	0.005139158
60	CREB3L2	cAMP responsive element binding protein 3-like 2	0.614	0.019321075
59	CDRT4	CMT1A duplicated region transcript 4	0.615	0.025168611
58	PPAPDC1B	phosphatidic acid phosphatase type 2 domain containing 1B	0.637	0.008748128
57	DNAJC3	DnaJ (Hsp40) homolog, subfamily C, member 3	0.641	0.002309772
56	NA	NA	0.645	0.042674281
55	TMEM39A	transmembrane protein 39A	0.651	0.001095584
54	NA	NA	0.652	0.019470183
53	FICD	FIC domain containing	0.665	0.001287642
52	SLC10A7	solute carrier family 10, member 7	0.678	0.000617907
51	GARS	glycyl-tRNA synthetase	0.685	0.000946563
50	SARS	seryl-tRNA synthetase	0.694	0.008748128
49	PDIA4	protein disulfide isomerase family A, member 4	0.695	0.000917712
48	EDEM2	ER degradation enhancer, mannosidase alpha-like 2	0.697	0.005634219
47	ARFGAP3	ADP-ribosylation factor GTPase activating protein 3	0.701	0.005847348
46	ASNS	asparagine synthetase (glutamine-hydrolyzing)	0.702	0.038698093
45	MTHFD2	methylenetetrahydrofolate dehydrogenase (NADP+ dependent) 2, methenyltetrahydrofolate cyclohydrolase	0.704	3.57E-05
44	HERPUD1	homocysteine-inducible, endoplasmic reticulum stress-inducible, ubiquitin-like domain member 1	0.710	0.020085983
43	SSR1	signal sequence receptor, alpha	0.711	2.08E-05
42	WIPI1	WD repeat domain, phosphoinositide interacting 1	0.715	0.001378825
41	RIMS3	regulating synaptic membrane exocytosis 3	0.722	0.037391237
40	SSR2	signal sequence receptor, beta (translocon-associated protein beta)	0.732	0.014777277
39	TARS	threonyl-tRNA synthetase	0.739	0.020574108
38	TIMM44	translocase of inner mitochondrial membrane 44 homolog (yeast)	0.748	0.025406677
37	PARM1	prostate androgen-regulated mucin-like protein 1	0.754	0.003467139
36	EDEM1	ER degradation enhancer, mannosidase alpha-like 1	0.760	0.002250795
35	GNL3	guanine nucleotide binding protein-like 3 (nucleolar)	0.765	0.00026869
34	SLC1A5	solute carrier family 1 (neutral amino acid transporter), member 5	0.777	0.016832394
33	ERLEC1	endoplasmic reticulum lectin 1	0.781	0.000455295
32	MANF	mesencephalic astrocyte-derived neurotrophic factor	0.786	0.005774258
31	PCK2	phosphoenolpyruvate carboxykinase 2 (mitochondrial)	0.798	0.015847846
30	HSPA5	heat shock 70kDa protein 5 (glucose-regulated protein, 78kDa)	0.799	0.009146536
29	SDF2L1	stromal cell-derived factor 2-like 1	0.808	0.001785335
28	NFE2L1	nuclear factor, erythroid 2-like 1	0.809	0.00131707
27	CHAC1	ChaC, cation transport regulator homolog 1 (E. coli)	0.809	0.042674281
26	DEPTOR	DEP domain containing MTOR-interacting protein	0.821	0.000946563
25	CARS	cysteinyl-tRNA synthetase	0.823	0.002543534
24	MTHFD1L	methylenetetrahydrofolate dehydrogenase (NADP+ dependent) 1-like	0.831	0.000150423
23	CTH	cystathionase (cystathionine gamma-lyase)	0.843	0.000156392
22	NA	NA	0.855	0.006675448
21	FKBP14	FK506 binding protein 14, 22 kDa	0.857	0.007429306
20	LAT2	linker for activation of T cells family, member 2	0.857	0.009146536
19	PSPH	phosphoserine phosphatase	0.879	0.000496868
18	SLC6A9	solute carrier family 6 (neurotransmitter transporter, glycine), member 9	0.883	0.029840227
17	HAX1	HCLS1 associated protein X-1	0.890	0.005139158
16	TMED10	transmembrane emp24-like trafficking protein 10 (yeast)	0.895	0.020193903
15	HYOU1	hypoxia up-regulated 1	0.917	0.039280693
14	VIMP	VCP-interacting membrane protein	0.951	0.000648233
13	SEC24D	SEC24 family member D	0.976	0.019470183
12	CTH	cystathionase (cystathionine gamma-lyase)	1.011	0.000138647
11	ATF4	activating transcription factor 4	1.099	0.025168611
10	CARS	cysteinyl-tRNA synthetase	1.132	0.0009649
9	TSC22D3	TSC22 domain family, member 3	1.166	0.006554991
8	DNAJB9	DnaJ (Hsp40) homolog, subfamily B, member 9	1.180	0.000914516
7	GPT2	glutamic pyruvate transaminase (alanine aminotransferase) 2	1.236	0.005223122
6	NA	NA	1.322	0.000374446
5	PSAT1	phosphoserine aminotransferase 1	1.421	2.02E-06
4	DDIT3	DNA-damage-inducible transcript 3	1.474	0.00026869
3	CTH	cystathionase (cystathionine gamma-lyase)	1.494	0.000295978
2	TSC22D3	TSC22 domain family, member 3	1.555	0.001880118
1	PCK2	phosphoenolpyruvate carboxykinase 2 (mitochondrial)	1.589	3.98E-05

Table 14 (Continued from previous page). Statistically significant genes differentially expressed in U2932 cells treated with CsA for 6hrs (unpaired data analysis). Columns indicate the gene symbols, names, log fold-change (logFC) and P values for statistically significant genes (adjusted P-value <0.05) differentially expressed upon treatment with CsA. Data in orange indicates genes downregulated by CsA and data in blue indicates genes upregulated by CsA. Gene numbers represent genes ordered by logFC, where 1 indicates the gene with the greatest logFC. Data includes gene probes marked as N/A.

U2932 6hr (paired data analysis)

Number	symbol	name	logFC	adjusted P value
1	NA	NA	-2.46024	1.33E-05
2	CCL4L1	chemokine (C-C motif) ligand 4-like 1	-2.20902	6.82E-06
3	CCL4L2	chemokine (C-C motif) ligand 4-like 2	-2.14727	1.33E-05
4	CCL3L3	chemokine (C-C motif) ligand 3-like 3	-1.25032	0.002786341
5	RILPL2	Rab interacting lysosomal protein-like 2	-1.07234	0.000896008
6	BATF	basic leucine zipper transcription factor, ATF-like	-1.06888	0.003367153
7	TNF	tumor necrosis factor	-1.05313	0.001776479
8	LRRC32	leucine rich repeat containing 32	-1.04826	0.006574593
9	NA	NA	-1.04768	0.00094904
10	SLA	Src-like-adaptor	-0.92831	0.000604875
11	SLA	Src-like-adaptor	-0.92184	0.002592167
12	NFKBIE	NA	-0.85271	0.001776479
13	CCL3	chemokine (C-C motif) ligand 3	-0.83513	0.003828764
14	ZYX	zyxin	-0.81341	0.005497236
15	MAP3K8	mitogen-activated protein kinase kinase kinase 8	-0.8095	0.003074677
16	NFKBIE	nuclear factor of kappa light polypeptide gene enhancer in B-cells inhibitor, epsilon	-0.79267	0.00387355
17	LOC285628	uncharacterized LOC285628	-0.77988	0.002093238
18	EGR3	early growth response 3	-0.77058	0.010619499
19	FKBP4	FK506 binding protein 4, 59kDa	-0.74933	0.01188207
20	NFATC1	nuclear factor of activated T-cells, cytoplasmic, calcineurin-dependent 1	-0.72798	0.003828764
21	EGR2	early growth response 2	-0.69989	0.003128221
22	ZBTB32	zinc finger and BTB domain containing 32	-0.69805	0.00668888
23	TPM4	tropomyosin 4	-0.69701	0.012554762
24	SCO2	SCO2 cytochrome c oxidase assembly protein	-0.69144	0.003817548
25	SRF	serum response factor (c-fos serum response element-binding transcription factor)	-0.67605	0.03266934
26	NFKBIA	nuclear factor of kappa light polypeptide gene enhancer in B-cells inhibitor, alpha	-0.66561	0.00387355
27	RBM14	RNA binding motif protein 14	-0.65338	0.047771027
28	WDR1	WD repeat domain 1	-0.64984	0.005591198
29	HILPDA	hypoxia inducible lipid droplet-associated	-0.64401	0.019056907
30	MIR155HG	MIR155 host gene (non-protein coding)	-0.6405	0.012554762
31	KIF26B	kinesin family member 26B	-0.63771	0.013911572
32	CCL3L1	chemokine (C-C motif) ligand 3-like 1	-0.62826	0.012233686
33	HES6	hes family bHLH transcription factor 6	-0.62456	0.017557919
34	RHPN2	rhophilin, Rho GTPase binding protein 2	-0.61989	0.006574593
35	IKZF1	IKAROS family zinc finger 1 (Ikaros)	-0.60894	0.03523105
36	EXO1	exonuclease 1	-0.59242	0.006697883
37	FANCG	Fanconi anemia, complementation group G	-0.59064	0.034405111
38	FST	follistatin	-0.58891	0.010773303
39	BCL2L11	BCL2-like 11 (apoptosis facilitator)	-0.58747	0.007775984
40	DNLZ	DNL-type zinc finger	-0.58674	0.01065754
41	PTGES2	prostaglandin E synthase 2	-0.58079	0.012233686
42	CCL3L1	chemokine (C-C motif) ligand 3-like 1	-0.57041	0.013953787
43	AGAP3	ArfGAP with GTPase domain, ankyrin repeat and PH domain 3	-0.56774	0.016756454
44	LIMA1	LIM domain and actin binding 1	-0.56619	0.033309286
45	SLC25A19	solute carrier family 25 (mitochondrial thiamine pyrophosphate carrier), member 19	-0.5593	0.025511885
46	BRK1	BRICK1, SCAR/WAVE actin-nucleating complex subunit	-0.55848	0.02373166
47	PDDC1	Parkinson disease 7 domain containing 1	-0.55658	0.028336008
48	LOC730101	uncharacterized LOC730101	-0.55523	0.044623686
49	NFKBID	nuclear factor of kappa light polypeptide gene enhancer in B-cells inhibitor, delta	-0.55507	0.023834561
50	AMY1B	amylase, alpha 1B (salivary)	-0.55434	0.032733413
51	BSPRY	B-box and SPRY domain containing	-0.55405	0.010619499
52	NA	NA	-0.55134	0.011174268
53	PSME3	proteasome (prosome, macropain) activator subunit 3 (PA28 gamma; Ki)	-0.55042	0.033845817
54	UPF3B	UPF3 regulator of nonsense transcripts homolog B (yeast)	-0.55038	0.021191687
55	BCL2L11	BCL2-like 11 (apoptosis facilitator)	-0.54896	0.034721721
56	CLDN14	claudin 14	-0.54857	0.018968968
57	CA2	carbonic anhydrase II	-0.54714	0.015294926
58	CCL3L1	chemokine (C-C motif) ligand 3-like 1	-0.54626	0.019031456
59	UBQLN4	ubiquilin 4	-0.54508	0.028336008
60	FAM65B	family with sequence similarity 65, member B	-0.53952	0.017557919
61	NA	NA	-0.53507	0.015280539
62	DHRS11	dehydrogenase/reductase (SDR family) member 11	-0.53497	0.013902319
63	TNFRSF1B	tumor necrosis factor receptor superfamily, member 1B	-0.53226	0.020831682
64	SAP30L	SAP30-like	-0.52613	0.013911572
65	DMAP1	DNA methyltransferase 1 associated protein 1	-0.52449	0.027958367
66	C9orf37	chromosome 9 open reading frame 37	-0.51835	0.047771027

U2932 6hr (paired data analysis) continued.

67	UPF3B	UPF3 regulator of nonsense transcripts homolog B (yeast)	-0.51632	0.012233686
68	NCOA1	nuclear receptor coactivator 1	-0.51273	0.015136811
69	LRRC20	leucine rich repeat containing 20	-0.50287	0.025910053
70	TUBA4A	tubulin, alpha 4a	-0.50287	0.031226285
71	CSTF3	cleavage stimulation factor, 3' pre-RNA, subunit 3, 77kDa	-0.50076	0.03523105
72	PPOX	protoporphyrinogen oxidase	-0.49994	0.049360192
73	PMS2P4	postmeiotic segregation increased 2 pseudogene 4	-0.49971	0.049762703
74	POLA2	polymerase (DNA directed), alpha 2, accessory subunit	-0.49952	0.025481384
75	ZAK	sterile alpha motif and leucine zipper containing kinase AZK	-0.49906	0.034721721
76	AMD1	adenosylmethionine decarboxylase 1	-0.49646	0.028336008
77	GPR137B	G protein-coupled receptor 137B	-0.49415	0.030661525
78	ZDHHC16	zinc finger, DHHC-type containing 16	-0.49275	0.033845817
79	NA	NA	-0.49153	0.028336008
80	HSPH1	heat shock 105kDa/110kDa protein 1	-0.49083	0.042792531
81	LPCAT3	lysophosphatidylcholine acyltransferase 3	-0.48911	0.014865142
82	PRPSAP1	phosphoribosyl pyrophosphate synthetase-associated protein 1	-0.4873	0.025511885
84	FAM136A	family with sequence similarity 136, member A	-0.48713	0.030649683
84	AMY1A	amylase, alpha 1A (salivary)	-0.48298	0.025474092
85	NA	NA	-0.47945	0.029010307
86	C16orf59	chromosome 16 open reading frame 59	-0.47764	0.034213914
87	DNAJA4	DnaJ (Hsp40) homolog, subfamily A, member 4	-0.47396	0.025511885
88	CAPRIN1	cell cycle associated protein 1	-0.47322	0.015717724
89	FANCL	Fanconi anemia, complementation group L	-0.47182	0.027958367
90	NA	NA	-0.46857	0.028336008
91	WWP1	WW domain containing E3 ubiquitin protein ligase 1	-0.46331	0.025666446
92	FAM133B	family with sequence similarity 133, member B	-0.46242	0.043284223
93	TRIOBP	TRIO and F-actin binding protein	-0.46034	0.02546761
94	COCH	cochlin	-0.45903	0.019775018
95	SDCBP	syndecan binding protein (syntenin)	-0.45804	0.049471046
96	CD24	CD24 molecule	-0.45444	0.033309286
97	CSRP2	cysteine and glycine-rich protein 2	-0.45405	0.03523105
98	ELL3	elongation factor RNA polymerase II-like 3	-0.45191	0.033465045
99	ADAP2	ArfGAP with dual PH domains 2	-0.45133	0.04508246
100	IER3	immediate early response 3	-0.44735	0.04702118
101	ACTG1	actin, gamma 1	-0.44715	0.034721721
102	PRRG4	proline rich Gla (G-carboxyglutamic acid) 4 (transmembrane)	-0.44499	0.023834561
103	CD58	CD58 molecule	-0.4445	0.022825104
104	NA	NA	-0.43586	0.036634046
105	BID	BH3 interacting domain death agonist	-0.43561	0.029010307
106	METTL13	methyltransferase like 13	-0.43511	0.042701416
107	SNX8	sorting nexin 8	-0.43508	0.0490733
108	LOC730101	uncharacterized LOC730101	-0.43149	0.026678785
109	NICN1	nicolin 1	-0.43102	0.039106595
110	CA2	carbonic anhydrase II	-0.43101	0.043284223
111	C22orf39	chromosome 22 open reading frame 39	-0.42995	0.025511885
112	RRP7A	ribosomal RNA processing 7 homolog A (S. cerevisiae)	-0.42923	0.025814373
113	TYMP	thymidine phosphorylase	-0.42622	0.027495256
114	SNHG9	small nucleolar RNA host gene 9 (non-protein coding)	-0.42589	0.032733413
115	NA	NA	-0.42561	0.048626688
116	C3orf70	chromosome 3 open reading frame 70	-0.42477	0.034213914
117	CLECL1	C-type lectin-like 1	-0.42387	0.041084607
118	PAM	peptidylglycine alpha-amidating monooxygenase	-0.42331	0.04021813
119	SUV420H1	suppressor of variegation 4-20 homolog 1 (Drosophila)	-0.42299	0.028336008
120	NA	NA	-0.42189	0.039106595
121	DDTL	D-dopachrome tautomerase-like	-0.42088	0.027330137
122	CD83	CD83 molecule	-0.40965	0.030649683
123	RPL29	ribosomal protein L29	-0.40906	0.048176288
124	RTCB	RNA 2',3'-cyclic phosphate and 5'-OH ligase	-0.40847	0.033975099
125	MCM10	minichromosome maintenance complex component 10	-0.4074	0.044623686
126	CD40	CD40 molecule, TNF receptor superfamily member 5	-0.40711	0.033153297
127	NA	NA	-0.40615	0.043961805
128	MPDU1	mannose-P-dolichol utilization defect 1	-0.4032	0.042792531
129	ABCC5	ATP-binding cassette, sub-family C (CFTR/MRP), member 5	-0.40242	0.036257109
130	WDR77	WD repeat domain 77	-0.40174	0.042792531
131	DUSP3	dual specificity phosphatase 3	-0.39127	0.044623686
132	LAMP2	lysosomal-associated membrane protein 2	-0.389	0.048791169
133	ACOT7	acyl-CoA thioesterase 7	-0.38534	0.048976659
214	SQLE	squalene epoxidase	0.388121	0.044623686

U2932 6hr (paired data analysis) continued.

213	SLC30A5	solute carrier family 30 (zinc transporter), member 5	0.388688	0.0490733
212	PDIA5	protein disulfide isomerase family A, member 5	0.390472	0.049471046
211	NA	NA	0.401922	0.039450906
210	SPCS3	signal peptidase complex subunit 3 homolog (S. cerevisiae)	0.413122	0.030728263
209	MMAB	methylmalonic aciduria (cobalamin deficiency) cblB type	0.413447	0.048976659
208	NA	NA	0.415339	0.038977112
207	SERPINA9	serpin peptidase inhibitor, clade A (alpha-1 antiproteinase, antitrypsin), member 9	0.415554	0.039450906
206	MYO9A	myosin IXA	0.419136	0.030649683
205	MAP1LC3B	microtubule-associated protein 1 light chain 3 beta	0.419286	0.029010307
204	ALKBH8	alkB, alkylation repair homolog 8 (E. coli)	0.419918	0.033309286
203	GPR89C	G protein-coupled receptor 89C	0.422361	0.028720756
202	UFM1	ubiquitin-fold modifier 1	0.422801	0.033309286
201	RAB24	RAB24, member RAS oncogene family	0.423	0.034347383
200	MGAT2	mannosyl (alpha-1,6-)-glycoprotein beta-1,2-N-acetylglucosaminyltransferase	0.426105	0.030638931
199	DERL1	derlin 1	0.428954	0.049471046
198	CHD2	chromodomain helicase DNA binding protein 2	0.430628	0.033455517
197	RNY1	RNA, Ro-associated Y1	0.431955	0.026678785
196	PAG1	phosphoprotein associated with glycosphingolipid microdomains 1	0.432002	0.034721721
195	ETV5	ets variant 5	0.432065	0.046852995
194	TVP23B	trans-golgi network vesicle protein 23 homolog B (S. cerevisiae)	0.437154	0.034213914
193	NFX1	nuclear transcription factor, X-box binding 1	0.438249	0.024495532
192	AKAP13	A kinase (PRKA) anchor protein 13	0.439217	0.048354392
191	FAM3C	family with sequence similarity 3, member C	0.43974	0.032605173
190	TCERG1	transcription elongation regulator 1	0.4429	0.042792531
189	DERL2	derlin 2	0.442967	0.043961805
188	NLRP7	NLR family, pyrin domain containing 7	0.444564	0.034133939
187	YPEL5	yippee-like 5 (Drosophila)	0.450595	0.044583427
186	GPR89B	G protein-coupled receptor 89B	0.451525	0.047283383
185	NA	NA	0.452246	0.038058521
184	HM13	histocompatibility (minor) 13	0.4546	0.034213914
183	TMED5	transmembrane emp24 protein transport domain containing 5	0.455088	0.023447568
182	ITGAL	integrin, alpha L (antigen CD11A (p180), lymphocyte function-associated antigen 1; alpha polypeptide)	0.455887	0.028336008
181	SLC7A6OS	solute carrier family 7, member 6 opposite strand	0.456045	0.028336008
180	CLCN6	chloride channel, voltage-sensitive 6	0.456884	0.034721721
179	EIF2S2	eukaryotic translation initiation factor 2, subunit 2 beta, 38kDa	0.457538	0.032871745
178	UGGT1	UDP-glucose glycoprotein glucosyltransferase 1	0.457557	0.02266537
177	SLC38A1	solute carrier family 38, member 1	0.457868	0.042792531
176	UGGT1	UDP-glucose glycoprotein glucosyltransferase 1	0.459498	0.025977079
175	RNA5S9	RNA, 5S ribosomal 9	0.460687	0.033309286
174	TMEM41B	transmembrane protein 41B	0.462287	0.025061667
173	CLPTM1L	CLPTM1-like	0.462569	0.029010307
172	PSMA8	proteasome (prosome, macropain) subunit, alpha type, 8	0.476483	0.034213914
171	NA	NA	0.477219	0.025814373
170	DNAJB11	DnaJ (Hsp40) homolog, subfamily B, member 11	0.477984	0.015280539
169	HMGCR	3-hydroxy-3-methylglutaryl-CoA reductase	0.48004	0.044130385
168	SRPRB	signal recognition particle receptor, B subunit	0.480555	0.017387647
167	NLRP7	NLR family, pyrin domain containing 7	0.48076	0.042792531
166	DHCR7	7-dehydrocholesterol reductase	0.480833	0.039106595
165	UBR4	ubiquitin protein ligase E3 component n-recognin 4	0.481429	0.04508246
164	XBP1	X-box binding protein 1	0.481721	0.021191687
163	RGS16	regulator of G-protein signaling 16	0.481775	0.025511885
162	FAM120C	family with sequence similarity 120C	0.48244	0.033465045
161	NSG1	neuron specific gene family member 1	0.482556	0.017557919
160	GOLGA3	golgin A3	0.484963	0.022364513
159	SC5D	sterol-C5-desaturase	0.488852	0.033309286
158	NA	NA	0.496974	0.021478771
157	OSTCP2	oligosaccharyltransferase complex subunit pseudogene 2	0.501738	0.021390993
156	NA	NA	0.502565	0.033309286
155	NA	NA	0.502647	0.016543045
154	SLC7A1	solute carrier family 7 (cationic amino acid transporter, y+ system), member 1	0.505211	0.018140838
153	OSTCP1	oligosaccharyltransferase complex subunit pseudogene 1	0.505459	0.026038902
152	GPR18	G protein-coupled receptor 18	0.507866	0.022364513
151	C7orf55	chromosome 7 open reading frame 55	0.508592	0.049471046
150	PGM3	phosphoglucomutase 3	0.509376	0.012554762
149	UGDH	UDP-glucose 6-dehydrogenase	0.509528	0.021564143
148	SNX29	sorting nexin 29	0.512102	0.030649683
147	SEC23B	Sec23 homolog B (S. cerevisiae)	0.515351	0.025511885
146	MSMO1	methylsterol monooxygenase 1	0.515463	0.027495256
145	ASNS	asparagine synthetase (glutamine-hydrolyzing)	0.518677	0.020915874
144	PREB	prolactin regulatory element binding	0.521182	0.039450906
143	ZCCHC8	zinc finger, CCHC domain containing 8	0.524404	0.034721721
142	CRELD2	cysteine-rich with EGF-like domains 2	0.525689	0.022364513

U2932 6hr (paired data analysis) continued.

141	FKBP2	FK506 binding protein 2, 13kDa	0.52575	0.044487281
140	SEL1L	sel-1 suppressor of lin-12-like (C. elegans)	0.531553	0.044623686
139	SYTL1	synaptotagmin-like 1	0.532337	0.048982213
138	YARS	tyrosyl-tRNA synthetase	0.535436	0.01794073
137	NLRP11	NLR family, pyrin domain containing 11	0.535728	0.025851479
136	LIPG	lipase, endothelial	0.536419	0.009673828
135	BET1	Bet1 golgi vesicular membrane trafficking protein	0.538502	0.010619499
134	OSTC	oligosaccharyltransferase complex subunit (non-catalytic)	0.544451	0.01741491
133	NA	NA	0.547035	0.037220693
132	STT3A	STT3A, subunit of the oligosaccharyltransferase complex (catalytic)	0.547063	0.008900982
131	DBNDD2	dysbindin (dystrobrevin binding protein 1) domain containing 2	0.549538	0.011932323
130	HAX1	HCLS1 associated protein X-1	0.555553	0.033845817
129	NA	NA	0.55761	0.028720756
128	WARS	tryptophanyl-tRNA synthetase	0.558349	0.027495256
127	SLC35B1	solute carrier family 35, member B1	0.558828	0.041372422
126	SGK1	serum/glucocorticoid regulated kinase 1	0.562749	0.013903108
125	FCAR	Fc fragment of IgA, receptor for	0.563287	0.037220693
124	XPOT	exportin, tRNA	0.564617	0.013903108
123	NA	NA	0.565596	0.020831682
122	PDIA3P1	protein disulfide isomerase family A, member 3 pseudogene 1	0.567463	0.016285318
121	LMAN1	lectin, mannose-binding, 1	0.568062	0.014865142
120	DEPTOR	DEP domain containing MTOR-interacting protein	0.568601	0.01714672
119	SELK	selenoprotein K	0.571773	0.007585682
118	ARMCX3	armadillo repeat containing, X-linked 3	0.573453	0.008148856
117	ZNF791	zinc finger protein 791	0.573947	0.030649683
116	NA	NA	0.576418	0.028336008
115	FAM129A	family with sequence similarity 129, member A	0.578746	0.029010307
114	DNASE2	deoxyribonuclease II, lysosomal	0.578976	0.033309286
113	NA	NA	0.5799	0.030649683
112	TXNIP	thioredoxin interacting protein	0.580446	0.032172513
111	GDPD5	glycerophosphodiester phosphodiesterase domain containing 5	0.581546	0.027380708
110	NA	NA	0.583244	0.015594172
109	SEC61A1	Sec61 alpha 1 subunit (S. cerevisiae)	0.583573	0.015280539
108	MARS	methionyl-tRNA synthetase	0.586618	0.012233686
107	NA	NA	0.588101	0.015717724
106	MSMO1	methylsterol monooxygenase 1	0.5902	0.010619499
105	PDIA3P1	protein disulfide isomerase family A, member 3 pseudogene 1	0.590922	0.01188207
104	SH2B3	SH2B adaptor protein 3	0.591453	0.033309286
103	TXNDC5	thioredoxin domain containing 5 (endoplasmic reticulum)	0.591672	0.042792531
102	SLC3A2	solute carrier family 3 (amino acid transporter heavy chain), member 2	0.59267	0.025851479
101	RELL1	RELT-like 1	0.593991	0.030661525
100	SLC30A7	solute carrier family 30 (zinc transporter), member 7	0.596284	0.011489243
99	DMTF1	cyclin D binding myb-like transcription factor 1	0.597786	0.017557919
98	SNORD96A	small nucleolar RNA, C/D box 96A	0.598306	0.012233686
97	GOT1	glutamic-oxaloacetic transaminase 1, soluble	0.60132	0.006697883
96	FAM84B	family with sequence similarity 84, member B	0.601527	0.025511885
95	IDI1	isopentenyl-diphosphate delta isomerase 1	0.60203	0.008675143
94	VIMP	VCP-interacting membrane protein	0.605458	0.012554762
93	DNAJC10	DnaJ (Hsp40) homolog, subfamily C, member 10	0.607169	0.00668888
92	MTHFD2	methylenetetrahydrofolate dehydrogenase (NADP+ dependent) 2, methenyltetrahydrofolate cyclohydrolase	0.610772	0.005591198
91	SLC3A2	solute carrier family 3 (amino acid transporter heavy chain), member 2	0.61197	0.007585682
90	FNDC3A	fibronectin type III domain containing 3A	0.612733	0.023358994
89	HERPUD1	homocysteine-inducible, endoplasmic reticulum stress-inducible, ubiquitin-like domain member 1	0.612898	0.010619499
88	CREB3L2	cAMP responsive element binding protein 3-like 2	0.613561	0.008643368
87	LDLR	low density lipoprotein receptor	0.614751	0.020831682
86	CDRT4	CMT1A duplicated region transcript 4	0.615341	0.013903108
85	PGM3	phosphoglucomutase 3	0.631624	0.008675143
84	SHROOM4	shroom family member 4	0.63568	0.033309286
83	PPAPDC1B	phosphatidic acid phosphatase type 2 domain containing 1B	0.636697	0.007585682
82	NA	NA	0.639376	0.004633017
81	DNAJC3	DnaJ (Hsp40) homolog, subfamily C, member 3	0.640713	0.005591198
80	SLC33A1	solute carrier family 33 (acetyl-CoA transporter), member 1	0.643859	0.010773303

U2932 6hr (paired data analysis) continued.

79	NA	NA	0.644729	0.022330056
78	HRK	harakiri, BCL2 interacting protein	0.645622	0.02179235
77	TMEM39A	transmembrane protein 39A	0.651069	0.006697883
76	NA	NA	0.651657	0.029010307
75	NA	NA	0.654071	0.034744431
74	NA	NA	0.65414	0.044936215
73	FICD	FIC domain containing	0.665024	0.009890445
72	CHRNA5	cholinergic receptor, nicotinic, alpha 5 (neuronal)	0.672513	0.025910053
71	C19orf10	chromosome 19 open reading frame 10	0.672907	0.023601336
70	SLC10A7	solute carrier family 10, member 7	0.678197	0.0036323
69	GARS	glycyl-tRNA synthetase	0.685334	0.007585682
68	NA	NA	0.688143	0.005180881
67	SARS	seryl-tRNA synthetase	0.694314	0.015594172
66	PDIA4	protein disulfide isomerase family A, member 4	0.69504	0.005951128
65	EDEM2	ER degradation enhancer, mannosidase alpha-like 2	0.697402	0.003033585
64	TM6SF1	transmembrane 6 superfamily member 1	0.698383	0.007107279
63	ARFGAP3	ADP-ribosylation factor GTPase activating protein 3	0.700789	0.012554762
62	ASNS	asparagine synthetase (glutamine-hydrolyzing)	0.702349	0.017387647
61	MTHFD2	methylenetetrahydrofolate dehydrogenase (NADP+ dependent) 2, methenyltetrahydrofolate cyclohydrolase	0.703636	0.006697883
60	SESN2	sestrin 2	0.709595	0.009449765
59	HERPUD1	homocysteine-inducible, endoplasmic reticulum stress-inducible, ubiquitin-like domain member 1	0.7098	0.005591198
58	SSR1	signal sequence receptor, alpha	0.710991	0.003038622
57	CDK2AP2	cyclin-dependent kinase 2 associated protein 2	0.711359	0.02373166
56	WIPI1	WD repeat domain, phosphoinositide interacting 1	0.715121	0.011174268
55	RIMS3	regulating synaptic membrane exocytosis 3	0.722443	0.005951128
54	NA	NA	0.726949	0.048976659
53	WARS	tryptophanyl-tRNA synthetase	0.729405	0.01188377
52	SSR2	signal sequence receptor, beta (translocon-associated protein beta)	0.732358	0.005194784
51	TARS	threonyl-tRNA synthetase	0.738811	0.007133845
50	LOC10019098	uncharacterized LOC100190986	0.744321	0.005591198
49	TIMM44	translocase of inner mitochondrial membrane 44 homolog (yeast)	0.748022	0.02179235
48	PARM1	prostate androgen-regulated mucin-like protein 1	0.753679	0.005497236
47	MZB1	marginal zone B and B1 cell-specific protein	0.757892	0.029125291
46	EDEM1	ER degradation enhancer, mannosidase alpha-like 1	0.759675	0.005964065
45	GNL3	guanine nucleotide binding protein-like 3 (nucleolar)	0.765224	0.002657337
44	SLC1A5	solute carrier family 1 (neutral amino acid transporter), member 5	0.776662	0.006574593
43	ERLEC1	endoplasmic reticulum lectin 1	0.780985	0.004815008
42	RGS1	regulator of G-protein signaling 1	0.785255	0.00387355
41	MANF	mesencephalic astrocyte-derived neurotrophic factor	0.785629	0.003128221
40	PCK2	phosphoenolpyruvate carboxykinase 2 (mitochondrial)	0.798453	0.003033585
39	HSPA5	heat shock 70kDa protein 5 (glucose-regulated protein, 78kDa)	0.798953	0.007693883
38	SDF2L1	stromal cell-derived factor 2-like 1	0.808028	0.00316128
37	NFE2L1	nuclear factor, erythroid 2-like 1	0.808684	0.006574593
36	CHAC1	ChaC, cation transport regulator homolog 1 (E. coli)	0.809486	0.003128221
35	EGR1	early growth response 1	0.80959	0.01065754
34	DEPTOR	DEP domain containing MTOR-interacting protein	0.821001	0.002093238
33	CARS	cysteinyl-tRNA synthetase	0.822985	0.01065754
32	MTHFD1L	methylenetetrahydrofolate dehydrogenase (NADP+ dependent) 1-like	0.830947	0.00387355
31	CDKN1A	cyclin-dependent kinase inhibitor 1A (p21, Cip1)	0.833289	0.008271467
30	CTH	cystathionase (cystathionine gamma-lyase)	0.843326	0.00387355
29	NA	NA	0.854598	0.003033585
28	FKBP14	FK506 binding protein 14, 22 kDa	0.85657	0.00316128
27	LAT2	linker for activation of T cells family, member 2	0.85687	0.005497236
26	ULBP1	UL16 binding protein 1	0.864554	0.007775984
25	PSPH	phosphoserine phosphatase	0.878546	0.003033585
24	SLC6A9	solute carrier family 6 (neurotransmitter transporter, glycine), member 9	0.88289	0.00668888
23	HAX1	HCLS1 associated protein X-1	0.889668	0.005497236
22	TMED10	transmembrane emp24-like trafficking protein 10 (yeast)	0.8946	0.006697883
21	INHBE	inhibin, beta E	0.912903	0.010699661
20	HYOU1	hypoxia up-regulated 1	0.916951	0.014865142
19	VIMP	VCP-interacting membrane protein	0.951048	0.003033585

U2932 6hr (paired data analysis) continued.

18	SLC3A2	solute carrier family 3 (amino acid transporter heavy chain), member 2	0.971069	0.005497236
17	SEC24D	SEC24 family member D	0.975646	0.003259562
16	ADM2	adrenomedullin 2	1.00892	0.010619499
15	CTH	cystathionase (cystathionine gamma-lyase)	1.010549	0.002802261
14	HYOU1	hypoxia up-regulated 1	1.02276	0.012759015
13	CEBPB	CCAAT/enhancer binding protein (C/EBP), beta	1.079577	0.005591198
12	ATF4	activating transcription factor 4	1.098727	0.000612591
11	CARS	cysteinyl-tRNA synthetase	1.132496	0.00316128
10	TSC22D3	TSC22 domain family, member 3	1.166124	0.001794099
9	DNAJB9	DnaJ (Hsp40) homolog, subfamily B, member 9	1.180008	0.000164111
8	TRIB3	tribbles pseudokinase 3	1.218832	0.001861368
7	GPT2	glutamic pyruvate transaminase (alanine aminotransferase) 2	1.235849	0.000593454
6	NA	NA	1.322123	0.000551401
5	PSAT1	phosphoserine aminotransferase 1	1.421133	0.000168502
4	DDIT3	DNA-damage-inducible transcript 3	1.474143	0.00017867
3	CTH	cystathionase (cystathionine gamma-lyase)	1.493669	0.000168502
2	TSC22D3	TSC22 domain family, member 3	1.554707	0.000551401
1	PCK2	phosphoenolpyruvate carboxykinase 2 (mitochondrial)	1.588798	0.000168502

Table 15 (Continued from previous five pages). Statistically significant genes differentially expressed in U2932 cells treated with CsA for 6hrs (paired data analysis). Columns indicate the gene symbols, names, log fold-change (logFC) and P values for statistically significant genes (adjusted P-value <0.05) differentially expressed upon treatment with CsA. Data in orange indicates genes downregulated by CsA and data in blue indicates genes upregulated by CsA. Gene numbers represent genes ordered by logFC, where 1 indicates the gene with the greatest logFC. Data includes gene probes marked as N/A.

HLY-1 2hr (unpaired data analysis)

Number	symbol	name	logFC	Adjusted p value
1	NA	NA	-1.55229	0.000490704
2	CCL4L2	chemokine (C-C motif) ligand 4-like 2	-1.54347	0.000440057
3	CCL4L1	chemokine (C-C motif) ligand 4-like 1	-1.35926	0.000785135
4	PDCD1	programmed cell death 1	-0.90421	0.001522435
5	RIN2	Ras and Rab interactor 2	-0.8322	0.005003284
6	PAX9	paired box 9	-0.80567	2.00E-06
7	IL10	interleukin 10	-0.73247	0.009463346
8	TNFSF14	tumor necrosis factor (ligand) superfamily, member 14	-0.67338	3.64E-05
9	PRF1	perforin 1 (pore forming protein)	-0.62594	0.007775043
10	ZNFX1	zinc finger, NFX1-type containing 1	-0.61761	0.015667893
11	GFI1	growth factor independent 1 transcription repressor	-0.61137	0.014837415
12	EVI2A	ecotropic viral integration site 2A	-0.43986	0.000785135
2	SOCS3	suppressor of cytokine signaling 3	0.612697	0.050001082
1	NUAK2	NUAK family, SNF1-like kinase, 2	0.643851	3.64E-05

Table 16. Statistically significant genes differentially expressed in HLY-1 cells treated with CsA for 2hrs (unpaired data analysis). Columns indicate the gene symbols, names, log fold-change (logFC) and P values for statistically significant genes (adjusted P-value <0.05) differentially expressed upon treatment with CsA. Data in orange indicates genes downregulated by CsA and data in blue indicates genes upregulated by CsA. Gene numbers represent genes ordered by logFC, where 1 indicates the gene with the greatest logFC. Data includes gene probes marked as N/A.

HLY-1 2hr (paired data analysis)

Number	symbol	name	logFC	adjusted p-value
1	NA	NA	-1.552	0.000945959
2	CCL4L2	chemokine (C-C motif) ligand 4-like 2	-1.543	0.000819302
3	CCL4L1	chemokine (C-C motif) ligand 4-like 1	-1.359	0.000945959
4	EGR2	early growth response 2	-1.219	0.000401285
5	CCL3L3	chemokine (C-C motif) ligand 3-like 3	-1.181	0.000583142
6	CCL3L1	chemokine (C-C motif) ligand 3-like 1	-1.016	0.005002719
7	CCL3L1	chemokine (C-C motif) ligand 3-like 1	-1.015	0.005993273
8	CCL3	chemokine (C-C motif) ligand 3	-0.988	0.003429333
9	CD69	CD69 molecule	-0.950	0.009742034
10	EGR3	early growth response 3	-0.946	0.013790183
11	PDCD1	programmed cell death 1	-0.904	0.009422215
12	HSPE1	heat shock 10kDa protein 1	-0.864	0.003429333
13	EVI2A	ecotropic viral integration site 2A	-0.811	0.00730127
14	PAX9	paired box 9	-0.806	0.003429333
15	RAB11FIP1	RAB11 family interacting protein 1 (class I)	-0.757	0.005002719
16	TNS3	tensin 3	-0.750	0.025770314
17	IL10	interleukin 10	-0.732	0.025770314
18	TNFAIP6	tumor necrosis factor, alpha-induced protein 6	-0.711	0.005002719
19	NFATC1	nuclear factor of activated T-cells, cytoplasmic, calcineurin-dependent 1	-0.682	0.011092949
20	TNF	tumor necrosis factor	-0.676	0.010843149
21	EVI2A	ecotropic viral integration site 2A	-0.654	0.042443215
22	NA	NA	-0.631	0.025770314
23	PTPN7	protein tyrosine phosphatase, non-receptor type 7	-0.622	0.035362512
24	ZNFX1	zinc finger, NFX1-type containing 1	-0.618	0.027488853
25	GFI1	growth factor independent 1 transcription repressor	-0.611	0.027488853
26	CLEC17A	C-type lectin domain family 17, member A	-0.588	0.02282443
27	FILIP1L	filamin A interacting protein 1-like	-0.582	0.025770314
28	CCL3L1	chemokine (C-C motif) ligand 3-like 1	-0.566	0.03667148
8	KLHL42	kelch-like family member 42	0.517	0.036539906
7	DCAF5	DDB1 and CUL4 associated factor 5	0.522	0.03667148
6	ID3	inhibitor of DNA binding 3, dominant negative helix-loop-helix protein	0.556	0.025770314
5	SOCS3	suppressor of cytokine signaling 3	0.613	0.037807413
4	NUAK2	NUAK family, SNF1-like kinase, 2	0.644	0.03667148
3	RGS12	regulator of G-protein signaling 12	0.664	0.041870692
2	TXNIP	thioredoxin interacting protein	0.726	0.025770314
1	NA	NA	0.754	0.035399725

Table 17 (Continued from previous page). Statistically significant genes differentially expressed in HLY-1 cells treated with CsA for 2hrs (paired data analysis). Columns indicate the gene symbols, names, log fold-change (logFC) and P values for statistically significant genes (adjusted P-value <0.05) differentially expressed upon treatment with CsA. Data in orange indicates genes downregulated by CsA and data in blue indicates genes upregulated by CsA. Gene numbers represent genes ordered by logFC, where 1 indicates the gene with the greatest logFC. Data includes gene probes marked as N/A.

HLY-1 6hr (unpaired data analysis)

Number	symbol	name	logFC	adjusted P value
1	NUP43	nucleoporin 43kDa	-0.870	0.036621561
2	DHRS3	dehydrogenase/reductase (SDR family) member 3	-0.823	0.006479651
3	SSR3	signal sequence receptor, gamma (translocon-associated protein gamma)	-0.805	0.026607204
4	LBH	limb bud and heart development	-0.789	0.011755439
5	NFATC1	nuclear factor of activated T-cells, cytoplasmic, calcineurin-dependent 1	-0.728	0.030097875
6	HLF	hepatic leukemia factor	-0.719	0.000301597
7	GBP1	guanylate binding protein 1, interferon-inducible	-0.676	0.009842981
8	CRY1	cryptochrome circadian clock 1	-0.672	0.009531744
9	EHD4	EH-domain containing 4	-0.651	0.036621561
10	CD36	CD36 molecule (thrombospondin receptor)	-0.612	0.005841722
11	NAMPT	nicotinamide phosphoribosyltransferase	-0.606	0.030097875
12	HNRNPH1	heterogeneous nuclear ribonucleoprotein H1 (H)	-0.584	0.005841722
13	GNG10	guanine nucleotide binding protein (G protein), gamma 10	-0.558	0.040294347
14	NA	NA	-0.545	0.021162023
15	C1orf186	chromosome 1 open reading frame 186	-0.544	0.011755439
16	LEF1	lymphoid enhancer-binding factor 1	-0.541	0.037655527
17	GBP2	guanylate binding protein 2, interferon-inducible	-0.492	0.011755439
12	NA	NA	0.418	0.030097875
11	SCN2A	sodium channel, voltage-gated, type II, alpha subunit	0.481	0.006479651
10	GUSBP11	glucuronidase, beta pseudogene 11	0.579	0.026607204
9	NA	NA	0.588	0.005841722
8	NA	NA	0.658	0.043990101
7	SNORD96A	small nucleolar RNA, C/D box 96A	0.693	0.008859118
6	SCART1	scavenger receptor protein family member	0.699	0.009531744
5	RALGPS2	Ral GEF with PH domain and SH3 binding motif 2	0.765	0.045460261
4	NA	NA	0.789	0.036621561
3	DDX17	DEAD (Asp-Glu-Ala-Asp) box helicase 17	0.801	0.047802366
2	RALGPS2	Ral GEF with PH domain and SH3 binding motif 2	0.910	0.005841722
1	SFN	stratifin	1.188	0.005841722

Table 18. Statistically significant genes differentially expressed in HLY-1 cells treated with CsA for 6hrs (unpaired data analysis). Columns indicate the gene symbols, names, log fold-change (logFC) and P values for statistically significant genes (adjusted P-value <0.05) differentially expressed upon treatment with CsA. Data in orange indicates genes downregulated by CsA and data in blue indicates genes upregulated by CsA. Genes numbers represent genes ordered by logFC, where 1 indicates the gene with the greatest logFC. Data includes gene probes marked as N/A.

HLY-1 6hr (paired data analysis)

Number	symbol	name	logFC	adjusted P value
1	TNF	tumor necrosis factor	-1.123	0.007625712
2	MAP3K8	mitogen-activated protein kinase kinase kinase 8	-1.023	0.006507769
3	NA	NA	-0.906	0.027633349
4	JUN	jun proto-oncogene	-0.879	0.007625712
5	NFKBIE	nuclear factor of kappa light polypeptide gene enhancer in B-cells inhibitor, epsilon	-0.873	0.020173855
6	NUP43	nucleoporin 43kDa	-0.870	0.035812526
7	SSR3	signal sequence receptor, gamma (translocon-associated protein gamma)	-0.805	0.017309688
8	EGR2	early growth response 2	-0.797	0.035812526
9	LBH	limb bud and heart development	-0.789	0.018836051
10	SRF	serum response factor (c-fos serum response element-binding transcription factor)	-0.778	0.018836051
11	RFWD3	ring finger and WD repeat domain 3	-0.736	0.043530578
12	FILIP1L	filamin A interacting protein 1-like	-0.728	0.019217247
13	NFATC1	nuclear factor of activated T-cells, cytoplasmic, calcineurin-dependent 1	-0.728	0.020173855
14	NFKBIA	nuclear factor of kappa light polypeptide gene enhancer in B-cells inhibitor, alpha	-0.727	0.027633349
15	PRPS1	phosphoribosyl pyrophosphate synthetase 1	-0.723	0.020173855
16	IGF2R	insulin-like growth factor 2 receptor	-0.723	0.035812526
17	HLF	hepatic leukemia factor	-0.719	0.022685527
18	CD1C	CD1c molecule	-0.715	0.027633349
19	ATP6V1F	ATPase, H+ transporting, lysosomal 14kDa, V1 subunit F	-0.709	0.027633349
20	FANCG	Fanconi anemia, complementation group G	-0.700	0.033798353
21	NA	NA	-0.680	0.027633349
22	GBP1	guanylate binding protein 1, interferon-inducible	-0.676	0.036227514
23	CIRH1A	cirrhosis, autosomal recessive 1A (cirhin)	-0.670	0.036784658
24	NA	NA	-0.668	0.031901152
25	NOL12	nucleolar protein 12	-0.666	0.029689317
26	CD83	CD83 molecule	-0.661	0.027633349
27	TRMT2B	tRNA methyltransferase 2 homolog B (S. cerevisiae)	-0.656	0.027633349
28	CD83	CD83 molecule	-0.655	0.029689317
29	EHD4	EH-domain containing 4	-0.651	0.031843488
30	PTGER4	prostaglandin E receptor 4 (subtype EP4)	-0.649	0.028928287
31	AMY1A	amylase, alpha 1A (salivary)	-0.645	0.037951338
32	DDX23	DEAD (Asp-Glu-Ala-Asp) box polypeptide 23	-0.640	0.031843488
33	PPP2R4	protein phosphatase 2A activator, regulatory subunit 4	-0.638	0.046021356
34	NFKBID	nuclear factor of kappa light polypeptide gene enhancer in B-cells inhibitor, delta	-0.633	0.036920475
35	FCF1	FCF1 rRNA-processing protein	-0.633	0.03348353
36	SGK223	homolog of rat pragma of Rnd2	-0.632	0.035812526
37	LTA	lymphotoxin alpha	-0.631	0.035812526
38	AGMAT	agmatine ureohydrolase (agmatinase)	-0.629	0.045294349
39	ZYX	zyxin	-0.618	0.037951338
40	DYRK1A	dual-specificity tyrosine-(Y)-phosphorylation regulated kinase 1A	-0.614	0.03333404
41	CD36	CD36 molecule (thrombospondin receptor)	-0.612	0.032717701
42	NAMPT	nicotinamide phosphoribosyltransferase	-0.606	0.03333404
43	SLX1A	SLX1 structure-specific endonuclease subunit homolog A (S. cerevisiae)	-0.605	0.035812526
44	MB21D1	Mab-21 domain containing 1	-0.599	0.035812526
45	NFKBIZ	nuclear factor of kappa light polypeptide gene enhancer in B-cells inhibitor, zeta	-0.594	0.037951338
46	MCRS1	microspherule protein 1	-0.589	0.036920475
47	NA	NA	-0.585	0.042392229
48	POLR2L	polymerase (RNA) II (DNA directed) polypeptide L, 7.6kDa	-0.564	0.047803903
49	GNG10	guanine nucleotide binding protein (G protein), gamma 10	-0.558	0.043958881
50	DNLZ	DNL-type zinc finger	-0.553	0.046091687
51	FBXL20	F-box and leucine-rich repeat protein 20	-0.550	0.046091687
52	GCLC	glutamate-cysteine ligase, catalytic subunit	-0.546	0.047317135
101	WASF2	WAS protein family, member 2	0.563	0.042392229
100	HSD17B7P2	hydroxysteroid (17-beta) dehydrogenase 7 pseudogene 2	0.563	0.047803903
99	UBA1	ubiquitin-like modifier activating enzyme 1	0.575	0.046021356

HLY-1 6hr (paired data analysis) continued.

98	FAM98B	family with sequence similarity 98, member B	0.576	0.047652546
97	GUSBP11	glucuronidase, beta pseudogene 11	0.579	0.036227514
96	VPREB3	pre-B lymphocyte 3	0.582	0.046021356
95	SMA5	glucuronidase, beta pseudogene	0.582	0.042417263
94	NEMF	nuclear export mediator factor	0.584	0.039488201
93	NA	NA	0.588	0.036607731
92	FAF1	Fas (TNFRSF6) associated factor 1	0.597	0.036920475
91	ORAI2	ORAI calcium release-activated calcium modulator 2	0.597	0.033658626
90	HMGCS1	3-hydroxy-3-methylglutaryl-CoA synthase 1 (soluble)	0.600	0.035812526
89	MVK	mevalonate kinase	0.604	0.035812526
88	NA	NA	0.609	0.042411387
87	NA	NA	0.610	0.035812526
86	SNORD3A	small nucleolar RNA, C/D box 3A	0.614	0.03333404
85	IDH1	isocitrate dehydrogenase 1 (NADP+), soluble	0.615	0.032717701
84	GUSBP2	glucuronidase, beta pseudogene 2	0.616	0.03333404
83	HNRNPA3	heterogeneous nuclear ribonucleoprotein A3	0.619	0.037951338
82	MZB1	marginal zone B and B1 cell-specific protein	0.623	0.032717701
81	GOLIM4	golgi integral membrane protein 4	0.626	0.03348353
80	USF2	upstream transcription factor 2, c-fos interacting	0.626	0.03312661
79	TCERG1	transcription elongation regulator 1	0.629	0.036068649
78	GINM1	glycoprotein integral membrane 1	0.629	0.030624744
77	TAF5L	TAF5-like RNA polymerase II, p300/CBP-associated factor (PCAF)-associated factor, 65kDa	0.632	0.032717701
76	VOPP1	vesicular, overexpressed in cancer, prosurvival protein 1	0.633	0.035369597
75	SORL1	sortilin-related receptor, L(DLR class) A repeats containing	0.637	0.038557508
74	NA	NA	0.639	0.032717701
73	ST6GALNAC4	ST6 (alpha-N-acetyl-neuraminyl-2,3-beta-galactosyl-1,3)-N-acetylgalactosaminide alpha-2,6-sialyltransferase 4	0.639	0.031843488
72	SNORA12	small nucleolar RNA, H/ACA box 12	0.640	0.032717701
71	NA	NA	0.649	0.03348353
70	GUSBP2	glucuronidase, beta pseudogene 2	0.650	0.031993965
69	NA	NA	0.653	0.027633349
68	CD79A	CD79a molecule, immunoglobulin-associated alpha	0.656	0.03333404
67	NA	NA	0.658	0.027633349
66	NA	NA	0.658	0.029689317
65	NA	NA	0.658	0.029689317
64	ITGB7	integrin, beta 7	0.658	0.028656323
63	TAF1	TAF1 RNA polymerase II, TATA box binding protein (TBP)-associated factor, 250kDa	0.660	0.038557508
62	SQLE	squalene epoxidase	0.660	0.029857453
61	KRI1	KRI1 homolog (S. cerevisiae)	0.666	0.027633349
60	LCMT1	leucine carboxyl methyltransferase 1	0.666	0.039645885
59	RN7SK	RNA, 7SK small nuclear	0.669	0.031843488
58	CDK5RAP3	CDK5 regulatory subunit associated protein 3	0.671	0.027028101
57	FAM102A	family with sequence similarity 102, member A	0.673	0.039920214
56	SDF4	stromal cell derived factor 4	0.678	0.036227514
55	SNORD96A	small nucleolar RNA, C/D box 96A	0.693	0.021634582
54	NA	NA	0.693	0.036920475
53	ADAP1	ArfGAP with dual PH domains 1	0.696	0.029689317
52	SCART1	scavenger receptor protein family member	0.699	0.027633349
51	NA	NA	0.701	0.033658626
50	RBM39	RNA binding motif protein 39	0.704	0.020173855
49	RBM38	RNA binding motif protein 38	0.710	0.020173855
48	NA	NA	0.717	0.031391766
47	SNORD56	small nucleolar RNA, C/D box 56	0.719	0.032717701
46	DDIT3	DNA-damage-inducible transcript 3	0.720	0.039645885
45	NLRP7	NLR family, pyrin domain containing 7	0.725	0.027028101
44	IDI1	isopentenyl-diphosphate delta isomerase 1	0.725	0.042417263
43	PPM1K	protein phosphatase, Mg2+/Mn2+ dependent, 1K	0.726	0.035812526
42	NA	NA	0.730	0.032717701
41	RAB5C	RAB5C, member RAS oncogene family	0.737	0.027633349

HLY-1 6hr (paired data analysis) continued.

40	SNHG4	small nucleolar RNA host gene 4 (non-protein coding)	0.742	0.01907066
39	PLEKHA2	pleckstrin homology domain containing, family A (phosphoinositide binding specific) member 2	0.742	0.020173855
38	ANP32AP1	acidic (leucine-rich) nuclear phosphoprotein 32 family, member A pseudogene 1	0.743	0.033658626
37	DHCR7	7-dehydrocholesterol reductase	0.744	0.027028101
36	MSMO1	methylsterol monooxygenase 1	0.748	0.018836051
35	LSP1	lymphocyte-specific protein 1	0.753	0.026873039
34	POU2F2	POU class 2 homeobox 2	0.753	0.020173855
33	FST	follistatin	0.757	0.027633349
32	TSC22D3	TSC22 domain family, member 3	0.761	0.027028101
31	RALGPS2	Ral GEF with PH domain and SH3 binding motif 2	0.765	0.018020406
30	NLRP7	NLR family, pyrin domain containing 7	0.765	0.020173855
29	NA	NA	0.770	0.027633349
28	PRKCSH	protein kinase C substrate 80K-H	0.774	0.017885243
27	DHCR7	7-dehydrocholesterol reductase	0.774	0.020173855
26	NA	NA	0.776	0.018020406
25	NA	NA	0.789	0.017309688
24	TMEM159	transmembrane protein 159	0.789	0.018836051
23	DDX17	DEAD (Asp-Glu-Ala-Asp) box helicase 17	0.801	0.020173855
22	MEF2BNB-MEF2B	MEF2BNB-MEF2B readthrough	0.808	0.027633349
21	NA	NA	0.815	0.013238241
20	UBE2E1	ubiquitin-conjugating enzyme E2E 1	0.827	0.010967044
19	LDLR	low density lipoprotein receptor	0.836	0.04535726
18	KPNA6	karyopherin alpha 6 (importin alpha 7)	0.850	0.010119927
17	AP1S1	adaptor-related protein complex 1, sigma 1 subunit	0.851	0.010119927
16	FADS1	fatty acid desaturase 1	0.862	0.027063976
15	DDX17	DEAD (Asp-Glu-Ala-Asp) box helicase 17	0.896	0.010119927
14	FBXW7	F-box and WD repeat domain containing 7, E3 ubiquitin protein ligase	0.910	0.007625712
13	RALGPS2	Ral GEF with PH domain and SH3 binding motif 2	0.910	0.007625712
12	NA	NA	0.912	0.028928287
11	CCDC71	coiled-coil domain containing 71	0.921	0.007625712
10	AP1S1	adaptor-related protein complex 1, sigma 1 subunit	0.924	0.007625712
9	KIAA1524	KIAA1524	0.924	0.010119927
8	MSMO1	methylsterol monooxygenase 1	0.952	0.006507769
7	COPG2	coatomer protein complex, subunit gamma 2	0.973	0.005970127
6	TSC22D3	TSC22 domain family, member 3	1.006	0.005413247
5	SFN	stratifin	1.188	0.0036354
4	PPP3R1	protein phosphatase 3, regulatory subunit B, alpha	1.197	0.005970127
3	ROCK1	Rho-associated, coiled-coil containing protein kinase 1	1.306	0.000925619
2	CTSZ	cathepsin Z	1.918	5.74E-05
1	NA	NA	3.068	0.000228568

Table 19 (Continued from previous two pages). Statistically significant genes differentially expressed in HLY-1 cells treated with CsA for 6hrs (paired data analysis). Columns indicate the gene symbols, names, log fold-change (logFC) and P values for statistically significant genes (adjusted P-value <0.05) differentially expressed upon treatment with CsA. Data in orange indicates genes downregulated by CsA and data in blue indicates genes upregulated by CsA. Gene numbers represent genes ordered by logFC, where 1 indicates the gene with the greatest logFC. Data includes gene probes marked as N/A.

WSU-NHL 6hr (unpaired data analysis)

Number	symbol	name	logFC	adjusted P value
1	UPF3B	UPF3 regulator of nonsense transcripts homolog B (yeast)	-0.678	0.021156406
3	SNORD96A	small nucleolar RNA, C/D box 96A	0.731	0.021156406
2	DNAJB11	DnaJ (Hsp40) homolog, subfamily B, member 11	0.826	0.023488487
1	HSPA5	heat shock 70kDa protein 5 (glucose-regulated protein, 78kDa)	1.063	0.021156406

Table 20. Statistically significant genes differentially expressed in WSU-NHL cells treated with CsA for 6hrs (unpaired data analysis). Columns indicate the gene symbols, names, log fold-change (logFC) and P values for statistically significant genes (adjusted P-value <0.05) differentially expressed upon treatment with CsA. Data in orange indicates genes downregulated by CsA and data in blue indicates genes upregulated by CsA. Gene numbers represent genes ordered by logFC, where 1 indicates the gene with the greatest logFC. Data includes gene probes marked as N/A.

4.2.7. Confirmation of array data target genes using qRT-PCR

To confirm the CsA-induced effects on gene expression observed in the microarray and to help decide whether paired or unpaired data analysis was most representative of the array, qRT-PCR analysis was conducted using the RNA array samples. Seven statistically significant, differentially expressed genes of interest were chosen for analysis, as described below. To further validate the findings of the microarray, the experiment was repeated in HLY-1 cells.

Moreover, to gain an understanding of the regulation of potential NFAT target genes in DLBCL, the effects of CsA treatment on an expanded panel of DLBCL cell lines was investigated. First, to confirm CsA-induced inhibition of NFAT2 in the panel, the subcellular localisation of NFAT2 was assessed by Western blot. As shown in figure 45, in the DMSO controls, NFAT2 was expressed at higher levels in the nucleus compared to the cytoplasm. When treated with CsA, a shift from the nucleus to the cytoplasm is observed in all cell lines. Moreover, CsA also caused an increase in the intensity of upper bands within each cluster and a decrease in the dephosphorylated (active) splice variants which is indicative of the rephosphorylation of the remaining NFAT2 protein in the nucleus.

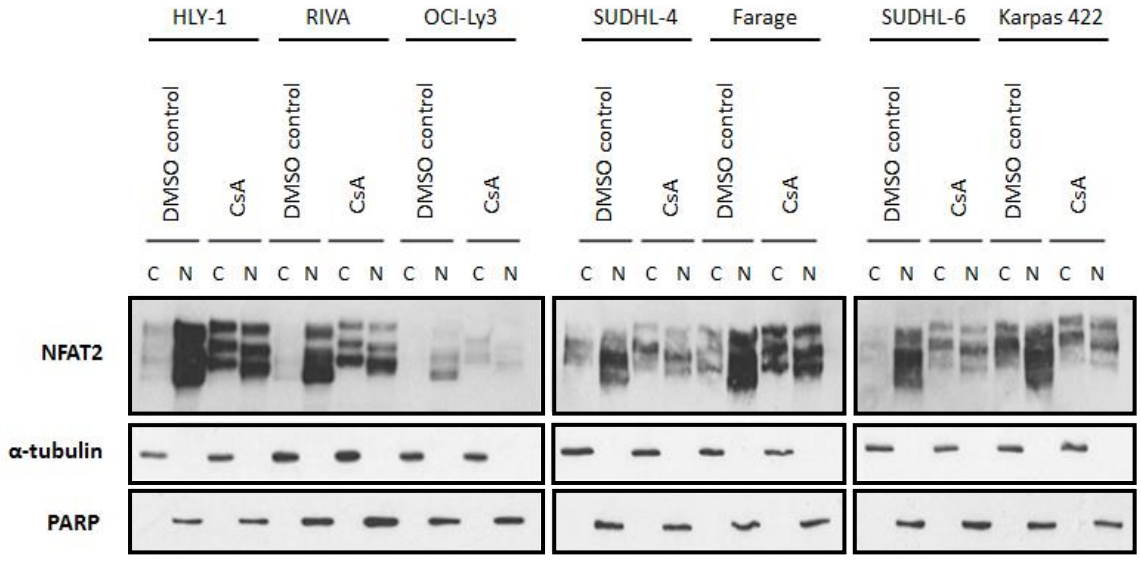

Figure 45. NFAT2 is inhibited by CsA in a panel of DLBCL cell lines. A panel of DLBCL cell lines were treated with their respective IC50 concentrations of CsA (HLY-1 7.4µg/ml, RIVA 13.5µg/ml, OCI-Ly3 10.6µg/ml, SUDHL-4 15.6µg/ml, Farage 11.8µg/ml, SUDHL-6 3.6µg/ml and Karpas 422 14.9µg/ml) for 2 hours before nuclear extracts were taken and the expression of NFAT2 analysed by Western blot. . A vehicle control sample (0.01% DMSO) was also included. Nuclear-cytoplasmic preparations illustrate the comparative subcellular localisation and activation of family members. Data is from one experiment.

4.2.7.1.Differential regulation of NFAT2 by calcineurin/NFAT signalling in DLBCL cell lines

As described in earlier sections of the study, NFAT2 is a calcium-responsive member of the NFAT family of transcription factors. Activated by stimulation of the BCR, constitutive expression and activation of NFAT2 has been demonstrated in patient samples and cell lines representative of DLBCL (Marafioti *et al.*, 2005; Pham *et al.*, 2005; Fu *et al.*, 2006; Pham *et al.*, 2010). Moreover, NFAT2 isoforms have demonstrated oncogenic characteristics in certain cell types, where autoregulation of the short NFAT2/Aα isoform is thought to play a key role (Chuvpilo *et al.*, 2002; Asagiri *et al.*, 2005; Serfling *et al.*, 2006a; Hock *et al.*, 2013).

Considering the known autoregulation of NFAT2 by other NFAT family members, it was anticipated that NFAT2 expression would be downregulated in the array and would therefore be suitable as a good positive control gene for confirmation of array findings by qRT-PCR analysis. Indeed, differential expression of NFAT2 was recurrently in the top 20 genes downregulated by CsA (tables 14-15 and 17-19) and NFAT2 was among the top 15 genes with the lowest adjusted P-value. Data in figure 46b-d demonstrates that CsA significantly downregulated the expression of NFAT2 in U2932 and HLY-1 cells after 6 hours incubation in the microarray, but no effect was observed in the GCB DLBCL cell line WSU-NHL. qRT-PCR analysis recapitulated these findings, demonstrating a time-dependent reduction of NFAT2 in the ABC lines but having little to no effect in WSU-NHL cells (figure 46b-d). Although not striking, NFAT2 was downregulated in HLY-1 cells treated with CsA for 2 hours, as indicated by paired, but not paired analysis. This suggests that paired analysis was slightly more representative of the array than unpaired analysis for this particular gene.

Despite NFAT2 being an excellent positive-control gene, the degree to which its expression was inhibited by CsA was less than expected, particularly across the cell line panel, as shown in figure 46e. This may be explained by the fact that ablation of calcineurin activity results in the inhibition of all calcium-responsive NFAT isoforms. The effects observed on one single family member (such as NFAT2) therefore, may not be substantial and may depend on which NFAT isoforms are expressed in particular cell lines and the extent to which a cell line utilised the NFAT2 autoregulatory mechanism. Moreover, autoregulation of NFAT2 has only been reported for the short NFAT2/Aα

isoform, however these experiments used a primer specific for all NFAT2 isoforms (Chuvpilo *et al.*, 2002; Hock *et al.*, 2013) . It is therefore possible that downregulation of the short NFAT2/Aα isoform may have been masked by the expression of other NFAT2 isoforms. Overall however, an interesting observation was that CsA-induced downregulation of NFAT2 was only observed in ABC DLBCL cell lines (apart from OCI-Ly3), whereas there was no apparent effect in all five GCB DLBCL cell lines tested. These data suggest that autoregulation of NFAT2 may be DLBCL subgroup-specific.

a.

NFAT2	2hr			6hr		
Cell line	Log FC	Unpaired p-value	Paired p-value	Log FC	Unpaired p-value	Paired p-value
U2932	-0.54	0.2171770383	0.8568731580	-0.73	0.0018681278	0.0038287636
WSU-NHL	-0.11	0.9360866390	0.8019760087	0.11	0.9656725194	0.9001941372
HLY-1	-0.68	0.6451650564	0.0110929489	-0.73	0.0300978747	0.0201738555

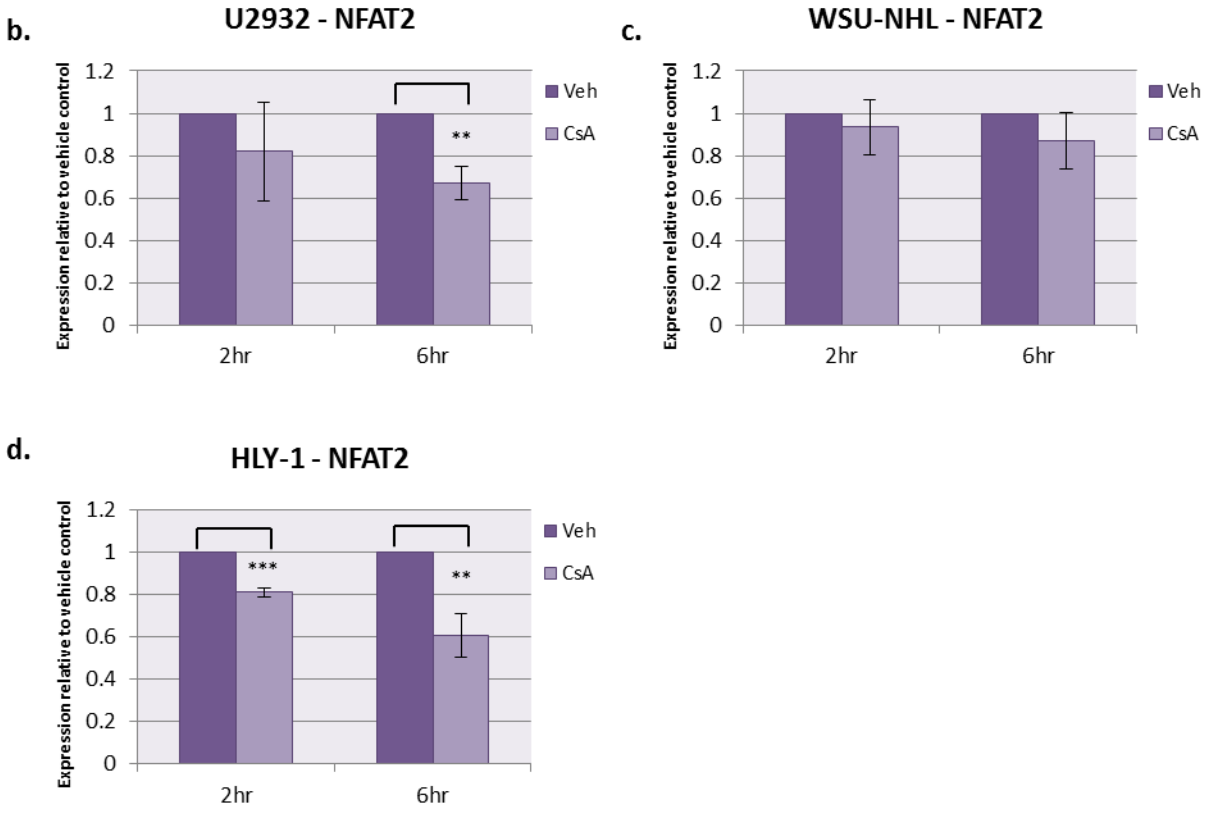

Figure 46. Differential regulation of NFAT2 by calcineurin/NFAT signalling in DLBCL cell lines. a) Table showing the microarray log FC expression of NFAT2 in cell lines treated with CsA for 2hrs or 6hrs, including respective adjusted p-values from unpaired and paired data analysis. Adjusted P-values highlighted in red are indicative of statistical significance (adjusted P-value <0.05). b-d) The ABC DLBCL cell lines U2932 and HLY-1 (b and d) and the GCB DLBCL cell line WSU-NHL (c) were treated with their respective IC50 concentrations of CsA (U2932 8.6µg/ml, HLY-1 7.4µg/ml and WSU-NHL10.4µg/ml) for 2 hours and 6 hours before the effects of treatment on NFAT2 mRNA expression were analysed by qRT-PCR (using RNA from gene expression microarray samples). Data is representative of four independent experiments where error bars indicate the standard error of the mean. P-values for qRT-PCR; U2932 2hr: 0.22 (insignificant) 6hr: 0.004, WSU-NHL 2hr: 0.390 (insignificant) 6hr: 0.148 (insignificant), HLY-1 2hr: <0.000 6hr: 0.005.

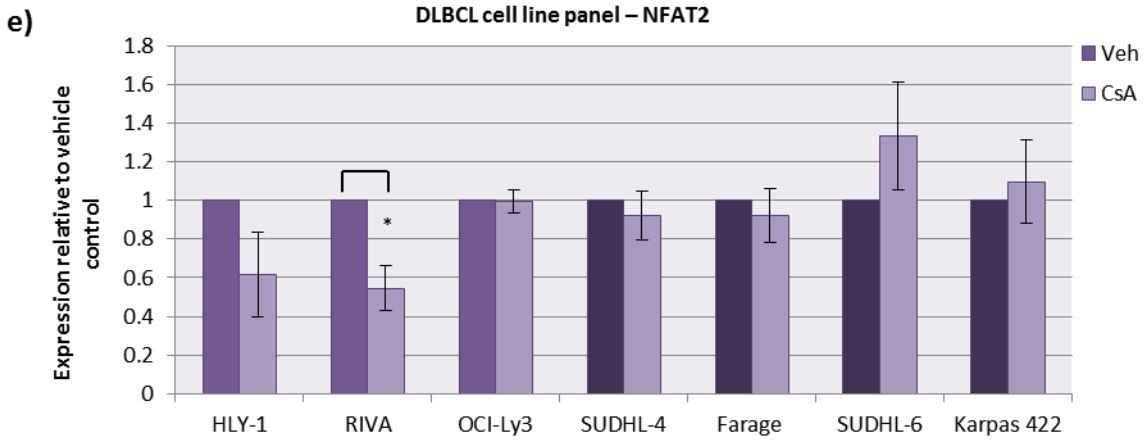

Figure 46 (Continued from previous page). Differential regulation of NFAT2 by calcineurin/NFAT signalling in DLBCL cell lines. e) A panel of DLBCL cell lines were treated with their respective IC50 concentrations of CsA (HLY-1 7.4µg/ml, RIVA 13.5µg/ml, OCI-Ly3 10.6µg/ml, SUDHL-4 15.6µg/ml, Farage 11.8µg/ml, SUDHL-6 3.6µg/ml and Karpas 422 14.9µg/ml) for 2 hours before the effects on NFAT2 mRNA expression were analysed by qRT-PCR. Lighter shaded bars indicate ABC DLBCL cell lines (HLY-1, RIVA and OCI-Ly3) whereas darker shaded bars represent GCB DLBCL cell lines (SUDHL-4, Farage, SUDHL-6 and Karpas 422). Data for b-e were normalised to the house-keeping gene GAPDH. Data for e is representative of three independent experiments where error bars indicate the standard error of the mean. P-values for qRT-PCR; HLY-1: 0.092 (insignificant), RIVA: 0.022, OCI-Ly3: 0.088 (insignificant), SUDHL-4: 0.389 (insignificant), Farage: 0.444 (insignificant), SUDHL-6: 0.173 (insignificant), Karpas 422: 0.517 (insignificant).

4.2.7.2. CsA has no effect on MYC and BCL6 mRNA expression

To confirm the accuracy of the array, the expression of the transcription factors BCL6 and MYC (which were unaffected by CsA treatment in the array analysis), were analysed by qRT-PCR using RNA samples used in the microarray. The log expression fold-change (logFC) for BCL6 probes in the data set for all three cell lines ranged from -0.13 to 0.29 and for MYC ranged from -0.36-0.3 (based on data from multiple MYC and BCL6 probes), indicating no change or only very little change in gene expression upon CsA treatment. Data in figure 47 demonstrates no effect of CsA on BCL6 expression in all three cell lines tested. Similarly, CsA treatment had little to no effect on the expression of MYC (figure 48). These data show that probe intensity and differential expression of genes were accurately reflected by qRT-PCR analysis, therefore providing confidence for the specificity and validity of the microarray.

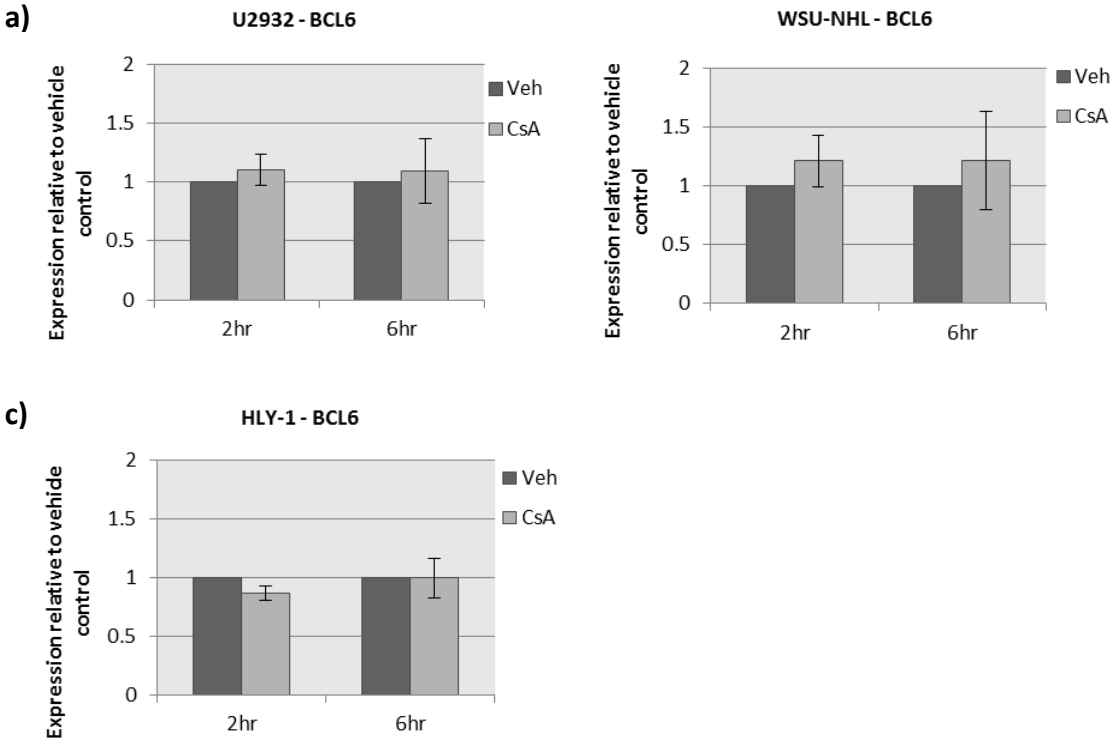

Figure 47. CsA has no effect on BCL6 mRNA expression. a-c) The ABC DLBCL cell lines U2932 and HLY-1 (a-b) and the GCB DLBCL cell line WSU-NHL (c) were treated with their respective IC50 concentrations of CsA (U2932 8.6µg/ml, HLY-1 7.4µg/ml and WSU-NHL10.4µg/ml) for 2 hours and 6 hours before the effects of treatment on BCL6 mRNA expression were analysed by qRT-PCR (using RNA from gene expression microarray samples). Data is representative of four independent experiments where error bars indicate the standard error of the mean.

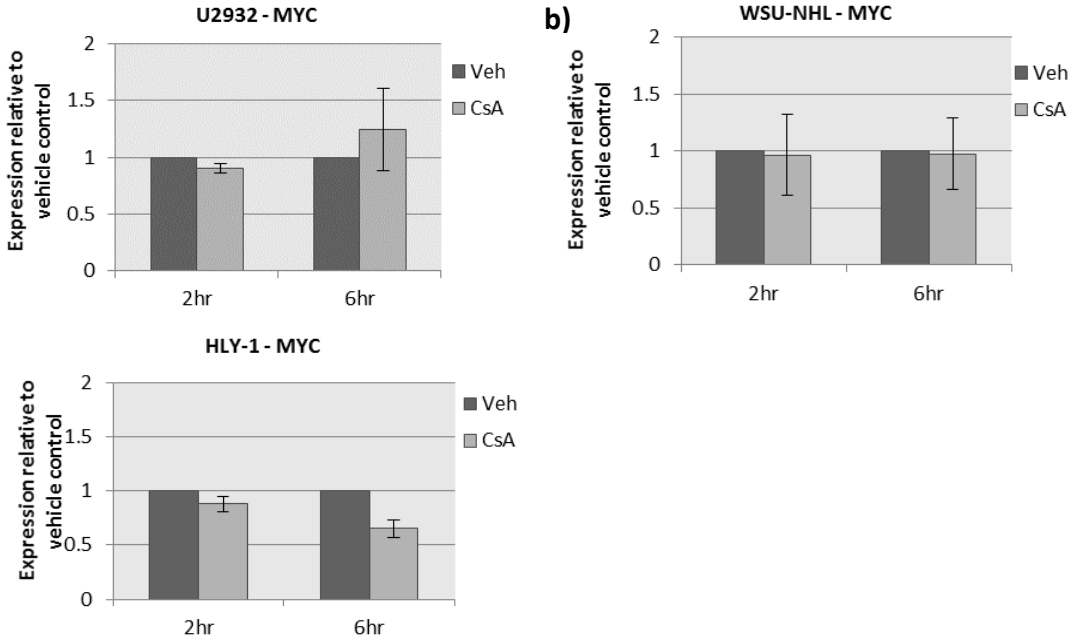

Figure 48. CsA has no effect on MYC mRNA expression. a-c) The ABC DLBCL cell lines U2932 and HLY-1 (a-b) and the GCB DLBCL cell line WSU-NHL (c) were treated with their respective IC50 concentrations of CsA (U2932 8.6µg/ml, HLY-1 7.4µg/ml and WSU-NHL10.4µg/ml) for 2 hours and 6 hours before the effects of treatment on MYC mRNA expression were analysed by qRT-PCR (using RNA from gene expression microarray samples). Data is representative of four independent experiments where error bars indicate the standard error of the mean.

4.2.7.3. Differential regulation of CCL4L2 by calcineurin/NFAT signalling in DLBCL cell lines

Given the key function of NFAT in the immune system, it was not surprising to see the downregulation of a number of cytokines upon CsA treatment. Cytokines are a family of small secreted proteins which play a key role in inflammation and immunoregulation. Chemokines are a subgroup of the cytokine family, mostly known for their recruitment of leukocytes to sites of inflammation, infection or injury (Howard *et al.*, 2004). Dysregulated expression of chemokines and their receptors has been shown to influence the proliferative and invasive properties of cancer cells. In breast cancer for example, chemokines are reported to mediate tumour metastasis and are being considered as targetable molecules for cancer treatment (Muller *et al.*, 2001; Mukaida *et al.*, 2014). Chemokine (C-C motif) ligand 4-like 2 (CCL4L2) is a gene encoding a chemokine known to induce chemotaxis of cells expressing the chemokine receptors CCR5 or CCR1 (Howard *et al.*, 2004). There are limited reports on CCL4L2, but it differs by only a single amino acid from the more characterised gene encoding CCL4, a major chemotactic and proinflammatory factor produced by macrophages (Irving *et al.*, 1990; Howard *et al.*, 2004). Moreover, CCL4L2 has an identical exonic sequence to the CCL4L1 chemokine

(which was also significantly downregulated in the array), even though these genes produce different patterns of mRNA expression (Colobran *et al.*, 2010).

CCL4L2 was chosen to confirm the array findings due to its presence in the top 5 statistically significant genes downregulated by CsA treatment in the two ABC DLBCL cell lines U2932 and HLY-1, as shown in figure 49a and tables 12-15 and 16-17. Moreover, CCL4L2 was among the top 15 statistically significant genes differentially expressed in these cell lines. Figure 49b-d illustrates downregulation of CCL4L2 by CsA in all three cell lines by qRT-PCR analysis, where expression was almost completely abolished by 6 hours treatment, particularly in U2932 (b) and HLY-1 (d) cell lines. For U2932 cell lines in particular, these data were consistent with the time-dependent logFC reduction in CCL4L2 gene expression, which was significant in both paired and unpaired analysis for both timepoints. Data from the microarray demonstrated no effect of CsA on CCL4L2 expression in WSU-NHL cells (figure 40), however qRT-PCR analysis showed significant depletion of expression. The Ct values obtained for CCL4L2 during qRT-PCR analysis of WSU-NHL cells were higher than those from HLY1 and U2932 cells, suggesting a lower abundance mRNA (not shown). It is possible that the gene expression microarray was not sensitive enough to detect changes in CCL4L2 expression in WSU-NHL RNA samples, unlike the qRT-PCR analysis.

To further validate data generated in the gene expression microarray and to more comprehensively understand calcineurin/NFAT-mediated expression of CCL4L2 in DLBCL, the expression of CCL4L2 was analysed in a larger panel of cell lines treated with CsA for 2 hours. qRT-PCR analysis demonstrated downregulation of CCL4L2 in almost all cell lines, however the effects were more prominent in DLBCL cell lines of the ABC subgroup (figure 49e). CsA had little effect on CCL4L2 expression in SUDHL-4 cells and appeared to increase expression in SUDHL-6 cells, but there was significant variability between experiments in this cell line, as indicated by the large error bars.

a.

CCL4L2	2hr			6hr		
Cell line	Log FC	Unpaired p-value	Paired p-value	Log FC	Unpaired p-value	Paired p-value
U2932	-1.69	0.0000064700	0.0093800517	-2.15	0.0000000032	0.0000013300
WSU-NHL	-0.15	0.9507057869	0.7170405370	-0.12	0.9790496946	0.8288739065
HLY-1	-1.54	0.0004400573	0.0008193020	-0.71	0.4559528755	0.1637981517

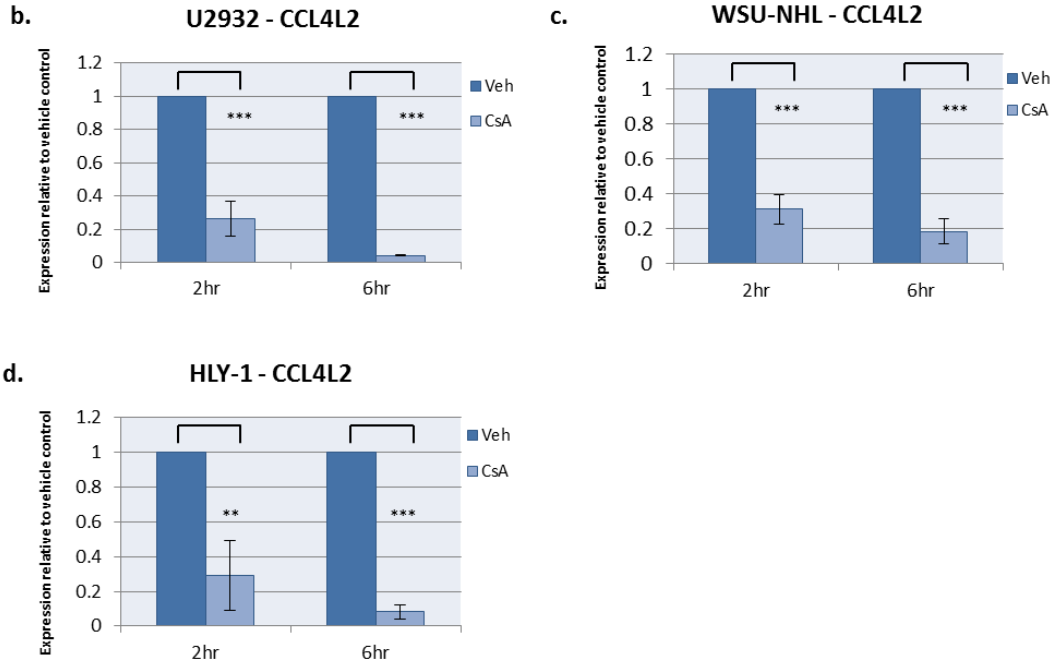

Figure 49. Differential regulation of CCL4L2 by calcineurin/NFAT signalling in DLBCL cell lines. a) Table showing the microarray log FC expression of CCL4L2 in cell lines treated with CsA for 2hrs or 6hrs, including respective adjusted p-values from unpaired and paired data analysis. Adjusted P-values highlighted in red are indicative of statistical significance (adjusted P-value <0.05). b-d) The ABC DLBCL cell lines U2932 and HLY-1 (b and d) and the GCB DLBCL cell line WSU-NHL (c) were treated with their respective IC50 concentrations of CsA (U2932 8.6µg/ml, HLY-1 7.4µg/ml and WSU-NHL10.4µg/ml) for 2 hours and 6 hours before the effects of treatment on CCL4L2 mRNA expression were analysed by qRT-PCR (using RNA from gene expression microarray samples). Data is representative of four independent experiments where error bars indicate the standard error of the mean. P-values for qRT-PCR; U2932 2hr: 0.001 6hr: <0.000, WSU-NHL 2hr: 0.001 6hr: <0.000, HLY-1 2hr: 0.006 6hr: <0.000.

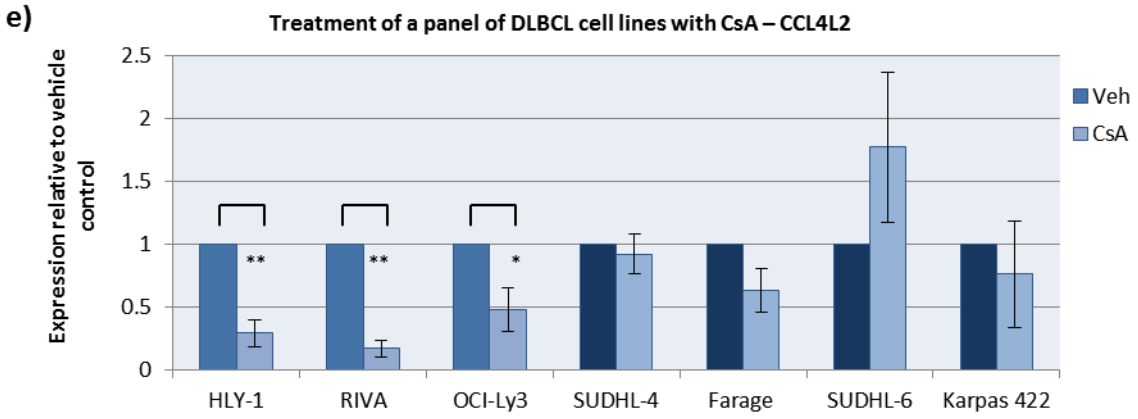

Figure 49 (Continued from previous page). Differential regulation of CCL4L2 by calcineurin/NFAT signalling in DLBCL cell lines. e) A panel of DLBCL cell lines were treated with their respective IC50 concentrations of CsA (HLY-1 7.4µg/ml, RIVA 13.5µg/ml, OCI-Ly3 10.6µg/ml, SUDHL-4 15.6µg/ml, Farage 11.8µg/ml, SUDHL-6 3.6µg/ml and Karpas 422 14.9µg/ml) for 2 hours before the effects on CCL4L2 mRNA expression were analysed by qRT-PCR. Lighter shaded bars indicate ABC DLBCL cell lines (HLY-1, RIVA and OCI-Ly3) whereas darker shaded bars represent GCB DLBCL cell lines (SUDHL-4, Farage, SUDHL-6 and Karpas 422). Data for b-e were normalised to the house-keeping gene GAPDH. Data for e is representative of three independent experiments where error bars indicate the standard error of the mean. P-values for qRT-PCR; HLY-1: 0.008, RIVA: 0.002, OCI-Ly3: 0.034, SUDHL-4: 0.481 (insignificant), Farage: 0.068 (insignificant), SUDHL-6: 0.154 (insignificant), Karpas 422: 0.427 (insignificant).

4.2.7.4.Differential regulation of TNFα by calcineurin/NFAT signalling in DLBCL cell lines

Tumour necrosis factor alpha (TNFα) is a cytokine that plays a pivotal role in the immune response and inflammation, however it is also involved with many other cellular processes such as proliferation, differentiation and apoptosis (Locksley *et al.*, 2001). Although TNFα displays a plethora of functions in the cell, it is mostly associated with regulation of the proinflammatory response, where it behaves as a ligand for TNF receptor activation and subsequent activation of downstream pathways such as NF-κB. Despite being critical for normal immune function, dysregulation of TNFα activity has been implicated in conditions such as cancer, autoimmune disorders, Alzheimer's disease, diabetes and osteoporosis (Chen *et al.*, 2002; Kollias *et al.*, 2002; Kodama *et al.*, 2005).

The table in figure 50a shows a significant downregulation of TNFα upon CsA treatment in U2932 and HLY-1 cell lines at both the 2 hour and 6 hour timepoints, whereas there was no effect in WSU-NHL cells. TNFα was in fact ranked the number one gene differentially expressed by calcineurin/NFAT inhibition in HLY-1 6 hour paired analysis and U2932 2 hour unpaired data analysis (table 19 and 12). In addition, TNFα was among

the top most statistically significant genes downregulated according to P-value, further supporting this gene as a candidate for array confirmation by qRT-PCR analysis.

qRT-PCR analysis correlated with these findings (figure 50b-d), showing the greatest reduction of TNFα after 2 hours treatment in U2932, followed by a slight increase in expression after 6 hours. Also in accordance with the array, a time-dependent depletion of TNFα was observed in HLY-1 cells, whereas TNFα expression in WSU-NHL cells did not change. Moreover, apart from U2932 cells treated with CsA for 2 hours, paired analysis seemed to reflect qRT-PCR analysis more consistently than unpaired analysis for this particular gene.

Apart from OCI-Ly3 cells, CsA-induced reduction in TNFα expression was largely correlated with the ABC subgroup of DLBCL, as shown in figure 50e. Interestingly, OCI-Ly3 was the only ABC DLBCL found to express low levels of NFAT2 protein (chapter 3, figure 15). TNFα expression in the GCB cell lines however did not appear to significantly change by CsA treatment, suggesting that TNFα may specifically be regulated by calcineurin/NFAT in ABC DLBCL cells. Although the large error bars for SUDHL-4 and SUDHL-6 indicate inconsistency between experiments, it is possible that this was due to the inability of qRT-PCR analysis to detect changes in expression of TNFα, which was apparent by the high Ct values recorded for these two cell lines (not shown).

a.

TNFα	2hr			6hr		
Cell line	Log FC	Unpaired p-value	Paired p-value	Log FC	Unpaired p-value	Paired p-value
U2932	-1.89	0.0047061881	0.0881162383	-1.05	0.2216086703	0.0017764787
WSU-NHL	-0.02	0.9975093920	0.9818637478	0.41	0.9656725194	0.5717083774
HLY-1	-0.68	0.9874205930	0.0108431493	-1.12	0.3743759006	0.0076257117

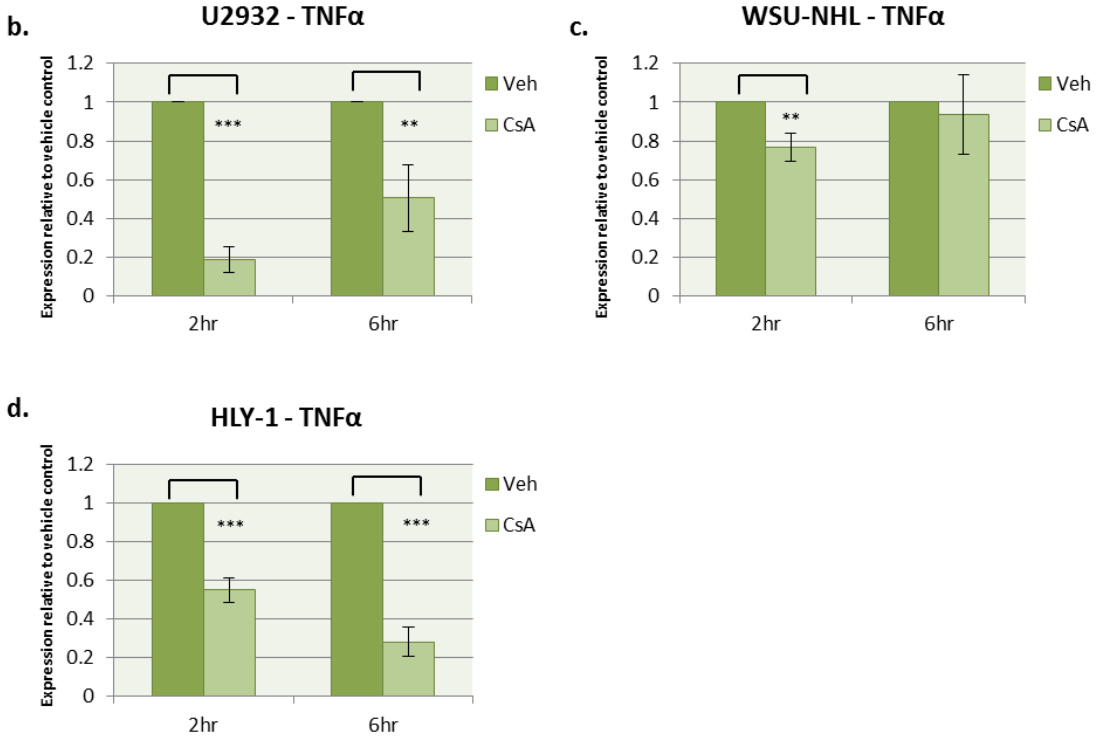

Figure 50. Differential regulation of TNFα by calcineurin/NFAT signalling in DLBCL cell lines. a) Table showing the microarray log FC expression of TNFα in cell lines treated with CsA for 2hrs or 6hrs, including respective adjusted p-values from unpaired and paired data analysis. Adjusted P-values highlighted in red are indicative of statistical significance (adjusted P-value <0.05). b-d) The ABC DLBCL cell lines U2932 and HLY-1 (b and d) and the GCB DLBCL cell line WSU-NHL (c) were treated with their respective IC50 concentrations of CsA (U2932 8.6µg/ml, HLY-1 7.4µg/ml and WSU-NHL10.4µg/ml) for 2 hours and 6 hours before the effects of treatment on TNFα mRNA expression were analysed by qRT-PCR (using RNA from gene expression microarray samples). Data is representative of four independent experiments where error bars indicate the standard error of the mean. P-values for qRT-PCR; U2932 2hr: <0.000 6hr: 0.010, WSU-NHL 2hr: 0.008 6hr: 0.579 (insignificant), HLY-1 2hr: 0.001 6hr: 0.000.

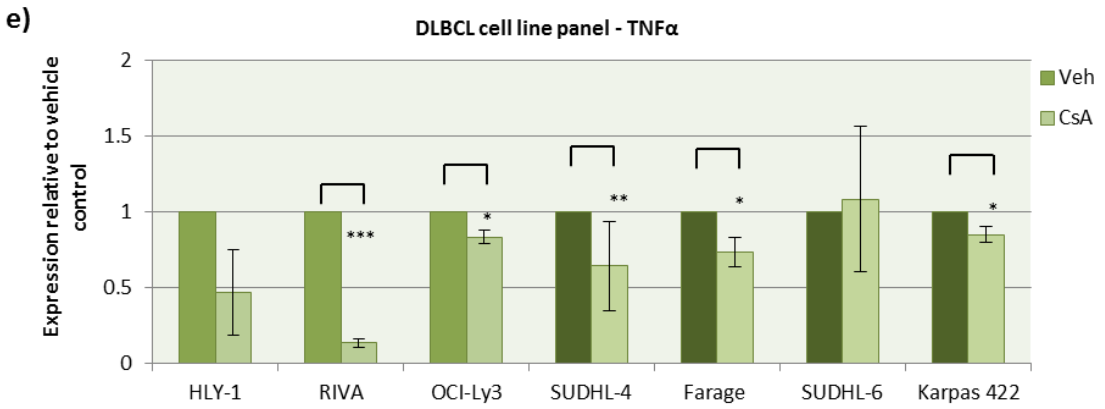

Figure 50 (Continued from previous page). Differential regulation of TNFα by calcineurin/NFAT signalling in DLBCL cell lines. e) A panel of DLBCL cell lines were treated with their respective IC50 concentrations of CsA (HLY-1 7.4μg/ml, RIVA 13.5μg/ml, OCI-Ly3 10.6μg/ml, SUDHL-4 15.6μg/ml, Farage 11.8μg/ml, SUDHL-6 3.6μg/ml and Karpas 422 14.9μg/ml) for 2 hours before the effects on TNFα mRNA expression were analysed by qRT-PCR. Lighter shaded bars indicate ABC DLBCL cell lines (HLY-1, RIVA and OCI-Ly3) whereas darker shaded bars represent GCB DLBCL cell lines (SUDHL-4, Farage, SUDHL-6 and Karpas 422). Data for b-e were normalised to the house-keeping gene GAPDH. Data for e is representative of three independent experiments where error bars indicate the standard error of the mean. P-values for qRT-PCR; HLY-1: 0.083, RIVA: <0.000, OCI-Ly3: 0.026, SUDHL-4: 0.004, Farage: 0.041, SUDHL-6: 0.799 (insignificant), Karpas 422: 0.036.

4.2.7.5. Differential regulation of NFKBIE by calcineurin/NFAT signalling in DLBCL cell lines

The protein encoded by the Nuclear Factor of Kappa Light Polypeptide Gene Enhancer in B cells Inhibitor Epsilon (NFKBIE) gene is a member of the IκB family of NF-κB inhibitory proteins. Along with other IκB proteins, IκBε binds to NF-κB subunits, masking their nuclear localisation sequence, keeping them sequestered in an inactive state in the cytoplasm. Phosphorylation of IκB proteins by IKK targets them for polyubiquitination and degradation by the 26S proteasome, activating NF-κB and allowing their translocation to the nucleus. Unlike IκBα, there is considerably less information regarding the specific role of IκBε. There is however evidence showing that IκBε functions differently to other IκB proteins (Whiteside *et al.*, 1997). First, IκBε is fairly inefficient at inhibiting the transcription of genes regulated by p50/p65 heterodimers, mostly functioning to sequester p65 and/or c-Rel homodimer in the cytoplasm (Whiteside *et al.*, 1997). Moreover, IκBε does not contain a PEST-like sequence (responsible for inhibition of DNA-binding), suggesting that IκBε may regulate the transient activation of a distinct subset of genes (Ernst *et al.*, 1995; Whiteside *et al.*, 1997). Additionally, in their report studying the temporal control and selective gene activation of IκB proteins, Hoffman and Baltimore (2002) describe IκBα to be responsible

for a fast turn-off of the NF-κB response, whereas IκBβ and IκBε control the oscillations of NF-κB in and out of the nucleus, stabilising NF-κB activity during longer periods of stimulation (Hoffmann *et al.*, 2002).

Interestingly, elevated expression of IκBε has been linked to oncogenesis in a number of malignancies, including ovarian, prostate and breast cancer (Qin *et al.*, 2010; Péant *et al.*, 2011; Hsu *et al.*, 2012). Moreover, in regard to blood malignancies, inactivating mutations of the *NFKBIE* gene have been identified in early haematopoietic cells and B cells of CLL patients, potentially contributing to the pathogenesis of CLL (Damm *et al.*, 2014).

IκBε expression was downregulated in the ABC DLBCL cell lines upon treatment with CsA, particularly after 6 hours of treatment where data was statistically significant by paired data analysis (figure 51a). Interestingly, IκBε was not the only IκB encoding gene differentially expressed in the microarray. In fact, IκBα (NFKBIA) and IκBδ (NFKBID) were significantly downregulated by CsA in HLY-1 and U2932 cells after 6 hours treatment and IκBζ (NFKBIZ) was downregulated in HLY-1 cells. These data suggest that the calcineurin/NFAT pathway may be associated with the transcriptional regulation of IκB proteins.

NFKBIE was chosen for qRT-PCR analysis due to it being the fifth most differentially expressed gene in HLY-1 cells (table 19) and the fourteenth most differentially expressed gene in U2932 after 6 hours CsA treatment (table 15). Moreover, the adjusted P-values for NFKBIE were among the 15 lowest in some samples. As shown in figure 51b and d, the expression of NFKBIE was reduced in a time-dependent manner in U2932 cells at both 2 hour and 6 hour timepoints and was downregulated in HLY-1 cells by 6 hours. Calcineurin/NFAT inhibition in WSU-NHL cells (figure 51c) had little to no effect on NFKBIE expression, which was in line with the microarray results. Overall, unpaired analysis did not appear to identify significant downregulation of NFKBIE in any samples, despite the obvious reduction observed by qRT-PCR analysis, suggesting that in this case paired analysis was more suitable.

When the experiment was repeated in a larger panel of cell lines, the effect of CsA on NFKBIE was highly variable and there were no obvious trends between DLBCL

subgroups (figure 51e). The presence of the large error bar on CsA-treated RIVA cells was due to inconsistency between each of the four repeat experiments, perhaps due to experimental error or maybe indicating NFKBIE to be highly sensitive to any fluctuations of CsA-treatment around the 2 hour timepoint.

a.

NFKBIE	2hr			6hr		
Cell line	Log FC	Unpaired p-value	Paired p-value	Log FC	Unpaired p-value	Paired p-value
U2932	-0.31	0.9133591693	0.8578505728	-0.79	0.0605885469	0.0038735497
WSU-NHL	0.18	0.9303989046	0.7214286634	0.27	0.9656725194	0.6489486583
HLY-1	-0.01	0.9965580857	0.9731426291	-0.87	0.1718207411	0.0201738555

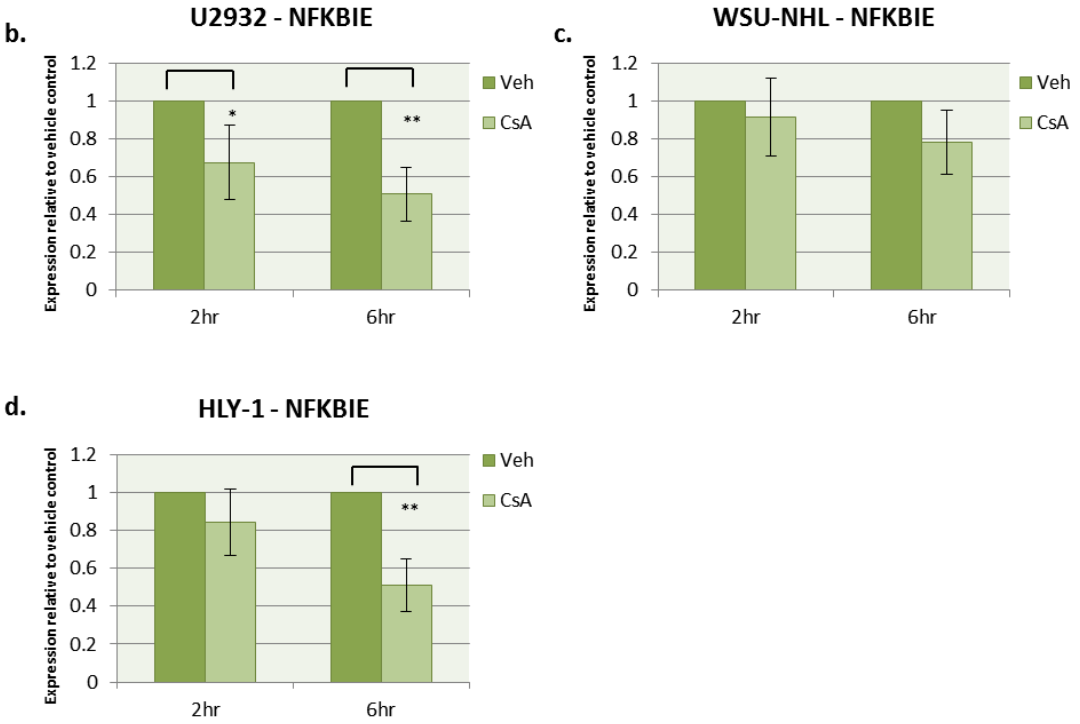

Figure 51. Differential regulation of NFKBIE by calcineurin/NFAT signalling in DLBCL cell lines. a) Table showing the microarray log FC expression of NFKBIE in cell lines treated with CsA for 2hrs or 6hrs, including respective adjusted p-values from unpaired and paired data analysis. Adjusted P-values highlighted in red are indicative of statistical significance (adjusted P-value <0.05). b-d) The ABC DLBCL cell lines U2932 and HLY-1 (b and d) and the GCB DLBCL cell line WSU-NHL (c) were treated with their respective IC50 concentrations of CsA (U2932 8.6µg/ml, HLY-1 7.4µg/ml and WSU-NHL10.4µg/ml) for 2 hours and 6 hours before the effects of treatment on NFKBIE mRNA expression were analysed by qRT-PCR (using RNA from gene expression microarray samples). Data is representative of four independent experiments where error bars indicate the standard error of the mean. P-values for qRT-PCR; U2932 2hr: 0.046 6hr: 0.006, WSU-NHL 2hr: 0.453 6hr: 0.082, HLY-1 2hr: 0.172 6hr: 0.006.

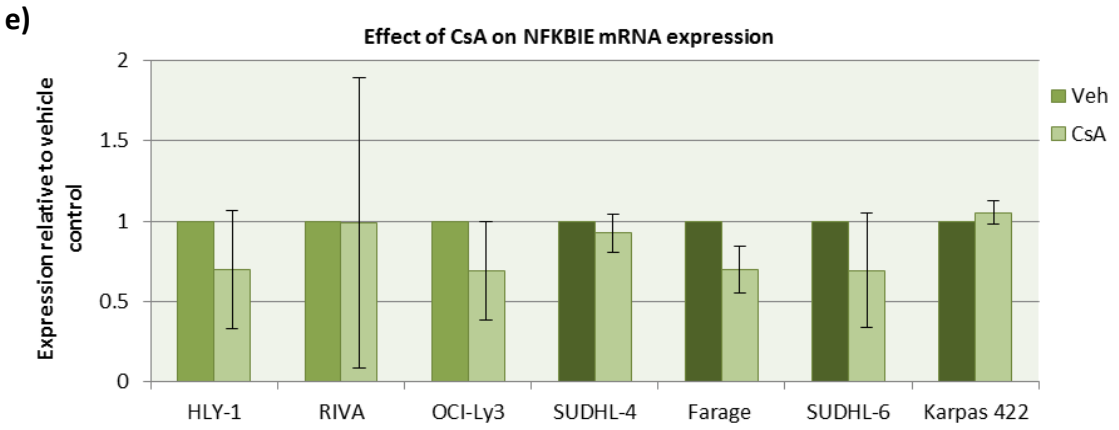

Figure 51 (Continued from previous page). Differential regulation of NFKBIE by calcineurin/NFAT signalling in DLBCL cell lines. e) A panel of DLBCL cell lines were treated with their respective IC50 concentrations of CsA (HLY-1 7.4μg/ml, RIVA 13.5μg/ml, OCI-Ly3 10.6μg/ml, SUDHL-4 15.6μg/ml, Farage 11.8μg/ml, SUDHL-6 3.6μg/ml and Karpas 422 14.9μg/ml) for 2 hours before the effects on NFKBIE mRNA expression were analysed by qRT-PCR. Lighter shaded bars indicate ABC DLBCL cell lines (HLY-1, RIVA and OCI-Ly3) whereas darker shaded bars represent GCB DLBCL cell lines (SUDHL-4, Farage, SUDHL-6 and Karpas 422). Data for b-e were normalised to the house-keeping gene GAPDH. Data for e is representative of three independent experiments where error bars indicate the standard error of the mean. P-values for qRT-PCR; HLY-1 0.293 (insignificant), RIVA: 0.741 (insignificant), OCI-Ly3: 0.220 (insignificant), SUDHL-4: 0.384 (insignificant), Farage: 0.068 (insignificant), SUDHL-6: 0.275 (insignificant), Karpas 422: 0.342 (insignificant).

4.2.7.6.Differential regulation of EGR2 by calcineurin/NFAT signalling in DLBCL cell lines

Early Growth Response 2 (EGR2) is a member of the zinc finger family of transcription factors induced by many mitotic signals on cells such as fibroblasts, and T and B-lymphocytes (Gómez-Martín *et al.*, 2010). The family is comprised of four members (EGR1, EGR2, EGR3 and EGR4), which have a key role in modulating the immune response, such as activating lymphocytes and monitoring central and peripheral tolerance. EGR1 is the family member most well-researched, its expression directly depending on antigen receptor signalling through the BCR and activation of PKC (Gómez-Martín *et al.*, 2010). Functioning as a positive regulatory factor for effector functions in T and B cells, EGR1 is known to interact with NFAT to modulate the transcription of IL-2 and TNFα after stimulation of the TCR (Skerka, 1995; Gómez-Martín *et al.*, 2010).

In contrast to EGR1, EGR2 and EGR3 function as regulators involved in the induction of anergy and apoptosis (Gómez-Martín *et al.*, 2010). Anergy is a state of immune unresponsiveness, induced when a cell's antigen receptor is stimulated in the absence of a second signal from an antigen presenting cell. A form of immune tolerance, anergy is a

useful mechanism used by normal lymphoid cells to avoid an undesirable immune response, such as to one's own immune system. However, in the malignant setting lymphocyte anergy can be deleterious, acting as an immunosuppressive mechanism in the tumour microenvironment, driving immune escape.

EGR2 was chosen as a candidate gene to confirm the array data due to its significant downregulation in U2932 (6 hours) and HLY-1 (2 hours and 6 hours) upon CsA treatment (figure 52a). EGR2 was in fact the fourth most downregulated gene in the 2 hour HLY-1 CsA treatment and the eighth most downregulated gene in the 6 hour HLY-1 treatment, as shown in tables 17 and 19. Moreover, EGR2 had one of the most statistically significant adjusted P-values. The downregulation of EGR2 expression observed by paired data analysis was confirmed by qRT-PCR, showing that paired analysis recapitulated the microarray more accurately than unpaired analysis.

The Ct values obtained for EGR2 during qRT-PCR analysis of WSU-NHL cells were higher than those from HLY1 and U2932 cells, suggesting a lower abundance mRNA (not shown). This could account for why an effect was observed by qRT-PCR in WSU-NHL cells, suggesting that qRT-PCR analysis was more sensitive than the array, which may not have been able to detect changes in the lower levels of EGR2 expressed by WSU-NHL. When expanded to a larger cell line panel, the effect of CsA on EGR2 expression was fairly heterogeneous, suggesting that EGR2 may be regulated to different degrees by calcineurin/NFAT in different DLBCL cells (figure 52e).

a.

EGR2	2hr			6hr		
Cell line	Log FC	Unpaired p-value	Paired p-value	Log FC	Unpaired p-value	Paired p-value
U2932	-1.33	0.1334870570	0.0902895460	-0.70	0.5943897564	0.0031282213
WSU-NHL	-0.32	0.3510649382	0.6465325859	0.00	0.9996975609	0.9976270149
HLY-1	-1.22	0.2015332576	0.0004012848	-0.80	0.5748233515	0.0358125265

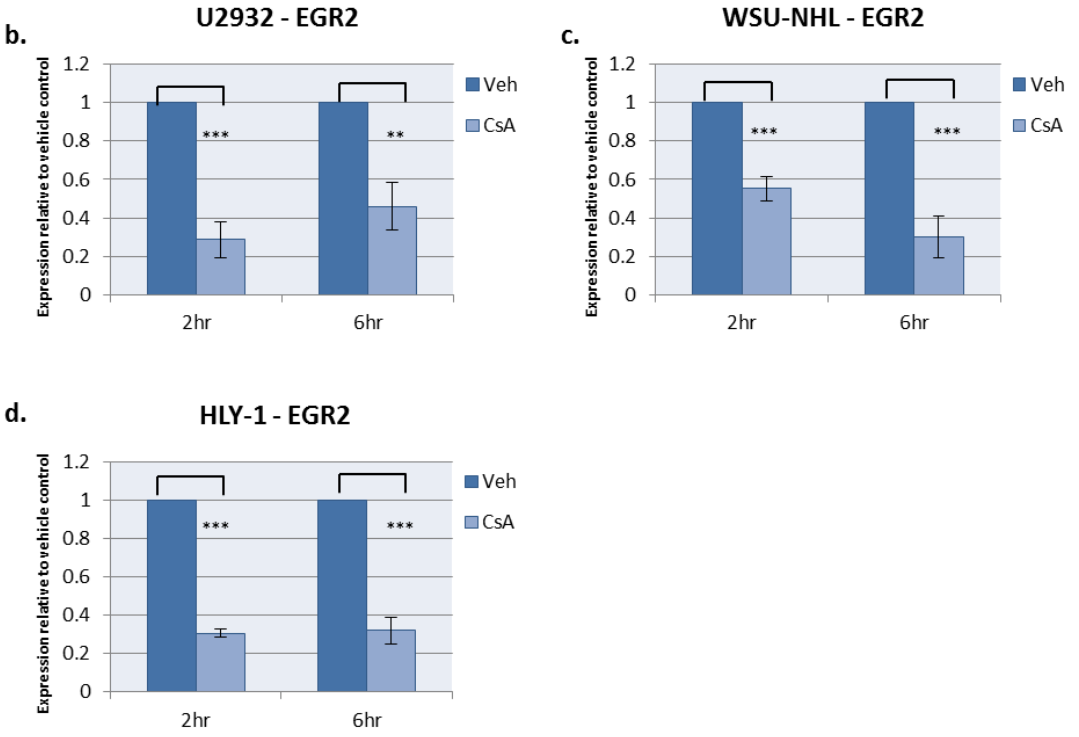

Figure 52. Differential regulation of EGR2 by calcineurin/NFAT signalling in DLBCL cell lines. a) Table showing the microarray log FC expression of EGR2 in cell lines treated with CsA for 2hrs or 6hrs, including respective adjusted p-values from unpaired and paired data analysis. Adjusted P-values highlighted in red are indicative of statistical significance (adjusted P-value <0.05). b-d) The ABC DLBCL cell lines U2932 and HLY-1 (b and d) and the GCB DLBCL cell line WSU-NHL (c) were treated with their respective IC50 concentrations of CsA (U2932 8.6µg/ml, HLY-1 7.4µg/ml and WSU-NHL10.4µg/ml) for 2 hours and 6 hours before the effects of treatment on EGR2 mRNA expression were analysed by qRT-PCR (using RNA from gene expression microarray samples). Data is representative of four independent experiments where error bars indicate the standard error of the mean. P-values for qRT-PCR; U2932 2hr: 0.001 6hr: 0.003, WSU-NHL 2hr: 0.001 6hr: 0.001, HLY-1 2hr: <0.000 6hr: <0.000.

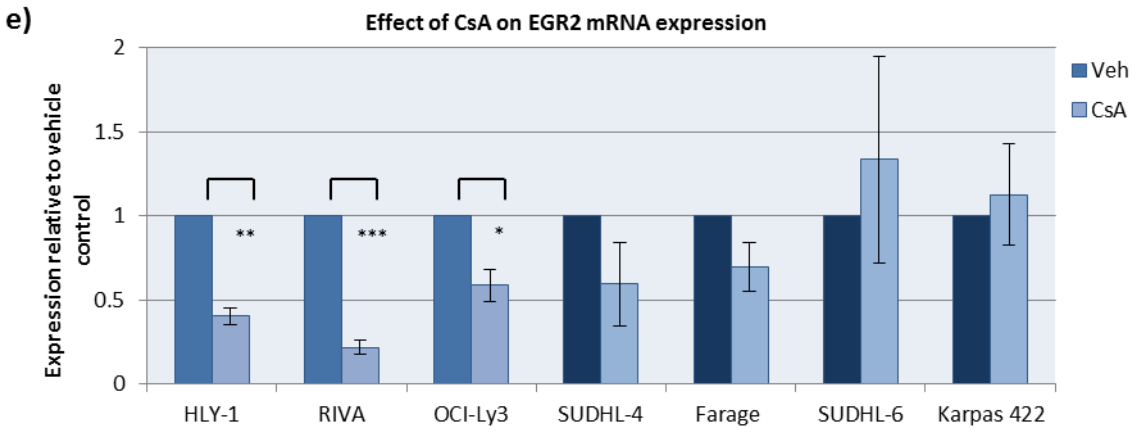

Figure 52 (Continued from previous page). Differential regulation of EGR2 by calcineurin/NFAT signalling in DLBCL cell lines. e) A panel of DLBCL cell lines were treated with their respective IC50 concentrations of CsA (HLY-1 7.4µg/ml, RIVA 13.5µg/ml, OCI-Ly3 10.6µg/ml, SUDHL-4 15.6µg/ml, Farage 11.8µg/ml, SUDHL-6 3.6µg/ml and Karpas 422 14.9µg/ml) for 2 hours before the effects on EGR2 mRNA expression were analysed by qRT-PCR. Lighter shaded bars indicate ABC DLBCL cell lines (HLY-1, RIVA and OCI-Ly3) whereas darker shaded bars represent GCB DLBCL cell lines (SUDHL-4, Farage, SUDHL-6 and Karpas 422). Data for b-e were normalised to the house-keeping gene GAPDH. Data for e is representative of three independent experiments where error bars indicate the standard error of the mean. P-values for qRT-PCR; HLY-1: 0.002, RIVA: <0.000, OCI-Ly3: 0.017, SUDHL-4: 0.106 (insignificant), Farage: 0.070 (insignificant), SUDHL-6: 0.445 (insignificant), Karpas 422: 0.547 (insignificant).

4.2.7.7. Differential regulation of EGR3 by calcineurin/NFAT signalling in DLBCL cell lines

Early Growth Response 3 (EGR3) is also a member of the zinc family of transcription factors described previously in section 5.2.7.6. EGR3 was also chosen for confirmation of the array data by qRT-PCR analysis due to its significant downregulation in HLY-1 cells after 2 hours (figure 53a), where it was the tenth most downregulated gene by paired analysis (table 17) and among the top 15 genes with the lowest adjusted P-values. Indeed, qRT-PCR analysis confirmed reduced expression of EGR3 by CsA treatment in HLY-1 cells and U2932 cells, suggesting that paired analysis was accurate. In line with the array data, there was no effect of calcineurin/NFAT inhibition on EGR3 in WSU-NHL cells. When the experiment was repeated in a large panel of cell lines, there was no trend between DLBCL subgroups. The error between experiments was generally high, as indicated by the large error bars, particularly in OCI-Ly3 and SUDHL-4 cells (figure 53e). Higher Ct values for EGR3 in these cell lines suggested a lower abundance mRNA (not shown), which appeared to correlate with the extent of the error, suggesting that EGR3 was difficult to detect by qRT-PCR analysis.

a)

EGR3	2hr			6hr		
Cell line	Log FC	Unpaired p-value	Paired p-value	Log FC	Unpaired p-value	Paired p-value
U2932	-1.65	0.1612041979	0.1206057538	-0.77	0.7479937303	0.0106194995
WSU-NHL	-0.08	0.9894820548	0.8675146783	-0.03	0.9975128677	0.9691745365
HLY-1	-0.95	0.9874205930	0.0137901830	-0.61	0.8383807383	0.0719254951

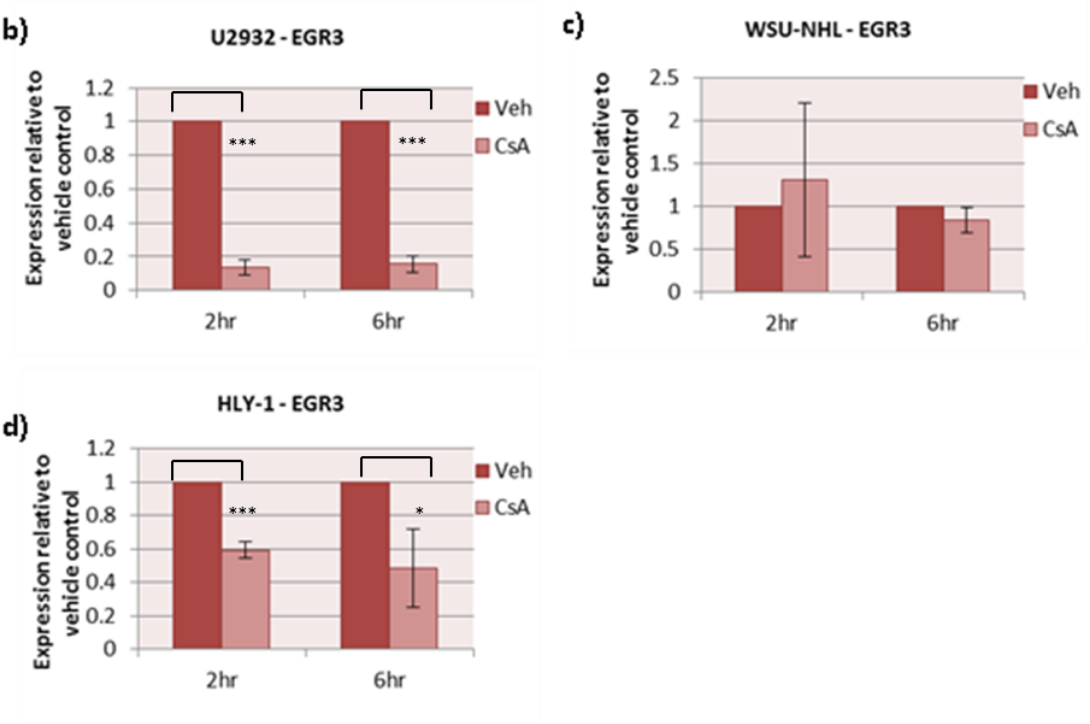

Figure 53. Differential regulation of EGR3 by calcineurin/NFAT signalling in DLBCL cell lines. a) Table showing the microarray log FC expression of EGR3 in cell lines treated with CsA for 2hrs or 6hrs, including respective adjusted p-values from unpaired and paired data analysis. Adjusted P-values highlighted in red are indicative of statistical significance (adjusted P-value <0.05). b-d) The ABC DLBCL cell lines U2932 and HLY-1 (b and d) and the GCB DLBCL cell line WSU-NHL (c) were treated with their respective IC50 concentrations of CsA (U2932 8.6µg/ml, HLY-1 7.4µg/ml and WSU-NHL10.4µg/ml) for 2 hours and 6 hours before the effects of treatment on EGR3 mRNA expression were analysed by qRT-PCR (using RNA from gene expression microarray samples). Data is representative of four independent experiments where error bars indicate the standard error of the mean. P-values for qRT-PCR; U2932 2hr: <0.000 6hr: <0.000, WSU-NHL 2hr: 0.541 (insignificant) 6hr: 0.401 (insignificant), HLY-1 2hr: <0.000 6hr: 0.022.

e)

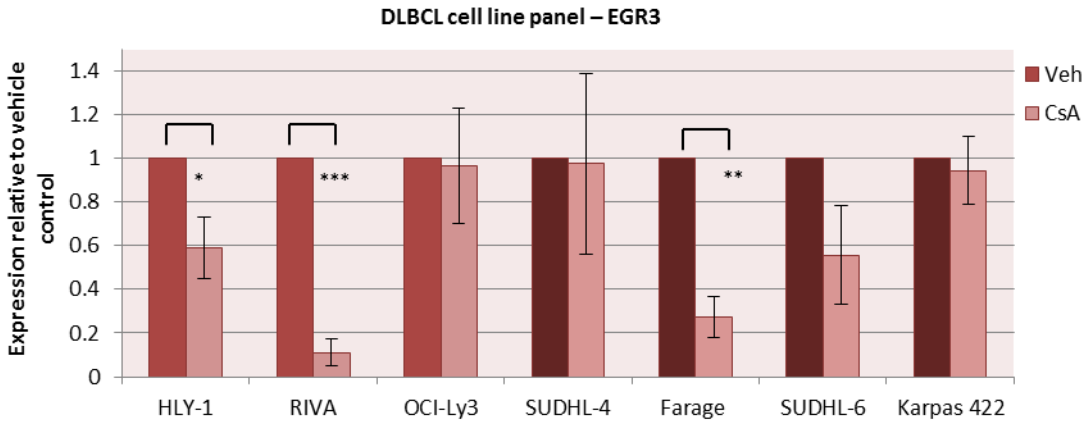

Figure 53 (Continued from previous page). Differential regulation of EGR3 by calcineurin/NFAT signalling in DLBCL cell lines. e) A panel of DLBCL cell lines were treated with their respective IC50 concentrations of CsA (HLY-1 7.4µg/ml, RIVA 13.5µg/ml, OCI-Ly3 10.6µg/ml, SUDHL-4 15.6µg/ml, Farage 11.8µg/ml, SUDHL-6 3.6µg/ml and Karpas 422 14.9µg/ml) for 2 hours before the effects on EGR3 mRNA expression were analysed by qRT-PCR. Lighter shaded bars indicate ABC DLBCL cell lines (HLY-1, RIVA and OCI-Ly3) whereas darker shaded bars represent GCB DLBCL cell lines (SUDHL-4, Farage, SUDHL-6 and Karpas 422). Data for b-e were normalised to the house-keeping gene GAPDH. Data for e is representative of three independent experiments where error bars indicate the standard error of the mean. P-values for qRT-PCR; HLY-1: 0.038, RIVA: <0.000, OCI-Ly3: 0.844 (insignificant), SUDHL4: 0.932 (insignificant), Farage: 0.005, SUDHL6: 0.077 (insignificant), Karpas 422: 0.593 (insignificant).

4.2.7.8. Differential regulation of PDCD1 by calcineurin/NFAT signalling in DLBCL cell lines

Programmed Cell Death 1 (PDCD1) (also commonly known to as PD1), is a cell surface immune check-point receptor. PDCD1 limits autoimmunity by reducing the activity of T cells in peripheral tissues during an inflammatory response (Rivoltini *et al.*, 2005; Keir *et al.*, 2008; Pardoll, 2012). During T-cell activation, engagement of the PDCD1 receptor causes inhibition of the kinases associated with T-cell activation (Bryan *et al.*, 2015). The PDCD1 receptor is highly expressed on infiltrating T_{Reg} cells and is thought to upregulate their proliferation (Pardoll, 2012). PDCD1 therefore functions as a major immune escape mechanism, which, when engaged frequently or constitutively, creates a tumour microenvironment that effectively avoids the anti-tumour immune response (Bryan *et al.*, 2015). Malignancies such as DLBCL have been shown to adopt this mechanism in order to escape the anti-tumour activity of surrounding lymphocytes (Fanoni *et al.*, 2011). PDCD1 ligands PD-L1 and PD-L2 have been found to be upregulated in various types of cancer, including DLBCL, where high levels of PD-L1 were associated with reduced overall survival (Rossille *et al.*, 2014). Blockade of PDCD-1 ligand binding using monoclonal antibodies such as Pidilizumab are an attractive therapeutic strategy and

clinical trials are currently in place for a range of malignancies, including DLBCL (Bryan *et al.*, 2014).

Although it is interesting that PDCD1 may potentially be upregulated by calcineurin/NFAT in DLBCL tumour cells, it is the increased engagement of PDCD1 on surrounding immune cells (rather than the cancer cells themselves) that is associated with the immune evasion reported in the tumour microenvironment. Interestingly however, PDCD1 has been reported to be an NFAT target gene in T cells (Oestreich *et al.*, 2008). Moreover, PDCD1 signalling has recently been shown to promote proliferation and survival in mouse models of melanoma (Kleffel *et al.*, 2015). Treatment with CsA was shown to reduce the expression of PDCD1, with ChIP analysis revealing an association with NFAT2 binding and activation of PDCD1 during stimulation of primary CD8 T cells (Oestreich *et al.*, 2008).

HLY-1 cells were the only cell line sensitive to CsA-induced downregulation of PDCD1 in the microarray. However, this was only statistically significant after 2 hours of treatment (figure 54a). qRT-PCR supported these findings, demonstrating around 50% reduction of PDCD1 expression. Interestingly, despite the array data indicating no significant effect in U2932 cells, qRT-PCR revealed CsA-induced downregulation of PDCD1 in U2932 cells. It is possible that this effect was undetectable in the array due to lower level mRNA expression of PDCD1 in U2932 compared to HLY1, as indicated by higher Ct values (not shown). Moreover, the Ct values for PDCD1 in WSU-NHL cells were even higher, suggesting very low abundant mRNA. PDCD1 was perhaps difficult for even the sensitivity of qRT-PCR analysis to detect, as suggested by the large error bars on figure 54c, where individual experiments produced highly variable expression data.

The effects observed in HLY-1 cells were validated by repeating the experiment in this cell line, where data repeatedly showed around 50% reduction of PDCD1 upon CsA treatment (figure 54e), demonstrating consistency between experiments. Although the array data and subsequent qRT-PCR analysis was suggestive of an ABC DLBCL-specific effect of CsA on PDCD1 expression, no trend was observed when the experiment was expanded to a larger cell line panel (figure 54e), suggesting similar regulation of PDCD1 by calcineurin/NFAT among DLBCL subtypes.

a.

PDCD1	2hr			6hr		
Cell line	Log FC	Unpaired p-value	Paired p-value	Log FC	Unpaired p-value	Paired p-value
U2932	-0.18	0.9272720177	0.8578505728	-0.12	0.9981600115	0.6462645895
WSU-NHL	-0.01	0.9955792092	0.9845512125	0.01	0.9987838161	0.9940330578
HLY-1	-0.90	0.0015224351	0.0094222152	-0.38	0.6119999424	0.3214580455

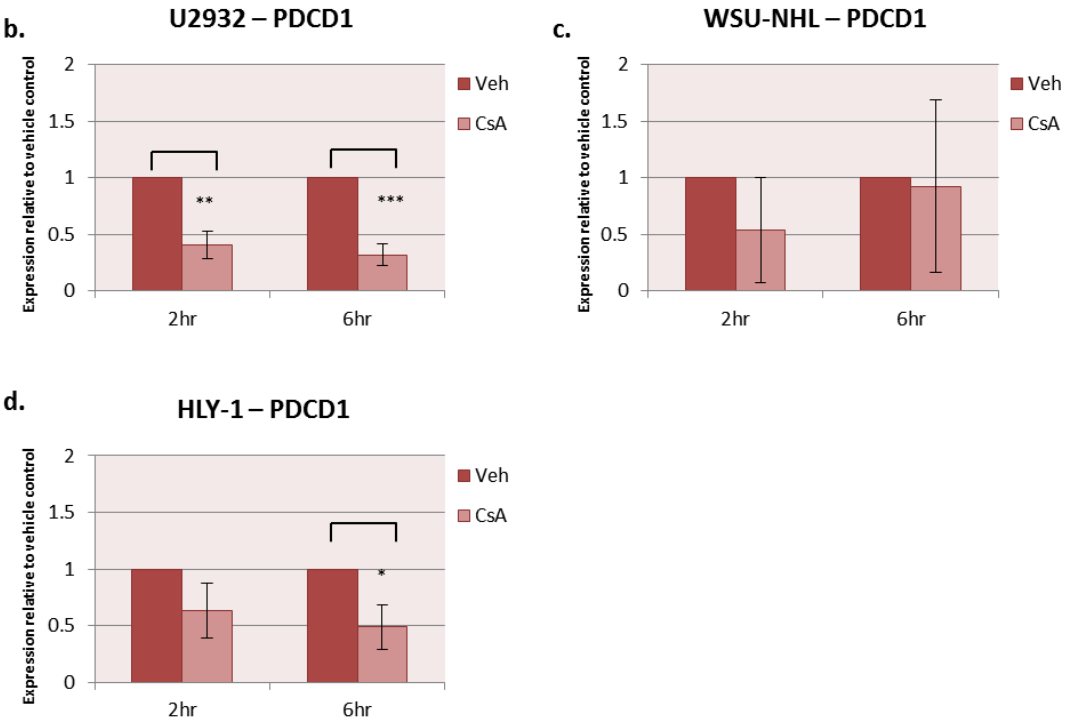

Figure 54. Differential regulation of PDCD1 by calcineurin/NFAT signalling in DLBCL cell lines. a) Table showing the microarray log FC expression of PDCD1 in cell lines treated with CsA for 2hrs or 6hrs, including respective adjusted p-values from unpaired and paired data analysis. Adjusted P-values highlighted in red are indicative of statistical significance (adjusted P-value <0.05). b-d) The ABC DLBCL cell lines U2932 and HLY-1 (b and d) and the GCB DLBCL cell line WSU-NHL (c) were treated with their respective IC50 concentrations of CsA (U2932 8.6µg/ml, HLY-1 7.4µg/ml and WSU-NHL10.4µg/ml) for 2 hours and 6 hours before the effects of treatment on PDCD1 mRNA expression were analysed by qRT-PCR (using RNA from gene expression microarray samples). Data is representative of four independent experiments where error bars indicate the standard error of the mean. P-values for qRT-PCR; U2932 2hr: 0.003 6hr: 0.001, WSU-NHL 2hr: 0.143 (insignificant) 6hr: 0.135 (insignificant), HLY-1 2hr: 0.057 (insignificant) 6hr: 0.014.

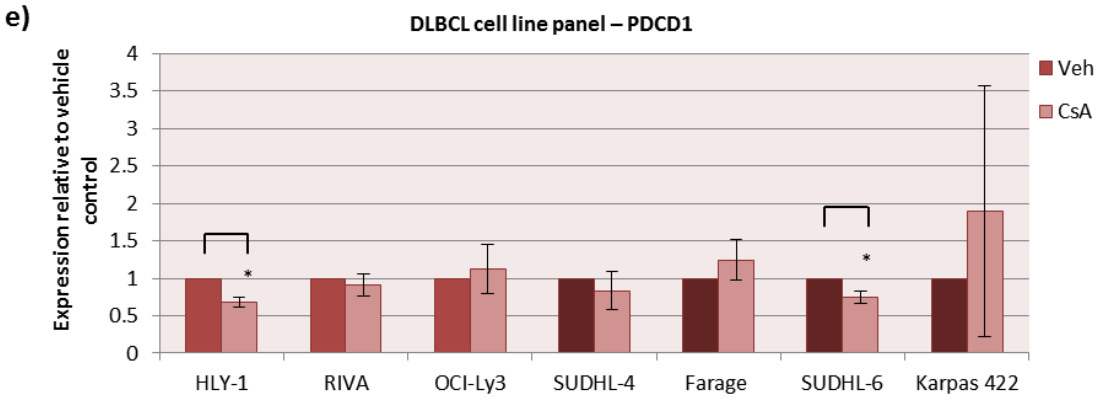

Figure 54 (Continued from previous page). Differential regulation of PDCD1 by calcineurin/NFAT signalling in DLBCL cell lines. e) A panel of DLBCL cell lines were treated with their respective IC50 concentrations of CsA (HLY-1 7.4µg/ml, RIVA 13.5µg/ml, OCI-Ly3 10.6µg/ml, SUDHL-4 15.6µg/ml, Farage 11.8µg/ml, SUDHL-6 3.6µg/ml and Karpas 422 14.9µg/ml) for 2 hours before the effects on PDCD1 mRNA expression were analysed by qRT-PCR. Lighter shaded bars indicate ABC DLBCL cell lines (HLY-1, RIVA and OCI-Ly3) whereas darker shaded bars represent GCB DLBCL cell lines (SUDHL-4, Farage, SUDHL-6 and Karpas 422). Data for b-e were normalised to the house-keeping gene GAPDH. Data for e is representative of three independent experiments where error bars indicate the standard error of the mean. P-values for qRT-PCR; HLY-1: 0.013, RIVA: 0.394 (insignificant), OCI-Ly3: 0.596 (insignificant), SUDHL4: 0.370 (insignificant), SUDHL-6: 0.029.

4.2.8. Gene Set Enrichment Analysis

To extract further information from the gene expression microarray, GSEA analysis was performed, as described in chapter 2, section 2.6. I aimed to utilise this powerful computational technique to determine whether a set of genes showed statistically significant differences between vehicle control and CsA-treated phenotypes. Considering that previous experiments confirming and validating the microarray suggested paired data analysis to be best, data derived from this method of analysis only was used for GSEA.

The Broad Institute of Harvard and MIT's molecular signatures database (MSigDB) was used for analysis (http://www.broadinstitute.org/gsea/index.jsp). Comprising 10,348 gene sets, the MSigDB are divided into eight major collections, from which the C2 curated gene set collection was chosen for this study (http://www.broadinstitute.org/gsea/index.jsp). This collection is composed of 4,725 genes obtained from various sources such as online pathway databases, publications in PubMed and the knowledge of domain experts. Within the collection are five subcategories of gene sets, including chemical and genetic permutations, canonical pathways, and the BioCarta, KEGG (Kyoto Encyclopaedia of Gene and Genomes) and

Reactome gene sets. These gene sets were believed suitable for this study due to their broad coverage of a range of biological activities, including well known pathways (such as NFAT) important for cellular function.

4.2.8.1. Enrichment of gene sets in DLBCL cell lines treated with CsA

During GSEA, the genes that were differentially expressed in our two experimental conditions (CsA and vehicle) were identified and compared to gene sets recorded in the C2 MSigDB to identify classes of genes enriched or depleted in our datasets. Gene sets analysed were given an enrichment score (ES), which is the principal result of gene set enrichment analysis, representing the degree to which a gene set is overrepresented at the top or the bottom of a ranked list of genes. The ES is calculated by the GSEA programme, which walks down the ranked list of genes, increasing a running-sum statistic when a gene is in the gene set and decreasing it when it is not (http://www.broadinstitute.org/gsea/index.jsp). The extent of the increment depends on how correlated the gene is with a particular phenotype. When walking the list of genes, the ES is the point at which the maximum deviation from zero is reached. Positive ES indicates enrichment of a gene set at the top of the ranked list of genes, whereas a negative ES value indicates gene set enrichment at the bottom of the ranked list (http://www.broadinstitute.org/gsea/index.jsp).

Although PARP cleavage was observed after 6 hours CsA treatment (figure 20), suggesting that changes relevant to DLBCL survival were seen at this timepoint, GSEA for the 2 hour timepoint was used in this study to look for more immediate gene targets. Importantly however, GSEA was also performed for the 6 hour timepoint (data not shown), which gave very similar findings.

Of the 4,725 gene sets in the C2 collection, 984 gene sets were filtered out by size preferences set (min = 15, max = 500 genes within a gene set), leaving 3,738 gene sets to be analysed. Two analysis reports were generated, one of which indicated the genes and gene sets enriched in the vehicle samples (but not in the CsA-treated samples) and the other report showing genes enriched in the CsA-treatment samples (but not in the vehicle samples). GSEA analysis of all three DLBCL cell lines treated with CsA for 2 hours produced a wealth of interesting data, as summarised in table 21.

	HLY-1		U2932		WSU-NHL	
	Vehicle	CsA	Vehicle	CsA	Vehicle	CsA
Gene sets significant at FDR <25%	569	216	451	387	466	328
Gene sets significant at FDR <5%	61	1	8	32	104	24

Table 21. Summary of GSEA in DLBCL cell lines treated with CsA for 2 hours. The data in the table shows the number of gene sets enriched in vehicle vs. CsA samples and CsA vs. vehicle samples with a FDR (False Discovery Rate) less than 25% and 5%. Data is from paired analysis.

The table also indicates the number of gene sets which had a False Discovery Rate (FDR) of less than 25% or less than 5%. The FDR is the estimated probability that a gene set represents a false positive finding. For example, an FDR of 25% indicates that the result is likely to be valid 3 out of 4 times. According to the Broad Institute GSEA user handbook, gene sets with an FDR less than 25% are those most likely to generate an interesting hypothesis and drive further research. However, if a small number of samples were used for GSEA, such as less than 7 samples for a phenotype (4 were used in this study), it is recommended to use a more stringent FDR cut-off, such as 5% (http://www.broadinstitute.org/gsea/index.jsp). Many of the gene sets generated in all three DLBCL cell lines had an FDR less than 25% and some cell lines, such as WSU-NHL, showed a respectable number of gene sets with an FDR less than 5%.

4.2.8.2. GSEA reveals enrichment of common gene sets between DLBCL cell lines treated with CsA

The top 50 potentially interesting genes sets are listed in appendix tables 10-15, many of which are likely to be groups of genes that share common biological characteristics, biochemical pathways or modes of regulation. Due to time restrictions, thorough analysis of all gene sets was not possible. Instead, I found that some gene sets were of particular interest due to the fact that they were highly supportive of some of the genes and pathways identified in the array.

These were best identified by investigating trends between the gene sets that arose between DLBCL cell lines. As shown in the Venn diagrams in figure 55 and 56, some cell lines shared common gene sets. Interestingly, many of the gene sets were associated with cancer, such as ‘Zhan, Multiple Myeloma, PR up’, ‘Pedersen, Metastasis, BY Erbb2 Isoform 3’ and ‘Nikolsky Breast Cancer 16Q24 Amplicon’. Gene sets associated with proliferation and immune function were also evident, including ‘Benporath, Proliferation’

and 'Seki, Inflammatory Response'. Moreover, in line with the large number of chemokines differentially expressed in the microarray, gene sets such as 'Kegg chemokine signalling pathway' arose as significant.

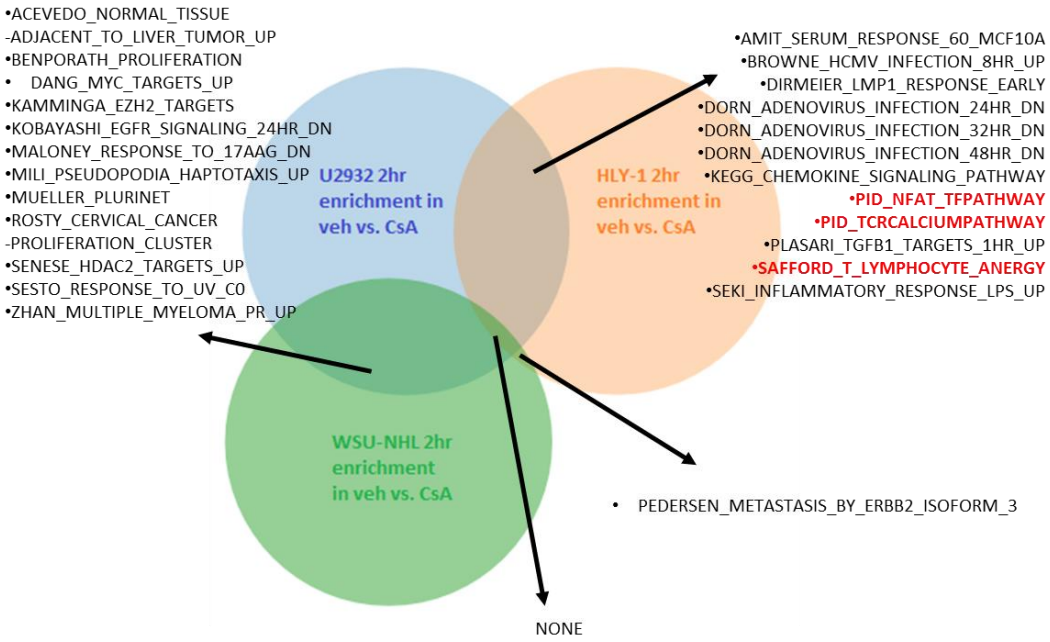

Figure 55. GSEA reveals enrichment of common gene sets between DLBCL cell lines treated with CsA for 2hrs (enrichment in vehicle vs. CsA). The Venn diagram compares common gene sets that are enriched in vehicle control samples compared to CsA-treated samples. Gene sets are derived from the top 50 enriched gene sets (ordered by FDR) for each cell line, including U2932 (blue), HLY-1 (orange) and WSU-NHL (green) DLBCL cells. Only overlapping gene sets are indicated on the diagram. Data is based on paired analysis. Gene sets highlighted in red are discussed in the following sections.

There were 6 gene sets which overlapped between all three cell lines in the analysis of enrichment in CsA-treated samples compared to vehicle samples (figure 56). However, there were no overlapping gene sets between all three cell lines when considering enrichment in the vehicle compared to CsA-treated samples (figure 55). Overall, the cell lines showed both unique and shared CsA-sensitive gene sets suggesting both commonalities and differences in calcineurin/NFAT regulated genes in the three cell lines.

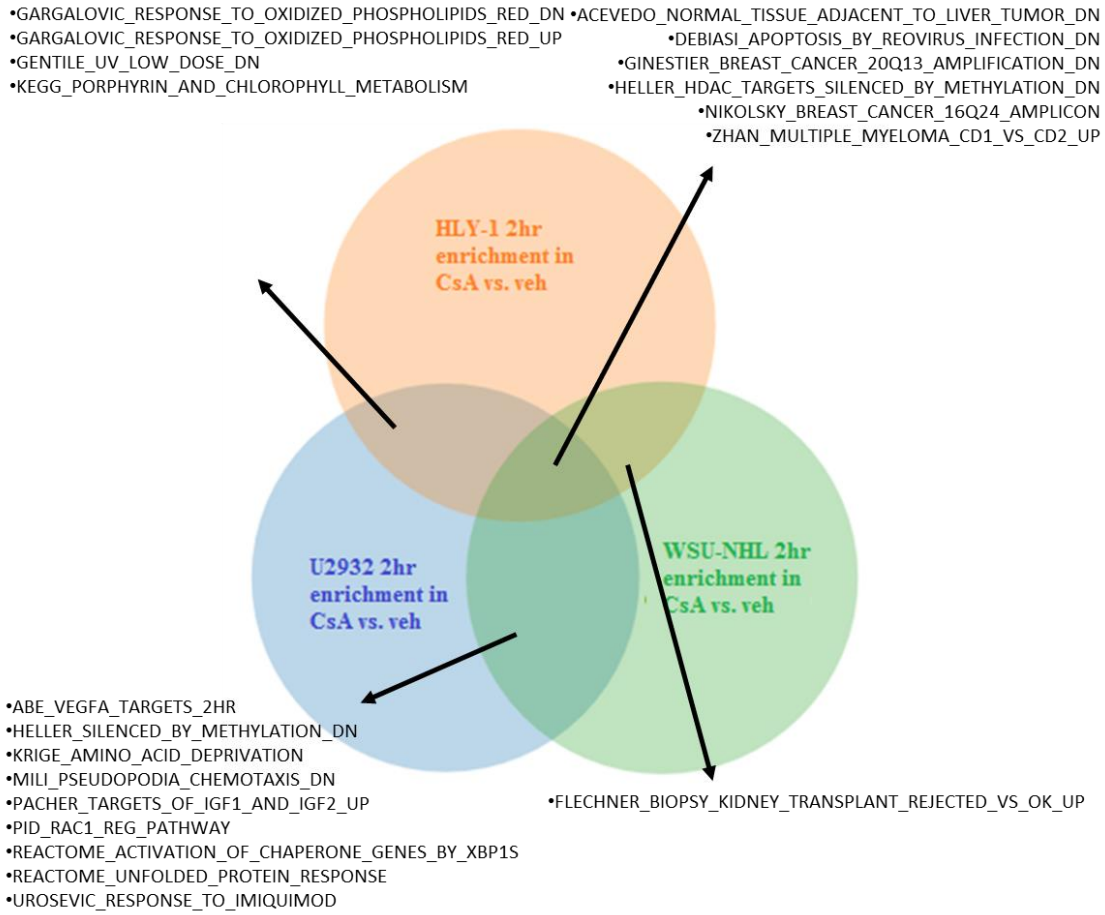

Figure 56. GSEA reveals enrichment of common gene sets between DLBCL cell lines treated with CsA for 2hrs (enrichment in CsA-treated samples vs. vehicle). The Venn diagram compares common gene sets that are enriched in vehicle control samples compared to CsA-treated samples. Gene sets are derived from the top 50 enriched gene sets (ordered by FDR) for each cell line, including U2932 (blue), HLY-1 (orange) and WSU-NHL (green) DLBCL cells. Only overlapping gene sets are indicated on the diagram. Data is based on paired analysis.

4.2.8.3. U2932 and HLY-1 cells demonstrate enrichment of gene sets associated with NFAT signalling

Importantly, some very interesting gene sets were shared between the two ABC DLBCL cell lines U2932 and HLY-1 (figure 55). These included two gene sets associated with TCR/NFAT signalling, 'PID NFAT TF Pathway' and 'PID TCR Calcium Pathway'. The enrichment plots for these gene sets are shown in figure 57. The top portion of the plot shows the running ES for the gene sets as the analysis walks down the ranked list. The score at the peak of the plot (the score furthest from zero) is the ES for the gene set.

The normalised enrichment scores (NES) is the main statistic for examining gene set enrichment results. The enrichment score is normalised, allowing GSEA to account for differences in gene set size and in correlations between gene sets and the expression dataset. The NES therefore allows comparisons to be made across gene sets. The NES for the 'PID NFAT TF pathway' gene set were 2.14 for U2932 cells with an FDR of 2.5% (figure 57a) and 2.15 for HLY-1 cells with an FDR of 0.6% (figure 57b). For the 'PID TCR calcium pathway' gene set, the ES for U2932 cells was 1.88 (FDR 10%) (figure 57c) and 2.22 for HLY-1 cells (FDR 0.2%) (figure 57d). The distinct peaks at the beginning of the ranked lists in these graphs indicate that these gene sets are potentially interesting.

The middle section of the plot shows where the members of the two NFAT-associated gene sets appear in the ranked list of genes. The bottom portion of the plot shows the value of the ranking metric as you move down the ranked list of genes, which measures a gene's correlation with a phenotype. The ranking metric value goes from positive to negative as you move down the list, where a positive value indicates a correlation with the first phenotype e.g. the vehicle and a negative value indicates correlation with the second phenotype e.g. CsA treated samples (http://www.broadinstitute.org/gsea/index.jsp).

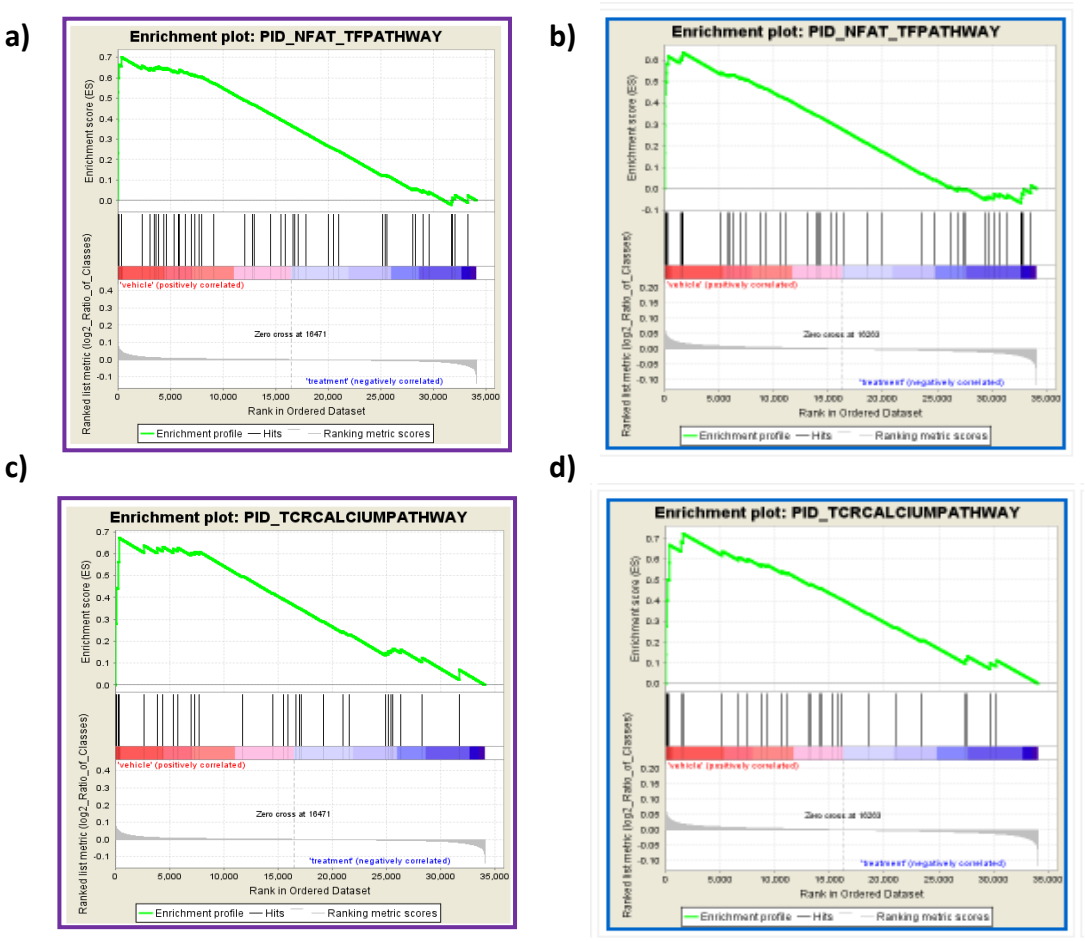

Figure 57. U2932 and HLY-1 cells demonstrate enrichment of gene sets associated with NFAT signalling. GSEA enrichment plots for U2932 (a and c) and HLY-1 cells (b and d) treated with CsA for 2 hours, showing enrichment of two gene sets associated with NFAT signalling in vehicle samples compared to CsA-treated samples. Data is based on paired analysis.

4.2.8.4. U2932 and HLY-1 cells demonstrate enrichment of gene sets associated with anergy

Another gene set that was significantly enriched in both U2932 and HLY-1 cells treated with CsA for 2 hours was the 'Safford T-Lymphocyte Anergy', as shown in figures 55 and 58. The NES for this gene set in U2932 cells was 2.08 (FDR 3%) and 2.20 in HLY-1 cells (FDR 0.3%). Identification of this gene set was interesting due to the downregulation of anergy-associated genes in the array, such as EGR2 and EGR3, as described in sections 5.2.7.6 and 5.2.7.7.

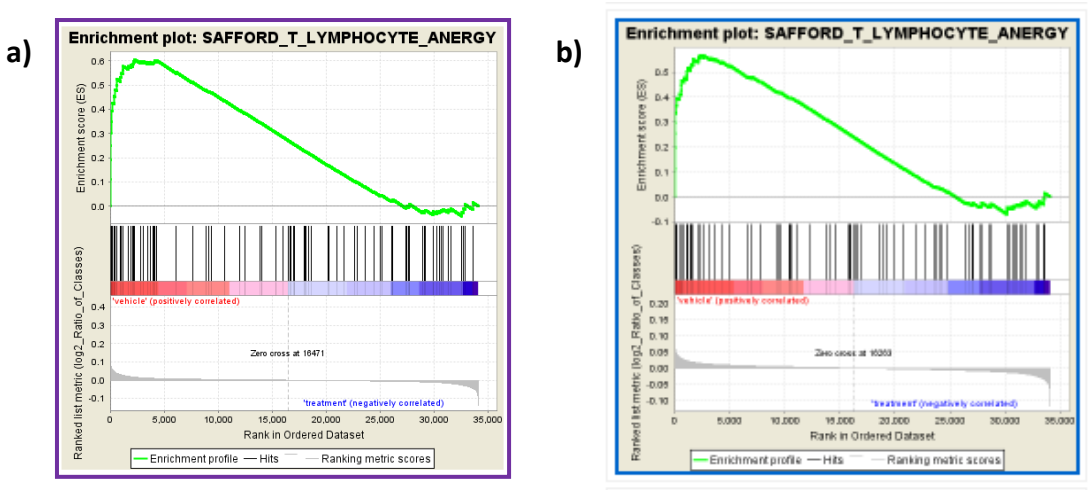

Figure 58. U2932 and HLY-1 cells demonstrate enrichment of gene sets associated with anergy. GSEA enrichment plots for U2932 (a) and HLY-1 cells (b) treated with CsA for 2 hours, showing enrichment of two gene sets associated with anergy in vehicle samples compared to CsA-treated samples. Data is based on paired analysis.

4.2.8.5. HLY-1 cells demonstrate enrichment of gene sets associated with TNFα signalling

Finally, although not shared between multiple cell lines, a gene set associated with TNFα was statistically significant. The 'Phong, TNF Targets Up' gene set had the 5th most significant FDR (0.2%), with an NES of 2.23 in HLY-1 cells treated with CsA for 2 hours. This gene set was also enriched in U2932 cells (NES 1.62), although its significance was much lower (FDR 14%). Overall however, GSEA was a useful tool for showing that TNFα signalling may be involved with the functions of the calcineurin/NFAT pathway in DLBCL (figure 59).

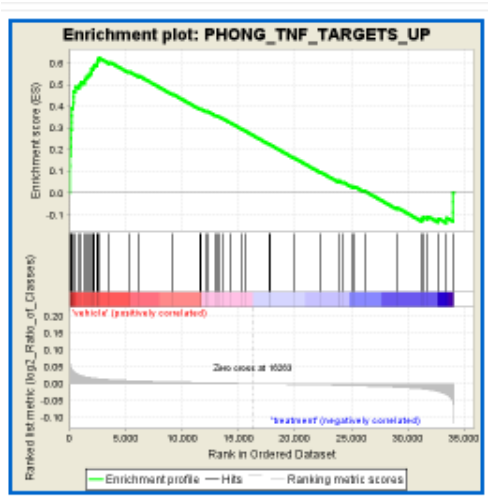

Figure 59. HLY-1 cells demonstrate enrichment of gene sets associated with TNFα signalling. GSEA enrichment plots for HLY-1 cells treated with CsA for 2 hours, showing enrichment of a gene associated with TNFα signalling in vehicle samples compared to CsA-treated samples. Data is based on paired analysis.

4.3. Discussion

4.3.1. Analysis of microarray data by qRT-PCR

qRT-PCR analysis (using RNA from samples sent for microarray analysis) was a useful way of confirming the effects of CsA on the expression of seven selected genes. Overall, the expression fold-change recorded in the array was highly reproducible by qRT-PCR analysis, demonstrating time-dependent changes in gene expression and differences between particular cell lines. There was great consistency between most experiments, however the degree of error was fairly high in some genes/cell lines. Analysis of the differential expression of genes between cell lines identified some cell lines (especially WSU-NHL) which had higher Ct values for specific genes, suggesting low abundance mRNA. This may have been difficult to detect by qRT-PCR analysis, increasing inter-experimental error. Often, the high error also correlated with data which did not reflect findings in the array, suggesting that the microarray may not have been sensitive enough to detect changes in the expression of some genes which were expressed at very low levels. Overall, these data provided sound evidence for the accuracy of the microarray. Although not shown, qRT-PCR analysis was also normalised to the TATA-binding protein (TBP) transcription factor, where results were consistent with data normalised to GAPDH.

During initial analysis of the array, there were differences in the genes identified as significant between paired, compared to unpaired methods of analysis. While the general direction of differential expression of genes was the same when paired and unpaired analysis were combined, it was important to investigate which method of analysis best reflected biological functions in the array samples. For most genes analysed by qRT-PCR, paired data analysis from the microarray was most accurate, which led to my decision to use the data from paired data analysis for GSEA. However, for some genes, it was not entirely clear cut as to which type of analysis was most accurate. Therefore genes identified as significantly significant by unpaired analysis were not entirely disregarded.

4.3.2. Investigation of the effects of CsA on potential calcineurin/NFAT target gene expression in an expanded panel of DLBCL cell lines

An interesting observation in the microarray was the lack of effects on gene expression in WSU-NHL cells. Perhaps a longer incubation period of CsA was required for inhibition of calcineurin/NFAT signalling in these cells. qRT-PCR analysis investigated a potential trend between CsA-induced changes in gene expression between ABC and GCB DLBCL cell lines. While some genes, such as NFKBIE, EGR2, EGR3, and PDCD1 were regulated similarly by calcineurin/NFAT, other genes including TNFα, CCL4L2 and NFAT2 were mostly depleted by CsA in cell lines of the ABC DLBCL subgroup only. In the future it would be interesting to perform gene expression analysis on the entire panel of cell lines and to further analyse the effects of CsA on different pathways in ABC versus GCB cell lines, such as by using ingenuity pathway analysis.

4.3.3. Summary of statistically significant genes differentially expressed by treatment with CsA

4.3.3.1. Genes associated with cancer and lymphoma

In addition to the functional subgroups of genes discussed below, a number of genes identified in the array analysis as regulated by CsA (in at least one cell line and at least one time point) were of interest due to their associations with lymphoma and cancer in general. The transcription factor paired-box 9 (PAX9) for example, was significantly downregulated in HLY-1 cells after 2 hours CsA treatment (unpaired analysis). Known for their role in early development, PAX family members have been found to be

frequently expressed and required for cell growth in malignancies such as breast cancer, lung cancer and lymphoma (Muratovska *et al.*, 2003).

Moreover, the type II transmembrane receptor CD69 was another top 10 gene downregulated in the microarray. Involved in lymphocyte activation, CD69 has been associated with haematological malignancies such as T-cell virus type-1 leukaemia's and non-Hodgkin B-cell lymphomas (Ishikawa *et al.*, 2013; Ishikawa, 1998). Moreover, upregulation of the suppressor of cytokine signalling-3 protein (SOCS3) by CsA (therefore normally downregulated by calcineurin/NFAT) was an interesting feature highlighted by the array due its known suppressive activity on pathways such as STAT3 and NF-κB (Starr *et al.*, 1997; Karlsen *et al.*, 2004; Lam *et al.*, 2008). SOCS family members have also demonstrated pivotal roles in inflammation and connections with cancer development (Inagaki-Ohara *et al.*, 2013). Overexpression of SOCS3 has now been implicated in an array of lymphomas, including *de novo* follicular lymphoma, T-cell lymphomas, classical Hodgkin lymphomas and mantle cell lymphomas (Brender *et al.*, 2001; Brender *et al.*, 2004; Baus *et al.*, 2006; Krishnadasan *et al.*, 2006; Molavi *et al.*, 2013). Another example of a cancer-associated gene upregulated by CsA treatment is the transcriptional regulator ID3 (inhibitor of DNA binding-3), which has recently been linked to oncogenesis of Burkitt's lymphoma in which inactivating ID3 mutations promote TCF3-mediated expression of BCR components (Schmitz *et al.*, 2014; Spender *et al.*, 2014).

Interestingly, CsA-induced downregulation of a number of genes encoding IκB proteins was apparent in the ABC DLBCL data analysis. Upregulation of these proteins by calcineurin/NFAT suggests that this signalling pathway in fact downregulates NF-κB signalling, which does not fit with the hypothesis that NFAT and NF-κB function by together promoting lymphomagenesis. However, expression of IκBζ, which is encoded by the NFKBIZ gene, has recently been shown to be upregulated in ABC DLBCL patient samples, but not GCB DLBCL samples or other NF-κB dependent malignancies such as multiple myeloma (Nogai *et al.*, 2013). Moreover, IκBζ expression was essential for the survival of ABC DLBCL cell lines as well as for nuclear NF-κB activity (Nogai *et al.*, 2013). Fascinatingly, gene expression profiling showed that IκBζ controls many NF-κB target genes by interacting with the NF-κB subunits p50 and p52 (Nogai *et al.*, 2013). Although IκBζ is a known NF-κB target gene itself, it is possible that other signalling

pathways, such as NFAT may also contribute to the elevated expression of IκBζ observed in some DLBCL. Unlike IκBα and IκBδ, IκBζ was significantly downregulated in just HLY-1 cells after 6 hours CsA treatment (paired analysis). Nevertheless, this is a potentially interesting result, which could be explored in greater depth in the future.

4.3.3.2. Cytokines and genes associated with the tumour microenvironment

A striking observation from the gene expression array was the significant downregulation of many cytokines. Due to the known involvement of NFAT in immune cell function this was perhaps not an unexpected result. The chemokines CCL4L1, CCL4L2, CCL3, CCL3L1 and CCL3L3 were frequently among the most statistically significant genes differentially expressed, however little is known about their function. Interestingly, a recent study reported high levels of secretion of CCL3 and CCL4 in the serum of patients with newly diagnosed DLBCL, where high CCL3 levels correlated with significantly shorter progression-free and overall survival (Takahashi *et al.*, 2015). Furthermore, *in vitro* studies demonstrated high levels of CCL3 and CCL4 after BCR triggering in ABC, but not GCB DLBCL cells, suggesting that these chemokines may be useful biomarkers in ABC DLBCL (Takahashi *et al.*, 2015).

Lymphotoxin alpha (LTA) and Interleukin 10 (IL-10) are examples of other cytokines downregulated by calcineurin/NFAT inhibition, IL-10 functioning as a known enhancer of B-cell survival and proliferation (Itoh *et al.*, 1995). Interestingly, high levels of circulating IL-10 have been reported in DLBCL patients, and IL-10 promotes the proliferation and survival of ABC DLBCL cell lines through an autocrine mechanism involving NF-κB and STAT3 (Lam *et al.*, 2008). IL-10 has in fact been reported a novel therapeutic target in DLBCL by Béguelin et al (2015), who also identified amplifications of the IL-10 surface receptor in primary DLBCLs (Beguelin *et al.*, 2015). Importantly, anti-IL-10-receptor therapy resulted in cell cycle arrest and induction of apoptosis in DLBCL cell lines (Beguelin *et al.*, 2015).

Furthermore, the proinflammatory cytokine Marginal Zone B and B1 Cell-Specific Protein (MZB1) was a gene significantly differentially expressed in the array. Interestingly, high expression of MZB1 has been predicted to cause adverse prognosis in CLL, follicular lymphoma and DLBCL (Herold, 2013). However, CsA caused an

upregulation of this gene in the array, suggesting that calcineurin/NFAT is not the underlying cause of the increased expression of this gene in these malignancies.

4.3.4. GSEA

It was encouraging to see the NFAT pathway among the most significant gene sets enriched in U2932 and HLY-1 vehicle control samples compared to CsA-treated samples. Data reassuringly pulled out genes and pathways previously associated with the biological function of NFAT signalling. Future analysis would ideally gain a greater insight into the genes which encompass the 'PID NFAT TF Pathway' and 'PID TCR Calcium Pathway' gene sets by using leading edge analysis.

The leading edge subset in a gene set include the genes that appear in the ranked list at or before the point where the running sum reached its maximum deviation from zero (http://www.broadinstitute.org/gsea/index.jsp). Therefore, the leading edge-subset can be regarded as the core genes that account for the gene set's enrichment signal. Analysis of genes that are commonly in the leading edge subsets are therefore more likely to be of interest and biological importance than a gene that is only in a small number of the leading-edge subsets. Appendix table 16 shows an example of the genes that form the leading edge analysis within the 'PID NFAT TF Pathway' gene set, which was enriched in U2932 cells treated with CsA for 2 hours. Interestingly, the core enrichment genes include EGR2 and EGR3, confirming that these genes have been associated with the biological activities of NFAT in already published data. Moreover, interferon regulatory factor 4 (IRF4) was also among the top ranked genes in this gene set. IRF4 is a transcription factor which plays a key role in lymphoid development, functioning to terminate the germinal centre transcriptional program, class switch recombination and plasma cell development (De Silva *et al.*, 2012). Of note, IRF4 is highly expressed in ABC DLBCL, due to constitutive active NF-κB signalling, and is required for the survival of this subgroup of DLBCL (Lam *et al.*, 2005; Yang *et al.*, 2012). Moreover, IRF4 is known to synergise with NFAT to regulate combined target genes, further supporting a potential association between these proteins in DLBCL (Rengarajan *et al.*, 2002)

Analysis of the C2 curated collection of gene sets also demonstrated enrichment of gene sets associated with the anergic phenotype and TNFα signalling. In the future, it would be of great interest to explore some of the other collections of gene sets. For example, the

C3 motif collection contains gene sets based upon shared cis-regulatory motifs that are conserved across human, mouse, rat and dog genomes (http://www.broadinstitute.org/gsea/index. jsp). The catalogued motifs represent known, or likely regulatory elements in promoters and 3'UTRs, thus allowing identification of other transcription factors that might regulate genes in cooperation with NFAT, such as NF-κB (Xie *et al.*, 2005).

4.3.5. Gene Expression Microarray Summary

Although analysis thus far has mainly been focused on early changes in gene expression to identify direct NFAT targets, some of the regulated genes described in this chapter were also identified as true targets of NFAT and NF-κB in EBV transformed lymphoblastoid cell lines. As explained in greater detail in Chapter 6, through access of previously published ChIP-sequencing data, binding of the NFAT and NF-κB transcription factors to the promoter regions of the TNFα gene in lymphoblastic cells were identified (appendix figure 20, provided by Professor Neil Perkins). Data was also generated for another potential NFAT target gene, PDCD-1 (not shown).

In summary, the gene expression array provided an abundance of interesting data, with which many avenues could be explored. One of the most exciting results from the array was the potential regulation of the cytokine TNFα by NFAT, which is investigated in the next chapter.

Chapter 6.

The role of TNFα in DLBCL

5. The role of TNFα in DLBCL

5.1. Introduction

Gene expression microarray analysis revealed TNFα to be a gene significantly downregulated by CsA treatment in the ABC DLBCL cell lines HLY-1 and U2932, but not in the GCB DLBCL cell line WSU-NHL. Given that TNFα activates pathways involved in proliferation and cell death, this suggested TNFα could be a potential NFAT target gene responsible for the killing of cells treated with CsA. Moreover, TNFα has recently been associated with reduced overall survival and reduced progression-free survival in patients with DLBCL, suggesting that its role should be further explored (Nakayama *et al.*, 2014a; Nakayama *et al.*, 2014b).

5.1.1. TNFα and TNFα receptors

TNFα is a cytokine that is highly involved in immune regulation and inflammation, playing a key role in cell proliferation, differentiation, apoptosis, and lipid metabolism (Locksley *et al.*, 2001). First coined as 'Lymphotoxin' by Dr Gale A Granger, TNF was first discovered to be a cytotoxic factor produced by lymphocytes and was later named 'TNF' by Dr Lloyd J. Old who reported macrophages to be the predominant cell-type of the immune system to produce this cytokine (Granger GA, 1969; Carswell *et al.*, 1975). The name tumour necrosis factor came from the discovery of TNF's ability to kill the mouse fibrosarcoma cell line L-929 (Carswell *et al.*, 1975). This interesting finding highlighted the potential involvement of TNF in anti-tumoural responses by the immune system, a theory which was first described by the physician William B. Coley (McCarthy, 2006).

Cloning of the cDNAs encoding Lymphotoxin and TNF in 1984 revealed the two proteins to be strikingly similar, also demonstrating significant functional homology in binding to the TNF receptor (Gray PW, 1984; Pennica D, 1984). These important discoveries led to the renaming of TNF to TNFα and Lymphotoxin to TNFβ (Aggarwal, 2003). Since these key discoveries, many other TNFR-related proteins have been identified to form a large TNF superfamily of 19 TNF ligands and 29 TNF receptors, which have been extensively reviewed (Smith *et al.*, 1994; Ashkenazi *et al.*, 1998; Idriss *et al.*, 2000; Aggarwal, 2003).

TNFα is a 212 amino acid type II transmembrane protein (Kriegler *et al.*, 1988). Forming a stable arrangement of homotrimers, TNFα integrates into the membrane; however proteolytic cleavage by the metalloprotease TNFα converting enzyme (TACE) allows a soluble TNF (sTNF) 51kDa trimeric complex to be secreted (Black *et al.*, 1997). The membrane-bound (mTNFα) and secreted, soluble forms of TNFα (sTNFα) are both biologically active, sharing some functionality, however *in vivo* models have revealed distinct roles for mTNFα and sTNFα. sTNFα is required for acute and chronic inflammation, whereas mTNFα is involved in the development of lymphoid tissues and provides protection from bacterial infection, chronic inflammation and autoimmunity (Ruuls *et al.*, 2001; Kollias *et al.*, 2002; Saunders *et al.*, 2004; Allenbach *et al.*, 2008). The differential effects of each form of TNFα generally imply protective immune functions for mTNFα, since it lacks the harmful effects of sTNFα (Locksley *et al.*, 2001; Richter *et al.*, 2012).

TNFα can bind to two receptors, either the TNFR1 (TNF receptor type 1) or TNFR2 (TNF receptor type 2) (Locksley *et al.*, 2001). TNFR1 is expressed in most tissues and can be activated by both the membrane-bound and soluble forms of TNFα (Grell *et al.*, 1995). TNFR2 on the other hand is distinctly found on immune cells and can only be activated by the membrane-bound form of TNFα (Grell *et al.*, 1995; Faustman *et al.*, 2010). While mTNFα-mediated signalling occurs in a juxtacrine manor, interacting in a cell-cell contact dependent fashion, sTNFα functions by both paracrine and systemic functions via TNFR1 (Grell *et al.*, 1995; Richter *et al.*, 2012).

In most cells, TNFR1 is the key mediator of TNFα signalling and plays an important role in apoptosis, whereas in the lymphoid system TNFR2 appears to play a more significant role, particularly for any function related to T-cell survival (Wajant et al., 2002; Faustman et al., 2010). There have been reports of crosstalk between the pathways that these receptors activate (Pimentel-Muiños et al., 1999; Naudé et al., 2011). Receptor crosstalk depends on the signalling kinetics between the two receptors, or the extent of their expression, which may result in agonistic or antagonistic effects on each other's signalling pathways (Naudé et al., 2011).

Ligand binding to the TNFα receptor forms a trimeric complex of receptors, initiating a conformational change, causing the inhibitory protein SODD (silencer of death domains) to dissociate from the intracellular death domain component of the TNF receptor (Kriegler et al., 1988; Tang et al., 1996; Locksley et al., 2001). In turn, the adaptor protein

TRADD (TNF Receptor type 1 Associated Death Domain) is permitted access to death domain binding, forming a platform for downstream protein domain activation (Wajant et al., 2002)

5.1.2. Signalling pathways initiated by TNFα

TNFα exhibits a large range of bioactivities in the cell but is mostly considered to function as a regulator of the proinflammatory response. In the pathological context however, TNFα can behave as a double-edged sword by exerting dual functionality. An early example of this is TNFα's role in liver regeneration after a partial hepatectomy (Yamada *et al.*, 1997). TNFα was shown to play a key role in liver regeneration, where mouse models deficient in TNFR1 showed severe impairment of hepatocyte DNA synthesis (Yamada *et al.*, 1997). In models of acute hepatotoxicity however, TNFα functions via TNFR1 by causing destruction of the liver (Yamada *et al.*, 1997). The ability of TNFα to play such opposing roles is likely due to engagement of different pathways downstream of the TNF receptors. Once activated, TNFRs use distinct, but partially overlapping signalling pathways. TNFR1 strongly enhances NF-κB signalling, but also has the ability to initiate cell death pathways via its cytoplasmic death domain (Naudé *et al.*, 2011; Richter *et al.*, 2012). TNFR2 on the other hand activates cytoprotective functions through canonical and non-canonical NF-κB signalling (Rauert *et al.*, 2010; Naudé *et al.*, 2011)

Two main signalling pathways are initiated by ligation of TNFα to its receptor, TNFR1, including the NF-κB pathway and the MAPK pathways. These transcriptional pathways are required for the expression of genes involved in cell growth, death, development and immune responses (Chen *et al.*, 2002). The molecular mechanisms of TNFα signal transduction are highly complex and in recent years there has been a wealth of information published involving molecules and pathways associated with TNFα (Locksley *et al.*, 2001; Aggarwal, 2003; Van Herreweghe *et al.*, 2010). Activation of the NF-κB and MAPK pathways (such as JNK) mediates an array of processes including cell proliferation, survival and inflammatory responses and anti-apoptotic factors. Generally speaking however, TNFα-induced NF-κB signalling leads to a pro-inflammatory and anti-apoptotic responses whereas JNK activation is largely pro-apoptotic (Wajant *et al.*, 2002).

In addition to induction of transcriptional pathways, the activation of death signalling pathways are also triggered by TNFα, where binding of TRADD to FADD (Fas-Associated protein with Death Domain) leads to the recruitment of caspase-8 and the

cleavage of downstream caspases, ultimately leading to apoptosis (Wilson *et al.*, 2009). When compared to other cell death inducing pathways, the induction of cell death by TNFα is fairly weak and is often masked by the anti-apoptotic influence from NF-κB (Wajant *et al.*, 2002).

5.1.3. Autocrine and paracrine signalling by TNFα

Many cytokines, including TNFα, can function by both autocrine and paracrine mechanisms. Autocrine signalling is a form of cell signalling in which a cell secretes a chemical, hormone or proteins such as cytokines that bind to autocrine receptors on that same cell, initiating downstream effects in the cell. During an immune response, autocrine functions often amplify signalling or gene expression in a cellular response to a given pathogen. For example, TNFα is a well-known autocrine regulator of inflammatory signalling in a number of cellular processes (Wu *et al.*, 1993; Blasi *et al.*, 1994; Xaus *et al.*, 2000; Coward *et al.*, 2002; Kuno *et al.*, 2005). TNFα and NF-κB form a positive autocrine feedback loop during the initiation of an allergic response in mast cells for example, where TNFα synthesised as a consequence of NF-κB activation is released into the extracellular environment to further augment the NF-κB response, leading to more TNFα production and so on (Coward *et al.*, 2002). If TNFα signalling in DLBCL functions in an autocrine manner it would be interesting to unravel the precise pathways TNFα targets and to investigate the effects of TNFα inhibition.

Paracrine signalling on the other hand, is a form of cell-cell communication where a cell produces a signal, such as a chemokine which then induces effects on surrounding cells, altering their behaviour. In the immune environment, paracrine signalling is critical for the amplification of an inflammatory response within a tissue or organ, involving a diverse variety of cell types (Caldwell *et al.*, 2014).

5.1.4. Dysregulation of TNFα

Now known to be produced by many cells of the immune system (including lymphoid cells, mast cells, cardiac cells and fibroblasts) (Locksley *et al.*, 2001), TNFα is a widely researched cytokine, due to its involvement in a vast array of diseases. Dysregulation of TNFα has been implicated in conditions such as cancer, autoimmune disorders, Alzheimer's disease, diabetes, osteoporosis and many more (Chen *et al.*, 2002; Kollias *et al.*, 2002; Kodama *et al.*, 2005). In normal, healthy, individuals, TNFα is released from

cells in a controlled fashion in response to various cytokines (such as IL-1) or by the presence of foreign substances (such as LPS or other bacterial products). In the disease setting however, TNFα production becomes dysregulated whereby excessive levels are produced. As a result, this creates a chronic state of inflammation in autoimmune disorders, while also having detrimental effects in cancer patients.

5.1.5. Inhibition of TNFα

Significant clinical improvements have been achieved by treating patients with autoimmune diseases such as rheumatoid arthritis with TNFα inhibitors (Taylor *et al.*, 2000). These have also been effective treatments for other conditions such as Crone's disease and inflammatory bowel disease, effectively suppressing overactivity of the immune system and dampening down the inflammatory response (Taylor *et al.*, 2000; Blam *et al.*, 2001). Inhibition is achieved by using monoclonal anti-TNFα antibodies, such as Infliximab (Remicade®) (Knight DM1, 1993), Adalimumab (Humira®) (Kempeni, 1999), Golimumab (Simponi®) (D. Shealy, 2007), or with Certolizumab pegol (Cimzia®) (Nesbitt A1, 2007), a pegylated Fab fragment of a humanised TNFα monoclonal antibody.

5.1.5.1. Infliximab

The TNFα neutralising antibody Infliximab was used in this study to investigate the effects of TNFα inhibition on DLBCL cell viability. Infliximab (trade name Remicade®) is a chimeric human-murine IgG monoclonal antibody against TNFα. Produced in Chinese hamster ovary cells by recombinant DNA technology, Infliximab is administered by intravenous infusion in the clinic to treat autoimmune diseases such as rheumatoid arthritis, psoriasis, Crohn's disease and ulcerative colitis. As shown in figure 60, the mechanism of action behind Infliximab's immunosuppressant effects are by high affinity binding to the soluble and membrane-bound forms of the TNFα cytokine, preventing TNFα from binding to the TNF receptor, thereby inhibiting the activation of downstream pro-inflammatory pathways.

5.1.5.2. Etanercept

Also used for the treatment of autoimmune diseases such as rheumatoid arthritis and psoriatic arthritis, Etanercept (Enbrel®) is an alternative approach used in the clinic to

antagonise TNFα. Although naturally occurring antagonists of TNFα receptor activation come in the form of soluble TNFα receptors, which compete with cell surface TNFα receptors for TNFα ligand binding, their actions are not sufficient to block the elevated levels of TNFα found in inflammatory diseases (D. Aderka, 1992; Goffe *et al.*, 2003).

Comprised of a recombinant, dimeric fusion protein, Etanercept consists of the human 75kDa TNFα receptor linked to the Fc portion of human IgG1 (Goffe *et al.*, 2003), allowing it to mimic the activity of naturally occurring soluble TNFα receptors. Etanercept therefore competes with membrane-bound TNFα receptors for binding to the TNFα cytokine, as shown in figure 60 (K. Peppel, 1991). In fact, Etanercept binds receptor bound molecules of TNFα at 50-1000 times that of soluble forms of the TNFα receptor, which is owed to the dimeric structure of the fusion protein, enabling high affinity binding of Etanercept to two free TNFα molecules or two receptor-bound molecules of TNFα (K. Peppel, 1991; Mohler *et al.*, 1993).

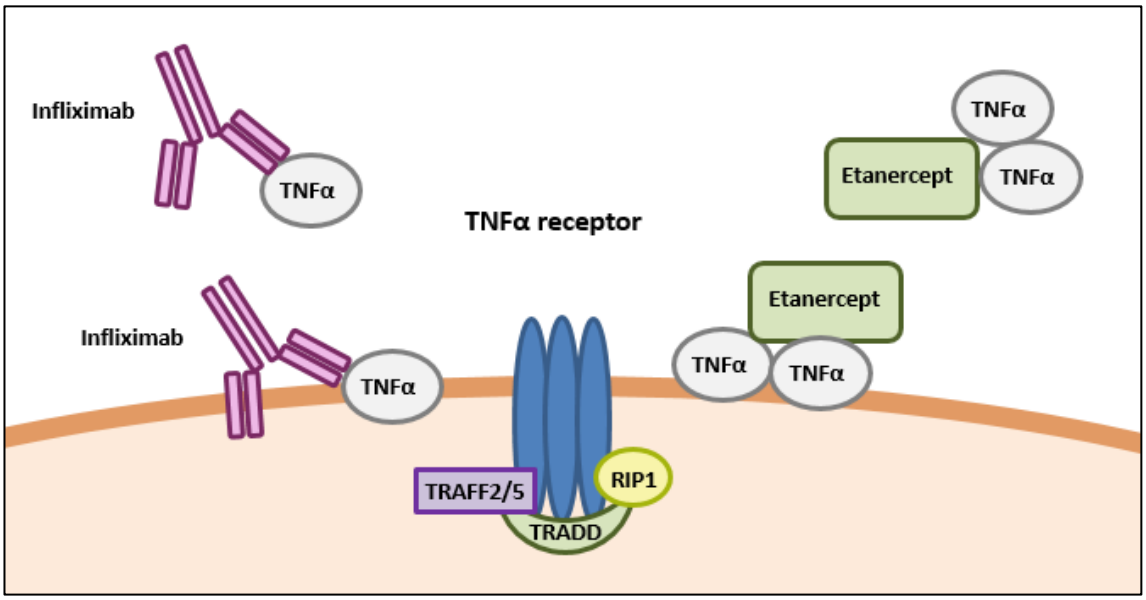

Figure 60. Mechanism of TNFα inhibition using Infliximab or Etanercept. The TNFα neutralising antibody Infliximab binds with high affinity to the soluble and membrane-bound forms of TNFα, preventing TNFα from binding to the TNF receptor. Etanercept is a dimeric fusion protein which mimics the activity of soluble TNFα receptors, competing with membrane-bound receptors for the binding of TNFα, therefore inhibiting the activation of downstream pro-inflammatory pathways.

5.1.6. Potential role for TNFα in DLBCL

As described previously, TNFα has been identified as an NFAT target in a number of biological contexts and in recent years their relationship has been described as potentially oncogenic (Pedersen *et al.*, 2009; Nakayama *et al.*, 2014a; Nakayama *et al.*, 2014b).

Recent studies have provided evidence supporting the addition of TNFα to the International Prognostic Index (IPI) to improve its predictive prognostic value for predicting the prognosis of patients with DLBCL (Nakayama *et al.*, 2014a). An investigation by Nakayama et al (2014), for example, evaluated TNFα expression in 62 lymphoma tissue samples from patients with not otherwise specified DLBCL (DLBCL, NOS), using immunostaining with an anti-TNFα antibody (Nakayama *et al.*, 2014a). Tumour specimens could be divided into two groups; TNFα positive (38 cases, 61%) and TNFα negative (24 cases, 39%). They found that TNFα positivity correlated with poorer overall survival and progression free survival (OS P=0.0005 and PFS P=0.0330) when compared with TNFα negative samples (Nakayama *et al.*, 2014a).

Furthermore, in a second study by the same research group, a cohort of 60 DLBCL NOS tissue specimens were evaluated for expression of the TNFR1 and TNFR2 by immunohistochemical staining (Nakayama *et al.*, 2014b). TNFR1 was expressed in 31 cases (52%) and correlated with poorer overall survival (P=0.0006) when compared to TNFR1-negative tumours (29 cases, 48%) and was confirmed a significant prognostic factor for OS, independent of the IPI (Nakayama *et al.*, 2014b). TNFR2 positive specimens were also predictive of a poorer OS, however this was not found to be statistically significant (Nakayama *et al.*, 2014b). Their data suggests that expression of the TNFα cytokine is associated with expression of the TNFR1, where 87% of TNFα positive cases showed positive expression of the TNFR1 and these cases were correlated with a poorer OS compared with the TNFα negative, TNFR1 negative cases (Nakayama *et al.*, 2014b). Moreover, a poorer prognosis for OS and progression-free survival, independent of the IPI was reported in 45% of TNFα positive, TNFR1 positive cases (Nakayama *et al.*, 2014b). These clinical report findings further support that the inclusion of TNFα, (with the addition of TNFR1) to the IPI may be a logical step to improve the prognosis of patients with DLBCL NOS more accurately.

Interestingly, previous studies by other research groups have shown that patients with ABC DLBCL display elevated serum levels of TNFα compared to patients with GCB DLBCL and other B-cell malignancies (Pedersen *et al.*, 2005). These findings have also been confirmed from an *in vitro* perspective. For example, in a study investigating elevated levels of oncogenic miR-155 in DLBCL, increased miR-155 levels and diminished expression of its target SHIP-1 were found to be a result of autocrine stimulation by TNFα (Pedersen *et al.*, 2009). Treatment of cells with Etanercept or

Infliximab was sufficient to reduce miR-155 levels and restore SHIP1 expression (Pedersen *et al.*, 2009). Interestingly, an anti-TNFα regimen also caused a reduction in cell proliferation and a decrease in DLBCL tumour xenograft burden in response to Etanercept (Pedersen *et al.*, 2009). These findings suggested that TNFα may be playing a key role in the survival of DLBCL cells and is indicative that anti-TNFα therapy may be a potential novel treatment for DLBCL.

In summary, there is sufficient clinical evidence, as well as mechanistic evidence, that NFAT regulates TNFα expression, which may be oncogenic in some contexts, such as in DLBCL. Should TNFα be an important NFAT target gene in DLBCL, essential for cell survival and other pro-tumour functions, it is important to decipher the precise mechanisms involved. Following on from the microarray, I aimed to investigate whether DLBCL cell lines were producing high levels of TNFα and whether calcineurin/NFAT-induced TNFα expression was driving the survival of DLBCL cells in an autocrine fashion, as shown in the model in figure 61. If TNFα were found to be a key cytokine required for DLBCL cell growth, I aimed to assess whether CsA-induced cell death could be rescued by the addition of exogenous TNFα. Should the calcineurin/NFAT-TNFα mechanism be effectively inhibited (and the viability of DLBCL cells reduced), this could reveal a potential treatment option for patients with DLBCL. Anti-TNFα treatments are already immediately accessible, so consequently their use as co-treatments with other therapeutic agents could be of potential benefit to patients in the near future.

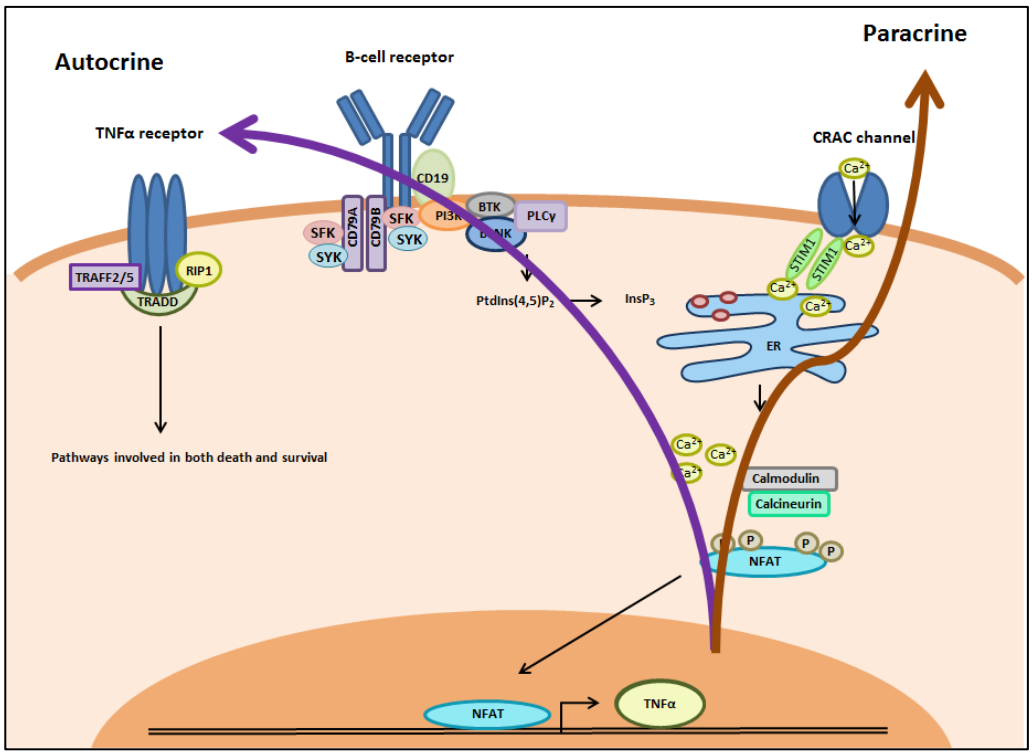

Figure 61. Model for TNFα signalling in DLBCL. TNFα is potentially an NFAT target gene in DLBCL, where upregulation of TNFα production by DLBCL cells may stimulate survival pathways in an autocrine manner. Alternatively, TNFα production may function in a paracrine fashion, affecting cells in the tumour microenvironment.

5.2. Results

5.2.1. TNFα production by DLBCL cell lines is variable and in some cell lines is dependent on the calcineurin-NFAT signalling pathway

To investigate whether DLBCL cell lines produce TNFα, either in soluble form or bound to soluble TNF receptors, cells were incubated for 2 days following the normal splitting procedure before their media supernatants were removed. The Quantikine TNFα assay was used to assess the quantity of TNFα produced from cells and to make a relative comparison of TNFα production between cell lines. Apart from when seeding cells, when harvesting supernatants cell counts were not performed to normalise TNFα expression in supernatants in relation to cell number per ml. Relative levels of TNFα produced are therefore only approximate.

Figure 62a illustrates heterogeneous production of TNFα among the panel of cell lines, ranging from 25pg/mL to 150pg/mL. Some cell lines such as RIVA and U2932 released greater than six-fold the levels of TNFα when compared to HLY-1, OCI-Ly3 and SUDHL-4, with some cell lines producing TNFα at intermediate levels.

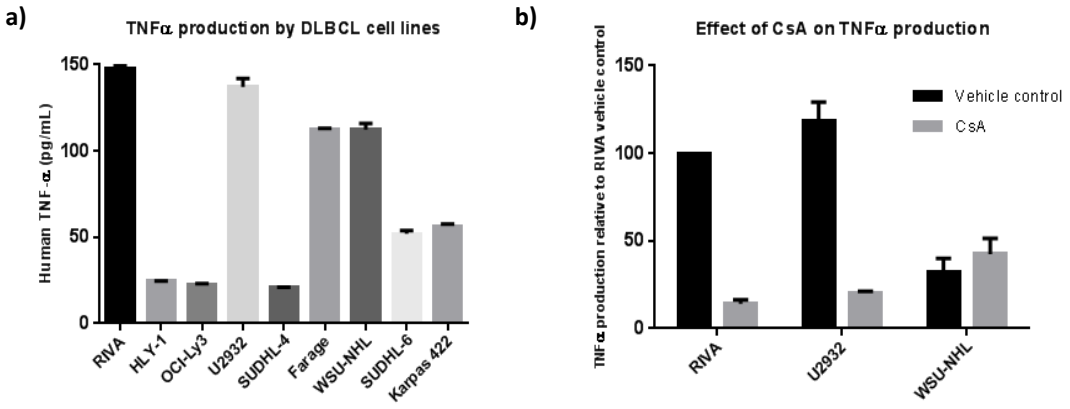

Figure 62. TNFα production by DLBCL cell lines is variable and in some cell lines is dependent on the calcineurin-NFAT signalling pathway. a) DLBCL cells were incubated for 2 days (following splitting as normal) before media supernatants were removed for use in a TNFα ELISA. Data is representative of one experiment repeated three times, where error bars represent the standard deviation of duplicate wells. b) RIVA, U2932 and WSU-NHL cells were treated with their respective IC50 concentrations of CsA (RIVA = 13.5μg/ml, U2932 = 8.6μg/ml and WSU-NHL = 10.4μg/ml) for 2 hours before removal of the media supernatants for use in the TNFα ELISA assay. Data is representative of two repeat experiments, where error bars indicate the standard error of the mean.

RIVA, U2932 and WSU-NHL cells were identified as high producers of TNFα in figure 62a and were treated with CsA for 2 hours to analyse the effects of calcineurin/NFAT inhibition on TNFα production (figure 62b). Of note, compared to figure 62a, WSU-NHL cells appeared to produce considerably lower concentrations of TNFα when compared to RIVA and U2932. This was a consequence of diluting the samples by a dilution factor of 4 with the aim of more accurately determining the effects of CsA treatment. CsA had a significant effect on TNFα production in the ABC DLBCL cell lines RIVA and U2932 cells, reducing its production around 5-fold. However, in the GCB DLBCL cell line WSU-NHL, TNFα production was not reduced upon treatment with CsA.

5.2.2. Infliximab and Etanercept are functioning appropriately by reducing the levels of TNFα-induced NF-κB activity

To ensure that Infliximab and Etanercept were having their desired effect on TNFα and pathways downstream of TNFα, a positive control experiment was performed using an NF-κB luciferase reporter assay. It is well known that TNFα is a common initiator of the NF-κB pathway, and for this reason the NF-κB luciferase reporter assay was an appropriate choice of control experiment to ensure Infliximab and Etanercept were inhibiting the transcriptional activation of NF-κB.

U2OS cells containing an NF-κB regulated promoter upstream of the firefly luciferase gene were treated with 10μg/ml TNFα (to induce NF-κB activity), followed immediately by treatment with 10μg/ml Infliximab or Etanercept. To make certain that any effects on NF-κB were due to inhibition of TNFα and not due to the addition of an antibody to cells, 10μg/ml human IgG was also added to cells accordingly. Cells were subsequently incubated for 2 hours before being lysed and a luciferase assay performed.

Figure 63 shows that the control human IgG had little to no effect on NF-κB activity when compared to the untreated -TNFα control. NF-κB activity was also similar in these

samples following the addition of TNFα, which (as expected) increased NF-κB activity substantially. Treatment of cells with Infliximab or Etanercept reduced NF-κB activity to levels comparable to the untreated –TNFα control. Addition of TNFα to samples treated with Infliximab and Etanercept demonstrated that the reduction of NF-κB activity was specifically by inhibition of TNFα and not due to off target effects of the anti-TNFα agents. This experiment was a useful tool to confirm that Infliximab, Etanercept and human IgG were functioning appropriately, allowing further experiments using these agents to be performed with confidence.

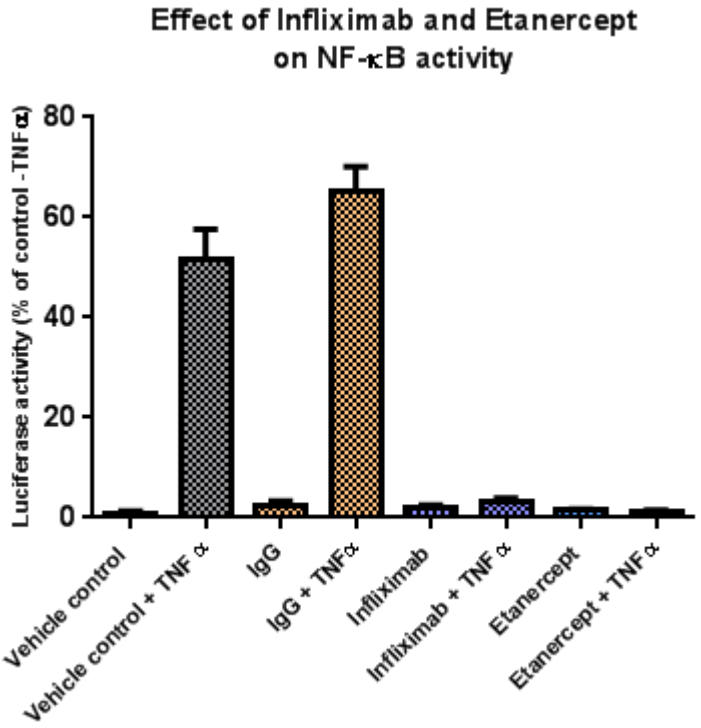

Figure 63. Infliximab and Etanercept are functioning appropriately by reducing the levels of TNFα-induced NF-κB activity. U2OS cells expressing the NF-κB gene regulatory region upstream of the firefly luciferase gene were treated with 10μg/ml TNFα, followed by immediate treatment with 10μg/ml of the TNFα neutralising antibody Infliximab, the TNFα antagonist Etanercept or a control human IgG, including a vehicle control (1% PBS + 0.05% FBS). Cells were incubated for 2 hours before being lysed and the luciferase reporter experiment performed. Data is representative of one experiment, where error bars indicate the standard deviation between triplicate wells.

5.2.3. TNFα produced by DLBCL cell lines is biologically active; however inhibition of TNFα signalling has no effect on p65 and c-Rel DNA binding activity

NF-κB signalling plays a fundamental role in DLBCL and (as described previously) TNFα is a well-known activator of the NF-κB pathway. Therefore I investigated whether the TNFα produced by DLBCL cells was sufficient to induce NF-κB. Media supernatants

from RIVA and HLY-1 cells were added to U2OS NF-κB luciferase reporter cells and the transcriptional activity of NF-κB analysed (figure 64a). As a positive control human TNFα was added to the cells, which demonstrated a substantial upregulation of NF-κB activity. Addition of RIVA cell medium (TNFα high) increased NF-κB activity almost two-fold and was statistically significant (P-value = 0.028) whereas addition of HLY-1 medium (TNFα low) had no effect on NF-κB activity. Activation of NF-κB by TNFα in RIVA cells was specifically due to TNFα and not due to other components of cell medium, as confirmed by the addition of Etanercept, which reduced NF-κB activity to levels similar to untreated –TNFα samples. Overall, these data confirm that TNFα produced by some DLBCL cell lines is biologically functional.

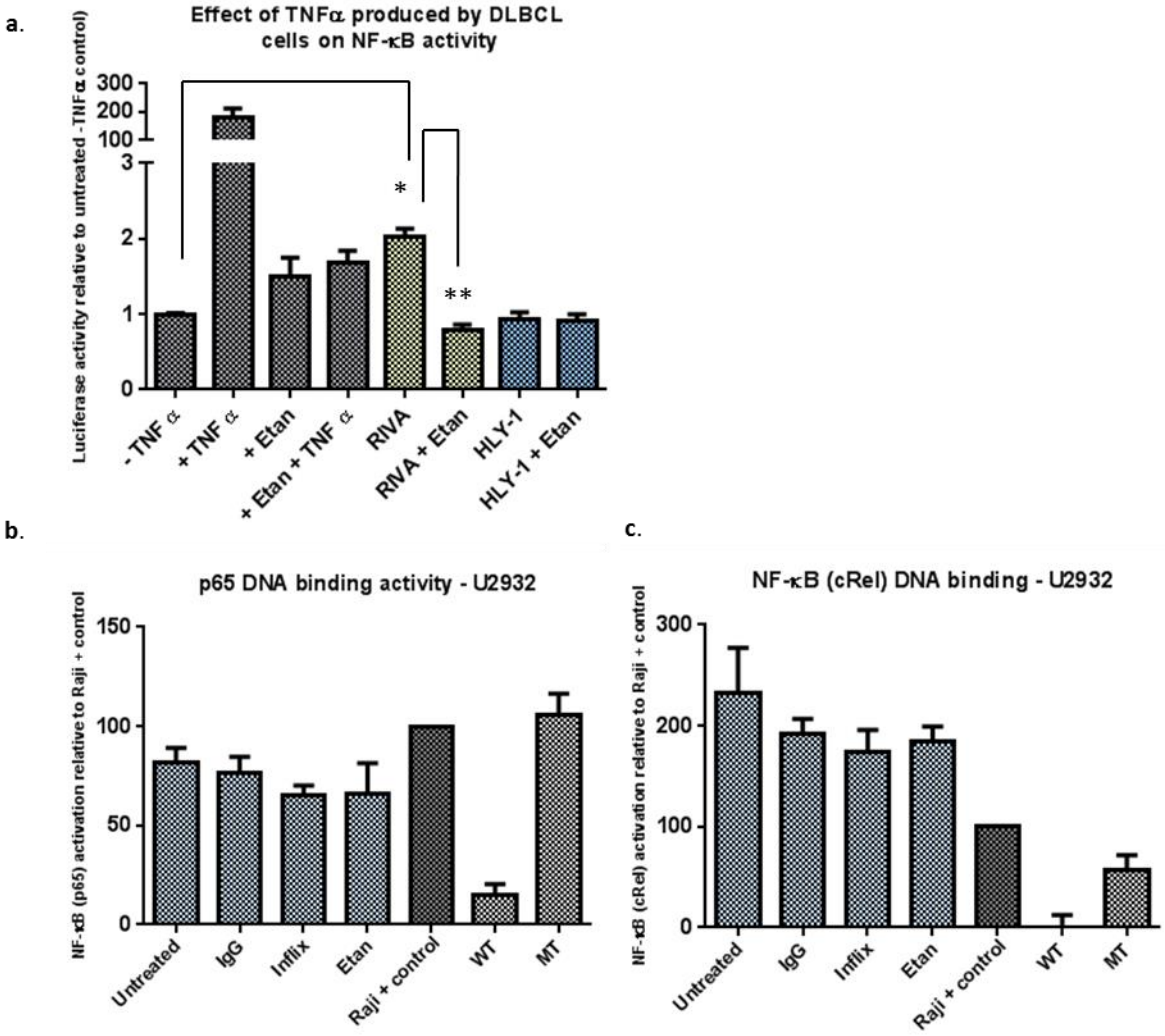

Figure 64. TNFα produced by DLBCL cell lines is biologically active; however inhibition of TNFα signalling has no effect on p65 and c-Rel DNA binding activity. a) The DLBCL cell lines RIVA and HLY-1 were incubated for 2 days (following splitting as normal) before media supernatants were removed. Media supernatants were immediately added to NF-κB luciferase reporter U2OS cells while 10μg/ml human TNFα was added to appropriate wells as a positive control for NF-κB activity. To confirm observed effects on NF-κB activity was specifically due to TNFα production, 10μg/ml of the TNFα antagonist Etanercept was also added to cells accordingly. Cells were incubated for 2 hours or 6 hours (showing very similar results) before NF-κB transcriptional activity was measured by a luciferase reporter assay. P-values: RIVA = 0.028, HLY-1 = insignificant. RIVA + Etanercept compared to RIVA P-value = 0.01. Data is representative of three individual biological repeat experiments performed in duplicate wells, where error bars represent the standard error of the mean. b-c) The DLBCL cell line U2932 was treated with 10μg/ml of the TNFα neutralising antibody Infliximab, the TNFα antagonist Etanercept or a control human IgG, including a vehicle control (1% PBS + 0.05% FBS). Cells were incubated for 2 hours before nuclear extraction and addition of nuclear samples to an NF-κB ELISA. To monitor the specificity of the assay, samples were run alongside a mutated (MT) consensus oligonucleotide and a wild-type (WT) consensus oligonucleotide (as a competitor for NF-κB binding). Data is representative of three independent biological repeat experiments (apart from the WT and MT controls (c) which represent one experiment), where error bars indicate the standard error of the mean.

I next aimed to assess whether inhibition of TNFα caused a downregulation of NF-κB DNA binding activity using ELISA assays specific for the p65 and c-Rel NF-κB family members. Treatment of U2932 cells with Infliximab and Etanercept had no significant effect on the DNA binding activity of either p65 or c-Rel compared to the vehicle control or human IgG (figure 64b and c). An explanation for this could be that the TNF that is produced by U2932 is not biologically active (as demonstrated in RIVA cells alone). Using U2932 cells for this particular experiment, rather than RIVA cells was indeed a limitation because we cannot be certain that the high levels of TNFα produced by U2932 cells is biologically active. If there had been sufficient time to investigate this, and the TNFα in U2932s was proven active, the results in figure 64 would indicate that although TNFα produced by DLBCL cells is biologically active, it may not be required for the transcriptional activity of the p65 and c-Rel NF-κB family members in DLBCL.

5.2.4. TNFα is an NFAT and NF-κB target gene

Although TPCA-1 was not the broad NF-κB inhibitor that we wanted for gene expression microarray analysis, its inhibitory effects (proven by ELISA) were useful for investigating potential interactions between the NF-κB and NFAT pathways in regards to cell viability and expression of joint target genes. Considering TNFα is a known NF-κB target gene and my recent discovery of NFAT as a mediator of TNFα expression in DLBCL, it was decided to confirm that TNFα was an NF-κB target gene in DLBCL cells. U2932 and RIVA cells were treated with increasing concentrations of TPCA-1 (figures 65a and b). Consistent with inhibition of IKK2, TPCA-1 caused a dose-dependent decrease in TNFα mRNA expression in both cell lines, confirming TNFα to be an NF-κB

target gene. Cells were also treated with increasing concentrations of CsA. Here, TNFα expression was considerably reduced even at concentrations representing $1/10^{th}$ of the IC50 concentration. When treated simultaneously with CsA and TPCA-1, the expression of TNFα and TNFα production in RIVA and U2932 cells was downregulated slightly more than treatment of CsA treatment alone (figure 65b and d). However, this was not significant enough for the effects to be considered additive or synergistic and was not observed in other cell lines.

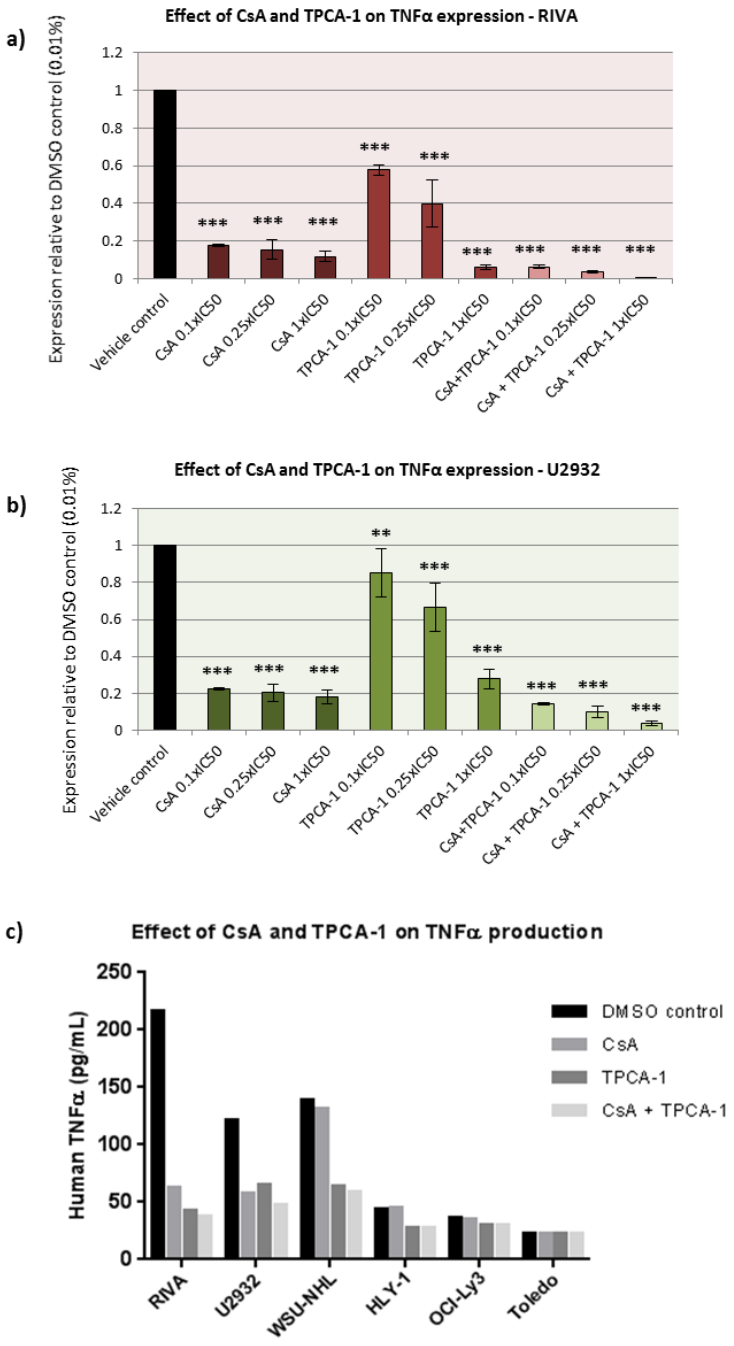

Figure 65. TNFα is a NFAT and NF-κB target gene. The DLBCL cells RIVA (a) and U2932 (b) were treated with increasing concentrations of CsA and TPCA-1, both alone and in combination for 2 hours before RNA was extracted, followed by reverse transcription to cDNA and analysis of TNFα mRNA expression by qRT-PCR analysis. A vehicle control was also included (0.01% DMSO). Concentrations of drugs included 1xIC50, 0.25xIC50 and 0.1xIC50 concentrations respectively. For RIVA cells, concentrations for CsA were as follows; 1xIC50=13.5μg/ml, 0.25xIC50=3.375μg/ml, 0.1xIC50=1.35μg/ml and for TPCA-1 included 1xIC50=4.2μM, 0.25xIC50=1.1μM and 0.1xIC50=0.11μM. For U2932 cells, concentrations of CsA were as follows; 1xIC50=8.6μg/ml, 0.25xIC50=2.15μg/ml, 0.1xIC50=0.86μg/ml and for TPCA-1 included 1xIC50=3.1μM, 0.25xIC50=0.775μM and 0.1xIC50=0.31μM. Data is representative of three repeat experiments where error bars represent the standard error of the mean. The effect of combined TPCA-1 and CsA treatment on TNFα production in U2932 cells was analysed by a TNFα ELISA (c). Cells were treated with their respective CsA and TPCA-1 IC50 concentrations, both alone and in combination. A vehicle control was also included (0.01% DMSO). Data is representative of one individual experiment. * marks the degree of significance compared to the vehicle control, where *≤0.05, **≤0.01, ***≤0.001.

5.2.5. DLBCL cell lines are insensitive to the TNFα neutralising agent Infliximab and the TNFα antagonist Etanercept

To investigate whether DLBCL cells rely on autocrine TNFα signalling for their survival, RIVA, U2932 and WSU-NHL cells were treated with a range of concentrations (0μg/ml-30μg/ml) of the TNFα neutralising agent Infliximab or the TNFα antagonist Etanercept for 72 hours before cell viability was recorded using the resazurin assay (figure 66). Human IgG was used as a control antibody. Inhibition of TNFα receptor binding and inhibition of downstream pathways did not significantly affect the viability of cells, even at high concentrations, suggesting that cell lines were not dependent on TNFα signalling for their survival.

It was next considered that perhaps the inhibition of simply one cytokine (TNFα) in these experiments may not have had an effect due to the multiple other growth factors and components in the cell medium supplemented with FBS. RIVA and U2932 cells were therefore stripped of serum factors by being cultured in either 10%, 5%, 1% or 0% FBS in addition to 20μg/ml Infliximab or human IgG for a timecourse of 24, 48 or 72 hours (figure 67). Reduction of serum concentrations did not have any effect on the viability of either cell line compared to the untreated or IgG control. The growth of cells plateaued out (U2932) or began to reduce (RIVA) after 48 hours of culture in 1% or 0% FBS, however this was not due to TNFα inhibition, but was rather due to deprivation of cells of essential nutrients in the FBS. This experiment was also performed using 20μg/ml Etanercept; however a similar lack of effect was observed (figure 68).

Considering the inhibitory effects of TNFα neutralisation on DLBCL proliferation reported by Pedersen et al (2009) in OCI-Ly3 and Toledo cell lines, the anti-TNFα regimen was also conducted using these two cell lines (figure 69a and b). Interestingly, in my analysis, OCI-Ly3 and Toledo cells were identified as having minimal TNFα production, while also expressing very low levels of NFAT2, a potential regulator of TNFα (figure 61a. 65c and figure 15). For these reasons, HLY-1 cells (which also demonstrated low TNFα production, but with high NFAT2 expression) were run alongside OCI-Ly3 and Toledo treatment with Infliximab and Etanercept (figure 69c). Surprisingly, all three cell lines were unresponsive to 72 hours treatment with TNFα neutralising agents.

In a final effort to investigate a potential growth inhibitory effect of Infliximab and Etanercept, OCI-Ly3 and RIVA cells were treated for shorter incubation periods to confirm that potential effects were not being missed (figure 69d-e and g-h). After 24 and 48 hours incubation, there was no significant effect on cell viability in OCI-Ly3 cells. A modest effect was observed in RIVA cells by 48 hours of treatment, however without repetition of this experiment, no solid conclusions can be drawn. Had there have been sufficient time for repetitions to be made, this effect may have become significant.

To assess whether Infliximab and Etanercept had an effect on the early stages of apoptosis, the expression of PARP and its cleaved apoptotic fragment were analysed by Western blot (figure 69f and i). The presence of just the upper band indicated PARP was expressed in its uncleaved form, indicating that anti-TNFα treatment had no effect on the apoptotic cellular machinery. Finally, as an additional measure of cell viability to the resazurin assay, manual cell counting by trypan blue exclusion was performed, but no effect of the anti-TNFα treatment was seen (figure 69j-k). Of note, anti-TNFα treatments were only tested in cell lines with high TNFα production, where NFAT and NF-κB inhibitors affected both TNFα expression and viability.

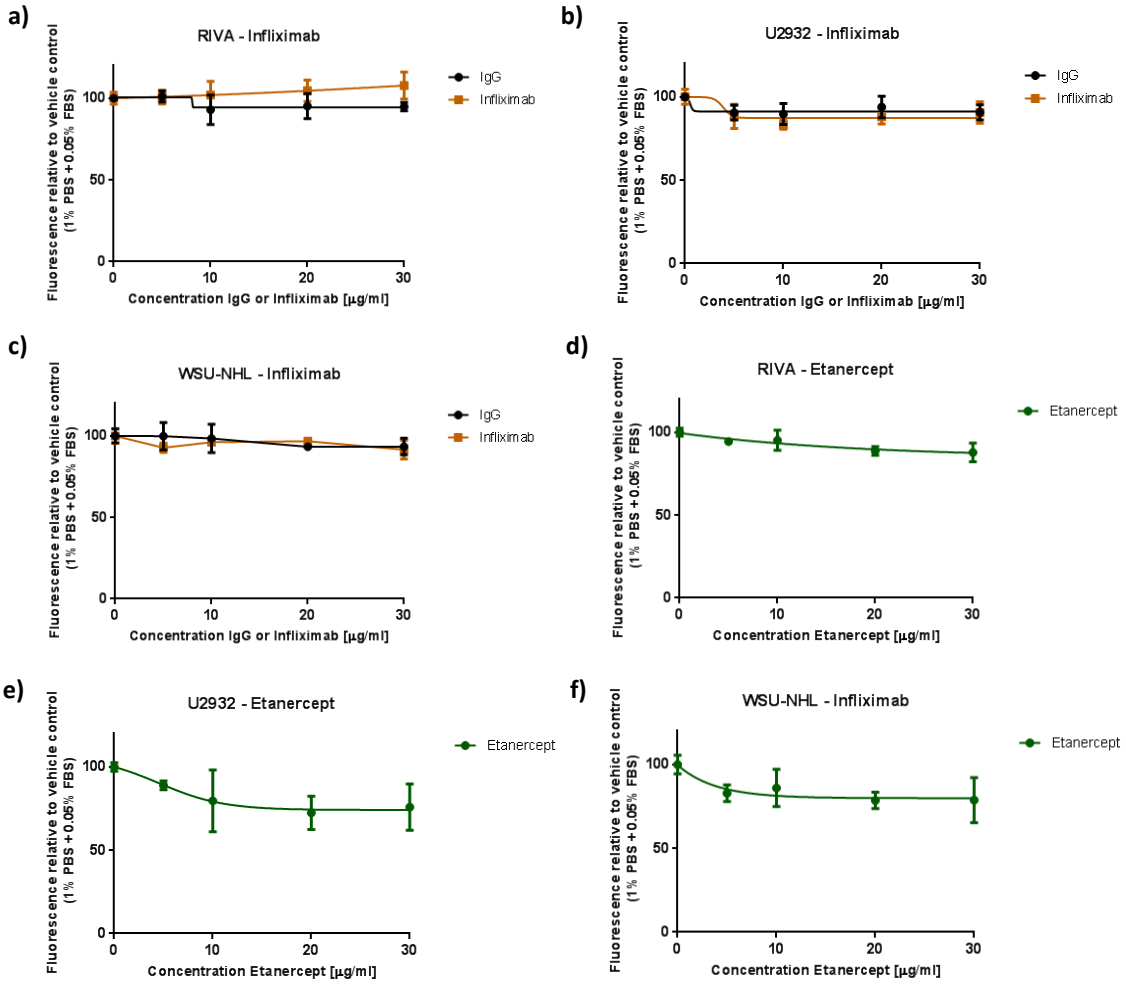

Figure 66. DLBCL cell lines are insensitive to the TNFα neutralising agent Infliximab and the TNFα antagonist Etanercept. a-c) The DLBCL cell lines RIVA, U2932 and WSU-NHL were treated with a range of concentrations of the TNFα neutralising antibody Infliximab and a control human IgG (0µg/ml-30µg/ml), including a vehicle control (1% PBS + 0.05% FBS). d-f) RIVA, U2932s and WSU-NHL were treated with a range of concentrations of the TNFα antagonist Etanercept (0µg/ml-30µg/ml), including a vehicle control (1% PBS + 0.05% FBS). Cells were incubated for 72 hours before cell viability was recorded using the resazurin assay. Data is representative of one experiment where error bars indicate the standard deviation of triplicate wells.

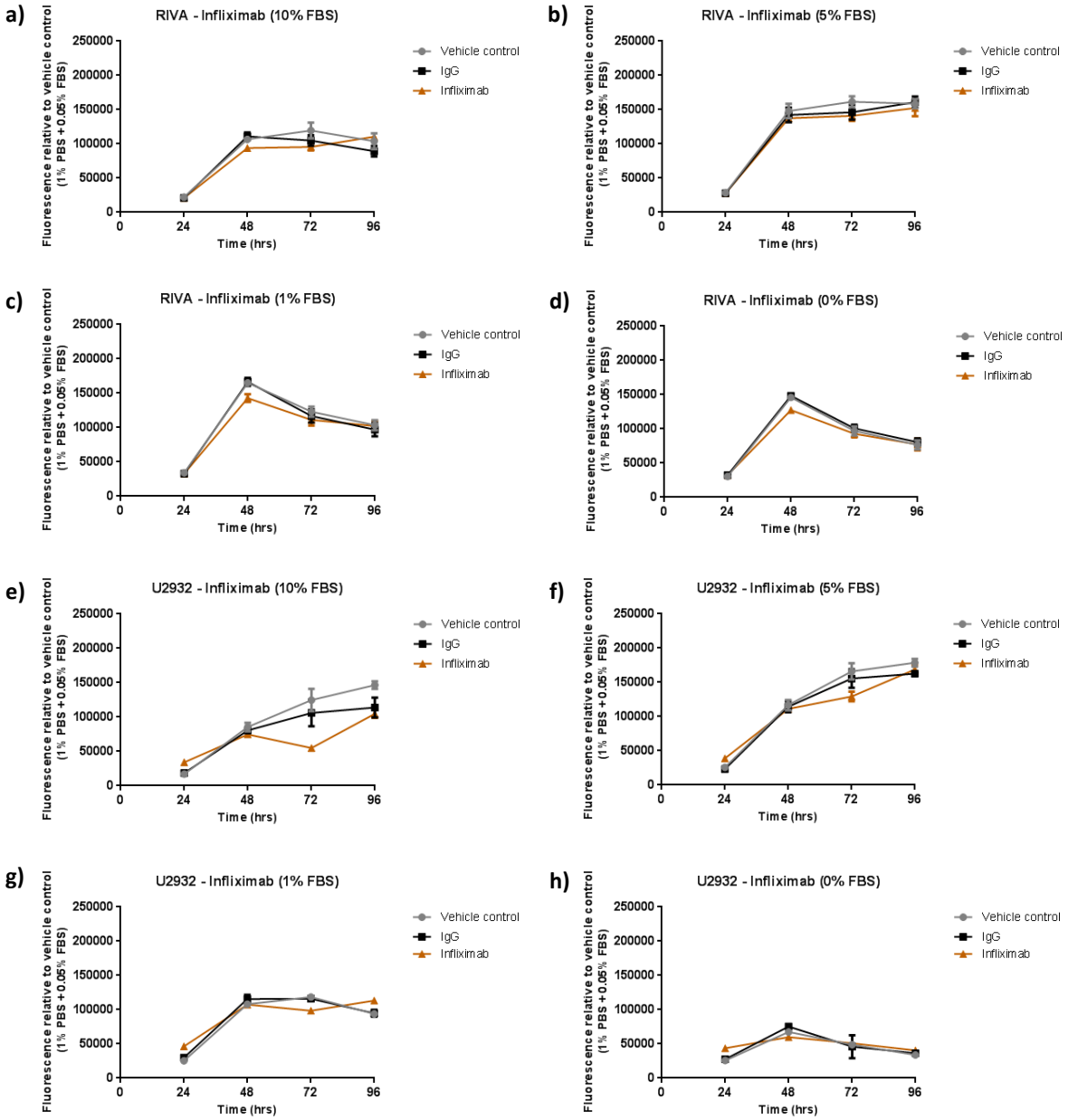

Figure 67. DLBCL cell lines deprived of serum factors are insensitive to the TNFα neutralising agent Infliximab. The DLBCL cell lines RIVA (a-d) and U2932 (e-h) were treated with 20µg/ml of the TNFα neutralising antibody Infliximab and a control human IgG, including a vehicle control (1% PBS + 0.05% FBS). Cells were cultured for 24, 48, 72 or 96 hours in a range of concentrations of FBS, including 10% (a and e), 5% (b and f), 1% (c and g) and 0% (d and h). Cell viability was then recorded using the resazurin assay. Data is representative of one experiment where error bars indicate the standard deviation of triplicate wells.

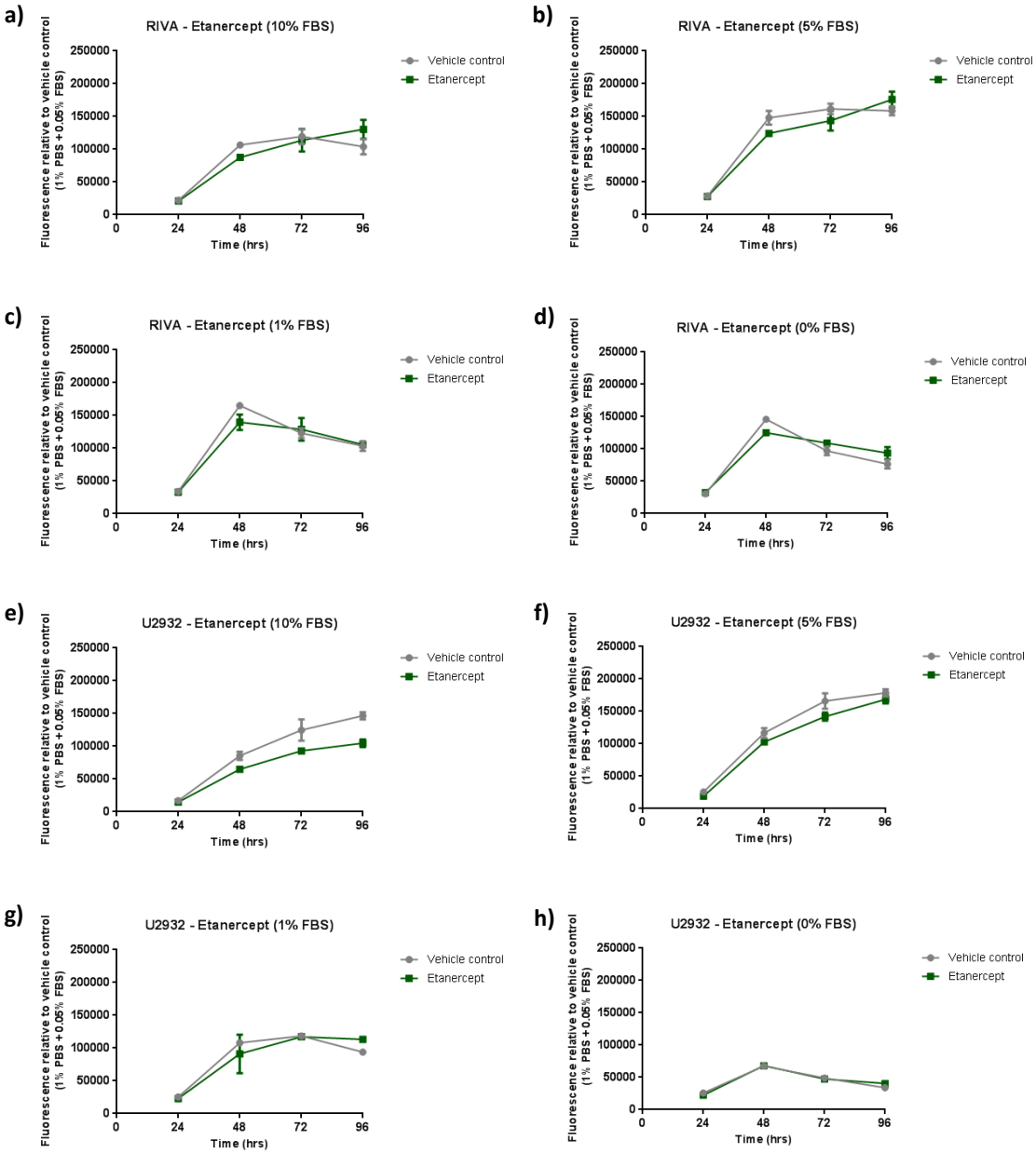

Figure 68. DLBCL cell lines deprived of serum factors are insensitive to the TNFα antagonist Etanercept. The DLBCL cell lines RIVA (a-d) and U2932 (e-h) were treated with 20µg/ml of the TNFα antagonist Etanercept, including a vehicle control (1% PBS + 0.05% FBS). Cells were cultured for 24, 48, 72 or 96 hours in a range of concentrations of FBS, including 10% (a and e), 5% (b and f), 1% (c and g) and 0% (d and h). Cell viability was then recorded using the resazurin assay. Data is representative of one experiment where error bars indicate the standard deviation of triplicate wells.

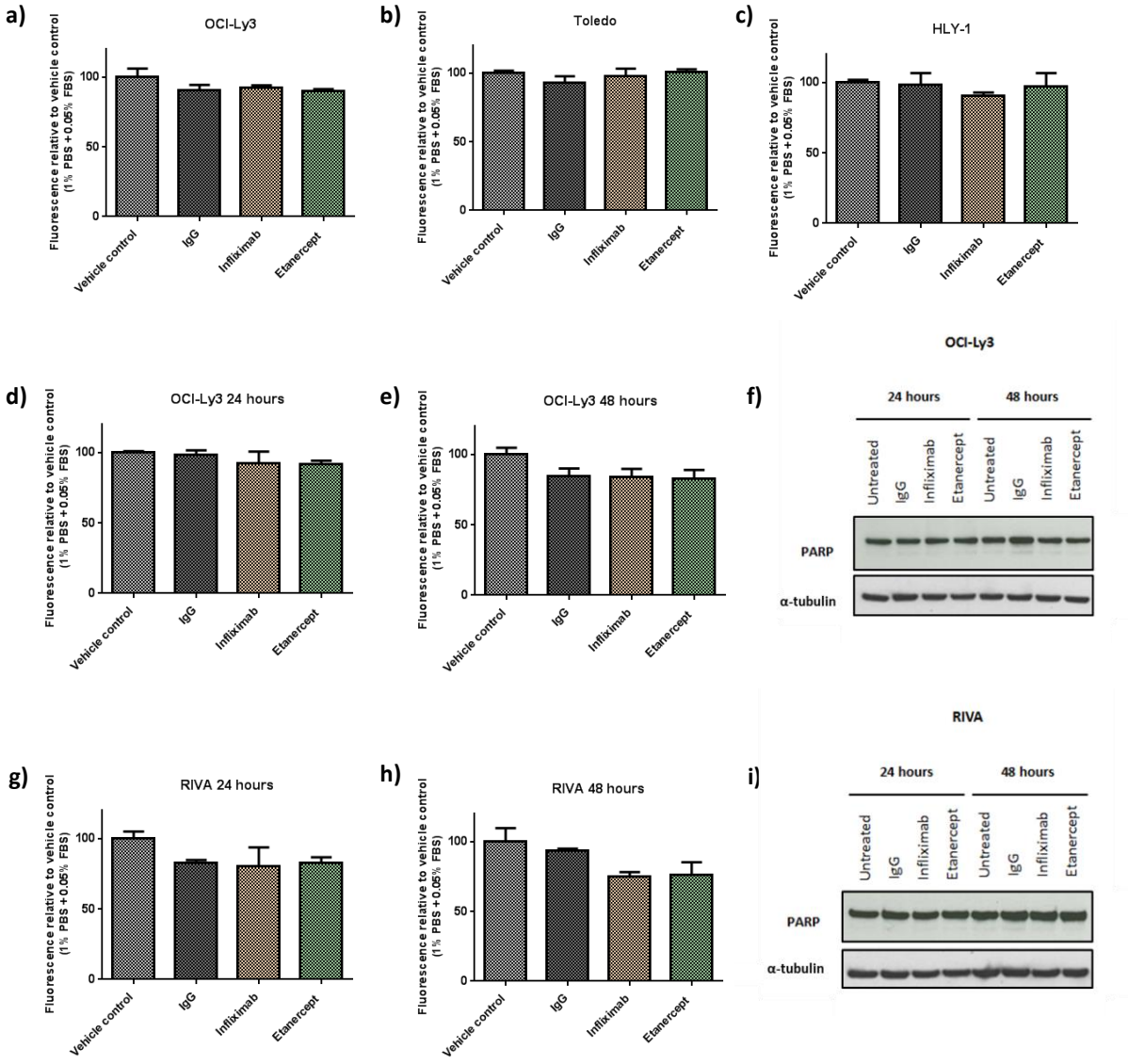

j)

Cell line	Treatment	Cell density ($x10^6$/ml)	
		24 hours	48 hours
RIVA	Vehicle control	0.77	1.56
RIVA	IgG	0.64	2
RIVA	Infliximab	0.57	1.47
RIVA	Etanercept	0.79	1.77

k)

Cell line	Treatment	Cell density ($x10^6$/ml)	
		24 hours	48 hours
OCI-Ly3	Vehicle control	0.49	1.4
OCI-Ly3	IgG	0.65	0.96
OCI-Ly3	Infliximab	0.58	1.14
OCI-Ly3	Etanercept	0.37	1.13

Figure 69 (Continued from previous page). Viability and apoptosis of 'Etanercept-sensitive' DLBCL cell lines used in the literature are unaffected by anti-TNFα treatment. a-c) The DLBCL cell lines OCI-Ly3, Toledo and HLY-1 were treated with 10μg/ml of the TNFα neutralising antibody Infliximab, the TNFα antagonist Etanercept or a control human IgG, including a vehicle control (1% PBS + 0.05% FBS). Cell viability was recorded after 72 hours incubation. d-e and f-g) DLBCL cell lines OCI-Ly3 and RIVA were treated with 10μg/ml of Infliximab, Etanercept or control human IgG, including a vehicle control (1% PBS + 0.05% FBS). After 24 hours (d and g) or 48 hours (e and h) cell viability was recorded using the resazurin assay. Data is representative of one experiment where error bars indicate the standard deviation of triplicate wells. f and i) Western blot analysis for OCI-Ly3 and RIVA cells treated with Infliximab, Etanercept or human IgG for 24 and 48 hours. The effect of 10μg/ml anti-TNFα treatment on apoptosis was analysed using an antibody specific for the PARP protein (116KDa) and its cleaved fragment (89KDa). Molecular weight marker lines to the right of the Western blot indicate the approximate location of antibody binding. α-tubulin was included as a loading control. Data is representative of one experiment. j-k) Trypan blue exclusion was used to investigate the effect of 10μg/ml anti-TNFα treatment on RIVA and OCI-Ly3 cell viability after 24 and 48 hours. Data in tables indicates manual cell counts for each treatment. Data is representative of one experiment.

5.3.Discussion

5.3.1. TNFα production by DLBCL cell lines

The Quantikine TNFα ELISA was a useful tool for confirming that DLBCL cell lines produce TNFα. TNFα was largely heterogeneous among the panel and no apparent correlation was observed between TNFα production and particular DLBCL subgroups. Half of the ABC cell lines, for example displayed high TNFα production (RIVA and U2932) whereas the remaining ABC lines generated much lower TNFα concentrations (HLY-1 and OCI-Ly3). The degree of heterogeneity observed may be due to alternative mechanisms of TNFα modulation by NFAT or other transcription factors in these cells.

If NFAT were a master regulator of TNFα induction in DLBCL it is possible that NFAT protein expression and activation in cell lines may correlate with the degree of TNFα produced. Analysis showed that although some cell lines expressed medium-high levels of NFAT1 and NFAT2 protein (chapter 3, figure 15 and 17a) in association with high production of TNFα (such as the four highest TNFα-producing cell lines RIVA, U2932, Farage and WSU-NHL), this correlation was not consistent among the cell line panel. HLY-1 for example, expressed substantially high levels of NFAT1 and NFAT2 protein, yet produced very little TNFα. SUDHL-4 on the other hand, also produced small quantities of TNFα, but expressed active NFAT1 and NFAT2 at considerably low levels.

Comparing cell line TNFα production with data in the literature is difficult due to differences between cell types tested, incubation periods, culture conditions and experimental setup. Generally speaking however, the concentrations of TNFα produced

by DLBCL cell lines (ranging from 20-150pg/ml) were considered relatively high, especially compared to non-cancerous cell lines. Basal expression of monocytes for example is around 25-50pg/ml, which can increase more than 10-fold after LPS stimulation (Guha *et al.*, 2001; Maus *et al.*, 2001). Moreover, Ebert et al (2006) found that TNFα production in human intestinal intraepithelial lymphocytes remained below 20pg/ml after 5 days culture (Ebert *et al.*, 2006). Cells were found to keep their TNFα levels low by low cell uptake of TNFα and negative feedback inhibition of transcription (Ebert *et al.*, 2006).

TNFα production in DLBCL cells appears to be either comparable or in some cell lines produced at higher levels compared to other cancer cell lines, for example, HT-29 human colon adenocarcinoma cells incubated for 48 hours in serum-free media were shown to produce 40-50pg/ml of TNFα (Scamuffa *et al.*, 2008). Moreover, the IGROV-1 ovarian cell line was reported to produce approximately 30pg/ml after 48 hours incubation (Kulbe *et al.*, 2012).

The effects of CsA treatment on TNFα production in these cell lines showed great consistency with the array results and qRT-PCR validation of samples used in the array. As seen in the array, where CsA treatment in U2932 cells at 2 hours caused a significant downregulation of TNFα mRNA, the ELISA assay also detected a substantial reduction in TNFα production. Also in line with the array, CsA had no effect on TNFα expression or production in WSU-NHL cells, further validating data from a number of different assay procedures.

Data shown in figure 62b also confirmed the DLBCL subtype-specific effects on TNFα observed between cell lines in the array and validation experiments. Inhibition of calcineurin/NFAT signalling had no effect on TNFα in the GCB cell line WSU-NHL compared to the two ABC cell lines RIVA and U2932, suggesting that calcineurin/NFAT may regulate the expression of TNFα differently in specific disease subsets. Data in the literature reports TNFα expression to be a significant prognostic factor for overall survival and progression free survival in addition to being an independent prognostic factor of the IPI (Nakayama *et al.*, 2014a; Nakayama *et al.*, 2014b). As of yet only one research group has published evidence for the differential distribution of TNFα expression between ABC and GCB DLBCL. Future experiments would aim to check the effects of TNFα expression with CsA treatment in more cell lines. Moreover, immunohistochemical analysis of TNFα expression in patient samples with ABC and GCB DLBCL would be a

very interesting avenue to explore given the heterogeneity of TNFα production between cell lines observed in this study.

5.3.2. Inhibition of TNFα signalling using Infliximab and Etanercept

The response of DLBCL cell lines to Infliximab and Etanercept was first tested using a broad range of concentrations, however even doses considered to be high did not have any additional effect on cell viability. The range of concentrations of Infliximab and Etanercept were similar to or exceeded those used in the literature and were therefore considered appropriate (Mitoma *et al.*, 2005; Teimourian *et al.*, 2015). In fact, in the publication described previously where the viability of non GC-cells was reduced upon Etanercept and Infliximab treatment, doses as low as 100ng/ml were used at an identical 72 hour timepoint (Pedersen *et al.*, 2009).

Before ruling out the hypothesis that cell lines depended on TNFα for survival, a number of alterations were made to the experimental procedure to see whether a potential effect was being missed. Of note, this series of optimisation experiments were performed as single experiments because it was not considered important to repeatedly produce negative results. After experimenting with different concentration of drug, cells were stripped of serum factors to allow the effects of TNFα inhibition to be more identifiable, however this had no effect on cell viability. Moreover, shorter incubation periods did not capture early effects of Infliximab or Etanercept, which also demonstrated a lack of impact on PARP cleavage. Together, the sum total of these data provided no evidence that anti-TNFα treatment impacts the viability of DLBCL cells, suggesting that calcineurin/NFAT-induced TNFα production does not promote the survival of cells in an autocrine fashion. A useful experiment in this study was confirmation that Etanercept and Infliximab were functioning appropriately, however a limitation of this assay was the use of U2OS cells rather than DLBCL cells. In hindsight, it may have been useful to have a cell line known to be sensitive to TNFα inhibition, although this effectively performed using Toledo and OCI-Ly3 cells used by Pedersen et al (2009) (Pedersen *et al.*, 2009).

A surprising observation was the lack of effect of Infliximab and Etanercept on the viability of OCI-Ly3 and Toledo cells, which were intended to complement our experiments by behaving as positive control cell lines. In their paper demonstrating autocrine stimulation of ABC DLBCL cell lines by TNFα, treatment of cells with 0.1µg/ml Etanercept caused significant antiproliferative effects compared to untreated

control cells (Pedersen *et al.*, 2009). Pedersen reported similar results using Infliximab; although these data were not shown. Growth inhibitory effects were observed in OCI-Ly3, OCI-Ly10 and Toledo cells but not SUDHL-4 or the BL cell line Daudi (Pedersen *et al.*, 2009). Sensitivity was concluded as being ABC DLBCL specific. However, Toledo cells in their study were wrongly classified and are in fact of GCB origin (Singh *et al.*, 2010). Nevertheless, to be absolutely sure that Etanercept and Infliximab were functional and to confirm published data, OCI-Ly3 and Toledo cells were treated with the anti-TNFα agents, but no anti-proliferative effects were observed.

There are a number of possible reasons that the effects reported by Pedersen et al (2009) were not repeated in our study. These include differences in cell culture, underlying genetic changes developed by passaging of continuous cell lines and dissimilarities in assay procedures. Pedersen for example, used a Beckman Coulter Counter for cell proliferation assays, whereas viability experiments in this study were performed using the resazurin assay, which measures the metabolic activity of cells. It is possible that the resazurin assay may not have been sensitive enough to detect subtle changes in cell viability, however trypan blue exclusion analysis also showed no effects. Future work may benefit from using colony forming assays to investigate whether Etanercept or Infliximab prevent the formation of a population of cells from one single cell.

Pedersen et al (2009) undoubtedly presented evidence for a clear mechanism proving that Onco-miR-155 targets SHIP1 to promote TNFα-dependent growth of DLBCL cells through autocrine stimulation by TNFα (Pedersen *et al.*, 2009). Their study even demonstrated a substantial decrease in tumour burden using xenograft models treated with Etanercept (Pedersen *et al.*, 2009). Despite this, it could be argued that their data lacked detailed investigation into the underlying production of TNFα by cell lines. Having investigated TNFα production in a comprehensive panel of DLBCL in this PhD study, it was recognised that OCI-Ly3 and Toledo cells were among the lowest producers of TNFα (and NFAT2 expression). It is possible that the small quantity of TNFα released from these cells is critical for autocrine survival mechanisms; although our data demonstrated no difference between cell line sensitivity and TNFα production.

5.3.3. TNFα and future work

In the future it would be useful to silence TNFα in DLBCL cell lines by shRNA knockdown. This would be a beneficial method for understanding the precise role of

TNFα in DLBCL, enabling further experiments to be conducted. Importantly, to pinpoint exactly which NFAT isoform upregulates TNFα in DLBCL cells, future experiments could use shRNA knockdown of individual NFAT family members. Similarly, ChIP experiments could be used to confirm TNFα as an NFAT target gene, where analysis of which NFAT isoforms bind to the TNFα promoter could be determined. As mentioned previously, TNFα is already a known NFAT1 target gene in other cellular systems, such as NIH/3T3 fibroblasts, where NFAT1 was demonstrated to induce cell death through cooperation with the Ras/Raf/MEK/ERK pathway and up-regulation of TNFα (Robbs *et al.*, 2013). Although NFAT1 was highly tumour suppressive in NIH/3T3 fibroblasts, regulation of TNFα in DLBCL may differ. A key question is whether regulation of TNFα by other NFAT isoforms may exert oncogenic roles in DLBCL. Ultimately, the relative balance of TNFα regulation by different NFAT isoforms may result in contrasting effects, some which may be tumour suppressive and others oncogenic.

Cooperative effects between NFAT and NF-κB signalling in DLBCL remains to be fully investigated. In chapter 4, analysis of combined CsA and TPCA-1 treatment demonstrated variable effects on cell viability, where additive effects were observed in select cell lines. Although a valid approach for investigating synergy between NF-κB and NFAT signalling, this data did not capture potentially interesting coordinate regulation of specific genes which may be important for DLBCL survival. After the NF-κB target gene TNFα was identified as a potential calcineurin/NFAT target gene by gene expression microarray analysis I investigated whether TNFα is also an NF-κB target gene in DLBCL cells. First I tested the effects of TPCA-1 on NF-κB, where ELISA assays proved to be a useful, sensitive tool for analysis, effectively showing a considerable reduction in p65 activity upon TPCA-1 treatment. Retrospectively, in previous TPCA-1 biochemical assays, where the conclusion was that TPCA-1 is an ineffective NF-κB inhibitor in DLBCL, additional assay techniques should have been used to confirm its effects. An interesting result was the differential effect of IKK2 inhibition on p65 and c-Rel activity. Although both subunits are highly involved in canonical NF-κB signalling, TPCA-1 exerted very mild effects on c-Rel activity compared to p65, suggesting that IKK2 inhibition may be subunit-specific. These data suggest that future investigation of NF-κB/NFAT synergy may require inhibition of both of these subunits. Interestingly, functional redundancy between c-Rel and p65 have in fact been reported in the literature, where mice lacking combinations of different NF-κB proteins demonstrated different haematopoietic and immune functions (Grossmann *et al.*, 1999).

TNFα was shown to be an NF-κB target gene by qRT-PCR analysis, however downregulation of TNFα mRNA expression by combined inhibition of NF-κB and NFAT was not significant enough for the effects to be considered additive or synergistic. Interestingly, through access of previously published ChIP-sequencing data, binding of the NFAT and NF-κB transcription factors to the promoter regions of the TNFα gene in lymphoblastic cells were identified (appendix figure 20, provided by Professor Neil Perkins). Transcription factor binding data was accessible through the ENCODE (Encyclopaedia of DNA Elements) consortium (http://www.ncbi.nlm.nih.gov/geo/query/acc.cgi?acc=GSE32465, accessed 18.09.15; http://www.ncbi.nlm.nih.gov/geo/query/acc.cgi?acc=GSM1010779, accessed 18.09.15). One study, which used ChIP-seq to investigate the genetic landscape of NF-κB binding, revealed strong peaks around the TNFα promoter regions and were particularly apparent for the RelA, RelB and c-Rel NF-κB subunits (Zhao *et al.*, 2014). Appendix figure 20, also shows ChIP-seq data for NFAT2, which was obtained from a study analysing the cell-type-specific DNA-binding of the oestrogen receptor (Gertz *et al.*, 2013). Importantly, both studies used EBV-transformed GM12878 lymphoblastic cells, allowing sensible comparisons to be made regarding the DNA binding of the NFAT and NF-κB transcription factors in lymphoma cells. Interestingly, the peaks also indicate binding of NFAT2 to the TNFα promoter, which occurred in similar areas to NF-κB. Additionally, strong NF-κB peaks were observed surrounding the LTB (TNFβ) gene, however this was not apparent for NFAT2.

Overall, there is undoubtedly evidence, both in literature and from this study, supporting a role for TNFα in DLBCL. Anti-TNFα therapy for DLBCL is a feasible novel co-treatment for DLBCL; however the function of TNFα and its precise mechanism action must first be better understood. Confirmation that TNFα is a direct target of NFAT remains to be elucidated and further investigation of cooperative regulation of TNFα between NFAT and NF-κB is required.

Chapter 7.

Discussion and Future Directions

6. Discussion and Future Directions

6.1. Exploration of NFAT pathway activation and inhibition

In this study, the expression of two lymphoid-specific NFAT family members, NFAT1 and NFAT2, were confirmed to be heterogeneously expressed in a large panel of DLBCL cell lines. In many cell lines, NFAT proteins were located in the nucleus in their activated state, which was also confirmed using an NFAT2 DNA-binding ELISA. These data were in line with studies in the literature, which showed expression of nuclear NFAT2 in DLBCL patient samples and cell lines (Marafioti *et al.*, 2005; Pham *et al.*, 2005). Similar to the heterogeneity of the disease, these data imply significant differences between DLBCL cell line expression and activation of NFAT.

Due to difficulties experienced with the small molecule compound INCA-6 and the peptide inhibitors VIVIT and MCV-1, the calcineurin inhibitor CsA was chosen as the best possible option for use in the microarray. It was accepted that, by using CsA, it could not be certain that differentially expressed genes were direct NFAT target genes. Changes in gene expression for example, could potentially be a downstream effect of calcineurin inhibition. Although far from perfect, it was anticipated that true NFAT target genes could later be identified by means of ChIP analysis or knockdown of NFAT family members, as described below.

This study demonstrated that CsA treatment reduced the viability of cells by inducing cell cycle arrest and apoptosis. Despite the use of CsA as an effective immunosuppressant in the clinic for the prevention of organ transplant rejections, its application for the treatment of cancer is unlikely (Kiani *et al.*, 2000). In addition to its off target effects on other pathways (such as NF-κB) and its neuro- and nephrotoxicity, CsA is also a reported inhibitor of multidrug resistance protein 2 (MRP2) (Kiani *et al.*, 2000; Rezzani, 2004; Hesselink *et al.*, 2005; El-Sheikh *et al.*, 2014). Similar to p-glycoprotein, which encodes the multidrug resistance protein 1 (MRP1), multidrug resistance proteins are derived from a superfamily of ATP-binding cassette (ABC) transporters that pump molecules out of cells (Gottesman *et al.*, 1993; Borst *et al.*, 2000). The presence of these transporters in tumour cells makes them key suspects for drug resistance in cancer treatment. CsA was demonstrated to interact with mycophenolic acid (MPA), (an immunosuppressant often used in combination with CsA as transplant therapy) by inhibiting MRP2, which targets MPA (Hesselink *et al.*, 2005; El-Sheikh *et al.*, 2014). CsA caused a reduction in cell exposure to MPA, which, should the same apply in cancer therapy, could prevent therapeutic agents from having their desired effect in the cell (Hesselink *et al.*, 2005).

Reports such as this imply that CsA is probably best used as a tool for research purposes only, such as by aiding our understanding of NFAT function in DLBCL.

There is demand for new, highly specific inhibitors of NFAT that are suitable for research purposes and are clinically applicable. To better understand the specific requirements and functions of specific NFAT family member isoforms, it is key that there be structural studies of the full-length phosphorylated and dephosphorylated proteins, to which inhibitors can subsequently be designed. Future efforts to inhibit NFAT may also be through upstream inhibition, such as by targeting components of the BCR. For this to be pursued however, a better understanding for the mechanisms by which NFAT is regulated in different diseases is required. Alternatively, NFAT may be inhibited by gaining a better understanding of its natural inhibitors. Activity of the NFAT export kinase GSK-3β, for example, is downregulated in some human solid tumours as a result of inhibition from hyperactivity of the PI3K/AKT pathway (Mancini *et al.*, 2009). Consequently, this leads to constitutive activation of NFAT in the nucleus, which may perhaps be reversed by effective inhibition of PI3K or AKT (Mancini *et al.*, 2009).

6.2. Gene expression microarray analysis

Characterisation of cell lines and sensitivities to CsA enabled selection of appropriate cell lines for gene expression microarray analysis. Despite producing a surprisingly low number of statistically significant genes, the microarray nonetheless generated a wealth information, highlighting potential NFAT target genes that may be important for lymphomagenesis. Analysis of some of the most significantly up- or downregulated genes from the array by qRT-PCR analysis validated the accuracy of the microarray. Given the differences observed between unpaired and paired analysis of the array data, these experiments were also a useful tool for proving that paired analysis was the best form of data analysis.

The molecular pathways on which the ABC and GCB DLBCL subgroups depend for survival and growth are vastly different and thus they represent two different disease entities with severely different outcomes (Lenz *et al.*, 2008c). It is therefore not surprising that distinct differences in transcriptional regulation are frequently observed between the subgroups. Initial analysis of the microarray suggested that the genes regulated by calcineurin/NFAT may be different between ABC and GCB cell lines. Subsequent

experiments treated a larger panel of DLBCL cell lines with CsA and found that indeed, specific genes, such as TNFα, were downregulated by CsA in mostly ABC cell lines only.

To further explore differences between the modes of gene regulation by NFAT in different subgroups of DLBCL, a gene expression microarray using a broader panel of cell lines would be required. Moreover, additional microarray analysis could include samples which have been treated with CsA for a longer period of incubation. This would generate a greater selection of genes to analyse, therefore providing a more comprehensive analysis of the primary and secondary effects of NFAT transcriptional regulation. Longer inhibition of calcineurin/NFAT could also be of particular use for understanding the role of NFAT in WSU-NHL/GCB cells, where few genes were differentially expressed after 2 or 6 hours CsA incubation. Should NFAT regulate select genes in ABC vs. GCB DLBCLs, and genes identified are proven critical for the development and maintenance of lymphoma, this could have a huge impact on a more stratified approach to the future treatment of these diseases.

6.3. Possible roles for the NFAT signalling pathway in DLBCL

Considering the significant effects of CsA on cell viability shown in previous experiments, it was anticipated that genes differentially expressed in the microarray were likely to represent genes associated with cell death, survival or cell cycle regulation. Interestingly, for the vast majority of statistically significant genes, this was not the case. Future analysis would benefit from Ingenuity Pathway Analysis, which could identify genes whose expression patterns and ontology suggest a critical role in cell death or survival. Interestingly, the gene expression array did reveal a small number of potential NFAT target genes that have previously been associated with cancer or lymphoma. In the future, it would be of interest to follow up some of these genes, such as PAX9, CD69, SOCS3 and NFKBIZ.

6.4. Induction of anergy

GSEA was a helpful tool for confirming that some of genes in the microarray were associated with previously published gene sets. For example, a gene set associated with anergy was statistically significant in U2932 and HLY-1 cells, but not in WSU-NHL cells.

Indeed, the array demonstrated downregulation of EGR2 in these two ABC DLBCLs and EGR3 in HLY-1 cells, suggesting that NFAT transcription factors normally upregulate the genes encoding these proteins.

EGR2 and EGR3 are well-documented regulators of the induction of anergy (Gómez-Martín *et al.*, 2010). In murine models for example, deficiency of EGR2 and ERG3 transcription factors have been associated with a phenotype resistant to anergy (Gómez-Martín *et al.*, 2010). Moreover, their expression has been shown to be highly upregulated by using microarray analysis of anergic T-cell clones (Safford *et al.*, 2005).

In the past ten years, NFAT transcription factors have been repeatedly reported to have a central role in the control of tolerance mechanisms. Formation of NFAT1 homodimers, for example, have been identified as transcriptional complexes responsible for the expression of anergy-inducing genes in T cells, such as *Grail* and *Caspase-3* (Noemi Soto-Nieves, 2009). NFAT1 has also recently been identified as a key mediator of the expression of anergy-associated genes in the context of cancer, where CD4+ T cells isolated from the draining lymph nodes of *Nfat1-/-* tumour-bearing mice lacked an anergic phenotype, which was observed in wild-type T cells (Abe *et al.*, 2012).

Interestingly, EGR family members are known to form stable heterodimers with NFAT and regulate the expression of proinflammatory cytokines, such as TNFα (Decker *et al.*, 2003). Interestingly, EGR2 and EGR3 have also been reported as NFAT target genes, suggesting that the interplay between these transcription factors could enhance an anergic phenotype (Rengarajan *et al.*, 2000). In the context of lymphoma, a study has shown EGR1 and NFAT2 to cooperate in the regulation of early stages of T-cell lymphoma development, however this was not found true for EGR2 and EGR3 (Koltsova, 2007).

Direct interaction with anergy-promoting proteins, and induction of anergy-inducing genes, could place NFAT as a key driver of immune unresponsiveness in the tumour microenvironment. NFAT may therefore assist evasion of immune destruction in lymphoma, thereby demonstrating the characteristics of one of Hanahan and Weinberg's most recent hallmarks of cancer (Hanahan *et al.*, 2011). Moreover, studies investigating the role of EGR2 and EGR3 in B-cell lymphomas are lacking and may be of great interest and therapeutic value.

6.5. Cooperation with the NF-κB pathway

One of the aims of this study was to investigate cooperativity between the NFAT and NF-κB signalling pathways in DLBCL. First, the effects of simultaneous inhibition of the two pathways using CsA and TPCA-1 were explored, although no strikingly obvious effects were observed. Considering the requirement of NF-κB and NFAT for the function of normal cells, this approach was not likely to ever translate to a clinical setting. It was possible however, that NFAT and NF-κB may still coordinate joint target genes which are important in lymphoma. For example, it was hypothesised NFAT and NF-κB may separately regulate genes whose simultaneous depletion creates a synthetic lethal phenotype, resulting from loss of in-built redundancy. Using a more specific approach therefore, the effects of CsA and TPCA-1 on TNFα mRNA expression were analysed. Inhibition of NF-κB confirmed TNFα to be an NF-κB target gene in DLBCL cells and when simultaneously treated with CsA, the expression of TNFα was downregulated slightly more than one treatment alone. However this was not significant enough for the effects to be considered additive or synergistic. Future work may investigate the effect of combined NFAT and NF-κB inhibition on other potential NFAT target genes that were generated from the microarray.

Due to time restrictions, a comprehensive analysis of known, databased NF-κB target genes were not cross-referenced with genes identified in the gene expression microarray. Although this would be an interesting avenue to explore, ChIP-seq analysis using DLBCL cell lines would be a superior experimental choice, allowing confirmed NFAT target genes in DLBCL cells to be considered as joint NF-κB target genes. Co-regulated NFAT and NF-κB target genes may represent important nodes of integration between NFAT and NF-κB signalling, where sequential ChIP analysis would ultimately be used to confirm simultaneous promoter occupancy and siRNA knockdown could be used to determine if NFAT and NF-κB promoter binding is interdependent. As described previously, there appear to be contrasting opinions as to the interaction of NFAT and NF-κB when they bind to DNA. While publications in the past have suggested coordinate regulation of genes such as CD154, some researchers are critical of the experimental approach taken to reach these conclusions (Pham *et al.*, 2005; Fu *et al.*, 2006; Muhammad *et al.*, 2014). Recently, evidence suggests that the connection between NF-κB and NFAT signalling in BCR-induced B cells is by induction of the NFAT2/αA short isoform by the p50 and c-Rel NF-κB subunits (Muhammad *et al.*, 2014). Although these two transcriptional pathways are individually important for DLBCL, the complexity with which they interact is likely to be very complex.

6.6. Tumour microenvironment

After 125 years, Stephen Paget's seed and soil hypothesis has finally been accepted, where relationships between cancer cells and the cells of the microenvironment are proving pivotal for the fate of the tumour (Paget, 1889). Recent evidence suggests that NFAT may be a key mediator in the creation of the tumour microenvironment and the potentiation of tumourigenesis (Mancini *et al.*, 2009; Tripathi *et al.*, 2013).

The gene expression array highlighted an abundance of potential NFAT target genes which are known to play key roles in immunity and possibly the tumour microenvironment. For example, among the genes significantly downregulated by CsA, were the chemokines CCL4L1, CCL4L2, CCL3, CCL3L1 and CCL3L3, and the cytokines LTA and IL-10. Interestingly, LTA, also known as TNFβ, has been linked to cancer, while IL-10 is known to function as an enhancer of B-cell survival and proliferation (Itoh *et al.*, 1995; Drutskaya *et al.*, 2010). Little is known about the functions of many of the chemokines generated by microarray analysis, suggesting future avenues for this project to be directed.

In addition to the induction of an array of inflammatory chemokines, NFAT family members appear to have a close relationship with macrophages. Upregulation of chemokines by NFAT in advanced breast cancer, for example, is known to stimulate macrophage infiltration and secretion of EGF and colony stimulating factor 1 (CSF1) (Muller *et al.*, 2001). In turn, EGF activates NFAT signalling in a feedforward paracrine loop, which consequently induces further production of CSF1 (Wyckoff *et al.*, 2004; Wang *et al.*, 2012). Specifically, NFAT2 has recently been shown to initiate primary tumour formation by establishment of a tumour microenvironment (Tripathi *et al.*, 2013). In addition to autonomous NFAT signalling, by upregulation of oncogenic proteins, Tripathi et al (2013) demonstrated that NFAT2 has non-cell autonomous effects on nearby cells (Tripathi *et al.*, 2013).

In this study, TNFα was identified as being one of the most significantly downregulated genes among ABC DLBCL cell lines and gene sets associated with TNFα signalling were identified by GSEA. Given the recently reported correlation between TNFα expression with worse overall survival and progression-free survival in some patients with DLBCL, I decided to investigate its role further. After demonstrating high levels of biologically active TNFα production in a select number of DLBCL cell lines, the sensitivity of cells

to inhibition of TNFα signalling were tested, as previously reported by Pedersen et al (2009) (Pedersen *et al.*, 2009). Overall, Infliximab and Etanercept had no effect on the viability of DLBCL cells, suggesting that calcineurin/NFAT-induced TNFα production does not promote the survival of cells in an autocrine fashion.

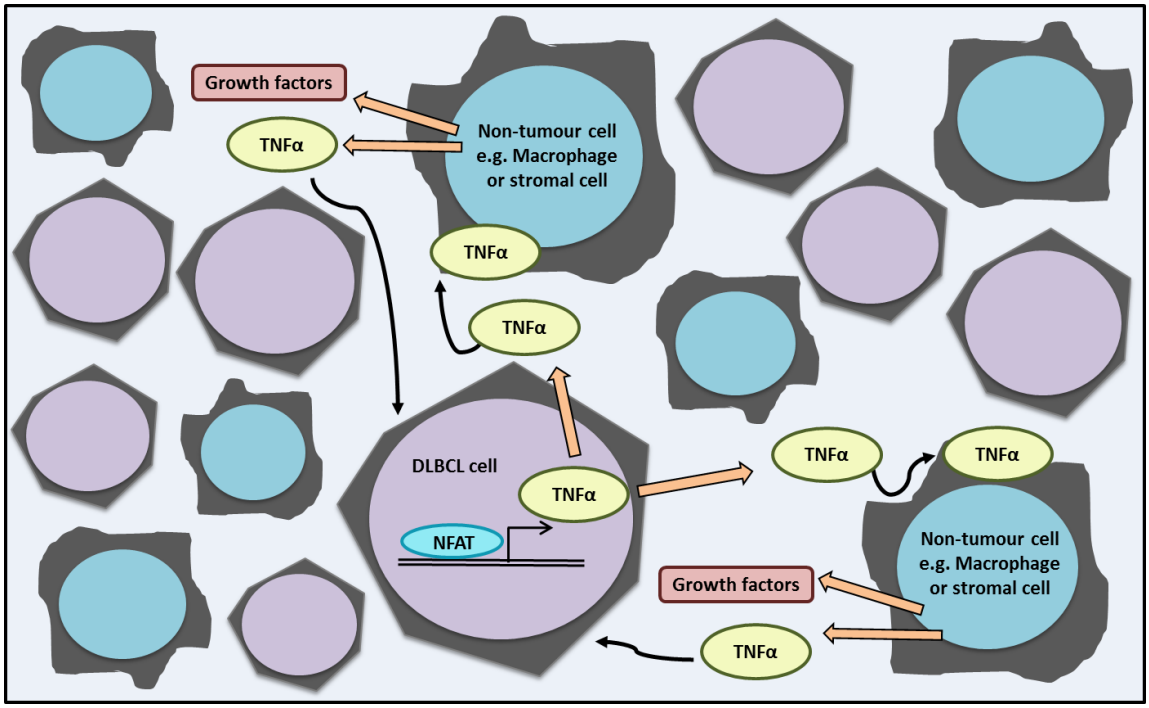

Figure 70. Proposed mechanism of action for NFAT in the tumour microenvironment. NFAT-mediated TNFα production by DLBCL cells (purple) is released into the tumour microenvironment before binding to TNFα receptors on non-tumour cells, such as macrophages or stromal cells in a paracrine fashion (blue). In turn, non-tumour cells produce TNFα and growth factors that allow surrounding cells to thrive. TNFα released by non-tumour cells may subsequently activate TNFα responsive pathways in DLBCL cells.

TNFα produced by DLBCL cells may however, be of functional relevance in a paracrine fashion, signalling to nearby cells in the tumour microenvironment. TNFα produced by DLBCL cells may stimulate signalling pathways of neighbouring non-tumour cells, such as macrophages, which in turn produce more TNFα and potentially increase the expression of growth factors. Growth factors produced by non-tumour cells may consequently activate signalling pathways in DLBCL cells. A similar phenomenon has been described in epithelial ovarian cancer, where TNFα produced by cancer cells was shown to sustain a tumour-promoting cytokine network in the microenvironment, which then promoted neovascularisation of tumour deposits in an autocrine and paracrine fashion (Kulbe *et al.*, 2007). Moreover, paracrine signalling has been shown to be important for tumour growth in mouse models of colon cancer (Greten *et al.*, 2004). For example, deletion of IKKβ in myeloid cells from colitis-associated mice inhibited tumour

growth and development by production of tumour-promoting paracrine factors, including TNFα (Greten *et al.*, 2004). Release of TNFα from DLBCL cells may therefore create a pro-proliferative tumour microenvironment, a proposed model for which is shown in figure 70.

In the future, this could be analysed by xenograft experiments where cells treated with or without TNFα neutralising agents could be injected into mouse models and the effects on nearby cells observed. Moreover, paracrine effects of TNFα could be investigated by trans-well assays, where the effects of TNFα (produced by DLBCL cell lines) on neighbouring cells could be evaluated, for example by analysing the effects on NF-κB target gene expression.

6.7. Future work/directions for the project

6.7.1. Knockdown of NFAT transcription factors

There is currently little understanding of the specific genes that NFAT family members and their isoforms regulate. ChIP-seq would be a suitable assay technique for identifying specific NFAT family member target genes in DLBCL cell lines, which would ultimately aid our understanding for the differential functions described in the literature.

Alternatively, shRNA knockdown of particular NFAT family members would have been a highly beneficial method for determining their function in cell line models of DLBCL. In fact, considerable time was spent during this study to achieve shRNA lentiviral knockdown of NFAT1 and NFAT2 by means of the PTRIPZ inducible system (Thermo-Scientific). For this, plasmid DNA was prepared and co-transfected into 293T cells before extraction of virus. DLBCL cell lines were subsequently transduced by spinfection and induced by addition of doxycycline. Unfortunately, considerable difficulty was experienced in transducing the DLBCL cell lines when compare to cell line models of T-cell lymphomas used in the laboratory. The expression of red fluorescent protein (RFP), detected by FACs analysis was used as a measure of percentage cells transduced and the DLBCL cell lines rarely demonstrated more than 5% transduction efficiency, as shown in appendix figure 21a. Using a potent non-silencing virus, the transduction of DLBCL cells were compared to two T-cell lines. After 72 hours of doxycycline induction, the T cells demonstrated transduction of over 80%. To decrease the chances of multiple integration of the shRNA into the DNA of cells, an ideal transduction efficiency of 30%

is usually required. With such ineffective transduction in the B cells, puromycin selection was challenging due to the high volume of death occurring in puromycin-sensitive cells. This was eventually overcome by considerably reducing the cell media volume, allowing healthy transduced cells to grow and eventually (after around three weeks of careful culture), become fully transduced. Interestingly, the difficulties of transducing these mature B cells have also been experienced by other well-known research groups, including the Louis Staudt laboratory (National Cancer Institute, USA), however the reasons for this are currently unknown.

Although stable cell lines were generated and knockdown of NFAT2 protein was achieved, as indicated by Western blot analysis (appendix figure 21b-c), the degree of protein knockdown was highly variable between experiments. In addition, the expression of NFAT2 mRNA was also variable between experiments and was often only slightly downregulated (appendix figure 21d). Furthermore, qRT-PCR experiments were performed to investigate the effect of NFAT2 knockdown on genes differentially expressed in the microarray. However, as illustrated in appendix figure 21e, expression of potential NFAT target genes in DLBCL cells were highly sensitive to doxycycline treatment alone, making the data inaccurate and unreliable. Interestingly, a recent paper was published showing that doxycycline accumulates in DLBCL cells to high concentrations and affects multiple signalling pathways crucial for lymphomagenesis (Pulvino *et al.*, 2015). For these reasons, and due to time restrictions, no further work regarding shRNA related studies were carried out.

In the future, this project would highly benefit from knockdown studies, both to investigate the role of NFAT transcription factors, but also to analyse the effects of TNFα depletion. While NFAT dominant negative constructs are available for purchase, it would be more ideal to optimise a method for shRNA knockdown, which can be used to investigate various proteins of interest, including NFAT, TNFα, or even NF-κB subunits. There are a number of different options available, including use of the GIPZ system for shRNA knockdown, which although is non-inducible, is smaller in size and known to achieve a higher degree of transduction into cells (www.dharmacon.com, 2015).

Alternatively, the CRISPR-Cas9 (clustered, regularly interspaced, short palindromic repeat-Cas9) system for gene knockdown is proving to revolutionise biomedical research and could be an advantageous technique for future work on this project. CRISPR/Cas is derived from a prokaryotic adaptive immune response, allowing organisms such as

bacteria and archaea to respond to and eliminate invading genetic material (Pyzocha *et al.*, 2014). The CRISPR/Cas approach generates RNA-guided nucleases, such as Cas9, which can cut any desired location of the genome in a highly targeted manor (Sander *et al.*, 2014).

6.7.2. Translational studies using tissue microarray analysis (TMA)

Finally, to gain insight into how this research project translates into the clinical setting, it would be interesting to obtain experimental data using DLBCL patient samples. A tissue microarray is in the process of being prepared within the lymphoma team, which will ultimately be used to analyse around 250 cases of *de novo* R-CHOP-treated DLBCL. It would be of great interest to stain for different NFAT family members and compare expression levels between different subgroups of patients with DLBCL.

In addition, the TMA would also be of value for confirming the high level of TNFα expression observed by Nakayama et al (2014) in DLBCL-NOS patient samples (Nakayama *et al.*, 2014a). Moreover, a particularly interesting analysis would involve probing for a selection of proteins associated with the tumour microenvironment, such as those revealed in the gene expression microarray. This would help gain an understanding of the nature of the tissue microenvironment surrounding different subgroups of lymphoma.

6.8. Study Summary

The data in this study has provided a strong foundation for future research regarding the role of the NFAT signalling pathway in DLBCL. Required for the survival of DLBCL cell lines, the calcineurin/NFAT pathway was demonstrated to regulate many genes associated with different aspects of cancer biology.

Data obtained from the gene expression microarray may act as a platform for future projects to be performed within the lymphoma team. In time, a greater understanding for the functions of other genes identified will be established, which may yet have a significant impact on our mission to understanding this devastating disease. Should the NFAT target genes investigated be oncogenic, or DLBCL subgroup –specific, there is opportunity to move towards a more stratified treatment approach.

Overall, the potential involvement of NFAT in the regulation of TNFα and the tumour microenvironment was a key finding in this study and could be of great importance. Ultimately, any new therapy targeting NFAT will need to consider the cell-dependent and context-dependent functions of NFAT within the microenvironment. Furthermore, treatment strategies will also need to comprehend the contribution of specific NFAT isoforms in different types of cancer.

Appendix.

7. Appendix

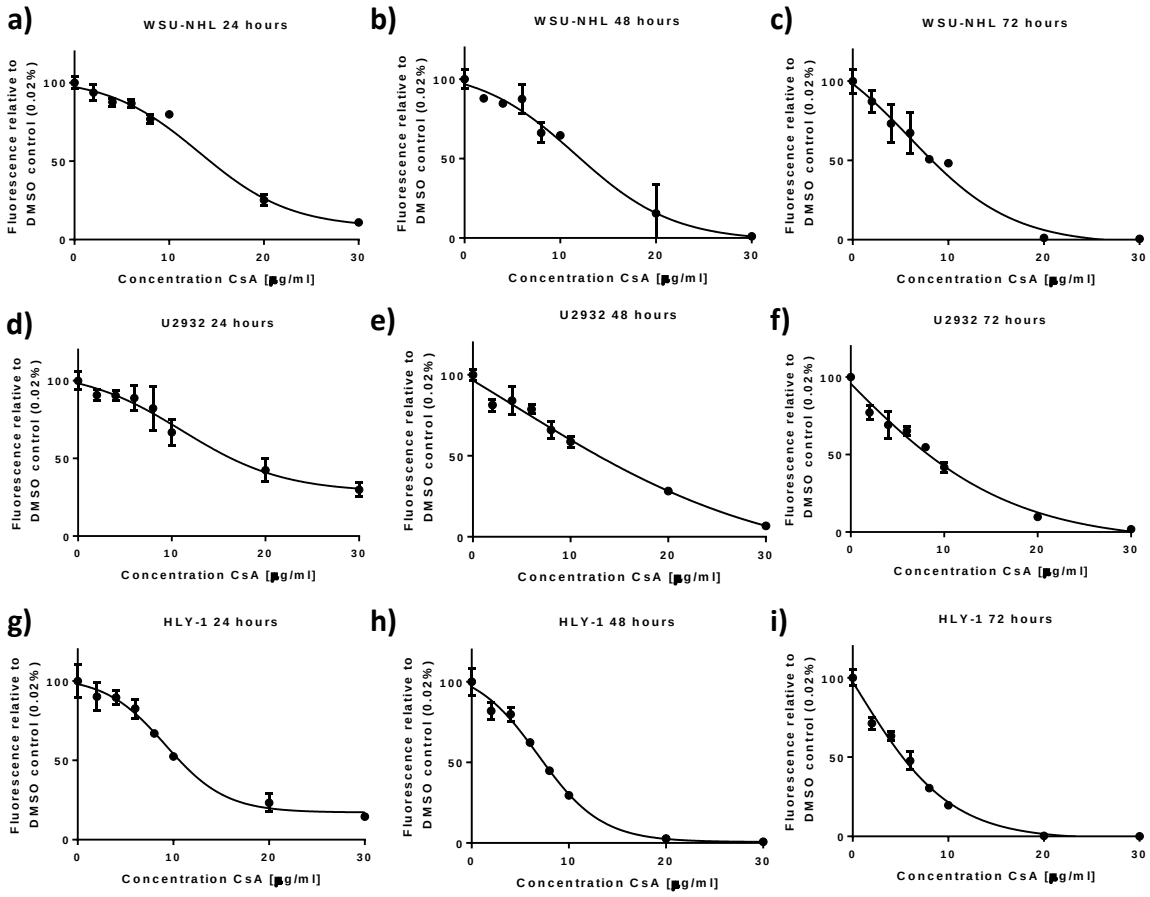

Appendix Figure 1. CsA causes a dose-dependent and time-dependent reduction in cell viability in DLBCL cell lines. The GCB DLBCL cell line WSU-NHL (a-c) and ABC DLBCL cell lines U2932 and HLY-1 (b-i) were treated with a range of concentrations of CsA (0µg/ml-30µg/ml), including a vehicle control (0.02% DMSO). Cells were incubated for 24, 48 and 72 hours before recording cell viability using the resazurin assay. Data is representative of one experiment where error bars indicate the standard deviation of triplicate wells.

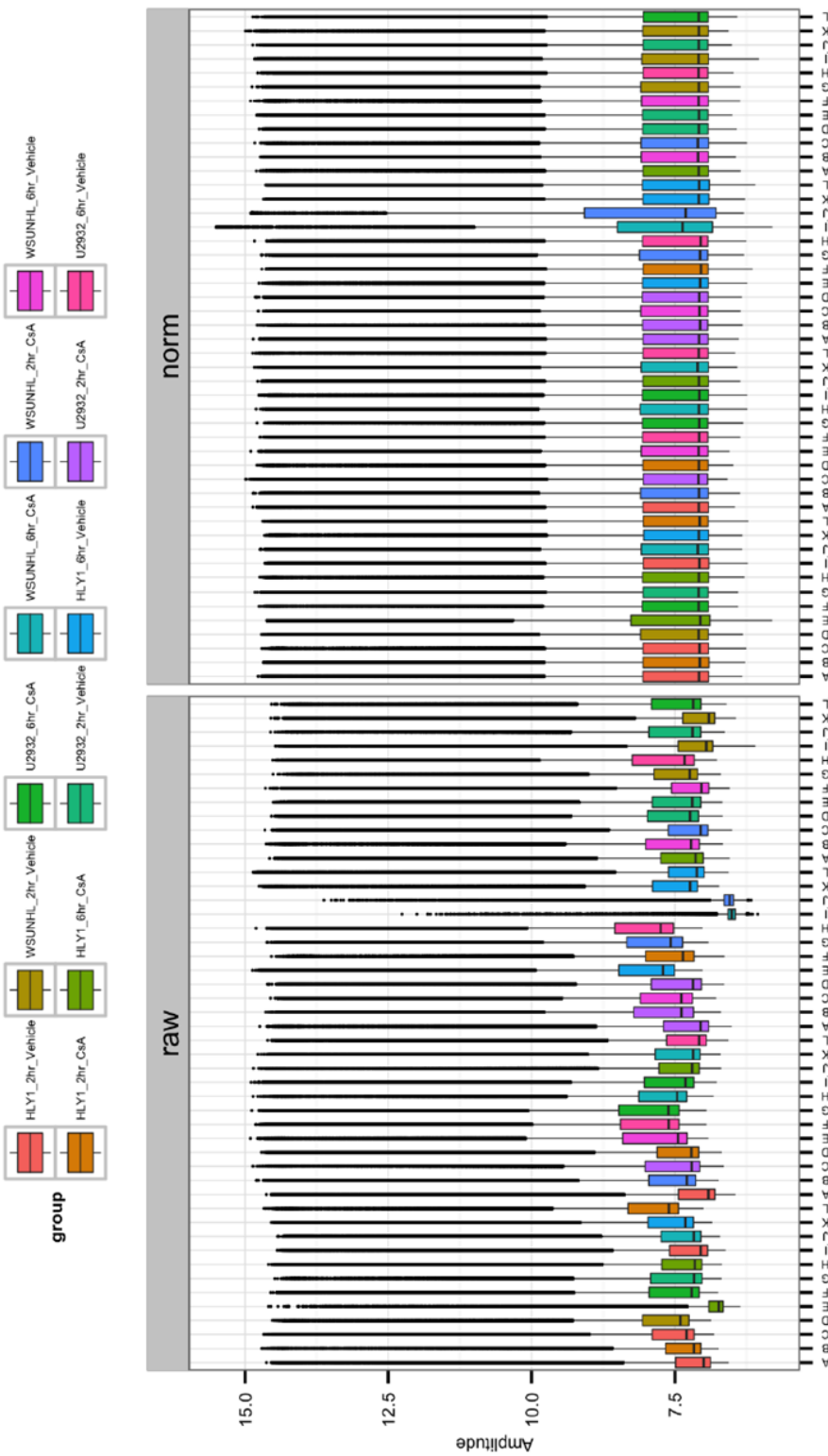

Appendix Figure 2. Box plot showing normalisation of microarray samples. All 48 samples from the gene expression microarray were normalised by transforming the data to log2 space via a variance stabilising transformation. Transformation takes advantage of the significant technical replication present on Illumina Bead-arrays resulting from the presence of multiple beads for each individual probe. Data is subsequently normalised by the robust spline normalisation algorithm that was designed for Bead-array data. The x-axis shows individual sample IDs and the y-axis shows the amplitude of the signal produced by samples. Data on the left indicates the raw data, whereas data on the right shows the normalised data. The colour-coded key at the top of the figure shows the various cell lines and their treatment conditions.

U2932 2hr (unpaired data analysis)

symbol	name	Family	Information based on GeneCard (www.genecards.org)
TNF	tumor necrosis factor	Cytokine	Encodes a multifunctional proinflammatory cytokine that belongs to the tumour necrosis factor superfamily. Mostly secreted by macrophages and is involved in cell proliferation, differentiation, apoptosis and many other cellular processes. Implicated in diseases such as cancer, autoimmune diseases and insulin resistance.
NA	NA	N/A	N/A
CCL4L1	chemokine (C-C motif) ligand 4-like 1	Chemokine	A chemokine that induces chemotaxis of cells expressing CCR5 or CCR1. One of several cytokine genes clustered on the q-arm of chromosome 17. This protein is similar to CCL4 which inhibits HIV entry by binding to the cell receptor CCR5 (protective role against HIV). Diseases associated include HIV and psoriasis.
CCL4L2	chemokine (C-C motif) ligand 4-like 2	Chemokine	A chemokine that induces chemotaxis of cells expressing CCR5 or CCR1. One of several cytokine genes clustered on the q-arm of chromosome 17. This protein is similar to CCL4 which inhibits HIV entry by binding to the cell receptor CCR5 (protective role against HIV). Diseases associated include HIV and psoriasis.
SLA	Src-like-adaptor	Adaptor protein	Negatively regulates T cell receptor signalling and inhibits NFAT signalling. Involved in the positive selection and mitosis of T cells.
CCL3L1	chemokine (C-C motif) ligand 3-like 1	Chemokine	A chemokine that binds to chemokine receptors such as CCR5.
PRRG4	proline rich Gla (G-carboxyglutamic acid) 4 (transmembrane)	Transmembrane protein	No information found
GCSAM	germinal center-associated, signaling and motility	No information found	Negatively regulates lymphocyte motility and is a regulator of B-cell receptor signalling via SYK kinase activation. The expression of this protein has been shown to be elevated in germinal centre B cells and is known to be induced by IL-4.
NA	NA	N/A	N/A

Appendix Table 1. Description of statistically significant genes differentially expressed in U2932 cells treated with CsA for 2hrs (unpaired data analysis). Columns indicate the gene symbols, names, family and function for statistically significant genes (adjusted P-value <0.05) differentially expressed upon treatment with CsA. Data in orange indicates genes downregulated by CsA and data in blue indicates genes upregulated by CsA. Data includes genes marked as N/A.

U2932 2hr (paired data analysis)

symbol	name	Family	Information based on GeneCard (www.genecards.org)
NA	NA	N/A	N/A
CCL4L2	chemokine (C-C motif) ligand 4-like 2	Chemokine	A chemokine that induces chemotaxis of cells expressing CCR5 or CCR1. One of several cytokine genes clustered on the q-arm of chromosome 17. This protein is similar to CCL4 which inhibits HIV entry by binding to the cell receptor CCR5 (protective role against HIV). Diseases associated include HIV and psoriasis.

Appendix Table 2. Description of statistically significant genes differentially expressed in U2932 cells treated with CsA for 2hrs (paired data analysis). Columns indicate the gene symbols, names, family and function for statistically significant genes (adjusted P-value <0.05) differentially expressed upon treatment with CsA. Data in orange indicates genes downregulated by CsA and data in blue indicates genes upregulated by CsA. Data includes genes marked as N/A.

U2932 6hr (unpaired data analysis)

symbol	name	Family	Information based on GeneCard (www.genecards.org)
NA	NA	N/A	N/A
CCL4L1	chemokine (C-C motif) ligand 4-like 1	Chemokine	A chemokine that induces chemotaxis of cells expressing CCR5 or CCR1. One of several cytokine genes clustered on the q-arm of chromosome 17. This protein is similar to CCL4 which inhibits HIV entry by binding to the cell receptor CCR5 (protective role against HIV). Diseases associated include HIV and psoriasis.
CCL4L2	chemokine (C-C motif) ligand 4-like 2	Chemokine	A chemokine that induces chemotaxis of cells expressing CCR5 or CCR1. One of several cytokine genes clustered on the q-arm of chromosome 17. This protein is similar to CCL4 which inhibits HIV entry by binding to the cell receptor CCR5 (protective role against HIV). Diseases associated include HIV and psoriasis.
RILPL2	Rab interacting lysosomal protein-like 2	Regulator of lysosome morphology	Plays a role in cellular transport.
NA	NA	N/A	N/A
SLA	Src-like-adaptor	Adaptor protein	Negatively regulates T cell receptor signalling and inhibits NFAT signalling. Involved in the positive selection and mitosis of T cells.
SLA	Src-like-adaptor	Adaptor protein	Negatively regulates T cell receptor signalling and inhibits NFAT signalling. Involved in the positive selection and mitosis of T cells.
NA	NA	N/A	N/A
LOC285628	uncharacterized	No information found	No information found
NFATC1	nuclear factor of activated T-cells, cytoplasmic, calcineurin-dependent 1	Transcription factor	DNA-binding transcription factor which plays a key role in inducible gene transcription during an immune response. Commonly known to induce the expression of genes such as IL-2 and IL-4 during T cell activation but now known to be expressed in many cell types. Recent studies suggest a role for this family of transcription factors in cancer. A central molecular target for the immunosuppresive drug CsA.
ZBTB32	zinc finger and BTB domain containing 32	Transcriptional transactivator or repressor	May function as a transcriptional transactivator or repressor. Thought to have a repressive effect by preventing GATA3 from binding to DNA
WDR1	WD repeat domain 1	F-actin binding protein	May induce the disassembley of actin filaments
KIF26B	kinesin family member	Kinesin family member	Essential for kidney development.
CCL3L1	chemokine (C-C motif) ligand 3-like 1	Chemokine	A chemokine that binds to chemokine receptors such as CCR5.
PDDC1	Parkinson disease 7 domain containing 1	No information found	No information found
BSPRY	B-box and SPRY domain containing	Calcium transporter	Involved in calcium transport
NA	NA	N/A	N/A
UPF3B	UPF3 regulator of nonsense transcripts	Component of a post-splicing multiprotein	Involved in nonsense mediated decay of mRNAs and mRNA nuclear export and surveillance
CLDN14	claudin 14	Claudin family member	Integral membrane protein and component of tight junction strands
CA2	carbonic anhydrase II	Enzyme	A carbonic anhydrase which catalyses the reversible hydration of carbon dioxide
UPF3B	UPF3 regulator of nonsense transcripts	Component of a post-splicing multiprotein	Involved in nonsense mediated decay of mRNAs and mRNA nuclear export and surveillance
CSTF3	cleavage stimulation factor, 3' pre-RNA,	Cleavage stimulation factor	Involved in the polyadenylation and 3-end cleavage of pre-mRNAs
CD58	CD58 molecule	Immunoglobulin protein	Encodes a ligand for the T lymphpcyte CD2 protein, functioning in adhesion and activation of T cells
LOC730101	uncharacterized	RNA gene	Affiliated with the lncRNA class of proteins
CLECL1	C-type lectin-like 1	Type II transmembrane protein	Highly expressed on dendritic and B cells, may act as a T-cell costimulatory protein which enhances IL4 production
NA	NA	N/A	N/A
BEND6	BEN domain containing 6	No information found	Associated with Notch signalling pathways
ZBTB8A	zinc finger and BTB domain containing 8A	Transcriptional regulator	Could be associated with gastric cancer
SOX7	SRY (sex determining region Y)-box 7	Transcription factor	Important in embryonic development and determination of cell fate. May play a role in tumourigenesis
NA	NA	N/A	N/A
ALKBH8	alkB, alkylation repair homolog 8 (E. coli)	Enzyme	Involved in RNA binding and has tRNA methyltransferase activity
RAB24	RAB24, member RAS oncogene family	Small GTPase	Member of the Rab subfamily of proteins that regulate intracellular protein trafficking
NA	NA	N/A	N/A
TMED5	transmembrane emp24 protein transport domain containing 5	Transmembrane transport protein	Associated with vesicular protein trafficking, GPCR and WNT signalling
EIF2S2	eukaryotic translation initiation factor 2, subunit 2 beta, 38kDa	No information found	Functions in the early stages of protein synthesis by forming a complex with GTP and initiator tRNA and binds to the 40S ribosomal subunit.
UGGT1	UDP-glucose glycoprotein	Enzyme	Soluble protein of the ER with a role in protein transport out of the ER
UGGT1	UDP-glucose glycoprotein	Enzyme	Soluble protein of the ER with a role in protein transport out of the ER

DNAJC12	DnaJ (Hsp40) homolog, subfamily C, member 12	Chaperone protein	Involved in protein folding
PSMA8	proteasome (prosome, macropain) subunit, alpha type, 8	Proteasome component	Part of the spermatoproteosome found in the testis. Associated with degradation of histones but also linked to downstream signalling events of the B-cell receptor
SRPRB	signal recognition particle receptor, B	Transmembrane GTPase	Anchors alpha subunit and peripheral membrane GTPase to the ER membrane
RGS16	regulator of G-protein signaling 16	G protein regulator	Inhibits signal transduction by increasing the GTPase activity of G protein alpha subunits
FAM120C	family with sequence similarity 120C	Transmembrane protein	Lies in a region where mutations and deletions are associated with disability and autism
PROSER1	proline and serine rich 1	No information found	A protein with serine and proline rich regions and may be associated with protein-protein interactions
OSTCP2	oligosaccharyltransferase complex subunit pseudogene 2	Pseudogene	No information found
PGM3	phosphoglucomutase 3	Phosphohexose mutase	Mediates glycogen formation
UGDH	UDP-glucose 6-dehydrogenase	Enzyme	Involved in the biosynthesis of components of the extracellular matrix
SEC23B	Sec23 homolog B (S. cerevisiae)	Vesicle trafficking protein	Involved in vesicle budding from the ER
SEL1L	sel-1 suppressor of lin-12-like (C. elegans)	No information found	Associated with the retrotranslocation or dislocation of misfolded proteins from the ER lumen to the cytosol
YARS	tyrosyl-tRNA synthetase	Enzyme	Thought to be among one of the first proteins that appeared in evolution. Involved with catalysing the aminoacetylation of tRNA by their cognate amino acid
BET1	Bet1 golgi vesicular membrane trafficking	Golgi-associated membrane protein	Involved in vesicle transport from the ER to the Golgi complex
STT3A	STT3A, subunit of the oligosaccharyltransferase complex (catalytic)	Integral membrane protein	Encodes the catalytic subunit of the N-oligosaccharyltransferase complex
LMAN1	lectin, mannose-	Type I integral membrane	A recyling protein located between the ER and the Golgi
DEPTOR	DEP domain containing MTOR-interacting	Kinase inhibitor	Negative regulator of mTORC1 and mTORC2 (inhibits kinase activity) and associated with Akt signalling
SELK	selenoprotein K	Selenoprotein	Signals translation termination
FAM129A	family with sequence similarity 129, member	No information found	Regulates the phosphorylation of a number of proteins such as EIF2A
GDPD5	glycerophosphodiester phosphodiesterase domain containing 5	Enzyme	Involved in glycerol metabolism
NA	NA	N/A	N/A
PDIA3P1	protein disulfide isomerase family A, member 3 pseudogene 1	Pseudogene	No information found
SH2B3	SH2B adaptor protein 3	SH2B adaptor protein	Negative regulator of cytokine signalling and plays a key role in haematopoesis
RELL1	RELT-like 1	No information found	No information found
SLC30A7	solute carrier family 30 (zinc transporter),	Enzyme cofactor	Involved in the transport of glucose and other sugars
SNORD96A	small nucleolar RNA, C/D box 96A	Small nucleolar RNA	Plays a role in the processing of ribosomal RNA precursors.
GOT1	glutamic-oxaloacetic transaminase 1, soluble	Enzyme	Involved in amino acid metabolism
FAM84B	family with sequence similarity 84, member B	No information found	Linked to gastroesophageal junction adenocarcimona and breast cancer
DNAJC10	DnaJ (Hsp40) homolog, subfamily C, member 10	Co-chaperone	ER co-chaperone involved in recogising and degrading misfolded proteins
CREB3L2	cAMP responsive element binding protein	Transcription factor	Transcriptional activator which regulates the transcription of unfolded protein response target genes
CDRT4	CMT1A duplicated region transcript 4	No information found	No information found
PPAPDC1B	phosphatidic acid phosphatase type 2 domain containing 1B	Enzyme	May be a metastatic suppressor in hepatocellular carcinoma
DNAJC3	DnaJ (Hsp40) homolog, subfamily C, member 3	Chaperone protein	Involved in the unfolded protein response during ER stress
NA	NA	N/A	N/A
TMEM39A	transmembrane protein	Transmembrane protein	No information found
NA	NA	N/A	N/A
FICD	FIC domain containing	Enzyme	Mediates the addition of AMP to target proteins and known to Inactivate Rho GTPases
SLC10A7	solute carrier family 10, member 7	No information found	No information found
GARS	glycyl-tRNA synthetase	Enzyme	Aminoaceyl-tRNA that charges tRNAs with their amino acids
SARS	seryl-tRNA synthetase	Enzyme	Catalyses the attachment of serine to tRNA (ser)

PDIA4	protein disulfide isomerase family A,	No information found	No information found
EDEM2	ER degradation enhancer, mannosidase	Enzyme	Involved in degradation of misfolded proteins
ARFGAP3	ADP-ribosylation factor GTPase activating	GTPase activating protein	Associates with the golgi apparatus and regulates the early secretory pathway of proteins
ASNS	asparagine synthetase (glutamine-hydrolyzing)	Enzyme	Involved in the synthesis of asparagine
MTHFD2	methylenetetrahydrofolate dehydrogenase (NADP+ dependent) 2, methenyltetrahydrofolate cyclohydrolase	Enzyme	Functions in the mitochondria and is involved in metabolism
HERPUD1	homocysteine-inducible, endoplasmic reticulum stress-inducible, ubiquitin-like	Enzyme	Functions in the mitochondria and is involved in metabolism
SSR1	signal sequence receptor, alpha	ER membrane receptor	Associated with protein translocation across the ER membrane
WIPI1	WD repeat domain, phosphoinositide interacting 1	WD40 repeat protein	Regulates the assembly of multiprotein complexes and plays a role in autophagy
RIMS3	regulating synaptic membrane exocytosis 3	No information found	Regulates synaptic membrane exocytosis
SSR2	signal sequence receptor, beta (translocon-associated	Enzyme	Associated with protein translocation across the ER membrane
TARS	threonyl-tRNA	Enzyme	Aminoacyl-tRNA that charges tRNAs with their amino acids
TIMM44	translocase of inner mitochondrial membrane 44 homolog	No information found	Translocation of proteins from the inner membrane to the mitochondrial matrix in an ATP-dependent manner
PARM1	prostate androgen-regulated mucin-like	No information found	May regulate telomerase activity
EDEM1	ER degradation enhancer, mannosidase	No information found	Targets misfolded proteins for degradation
GNL3	guanine nucleotide binding protein-like 3 (nucleolar)	No information found	May interact with p53 and therefore be involved in tumourigenesis. Known to stabilise MDM2 by preventing its ubiquitination and degradation. Also thought to be important in stem cell proliferation and associated with ribosome biosynthesis
SLC1A5	solute carrier family 1 (neutral amino acid transporter), member 5	Amino acid transporter	Associated with metabolism
ERLEC1	endoplasmic reticulum lectin 1	ER protein	ER protein that functions in N-glycan recognition. Involved in ER-associated degradation and stress-response pathways. May promote metastatic cell survival
MANF	mesencephalic astrocyte-derived neurotrophic factor	No information found	Reducing the expression of this gene has been shown to increase susceptibility to ER stress-induced death and results in proliferation.
PCK2	phosphoenolpyruvate carboxykinase 2 (mitochondrial)	Mitochondrial enzyme	The main enzyme involved with gluconeogenesis in the liver
HSPA5	heat shock 70kDa protein 5 (glucose-regulated protein,	Heat shock family protein	Located in the ER this protein is involved in protein folding and assembly
SDF2L1	stromal cell-derived factor 2-like 1	No information found	No information found
NFE2L1	nuclear factor, erythroid 2-like 1	Transcription factor	Involved in globin gene expression in erythrocytes. Also associated with ERK signalling.
CHAC1	ChaC, cation transport regulator homolog 1 (E. coli)	Enzyme	Role as a pro-apoptotic protein by mediating the pro-apoptotic effects of the ATF4-ATF3-DDIT3/CHOP cascade. Also involved in NOTCH signalling
DEPTOR	DEP domain containing MTOR-interacting	Kinase inhibitor	Negative regulator of mTORC1 and mTORC2 (inhibits kinase activity) and associated with Akt signalling
CARS	cysteinyl-tRNA synthetase	Aminoacyl-tRNA synthetase	Catalyses the aminoacylation of tRNAs with their cognate amino acid. Associated with lung, breast and ovarian cancers.
MTHFD1L	methylenetetrahydrofolate dehydrogenase (NADP+ dependent) 1-	Enzyme	De novo synthesis of purines and thymidylate. Involved in metabolism
CTH	cystathionase (cystathionine gamma-	Enzyme	Cytoplasmic enzyme involved in trans-sulfuration of methionine into cysteine. Role in metabolism.
NA	NA	N/A	N/A
FKBP14	FK506 binding protein 14, 22 kDa	Enzyme	Peptidyl-prolyl cis-trans isomerase found in the lumen of the ER. May have a role in protein folding.
LAT2	linker for activation of T cells family, member 2	Adaptor protein	Involved in signalling in mast cells and is associated with Williams's disease (developmental disorder). May be associated with BCR signalling
PSPH	phosphoserine	Enzyme	Phosphotransferase protein involved in L-serine formation
SLC6A9	solute carrier family 6 (neurotransmitter transporter, glycine), member 9	No information found	Involved in the transport of glucose and other sugars

HAX1	HCLS1 associated protein X-1	No information found	Known to associate with a Src family member of kinases named haematopoetic cell-specific Lyn substrate 1. Also interacts with the polycystic kidney disease gene . Known to promote cell survival and involved with intracellular calcium pools
TMED10	transmembrane emp24-like trafficking protein	Type I membrane protein	Involved in vesicular protein trafficking
HYOU1	hypoxia up-regulated 1	Heat shock family protein	Protein folding and secretion in the ER. Associated with increasing apoptosis and has been linked to increased invasiveness in breast tumours
VIMP	VCP-interacting membrane protein	Selenoprotein	May regulate cytokine production and the inflammatory response. Involved in the degradation of misfolded ER proteins.
SEC24D	SEC24 family member D	No information found	Involved in vesicle trafficking
CTH	cystathionase (cystathionine gamma-	Enzyme	Cytoplasmic enzyme involved in trans-sulfuration of methionine into cysteine. Role in metabolism.
ATF4	activating transcription factor 4	Transcription factor	Belongs to a family of DNA binding proteins which include AP-1, cAMP-response element binding proteins (CREB) and CREB-like proteins. Presence of leucine-zipper elements allow this protein to interact with other proteins. Associated with glucose homeostatisis in osteoblasts and the induction of asparagine synthetase in response to ER stress. Also regulates proteins associated with the circadian clock.
CARS	cysteinyl-tRNA synthetase	Aminoacyl-tRNA synthetase	Catalyses the aminoacylation of tRNAs with their cognate amino acid. Associated with lung, breast and ovarian cancers.
TSC22D3	TSC22 domain family, member 3	Transcriptional regulator	Stimulated by glucocorticoids and IL10. Plays a role in the anti-inflammatory response and immunosuppressive activities
DNAJB9	DnaJ (Hsp40) homolog, subfamily B, member 9	J protein family member	Regulated ATPase activity of 70kDa heat shock proteins. Induced by ER stress and plays a role protecting cells from apoptosis
GPT2	glutamic pyruvate transaminase (alanine aminotransferase) 2	Enzyme	Encodes a mitochondrial alanine transaminase. Involved in metabolism. Upregulated by ATF4 under metabolic stress in hepatocyte cells
NA	NA	N/A	N/A
PSAT1	phosphoserine aminotransferase 1	Enzyme	Aminotransferase Involved in metabolism
DDIT3	DNA-damage-inducible transcript 3	Transcription factor	CCAAT/enhancer-binding protein (C/EBP) family of transcription factors involved in the ER stress response. Known to induce cell cycle arrest and apoptosis in response to ER stress
CTH	cystathionase (cystathionine gamma-	Enzyme	Cytoplasmic enzyme involved in trans-sulfuration of methionine into cysteine. Role in metabolism.
TSC22D3	TSC22 domain family, member 3	Transcriptional regulator	Stimulated by glucocorticoids and IL10. Plays a role in the anti-inflammatory response and immunosuppressive activities
PCK2	phosphoenolpyruvate carboxykinase 2 (mitochondrial)	Mitochondrial enzyme	The main enzyme involved with gluconeogenesis in the liver

Appendix Table 3 (Continued from previous three pages). Description of statistically significant genes differentially expressed in U2932 cells treated with CsA for 6hrs (unpaired data analysis). Columns indicate the gene symbols, names, family and function for statistically significant genes (adjusted P-value <0.05) differentially expressed upon treatment with CsA. Data in orange indicates genes downregulated by CsA and data in blue indicates genes upregulated by CsA. Data includes genes marked as N/A.

U2932 6hr (paired data analysis)

symbol	name	Family	Information based on GeneCard (www.genecards.org)
NA	NA	NA	NA
CCL4L1	chemokine (C-C motif) ligand 4-like 1	Chemokine	A chemokine that induces chemotaxis of cells expressing CCR5 or CCR1. One of several cytokine genes clustered on the q-arm of chromosome 17. This protein is similar to CCL4 which inhibits HIV entry by binding to the cell receptor CCR5 (protective role against HIV). Diseases associated include HIV and psoriasis.
CCL4L2	chemokine (C-C motif) ligand 4-like 2	Chemokine	A chemokine that induces chemotaxis of cells expressing CCR5 or CCR1. One of several cytokine genes clustered on the q-arm of chromosome 17. This protein is similar to CCL4 which inhibits HIV entry by binding to the cell receptor CCR5 (protective role against HIV). Diseases associated include HIV and psoriasis.
CCL3L3	chemokine (C-C motif) ligand 3-like 3	Chemokine	A chemokine that binds to chemokine receptors such as CCR5.
RILPL2	Rab interacting lysosomal protein-like 2	Regulator of lysosome morphology	Plays a role in cellular transport.
BATF	basic leucine zipper transcription factor, ATF-like	Transcription factor	An AP-1 family transcription factor which dimerises with members of the Jun family
TNF	tumor necrosis factor	Cytokine	Encodes a multifunctional proinflammatory cytokine that belongs to the tumour necrosis factor superfamily. Mostly secreted by macrophages and is involved in cell proliferation, differentiation, apoptosis and many other cellular processes. Implicated in diseases such as cancer, autoimmune diseases and insulin resistance.
LRRC32	leucine rich repeat containing 32	Type I membrane protein	No information found
NA	NA	NA	NA
SLA	Src-like-adaptor	Adaptor protein	Negatively regulates T cell receptor signalling and inhibits NFAT signalling. Involved in the positive selection and mitosis of T cells.
SLA	Src-like-adaptor	Adaptor protein	Negatively regulates T cell receptor signalling and inhibits NFAT signalling. Involved in the positive selection and mitosis of T cells.
NFKBIE	nuclear factor of kappa light polypeptide gene enhancer in B-cells inhibitor, epsilon	IkB protein which inhibits nuclear localisation and activation of NF-κB alongside IκBa and IκBb	The protein encoded by this gene binds to components of NF-kappa-B, trapping the complex in the cytoplasm and preventing it from activating genes in the nucleus. Phosphorylation of the encoded protein targets it for desruction by the ubiquitin pathway, which activates NF-kappa-B by making it available to translocate to the nucleus
CCL3	chemokine (C-C motif) ligand 3	Chemokine	A small inducible cytokine also known as macrophage inflammatory protein 1 alpha which plays a role in inflammatory responses by binding to the receptor CCR1, CCR4 and CCR5.
ZYX	zyxin	Zinc-binding phosphoprotein	Concentrates at focal adhesions and along the actin cytoskeleton
MAP3K8	mitogen-activated protein kinase kinase kinase 8	Serine/threonine kinase	Encodes a serine/threonine kinase which localises to the cytoplasm and can activate both the MAP kinase and JNK kinase pathways. Known to activate NF-κB via activation of I kappa B kinases. Also reported to promote the production of TNF-alpha and IL-2 during lymphocyte activation.
NFKBIE	nuclear factor of kappa light polypeptide gene enhancer in B-cells inhibitor, epsilon	IkB protein which inhibits nuclear localisation and activation of NF-κB alongside IκBa and IκBb	The protein encoded by this gene binds to components of NF-kappa-B, trapping the complex in the cytoplasm and preventing it from activating genes in the nucleus. Phosphorylation of the encoded protein targets it for desruction by the ubiquitin pathway, which activates NF-kappa-B by making it available to translocate to the nucleus
LOC285628	uncharacterized LOC285628	No information found	No information found
EGR3	early growth response 3	Transcription factor	Encodes a transcription factor from the three tandem C2H2-type zinc finger family.
FKBP4	FK506 binding protein 4, 59kDa	Immunophilin	Plays a role in protein trafficking
NFATC1	nuclear factor of activated T-cells, cytoplasmic, calcineurin-dependent 1	Transcription factor	DNA-binding transcription factor which plays a key role in inducible gene transcription during an immune response. Commonly known to induce the expression of genes such as IL-2 and IL-4 during T cell activation but now known to be expressed in many cell types. Recent studies suggest a role for this family of transcription factors in cancer. A central molecular target for the immunosuppresive drug CsA.
EGR2	early growth response 2	Transcription factor	Encodes a transcription factor from the three tandem C2H2-type zinc finger family.
ZBTB32	zinc finger and BTB domain containing 32	Transcriptional transactivator or repressor	May function as a transcriptional transactivator or repressor. Thought to have a repressive effect by preventing GATA3 from binding to DNA
TPM4	tropomyosin 4	Actin binding protein	Important for muscle structure and function
SCO2	SCO2 cytochrome c oxidase assembly protein	Enzyme	Maintains proton gradient across the inner mitrochondrial membrane
SRF	serum response factor (c-fos serum response element-binding transcription factor)	Ubiquitous nuclear protein	Involved in proilferation and differentiation
NFKBIA	nuclear factor of kappa light polypeptide gene enhancer in B-cells inhibitor, alpha	IkB protein which inhibits nuclear localisation and activation of NF-κB alongside IκBa and IκBb	The protein encoded by this gene binds to components of NF-kappa-B, trapping the complex in the cytoplasm and preventing it from activating genes in the nucleus. Phosphorylation of the encoded protein targets it for desruction by the ubiquitin pathway, which activates NF-kappa-B by making it available to translocate to the nucleus
RBM14	RNA binding motif protein 14	Nuclear coactivator	Nuclear coactivator and RNA splicing modulator
WDR1	WD repeat domain 1	F-actin binding protein	May induce the disassembley of actin filaments
HILPDA	hypoxia inducible lipid droplet-associated	No information found	Involved in growth and proliferation. Known to stimulate some cytokines
MIR155HG	MIR155 host gene (non-protein coding)	Micro RNA	No information found
KIF26B	kinesin family member 26B	Kinesin family member	Essential for kidney development.

CCL3L1	chemokine (C-C motif) ligand 3-like 1	Chemokine	A chemokine that binds to chemokine receptors such as CCR5.
HES6	hes family bHLH transcription factor 6	Transcriptional repressor	Regulates cell differentiation
RHPN2	rhophilin, Rho GTPase binding protein 2	GTPase binding protein	Involved in organisation of the actin cytoskeleton
IKZF1	IKAROS family zinc finger 1 (Ikaros)	Transcription factor	Regulator of lymphocyte differentiation
EXO1	exonuclease 1	Enzyme	Require for SHM and CSR
FANCG	Fanconi anemia, complementation group G	No information found	Involved in DNA repair
FST	follistatin	Gonadal protein	Inhibits follicle stimulating hormone release
BCL2L11	BCL2-like 11 (apoptosis facilitator)	BCL-2 family member	Acts as an apoptotic activator
DNLZ	DNL-type zinc finger	No information found	No information found
PTGES2	prostaglandin E synthase 2	Enzyme	Catalyzes the conversion of prostaglandin H2 to prostaglandin E2
CCL3L1	chemokine (C-C motif) ligand 3-like 1	Chemokine	A chemokine that binds to chemokine receptors such as CCR5.
AGAP3	ArfGAP with GTPase domain, ankyrin repeat and PH domain 3	No information found	Involved in endocytosis
LIMA1	LIM domain and actin binding 1	Cytoskeleton-associated protein	Inhibits actin filament polymerisation
SLC25A19	solute carrier family 25 (mitochondrial thiamine pyrophosphate carrier), member 19	Solute carrier protein	Solute carrier protein in the mitochondria
BRK1	BRICK1, SCAR/WAVE actin-nucleating complex subunit	No information found	Regulates the actin cytoskeleton
PDDC1	Parkinson disease 7 domain containing 1	No information found	No information found
LOC730101	uncharacterized LOC730101	RNA gene	Affiliated with the lncRNA class of proteins
NFKBID	nuclear factor of kappa light polypeptide gene enhancer in B-cells inhibitor, delta	IkB protein which inhibits nuclear localisation and activation of NF-κB alongside IκBa and IκBb	The protein encoded by this gene binds to components of NF-kappa-B, trapping the complex in the cytoplasm and preventing it from activating genes in the nucleus. Phosphorylation of the encoded protein targets it for desruction by the ubiquitin pathway, which activates NF-kappa-B by making it available to translocate to the nucleus
AMY1B	amylase, alpha 1B (salivary)	Enzyme	Produced by the salvary gland
BSPRY	B-box and SPRY domain containing	Calcium transporter	Involved in calcium transport
NA	NA	NA	NA
PSME3	proteasome (prosome, macropain) activator subunit 3 (PA28 gamma; Ki)	Proteasome component	Subunit of the proteasome
UPF3B	UPF3 regulator of nonsense transcripts homolog B (yeast)	Component of a post-splicing multiprotein complex	Involved in nonsense mediated decay of mRNAs and mRNA nuclear export and surveillance
BCL2L11	BCL2-like 11 (apoptosis facilitator)	BCL-2 family member	Acts as an apoptotic activator
CLDN14	claudin 14	Claudin family member	Integral membrane protein and component of tight junction strands
CA2	carbonic anhydrase II	Enzyme	A carbonic anhydrase which catalyses the reversible hydration of carbon dioxide
CCL3L1	chemokine (C-C motif) ligand 3-like 1	Chemokine	A chemokine that binds to chemokine receptors such as CCR5.
UBQLN4	ubiquilin 4	Nuclear hormone receptor	Acts as a transcriptional coactivator for steroid hormones
FAM65B	family with sequence similarity 65, member B	No information found	Involved in proteasomal protein degradation
NA	NA	NA	NA
DHRS11	dehydrogenase/reductase (SDR family) member 11	Enzyme	No information found
TNFRSF1B	tumor necrosis factor receptor superfamily, member 1B	TNF-receptor superfamily member	Mediates the recruitment of anti-apoptotic proteins
SAP30L	SAP30-like	No information found	Involved in the recruitment of HDACs to the nucleus
DMAP1	DNA methyltransferase 1 associated protein 1	Transcriptional regulator	Transcriptional activator and repressor. Interacts with HDACs
C9orf37	chromosome 9 open reading frame 37	No information found	No information found
UPF3B	UPF3 regulator of nonsense transcripts homolog B (yeast)	Component of a post-splicing multiprotein complex	Involved in nonsense mediated decay of mRNAs and mRNA nuclear export and surveillance
NCOA1	nuclear receptor coactivator 1	Transcriptional coactivator	Transcriptional coactivator for steroid hormones
LRRC20	leucine rich repeat containing 20	No information found	No information found
TUBA4A	tubulin, alpha 4a	Tubulin	Member of the tubulin family of microtubles
CSTF3	cleavage stimulation factor, 3' pre-RNA, subunit 3, 77kDa	Cleavage stimulation factor	Involved in the polyadenylation and 3-end cleavage of pre-mRNAs
PPOX	protoporphyrinogen oxidase	Enzyme	Catalyzes the 6-electron oxidation of protoporphyrinogen-IX to form protoporphyrin-IX.
PMS2P4	postmeiotic segregation increased 2 pseudogene 4	Pseudogene	No information found
POLA2	polymerase (DNA directed), alpha 2, accessory subunit	Polymerase subunit	Involved in the cell cycle

NA	NA	NA	NA
NA	NA	NA	NA
NA	NA	NA	NA
FICD	FIC domain containing	Enzyme	Mediates the addition of AMP to target proteins and known to Inactivate Rho GTPases
CHRNA5	cholinergic receptor, nicotinic, alpha 5 (neuronal)	Ligand-gated ion channel	Nicotinic receptor subunit. Mediates fast signals at synapses.
C19orf10	chromosome 19 open reading frame 10	No information found	No information found
SLC10A7	solute carrier family 10, member 7	No information found	No information found
GARS	glycyl-tRNA synthetase	Enzyme	Aminoacyl-tRNA that charges tRNAs with their amino acids
NA	NA	NA	NA
SARS	seryl-tRNA synthetase	Enzyme	Catalyses the attachment of serine to tRNA (ser)
PDIA4	protein disulfide isomerase family A, member 4	No information found	No information found
EDEM2	ER degradation enhancer, mannosidase alpha-like 2	No information found	Involved in glycoprotein degradation
TM6SF1	transmembrane 6 superfamily member 1	Transmembrane protein	No information found
ARFGAP3	ADP-ribosylation factor GTPase activating protein 3	GTPase activating protein	Associates with the golgi apparatus and regulates the early secretory pathway of proteins
ASNS	asparagine synthetase (glutamine-hydrolyzing)	Enzyme	Involved in the synthesis of asparagine
MTHFD2	methylenetetrahydrofolate dehydrogenase (NADP+ dependent) 2, methenyltetrahydrofolate cyclohyd	Enzyme	Functions in the mitochondria
SESN2	sestrin 2	PA2 related protein	Regulation of growth and survival
HERPUD1	homocysteine-inducible, endoplasmic reticulum stress-inducible, ubiquitin-like domain member 1	Enzyme	Functions in the mitochondria and is involved in metabolism
SSR1	signal sequence receptor, alpha	Membrane receptor	Binds calcium to the ER membrane
CDK2AP2	cyclin-dependent kinase 2 associated protein 2	Cyclin -dependent kinase associated protein	Diseases associated include oral cancer
WIPI1	WD repeat domain, phosphoinositide interacting 1	WD40 repeat protein	Regulates the assembly of multiprotein complexes and plays a role in autophagy
RIMS3	regulating synaptic membrane exocytosis 3	No information found	Regulates synaptic membrane exocytosis
NA	NA	NA	NA
WARS	tryptophanyl-tRNA synthetase	Enzyme	tRNA synthetase
SSR2	signal sequence receptor, beta (translocon-associated protein beta)	Enzyme	Associated with protein translocation across the ER membrane
TARS	threonyl-tRNA synthetase	Enzyme	Aminoacyl-tRNA that charges tRNAs with their amino acids
LOC100190986	uncharacterized LOC100190986	No information found	No information found
TIMM44	translocase of inner mitochondrial membrane 44 homolog (yeast)	No information found	Translocation of proteins from the inner membrane to the mitochondrial matrix in an ATP-dependent manner

PARM1	prostate androgen-regulated mucin-like protein 1	No information found	May regulate telomerase activity
MZB1	marginal zone B and B1 cell-specific protein		
EDEM1	ER degradation enhancer, mannosidase alpha-like 1	No information found	Targets misfolded proteins for degradation
GNL3	guanine nucleotide binding protein-like 3 (nucleolar)	No information found	May interact with p53 and be linked to stem cell proliferation and tumourigenesis
SLC1A5	solute carrier family 1 (neutral amino acid transporter), member 5	Amino acid transporter	Associated with metabolism
ERLEC1	endoplasmic reticulum lectin 1	No information found	Degradation of the ER and a regulator of cell stress-response pathways
RGS1	regulator of G-protein signaling 1	Regulator of G-protein signalling	Inhibitis transduction of signals by increasing the GTPase activity of G-protein alpha subunits, causing them to turn into their inactive GDP-bound form. May also be involved in regulation of B-cell activation and proliferation.
MANF	mesencephalic astrocyte-derived neurotrophic factor	No information found	Reducing the expression of this gene has been shown to increase susceptibility to ER stress-induced death and results in proliferation.
PCK2	phosphoenolpyruvate carboxykinase 2 (mitochondrial)	Mitochondrial enzyme	Catalyses the conversion of oxaloacetate to phosphoenolpyruvate in the presence of GTP
HSPA5	heat shock 70kDa protein 5 (glucose-regulated protein, 78kDa)	Heat shock family protein	Located in the ER this protein is involved in protein folding and assembly
SDF2L1	stromal cell-derived factor 2-like 1	No information found	No information found
NFE2L1	nuclear factor, erythroid 2-like 1	Transcription factor	Involved in globin gene expression in erythrocytes. Also associated with ERK signalling.
CHAC1	ChaC, cation transport regulator homolog 1 (E. coli)	Enzyme	Pro-apoptotic component of the unfolded protein response pathway
EGR1	early growth response 1	Early growth response protein	Transcriptional regulator involved in anergy
DEPTOR	DEP domain containing MTOR-interacting protein	No information found	Negative regulator of the mTORC1 and mTORC2 signalling pathways
CARS	cysteinyl-tRNA synthetase	Aminoacyl-tRNA synthetase	Catalyses the aminoacylation of tRNAs with their cognate amino acid. Associated with lung, breast and ovarian cancers.
MTHFD1L	methylenetetrahydrofolate dehydrogenase (NADP+ dependent) 1-like	Enzyme	De novo synthesis of purines
CDKN1A	cyclin-dependent kinase inhibitor 1A (p21, Cip1)	Cyclin dependent kinase inhibitor	Regulator of cell cycle checkpoint at G1. Controlled by p53.
CTH	cystathionase (cystathionine gamma-lyase)	Enzyme	Catalyses the final step in the trans-sulfuration process
NA	NA	NA	NA
FKBP14	FK506 binding protein 14, 22 kDa	Peptidyl-prolyl cis-trans isomerase	Found in the lumen of the ER, this protein may accelerate protein folding
LAT2	linker for activation of T cells family, member 2	Adaptor protein	Involved in signalling in mast cells and is associated with Williams's disease (developmental disorder). May be associated with BCR signalling
ULBP1	UL16 binding protein 1	No information found	Involved in class 1 MHC mediated antigen processing and presentation
PSPH	phosphoserine phosphatase	Enzyme	Phosphotransferase protein involved in L-serine formation
SLC6A9	solute carrier family 6 (neurotransmitter transporter, glycine), member 9	No information found	Involved in the transport of glucose and other sugars
HAX1	HCLS1 associated protein X-1	No information found	Known to associate with a Src family member of kinases named haematopoetic cell-specific Lyn substrate 1. Also interacts with the polycystic kidney disease gene . Known to promote cell survival and involved with intracellular calcium pools
TMED10	transmembrane emp24-like trafficking protein 10 (yeast)	Type I membrane protein	Involved in vesicular protein trafficking
INHBE	inhibin, beta E	Inhibin	Pancreatic cell growth and many other diverse roles
HYOU1	hypoxia up-regulated 1	Heat shock family protein	Protein folding and secretion in the ER. Associated with increasing apoptosis and has been linked to increased invasiveness in breast tumours
VIMP	VCP-interacting membrane protein	Selenoprotein	May regulate cytokine production and the inflammatory response. Involved in the degradation of misfolded ER proteins.
SLC3A2	solute carrier family 3 (amino acid transporter heavy chain), member 2	Cell surface transmembrane protein	Required for the function of light chain amino-acid transporters
SEC24D	SEC24 family member D	Phosphotransferase	L-serine formation
ADM2	adrenomedullin 2	No information found	No information found
CTH	cystathionase (cystathionine gamma-lyase)	Enzyme	Catalyses the final step in the trans-sulfuration process
HYOU1	hypoxia up-regulated 1	Heat shock family protein	Protein folding and secretion in the ER. Associated with increasing apoptosis and has been linked to increased invasiveness in breast tumours
CEBPB	CCAAT/enhancer binding protein (C/EBP), beta	Transcription factor	Involed in immune function
ATF4	activating transcription factor 4	Transcription factor	Belongs to a family of DNA binding proteins which include AP-1, cAMP-response element binding proteins (CREB) and CREB-like proteins. Presence of leucine-zipper elements allow this protein to interact with other proteins. Associated with glucose homeostatisis in osteoblasts and the induction of asparagine synthetase in response to ER stress. Also regulates proteins associated with the circadian clock.

CARS	cysteinyl-tRNA synthetase	Class I aminoacyl-tRNA synthetase	Associated with lung, ovarian and breast cancers
TSC22D3	TSC22 domain family, member 3	Transcriptional regulator	Known to inhibit NF-kappa B DNA binding activity
DNAJB9	DnaJ (Hsp40) homolog, subfamily B, member 9	Regulator of ATPase activity	Regulates ATPase activity in heat shock proteins and plays a role in protecting stressed cells from apoptosis
TRIB3	tribbles pseudokinase 3	Kinase	Induced by NF-κB, but is also a negative regulator of NF-κB by interacting with p65.
GPT2	glutamic pyruvate transaminase (alanine aminotransferase) 2	Enzyme	Roles in amino acid metabolism. Upregulated by ATF4 under metabolic stress in hepatocyte cell lines
NA	NA	NA	NA
PSAT1	phosphoserine aminotransferase 1	Enzyme	Encodes a protein associated with metabolism
DDIT3	DNA-damage-inducible transcript 3	Transcription factor	This gene encodes a member of the C/EBP family of transcription factors. The protein functions as a dominant negative inhibitor. This multifunctional transcription factor is involved in the ER stress response and plays a wide role in cell stresses and induces cell cycle arrest and apoptosis in response to ER stress. Negatively regulates expression of BCL2, ATF4-dependent transcriptional activation of asparagine synthetase and other genes. Inhibits Wnt signalling and plays a role in the inflammatory response through the induction of caspase 11.
CTH	cystathionase (cystathionine gamma-lyase)	Enzyme	Involved in the trans-sulphuration pathway from methionine to cysteine
TSC22D3	TSC22 domain family, member 3	Transcriptional regulator	Known to inhibit NF-kappa B DNA binding activity
PCK2	phosphoenolpyruvate carboxykinase 2 (mitochondrial)	Enzyme	Encodes a mitochondrial enzyme

Appendix Table 4 (Continued from previous 3 pages). Description of statistically significant genes differentially expressed in U2932 cells treated with CsA for 6hrs (paired data analysis). Columns indicate the gene symbols, names, family and function for statistically significant genes (adjusted P-value <0.05) differentially expressed upon treatment with CsA. Data in orange indicates genes downregulated by CsA and data in blue indicates genes upregulated by CsA. Data includes genes marked as N/A

HLY-1 2hr (unpaired data analysis)

symbol	name	Family	Information based on GeneCard (www.genecards.org)
NA	NA	N/A	N/A
CCL4L2	chemokine (C-C motif) ligand 4-like 2	Chemokine	A chemokine that induces chemotaxis of cells expressing CCR5 or CCR1. One of several cytokine genes clustered on the q-arm of chromosome 17. This protein is similar to CCL4 which inhibits HIV entry by binding to the cell receptor CCR5 (protective role against HIV). Diseases associated include HIV and psoriasis.
CCL4L1	chemokine (C-C motif) ligand 4-like 1	Chemokine	A chemokine that induces chemotaxis of cells expressing CCR5 or CCR1. One of several cytokine genes clustered on the q-arm of chromosome 17. This protein is similar to CCL4 which inhibits HIV entry by binding to the cell receptor CCR5 (protective role against HIV). Diseases associated include HIV and psoriasis.
PDCD1	programmed cell death 1	Immune checkpoint receptor expressed by activated T cells	This gene encodes a cell surface membrane protein of the immunoglobulin superfamily. It is expressed in pro-B-cells and is thought to play a role in their differentiation and the immune response. Diseases associated with PDCD1 include indolent b cell lymphoma and nodular lymphocyte predominant hodgkin lymphoma
RIN2	Ras and Rab interactor 2	Small GTPase	Involved in membrane trafficking in the early endocytic pathway. The protein encoded by the RIN2 gene binds the GTP-bound form of the RAB5 protein and functions as a guanine exchange factor for RAB5. Found as a tetramer in the cytoplasm RIN2 does not. Mutations in this gene cause macrocephaly alopecia cutis laxa and scoliosis (MACS) syndrome (an elastic tissue disorder) as well as the related connective tissue disorder, RIN2 syndrome.
PAX9	paired box 9	Transcription factor	Encodes a member of the paired box (PAX) family of transcription factors. PAX family members are important regulators in early development. Critical role in cancer growth.
IL10	interleukin 10	Cytokine	Role in immune regulation and inflammation. Known to enhance B-cell survival
TNFSF14	tumor necrosis factor (ligand) superfamily, member 14	Member of the TNF ligand superfamily	May function as a costimulatory factor for the activation of lymphoid cells. Has been shown to stimulate T cell proliferation and trigger the apoptosis of malignant cells.
PRF1	perforin 1 (pore forming protein)	Transmembrane tubule protein	Forms part of the transmembrane tubule
ZNFX1	zinc finger, NFX1-type containing 1	No information found	No information found
GFI1	growth factor independent 1 transcription repressor	Transcriptional repressor	Encodes a nuclear zinc finger protein that plays a role in oncogenesis
EVI2A	ecotropic viral integration site 2A	Gene encoding a viral integration site.	Thought to complex with itself or other proteins within the cell membrane, perhaps functioning as a cell-surface receptor.
SOCS3	suppressor of cytokine signaling 3	Negative regulator of cytokine signalling	Member of the STAT induced STAT inhibitors. Induced by IL10 and can inhibit JAK kinase
NUAK2	NUAK family, SNF1-like kinase, 2	Stress-activated kinase involved in tolerance to glucose starvation	A stress-activated kinase involved in tolerance to glucose stravation and cytoskeletal signalling. Expression is induced by TNF-alpha via NF-κB. Also protects cells from Fas-mediated apoptosis and is required for increased motility and invasiveness in fas-mediated tumour cells.

Appendix Table 5. Description of statistically significant genes differentially expressed in HLY-1 cells treated with CsA for 2hrs (unpaired data analysis). Columns indicate the gene symbols, names, family and function for statistically significant genes (adjusted P-value <0.05) differentially expressed upon treatment with CsA. Data in orange indicates genes downregulated by CsA and data in blue indicates genes upregulated by CsA. Data includes genes marked as N/A.

HLY-1 2hr (paired data analysis)

symbol	name	Family	Information based on GeneCard (www.genecards.org)
NA	NA	N/A	N/A
CCL4L2	chemokine (C-C motif) ligand 4-like 2	Chemokine	A chemokine that induces chemotaxis of cells expressing CCR5 or CCR1. One of several cytokine genes clustered on the q-arm of chromosome 17. This protein is similar to CCL4 which inhibits HIV entry by binding to the cell receptor CCR5 (protective role against HIV). Diseases associated include HIV and psoriasis.
CCL4L1	chemokine (C-C motif) ligand 4-like 1	Chemokine	A chemokine that induces chemotaxis of cells expressing CCR5 or CCR1. One of several cytokine genes clustered on the q-arm of chromosome 17. This protein is similar to CCL4 which inhibits HIV entry by binding to the cell receptor CCR5 (protective role against HIV). Diseases associated include HIV and psoriasis.
EGR2	early growth response 2	Transcription factor	Encodes a transcription factor from the three tandem C2H2-type zinc finger family. Early growth response gene induced by mitogenic stimulation and is involved in muscle development, lymphocyte development and many other cellular processes.
CCL3L3	chemokine (C-C motif) ligand 3-like 3	Chemokine	A chemokine that binds to chemokine receptors such as CCR5.
CCL3L1	chemokine (C-C motif) ligand 3-like 1	Chemokine	A chemokine that binds to chemokine receptors such as CCR5.
CCL3L1	chemokine (C-C motif) ligand 3-like 1	Chemokine	A chemokine that binds to chemokine receptors such as CCR5.
CCL3	chemokine (C-C motif) ligand 3	Chemokine	A small inducible cytokine also known as macrophage inflammatory protein 1 alpha which plays a role in inflammatory responses by binding to the receptor CCR1, CCR4 and CCR5.
CD69	CD69 molecule	Type II transmembrane receptor	Encodes a member of the calcium-dependent lectin superfamily of type II transmembrane receptors. Expression is induced during activation of T lymphocytes and may play a role in lymphocyte proliferation.
EGR3	early growth response 3	Transcription factor	Encodes a transcription factor from the three tandem C2H2-type zinc finger family.
PDCD1	programmed cell death 1	Immune checkpoint receptor expressed by activated T cells	This gene encodes a cell surface membrane protein of the immunoglobulin superfamily. It is expressed in pro-B-cells and is thought to play a role in their differentiation and the immune response. Diseases associated with PDCD1 include indolent b cell lymphoma and nodular lymphocyte predominant hodgkin lymphoma
HSPE1	heat shock 10kDa protein 1	Heat shock protein	Encodes a major heat shock protein which functions as a chaperonin. Binds to other heat shock proteins to enhance ATP-dependent protein folding
EVI2A	ecotropic viral integration site 2A	Gene encoding a viral integration site.	Thought to complex with itself or other proteins within the cell membrane, perhaps functioning as a cell-surface receptor.
PAX9	paired box 9	B cell specific transcription factor	Encodes a member of the paired box (PAX) family of transcription factors. PAX family members are important regulators in early development. Altered expression of these genes are thought to contribute to neoplastic transformation. Expressed at early (but not late) stages of B-cell differentiation. Dysregulation of this gene is known to contribute to the pathogenesis of large-cell lymphomas.
RAB11FIP1	RAB11 family interacting protein 1 (class I)	Vesicle recycling protein	Plays a role in Rab-11 mediated recycling of vesicles and may be involved in endocytic sorting and trafficking of proteins such as epidermal growth factor receptor (EGFR)
TNS3	tensin 3	Actin remodelling	May play a role in the remodelling of actin and the dissociation of the integrin-tensin-actin complex
IL10	interleukin 10	Cytokine	Encodes a cytokine which is primarily produced by monocytes and to a lesser extent by lymphocytes. IL10 functions in immunoregulation and inflammation and downregulates the expression of Th1 cytokines, MHC class II Ags and costimulatory molecules on macrophages. This cytokine is also known to enhance B cell survival, proliferation and antibody production and is also known to inhibit NF-κB production. Also involved in the regulation of the JAK-STAT signalling pathway.

TNFAIP6	tumor necrosis factor, alpha-induced protein 6	Hyaluronan-binding secretory pr	A secretory protein which contains a hyaluronan-binding domain and is known to be involved in extracellular matrix stability and cell migration. Induced by proinflammatory cytokines such as TNF-alpha and interleukin-1. Important in the protease network associated with inflammation. Enhanced levels of TNFAIP6 have been found in the synovial fluid of patients with osteoarthritis and rheumatoid arthritis. Some evidence of involvement in cell-cell and cell-matrix interactions during inflammation and tumourigenesis.
NFATC1	nuclear factor of activated T-cells, cytoplasmic, calcineurin-dependent 1	Transcription factor	DNA-binding transcription factor which plays a key role in inducible gene transcription during an immune response. Commonly known to induce the expression of genes such as IL-2 and IL-4 during T cell activation but now known to be expressed in many cell types. Recent studies suggest a role for this family of transcription factors in cancer. A central molecular target for the immunosuppresive drug CsA.
TNF	tumor necrosis factor	Cytokine	Encodes a multifunctional proinflammatory cytokine that belongs to the tumour necrosis factor superfamily. Mostly secreted by macrophages and is involved in cell proliferation, differentiation, apoptosis and many other cellular processes. Implicated in diseases such as cancer, autoimmune diseases and insulin resistance.
EVI2A	ecotropic viral integration site 2A	Gene encoding a viral integration site	Thought to complex with itself or other proteins within the cell membrane, perhaps functioning as a cell-surface receptor.
NA	NA	N/A	N/A
PTPN7	protein tyrosine phosphatase, non-receptor type 7	Protein tyrosine phosphatase	A member of the protein tyrosine phosphatase (PTP) family which are known to regulate cell growth, differentiation and the cell cycle. Also implicated in oncogenesis. PTPN7 is mostly expressed in haematopoietic cells and is an early response gene in activated T and B lymphocytes
ZNFX1	zinc finger, NFX1-type containing 1	No information found	No information found
GFI1	growth factor independent 1 transcription repressor	Transcriptional repressor	A zinc finger protein that functions as a transcriptional repressor in haematopoiesis and oncgenesis. Functions as a complex to control histone modifications that lead to silencing of specific target gene promoters. Mutations in this gene cause autosomal dominant congenital neutropenia and dominant nonimmune chronic idiopathic neutropenia, which predispose patients to leukaemia. Reported to regulate TLR reponses such as by antagonising RELA.
CLEC17A	C-type lectin domain family 17, member A	Cell surface receptor	A cell surface receptor which may play a role in carbohydrate-mediated communication between cells in the germinal centre. Known to bind glycans such as mannose and fucose residues.
FILIP1L	filamin A interacting protein 1-like	Regulator of endothelial antiapoptotic activity	Regulates antiangiogenic activity on endothelial cells and when overexpressed, leads to inhibition of proliferation, migration and apoptosis. Also demonstrated to inhibit melanoma growth when expressed in tumour-associated vasculature.
CCL3L1	chemokine (C-C motif) ligand 3-like 1	Cytokine	Encodes a cytokine which binds to chemokine receptors such as CCR5. Known to be involved in chemotaxis of monocytes and lymphocytes
KLHL42	kelch-like family member 42	BCR E3 ubiquitin-protein ligase complex adaptor	Encodes an adaptor for a BCR (BTB-CUL3-RBX1) E3 ubiquitin-protein ligase complex required for mitotic progression and cytokinesis. Also involved in microtubule dynamics during mitosis.
DCAF5	DDB1 and CUL4 associated factor 5	Substrate receptor	May function as a substrate receptor for a CLU4-DDB1 E3 ubiquitin-protein ligase complex
ID3	inhibitor of DNA binding 3, dominant negative helix-loop-helix protein	Transcriptional regulator	Encodes a transcriptional regulator (lacking a basic DNA binding domain) which negatively regulates the basic helix-loop-helix transcription factors by inhibiting their transcriptional activity. Involved in many cellular processes such as proliferation, growth, senescence, apoptosis, differentiation and neoplastic transformation. Also involved in myogenesis and regulation of the circadian clock.

SOCS3	suppressor of cytokine signaling 3	Suppressor of cytokine signalling	Encodes a member of the STAT-induced STAT inhibitor, known as the suppressor of cytokine signalling family which are cytokine-inducible negative regulators of cytokine signalling. The expression of SOCS3 is induced by IL6, IL10 and interferon gamma.
NUAK2	NUAK family, SNF1-like kinase, 2	Stress-activated kinase involved in tolerance to glucose starvation	A stress-activated kinase involved in tolerance to glucose stravation and cytoskeletal signalling. Expression is induced by TNF-alpha via NF-κB. Also protects cells from Fas-mediated apoptosis and is required for increased motility and invasiveness in fas-mediated tumour cells.
RGS12	regulator of G-protein signaling 12	GTPase-activating protein	Functions as a guanosine triphosphatase (GTPase) -activating protein and a transcriptional repressor. May play a role in tumourigenesis.
TXNIP	thioredoxin interacting protein	Mediator of oxidative stress	May function as a mediator of oxidative stress by inhibiting the activity of thioredoxin. Also plays a role as a transcriptional repressor by acting as a molecular bridge between trascription factors and corepressor complexes. Also known to suppress tumour cell growth.
NA	NA	N/A	N/A

Appendix Table 6 (continued from previous two pages). Description of statistically significant genes differentially expressed in HLY-1 cells treated with CsA for 2hrs (paired data analysis). Columns indicate the gene symbols, names, family and function for statistically significant genes (adjusted P-value <0.05) differentially expressed upon treatment with CsA. Data in orange indicates genes downregulated by CsA and data in blue indicates genes upregulated by CsA. Data includes genes marked as N/A.

HLY-1 6hr (unpaired data analysis)

symbol	name	Family	Information based on GeneCard (www.genecards.org)
NUP43	nucleoporin 43kDa	Nuclear pore complex transporter	Encodes a protein involved in the bidirectional transport of macromolecules between the cytoplasm and the nucleus through nuclear pore complexes embedded in the nuclear envelope. NUP43 is part of a subcomplex which composes a nuclear pore complex.
DHRS3	dehydrogenase/reductase (SDR family) member 3	Short-chain dehydrogenases/reductase	Catalyses the oxidation/reduction of a wide range of substrates such as retinoids and steroids
SSR3	signal sequence receptor, gamma (translocon-associated protein gamma)	Signal-sequence receptor	Encodes a gamma subunit of a signal sequence receptor which forms a glycosylated endoplasmic reticulum (ER) membrane receptor which aids the translocation of proteins across the ER membrane.
LBH	limb bud and heart development	Transcriptional regulator/cofactor	Diseases associated are rheumatoid arthritus and celiacs disease
NFATC1	nuclear factor of activated T-cells, cytoplasmic, calcineurin-dependent 1	Transcription factor	DNA-binding transcription factor which plays a key role in inducible gene transcription during an immune response. Commonly known to induce the expression of genes such as IL-2 and IL-4 during T cell activation but now known to be expressed in many cell types. Recent studies suggest a role for this family of transcription factors in cancer. A central molecular target for the immunosuppresive drug CsA.
HLF	hepatic leukemia factor	Transcription factor	Encodes a member of the proline and acidic-rich (PAR) protein family, a subset of the bZIP transcription factors. HLF forms homo- or heterodimers with other PAR family members and activates transcription. Chromosomal translocations fusing portions of this gene with the E2A gene are known to cause a subset of childhood B-lineage acute lymphoid leukaemias.

GBP1	guanylate binding protein 1, interferon-inducible	Guanylate binding protein	Induced by interferon, this guanylate binding protein binds guanine nucleotides such as GMP, GDP and GTP.
CRY1	cryptochrome circadian clock 1	Protein involved in regulating the circadian clock	This gene encodes a flavin adenine dinucleotide-binding protein that is a key component of the circadian core oscillator complex, which regulates the circadian clock. Polymorphisms in this gene have been associated with altered sleep patterns. Diseases associated include sleep disorders and anxiety disorder.
EHD4	EH-domain containing 4	Endocytic trafficking protein	Associated with endocytosis and Trk receptor signalling mediated by the MAPK pathway. Also associated with hepatocellular carcinoma.
CD36	CD36 molecule (thrombospondin receptor)	Glycoprotein	A major glycoprotein on the surface of platelets which acts as a receptor for thrombospondin.
NAMPT	nicotinamide phosphoribosyltransferase	Nicotinic acid phosphoribosyltransferase (NAPRTase)	Catalyses the condensation of nicotinamide with 5-phosphoribosyl-1-pyrophosphate to yield nicotinamide mononucleotide. Involved in metabolism, the stress-response and aging.
HNRNPH1	heterogeneous nuclear ribonucleoprotein H1 (H)	Heterogeneous nuclear ribonucleoprotein (hnRNP)	RNA binding protein that complex with heterogeneous nuclear RNA. Associated with pre-mRNA processing and other functions related to mRNA metabolism and transport.
GNG10	guanine nucleotide binding protein (G protein), gamma 10	Heterotrimeric G protein	Encodes a heterotrimeric G protein activates PLA2 and Gbetagamma coupled to M1 receptors
NA	NA	N/A	N/A
C1orf186	chromosome 1 open reading frame 186	No information found	No information found
LEF1	lymphoid enhancer-binding factor 1	Transcription factor	Encodes a transcription factor which shares homology with the high mobility group protein-1. Binds to a key site in the T-cell receptor-alpha enhancer. Also involved in the Wnt signalling pathway and has been linked to various cancers including prostate cancer.
GBP2	guanylate binding protein 2, interferon-inducible	GTPase	Encodes a guanine-binding protein which includes interferon-induced proteins that can bind gaunine nucleotides such as GMP, GDP and GTP. May play a role as a marker of squamous cell carcinomas
NA	NA	N/A	N/A
SCN2A	sodium channel, voltage-gated, type II, alpha subunit	Voltage-gated sodium channel	Encodes one member of the sodium channel alpha subunit gene family.
GUSBP11	glucuronidase, beta pseudogene 11	Pseudogene	Pseudogene similar to glucuronidase beta and immunoglobulin lambda-like polypeptide 1
NA	NA	N/A	N/A
NA	NA	N/A	N/A
SNORD96A	small nucleolar RNA, C/D box 96A	Small nucleolar RNA	Plays a role in the processing of ribosomal RNA precursors.
SCART1	scavenger receptor protein family member	Type I transmembrane molecule	Scavenger receptor cysteine-rich type I transmembrane molecule.
RALGPS2	Ral GEF with PH domain and SH3 binding motif 2	Guanine nucleotide exchange factor	A guanine nucleotide exchange factor for the small GTPase RALA. May be involved in cytoskeletal organisation and the stimulation of transcription in a Ras-independent way. Diseases associated are tonsillitus and Alzheimers disease
NA	NA	N/A	N/A
DDX17	DEAD (Asp-Glu-Ala-Asp) box helicase 17	RNA helicase	DEAD box proteins are characterised by the conserved motif Asp-Glu-Ala-Asp and their role as RNA helicases allows them to aid initiation of translation and assembly of ribosomes and splicesosome. Some family members are thought to have a role in cellular growth and division.
RALGPS2	Ral GEF with PH domain and SH3 binding motif 2	Guanine nucleotide exchange factor	Guanine nucleotide exchange factor for the small GTPase RALA. May be involved in transcription.
SFN	stratifin	Adaptor protein	Adaptor protein implicated in the regulation of a large spectrum of both general and specialised signalling pathways. Binds to a large number of partners and usually results in the modulation of activity of the binding partner. Involved in stimulation of the AkT/mTOR pathway and may activate p53 via MDM2 regulation. Diseases associated include phlebotomus fever and bladder squamous cell carcinoma

Appendix Table 7 (Continued from previous page). Description of statistically significant genes differentially expressed in HLY-1 cells treated with CsA for 6hrs (unpaired data analysis). Columns indicate the gene symbols, names, family and function for statistically significant genes (adjusted P-value <0.05) differentially expressed upon treatment with CsA. Data in orange indicates genes downregulated by CsA and data in blue indicates genes upregulated by CsA. Data includes genes marked as N/A.

HLY-1 6hr (paired data analysis)

symbol	name	Family	Information based on GeneCard (www.genecards.org)
TNF	tumor necrosis factor	Cytokine	Encodes a multifunctional proinflammatory cytokine that belongs to the tumour necrosis factor superfamily. Mostly secreted by macrophages and is involved in cell proliferation, differentiation, apoptosis and many other cellular processes. Implicated in diseases such as cancer, autoimmune diseases and insulin resistance.
MAP3K8	mitogen-activated protein kinase kinase kinase 8	Serine/threonine kinase	Encodes a serine/threonine kinase which localises to the cytoplasm and can activate both the MAP kinase and JNK kinase pathways. Known to activate NF-κB via activation of I kappa B kinases. Also reported to promote the production of TNF-alpha and IL-2 during lymphocyte activation.
NA	NA	N/A	N/A
JUN	jun proto-oncogene	Transcription factor	Known as the transforming gene of avian sarcoma virus 17. Encodes a tramscription factor which binds DNA and regulates gene transcription. Associated with PI3K and MAPK signalling pathways and involved in cell cycle progression and anti-apoptosis.
NFKBIE	nuclear factor of kappa light polypeptide gene enhancer in B-cells inhibitor, epsilon	IkB protein which inhibits nuclear localisation and activation of NF-κB alongside IκBa and IκBb	The protein encoded by this gene binds to components of NF-kappa-B, trapping the complex in the cytoplasm and preventing it from activating genes in the nucleus. Phosphorylation of the encoded protein targets it for desruction by the ubiquitin pathway, which activates NF-kappa-B by making it available to translocate to the nucleus
NUP43	nucleoporin 43kDa	Nuclear pore complex transporter	Encodes a protein involved in the bidirectional transport of macromolecules between the cytoplasm and the nucleus through nuclear pore complexes embedded in the nuclear envelope. NUP43 is part of a subcomplex which composes a nuclear pore complex.
SSR3	signal sequence receptor, gamma (translocon-associated protein gamma)	Signal-sequence receptor	Encodes a gamma subunit of a signal sequence receptor which forms a glycosylated endoplasmic reticulum (ER) membrane receptor which aids the translocation of proteins across the ER membrane.
EGR2	early growth response 2	Transcription factor	Encodes a transcription factor from the three tandem C2H2-type zinc finger family.
LBH	limb bud and heart development	Transcriptional regulator/cofactor	Diseases associated are rheumatoid arthritus and celiacs disease. LBH encodes a nuclear protein which possesses a transcriptional activator function in tissue culture cells. Expressed during limb and heart development in the embryo.
SRF	serum response factor (c-fos serum response element-binding transcription factor)	Transcription factor	Encodes a nuclear protein that stimulates cell proliferation and differentiation and is a member of the MCM1, Agamous, Deficiens and SRF (MADS) box family of transcription factors. Binds to the serum response element in the promoter region of target genes and regulates many immediate to early genes. Examples of genes regulated include c-fos, therefore having involvement in the cell cycle, apoptosis and many other processes. SRF is also a downstream target for many pathways such as the MAPK pathway.
RFWD3	ring finger and WD repeat domain 3	E3 ubiquitin ligase	Mediates the ubiquitination of p53/TP53 in the late response to DNA damage and acts as a positive regulator of p53/TP53 stability by regulating the G1/A DNA damage checkpoint.
FILIP1L	filamin A interacting protein 1-like	Regulator of endothelial antiapoptotic activity	Regulates antiangiogenic activity on endothelial cells and when overexpressed, leads to inhibition of proliferation, migration and apoptosis. Also demonstrated to inhibit melanoma growth when expressed in tumour-associated vasculature.
NFATC1	nuclear factor of activated T-cells, cytoplasmic, calcineurin-dependent 1	Transcription factor	DNA-binding transcription factor which plays a key role in inducible gene transcription during an immune response. Commonly known to induce the expression of genes such as IL-2 and IL-4 during T cell activation but now known to be expressed in many cell types. Recent studies suggest a role for this family of transcription factors in cancer. A central molecular target for the immunosuppresive drug CsA.
NFKBIA	nuclear factor of kappa light polypeptide gene enhancer in B-cells inhibitor, alpha	IkB protein which inhibits nuclear localisation and activation of NF-κB alongside IκBa and IκBb	The protein encoded by this gene binds to components of NF-kappa-B, trapping the complex in the cytoplasm and preventing it from activating genes in the nucleus. Phosphorylation of the encoded protein targets it for desruction by the ubiquitin pathway, which activates NF-kappa-B by making it available to translocate to the nucleus
PRPS1	phosphoribosyl pyrophosphate synthetase 1	Enzyme	Catalyses the phosphoribosylation of ribose 5-phosphate to 5-phosphoribosyl-1-pyrophosphate, which is required for metabolism and synthesis of nucleotides.
IGF2R	insulin-like growth factor 2 receptor	Receptor	Encodes a receptor for insulin-like growth factor 2 and mannose 6-phosphate, functioning in intracellular trafficking of lysosomal enzymes and the activation of transforming growth factor.
HLF	hepatic leukemia factor	Transcription factor	Encodes a member of the proline and acidic-rich (PAR) protein family, a subset of the bZIP transcription factors. HLF forms homo- or heterodimers with other PAR family members and activates transcription. Chromosomal translocations fusing portions of this gene with the E2A gene are known to cause a subset of childhood B-lineage acute lymphoid leukaemias.
CD1C	CD1c molecule	Transmembrane glycoprotein, similar to the MHC proteins and involved in antigen presentation	This gene encodes a member of the CD1 family of CD1 family of transmembrane glycoproteins, structurally related to the MHC proteins and form heterodimers with beta-2-microglobulin. The CD1 proteins mediate the presentation of antigens to T cells.
ATP6V1F	ATPase, H+ transporting, lysosomal 14kDa, V1 subunit	Vacuolar ATPase	Encodes a vacuolar ATPase which mediates acidification of eukaryotic intracellular organelles.
FANCG	Fanconi anemia, complementation group G	DNA repair protein	May function in post replication repair or during cell cycle checkpoints. Also thought to be a tumour suppressor gene.

NA	NA	N/A	N/A
GBP1	guanylate binding protein 1, interferon-inducible	Guanylate binding protein	Induced by interferon, this guanylate binding protein binds guanine nucleotides such as GMP, GDP and GTP.
CIRH1A	cirrhosis, autosomal recessive 1A (cirhin)	Transcriptional regulator	Positive regulator of HIVEP1 which locates to viral promoters such as HIV-1.
NA	NA	N/A	N/A
NOL12	nucleolar protein 12	No information found	No information found
CD83	CD83 molecule	Type I transmembrane molecule	Encodes a single-pass type I membrane protein and may be involved in antigen presentation.
TRMT2B	tRNA methyltransferase 2 homolog B (S. cerevisiae)	tRNA methyltransferase	Plays a role in tRNA maturation
CD83	CD83 molecule	Type I transmembrane molecule	Encodes a single-pass type I membrane protein and may be involved in antigen presentation.
EHD4	EH-domain containing 4	Endocytic trafficking protein	Associated with endocytosis and Trk receptor signalling mediated by the MAPK pathway. Also associated with hepatocellular carcinoma.
PTGER4	prostaglandin E receptor 4 (subtype EP4)	G-protein coupled receptor	Encodes a G-protein coupled receptor for prostaglandin E2 (PGE2) and has been shown to mediate PGE2 induced expression of early growth response 1.
AMY1A	amylase, alpha 1A (salivary)	Amylase	Encodes the secretory protein amylase which plays an important role in catalysing the first steps of digestion of dietary starch and glycogen.
DDX23	DEAD (Asp-Glu-Ala-Asp) box polypeptide 23	RNA helicase	DEAD box proteins are characterised by the conserved motif Asp-Glu-Ala-Asp and their role as RNA helicases allows them to aid initiation of translation and assembly of ribosomes and splicesosome. Some family members are thought to have a role in cellular growth and division.
PPP2R4	protein phosphatase 2A activator, regulatory subunit	Serine/threonine kinase	Encodes a serine/threonine kinase which is implicated in the negative control of cell growth and division.
NFKBID	nuclear factor of kappa light polypeptide gene enhancer in B-cells inhibitor, delta	IkB protein which inhibits nuclear localisation and activation of NF-κB alongside IκBa and IκBb	The protein encoded by this gene binds to components of NF-kappa-B, trapping the complex in the cytoplasm and preventing it from activating genes in the nucleus. Phosphorylation of the encoded protein targets it for desruction by the ubiquitin pathway, which activates NF-kappa-B by making it available to translocate to the nucleus
FCF1	FCF1 rRNA-processing protein	rRNA processing protein	Plays an essential role in pre-rRNA processing and 40S ribosomal subunit assembly
SGK223	homolog of rat pragma of	Tyrosine kinase	Encodes a tyrosine kinase protein which in rats binds to Rho GTPase 2
LTA	lymphotoxin alpha	Cytokine	Encodes a cytokine which is a member of the TNF family. Produced by lymphocytes, LTA is highly inducible and plays a role in inflammation, immune stimulation and apoptosis. Genetic mutations of this gene are associated with increased susceptibility of non-Hodgkin's lymphoma.
AGMAT	agmatine ureohydrolase (agmatinase)	Hydrolase enzyme	Involved in metabolism
SOCS3	Supressor of cytokine signalling-3	Zinc-binding phosphoprotein	This protein concentrates at focal adhesions (actin-rich structures that allow cells to adhere to the extracellular matrix) and along the actin cytoskeleton. The function of ZYX may be to interact with SH3 domains to aid initiation of downstream siganalling pathways. Thought to act as a messenger in signalling pathways that mediate adhesion-related genes.
DYRK1A	dual-specificity tyrosine-(Y)-phosphorylation regulated kinase 1A	Kinase	Encodes a member of the dual-specifity tyrosine phosphorylation-regulated kinase (DYRK) family. Catalyses its autophosphorylation on serine/threonine and tyrosine residues and plays a key role in regulating cell proliferation in signalling pathways such as NFAT. Homolog of the Drosophila mnb (minibrain) gene and rat Dyrk gene and is localised in the Down syndrome region of chromosome 21. Also an important target for learning defects associated in Down syndrome.
CD36	CD36 molecule (thrombospondin receptor)	Glycoprotein	A major glycoprotein on the surface of platelets which acts as a receptor for thrombospondin.
NAMPT	nicotinamide phosphoribosyltransferase	Cytokine/adipokine	Encodes a protein which catalyses the condensation of nicrotinamide with 5-phosphoribosyl-1-pyrophosphate to yield an intermedate in the biosynthesis of NAD (nicotinamide mononucleotide). Plays a role in regulation of the circadian clock.
SLX1A	SLX1 structure-specific endonuclease subunit homolog A (S. cerevisiae)	Endonuclease subunit	Encodes the catalytic subunit for the SLX-SLX4 structure-specific endonuclease which plays a role in the repair and recombination of secondary DNA structures
MB21D1	Mab-21 domain containing 1	Nucleotidyltransferase	Catalyses the formation of cyclic GMP-AMP from ATP and GTP. A key cytosolic DNA sensor with antiviral activity.
NFKBIZ	nuclear factor of kappa light polypeptide gene enhancer in B-cells inhibitor, zeta	IkB protein which inhibits nuclear localisation and activation of NF-κB alongside IκBa and IκBb	The protein encoded by this gene binds to components of NF-kappa-B, trapping the complex in the cytoplasm and preventing it from activating genes in the nucleus. Phosphorylation of the encoded protein targets it for desruction by the ubiquitin pathway, which activates NF-kappa-B by making it available to translocate to the nucleus
MCRS1	microspherule protein 1	Component of the chromatin remodeling complex	Regulatory component of the INO80 complex which is involved in transcriptional regulation and DNA replication. Associated with pigmented basal cell carcinoma.
NA	NA	N/A	N/A
POLR2L	polymerase (RNA) II (DNA directed) polypeptide L,	RNA polymerase II subunit	Encodes a subunit for RNA polymerase II which is responsible for the synthesis of mRNA
GNG10	guanine nucleotide binding protein (G protein), gamma	GTPase	Heterotrimeric G protein involved in PI3K-Akt and Ras signalling pathways
DNLZ	DNL-type zinc finger	Co-chaperone protein	May function as a co-chaperone for HSPA9/mortalin.
FBXL20	F-box and leucine-rich repeat protein 20	Ubiquitin ligase	Substrate-recognition component of the SCF-type E3 ubiquitin ligase complex with a role in neural transmission.
GCLC	glutamate-cysteine ligase, catalytic subunit	Glutamate-cysteine ligase	Functions as the first rate-limiting enzyme of glutathione synthesis.
WASF2	WAS protein family, member 2	Linker of receptor kinases and actin	Encodes a member of the Wiskott-Aldrich syndrome protein family and functions by linking receptor kinases and actin to aid changes in cell shape, motility and function.

HSD17B7P2	hydroxysteroid (17-beta) dehydrogenase 7 pseudogene	Pseudogene	Involved in metabolism
UBA1	ubiquitin-like modifier activating enzyme 1	Activator of ubiquitin	Catalyses the first step in ubiquitin conjugation to mark proteins for degradation.
FAM98B	family with sequence similarity 98, member B	No information found	No information found
GUSBP11	glucuronidase, beta pseudogene 11	Pseudogene	Pseudogene similar to glucuronidase beta and immunoglobulin lambda-like polypeptide 1
VPREB3	pre-B lymphocyte 3	Related to the immunoglobin supergene family	Associates with membrane Ig-mu heavy chains during pre-B cell receptor biosynthesis.
SMA5	glucuronidase, beta pseudogene	Pseudogene	Related pathways are involved in protein processing in the endoplasmic reticulum
NEMF	nuclear export mediator factor	Component of the ribosome quality control complex	Part of a ribosome-associated complex that regulates ubiquitination.
NA	NA	N/A	N/A
FAF1	Fas (TNFRSF6) associated	Initiator of apoptosis	Interacts with Fas antigen and initiate apoptosis.
ORAI2	ORAI calcium release-activated calcium modulator	ER calcium sensor	CRAC-like channel subunit which mediates calcium influx from the ER
HMGCS1	3-hydroxy-3-methylglutaryl-CoA synthase 1 (soluble)	Enzyme	Regulation of cholesterol biosythesis
MVK	mevalonate kinase	Kinase	Encodes a peroxisomal enzyme mevalonate kinase which is involved in metabolism.
NA	NA	N/A	N/A
NA	NA	N/A	N/A
SNORD3A	small nucleolar RNA, C/D box	Small nucleolar RNA	Plays a role in the processing of ribosomal RNA precursors.
IDH1	isocitrate dehydrogenase 1 (NADP+), soluble	Isocitrate dehydrogenase	Functions by catalysing the oxidative decarboxylation of isocitrate to 2-oxoglutarate.
GUSBP2	glucuronidase, beta	Pseudogene	No information found
HNRNPA3	heterogeneous nuclear ribonucleoprotein A3	Cytoplasmic trafficking protein	Functions in the cytoplasmic trafficking of RNA and is involved in gene expression pathways and the spliceosome.
MZB1	marginal zone B and B1 cell-specific protein	Cytokine	Diversifies peripheral B-cell functons by regulating Calcium stores, antibody secretion and integrin activation. Functions as a proinflammatory cytokine associated with chronic inflammation.
GOLIM4	golgi integral membrane protein 4	Type II Golgi-resident protein	Functions in endosome to Golgi trafficking by mediating protein transport along the late endosome-bypass pathway
USF2	upstream transcription factor 2, c-fos interacting	Transcription factor	Encodes a member of the basic helix-loop-helix leucine zipper family. Functions as a trancription factor and is associated with the transcriptional targets of AP1 family members
TCERG1	transcription elongation regulator 1	Transcription factor	Regulates transcriptional elongation and pre-RNA splicing.
GINM1	glycoprotein integral	Integral membrane protein	No information found
TAF5L	TAF5-like RNA polymerase II, p300/CBP-associated factor (PCAF)-associated factor,	Component of the PCAF histone acetylase complex	Required for myognic transcription and differentiation.
VOPP1	vesicular, overexpressed in cancer, prosurvival protein 1	Regulator of NF-κB	Increases the transcriptional activity of NFKB1 by facilitating its nuclear translocation, DNA-binding and associated apoptotic response when overexpressed.
SORL1	sortilin-related receptor, L(DLR class) A repeats	Endocytic endocytic receptor	Involved in the uptake of lipoproteins and proteases.
NA	NA	N/A	N/A
ST6GALNAC4	ST6 (alpha-N-acetyl-neuraminyl-2,3-beta-galactosyl-1,3)-N-acetylgalactosaminide alpha-	Type II membrane protein	Located in the golgi apparatus and functions to catalyse the transfer of sialic acid from CMP-sialic acid to galactose-containing substrates.
SNORA12	small nucleolar RNA, H/ACA box 12	Small nucleolar RNA	Small noncoding RNA involved in RNA processing
NA	NA	N/A	N/A
GUSBP2	glucuronidase, beta	Pseudogene	No information found
NA	NA	N/A	N/A
CD79A	CD79a molecule, immunoglobulin-associated alpha	Associated with membrane-bound immunoglobulin in B cells	Encodes the Ig-alpha protein of the B-cell receptor antigen component. Needed in cooperation with CD79B for initiation of the signal transduction cascade downstream of the BCR. Also required for BCR surface expression and differentiation of pro- and pre- B cells. Stimulates SYK autophosphprylation and interacts with Src-family kinases.
NA	NA	N/A	N/A
NA	NA	N/A	N/A
NA	NA	N/A	N/A
ITGB7	integrin, beta 7	Integrin	Dimerises with other proteins to form a homing receptor for migration of lymphocytes to the intestinal mucosa and Peyer's patches.
TAF1	TAF1 RNA polymerase II, TATA box binding protein (TBP)-associated factor, 250kDa	Transcription factor complex protein	Facilitates transcription by acting as a large subunit of the transcription factor TFIID.
SQLE	squalene epoxidase	Enzyme	Cataluses the first oxygenation step in sterol synthesis
KRI1	KRI1 homolog (S. cerevisiae)	No information found	No information found
LCMT1	leucine carboxyl methyltransferase 1	Methyltransferase	Methylates the carboxyl group of the C-terminal leucine residue of protein phosphatase 2A catalytic subunits to form alpha-leucine ester residues
RN7SK	RNA, 7SK small nuclear	No information found	No information found
CDK5RAP3	CDK5 regulatory subunit associated protein 3	No information found	Associated with signalling pathways involved in transcriptional regulation and the cell cycle (potential regulator of CDK5). May be linked to tumourigenesis and metastasis.

FAM102A	family with sequence similarity 102, member A	No information found	May play a role in oestrogen action
SDF4	stromal cell derived factor 4	Calcium binding protein	Encodes a stromal cell derived factor that is localised in the Golgi lumen and may regulate calcium-dependent processes.
SNORD96A	small nucleolar RNA, C/D box	Small nucleolar RNA	Small noncoding RNA involved in RNA processing
NA	NA	N/A	N/A
ADAP1	ArfGAP with dual PH domains 1	GTPase-activating protein	GTPase-activating protein for the ADP ribosylation factor family. Binds PtdInsP3 and InsP4). Diseases associated include childhood leukaemia and alzheimers disease
SCART1	scavenger receptor protein family member	Type I transmembrane molecule	Scavenger receptor cysteine-rich type I transmembrane molecule.
NA	NA	N/A	N/A
RBM39	RNA binding motif protein 39	Transcriptional coactivator	Involved in transcription of steroid hormones and is a transcriptional coregulator of the viral oncoprotein v-Rel.
RBM38	RNA binding motif protein 38	RNA-binding protein	Binds CDKN1A transcripts to mediate p53/TP53
NA	NA	N/A	N/A
SNORD56	small nucleolar RNA, C/D box	Small nucleolar RNA	Small noncoding RNA involved in RNA processing
DDIT3	DNA-damage-inducible transcript 3	Transcription factor	This gene encodes a member of the C/EBP family of transcription factors. The protein functions as a dominant negative inhibitor. This multifunctional transcription factor is involved in the ER stress response and plays a wide role in cell stresses and induces cell cycle arrest and apoptosis in response to ER stress. Negatively regulates expression of BCL2, ATF4-dependent transcriptional activation of asparagine synthetase and other genes. Inhibits Wnt signalling and plays a role in the inflammatory response through the induction of caspase 11.
NLRP7	NLR family, pyrin domain containing 7	Leucine rich repeat protein	Encodes a protein involved in the activation of proinflammatory cytokines
IDI1	isopentenyl-diphosphate delta isomerase 1	Isocitrate dehydrogenase	Functions by catalysing the oxidative decarboxylation of isocitrate to 2-oxoglutarate.
PPM1K	protein phosphatase, Mg2+/Mn2+ dependent, 1K	Phosphatase	Regulation of the mitochondrial permeability transition pore and is essential for cell survival and development.
NA	NA	N/A	N/A
RAB5C	RAB5C, member RAS oncogene family	Small GTPase	Involved in endocytosis and the Ras signalling pathway
SNHG4	small nucleolar RNA host gene 4 (non-protein coding)	Non-coding gene	N/A
PLEKHA2	pleckstrin homology domain containing, family A (phosphoinositide binding specific) member 2	No information found	Recruits proteins to the plasma membrane and is associated with the PI3K and B-cell receptor signalling pathways
ANP32AP1	acidic (leucine-rich) nuclear phosphoprotein 32 family, member A pseudogene 1	Pseudogene	No information found
DHCR7	7-dehydrocholesterol		
MSMO1	methylsterol monooxygenase	Enzyme	Cholesterol synthesis
LSP1	lymphocyte-specific protein 1	Intracellular F-actin binding protein	Regulates chemotaxis
POU2F2	POU class 2 homeobox 2	Transcription factor	Binds octomer sequences which are common in immunoglobulin gene promoters. Associated with B-cell receptor signalling pathways. Diseases associated include nodular lymphocyte predominant hodgkin lymphoma.
FST	follistatin	Gonadal protein	Inhibits follicle-stimulating hormone release. Diseases associated include endometriosis
TSC22D3	TSC22 domain family,	Transcriptional regulator	Known to inhibit NF-kappa B DNA binding activity
RALGPS2	Ral GEF with PH domain and SH3 binding motif 2	Guanine nucleotide exchange factor	A guanine nucleotide exchange factor for the small GTPase RALA. May be involved in cytoskeletal organisation and the stimulation of transcription in a Ras-independent way. Diseases associated are tonsillitus and Alzheimers disease
NLRP7	NLR family, pyrin domain containing 7	Leucine rich repeat protein	Encodes a protein involved in the activation of proinflammatory cytokines
NA	NA	N/A	N/A
PRKCSH	protein kinase C substrate	Enzyme	Associated with liver disease
DHCR7	7-dehydrocholesterol	Enzyme	Cholesterol synthesis
NA	NA	N/A	N/A
NA	NA	N/A	N/A
TMEM159	transmembrane protein 159	Transmembrane protein	No information found
DDX17	DEAD (Asp-Glu-Ala-Asp) box helicase 17	RNA helicase	DEAD box proteins are characterised by the conserved motif Asp-Glu-Ala-Asp and their role as RNA helicases allows them to aid initiation of translation and assembly of ribosomes and splicesosome. Some family members are thought to have a role in cellular growth and division.
MEF2BNB-MEF2B	MEF2BNB-MEF2B readthrough	Non-coding nonsense-mediated decay candidates.	MEF2C is an important paralog of this gene.
NA	NA	N/A	N/A
UBE2E1	ubiquitin-conjugating enzyme E2E 1	E2 ubiquitin-conjugating enzyme	Accepts ubiquitin from the E1 complex and catalyses its covalent attachment to other proteins,
LDLR	low density lipoprotein	Lipoprotein receptor	Binds low density lipoprotein receptor and transports it into cells.
KPNA6	karyopherin alpha 6 (importin alpha 7)	Nuclear import protein	Functions in nuclear import of proteins by acting as an adapter protein for nuclear receptor KPNB1
AP1S1	adaptor-related protein complex 1, sigma 1 subunit	Component of the clathrin coat assembly complex	Plays a role in protein sorting in the Golgi.

FADS1	fatty acid desaturase 1	Fatty acid desaturase	Regulates unsaturation of fatty acids.
DDX17	DEAD (Asp-Glu-Ala-Asp) box helicase 17	RNA helicase	DEAD box proteins are characterised by the conserved motif Asp-Glu-Ala-Asp and their role as RNA helicases allows them to aid initiation of translation and assembly of ribosomes and splicesosome. Some family members are thought to have a role in cellular growth and division.
FBXW7	F-box and WD repeat domain containing 7, E3 ubiquitin protein ligase	Component of the E3 ubiquitin ligase complex	Mediates the ubiquitination of proteins including MYC and JUN.
RALGPS2	Ral GEF with PH domain and SH3 binding motif 2	Guanine nucleotide exchange factor	Guanine nucleotide exchange factor for the small GTPase RALA, involved in metabolism.
NA	NA	N/A	N/A
CCDC71	coiled-coil domain	No information found	No information found
AP1S1	adaptor-related protein complex 1, sigma 1 subunit	Component of the clathrin coat assembly complex	Plays a role in protein sorting in the Golgi.
KIAA1524	KIAA1524	Phosphatase	Known to be an oncoprotein that stabilises MYC in human malignancies. Also known to promote tumour formation and cell growth.
MSMO1	methylsterol monooxygenase	Enzyme	Role in cholesterol biosynthesis
COPG2	coatomer protein complex, subunit gamma 2	Coatomer	Encodes a cytosolic protein complex which associates with the golgi and mediates protein transport from the ER
TSC22D3	TSC22 domain family,	Transcriptional regulator	Known to inhibit NF-kappa B DNA binding activity
SFN	stratifin	Adaptor protein	Adaptor protein implicated in the regulation of a large spectrum of both general and specialised signalling pathways. Binds to a large number of partners and usually results in the modulation of activity of the binding partner. Involved in stimulation of the AkT/mTOR pathway and may activate p53 via MDM2 regulation. Diseases associated include phlebotomus fever and bladder squamous cell carcinoma
PPP3R1	protein phosphatase 3, regulatory subunit B, alpha	Phosphatase	Associated with the PI3K and MAPK pathways.
ROCK1	Rho-associated, coiled-coil containing protein kinase 1	Serine/threonine kinase	Activated when bound to the GTP-bound form of Rho, allowing it to activate LIM kinase which phosphorylates cofilin and therefore inhibiting actin-depolymerisation.
CTSZ	cathepsin Z	Carboxypeptidase	Encodes a lysosomal cysteine proteinase and is expressed ubiquitously in tumours and may be involved in tumourigenesis.
NA	NA	N/A	N/A

Appendix Table 8 (Continued from previous four pages). Description of statistically significant genes differentially expressed in HLY-1 cells treated with CsA for 6hrs (paired data analysis). Columns indicate the gene symbols, names, family and function for statistically significant genes (adjusted P-value <0.05) differentially expressed upon treatment with CsA. Data in orange indicates genes downregulated by CsA and data in blue indicates genes upregulated by CsA. Data includes genes marked as N/A.

WSU-NHL 6hr (unpaired data analysis)

symbol	name	Family	Information based on GeneCard (www.genecards.org)
UPF3B	UPF3 regulator of nonsense transcripts homolog B	Component of a post-splicing multiprotein	Involved in mRNA nuclear export and immunsurveillance
SNORD96A	small nucleolar RNA, C/D	Small nucleolar RNA	Plays a role in the processing of ribosomal RNA precursors.
DNAJB11	DnaJ (Hsp40) homolog, subfamily B, member 11	Glycoprotein	Co-chaperone for binding immunoglobulin protein in the ER lumen
HSPA5	heat shock 70kDa protein 5 (glucose-regulated protein,	Heat shock protein	Encodes a protein involved in protein folding and degradation of misfolded proteins.

Appendix Table 9. Description of statistically significant genes differentially expressed in WSU-NHL cells treated with CsA for 6hrs (unpaired data analysis). Columns indicate the gene symbols, names, family and function for statistically significant genes (adjusted P-value <0.05) differentially expressed upon treatment with CsA. Data in orange indicates genes downregulated by CsA and data in blue indicates genes upregulated by CsA. Data includes genes marked as N/A.

U2932 2hr (unpaired data analysis)

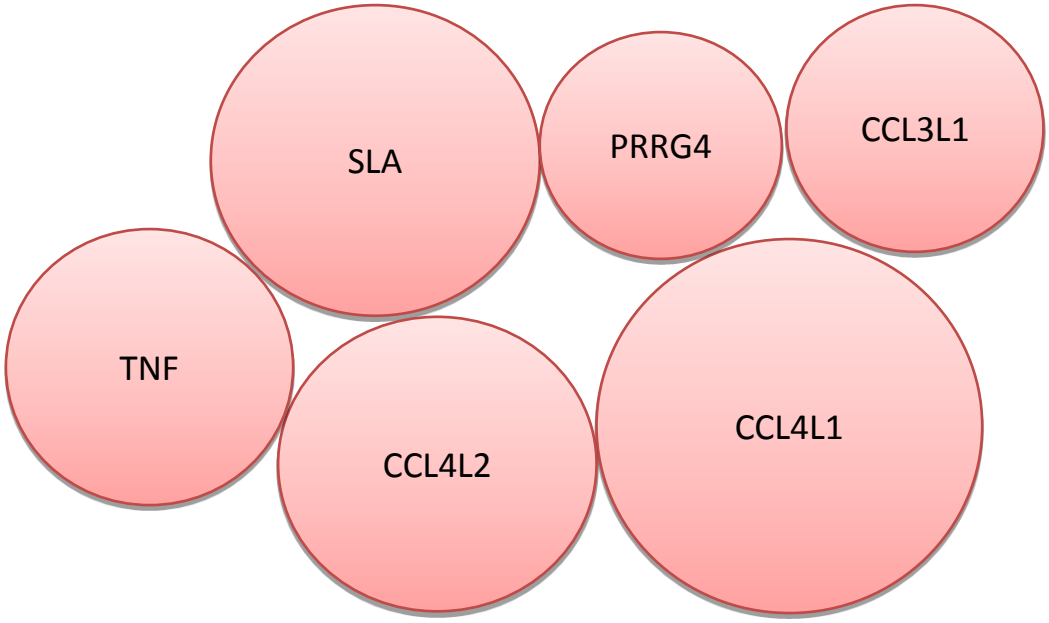

Appendix Figure 3. The top 6 statistically significant genes (ranked by adjusted P-value) downregulated in U2932 cells treated with CsA for 2 hours (unpaired analysis). Each bubble in the figure represents one of most highly significant genes differentially expressed upon treatment with CsA. The larger the bubble the lower the adjusted P-value. Data excludes genes marked as N/A.

Appendix Figure 4. The top statistically significant gene (ranked by adjusted P-value) upregulated in U2932 cells treated with CsA for 2 hours (unpaired analysis). Each bubble in the figure represents one of most highly significant genes differentially expressed upon treatment with CsA. The larger the bubble the lower the adjusted P-value. Data excludes genes marked as N/A.

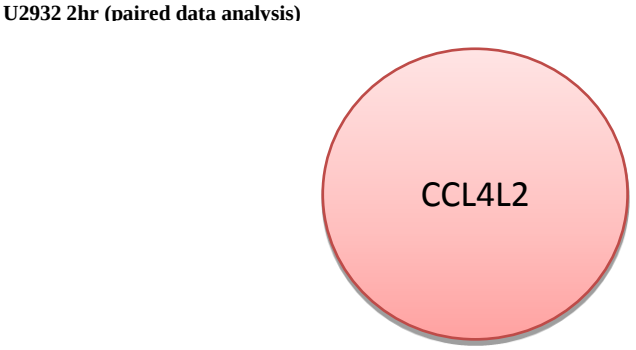

Appendix Figure 5. The top statistically significant gene (ranked by adjusted P-value) downregulated in U2932 cells treated with CsA for 2 hours (paired analysis). Each bubble in the figure represents one of most highly significant genes differentially expressed upon treatment with CsA. The larger the bubble the lower the adjusted P-value. Data excludes genes marked as N/A.

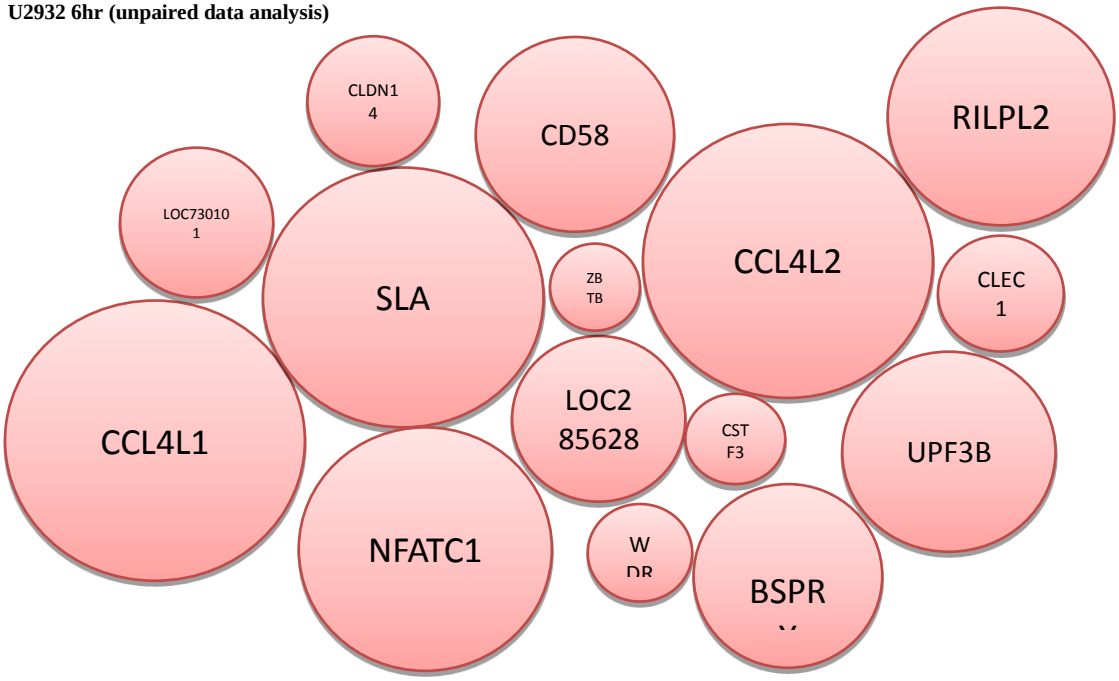

Appendix Figure 6. The top 15 statistically significant genes (ranked by adjusted P-value) downregulated in U2932 cells treated with CsA for 6 hours (unpaired analysis). Each bubble in the figure represents one of most highly significant genes differentially expressed upon treatment with CsA. The larger the bubble the lower the adjusted P-value. Data excludes genes marked as N/A.

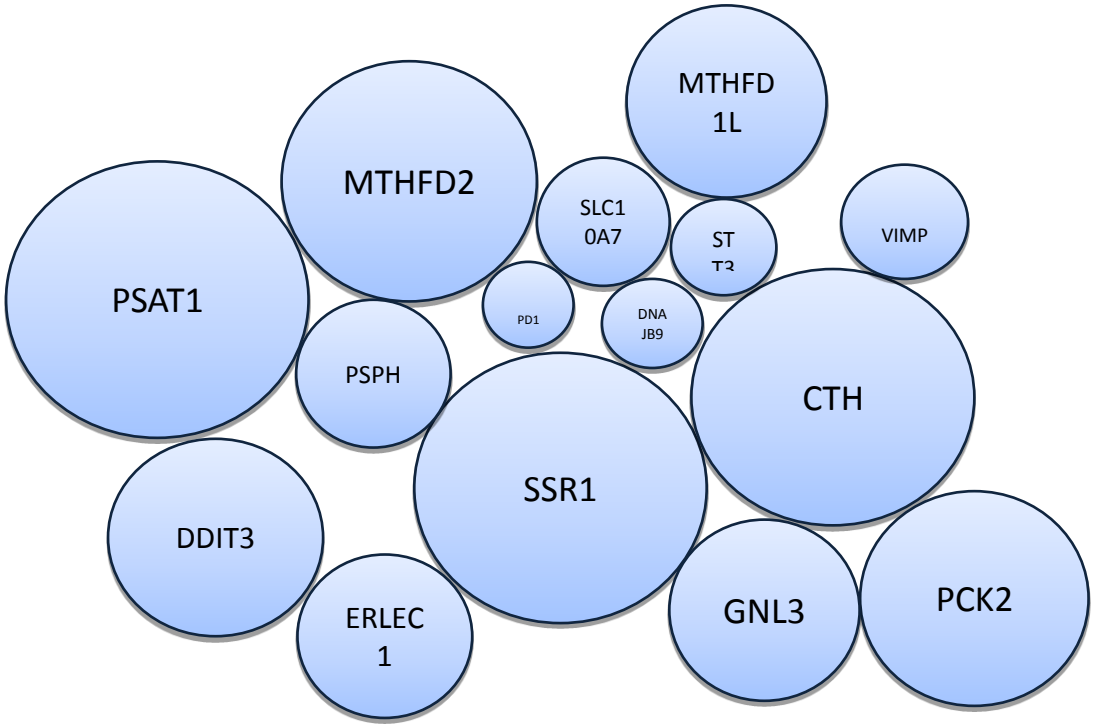

Appendix Figure 7. The top 15 statistically significant genes (ranked by adjusted P-value) upregulated in U2932 cells treated with CsA for 6 hours (unpaired analysis). Each bubble in the figure represents one of most highly significant genes differentially expressed upon treatment with CsA. The larger the bubble the lower the adjusted P-value. Data excludes genes marked as N/A.

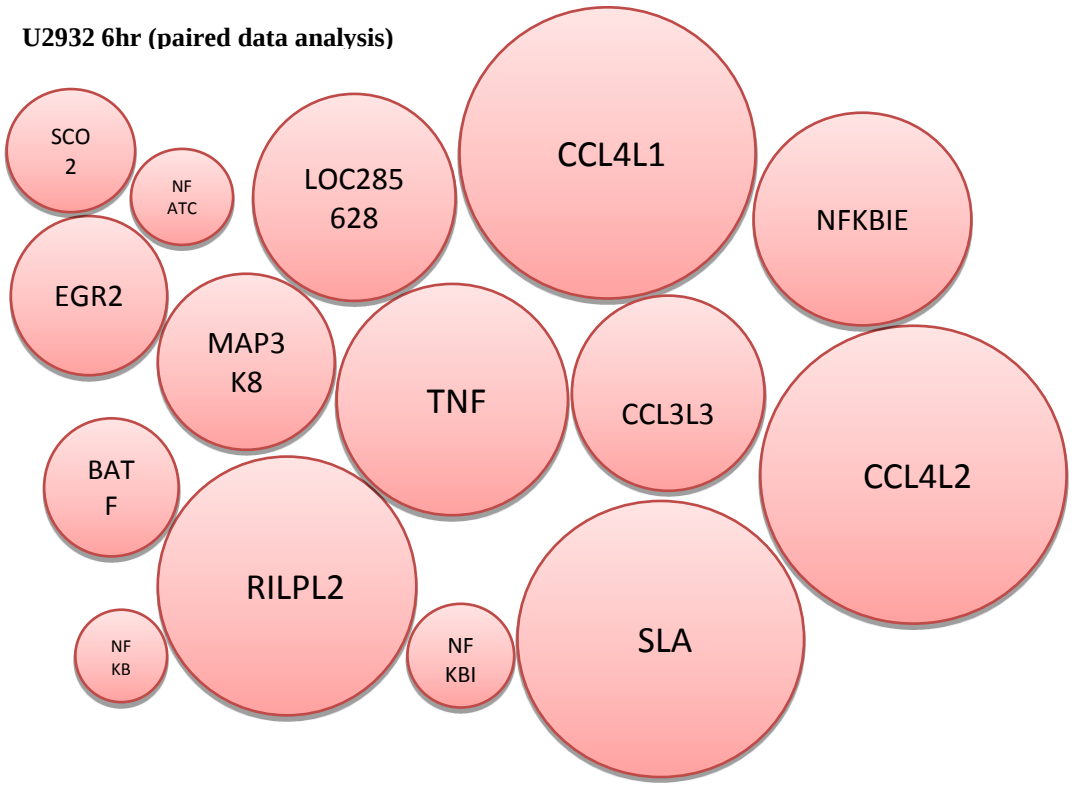

Appendix Figure 8. The top 15 statistically significant genes (ranked by adjusted P-value) downregulated in U2932 cells treated with CsA for 6 hours (paired analysis). Each bubble in the figure represents one of most highly significant genes differentially expressed upon treatment with CsA. The larger the bubble the lower the adjusted P-value. Data excludes genes marked as N/A.

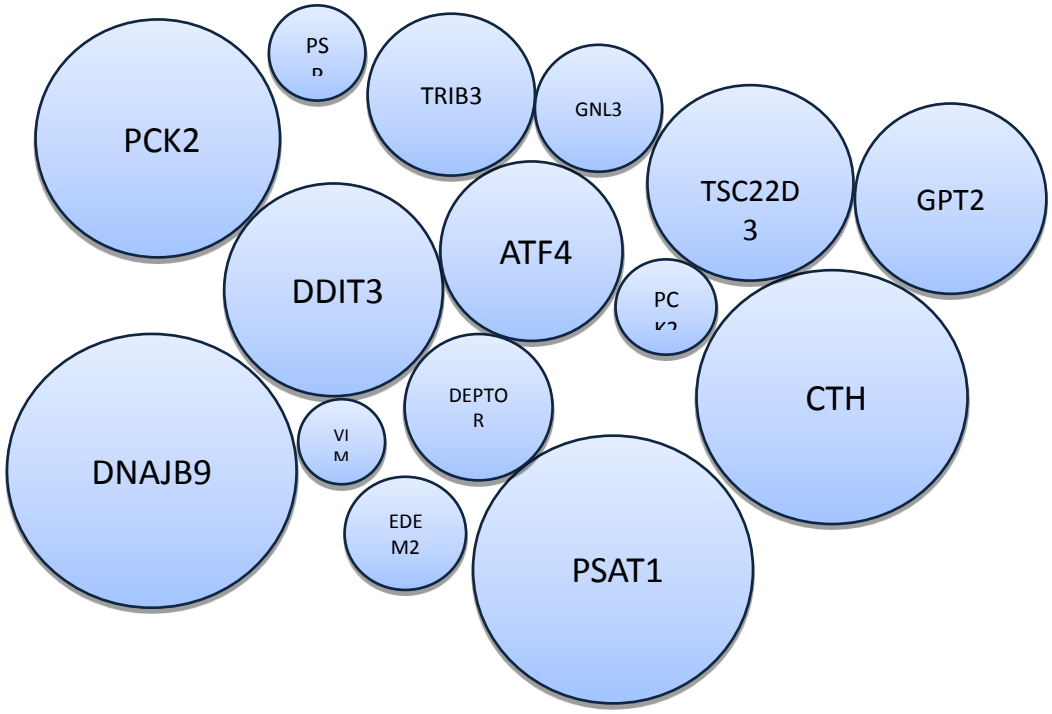

Appendix Figure 9. The top 15 statistically significant genes (ranked by adjusted P-value) upregulated in U2932 cells treated with CsA for 6 hours (paired analysis). Each bubble in the figure represents one of most highly significant genes differentially expressed upon treatment with CsA. The larger the bubble the lower the adjusted P-value. Data excludes genes marked as N/A.

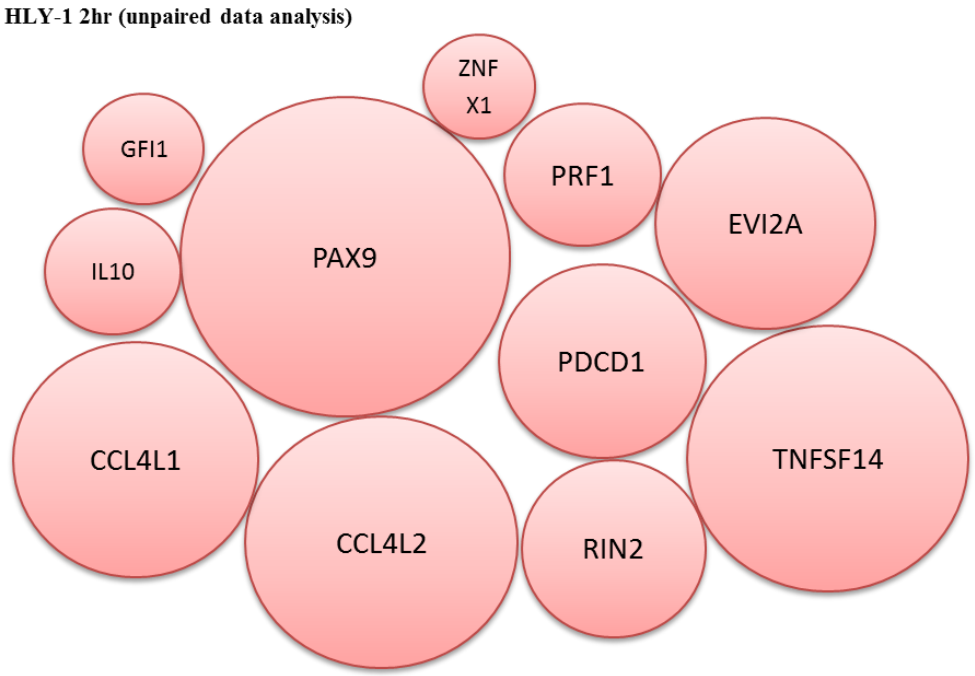

Appendix Figure 10. The top 11 statistically significant genes (ranked by adjusted P-value) downregulated in HLY-1 cells treated with CsA for 2 hours (unpaired analysis). Each bubble in the figure represents one of most highly significant genes differentially expressed upon treatment with CsA. The larger the bubble the lower the adjusted P-value. Data excludes genes marked as N/A.

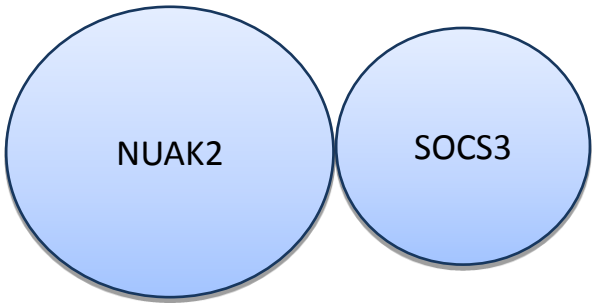

Appendix Figure 11. The top 2 statistically significant genes (ranked by adjusted P-value) upregulated in HLY-1 cells treated with CsA for 2 hours (unpaired analysis). Each bubble in the figure represents one of most highly significant genes differentially expressed upon treatment with CsA. The larger the bubble the lower the adjusted P-value. Data excludes genes marked as N/A.

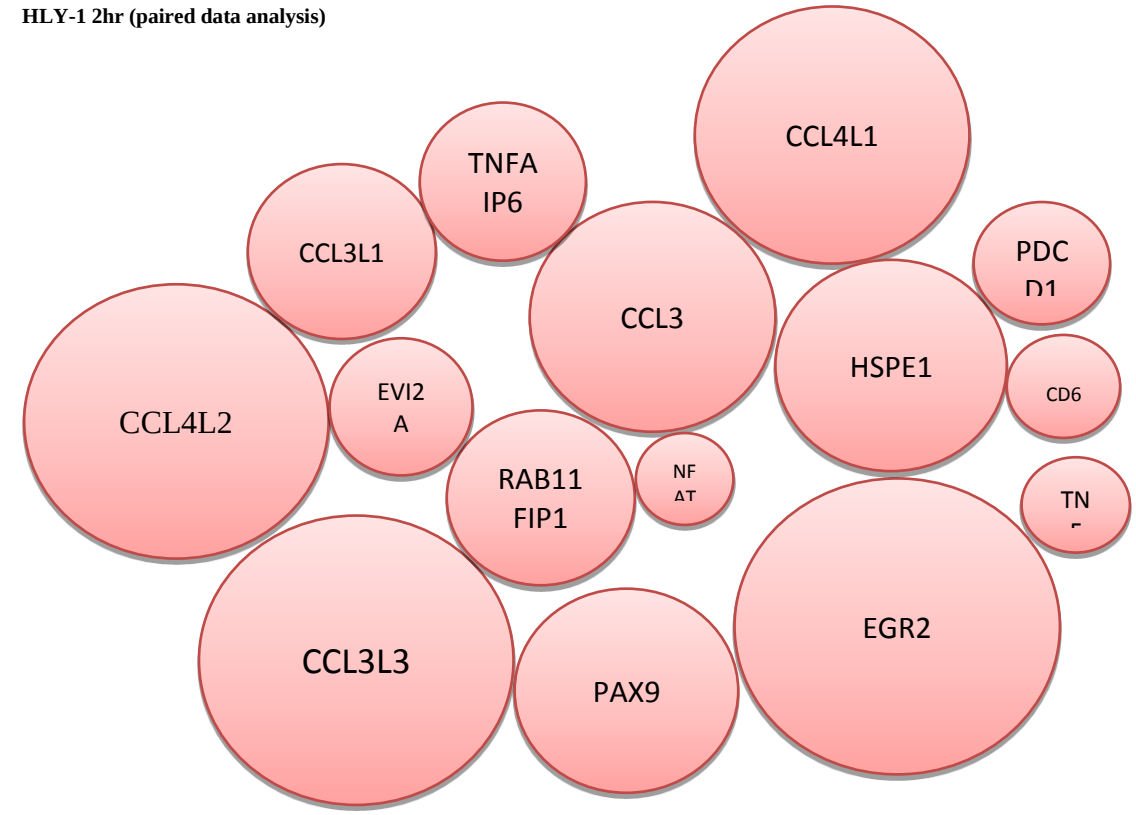

Appendix Figure 12. The top 15 statistically significant genes (ranked by adjusted P-value) downregulated in HLY-1 cells treated with CsA for 2 hours (paired analysis). Each bubble in the figure represents one of most highly significant genes differentially expressed upon treatment with CsA. The larger the bubble the lower the adjusted P-value. Data excludes genes marked as N/A.

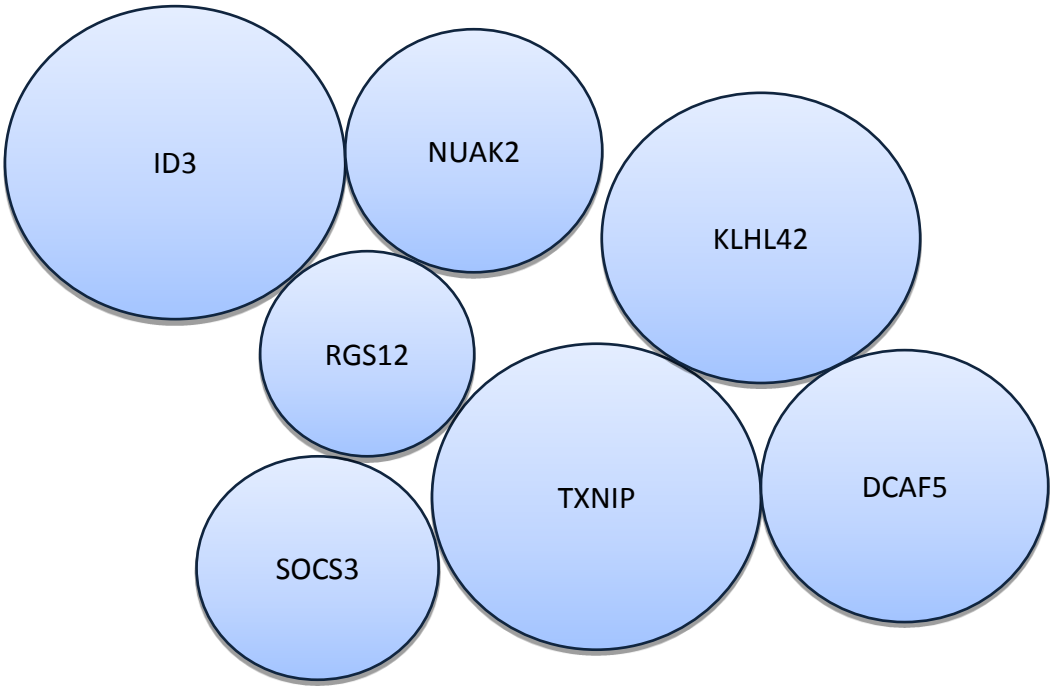

Appendix Figure 13. The top 7 statistically significant genes (ranked by adjusted P-value) upregulated in HLY-1 cells treated with CsA for 2 hours (paired analysis). Each bubble in the figure represents one of most highly significant genes differentially expressed upon treatment with CsA. The larger the bubble the lower the adjusted P-value. Data excludes genes marked as N/A.

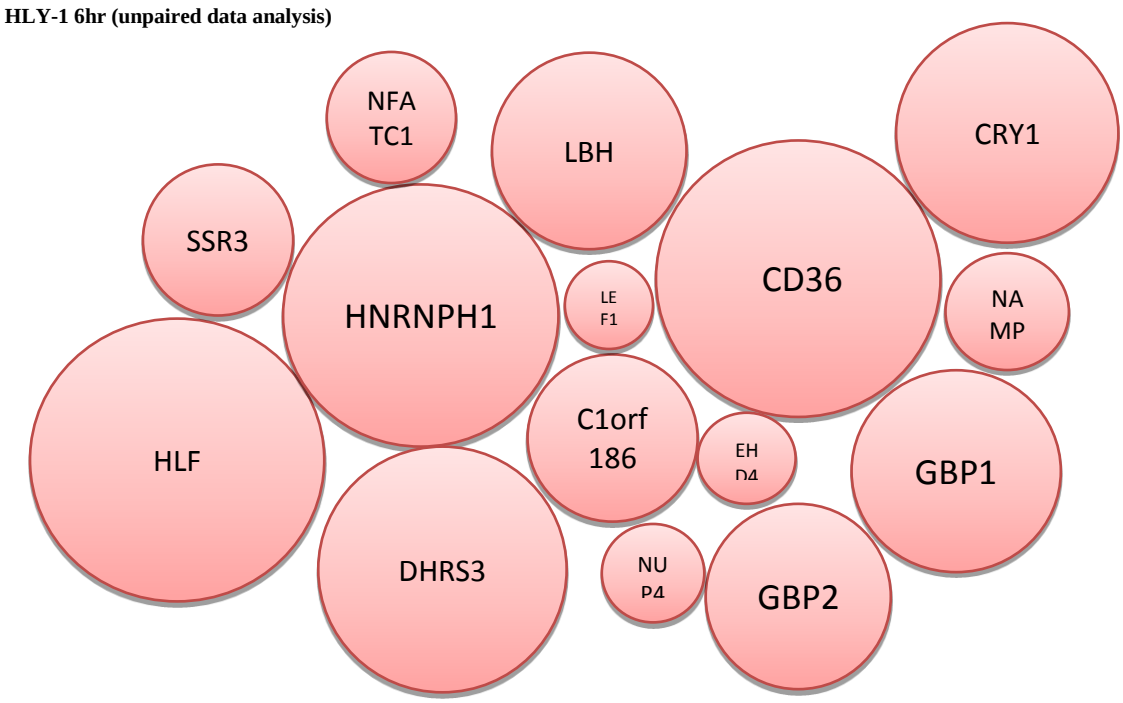

Appendix Figure 14. The top 15 statistically significant genes (ranked by adjusted P-value) downregulated in HLY-1 cells treated with CsA for 6 hours (unpaired analysis). Each bubble in the figure represents one of most highly significant genes differentially expressed upon treatment with CsA. The larger the bubble the lower the adjusted P-value. Data excludes genes marked as N/A.

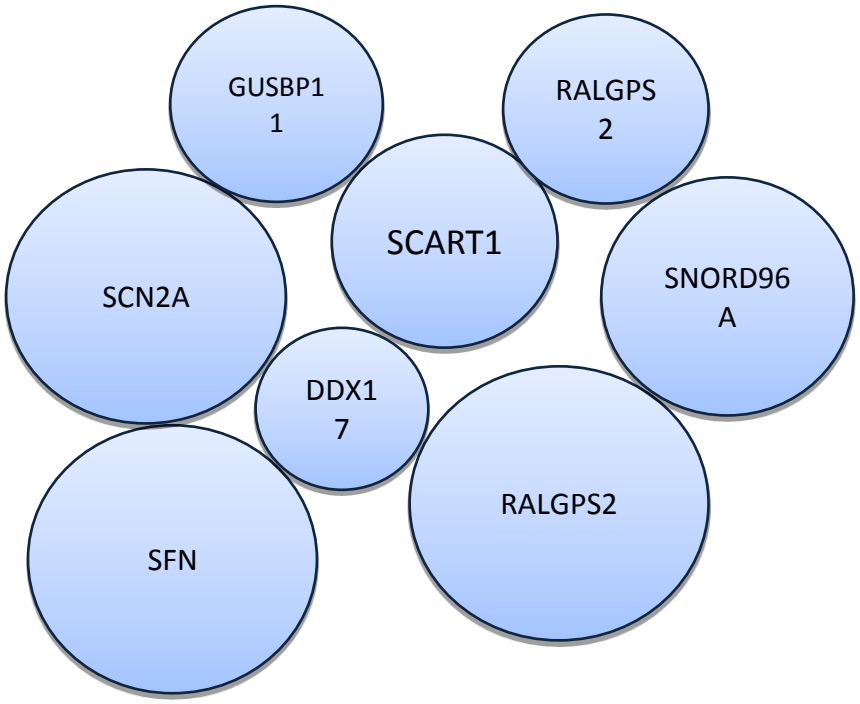

Appendix Figure 15. The top 8 statistically significant genes (ranked by adjusted P-value) upregulated in HLY-1 cells treated with CsA for 6 hours (unpaired analysis). Each bubble in the figure represents one of most highly significant genes differentially expressed upon treatment with CsA. The larger the bubble the lower the adjusted P-value. Data excludes genes marked as N/A.

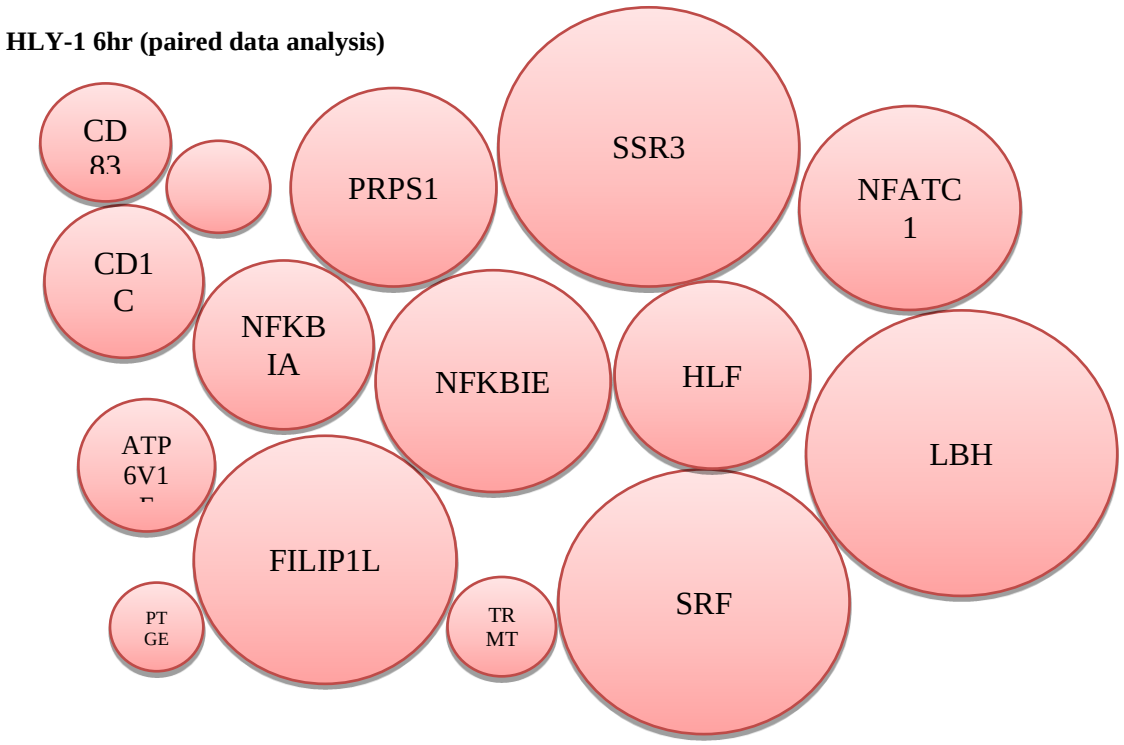

Appendix Figure 16. The top 15 statistically significant genes (ranked by adjusted P-value) downregulated in HLY-1 cells treated with CsA for 6 hours (paired analysis). Each bubble in the figure represents one of most highly significant genes differentially expressed upon treatment with CsA. The larger the bubble the lower the adjusted P-value Data excludes genes marked as N/A..

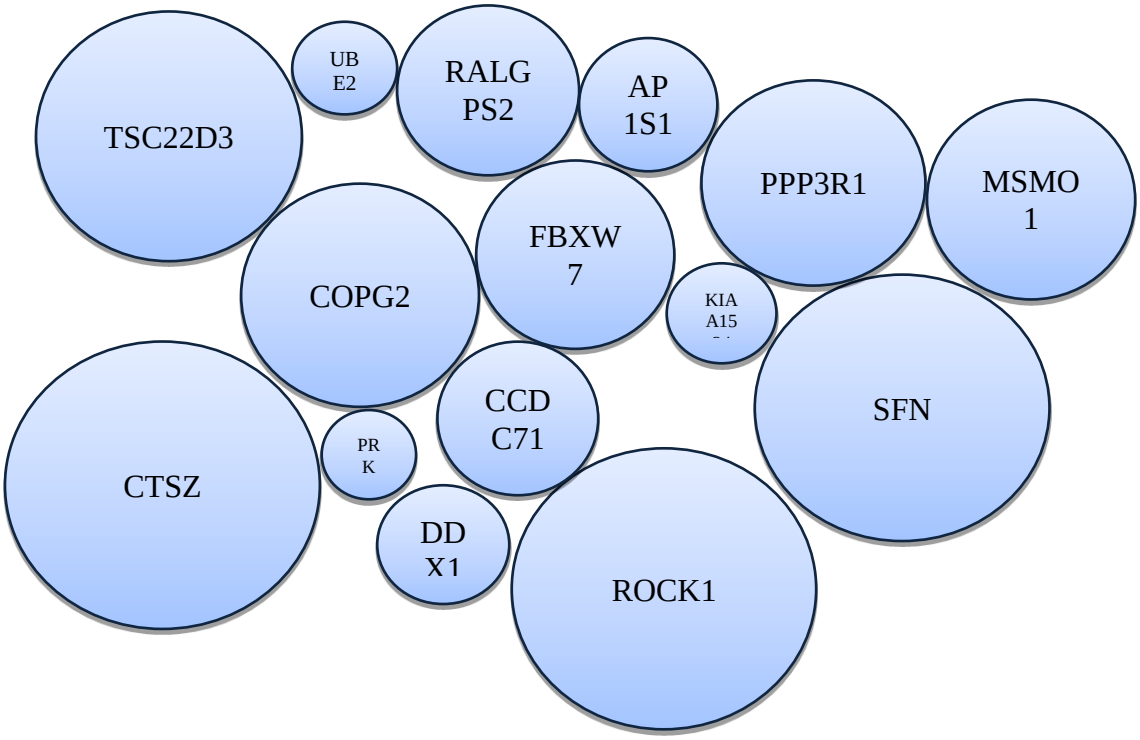

Appendix Figure 17. The top 15 statistically significant genes (ranked by P-value) upregulated in HLY-1 cells treated with CsA for 6 hours (paired analysis). Each bubble in the figure represents one of most highly significant genes differentially expressed upon treatment with CsA. The larger the bubble the lower the adjusted P-value. Data excludes genes marked as N/A.

WSU-NHL 6hr (unpaired data analysis)

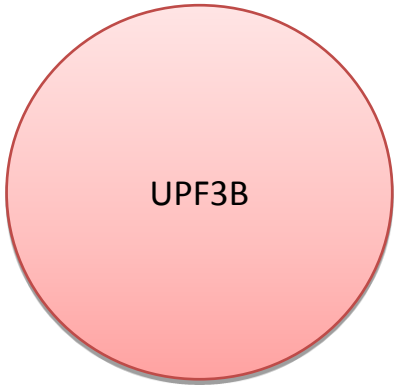

Appendix Figure 18. The top statistically significant gene (ranked by adjusted P-value) downregulated in WSU-NHL cells treated with CsA for 6 hours (unpaired analysis). Each bubble in the figure represents one of most highly significant genes differentially expressed upon treatment with CsA. The larger the bubble the lower the adjusted P-value. Data excludes genes marked as N/A.

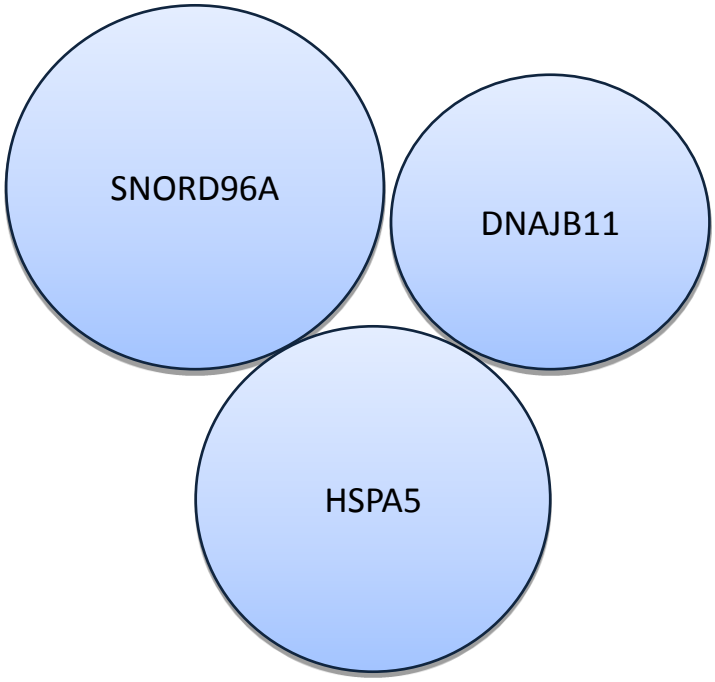

Appendix Figure 19. The top 3 statistically significant genes (ranked by adjusted P-value) upregulated in WSU-NHL cells treated with CsA for 6 hours (unpaired analysis). Each bubble in the figure represents one of most highly significant genes differentially expressed upon treatment with CsA. The larger the bubble the lower the adjusted P-value. Data excludes genes marked as N/A.

Gene sets enriched in vehicle phenotype vs. CsA – HLY-1 2hrs (4 samples)

	GS follow link to MSigDB	SIZE	ES	NES	NOM p-val	FDR q-val	FWER p-val	RANK AT MAX	LEADING EDGE
1	UZONYI_RESPONSE_TO_LEUKOTRIENE_AND_THROMBIN	37	0.79	2.53	0.000	0.000	0.000	1952	tags=41%, list=6%, signal=43%
2	NAGASHIMA_EGF_SIGNALING_UP	56	0.67	2.35	0.000	0.000	0.000	2132	tags=45%, list=6%, signal=48%
3	SEKI_INFLAMMATORY_RESPONSE_LPS_UP	74	0.62	2.32	0.000	0.000	0.000	2500	tags=27%, list=7%, signal=29%
4	DIRMEIER_LMP1_RESPONSE_EARLY	66	0.64	2.29	0.000	0.000	0.000	1900	tags=33%, list=6%, signal=35%
5	PHONG_TNF_TARGETS_UP	61	0.62	2.23	0.000	0.002	0.008	2574	tags=43%, list=8%, signal=46%
6	PID_TCRCALCIUMPATHWAY	29	0.72	2.22	0.000	0.002	0.010	1587	tags=28%, list=5%, signal=29%
7	SAFFORD_T_LYMPHOCYTE_ANERGY	87	0.57	2.20	0.000	0.003	0.016	2605	tags=26%, list=8%, signal=29%
8	AMIT_SERUM_RESPONSE_60_MCF10A	55	0.63	2.20	0.000	0.003	0.018	2490	tags=33%, list=7%, signal=35%
9	ABE_VEGFA_TARGETS	20	0.76	2.19	0.002	0.003	0.022	871	tags=25%, list=3%, signal=26%
10	PID_NFAT_TFPATHWAY	47	0.64	2.15	0.000	0.006	0.053	1696	tags=23%, list=5%, signal=25%
11	AMIT_EGF_RESPONSE_120_MCF10A	42	0.66	2.14	0.000	0.007	0.063	3017	tags=36%, list=9%, signal=39%
12	BROWNE_HCMV_INFECTION_2HR_UP	39	0.65	2.13	0.000	0.007	0.071	2500	tags=33%, list=7%, signal=36%
13	DORN_ADENOVIRUS_INFECTION_32HR_DN	37	0.66	2.09	0.000	0.011	0.116	1697	tags=32%, list=5%, signal=34%
14	DORN_ADENOVIRUS_INFECTION_48HR_DN	38	0.64	2.09	0.000	0.011	0.129	1697	tags=32%, list=5%, signal=33%
15	ZHOU_TNF_SIGNALING_30MIN	53	0.60	2.08	0.000	0.012	0.144	2697	tags=36%, list=8%, signal=39%
16	ABE_VEGFA_TARGETS_30MIN	29	0.67	2.06	0.000	0.015	0.197	1542	tags=24%, list=5%, signal=25%
17	SMIRNOV_RESPONSE_TO_IR_2HR_UP	48	0.61	2.05	0.000	0.015	0.200	3555	tags=40%, list=10%, signal=44%
18	LIN_NPAS4_TARGETS_DN	62	0.56	2.05	0.000	0.015	0.210	1696	tags=13%, list=5%, signal=14%
19	REACTOME_NONSENSE_MEDIATED_DECAY_ENHANCED_BY_THE_EXON_JUNCTION_COMPLEX	111	0.52	2.05	0.000	0.015	0.221	5158	tags=48%, list=15%, signal=56%
20	REACTOME_PD1_SIGNALING	18	0.74	2.04	0.000	0.016	0.248	1955	tags=33%, list=6%, signal=35%
21	PEDERSEN_METASTASIS_BY_ERBB2_ISOFORM_1	44	0.61	2.03	0.000	0.016	0.271	909	tags=18%, list=3%, signal=19%
22	AMIT_EGF_RESPONSE_120_HELA	67	0.57	2.02	0.000	0.019	0.315	2871	tags=34%, list=8%, signal=37%
23	ST_DIFFERENTIATION_PATHWAY_IN_PC12_CELLS	45	0.58	2.00	0.000	0.023	0.378	4956	tags=38%, list=15%, signal=44%
24	PLASARI_TGFB1_TARGETS_1HR_UP	32	0.63	1.99	0.000	0.024	0.406	2574	tags=31%, list=8%, signal=34%
25	SCHLOSSER_SERUM_RESPONSE_AUGMENTED_BY_MYC	100	0.51	1.99	0.000	0.023	0.407	2747	tags=29%, list=8%, signal=31%

Gene sets enriched in vehicle phenotype vs. CsA – HLY-1 2hrs (4 samples)

	GS follow link to MSigDB	SIZE	ES	NES	NOM p-val	FDR q-val	FWER p-val	RANK AT MAX	LEADING EDGE
26	KYNG_WERNER_SYNDROM_AND_NORMAL_AGING_UP	86	0.52	1.99	0.000	0.022	0.407	4657	tags=35%, list=14%, signal=40%
27	ZWANG_CLASS_2_TRANSIENTLY_INDUCED_BY_EGF	46	0.60	1.99	0.000	0.023	0.428	3162	tags=24%, list=9%, signal=26%
28	JOHNSTONE_PARVB_TARGETS_2_UP	135	0.49	1.97	0.000	0.029	0.529	3719	tags=34%, list=11%, signal=38%
29	PICCALUGA_ANGIOIMMUNOBLASTIC_LYMPHOMA_DN	124	0.49	1.97	0.000	0.029	0.533	4221	tags=39%, list=12%, signal=44%
30	BROWNE_HCMV_INFECTION_8HR_UP	102	0.51	1.96	0.000	0.028	0.537	2991	tags=28%, list=9%, signal=31%
31	WOOD_EBV_EBNA1_TARGETS_DN	47	0.58	1.96	0.000	0.028	0.546	2663	tags=26%, list=8%, signal=28%
32	LU_TUMOR_VASCULATURE_UP	29	0.64	1.96	0.000	0.028	0.558	4093	tags=31%, list=12%, signal=35%
33	KEGG_CHEMOKINE_SIGNALING_PATHWAY	188	0.45	1.96	0.000	0.027	0.559	1845	tags=13%, list=5%, signal=13%
34	AMIT_EGF_RESPONSE_40_HELA	41	0.59	1.96	0.000	0.027	0.561	3426	tags=44%, list=10%, signal=49%
35	WIERENGA_STAT5A_TARGETS_GROUP2	56	0.55	1.95	0.000	0.029	0.614	1758	tags=16%, list=5%, signal=17%
36	DORN_ADENOVIRUS_INFECTION_24HR_DN	41	0.59	1.94	0.003	0.030	0.636	1697	tags=29%, list=5%, signal=31%
37	OSWALD_HEMATOPOIETIC_STEM_CELL_IN_COLLAGEN_GEL_UP	225	0.45	1.94	0.000	0.030	0.645	2694	tags=22%, list=8%, signal=24%
38	AMIT_EGF_RESPONSE_40_MCF10A	18	0.70	1.94	0.000	0.030	0.654	4403	tags=61%, list=13%, signal=70%
39	KEGG_RIBOSOME	87	0.51	1.93	0.000	0.032	0.682	5034	tags=48%, list=15%, signal=56%
40	REACTOME_PEPTIDE_CHAIN_ELONGATION	90	0.50	1.93	0.000	0.032	0.698	5900	tags=52%, list=17%, signal=63%
41	NAGASHIMA_NRG1_SIGNALING_UP	169	0.46	1.92	0.000	0.033	0.705	3539	tags=33%, list=10%, signal=36%
42	PEDERSEN_METASTASIS_BY_ERBB2_ISOFORM_3	18	0.72	1.92	0.000	0.033	0.714	6549	tags=61%, list=19%, signal=76%
43	AMUNDSON_GENOTOXIC_SIGNATURE	101	0.50	1.92	0.000	0.032	0.714	2880	tags=29%, list=8%, signal=31%
44	AMIT_DELAYED_EARLY_GENES	17	0.70	1.92	0.002	0.032	0.715	4231	tags=53%, list=12%, signal=60%
45	BROCKE_APOPTOSIS_REVERSED_BY_IL6	139	0.46	1.92	0.000	0.033	0.740	2696	tags=28%, list=8%, signal=30%
46	BORLAK_LIVER_CANCER_EGF_UP	56	0.54	1.91	0.000	0.034	0.744	3000	tags=29%, list=9%, signal=31%
47	JECHLINGER_EPITHELIAL_TO_MESENCHYMAL_TRANSITION_DN	66	0.53	1.91	0.000	0.034	0.749	4117	tags=35%, list=12%, signal=40%
48	REACTOME_INFLUENZA_LIFE_CYCLE	140	0.46	1.91	0.000	0.033	0.749	5158	tags=44%, list=15%, signal=51%
49	REACTOME_CHEMOKINE_RECEPTORS_BIND_CHEMOKINES	55	0.55	1.91	0.000	0.033	0.752	1607	tags=11%, list=5%, signal=11%
50	REACTOME_G_BETA_GAMMA_SIGNALLING_THROUGH_PI3KGAMMA	25	0.64	1.90	0.002	0.034	0.764	4726	tags=48%, list=14%, signal=56%

Appendix Table 10 (Continued from previous page). Top 50 gene sets enriched in HLY-1 cells treated with CsA for 2hrs (enrichment in vehicle sample phenotypes compared to CsA-treated samples). The table shows the top 50 enriched gene sets (ordered by false discovery rate FDR) for HLY-1 cells treated with CsA for 2hrs. Columns indicate gene set name, size, enrichment score (ES), normalised enrichment score (NES), nominal P-value (NOM), family-wise error rate (FWER), rank at maximum enrichment score and definition of the leading edge subset. Data is based on paired microarray analysis.

Gene sets enriched in CsA treatment phenotype vs. vehicle – HLY-1 2hrs (4 samples)

	GS follow link to MSigDB	SIZE	ES	NES	NOM p-val	FDR q-val	FWER p-val	RANK AT MAX	LEADING EDGE
1	VALK_AML_CLUSTER_5	32	-0.71	-2.16	0.000	0.002	0.002	1431	tags=28%, list=4%, signal=29%
2	YAN_ESCAPE_FROM_ANOIKIS	24	-0.69	-1.95	0.000	0.096	0.187	2475	tags=42%, list=7%, signal=45%
3	ZHAN_MULTIPLE_MYELOMA_CD1_VS_CD2_UP	64	-0.57	-1.95	0.000	0.066	0.193	3622	tags=31%, list=11%, signal=35%
4	ACEVEDO_NORMAL_TISSUE_ADJACENT_TO_LIVER_TUMOR_DN	336	-0.45	-1.95	0.000	0.055	0.213	3994	tags=30%, list=12%, signal=34%
5	COATES_MACROPHAGE_M1_VS_M2_DN	70	-0.56	-1.94	0.000	0.052	0.242	6401	tags=41%, list=19%, signal=51%
6	HORTON_SREBF_TARGETS	25	-0.68	-1.93	0.002	0.050	0.279	1520	tags=36%, list=4%, signal=38%
7	REICHERT_MITOSIS_LIN9_TARGETS	26	-0.67	-1.92	0.002	0.054	0.336	4045	tags=42%, list=12%, signal=48%
8	GINESTIER_BREAST_CANCER_20Q13_AMPLIFICATION_DN	147	-0.49	-1.90	0.000	0.059	0.393	4189	tags=37%, list=12%, signal=42%
9	REACTOME_RNA_POL_III_TRANSCRIPTION_INITIATION_FROM_TYPE_3_PROMOTER	26	-0.66	-1.90	0.000	0.054	0.403	3711	tags=54%, list=11%, signal=60%
10	REACTOME_YAP1_AND_WWTR1_TAZ_STIMULATED_GENE_EXPRESSION	24	-0.67	-1.89	0.002	0.057	0.459	2227	tags=33%, list=7%, signal=36%
11	GENTILE_UV_RESPONSE_CLUSTER_D8	38	-0.59	-1.85	0.002	0.103	0.714	3124	tags=34%, list=9%, signal=38%
12	BIOCARTA_WNT_PATHWAY	25	-0.65	-1.85	0.000	0.095	0.714	6127	tags=48%, list=18%, signal=58%
13	FARDIN_HYPOXIA_11	28	-0.64	-1.84	0.002	0.102	0.756	1377	tags=32%, list=4%, signal=33%
14	PYEON_HPV_POSITIVE_TUMORS_UP	82	-0.52	-1.83	0.000	0.099	0.768	7035	tags=46%, list=21%, signal=58%
15	DEBIASI_APOPTOSIS_BY_REOVIRUS_INFECTION_DN	276	-0.43	-1.81	0.000	0.122	0.862	3924	tags=26%, list=12%, signal=29%
16	KEGG_BLADDER_CANCER	42	-0.57	-1.81	0.004	0.115	0.862	3483	tags=29%, list=10%, signal=32%
17	KEGG_PORPHYRIN_AND_CHLOROPHYLL_METABOLISM	41	-0.58	-1.81	0.000	0.108	0.863	5337	tags=37%, list=16%, signal=43%
18	LE_NEURONAL_DIFFERENTIATION_DN	19	-0.69	-1.81	0.000	0.105	0.871	1784	tags=42%, list=5%, signal=44%
19	GENTILE_UV_LOW_DOSE_DN	64	-0.52	-1.79	0.002	0.130	0.934	3505	tags=30%, list=10%, signal=33%
20	STAMBOLSKY_RESPONSE_TO_VITAMIN_D3_DN	23	-0.65	-1.79	0.000	0.129	0.939	4115	tags=30%, list=12%, signal=35%
21	REACTOME_ANTIGEN_PROCESSING_UBIQUITINATION_PROTEASOME_DEGRADATION	206	-0.44	-1.78	0.000	0.137	0.957	4835	tags=31%, list=14%, signal=35%
22	SARTIPY_NORMAL_AT_INSULIN_RESISTANCE_DN	16	-0.69	-1.77	0.005	0.142	0.966	6399	tags=50%, list=19%, signal=62%
23	KEGG_UBIQUITIN_MEDIATED_PROTEOLYSIS	137	-0.46	-1.76	0.000	0.157	0.982	4557	tags=34%, list=13%, signal=39%
24	GARGALOVIC_RESPONSE_TO_OXIDIZED_PHOSPHOLIPIDS_RED_DN	24	-0.62	-1.76	0.007	0.150	0.983	6345	tags=46%, list=19%, signal=56%
25	KEGG_BUTANOATE_METABOLISM	34	-0.58	-1.76	0.003	0.146	0.984	4798	tags=32%, list=14%, signal=38%

Gene sets enriched in CsA treatment phenotype vs. vehicle – HLY-1 2hrs (4 samples)

	GS follow link to MSigDB	SIZE	ES	NES	NOM p-val	FDR q-val	FWER p-val	RANK AT MAX	LEADING EDGE
26	NIKOLSKY_BREAST_CANCER_16Q24_AMPLICON	46	-0.55	-1.75	0.005	0.157	0.990	2393	tags=26%, list=7%, signal=28%
27	BIOCARTA_TH1TH2_PATHWAY	19	-0.66	-1.75	0.005	0.154	0.991	3224	tags=32%, list=9%, signal=35%
28	GARGALOVIC_RESPONSE_TO_OXIDIZED_PHOSPHOLIPIDS_RED_UP	16	-0.69	-1.75	0.004	0.149	0.991	3442	tags=56%, list=10%, signal=63%
29	REACTOME_CONVERSION_FROM_APC_C_CDC20_TO_APC_C_CDH1_IN_LATE_ANAPHASE	20	-0.64	-1.75	0.000	0.145	0.991	4149	tags=35%, list=12%, signal=40%
30	TOOKER_GEMCITABINE_RESISTANCE_DN	121	-0.46	-1.75	0.000	0.140	0.991	3528	tags=31%, list=10%, signal=35%
31	CHARAFE_BREAST_CANCER_LUMINAL_VS_BASAL_UP	345	-0.41	-1.75	0.000	0.136	0.991	4544	tags=26%, list=13%, signal=29%
32	PID_RB_1PATHWAY	65	-0.50	-1.74	0.003	0.148	0.993	2488	tags=29%, list=7%, signal=31%
33	REACTOME_CLASS_I_MHC_MEDIATED_ANTIGEN_PROCESSING_PRESENTATION	244	-0.42	-1.74	0.000	0.144	0.993	4835	tags=30%, list=14%, signal=34%
34	HALMOS_CEBPA_TARGETS_DN	45	-0.53	-1.73	0.002	0.145	0.993	4047	tags=33%, list=12%, signal=38%
35	REACTOME_APC_C_CDH1_MEDIATED_DEGRADATION_OF_CDC20_AND_OTHER_APC_C_CDH1_TARGETED_PROTEINS_IN_LATE_MITOSIS_EARLY_G1	69	-0.49	-1.73	0.002	0.142	0.993	4791	tags=35%, list=14%, signal=40%
36	SILIGAN_TARGETS_OF_EWS_FLI1_FUSION_DN	17	-0.66	-1.73	0.002	0.139	0.993	3446	tags=35%, list=10%, signal=39%
37	FLECHNER_BIOPSY_KIDNEY_TRANSPLANT_REJECTED_VS_OK_UP	85	-0.48	-1.73	0.000	0.135	0.994	3858	tags=28%, list=11%, signal=32%
38	REACTOME_RNA_POL_III_TRANSCRIPTION	33	-0.58	-1.73	0.002	0.135	0.995	3721	tags=48%, list=11%, signal=54%
39	REACTOME_ENERGY_DEPENDENT_REGULATION_OF_MTOR_BY_LKB1_AMPK	17	-0.67	-1.73	0.007	0.132	0.996	3281	tags=41%, list=10%, signal=46%
40	MARIADASON_RESPONSE_TO_CURCUMIN_SULINDAC_5	23	-0.61	-1.73	0.007	0.130	0.997	6233	tags=52%, list=18%, signal=64%
41	DEMAGALHAES_AGING_DN	15	-0.68	-1.72	0.003	0.138	0.999	7857	tags=60%, list=23%, signal=78%
42	KEGG_MTOR_SIGNALING_PATHWAY	51	-0.52	-1.72	0.002	0.140	0.999	2755	tags=25%, list=8%, signal=28%
43	XU_HGF_SIGNALING_NOT_VIA_AKT1_48HR_DN	17	-0.66	-1.72	0.004	0.137	0.999	4623	tags=47%, list=14%, signal=54%
44	ZHAN_VARIABLE_EARLY_DIFFERENTIATION_GENES_DN	29	-0.59	-1.72	0.007	0.141	1.000	3505	tags=41%, list=10%, signal=46%
45	STARK_HYPPOCAMPUS_22Q11_DELETION_UP	48	-0.52	-1.71	0.002	0.141	1.000	5018	tags=42%, list=15%, signal=49%
46	GUENTHER_GROWTH_SPHERICAL_VS_ADHERENT_DN	26	-0.61	-1.71	0.003	0.144	1.000	2099	tags=31%, list=6%, signal=33%
47	DING_LUNG_CANCER_BY_MUTATION_RATE	20	-0.63	-1.71	0.007	0.141	1.000	2896	tags=25%, list=8%, signal=27%
48	SA_G1_AND_S_PHASES	15	-0.68	-1.70	0.007	0.157	1.000	2614	tags=33%, list=8%, signal=36%
49	BRACHAT_RESPONSE_TO_CAMPTOTHECIN_UP	26	-0.59	-1.70	0.007	0.154	1.000	2745	tags=31%, list=8%, signal=33%
50	HELLER_HDAC_TARGETS_SILENCED_BY_METHYLATION_DN	266	-0.41	-1.70	0.000	0.155	1.000	3664	tags=26%, list=11%, signal=29%

Appendix Table 11 (Continued from previous page). Top 50 gene sets enriched in HLY-1 cells treated with CsA for 2hrs (enrichment in CsA treated sample phenotypes compared to vehicle samples). The table shows the top 50 enriched gene sets (ordered by false discovery rate FDR) for HLY-1 cells treated with CsA for 2hrs. Columns indicate gene set name, size, enrichment score (ES), normalised enrichment score (NES), nominal P-value (NOM), family-wise error rate (FWER), rank at maximum enrichment score and definition of the leading edge subset. Data is based on paired microarray analysis.

Gene sets enriched in vehicle phenotype vs. CsA – U2932 2hrs (4 samples)

	GS follow link to MSigDB	SIZE	ES	NES	NOM p-val	FDR q-val	FWER p-val	RANK AT MAX	LEADING EDGE
1	DIRMEIER_LMP1_RESPONSE_EARLY	66	0.72	2.33	0.000	0.000	0.000	2224	tags=38%, list=7%, signal=40%
2	DORN_ADENOVIRUS_INFECTION_24HR_DN	41	0.74	2.21	0.000	0.012	0.023	2265	tags=41%, list=7%, signal=44%
3	PID_NFAT_TFPATHWAY	47	0.70	2.14	0.000	0.025	0.073	344	tags=13%, list=1%, signal=13%
4	FRASOR_RESPONSE_TO_ESTRADIOL_UP	37	0.71	2.10	0.000	0.042	0.159	3302	tags=24%, list=10%, signal=27%
5	DORN_ADENOVIRUS_INFECTION_48HR_DN	38	0.71	2.10	0.000	0.035	0.165	2265	tags=37%, list=7%, signal=39%
6	SEKI_INFLAMMATORY_RESPONSE_LPS_UP	74	0.61	2.08	0.000	0.034	0.188	2749	tags=26%, list=8%, signal=28%
7	SAFFORD_T_LYMPHOCYTE_ANERGY	87	0.60	2.08	0.000	0.033	0.208	2272	tags=23%, list=7%, signal=25%
8	DORN_ADENOVIRUS_INFECTION_32HR_DN	37	0.71	2.08	0.000	0.029	0.209	2265	tags=38%, list=7%, signal=40%
9	VILIMAS_NOTCH1_TARGETS_UP	52	0.65	2.06	0.000	0.033	0.258	1590	tags=25%, list=5%, signal=26%
10	MORI_PLASMA_CELL_DN	30	0.73	2.01	0.000	0.053	0.410	2271	tags=40%, list=7%, signal=43%
11	ACEVEDO_NORMAL_TISSUE_ADJACENT_TO_LIVER_TUMOR_UP	160	0.54	2.01	0.000	0.049	0.418	3117	tags=35%, list=9%, signal=38%
12	DEBOSSCHER_NFKB_TARGETS_REPRESSED_BY_GLUCOCORTICOIDS	24	0.75	1.98	0.000	0.063	0.528	9	tags=8%, list=0%, signal=8%
13	DUTTA_APOPTOSIS_VIA_NFKB	32	0.69	1.96	0.002	0.071	0.586	2224	tags=34%, list=7%, signal=37%
14	PLASARI_TGFB1_TARGETS_1HR_UP	32	0.68	1.95	0.000	0.075	0.639	1674	tags=25%, list=5%, signal=26%
15	DORN_ADENOVIRUS_INFECTION_12HR_DN	32	0.69	1.94	0.000	0.084	0.714	2633	tags=41%, list=8%, signal=44%
16	ZHAN_EARLY_DIFFERENTIATION_GENES_DN	42	0.64	1.94	0.000	0.081	0.728	1544	tags=24%, list=5%, signal=25%
17	BASSO_CD40_SIGNALING_UP	101	0.55	1.92	0.000	0.091	0.787	2067	tags=30%, list=6%, signal=32%
18	JIANG_AGING_CEREBRAL_CORTEX_UP	34	0.67	1.92	0.000	0.088	0.791	4481	tags=47%, list=13%, signal=54%
19	MILI_PSEUDOPODIA_HAPTOTAXIS_UP	474	0.46	1.91	0.000	0.086	0.803	3113	tags=28%, list=9%, signal=31%
20	MUELLER_PLURINET	282	0.48	1.91	0.000	0.083	0.806	2915	tags=32%, list=9%, signal=35%
21	BIOCARTA_PML_PATHWAY	17	0.76	1.90	0.000	0.089	0.853	1663	tags=24%, list=5%, signal=25%
22	PID_TCRCALCIUMPATHWAY	29	0.67	1.88	0.002	0.102	0.907	344	tags=14%, list=1%, signal=14%
23	LINDSTEDT_DENDRITIC_CELL_MATURATION_A	66	0.57	1.87	0.000	0.108	0.926	2315	tags=20%, list=7%, signal=21%
24	BENPORATH_PROLIFERATION	137	0.51	1.87	0.000	0.107	0.929	5657	tags=50%, list=17%, signal=59%
25	REACTOME_RNA_POL_II_TRANSCRIPTION_PRE_INITIATION_AND_PROMOTER_OPENING	41	0.62	1.86	0.007	0.107	0.936	2567	tags=46%, list=8%, signal=50%

Gene sets enriched in vehicle phenotype vs. CsA – U2932 2hrs (4 samples)

	GS follow link to MSigDB	SIZE	ES	NES	NOM p-val	FDR q-val	FWER p-val	RANK AT MAX	LEADING EDGE
26	LE_EGR2_TARGETS_UP	105	0.53	1.86	0.000	0.105	0.940	2616	tags=34%, list=8%, signal=37%
27	GALINDO_IMMUNE_RESPONSE_TO_ENTEROTOXIN	83	0.56	1.86	0.000	0.102	0.940	1232	tags=20%, list=4%, signal=21%
28	DANG_MYC_TARGETS_UP	138	0.51	1.86	0.000	0.100	0.943	6143	tags=41%, list=18%, signal=49%
29	SESTO_RESPONSE_TO_UV_C0	106	0.53	1.86	0.000	0.097	0.943	4721	tags=42%, list=14%, signal=48%
30	BIOCARTA_VIP_PATHWAY	26	0.67	1.85	0.005	0.100	0.957	98	tags=15%, list=0%, signal=15%
31	PID_WNT_NONCANONICAL_PATHWAY	30	0.66	1.85	0.000	0.102	0.963	3342	tags=33%, list=10%, signal=37%
32	BROWNE_HCMV_INFECTION_8HR_UP	102	0.53	1.84	0.000	0.101	0.963	2146	tags=25%, list=6%, signal=26%
33	KEGG_CHEMOKINE_SIGNALING_PATHWAY	188	0.49	1.83	0.000	0.111	0.974	2068	tags=12%, list=6%, signal=13%
34	BIOCARTA_CDC42RAC_PATHWAY	16	0.76	1.83	0.002	0.108	0.974	3004	tags=50%, list=9%, signal=55%
35	PUJANA_BREAST_CANCER_WITH_BRCA1_MUTATED_UP	52	0.59	1.83	0.005	0.105	0.975	2616	tags=40%, list=8%, signal=44%
36	HINATA_NFKB_TARGETS_FIBROBLAST_UP	83	0.54	1.83	0.000	0.105	0.976	2749	tags=27%, list=8%, signal=29%
37	ROSTY_CERVICAL_CANCER_PROLIFERATION_CLUSTER	137	0.50	1.83	0.003	0.102	0.977	2793	tags=34%, list=8%, signal=36%
38	SENESE_HDAC2_TARGETS_UP	108	0.51	1.82	0.000	0.104	0.981	5914	tags=39%, list=17%, signal=47%
39	MALONEY_RESPONSE_TO_17AAG_DN	76	0.55	1.82	0.002	0.105	0.984	2390	tags=30%, list=7%, signal=32%
40	SONG_TARGETS_OF_IE86_CMV_PROTEIN	58	0.57	1.82	0.003	0.103	0.984	2016	tags=38%, list=6%, signal=40%
41	BIOCARTA_GATA3_PATHWAY	16	0.73	1.81	0.005	0.104	0.986	5781	tags=50%, list=17%, signal=60%
42	KOBAYASHI_EGFR_SIGNALING_24HR_DN	239	0.47	1.81	0.000	0.103	0.987	3182	tags=33%, list=9%, signal=36%
43	CROONQUIST_NRAS_SIGNALING_DN	71	0.55	1.81	0.005	0.101	0.988	3065	tags=42%, list=9%, signal=46%
44	ST_TUMOR_NECROSIS_FACTOR_PATHWAY	28	0.64	1.81	0.012	0.100	0.988	1254	tags=25%, list=4%, signal=26%
45	NEMETH_INFLAMMATORY_RESPONSE_LPS_UP	87	0.53	1.81	0.000	0.098	0.988	3487	tags=33%, list=10%, signal=37%
46	KAMMINGA_EZH2_TARGETS	41	0.59	1.81	0.002	0.098	0.989	2616	tags=34%, list=8%, signal=37%
47	PID_HDAC_CLASSI_PATHWAY	66	0.55	1.81	0.000	0.097	0.991	3335	tags=33%, list=10%, signal=37%
48	ABRAMSON_INTERACT_WITH_AIRE	42	0.60	1.81	0.003	0.096	0.991	3493	tags=48%, list=10%, signal=53%
49	AMIT_SERUM_RESPONSE_60_MCF10A	55	0.57	1.80	0.005	0.094	0.991	3164	tags=22%, list=9%, signal=24%
50	ZHAN_MULTIPLE_MYELOMA_PR_UP	44	0.59	1.80	0.005	0.097	0.993	3919	tags=41%, list=12%, signal=46%

Appendix Table 12 (Continued from previous page). Top 50 gene sets enriched in U2932 cells treated with CsA for 2hrs (enrichment in vehicle sample phenotypes compared to CsA-treated samples). The table shows the top 50 enriched gene sets (ordered by false discovery rate FDR) for U2932 cells treated with CsA for 2hrs. Columns indicate gene set name, size, enrichment score (ES), normalised enrichment score (NES), nominal P-value (NOM), family-wise error rate (FWER), rank at maximum enrichment score and definition of the leading edge subset. Data is based on paired microarray analysis.

Gene sets enriched in CsA treatment phenotype vs. vehicle – U2932 2hrs (4 samples)

	GS follow link to MSigDB	SIZE	ES	NES	NOM p-val	FDR q-val	FWER p-val	RANK AT MAX	LEADING EDGE
1	NIKOLSKY_BREAST_CANCER_16Q24_AMPLICON	46	-0.75	-2.21	0.000	0.000	0.000	3469	tags=41%, list=10%, signal=46%
2	KRIGE_AMINO_ACID_DEPRIVATION	29	-0.79	-2.14	0.000	0.000	0.000	2519	tags=48%, list=7%, signal=52%
3	DEBIASI_APOPTOSIS_BY_REOVIRUS_INFECTION_DN	276	-0.56	-2.12	0.000	0.000	0.000	4864	tags=41%, list=14%, signal=48%
4	ACEVEDO_NORMAL_TISSUE_ADJACENT_TO_LIVER_TUMOR_DN	336	-0.54	-2.09	0.000	0.000	0.001	4568	tags=39%, list=13%, signal=45%
5	HELLER_SILENCED_BY_METHYLATION_DN	102	-0.61	-2.06	0.000	0.001	0.006	2746	tags=29%, list=8%, signal=32%
6	FERRARI_RESPONSE_TO_FENRETINIDE_UP	19	-0.82	-2.01	0.000	0.003	0.019	2605	tags=42%, list=8%, signal=46%
7	WANG_NEOPLASTIC_TRANSFORMATION_BY_CCND1_MYC	21	-0.79	-1.98	0.000	0.006	0.043	357	tags=19%, list=1%, signal=19%
8	GARGALOVIC_RESPONSE_TO_OXIDIZED_PHOSPHOLIPIDS_RED_DN	24	-0.75	-1.98	0.000	0.006	0.046	3557	tags=33%, list=10%, signal=37%
9	ZHAN_MULTIPLE_MYELOMA_CD1_UP	45	-0.68	-1.96	0.000	0.009	0.075	2140	tags=27%, list=6%, signal=28%
10	ZHANG_TLX_TARGETS_60HR_UP	286	-0.51	-1.96	0.000	0.008	0.076	3603	tags=24%, list=11%, signal=27%
11	SENGUPTA_EBNA1_ANTICORRELATED	150	-0.55	-1.96	0.000	0.007	0.077	4217	tags=27%, list=12%, signal=30%
12	TANG_SENESCENCE_TP53_TARGETS_UP	33	-0.70	-1.94	0.000	0.009	0.099	1252	tags=18%, list=4%, signal=19%
13	GENTILE_UV_LOW_DOSE_DN	64	-0.61	-1.93	0.000	0.010	0.123	4290	tags=38%, list=13%, signal=43%
14	REACTOME_ACTIVATION_OF_CHAPERONE_GENES_BY_XBP1S	44	-0.66	-1.93	0.000	0.009	0.124	4185	tags=43%, list=12%, signal=49%
15	REACTOME_UNFOLDED_PROTEIN_RESPONSE	76	-0.60	-1.90	0.000	0.016	0.222	4185	tags=42%, list=12%, signal=48%
16	KEGG_PORPHYRIN_AND_CHLOROPHYLL_METABOLISM	41	-0.65	-1.89	0.002	0.020	0.283	1882	tags=27%, list=6%, signal=28%
17	LEE_AGING_MUSCLE_DN	44	-0.64	-1.89	0.000	0.020	0.294	5479	tags=45%, list=16%, signal=54%
18	ROYLANCE_BREAST_CANCER_16Q_COPY_NUMBER_UP	53	-0.62	-1.89	0.000	0.019	0.294	3725	tags=28%, list=11%, signal=32%
19	ZHAN_MULTIPLE_MYELOMA_CD1_VS_CD2_UP	64	-0.60	-1.86	0.000	0.029	0.437	3594	tags=33%, list=11%, signal=37%
20	HELLER_HDAC_TARGETS_SILENCED_BY_METHYLATION_DN	266	-0.50	-1.86	0.000	0.029	0.450	2875	tags=27%, list=8%, signal=30%
21	BLUM_RESPONSE_TO_SALIRASIB_UP	239	-0.50	-1.85	0.000	0.030	0.477	3683	tags=33%, list=11%, signal=37%
22	YOKOE_CANCER_TESTIS_ANTIGENS	33	-0.66	-1.85	0.000	0.031	0.507	3141	tags=36%, list=9%, signal=40%
23	VARELA_ZMPSTE24_TARGETS_UP	39	-0.64	-1.84	0.000	0.035	0.573	3156	tags=44%, list=9%, signal=48%
24	NIKOLSKY_BREAST_CANCER_16P13_AMPLICON	111	-0.54	-1.84	0.000	0.033	0.573	3549	tags=30%, list=10%, signal=33%
25	MARCINIAK_ER_STRESS_RESPONSE_VIA_CHOP	25	-0.69	-1.84	0.002	0.033	0.578	2583	tags=36%, list=8%, signal=39%

Gene sets enriched in CsA treatment phenotype vs. vehicle – U2932 2hrs (4 samples)

	GS follow link to MSigDB	SIZE	ES	NES	NOM p-val	FDR q-val	FWER p-val	RANK AT MAX	LEADING EDGE
26	GINESTIER_BREAST_CANCER_20Q13_AMPLIFICATION_DN	147	-0.52	-1.84	0.000	0.032	0.584	4050	tags=38%, list=12%, signal=43%
27	MARSON_FOXP3_TARGETS_UP	63	-0.59	-1.83	0.000	0.039	0.661	4884	tags=41%, list=14%, signal=48%
28	WELCH_GATA1_TARGETS	22	-0.71	-1.82	0.004	0.038	0.667	2121	tags=27%, list=6%, signal=29%
29	YOSHIOKA_LIVER_CANCER_EARLY_RECURRENCE_UP	35	-0.64	-1.82	0.000	0.038	0.681	4114	tags=40%, list=12%, signal=45%
30	MILI_PSEUDOPODIA_CHEMOTAXIS_DN	441	-0.46	-1.82	0.000	0.038	0.689	3651	tags=29%, list=11%, signal=33%
31	PACHER_TARGETS_OF_IGF1_AND_IGF2_UP	34	-0.65	-1.81	0.003	0.041	0.718	2519	tags=44%, list=7%, signal=48%
32	KANG_FLUOROURACIL_RESISTANCE_DN	16	-0.76	-1.80	0.004	0.049	0.795	3921	tags=44%, list=12%, signal=49%
33	HELLER_HDAC_TARGETS_DN	283	-0.48	-1.79	0.000	0.051	0.819	3166	tags=28%, list=9%, signal=31%
34	SABATES_COLORECTAL_ADENOMA_SIZE_UP	21	-0.69	-1.79	0.005	0.052	0.839	1429	tags=24%, list=4%, signal=25%
35	NIKOLSKY_MUTATED_AND_AMPLIFIED_IN_BREAST_CANCER	89	-0.54	-1.78	0.000	0.056	0.869	5381	tags=33%, list=16%, signal=39%
36	ABE_VEGFA_TARGETS_2HR	34	-0.63	-1.77	0.000	0.062	0.916	2088	tags=26%, list=6%, signal=28%
37	KEGG_GALACTOSE_METABOLISM	26	-0.68	-1.77	0.000	0.062	0.919	4085	tags=42%, list=12%, signal=48%
38	REACTOME_NRAGE_SIGNALS_DEATH_THROUGH_JNK	43	-0.61	-1.77	0.002	0.065	0.937	2089	tags=26%, list=6%, signal=27%
39	UROSEVIC_RESPONSE_TO_IMIQUIMOD	23	-0.68	-1.77	0.004	0.066	0.940	5420	tags=48%, list=16%, signal=57%
40	BIOCARTA_CCR3_PATHWAY	23	-0.68	-1.76	0.007	0.066	0.942	4238	tags=43%, list=12%, signal=50%
41	PENG_LEUCINE_DEPRIVATION_UP	137	-0.51	-1.76	0.000	0.065	0.945	3594	tags=30%, list=11%, signal=33%
42	BIOCARTA_SPPA_PATHWAY	22	-0.69	-1.76	0.004	0.064	0.952	2721	tags=36%, list=8%, signal=39%
43	MULLIGHAN_MLL_SIGNATURE_2_UP	392	-0.45	-1.76	0.000	0.063	0.954	3550	tags=29%, list=10%, signal=32%
44	GARGALOVIC_RESPONSE_TO_OXIDIZED_PHOSPHOLIPIDS_RED_UP	16	-0.74	-1.76	0.003	0.062	0.954	3082	tags=63%, list=9%, signal=69%
45	PID_RAC1_REG_PATHWAY	37	-0.62	-1.76	0.000	0.061	0.956	3092	tags=38%, list=9%, signal=42%
46	LIU_SMARCA4_TARGETS	58	-0.58	-1.76	0.003	0.061	0.958	5423	tags=38%, list=16%, signal=45%
47	KEGG_LYSOSOME	121	-0.51	-1.76	0.000	0.062	0.963	4217	tags=37%, list=12%, signal=42%
48	SHI_SPARC_TARGETS_UP	23	-0.69	-1.75	0.004	0.063	0.967	2280	tags=22%, list=7%, signal=23%
49	ZHANG_TLX_TARGETS_DN	106	-0.52	-1.75	0.000	0.068	0.977	3603	tags=26%, list=11%, signal=29%
50	MARTENS_BOUND_BY_PML_RARA_FUSION	428	-0.45	-1.75	0.000	0.067	0.978	3617	tags=25%, list=11%, signal=28%

Appendix Table 13 (Continued from previous page). Top 50 gene sets enriched in U2932 cells treated with CsA for 2hrs (enrichment in CsA treated sample phenotypes compared to vehicle samples). The table shows the top 50 enriched gene sets (ordered by false discovery rate FDR) for U2932 cells treated with CsA for 2hrs. Columns indicate gene set name, size, enrichment score (ES), normalised enrichment score (NES), nominal P-value (NOM), family-wise error rate (FWER), rank at maximum enrichment score and definition of the leading edge subset. Data is based on paired microarray analysis.

Gene sets enriched in vehicle phenotype vs. CsA – WSU-NHL 2hrs (3 samples)

	GS follow link to MSigDB	SIZE	ES	NES	NOM p-val	FDR q-val	FWER p-val	RANK AT MAX	LEADING EDGE
1	MILI_PSEUDOPODIA_HAPTOTAXIS_UP	474	0.59	2.61	0.000	0.000	0.000	2946	tags=36%, list=9%, signal=39%
2	ACEVEDO_NORMAL_TISSUE_ADJACENT_TO_LIVER_TUMOR_UP	160	0.60	2.38	0.000	0.000	0.000	2179	tags=36%, list=6%, signal=39%
3	SEIDEN_ONCOGENESIS_BY_MET	83	0.64	2.29	0.000	0.000	0.000	2921	tags=42%, list=9%, signal=46%
4	ZHANG_TLX_TARGETS_36HR_DN	174	0.56	2.25	0.000	0.000	0.000	2859	tags=37%, list=8%, signal=41%
5	SHEN_SMARCA2_TARGETS_UP	402	0.51	2.23	0.000	0.000	0.000	3264	tags=37%, list=10%, signal=40%
6	ROSTY_CERVICAL_CANCER_PROLIFERATION_CLUSTER	137	0.56	2.16	0.000	0.000	0.003	2732	tags=39%, list=8%, signal=43%
7	GRAHAM_NORMAL_QUIESCENT_VS_NORMAL_DIVIDING_DN	85	0.59	2.15	0.000	0.000	0.003	2732	tags=39%, list=8%, signal=42%
8	KOBAYASHI_EGFR_SIGNALING_24HR_DN	239	0.50	2.08	0.000	0.005	0.040	3049	tags=33%, list=9%, signal=36%
9	KAMMINGA_EZH2_TARGETS	41	0.66	2.07	0.000	0.005	0.048	1705	tags=34%, list=5%, signal=36%
10	WANG_SMARCE1_TARGETS_DN	350	0.47	2.06	0.000	0.005	0.053	2821	tags=24%, list=8%, signal=26%
11	BENPORATH_PROLIFERATION	137	0.53	2.06	0.000	0.004	0.053	2859	tags=36%, list=8%, signal=40%
12	DANG_MYC_TARGETS_UP	138	0.53	2.05	0.000	0.005	0.061	3617	tags=33%, list=11%, signal=37%
13	MARKEY_RB1_ACUTE_LOF_DN	214	0.50	2.05	0.000	0.005	0.063	2305	tags=26%, list=7%, signal=27%
14	DING_LUNG_CANCER_EXPRESSION_BY_COPY_NUMBER	96	0.56	2.05	0.000	0.004	0.065	3360	tags=33%, list=10%, signal=37%
15	WANG_TARGETS_OF_MLL_CBP_FUSION_DN	44	0.64	2.04	0.000	0.005	0.074	3538	tags=48%, list=10%, signal=53%
16	SOTIRIOU_BREAST_CANCER_GRADE_1_VS_3_UP	143	0.52	2.04	0.000	0.005	0.077	3203	tags=39%, list=9%, signal=43%
17	BIDUS_METASTASIS_UP	201	0.50	2.04	0.000	0.004	0.078	2732	tags=33%, list=8%, signal=35%
18	CHANG_CYCLING_GENES	138	0.53	2.04	0.000	0.004	0.078	3270	tags=39%, list=10%, signal=43%
19	WINNEPENNINCKX_MELANOMA_METASTASIS_UP	148	0.52	2.03	0.000	0.004	0.083	4643	tags=41%, list=14%, signal=48%
20	MUELLER_PLURINET	282	0.48	2.03	0.000	0.005	0.093	3370	tags=33%, list=10%, signal=36%
21	YU_MYC_TARGETS_UP	41	0.64	2.02	0.000	0.005	0.095	1638	tags=44%, list=5%, signal=46%
22	SESTO_RESPONSE_TO_UV_C0	106	0.54	2.02	0.000	0.005	0.102	2924	tags=35%, list=9%, signal=38%
23	MALONEY_RESPONSE_TO_17AAG_DN	76	0.57	2.01	0.000	0.005	0.110	4157	tags=39%, list=12%, signal=45%
24	MARTINEZ_RESPONSE_TO_TRABECTEDIN_DN	255	0.48	2.01	0.000	0.005	0.118	2807	tags=29%, list=8%, signal=31%
25	PUIFFE_INVASION_INHIBITED_BY_ASCITES_DN	135	0.52	1.99	0.000	0.006	0.142	2357	tags=30%, list=7%, signal=32%

Gene sets enriched in vehicle phenotype vs. CsA – WSU-NHL 2hrs (3 samples)

	GS follow link to MSigDB	SIZE	ES	NES	NOM p-val	FDR q-val	FWER p-val	RANK AT MAX	LEADING EDGE
26	GRAHAM_CML_DIVIDING_VS_NORMAL_QUIESCENT_UP	177	0.49	1.97	0.000	0.007	0.187	2510	tags=27%, list=7%, signal=29%
27	ENK_UV_RESPONSE_KERATINOCYTE_DN	470	0.44	1.97	0.000	0.008	0.220	2946	tags=27%, list=9%, signal=29%
28	FARMER_BREAST_CANCER_CLUSTER_2	32	0.66	1.96	0.000	0.009	0.236	2732	tags=53%, list=8%, signal=58%
29	CHANDRAN_METASTASIS_TOP50_UP	34	0.63	1.95	0.000	0.010	0.278	3146	tags=38%, list=9%, signal=42%
30	FERREIRA_EWINGS_SARCOMA_UNSTABLE_VS_STABLE_UP	158	0.49	1.94	0.000	0.011	0.308	3148	tags=33%, list=9%, signal=36%
31	LEE_LIVER_CANCER_SURVIVAL_DN	169	0.49	1.94	0.000	0.011	0.319	3850	tags=37%, list=11%, signal=42%
32	HAHTOLA_MYCOSIS_FUNGOIDES_CD4_DN	112	0.51	1.93	0.000	0.011	0.327	3385	tags=37%, list=10%, signal=41%
33	HOWLIN_CITED1_TARGETS_1_DN	37	0.64	1.92	0.000	0.013	0.391	3797	tags=35%, list=11%, signal=39%
34	SHEDDEN_LUNG_CANCER_POOR_SURVIVAL_A6	433	0.43	1.92	0.000	0.013	0.393	3270	tags=29%, list=10%, signal=31%
35	ZHANG_TLX_TARGETS_UP	84	0.53	1.92	0.000	0.013	0.409	2859	tags=37%, list=8%, signal=40%
36	GARY_CD5_TARGETS_DN	416	0.43	1.91	0.000	0.014	0.423	3049	tags=31%, list=9%, signal=33%
37	LINDGREN_BLADDER_CANCER_CLUSTER_3_UP	308	0.45	1.91	0.000	0.013	0.427	3335	tags=30%, list=10%, signal=33%
38	SENESE_HDAC2_TARGETS_UP	108	0.50	1.91	0.000	0.014	0.445	2081	tags=23%, list=6%, signal=25%
39	GOLDRATH_HOMEOSTATIC_PROLIFERATION	163	0.49	1.90	0.000	0.016	0.493	3121	tags=28%, list=9%, signal=30%
40	REACTOME_GLOBAL_GENOMIC_NER_GG_NER	35	0.62	1.89	0.000	0.017	0.523	1602	tags=34%, list=5%, signal=36%
41	ZHAN_MULTIPLE_MYELOMA_PR_UP	44	0.60	1.88	0.000	0.020	0.588	5403	tags=50%, list=16%, signal=59%
42	ZHOU_CELL_CYCLE_GENES_IN_IR_RESPONSE_24HR	120	0.49	1.87	0.000	0.022	0.628	3146	tags=33%, list=9%, signal=37%
43	ZHANG_BREAST_CANCER_PROGENITORS_UP	400	0.43	1.87	0.000	0.022	0.640	3150	tags=29%, list=9%, signal=32%
44	TIEN_INTESTINE_PROBIOTICS_2HR_DN	83	0.52	1.86	0.000	0.022	0.646	3345	tags=35%, list=10%, signal=39%
45	PEDERSEN_METASTASIS_BY_ERBB2_ISOFORM_3	18	0.70	1.86	0.002	0.023	0.678	1823	tags=28%, list=5%, signal=29%
46	RIGGINS_TAMOXIFEN_RESISTANCE_DN	214	0.44	1.85	0.000	0.025	0.705	3889	tags=24%, list=11%, signal=27%
47	HOLLEMAN_ASPARAGINASE_RESISTANCE_ALL_DN	23	0.66	1.85	0.002	0.025	0.713	3737	tags=43%, list=11%, signal=49%
48	HORIUCHI_WTAP_TARGETS_DN	289	0.43	1.84	0.000	0.026	0.738	4207	tags=33%, list=12%, signal=38%
49	SARRIO_EPITHELIAL_MESENCHYMAL_TRANSITION_UP	165	0.46	1.84	0.000	0.026	0.739	2859	tags=27%, list=8%, signal=30%
50	PUJANA_XPRSS_INT_NETWORK	160	0.47	1.84	0.000	0.026	0.751	3150	tags=33%, list=9%, signal=36%

Appendix Table 14 (Continued from previous page). Top 50 gene sets enriched in WSU-NHL cells treated with CsA for 2hrs (enrichment in vehicle sample phenotypes compared to CsA-treated samples). The table shows the top 50 enriched gene sets (ordered by false discovery rate FDR) for WSU-NHL cells treated with CsA for 2hrs. Columns indicate gene set name, size, enrichment score (ES), normalised enrichment score (NES), nominal P-value (NOM), family-wise error rate (FWER), rank at maximum enrichment score and definition of the leading edge subset. Data is based on paired microarray analysis.

Gene sets enriched in CsA treatment phenotype vs. vehicle – WSU-NHL 2hrs (3 samples)

	GS follow link to MSigDB	SIZE	ES	NES	NOM p-val	FDR q-val	FWER p-val	RANK AT MAX	LEADING EDGE
1	ACEVEDO_NORMAL_TISSUE_ADJACENT_TO_LIVER_TUMOR_DN	336	-0.56	-2.34	0.000	0.000	0.000	5190	tags=38%, list=15%, signal=44%
2	NIKOLSKY_BREAST_CANCER_16Q24_AMPLICON	46	-0.71	-2.25	0.000	0.000	0.000	3283	tags=37%, list=10%, signal=41%
3	DEBIASI_APOPTOSIS_BY_REOVIRUS_INFECTION_DN	276	-0.53	-2.16	0.000	0.000	0.000	4496	tags=34%, list=13%, signal=39%
4	REACTOME_ACTIVATION_OF_CHAPERONE_GENES_BY_XBP1S	44	-0.68	-2.12	0.000	0.001	0.002	3895	tags=48%, list=11%, signal=54%
5	REACTOME_AMINO_ACID_SYNTHESIS_AND_INTERCONVERSION_TRANSAMINATION	16	-0.81	-2.03	0.000	0.006	0.025	4046	tags=69%, list=12%, signal=78%
6	KRIGE_AMINO_ACID_DEPRIVATION	29	-0.71	-2.02	0.000	0.008	0.041	4049	tags=48%, list=12%, signal=55%
7	NOJIMA_SFRP2_TARGETS_UP	31	-0.68	-2.00	0.000	0.008	0.049	4926	tags=52%, list=14%, signal=60%
8	FLECHNER_BIOPSY_KIDNEY_TRANSPLANT_REJECTED_VS_OK_UP	85	-0.56	-1.94	0.000	0.023	0.158	3857	tags=33%, list=11%, signal=37%
9	GINESTIER_BREAST_CANCER_ZNF217_AMPLIFIED_DN	296	-0.47	-1.93	0.000	0.025	0.189	4128	tags=28%, list=12%, signal=32%
10	FERRARI_RESPONSE_TO_FENRETINIDE_UP	19	-0.76	-1.92	0.000	0.027	0.228	2871	tags=37%, list=8%, signal=40%
11	ZHAN_MULTIPLE_MYELOMA_CD1_VS_CD2_UP	64	-0.58	-1.92	0.000	0.025	0.234	6482	tags=39%, list=19%, signal=48%
12	KASLER_HDAC7_TARGETS_2_DN	31	-0.66	-1.92	0.000	0.024	0.243	1064	tags=23%, list=3%, signal=23%
13	ABE_VEGFA_TARGETS_2HR	34	-0.64	-1.91	0.000	0.027	0.288	3310	tags=29%, list=10%, signal=33%
14	LU_EZH2_TARGETS_UP	261	-0.47	-1.91	0.000	0.026	0.289	4682	tags=32%, list=14%, signal=37%
15	UROSEVIC_RESPONSE_TO_IMIQUIMOD	23	-0.71	-1.90	0.000	0.026	0.306	4186	tags=43%, list=12%, signal=50%
16	LEE_DIFFERENTIATING_T_LYMPHOCYTE	181	-0.48	-1.90	0.000	0.026	0.322	4481	tags=35%, list=13%, signal=40%
17	REACTOME_UNFOLDED_PROTEIN_RESPONSE	76	-0.54	-1.87	0.000	0.040	0.474	3895	tags=42%, list=11%, signal=47%
18	LEE_CALORIE_RESTRICTION_MUSCLE_UP	41	-0.60	-1.87	0.000	0.039	0.480	3371	tags=37%, list=10%, signal=41%
19	BURTON_ADIPOGENESIS_8	86	-0.53	-1.86	0.000	0.043	0.538	5828	tags=36%, list=17%, signal=43%
20	DIRMEIER_LMP1_RESPONSE_LATE_DN	31	-0.64	-1.85	0.000	0.043	0.556	3483	tags=45%, list=10%, signal=50%
21	CREIGHTON_AKT1_SIGNALING_VIA_MTOR_DN	22	-0.69	-1.85	0.000	0.045	0.588	2297	tags=45%, list=7%, signal=49%
22	GRATIAS_RETINOBLASTOMA_16Q24	17	-0.74	-1.84	0.000	0.046	0.618	2529	tags=41%, list=7%, signal=44%
23	PID_ATF2_PATHWAY	59	-0.56	-1.84	0.000	0.046	0.630	6580	tags=41%, list=19%, signal=50%
24	LAIHO_COLORECTAL_CANCER_SERRATED_DN	75	-0.54	-1.84	0.000	0.044	0.632	4067	tags=36%, list=12%, signal=41%
25	ZHANG_RESPONSE_TO_CANTHARIDIN_DN	68	-0.54	-1.82	0.002	0.061	0.761	5533	tags=43%, list=16%, signal=51%

Gene sets enriched in CsA treatment phenotype vs. vehicle – WSU-NHL 2hrs (3 samples)

	GS follow link to MSigDB	SIZE	ES	NES	NOM p-val	FDR q-val	FWER p-val	RANK AT MAX	LEADING EDGE
26	WANG_METHYLATED_IN_BREAST_CANCER	35	-0.61	-1.82	0.002	0.061	0.771	4691	tags=31%, list=14%, signal=36%
27	KIM_ALL_DISORDERS_DURATION_CORR_DN	140	-0.48	-1.81	0.000	0.060	0.779	4924	tags=35%, list=14%, signal=41%
28	MAHADEVAN_RESPONSE_TO_MP470_DN	18	-0.71	-1.81	0.004	0.064	0.813	5456	tags=44%, list=16%, signal=53%
29	HELLER_SILENCED_BY_METHYLATION_DN	102	-0.49	-1.79	0.002	0.078	0.871	2928	tags=25%, list=9%, signal=28%
30	HELLER_HDAC_TARGETS_SILENCED_BY_METHYLATION_DN	266	-0.44	-1.78	0.000	0.082	0.901	3642	tags=27%, list=11%, signal=30%
31	PID_REG_GR_PATHWAY	82	-0.51	-1.78	0.000	0.081	0.910	4510	tags=32%, list=13%, signal=36%
32	MILI_PSEUDOPODIA_CHEMOTAXIS_DN	441	-0.42	-1.77	0.000	0.094	0.944	3937	tags=26%, list=12%, signal=29%
33	MAGRANGEAS_MULTIPLE_MYELOMA_IGG_VS_IGA_UP	20	-0.67	-1.76	0.006	0.096	0.954	5095	tags=40%, list=15%, signal=47%
34	MAYBURD_RESPONSE_TO_L663536_UP	26	-0.62	-1.76	0.002	0.102	0.964	2465	tags=27%, list=7%, signal=29%
35	JAIN_NFKB_SIGNALING	73	-0.51	-1.76	0.000	0.101	0.967	2273	tags=32%, list=7%, signal=34%
36	MAGRANGEAS_MULTIPLE_MYELOMA_IGLL_VS_IGLK_DN	23	-0.65	-1.75	0.002	0.100	0.968	3462	tags=30%, list=10%, signal=34%
37	BIOCARTA_IL12_PATHWAY	21	-0.65	-1.75	0.005	0.098	0.969	1634	tags=29%, list=5%, signal=30%
38	GARY_CD5_TARGETS_UP	454	-0.41	-1.75	0.000	0.096	0.969	4627	tags=34%, list=14%, signal=38%
39	ST_GRANULE_CELL_SURVIVAL_PATHWAY	26	-0.62	-1.75	0.004	0.096	0.970	6169	tags=46%, list=18%, signal=56%
40	GAUSSMANN_MLL_AF4_FUSION_TARGETS_E_DN	22	-0.66	-1.74	0.007	0.102	0.976	5319	tags=41%, list=16%, signal=48%
41	VERHAAK_GLIOBLASTOMA_MESENCHYMAL	197	-0.44	-1.74	0.000	0.105	0.980	5286	tags=27%, list=16%, signal=32%
42	PACHER_TARGETS_OF_IGF1_AND_IGF2_UP	34	-0.59	-1.74	0.002	0.109	0.985	3977	tags=32%, list=12%, signal=37%
43	REACTOME_AMINE_COMPOUND_SLC_TRANSPORTERS	27	-0.61	-1.73	0.005	0.110	0.986	2653	tags=19%, list=8%, signal=20%
44	REACTOME_CHOLESTEROL_BIOSYNTHESIS	23	-0.65	-1.73	0.006	0.109	0.987	3569	tags=48%, list=10%, signal=53%
45	ZHAN_MULTIPLE_MYELOMA_UP	64	-0.52	-1.73	0.000	0.108	0.989	4683	tags=44%, list=14%, signal=51%
46	ROSS_AML_WITH_MLL_FUSIONS	77	-0.50	-1.73	0.000	0.106	0.989	4677	tags=38%, list=14%, signal=44%
47	GINESTIER_BREAST_CANCER_20Q13_AMPLIFICATION_DN	147	-0.46	-1.73	0.000	0.105	0.989	3850	tags=33%, list=11%, signal=37%
48	PID_RAC1_REG_PATHWAY	37	-0.57	-1.73	0.002	0.103	0.990	4625	tags=35%, list=14%, signal=41%
49	ST_WNT_CA2_CYCLIC_GMP_PATHWAY	20	-0.67	-1.73	0.010	0.104	0.990	2353	tags=25%, list=7%, signal=27%
50	BIOCARTA_MCALPAIN_PATHWAY	25	-0.63	-1.72	0.000	0.107	0.991	3212	tags=36%, list=9%, signal=40%

Appendix Table 15 (Continued from previous page). Top 50 gene sets enriched in WSU-NHL cells treated with CsA for 2hrs (enrichment in CsA treated sample phenotypes compared to vehicle samples). The table shows the top 50 enriched gene sets (ordered by false discovery rate FDR) for WSU-NHL cells treated with CsA for 2hrs. Columns indicate gene set name, size, enrichment score (ES), normalised enrichment score (NES), nominal P-value (NOM), family-wise error rate (FWER), rank at maximum enrichment score and definition of the leading edge subset. Data is based on paired microarray analysis.

	PROBE	GENE SYMBOL	GENE_TITLE	RANK IN GENE LIST	RANK METRIC SCORE	RUNNING ES	CORE ENRICHMENT
1	TNF	TNF Entrez, Source	tumor necrosis factor (TNF superfamily, member 2)	1	0.252	0.2326	Yes
2	EGR2	EGR2 Entrez, Source	early growth response 2 (Krox-20 homolog, Drosophila)	5	0.169	0.3880	Yes
3	EGR3	EGR3 Entrez, Source	early growth response 3	7	0.153	0.5292	Yes
4	IRF4	IRF4 Entrez, Source	interferon regulatory factor 4	69	0.079	0.6001	Yes
5	NFATC1	NFATC1 Entrez, Source	nuclear factor of activated T-cells, cytoplasmic, calcineurin-dependent 1	98	0.070	0.6640	Yes
6	JUNB	JUNB Entrez, Source	jun B proto-oncogene	344	0.048	0.7010	Yes
7	EGR4	EGR4 Entrez, Source	early growth response 4	2286	0.016	0.6588	No
8	PPARG	PPARG Entrez, Source	peroxisome proliferative activated receptor, gamma	3075	0.012	0.6471	No
9	GBP3	GBP3 Entrez, Source	guanylate binding protein 3	3438	0.011	0.6469	No
10	EGR1	EGR1 Entrez, Source	early growth response 1	3619	0.011	0.6516	No
11	DGKA	DGKA Entrez, Source	diacylglycerol kinase, alpha 80kDa	3846	0.010	0.6544	No
12	CREM	CREM Entrez, Source	cAMP responsive element modulator	4403	0.009	0.6467	No
13	MAF	MAF Entrez, Source	v-maf musculoaponeurotic fibrosarcoma oncogene homolog (avian)	4604	0.009	0.6490	No
14	FOS	FOS Entrez, Source	v-fos FBJ murine osteosarcoma viral oncogene homolog	5324	0.008	0.6352	No
15	NFATC2	NFATC2 Entrez, Source	nuclear factor of activated T-cells, cytoplasmic, calcineurin-dependent 2	5781	0.007	0.6286	No

Appendix Table 16. Leading edge genes in the PID NFAT TF PATHWAY gene set. GSEA analysis data showing the leading edge genes in the PID NFAT TF PATHWAY gene set which was enriched in U2932 treated with CsA for 2 hours (enrichment in vehicle compared to CsA-treated samples. Core enrichment genes are highlighted in green. Data is from paired analysis.

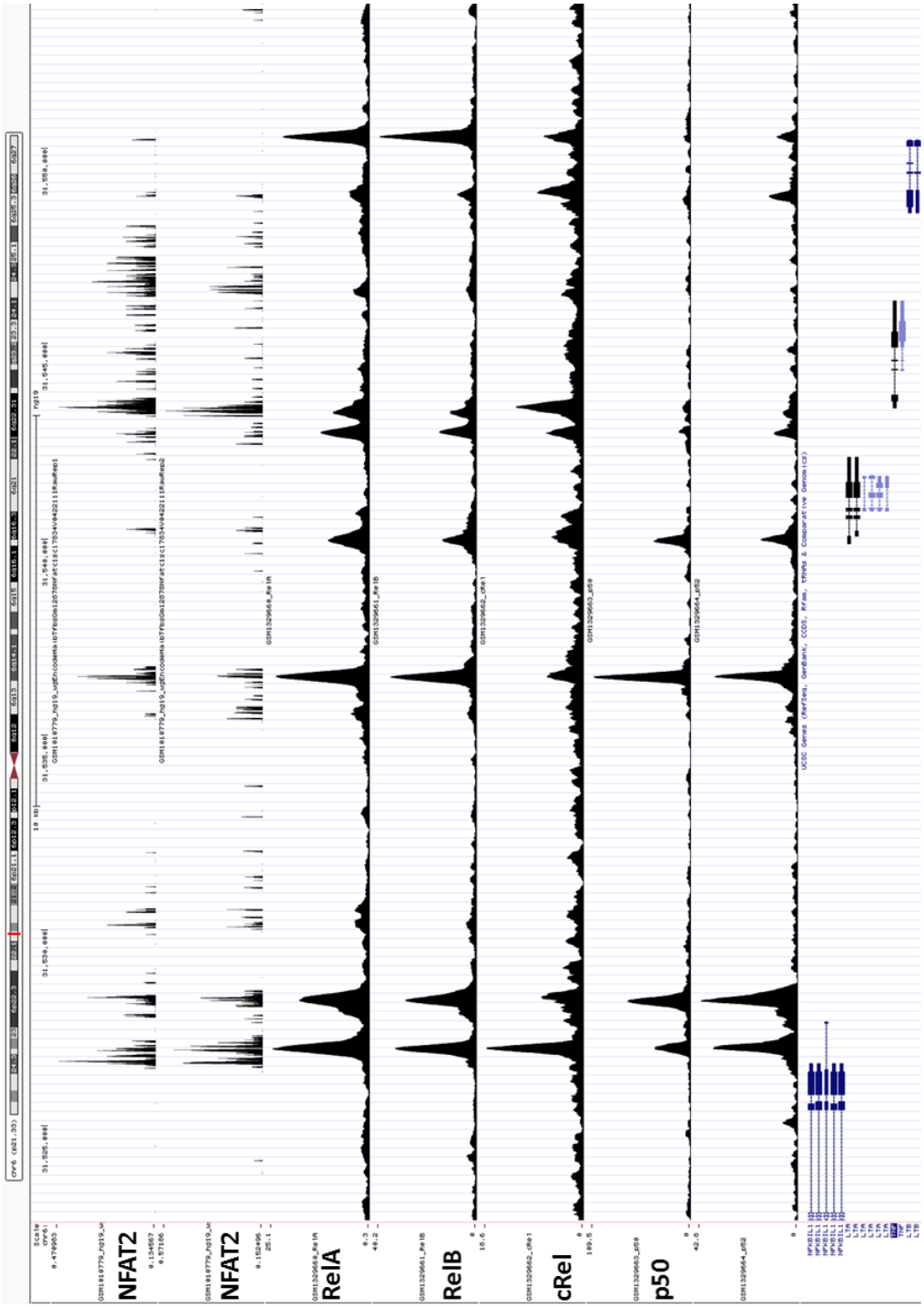

Appendix Figure 20. NFAT and NF-κB bind to the promoter of the TNFα gene in EBV-transformed B-cells. Previously published ChIP-sequencing data indicates that the NFAT2 isoform and NF-κB family members bind in the promoter regions of the TNFα gene in EBV-transformed B-cells. The *x*-axis shows the genomic location of the TNFα gene, where the location of peaks represent areas of transcription factor binding. The degree of DNA-binding is shown by the height of the peaks on the y-axis for NFAT2 or NF-κB family members respectively.

a)

Cell line	Cell type	24 hours induction NS virus (% RFP positive)	72 hours induction NS virus (% RFP positive)
SUDHL-1	T-cell	32%	83%
Jurkat	T-cell	26%	90%
HLY-1	B-cell	5%	9%
OCI-Ly3	B-cell	0%	0%
U2932	B-cell	0%	5%
SUDHL-4	B-cell	4%	32%
Farage	B-cell	0%	0%
WSU-NHL	B-cell	1%	5%
SUDHL-6	B-cell	0%	0%
OCI-Ly18	B-cell	0%	19%

b)

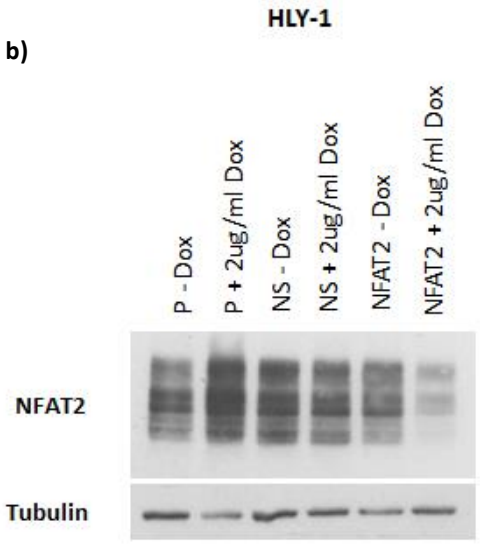

c)

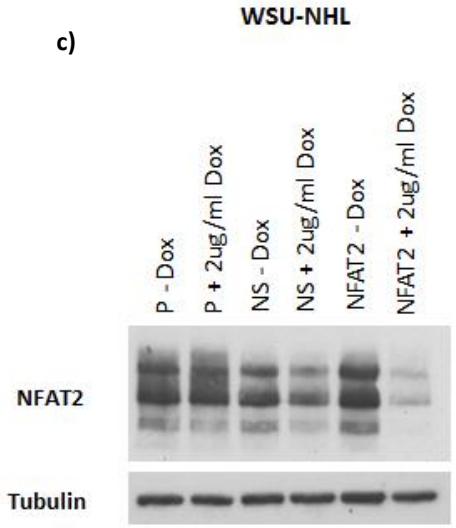

d)

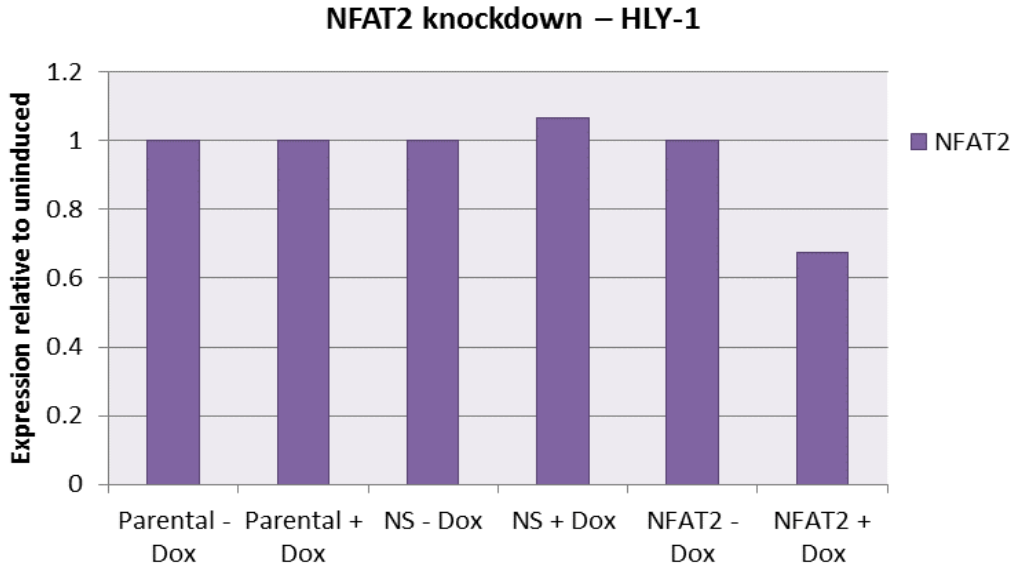

e)

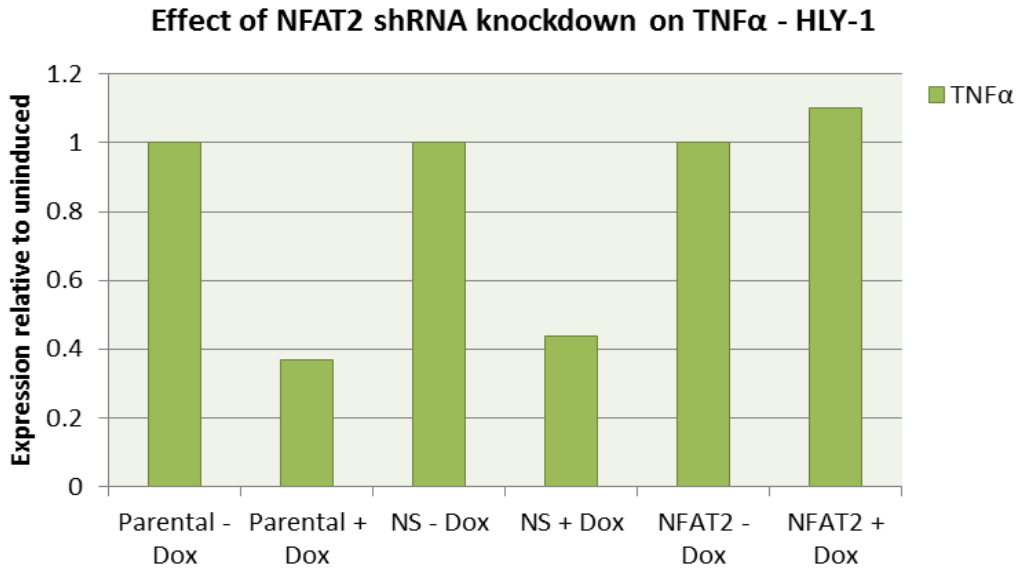

Appendix Figure 21 (Continued from previous page). shRNA knockdown of NFAT2 in DLBCL cell lines. (a) The transducibility of B-cells and T cells were compared by spinfection of a potent non-silencing (NS) virus into cells, followed by induction by 2μg/ml doxycycline (dox) for 24 and 72 hours. The percentage RFP-positive cells were analysed by FACs analysis as a measure of transduction. Data is from one experiment (b-c) Fully transduced HLY-1 and WSU-NHL cells which stably expressed the shRNA construct were induced with 2μg/ml dox for one week before the level of NFAT2 protein was analysed by Western blot analysis. α-tubulin was used as a positive loading control. Data is representative of three individual experiments. (d) The expression of NFAT2 mRNA in HLY-1 cells was analysed by qRT-PCR analysis following one week induction with 2μg/ml dox. (e) The effect of NFAT2 knockdown on TNFα mRNA expression was analysed by qRT-PCR analysis following one week induction with 2μg/ml dox. For d-e, expression is relative to the uninduced control sample and data were normalised to the house-keeping gene GAPDH. Data is representative of one experiment from three independent experiments.

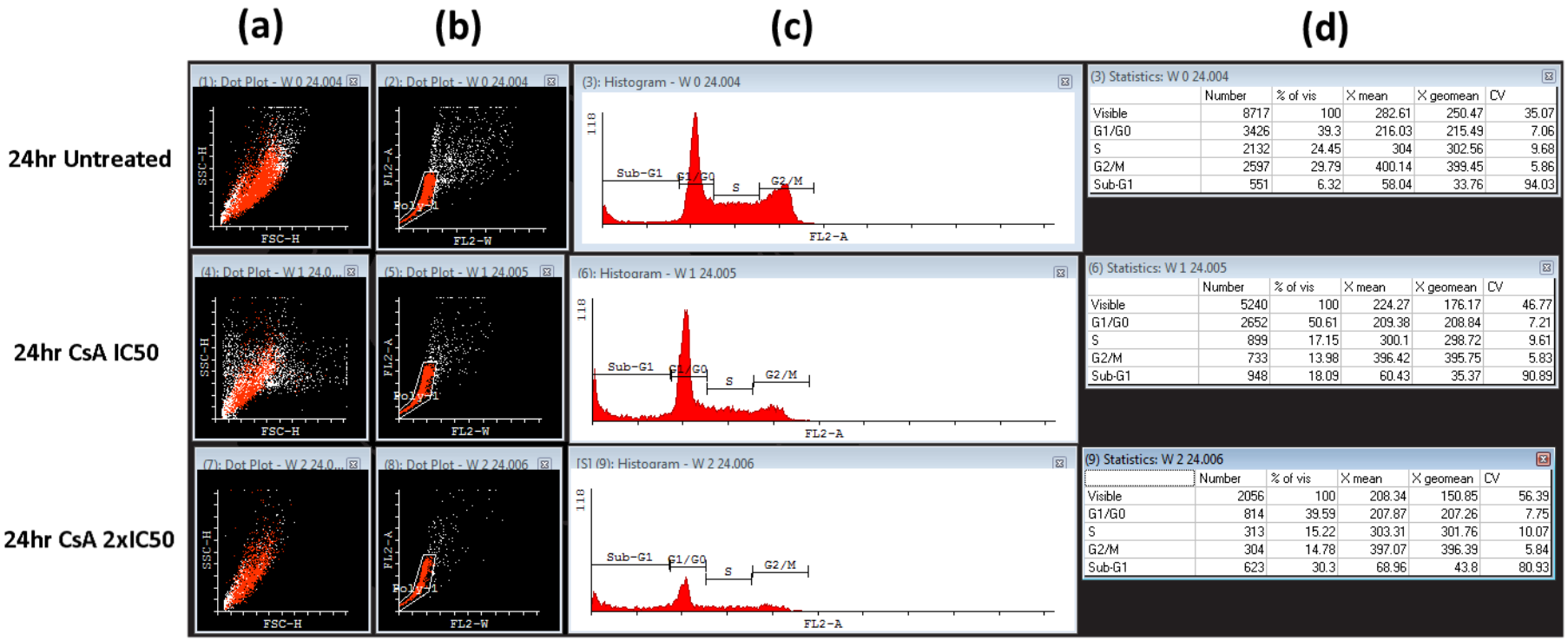

Appendix Figure 22. Example of FACs gating strategy for Propidium Iodide analysis. Using Cyflogic Software, a dot plot was drawn with side scatter (SSC-H) on the y-axis and forward scatter on the x-axis (FSC-H) (a). A single population of cells of interest (the main bulk of the cells) were gated. This removed any cells with high SSC-H and FSC-H which may be doublets/triplets or even clumps of cells. Cells with low SSC-H and FSC-H were debris and were also removed by gating. A second dot plot was draw (b), this time with FL2-A on the y-axis and FL2-W on the x-axis. The further along the x-axis in this graph represents cells in different stages of the cell cycle e.g. sub-G1, G1, S-phase, G2 etc. A gate was also made on this plot. Next, the gates were combined to form the Propidium Iodide histogram (c). The percentage of cells in each cell cycle phase were quantified by setting pre-set parameters (representing the populations of cells in each stage of the cell cycle) along the x-axis, optimised previously within the lab. The percentage of cells within each phase of the cell cycle are indicated in the third column in the statistics tables (d).

8. References

Abe, B.T., et al. (2012) 'NFAT1 supports tumor-induced anergy of CD4+ T cells', *Cancer research*, 72(18), pp. 4642-4651.

Abou Zahr, A., et al. (2015) 'Clinical utility of lenalidomide in the treatment of myelodysplastic syndromes', *Journal of Blood Medicine*, 6, pp. 1-16.

Advani, R., et al. (2007) 'Angioimmunoblastic T cell lymphoma: Treatment experience with cyclosporine', *Leukemia & Lymphoma*, 48(3), pp. 521-525.

Agalioti, T., et al. (2000) 'Ordered Recruitment of Chromatin Modifying and General Transcription Factors to the IFN-β Promoter', *Cell*, 103(4), pp. 667-678.

Aggarwal, B.B. (2003) 'Signalling pathways of the TNF superfamily: a double-edged sword', *Nat Rev Immunol*, 3(9), pp. 745-756.

Alizadeh, A.A., et al. (2000) 'Distinct types of diffuse large B-cell lymphoma identified by gene expression profiling', *Nature*, 403(6769), pp. 503-511.

Allavena, P., et al. (2008) 'The inflammatory micro-environment in tumor progression: The role of tumor-associated macrophages', *Critical Reviews in Oncology/Hematology*, 66(1), pp. 1-9.

Allenbach, C., et al. (2008) 'An essential role for transmembrane TNF in the resolution of the inflammatory lesion induced by Leishmania major infection', *European Journal of Immunology*, 38(3), pp. 720-731.

Ansell, S.M., et al. (2014) 'Activation of TAK1 by MYD88 L265P drives malignant B-cell Growth in non-Hodgkin lymphoma', *Blood Cancer Journal*, 4(2), p. e183.

Aramburu, J., et al. (1998) 'Selective Inhibition of NFAT Activation by a Peptide Spanning the Calcineurin Targeting Site of NFAT', *Molecular Cell*, 1(5), pp. 627-637.

Aramburu, J., et al. (1999) 'Affinity-Driven Peptide Selection of an NFAT Inhibitor More Selective Than Cyclosporin A', *Science*, 285(5436), pp. 2129-2133.

Arbajian, E., et al. (2013) 'A Benign Vascular Tumor With a New Fusion Gene: EWSR1-NFATC1 in Hemangioma of the Bone', *The American Journal of Surgical Pathology*, 37(4), pp. 613-616.

Arron, J.R., et al. (2006) 'NFAT dysregulation by increased dosage of DSCR1 and DYRK1A on chromosome 21', *Nature*, 441(7093), pp. 595-600.

Asagiri, M., et al. (2005) 'Autoamplification of NFATc1 expression determines its essential role in bone homeostasis', *The Journal of Experimental Medicine*, 202(9), pp. 1261-1269.

Ashkenazi, A., et al. (1998) 'Death Receptors: Signaling and Modulation', *Science*, 281(5381), pp. 1305-1308.

Aspeslet, L., et al. (2001) 'ISATX247: a novel calcineurin inhibitor', *Transplantation Proceedings*, 33(1–2), pp. 1048-1051.

Aukema, S.M., et al. (2011) 'Double-hit B-cell lymphomas', *Blood*, 117(8), pp. 2319-2331.

Baksh, S., et al. (2002) 'NFATc2-Mediated Repression of Cyclin-Dependent Kinase 4 Expression', *Molecular Cell*, 10(5), pp. 1071-1081.

Baldwin, A.S. (2001) 'Control of oncogenesis and cancer therapy resistance by the transcription factor NF-κB', *The Journal of Clinical Investigation*, 107(3), pp. 241-246.

Barik, S. (2006) 'Immunophilins: for the love of proteins', *Cellular and Molecular Life Sciences CMLS*, 63(24), pp. 2889-2900.

Basso, K., et al. (2012) 'Roles of BCL6 in normal and transformed germinal center B cells', *Immunological Reviews*, 247(1), pp. 172-183.

Baumgart, S., et al. (2012) 'Restricted Heterochromatin Formation Links NFATc2 Repressor Activity With Growth Promotion in Pancreatic Cancer', *Gastroenterology*, 142(2), pp. 388-98.e1-7.

Baus, D., et al. (2006) 'Specific function of STAT3, SOCS1, and SOCS3 in the regulation of proliferation and survival of classical Hodgkin lymphoma cells', *International Journal of Cancer*, 118(6), pp. 1404-1413.

Beals, C.R., et al. (1997) 'Nuclear Export of NF-ATc Enhanced by Glycogen Synthase Kinase-3', *Science*, 275(5308), pp. 1930-1933.

Béguelin, W., et al. (2013) 'EZH2 Is Required for Germinal Center Formation and Somatic EZH2 Mutations Promote Lymphoid Transformation', *Cancer Cell*, 23(5), pp. 677-692.

Beguelin, W., et al. (2015) 'IL10 receptor is a novel therapeutic target in DLBCLs', *Leukemia*, 29(8), pp. 1684-1694.

Benjamini (1995) 'Controlling the False Discovery Rate: A practical and Powerful Approach to Multiple Testing ', *Journal of the Royal Statistical Society Series B (methological)*, 57(1), pp. 289-300.

Berek, C., et al. (1991) 'Maturation of the immune response in germinal centers', *Cell*, 67(6), pp. 1121-1129.

Bert, A.G., et al. (2000) 'Reconstitution of T Cell-Specific Transcription Directed by Composite NFAT/Oct Elements', *The Journal of Immunology*, 165(10), pp. 5646-5655.

Bertoni, F., et al. (2007) 'The cellular origin of mantle cell lymphoma', *The International Journal of Biochemistry & Cell Biology*, 39(10), pp. 1747-1753.

Bikoff, E.K., et al. (2009) 'An expanding job description for Blimp-1/PRDM1', *Current Opinion in Genetics & Development*, 19(4), pp. 379-385.

Biswas, G., et al. (2003) 'Mitochondria to nucleus stress signaling: a distinctive mechanism of NFκB/Rel activation through calcineurin-mediated inactivation of IκBβ', *The Journal of Cell Biology*, 161(3), pp. 507-519.

Black, R.A., et al. (1997) 'A metalloproteinase disintegrin that releases tumour-necrosis factor-[alpha] from cells', *Nature*, 385(6618), pp. 729-733.

Blam, M.E., et al. (2001) 'Integrating anti-tumor necrosis factor therapy in inflammatory bowel disease: current and future perspectives', *Am J Gastroenterol*, 96(7), pp. 1977-1997.

Blasi, E., et al. (1994) 'Tumor necrosis factor as an autocrine and paracrine signal controlling the macrophage secretory response to Candida albicans', *Infection and Immunity*, 62(4), pp. 1199-1206.

Blumenthal, D.K., et al. (1986) 'Dephosphorylation of cAMP-dependent protein kinase regulatory subunit (type II) by calmodulin-dependent protein phosphatase. Determinants of substrate specificity', *Journal of Biological Chemistry*, 261(18), pp. 8140-5.

Bonizzi, G., et al. (2004) 'The two NF-κB activation pathways and their role in innate and adaptive immunity', *Trends in Immunology*, 25(6), pp. 280-288.

Borst, P., et al. (2000) 'A Family of Drug Transporters: the Multidrug Resistance-Associated Proteins', *Journal of the National Cancer Institute*, 92(16), pp. 1295-1302.

Bose, P., et al. (2014) 'Bortezomib for the treatment of non-Hodgkin's lymphoma', *Expert Opinion on Pharmacotherapy*, 15(16), pp. 2443-2459.

Brender, C., et al. (2004) 'Constitutive SOCS-3 expression protects T-cell lymphoma against growth inhibition by IFN[alpha]', *Leukemia*, 19(2), pp. 209-213.

Brender, C., et al. (2001) *STAT3-mediated constitutive expression of SOCS-3 in cutaneous T-cell lymphoma*.

Bretz, C.A., et al. (2013) 'The Role of the NFAT Signaling Pathway in Retinal Neovascularization', *Investigative Ophthalmology & Visual Science*, 54(10), pp. 7020-7027.

Brockman, J.A., et al. (1995) 'Coupling of a signal response domain in I kappa B alpha to multiple pathways for NF-kappa B activation', *Molecular and Cellular Biology*, 15(5), pp. 2809-2818.

Bronk, C.C., et al. (2014) 'NF-κB is crucial in proximal T-cell signaling for calcium influx and NFAT activation', *European Journal of Immunology*, pp. n/a-n/a.

Bryan, L.J., et al. (2014) 'Pidilizumab in the treatment of diffuse large B-cell lymphoma', *Expert Opinion on Biological Therapy*, 14(9), pp. 1361-1368.

Bryan, L.J., et al. (2015) 'Blocking tumor escape in hematologic malignancies: The anti-PD-1 strategy', *Blood Reviews*, 29(1), pp. 25-32.

Buchholz, M., et al. (2006) 'Overexpression of c-myc in pancreatic cancer caused by ectopic activation of NFATc1 and the Ca2+/calcineurin signaling pathway', *EMBO J*, 25(15), pp. 3714-3724.

Burkitt (1958) 'A sarcoma involving the jaws in African children', *Br J Surg*, 46(197), pp. 218-23.

C R Beals, N.A.C., S N Ho, and G R Crabtree (1997) 'Nuclear localization of NF-ATc by a calcineurin-dependent, cyclosporin-sensitive intramolecular interaction.

', *Genes Dev*, 11, pp. 824-834.

Cai, T.X.L., J. Ding, W. Luo, J. Li and C. Huang (2011) 'A Cross-Talk Between NFAT and NF-κB Pathways is Crucial for Nickel- Induced COX-2 Expression in Beas-2B Cells', *Current Cancer Drug Targets*, 11(5), pp. 548-59.

Cai, Y., et al. (2013) 'The effects of a histone deacetylase inhibitor on biological behavior of diffuse large B-cell lymphoma cell lines and insights into the underlying mechanisms', *Cancer Cell International*, 13, pp. 57-57.

Caldwell, A.B., et al. (2014) 'Network dynamics determine the autocrine and paracrine signaling functions of TNF', *Genes & Development*, 28(19), pp. 2120-2133.

Cameron, A.M., et al. (1995) 'Calcineurin associated with the inositol 1,4,5-trisphosphate receptor-FKBP12 complex modulates Ca2+ flux', *Cell*, 83(3), pp. 463-472.

Cancer Research UK (2012) *Non-Hodgkin Lymphoma – UK Incidence statistics* [Webpage]. Available at: http://info.cancerresearchuk.org/cancerstats/types/nhl/incidence/ (Accessed: 26/07/2012).

Carswell, E.A., et al. (1975) 'An endotoxin-induced serum factor that causes necrosis of tumors', *Proceedings of the National Academy of Sciences of the United States of America*, 72(9), pp. 3666-3670.

Carvalho, L.D.S., et al. (2007) 'The NFAT1 Transcription Factor is a Repressor of Cyclin A2 Gene Expression', *Cell Cycle*, 6(14), pp. 1789-1795.

Casolaro, V., et al. (1995) 'Inhibition of NF-AT-dependent transcription by NF-kappa B: implications for differential gene expression in T helper cell subsets', *Proceedings of the National Academy of Sciences*, 92(25), pp. 11623-11627.

Cattoretti, G., et al. (2005) 'Deregulated BCL6 expression recapitulates the pathogenesis of human diffuse large B cell lymphomas in mice', *Cancer Cell*, 7(5), pp. 445-455.

Chen, D., et al. (2011a) 'Bortezomib as the First Proteasome Inhibitor Anticancer Drug: Current Status and Future Perspectives', *Current Cancer Drug Targets*, 11(3), pp. 239-253.

Chen, G., et al. (2002) 'TNF-R1 Signaling: A Beautiful Pathway', *Science*, 296(5573), pp. 1634-1635.

Chen, L., et al. (1998) 'Structure of the DNA-binding domains from NFAT, Fos and Jun bound specifically to DNA', *Nature*, 392(6671), pp. 42-48.

Chen, L., et al. (2008) 'SYK-dependent tonic B-cell receptor signaling is a rational treatment target in diffuse large B-cell lymphoma', *Blood*, 111(4), pp. 2230-2237.

Chen, L., et al. (2013) 'SYK Inhibition Modulates Distinct PI3K/AKT- Dependent Survival Pathways and Cholesterol Biosynthesis in Diffuse Large B Cell Lymphomas', *Cancer Cell*, 23(6), pp. 826-838.

Chen, M., et al. (2005) 'Integrin [alpha]6[beta]4 promotes expression of autotaxin//ENPP2 autocrine motility factor in breast carcinoma cells', *Oncogene*, 24(32), pp. 5125-5130.

Chen, X.-G., et al. (2011b) 'Cyclosporine, prednisone, and high-dose immunoglobulin treatment of angioimmunoblastic T-cell lymphoma refractory to prior CHOP or CHOP-like regimen', *Chinese Journal of Cancer*, 30(10), pp. 731-738.

Chen, Z.-L., et al. (2011c) 'Expression and unique functions of four nuclear factor of activated T cells isoforms in non-small cell lung cancer', *Chinese Journal of Cancer*, 30(1), pp. 62-68.

Chen, Z.J., et al. (1996) 'Site-Specific Phosphorylation of IκBα by a Novel Ubiquitination-Dependent Protein Kinase Activity', *Cell*, 84(6), pp. 853-862.

Chiappella, A., et al. (2013) *Lenalidomide plus cyclophosphamide, doxorubicin, vincristine, prednisone and rituximab is safe and effective in untreated, elderly patients with diffuse large B-cell lymphoma: a phase I study by the Fondazione Italiana Linfomi*.

Choi, W.W.L., et al. (2009) 'A New Immunostain Algorithm Classifies Diffuse Large B-Cell Lymphoma into Molecular Subtypes with High Accuracy', *Clinical Cancer Research*, 15(17), pp. 5494-5502.

Chou, T.-C. (1974) 'Relationships between inhibition Constants and Fractional Inhibition in Enzyme-Catalyzed Reactions with Different Numbers of Reactants, Different Reaction Mechanisms, and Different Types and Mechanisms of Inhibition', *Molecular Pharmacology*, 10(2), pp. 235-247.

Chou TC, T.P. (1984) 'Quantitative analysis of dose-effect relationships: the combined effects of multiple drugs or enzyme inhibitors', *Adv Enzyme Regul* 22, pp. 27-55.

Chuvpilo, S., et al. (1999a) 'Multiple NF-ATc Isoforms with Individual Transcriptional Properties Are Synthesized in T Lymphocytes', *The Journal of Immunology*, 162(12), pp. 7294-7301.

Chuvpilo, S., et al. (2002) 'Autoregulation of NFATc1/A Expression Facilitates Effector T Cells to Escape from Rapid Apoptosis', *Immunity*, 16(6), pp. 881-895.

Chuvpilo, S., et al. (1999b) 'Alternative Polyadenylation Events Contribute to the Induction of NF-ATc in Effector T Cells', *Immunity*, 10(2), pp. 261-269.

Ci, W., et al. (2009) *The BCL6 transcriptional program features repression of multiple oncogenes in primary B cells and is deregulated in DLBCL*.

Cockerill, P.N., et al. (1995) 'Human granulocyte-macrophage colony-stimulating factor enhancer function is associated with cooperative interactions between AP-1 and NFATp/c', *Molecular and Cellular Biology*, 15(4), pp. 2071-2079.

Cockerill, P.N., et al. (1993) 'The granulocyte-macrophage colony-stimulating factor/interleukin 3 locus is regulated by an inducible cyclosporin A-sensitive enhancer', *Proceedings of the National Academy of Sciences of the United States of America*, 90(6), pp. 2466-2470.

Coiffier, B., et al. (2002) 'CHOP Chemotherapy plus Rituximab Compared with CHOP Alone in Elderly Patients with Diffuse Large-B-Cell Lymphoma', *New England Journal of Medicine*, 346(4), pp. 235-242.

Coiffier, B., et al. (2010) *Long-term outcome of patients in the LNH-98.5 trial, the first randomized study comparing rituximab-CHOP to standard CHOP chemotherapy in DLBCL patients: a study by the Groupe d'Etudes des Lymphomes de l'Adulte*.

Colobran, R., et al. (2010) 'Copy number variation in chemokine superfamily: the complex scene of CCL3L–CCL4L genes in health and disease', *Clinical and Experimental Immunology*, 162(1), pp. 41-52.

Compagno, M., et al. (2009) 'Mutations of multiple genes cause deregulation of NF-[kgr]B in diffuse large B-cell lymphoma', *Nature*, 459(7247), pp. 717-721.

Cook, I.H., et al. (2010) 'Prokineticin-1 (PROK1) modulates interleukin (IL)-11 expression via prokineticin receptor 1 (PROKR1) and the calcineurin/NFAT signalling pathway', *Molecular Human Reproduction*, 16(3), pp. 158-169.

Courtwright, A., et al. (2009) 'SFRP2 Stimulates Angiogenesis via a Calcineurin/NFAT Signaling Pathway', *Cancer research*, 69(11), pp. 4621-4628.

Coward, W.R., et al. (2002) 'NF-κB and TNF-α: A Positive Autocrine Loop in Human Lung Mast Cells?', *The Journal of Immunology*, 169(9), pp. 5287-5293.

Crabtree, G.R., et al. (2002) 'NFAT Signaling: Choreographing the Social Lives of Cells', *Cell*, 109(2, Supplement 1), pp. S67-S79.

Crist, S.A., et al. (2008) *Nuclear factor of activated T cells (NFAT) mediates CD154 expression in megakaryocytes*.

CRUK (2015) *Cancer Research UK statistics*.

D. Aderka, H.E., Y. Maor, C. Brakebusch, D. Wallach (1992) 'Stabilization of the bioactivity of tumor necrosis factor by its soluble receptors', *The Journal of Experimental Medicine*, 175(2), pp. 323-329.

D. Shealy, A.C., E. Lacy, T. Nesspor, K. Staquet, L. Johns, et al. (2007) 'Characterisation of golimumab (CNTO 148), a novel monoclonal antibody specific for human TNFα', *Ann Rheum Dis*, 66, p. 151.

Dal Porto, J.M., et al. (2004) 'B cell antigen receptor signaling 101', *Molecular Immunology*, 41(6–7), pp. 599-613.

Damm, F., et al. (2014) 'Acquired Initiating Mutations in Early Hematopoietic Cells of CLL Patients', *Cancer Discovery*, 4(9), pp. 1088-1101.

Dantal, J., et al. (2005) 'Immunosuppressive Drugs and the Risk of Cancer after Organ Transplantation', *New England Journal of Medicine*, 352(13), pp. 1371-1373.

Davis, R.E., et al. (2001) 'Constitutive Nuclear Factor κB Activity Is Required for Survival of Activated B Cell–like Diffuse Large B Cell Lymphoma Cells', *The Journal of Experimental Medicine*, 194(12), pp. 1861-1874.

Davis, R.E., et al. (2010) 'Chronic active B-cell-receptor signalling in diffuse large B-cell lymphoma', *Nature*, 463(7277), pp. 88-92.

Dawson, V.L., et al. (1993) 'Human immunodeficiency virus type 1 coat protein neurotoxicity mediated by nitric oxide in primary cortical cultures', *Proceedings of the National Academy of Sciences of the United States of America*, 90(8), pp. 3256-3259.

de la Pompa, J.L., et al. (1998) 'Role of the NF-ATc transcription factor in morphogenesis of cardiac valves and septum', *Nature*, 392(6672), pp. 182-186.

de Lumley, M., et al. (2004) 'A Biophysical Characterisation of Factors Controlling Dimerisation and Selectivity in the NF-κB and NFAT Families', *Journal of Molecular Biology*, 339(5), pp. 1059-1075.

De Silva, N.S., et al. (2012) 'The diverse roles of IRF4 in late germinal center B-cell differentiation', *Immunological Reviews*, 247(1), pp. 73-92.

Decker, E.L., et al. (2003) 'Early growth response proteins (EGR) and nuclear factors of activated T cells (NFAT) form heterodimers and regulate proinflammatory cytokine gene expression', *Nucleic Acids Research*, 31(3), pp. 911-921.

Decker, E.L., et al. (1998) 'The Early Growth Response Protein (EGR-1) Regulates Interleukin-2 Transcription by Synergistic Interaction with the Nuclear Factor of Activated T Cells', *Journal of Biological Chemistry*, 273(41), pp. 26923-26930.

Ding, B.B., et al. (2008) 'Constitutively activated STAT3 promotes cell proliferation and survival in the activated B-cell subtype of diffuse large B-cell lymphomas', *Blood*, 111(3), pp. 1515-1523.

dos Santos, N.R., et al. (2010) 'NF-κB in T-cell Acute Lymphoblastic Leukemia: Oncogenic Functions in Leukemic and in Microenvironmental Cells', *Cancers*, 2(4), pp. 1838-1860.

Drutskaya, M.S., et al. (2010) 'Tumor necrosis factor, lymphotoxin and cancer', *IUBMB Life*, 62(4), pp. 283-289.

Du, P., et al. (2008) 'lumi: a pipeline for processing Illumina microarray', *Bioinformatics*, 24(13), pp. 1547-1548.

Dubois, S.M., et al. (2014) *A catalytic-independent role for the LUBAC in NF-κB activation upon antigen receptor engagement and in lymphoma cells*.

Dunleavy, K., et al. (2009) *Differential efficacy of bortezomib plus chemotherapy within molecular subtypes of diffuse large B-cell lymphoma*.

Duque, J., et al. (2005) 'Expression and Function of the Nuclear Factor of Activated T Cells in Colon Carcinoma Cells: INVOLVEMENT IN THE REGULATION OF CYCLOOXYGENASE-2', *Journal of Biological Chemistry*, 280(10), pp. 8686-8693.

Dvorak, H.F. (2006) 'Discovery of vascular permeability factor (VPF)', *Experimental Cell Research*, 312(5), pp. 522-526.

Ebert, E.C., et al. (2006) 'Human intestinal intraepithelial lymphocytes keep TNFα levels low by cell uptake and feedback inhibition of transcription', *Cellular Immunology*, 241(1), pp. 7-13.

El-Sheikh, A.A.K., et al. (2014) 'Renal glucuronidation and multidrug resistance protein 2-/ multidrug resistance protein 4-mediated efflux of mycophenolic acid: interaction with cyclosporine and tacrolimus', *Translational Research*, 164(1), pp. 46-56.

Ernst, M.K., et al. (1995) 'The PEST-like sequence of I kappa B alpha is responsible for inhibition of DNA binding but not for cytoplasmic retention of c-Rel or RelA homodimers', *Molecular and Cellular Biology*, 15(2), pp. 872-882.

Fanoni, D., et al. (2011) 'New monoclonal antibodies against B-cell antigens: Possible new strategies for diagnosis of primary cutaneous B-cell lymphomas', *Immunology Letters*, 134(2), pp. 157-160.

Faralli, J.A., et al. (2015) 'NFATc1 activity regulates the expression of myocilin induced by dexamethasone', *Experimental Eye Research*, 130(0), pp. 9-16.

Faustman, D., et al. (2010) 'TNF receptor 2 pathway: drug target for autoimmune diseases', *Nat Rev Drug Discov*, 9(6), pp. 482-493.

Ferch, U., et al. (2009) 'Inhibition of MALT1 protease activity is selectively toxic for activated B cell–like diffuse large B cell lymphoma cells', *The Journal of Experimental Medicine*, 206(11), pp. 2313-2320.

Ferraccioli, G.F., et al. (2005) 'Rationale for T Cell Inhibition by Cyclosporin A in Major Autoimmune Diseases', *Annals of the New York Academy of Sciences*, 1051(1), pp. 658-665.

Ferrara, N.a.a.t.t.i.c. (2005) 'VEGF as a therapeutic target in cancer', *Oncology*, 69, pp. 11-16.

Finco, T.S., et al. (1994) 'Inducible phosphorylation of I kappa B alpha is not sufficient for its dissociation from NF-kappa B and is inhibited by protease inhibitors', *Proceedings of the National Academy of Sciences of the United States of America*, 91(25), pp. 11884-11888.

Flockhart, R.J., et al. (2009) 'NFAT signalling is a novel target of oncogenic BRAF in metastatic melanoma', *British Journal of Cancer*, 101(8), pp. 1448-1455.

Fontan, L., et al. (2012) 'MALT1 Small Molecule Inhibitors Specifically Suppress ABC-DLBCL In Vitro and In Vivo', *Cancer Cell*, 22(6), pp. 812-824.

Fric, J., et al. (2012) 'NFAT control of innate immunity', *Blood*, 120(7), pp. 1380-1389.

Friedberg, J.W., et al. (2010) *Inhibition of Syk with fostamatinib disodium has significant clinical activity in non-Hodgkin lymphoma and chronic lymphocytic leukemia*.

Frischbutter, S., et al. (2011) 'Dephosphorylation of Bcl-10 by calcineurin is essential for canonical NF-κB activation in Th cells', *European Journal of Immunology*, 41(8), pp. 2349-2357.

Fu, L., et al. (2006) 'Constitutive NF-κB and NFAT activation leads to stimulation of the BLyS survival pathway in aggressive B-cell lymphomas', *Blood*, 107(11), pp. 4540-4548.

Fuentes, J.J., et al. (2000) 'DSCR1, overexpressed in Down syndrome, is an inhibitor of calcineurin-mediated signaling pathways', *Human Molecular Genetics*, 9(11), pp. 1681-1690.

Gachet, S., et al. (2013) 'Leukemia-initiating cell activity requires calcineurin in T-cell acute lymphoblastic leukemia', *Leukemia*, 27(12), pp. 2289-2300.

Gauld, S.B., et al. (2002) 'B Cell Antigen Receptor Signaling: Roles in Cell Development and Disease', *Science*, 296(5573), pp. 1641-1642.

Gerlach, K., et al. (2012) 'Transcription Factor NFATc2 Controls the Emergence of Colon Cancer Associated with IL-6–Dependent Colitis', *Cancer Research*, 72(17), pp. 4340-4350.

Gerondakis, S., et al. (2010) 'Roles of the NF-kappaB pathway in lymphocyte development and function', *Cold Spring Harbor perspectives in biology*, 2(5), p. a000182.

Gertz, J., et al. (2013) 'Distinct properties of cell type-specific and shared transcription factor binding sites', *Molecular cell*, 52(1), p. 10.1016/j.molcel.2013.08.037.

Ghosh, G., et al. (1995) 'Structure of NF-[kappa]B p50 homodimer bound to a [kappa]B site', *Nature*, 373(6512), pp. 303-310.

Ghosh, N., et al. (2015) 'Expanding role of lenalidomide in hematologic malignancies', *Cancer Management and Research*, 7, pp. 105-119.

Gilmore (1999) 'Mulitple mutations contribute to the oncogenicity of the retroviral oncoprotein v-Rel', *Oncogene*, 18(49), pp. 6925-6937.

Gilmore, T.D., et al. (2004) 'The c-Rel transcription factor and B-cell proliferation: a deal with the devil', *Oncogene*, 23(13), pp. 2275-2286.

Glud, S.Z., et al. (2005) 'A tumor-suppressor function for NFATc3 in T-cell lymphomagenesis by murine leukemia virus', *Blood*, 106(10), pp. 3546-3552.

Goffe, B., et al. (2003) 'Etanercept: An overview', *Journal of the American Academy of Dermatology*, 49(2, Supplement), pp. 105-111.

Gómez-Martín, D., et al. (2010) 'Early growth response transcription factors and the modulation of immune response: Implications towards autoimmunity', *Autoimmunity Reviews*, 9(6), pp. 454-458.

González-Guerrero, C., et al. (2013) 'Calcineurin inhibitors recruit protein kinases JAK2 and JNK, TLR signaling and the UPR to activate NF-κB-mediated inflammatory responses in kidney tubular cells', *Toxicology and Applied Pharmacology*, 272(3), pp. 825-841.

Gooch, J.L., et al. (2004) 'Involvement of Calcineurin in Transforming Growth Factor-β-mediated Regulation of Extracellular Matrix Accumulation', *Journal of Biological Chemistry*, 279(15), pp. 15561-15570.

Gottesman, M.M., et al. (1993) 'Biochemistry of Multidrug Resistance Mediated by the Multidrug Transporter', *Annual Review of Biochemistry*, 62(1), pp. 385-427.

Goy, A., et al. (2011) 'Mantle cell lymphoma: The promise of new treatment options', *Critical Reviews in Oncology/Hematology*, 80(1), pp. 69-86.

Graef, I.A., et al. (2001) 'Signals Transduced by Ca2+/Calcineurin and NFATc3/c4 Pattern the Developing Vasculature', *Cell*, 105(7), pp. 863-875.

Granger GA, S.S., Williams TW, Kolb WP. (1969) 'Lymphocyte in vitro cytotoxicity: specific release of lymphotoxin-like materials from tuberculin-sensitive lymphoid cells', *Nature*, 22(221 (5186)), pp. 1155-7.

Gray PW, A.B., Benton CV, Bringman TS, Henzel WJ, Jarrett JA, Leung DW, Moffat B, Ng P, Svedersky LP, et al. (1984) 'Cloning and expression of cDNA for human lymphotoxin, a lymphokine with tumour necrosis activity.', *Nature*, 312 (5996), pp. 721-4.

Greenhough, A., et al. (2009) 'The COX-2/PGE2 pathway: key roles in the hallmarks of cancer and adaptation to the tumour microenvironment', *Carcinogenesis*, 30(3), pp. 377-386.

Gregory, M.A., et al. (2010) 'Wnt/Ca(2+)/NFAT signaling maintains survival of Ph(+) leukemia cells upon inhibition of Bcr-Abl', *Cancer cell*, 18(1), pp. 74-87.

Grell, M., et al. (1995) 'The transmembrane form of tumor necrosis factor is the prime activating ligand of the 80 kDa tumor necrosis factor receptor', *Cell*, 83(5), pp. 793-802.

Greten, F.R., et al. (2004) 'IKKβ Links Inflammation and Tumorigenesis in a Mouse Model of Colitis-Associated Cancer', *Cell*, 118(3), pp. 285-296.

Grossmann, M., et al. (1999) 'New insights into the roles of ReL/NF-κB transcription factors in immune function, hemopoiesis and human disease', *The International Journal of Biochemistry & Cell Biology*, 31(10), pp. 1209-1219.

Grumont, R., et al. (2004) 'The Mitogen-Induced Increase in T Cell Size Involves PKC and NFAT Activation of Rel/NF-κB-Dependent c-myc Expression', *Immunity*, 21(1), pp. 19-30.

Guha, M., et al. (2001) *Lipopolysaccharide activation of the MEK-ERK1/2 pathway in human monocytic cells mediates tissue factor and tumor necrosis factor α expression by inducing Elk-1 phosphorylation and Egr-1 expression.*

Gupta, N., et al. (2007) 'Lipid rafts and B cell signaling', *Seminars in cell & developmental biology*, 18(5), pp. 616-626.

Gwack, Y., et al. (2007) 'Signalling to transcription: Store-operated Ca2+ entry and NFAT activation in lymphocytes', *Cell Calcium*, 42(2), pp. 145-156.

Gwack, Y., et al. (2006) 'A genome-wide Drosophila RNAi screen identifies DYRK-family kinases as regulators of NFAT', *Nature*, 441(7093), pp. 646-650.

Haagensen, E.J., et al. (2012) 'The synergistic interaction of MEK and PI3K inhibitors is modulated by mTOR inhibition', *Br J Cancer*, 106(8), pp. 1386-1394.

Habermann, T.M., et al. (2006) 'Rituximab-CHOP Versus CHOP Alone or With Maintenance Rituximab in Older Patients With Diffuse Large B-Cell Lymphoma', *Journal of Clinical Oncology*, 24(19), pp. 3121-3127.

Habib, T., et al. (2007) 'Myc stimulates B lymphocyte differentiation and amplifies calcium signaling', *The Journal of Cell Biology*, 179(4), pp. 717-731.

Hailfinger, S., et al. (2009) 'Essential role of MALT1 protease activity in activated B cell-like diffuse large B-cell lymphoma', *Proceedings of the National Academy of Sciences*, 106(47), pp. 19946-19951.

Hanahan, D., et al. (2000) 'The Hallmarks of Cancer', *Cell*, 100(1), pp. 57-70.

Hanahan, D., et al. (2011) 'Hallmarks of Cancer: The Next Generation', *Cell*, 144(5), pp. 646-674.

Hans, C.P., et al. (2004) *Confirmation of the molecular classification of diffuse large B-cell lymphoma by immunohistochemistry using a tissue microarray*.

Hatchi, E.M., et al. (2014) 'Participation of the E3-ligase TRIM13 in NF-κB p65 activation and NFAT-dependent activation of c-Rel upon T-cell receptor engagement', *The International Journal of Biochemistry & Cell Biology*, 54(0), pp. 217-222.

Hayden, M.S., et al. (2008) 'Shared Principles in NF-κB Signaling', *Cell*, 132(3), pp. 344-362.

Heineke, J., et al. (2006) 'Regulation of cardiac hypertrophy by intracellular signalling pathways', *Nat Rev Mol Cell Biol*, 7(8), pp. 589-600.

Heit, J.J., et al. (2006) 'Calcineurin/NFAT signalling regulates pancreatic [beta]-cell growth and function', *Nature*, 443(7109), pp. 345-349.

Herman, S.E.M., et al. (2011) 'Bruton tyrosine kinase represents a promising therapeutic target for treatment of chronic lymphocytic leukemia and is effectively targeted by PCI-32765', *Blood*, 117(23), pp. 6287-6296.

Hernandez-Ilizaliturri, F.J., et al. (2011) 'Higher response to lenalidomide in relapsed/refractory diffuse large B-cell lymphoma in nongerminal center B-cell–like than in germinal center B-cell–like phenotype', *Cancer*, 117(22), pp. 5058-5066.

Herold, M., Jurinovic, Seiler, Metzeler, Dufour, Schneider, Kakadia, Spiekermann, Mansmann, Hiddemann, Buske, Dreyling, Bohlander (2013) 'High expression of MZB1 predicts adverse prognosis in chronic lymphocytic leukemia, follicular lymphoma and diffuse large B-cell lymphoma and is associated with a unique gene expression signature', *Leukaemia and Lymphoma*, 54(8), pp. 1652-1657.

Hesselink, D.A., et al. (2005) 'Cyclosporine Interacts with Mycophenolic Acid by Inhibiting the Multidrug Resistance-Associated Protein 2', *American Journal of Transplantation*, 5(5), pp. 987-994.

Ho, S.N., et al. (1995) 'NFATc3, a Lymphoid-specific NFATc Family Member That Is Calcium-regulated and Exhibits Distinct DNA Binding Specificity', *Journal of Biological Chemistry*, 270(34), pp. 19898-19907.

Hock, M., et al. (2013) 'NFATc1 Induction in Peripheral T and B Lymphocytes', *The Journal of Immunology*, 190(5), pp. 2345-2353.

Hoey T, S.Y., Williamson K, Xu X (1995) 'Isolation of two new members of the NF-AT gene family and functional characterization of the NF-AT proteins', *Immunity*, 2(5), pp. 461-72.

Hoffmann, A., et al. (2002) 'The IκB-NF-κB Signaling Module: Temporal Control and Selective Gene Activation', *Science*, 298(5596), pp. 1241-1245.

Hogan, P.G., et al. (2003) 'Transcriptional regulation by calcium, calcineurin, and NFAT', *Genes & Development*, 17(18), pp. 2205-2232.

Holzmann, K., et al. (2004) 'Genomic DNA-Chip Hybridization Reveals a Higher Incidence of Genomic Amplifications in Pancreatic Cancer than Conventional

Comparative Genomic Hybridization and Leads to the Identification of Novel Candidate Genes', *Cancer Research*, 64(13), pp. 4428-4433.

Horsley, V., et al. (2008) 'NFATc1 balances quiescence and proliferation of skin stem cells', *Cell*, 132(2), pp. 299-310.

Howard, O.M., et al. (2004) 'Functional redundancy of the human CCL4 and CCL4L1 chemokine genes', *Biochemical and Biophysical Research Communications*, 320(3), pp. 927-931.

Hozumi, N., et al. (1976) 'Evidence for somatic rearrangement of immunoglobulin genes coding for variable and constant regions', *Proceedings of the National Academy of Sciences of the United States of America*, 73(10), pp. 3628-3632.

Hsu, S., et al. (2012) 'IKKε coordinates invasion and metastasis of ovarian cancer', *Cancer research*, 72(21), pp. 5494-5504.

http://www.broadinstitute.org/gsea/index.jsp 'Accessed 30.08.15'.

http://www.kinase-screen.mrc.ac.uk/kinase-inhibitors (2015).

http://www.ncbi.nlm.nih.gov/geo/query/acc.cgi?acc=GSE32465 (accessed 18.09.15) *NF-kB ChIP-sequencing data*.

http://www.ncbi.nlm.nih.gov/geo/query/acc.cgi?acc=GSM1010779 (accessed 18.09.15) *NFAT2 ChIp-sequencing data*.

Hu, C.-M., et al. (2002) 'Modulation of T Cell Cytokine Production by Interferon Regulatory Factor-4', *Journal of Biological Chemistry*, 277(51), pp. 49238-49246.

Huang, J.Z., et al. (2002) *The t(14;18) defines a unique subset of diffuse large B-cell lymphoma with a germinal center B-cell gene expression profile*.

Idriss, H.T., et al. (2000) 'TNFα and the TNF receptor superfamily: Structure-function relationship(s)', *Microscopy Research and Technique*, 50(3), pp. 184-195.

Imamura, R., et al. (1998) 'Carboxyl-Terminal 15-Amino Acid Sequence of NFATx1 Is Possibly Created by Tissue-Specific Splicing and Is Essential for Transactivation Activity in T Cells', *The Journal of Immunology*, 161(7), pp. 3455-3463.

Inagaki-Ohara, K., et al. (2013) 'SOCS, inflammation, and cancer', *JAK-STAT*, 2(3), p. e24053.

Iqbal, J., et al. (2007) 'Distinctive patterns of BCL6 molecular alterations and their functional consequences in different subgroups of diffuse large B-cell lymphoma', *Leukemia*, 21(11), pp. 2332-2343.

Iqbal, J., et al. (2006) 'BCL2 Expression Is a Prognostic Marker for the Activated B-Cell–Like Type of Diffuse Large B-Cell Lymphoma', *Journal of Clinical Oncology*, 24(6), pp. 961-968.

Iqbal, J., et al. (2004) 'BCL2 Translocation Defines a Unique Tumor Subset within the Germinal Center B-Cell-Like Diffuse Large B-Cell Lymphoma', *The American Journal of Pathology*, 165(1), pp. 159-166.

Irving, S.G., et al. (1990) 'Two inflammatory mediator cytokine genes are closely linked and variably amplified on chromosome 17q', *Nucleic Acids Research*, 18(11), pp. 3261-3270.

Ishikawa, C., et al. (2013) 'CD69 overexpression by human T-cell leukemia virus type 1 Tax transactivation', *Biochimica et Biophysica Acta (BBA) - Molecular Cell Research*, 1833(6), pp. 1542-1552.

Ishikawa, K.H., Uchihara JN, Senba M, Mori N. (1998) 'Expression of activation markers CD23 and CD69 in B-cell non-Hodgkin's lymphoma', *Eur J Haematol.*, 60(2), pp. 125-32.

Itoh, K., et al. (1995) 'The role of IL-10 in human B cell activation, proliferation, and differentiation', *The Journal of Immunology*, 154(9), pp. 4341-50.

Jacob, J., et al. (1991) 'Intraclonal generation of antibody mutants in germinal centres', *Nature*, 354(6352), pp. 389-392.

Jain, J., et al. (1992) 'Nuclear factor of activated T cells contains Fos and Jun', *Nature*, 356(6372), pp. 801-804.

Jash, A., et al. (2012) 'Nuclear Factor of Activated T Cells 1 (NFAT1)-induced Permissive Chromatin Modification Facilitates Nuclear Factor-κB (NF-κB)-mediated Interleukin-9 (IL-9) Transactivation', *Journal of Biological Chemistry*, 287(19), pp. 15445-15457.

Jauliac, S., et al. (2002) 'The role of NFAT transcription factors in integrin-mediated carcinoma invasion', *Nat Cell Biol*, 4(7), pp. 540-544.

Jinnin, M., et al. (2008) 'Suppressed NFAT-dependent VEGFR1 expression and constitutive VEGFR2 signaling in infantile hemangioma', *Nature medicine*, 14(11), pp. 1236-1246.

Jost, P.J., et al. (2007) 'Aberrant NF-κB signaling in lymphoma: mechanisms, consequences, and therapeutic implications', *Blood*, 109(7), pp. 2700-2707.

Jurado, S., et al. (2010) 'A calcineurin/AKAP complex is required for NMDA receptor-dependent long-term depression', *Nat Neurosci*, 13(9), pp. 1053-1055.

K. Peppel, D.C., B. Beutler (1991) 'A tumor necrosis factor (TNF) receptor-IgG heavy chain chimeric protein as a bivalent antagonist of TNF activity', *The Journal of Experimental Medicine*, 174(6), pp. 1483-1489.

Kang, S., et al. (2005) 'Inhibition of the Calcineurin-NFAT Interaction by Small Organic Molecules Reflects Binding at an Allosteric Site', *Journal of Biological Chemistry*, 280(45), pp. 37698-37706.

Karanam, B.V., et al. (1998) 'Disposition of L-732,531, a Potent Immunosuppressant, in Rats and Baboons', *Drug Metabolism and Disposition*, 26(10), pp. 949-957.

Karin, M. (2006) 'Nuclear factor-[kappa]B in cancer development and progression', *Nature*, 441(7092), pp. 431-436.

Karin, M. (2009) 'NF-κB as a Critical Link Between Inflammation and Cancer', *Cold Spring Harb Perspect Biol.* .

Karin, M., et al. (2000) 'Phosphorylation Meets Ubiquitination: The Control of NF-κB Activity', *Annual Review of Immunology*, 18(1), pp. 621-663.

Karin, M., et al. (2002) 'NF-[kappa]B in cancer: from innocent bystander to major culprit', *Nat Rev Cancer*, 2(4), pp. 301-310.

Karlsen, A.E., et al. (2004) 'Suppressor of cytokine signalling (SOCS)-3 protects beta cells against IL-1β-mediated toxicity through inhibition of multiple nuclear factor-κB-regulated proapoptotic pathways', *Diabetologia*, 47(11), pp. 1998-2011.

Karpanen, T., et al. (2001) 'Lymphatic Vessels as Targets of Tumor Therapy?', *The Journal of Experimental Medicine*, 194(6), pp. f37-f42.

Kato, M., et al. (2009) 'Frequent inactivation of A20 in B-cell lymphomas', *Nature*, 459(7247), pp. 712-716.

Keir, M.E., et al. (2008) 'PD-1 and Its Ligands in Tolerance and Immunity', *Annual Review of Immunology*, 26(1), pp. 677-704.

Kempeni, J. (1999) 'Preliminary results of early clinical trials with the fully human anti-TNFα monoclonal antibody D2E7', *Annals of the Rheumatic Diseases*, 58(Suppl 1), pp. I70-I72.

Kenkre, V., et al. (2012) 'The Future of B-Cell Lymphoma Therapy: The B-Cell Receptor and its Downstream Pathways', *Current Hematologic Malignancy Reports*, pp. 1-5.

Kiani, A., et al. (2000) 'Manipulating Immune Responses with Immunosuppressive Agents that Target NFAT', *Immunity*, 12(4), pp. 359-372.

Kim, H.J., et al. (2006) 'NF-[kappa]B and IKK as therapeutic targets in cancer', *Cell Death Differ*, 13(5), pp. 738-747.

Klapper, W., et al. (2008) 'Structural aberrations affecting the MYC locus indicate a poor prognosis independent of clinical risk factors in diffuse large B-cell lymphomas treated within randomized trials of the German High-Grade Non-Hodgkin's Lymphoma Study Group (DSHNHL)', *Leukemia*, 22(12), pp. 2226-2229.

Kleffel, S., et al. (2015) 'Melanoma Cell-Intrinsic PD-1 Receptor Functions Promote Tumor Growth', *Cell*, 162(6), pp. 1242-1256.

Kloo, B., et al. (2011) 'Critical role of PI3K signaling for NF-κB–dependent survival in a subset of activated B-cell–like diffuse large B-cell lymphoma cells', *Proceedings of the National Academy of Sciences of the United States of America*, 108(1), pp. 272-277.

Knight DM1, T.H., Le J, Siegel S, Shealy D, McDonough M, Scallon B, Moore MA, Vilcek J, Daddona P, et al. (1993) 'Construction and initial characterization of a mouse-human chimeric anti-TNF antibody.', *Mol Immunol*, 30(16), pp. 1443-53.

Knutson, S.K., et al. (2012) 'A selective inhibitor of EZH2 blocks H3K27 methylation and kills mutant lymphoma cells', *Nat Chem Biol*, 8(11), pp. 890-896.

Kodama, S., et al. (2005) 'The therapeutic potential of tumor necrosis factor for autoimmune disease: a mechanistically based hypothesis', *Cellular and Molecular Life Sciences CMLS*, 62(16), pp. 1850-1862.

Kollias, G., et al. (2002) 'Role of TNF/TNFR in autoimmunity: specific TNF receptor blockade may be advantageous to anti-TNF treatments', *Cytokine & Growth Factor Reviews*, 13(4–5), pp. 315-321.

Koltsova, W.D., Vavilova TP. (2007) 'Transcription factors NFAT2 and Egr1 cooperatively regulate the maturation of T-lymphoma in vitro.', *Biochemistry (Mosc)*, 72(9), pp. 954-61.

Köntgen, F., et al. (1995) 'Mice lacking the c-rel proto-oncogene exhibit defects in lymphocyte proliferation, humoral immunity, and interleukin-2 expression', *Genes & Development*, 9(16), pp. 1965-1977.

Kraus, M., et al. (2004) 'Survival of Resting Mature B Lymphocytes Depends on BCR Signaling via the Igα/β Heterodimer', *Cell*, 117(6), pp. 787-800.

Kriegler, M., et al. (1988) 'A novel form of TNF/cachectin is a cell surface cytotoxic transmembrane protein: Ramifications for the complex physiology of TNF', *Cell*, 53(1), pp. 45-53.

Krishnadasan, R., et al. (2006) 'Overexpression of SOCS3 is associated with decreased survival in a cohort of patients with de novo follicular lymphoma', *British Journal of Haematology*, 135(1), pp. 72-75.

Kulbe, H., et al. (2012) 'A dynamic inflammatory cytokine network in the human ovarian cancer microenvironment', *Cancer research*, 72(1), pp. 66-75.

Kulbe, H., et al. (2007) 'The Inflammatory Cytokine Tumor Necrosis Factor-α Generates an Autocrine Tumor-Promoting Network in Epithelial Ovarian Cancer Cells', *Cancer Research*, 67(2), pp. 585-592.

Kulkarni, R.M., et al. (2009) 'NFATc1 regulates lymphatic endothelial development', *Mechanisms of development*, 126(5-6), pp. 350-365.

Kumar, A., et al. (2004) 'Nuclear factor-κB: its role in health and disease', *Journal of Molecular Medicine*, 82(7), pp. 434-448.

Kuno, R., et al. (2005) 'Autocrine activation of microglia by tumor necrosis factor-α', *Journal of Neuroimmunology*, 162(1–2), pp. 89-96.

Kuppers, R. (2005) 'Mechanisms of B-cell lymphoma pathogenesis', *Nat Rev Cancer*, 5(4), pp. 251-262.

Küppers, R., et al. (2012) 'Hodgkin lymphoma', *The Journal of Clinical Investigation*, 122(10), pp. 3439-3447.

Kuroda, Y., et al. (2012) 'Cot Kinase Promotes Ca(2+) Oscillation/Calcineurin-Independent Osteoclastogenesis by Stabilizing NFATc1 Protein', *Molecular and Cellular Biology*, 32(14), pp. 2954-2963.

Kuroda, Y., et al. (2008) 'Osteoblasts induce Ca(2+) oscillation-independent NFATc1 activation during osteoclastogenesis', *Proceedings of the National Academy of Sciences of the United States of America*, 105(25), pp. 8643-8648.

Lagunas, L., et al. (2009) 'Deregulated NFATc1 activity transforms murine fibroblasts via an autocrine growth factor-mediated Stat3-dependent pathway', *Journal of Cellular Biochemistry*, 108(1), pp. 237-248.

Lai, M.M., et al. (1998) 'Cain, A Novel Physiologic Protein Inhibitor of Calcineurin', *Journal of Biological Chemistry*, 273(29), pp. 18325-18331.

Lam, K.-P., et al. (1997) 'In Vivo Ablation of Surface Immunoglobulin on Mature B Cells by Inducible Gene Targeting Results in Rapid Cell Death', *Cell*, 90(6), pp. 1073-1083.

Lam, L.T., et al. (2005) 'Small Molecule Inhibitors of IκB Kinase Are Selectively Toxic for Subgroups of Diffuse Large B-Cell Lymphoma Defined by Gene Expression Profiling', *Clinical Cancer Research*, 11(1), pp. 28-40.

Lam, L.T., et al. (2008) 'Cooperative signaling through the signal transducer and activator of transcription 3 and nuclear factor-κB pathways in subtypes of diffuse large B-cell lymphoma', *Blood*, 111(7), pp. 3701-3713.

Le Roy, C., et al. (2012) *The degree of BCR and NFAT activation predicts clinical outcomes in chronic lymphocytic leukemia*.

Lehen'Kyi, V., et al. (2007) 'TRPV6 channel controls prostate cancer cell proliferation via Ca2+//NFAT-dependent pathways', *Oncogene*, 26(52), pp. 7380-7385.

Lenz, G., et al. (2008a) 'Oncogenic CARD11 Mutations in Human Diffuse Large B Cell Lymphoma', *Science*, 319(5870), pp. 1676-1679.

Lenz, G., et al. (2010) 'Aggressive Lymphomas', *New England Journal of Medicine*, 362(15), pp. 1417-1429.

Lenz, G., et al. (2008b) 'Stromal Gene Signatures in Large-B-Cell Lymphomas', *New England Journal of Medicine*, 359(22), pp. 2313-2323.

Lenz, G., et al. (2008c) 'Molecular subtypes of diffuse large B-cell lymphoma arise by distinct genetic pathways', *Proceedings of the National Academy of Sciences*, 105(36), pp. 13520-13525.

Li-Weber, M., et al. (2004) 'NF-κB synergizes with NF-AT and NF-IL6 in activation of the IL-4 gene in T cells', *European Journal of Immunology*, 34(4), pp. 1111-1118.

Li, Q., et al. (2012) 'Constitutive Nuclear Localization of NFAT in Foxp3+ Regulatory T Cells Independent of Calcineurin Activity', *The Journal of Immunology*, 188(9), pp. 4268-4277.

Liao, G., et al. (2004) 'Regulation of the NF-κB-inducing Kinase by Tumor Necrosis Factor Receptor-associated Factor 3-induced Degradation', *Journal of Biological Chemistry*, 279(25), pp. 26243-26250.

Lin, S.-C., et al. (2010) 'Helical assembly in the MyD88–IRAK4–IRAK2 complex in TLR/IL-1R signalling', *Nature*, 465(7300), pp. 885-890.

Lin, S.M., et al. (2008) 'Model-based variance-stabilizing transformation for Illumina microarray data', *Nucleic Acids Research*, 36(2), pp. e11-e11.

Lin, X., et al. (1999) 'Inhibition of Calcineurin Phosphatase Activity by a Calcineurin B Homologous Protein', *Journal of Biological Chemistry*, 274(51), pp. 36125-36131.

Lin, Y., et al. (1997) 'Repression of c-myc Transcription by Blimp-1, an Inducer of Terminal B Cell Differentiation', *Science*, 276(5312), pp. 596-599.

Liu, J., et al. (1991) 'Calcineurin is a common target of cyclophilin-cyclosporin A and FKBP-FK506 complexes', *Cell*, 66(4), pp. 807-815.

Liu, Q., et al. (2012) 'Interaction Between NFκB and NFAT Coordinates Cardiac Hypertrophy and Pathological Remodeling', *Circulation Research*, 110(8), pp. 1077-1086.

Locksley, R.M., et al. (2001) 'The TNF and TNF Receptor Superfamilies: Integrating Mammalian Biology', *Cell*, 104(4), pp. 487-501.

Lohr, J.G., et al. (2012) 'Discovery and prioritization of somatic mutations in diffuse large B-cell lymphoma (DLBCL) by whole-exome sequencing', *Proceedings of the National Academy of Sciences*, 109(10), pp. 3879-3884.

López-Rodríguez, C., et al. (2001) 'Bridging the NFAT and NF-κB Families: NFAT5 Dimerization Regulates Cytokine Gene Transcription in Response to Osmotic Stress', *Immunity*, 15(1), pp. 47-58.

López-Rodríguez, C., et al. (1999) 'NFAT5, a constitutively nuclear NFAT protein that does not cooperate with Fos and Jun', *Proceedings of the National Academy of Sciences*, 96(13), pp. 7214-7219.

Lynch, J., et al. (2005) 'Calreticulin signals upstream of calcineurin and MEF2C in a critical Ca2+-dependent signaling cascade', *The Journal of Cell Biology*, 170(1), pp. 37-47.

Macian, F. (2001) 'Partners in transcription: NFAT and AP-1', *Oncogene*, 20(19), pp. 2476-2489.

Macian, F. (2005) 'NFAT proteins: key regulators of T-cell development and function', *Nat Rev Immunol*, 5(6), pp. 472-484.

MacLennan, I.C.M. (1994) 'Germinal Centers', *Annual Review of Immunology*, 12(1), pp. 117-139.

Maggirwar, S.B., et al. (1997) 'Regulation of the interleukin-2 CD28-responsive element by NF-ATp and various NF-kappaB/Rel transcription factors', *Molecular and Cellular Biology*, 17(5), pp. 2605-14.

Mancini, M., et al. (2009) 'NFAT proteins: emerging roles in cancer progression', *Nat Rev Cancer*, 9(11), pp. 810-820.

Mandelbaum, J., et al. (2010) 'BLIMP1 Is a Tumor Suppressor Gene Frequently Disrupted in Activated B Cell-like Diffuse Large B Cell Lymphoma', *Cancer Cell*, 18(6), pp. 568-579.

Mani, S.A., et al. (2008) 'The epithelial-mesenchymal transition generates cells with properties of stem cells', *Cell*, 133(4), pp. 704-715.

Manninen, A., et al. (2000) 'Synergistic Activation of NFAT by HIV-1 Nef and the Ras/MAPK Pathway', *Journal of Biological Chemistry*, 275(22), pp. 16513-16517.

Marafioti, T., et al. (2005) 'The NFATc1 transcription factor is widely expressed in white cells and translocates from the cytoplasm to the nucleus in a subset of human lymphomas', *British Journal of Haematology*, 128(3), pp. 333-342.

Masuda, E.S., et al. (1995) 'NFATx, a novel member of the nuclear factor of activated T cells family that is expressed predominantly in the thymus', *Molecular and Cellular Biology*, 15(5), pp. 2697-706.

Masuda, E.S., et al. (1993) 'The granulocyte-macrophage colony-stimulating factor promoter cis-acting element CLE0 mediates induction signals in T cells and is recognized by factors related to AP1 and NFAT', *Molecular and Cellular Biology*, 13(12), pp. 7399-7407.

Mathot, L., et al. (2012) 'Behavior of seeds and soil in the mechanism of metastasis: A deeper understanding', *Cancer Science*, 103(4), pp. 626-631.

Matsuda, S., et al. (2000) 'Mechanisms of action of cyclosporine', *Immunopharmacology*, 47(2–3), pp. 119-125.

Maus, U., et al. (2001) 'Monocytes recruited into the alveolar air space of mice show a monocytic phenotype but upregulate CD14', *American Journal of Physiology - Lung Cellular and Molecular Physiology*, 280(1), pp. L58-L68.

Maxeiner, J.H., et al. (2009) 'A Key Regulatory Role of the Transcription Factor NFATc2 in Bronchial Adenocarcinoma via CD8+ T Lymphocytes', *Cancer Research*, 69(7), pp. 3069-3076.

McCabe, M.T., et al. (2012) 'EZH2 inhibition as a therapeutic strategy for lymphoma with EZH2-activating mutations', *Nature*, 492(7427), pp. 108-112.

McCaffrey PG, L.C., Kerppola TK, Jain J, Badalian TM, Ho AM, Burgeon E, Lane WS, Lambert JN, Curran T, et al (1993) 'Isolation of the cyclosporin-sensitive T cell transcription', *Science*, 262(5134), p. 750.

McCarthy, E.F. (2006) 'The Toxins of William B. Coley and the Treatment of Bone and Soft-Tissue Sarcomas', *The Iowa Orthopaedic Journal*, 26, pp. 154-158.

Medyouf, H., et al. (2007) 'Targeting calcineurin activation as a therapeutic strategy for T-cell acute lymphoblastic leukemia', *Nat Med*, 13(6), pp. 736-741.

Meyer, P.N., et al. (2011) 'Immunohistochemical Methods for Predicting Cell of Origin and Survival in Patients With Diffuse Large B-Cell Lymphoma Treated With Rituximab', *Journal of Clinical Oncology*, 29(2), pp. 200-207.

Minami, T., et al. (2013) 'The Calcineurin-NFAT-Angiopoietin 2 signaling axis in lung endothelium is critical for the establishment of lung metastases', *Cell reports*, 4(4), pp. 709-723.

Mitoma, H., et al. (2005) 'Infliximab induces potent anti-inflammatory responses by outside-to-inside signals through transmembrane TNF-α', *Gastroenterology*, 128(2), pp. 376-392.

Miyakawa, H., et al. (1999) 'Tonicity-responsive enhancer binding protein, a Rel-like protein that stimulates transcription in response to hypertonicity', *Proceedings of the National Academy of Sciences*, 96(5), pp. 2538-2542.

Mohler, K.M., et al. (1993) 'Soluble tumor necrosis factor (TNF) receptors are effective therapeutic agents in lethal endotoxemia and function simultaneously as both TNF carriers and TNF antagonists', *The Journal of Immunology*, 151(3), pp. 1548-61.

Molavi, O., et al. (2013) 'Gene methylation and silencing of SOCS3 in mantle cell lymphoma', *British Journal of Haematology*, 161(3), pp. 348-356.

Monroe, J.G. (2004) 'Ligand-independent tonic signaling in B-cell receptor function', *Current Opinion in Immunology*, 16(3), pp. 288-295.

Monti, S., et al. (2005) 'Molecular profiling of diffuse large B-cell lymphoma identifies robust subtypes including one characterized by host inflammatory response', *Blood*, 105(5), pp. 1851-1861.

Morin, R.D., et al. (2010) 'Somatic mutations altering EZH2 (Tyr641) in follicular and diffuse large B-cell lymphomas of germinal-center origin', *Nat Genet*, 42(2), pp. 181-185.

Morin, R.D., et al. (2011) 'Frequent mutation of histone-modifying genes in non-Hodgkin lymphoma', *Nature*, 476(7360), pp. 298-303.

Mott, J.D., et al. (2004) 'Regulation of matrix biology by matrix metalloproteinases', *Current opinion in cell biology*, 16(5), pp. 558-564.

Mueller, K., et al. (2013) 'Octamer-dependent transcription in T cells is mediated by NFAT and NF-κB', *Nucleic Acids Research*, 41(4), pp. 2138-2154.

Muhammad, K., et al. (2014) 'NF-κB factors control the induction of NFATc1 in B lymphocytes', *European Journal of Immunology*, pp. n/a-n/a.

Mukaida, N., et al. (2014) 'Chemokines in Cancer Development and Progression and Their Potential as Targeting Molecules for Cancer Treatment', *Mediators of Inflammation*, 2014, p. 170381.

Muller, A., et al. (2001) 'Involvement of chemokine receptors in breast cancer metastasis', *Nature*, 410(6824), pp. 50-56.

Muller, C.W., et al. (1995) 'Structure of the NF-[kappa]B p50 homodimer bound to DNA', *Nature*, 373(6512), pp. 311-317.

Müller, M.R., et al. (2010) 'NFAT, immunity and cancer: a transcription factor comes of age', *Nat Rev Immunol*, 10(9), pp. 645-656.

Muramatsu, M., et al. (2000) 'Class Switch Recombination and Hypermutation Require Activation-Induced Cytidine Deaminase (AID), a Potential RNA Editing Enzyme', *Cell*, 102(5), pp. 553-563.

Muramatsu, M., et al. (1999) 'Specific Expression of Activation-induced Cytidine Deaminase (AID), a Novel Member of the RNA-editing Deaminase Family in Germinal Center B Cells', *Journal of Biological Chemistry*, 274(26), pp. 18470-18476.

Muratovska, A., et al. (2003) 'Paired-Box genes are frequently expressed in cancer and often required for cancer cell survival', *Oncogene*, 22(39), pp. 7989-7997.

Nakayama, S., et al. (2014a) 'TNF-α Expression in Tumor Cells as a Novel Prognostic Marker for Diffuse Large B-cell Lymphoma, Not Otherwise Specified', *The American Journal of Surgical Pathology*, 38(2), pp. 228-234 10.1097/PAS.0000000000000094.

Nakayama, S., et al. (2014b) 'TNF-α Receptor 1 Expression Predicts Poor Prognosis of Diffuse Large B-cell Lymphoma, Not Otherwise Specified', *The American Journal of Surgical Pathology*, 38(8), pp. 1138-1146.

Nan, J., et al. (2014) 'TPCA-1 Is a Direct Dual Inhibitor of STAT3 and NF-κB and Regresses Mutant EGFR-Associated Human Non–Small Cell Lung Cancers', *Molecular Cancer Therapeutics*, 13(3), pp. 617-629.

Naudé, P.J.W., et al. (2011) 'Tumor necrosis factor receptor cross-talk', *FEBS Journal*, 278(6), pp. 888-898.

Nayak, A., et al. (2009) 'Sumoylation of the Transcription Factor NFATc1 Leads to Its Subnuclear Relocalization and Interleukin-2 Repression by Histone Deacetylase', *Journal of Biological Chemistry*, 284(16), pp. 10935-10946.

Neal, J.W., et al. (2003) 'A Constitutively Active NFATc1 Mutant Induces a Transformed Phenotype in 3T3-L1 Fibroblasts', *Journal of Biological Chemistry*, 278(19), pp. 17246-17254.

Negishi-Koga, T., et al. (2009) 'Ca2+-NFATc1 signaling is an essential axis of osteoclast differentiation', *Immunological Reviews*, 231(1), pp. 241-256.

Nemer, G., et al. (2002) 'Cooperative interaction between GATA5 and NF-ATc regulates endothelial-endocardial differentiation of cardiogenic cells', *Development*, 129(17), pp. 4045-4055.

Nesbitt A1, F.G., Bergin M, Stephens P, Stephens S, Foulkes R, Brown D, Robinson M, Bourne T. (2007) 'Mechanism of action of certolizumab pegol (CDP870): in vitro comparison with other anti-tumor necrosis factor alpha agents.', *Inflamm Bowel Dis.*, 13(11), pp. 1323-32.

Ngo, V.N., et al. (2006) 'A loss-of-function RNA interference screen for molecular targets in cancer', *Nature*, 441(7089), pp. 106-110.

Ngo, V.N., et al. (2011) 'Oncogenically active MYD88 mutations in human lymphoma', *Nature*, 470(7332), pp. 115-119.

Noemi Soto-Nieves, I.P., 1 Brian T. Abe,1 Sanmay Bandyopadhyay,1 Ian Baine,1 Anjana Rao,2 and Fernando Macian1 (2009) 'Transcriptional complexes formed by NFAT dimers regulate the induction of T cell tolerance', *J Exp Med*, 206(4), pp. 867-876.

Nogai, H., et al. (2011) 'Pathogenesis of Non-Hodgkin's Lymphoma', *Journal of Clinical Oncology*, 29(14), pp. 1803-1811.

Nogai, H., et al. (2013) *IκB-ζ controls the constitutive NF-κB target gene network and survival of ABC DLBCL*.

Noguchi (2004) 'A new cell-permeable peptide allows successful allogenic islet transplantation in mice ', *Nature Medicine*, 10, pp. 305-309.

Norrmén, C., et al. (2009) 'FOXC2 controls formation and maturation of lymphatic collecting vessels through cooperation with NFATc1', *The Journal of Cell Biology*, 185(3), pp. 439-457.

Northrop, J.P., et al. (1994) 'NF-AT components define a family of transcription factors targeted in T-cell activation', *Nature*, 369(6480), pp. 497-502.

Nowakowski, G.S., et al. (2011) 'Lenalidomide can be safely combined with R-CHOP (R2CHOP) in the initial chemotherapy for aggressive B-cell lymphomas: phase I study', *Leukemia*, 25(12), pp. 1877-1881.

Oestreich, K.J., et al. (2008) 'NFATc1 Regulates PD-1 Expression upon T Cell Activation', *The Journal of Immunology*, 181(7), pp. 4832-4839.

Okamura, H., et al. (2000) 'Concerted Dephosphorylation of the Transcription Factor NFAT1 Induces a Conformational Switch that Regulates Transcriptional Activity', *Molecular Cell*, 6(3), pp. 539-550.

Okamura H, C.G.-R., 1,† Holly Martinson,1 Jun Qin,2 David M. Virshup,3 and Anjana Rao1,* (2004) 'A Conserved Docking Motif for CK1 Binding Controls the Nuclear Localization of NFAT1', *Mol Cell Biol*, 24(10), pp. 4184-4195.

Olabisi, O.A., et al. (2008) 'Regulation of Transcription Factor NFAT by ADP-Ribosylation', *Molecular and Cellular Biology*, 28(9), pp. 2860-2871.

Oro, A.E. (2008) 'A New Role for an Old Friend: NFAT and Stem Cell Quiescence', *Cell stem cell*, 2(2), p. 10.1016/j.stem.2008.01.008.

Oukka, M., et al. (1998) 'The Transcription Factor NFAT4 Is Involved in the Generation and Survival of T Cells', *Immunity*, 9(3), pp. 295-304.

Paget, S. (1889) 'The distribution of secondary growths in cancer of the breast.', *Cancer Metastasis Rev.*, 8(2), pp. 98-101.

Palkowitsch, L., et al. (2011) 'The Ca2+-dependent Phosphatase Calcineurin Controls the Formation of the Carma1-Bcl10-Malt1 Complex during T Cell Receptor-induced NF-κB Activation', *Journal of Biological Chemistry*, 286(9), pp. 7522-7534.

Palumbo, A., et al. (2011) 'Multiple Myeloma', *New England Journal of Medicine*, 364(11), pp. 1046-1060.

Pan, M.G., et al. (2013) 'NFAT Gene Family in Inflammation and Cancer', *Current molecular medicine*, 13(4), pp. 543-554.

Pan, Z., et al. (2007) 'Discovery of Selective Irreversible Inhibitors for Bruton's Tyrosine Kinase', *ChemMedChem*, 2(1), pp. 58-61.

Pardoll, D.M. (2012) 'The blockade of immune checkpoints in cancer immunotherapy', *Nat Rev Cancer*, 12(4), pp. 252-264.

Park, J., et al. (1996) 'Characterization of a New Isoform of the NFAT (Nuclear Factor of Activated T Cells) Gene Family Member NFATc', *Journal of Biological Chemistry*, 271(34), pp. 20914-20921.

Pasqualucci, L. (2013) 'The Genetic Basis of Diffuse Large B Cell Lymphoma', *Current opinion in hematology*, 20(4), pp. 336-344.

Pasqualucci, L., et al. (2006) 'Inactivation of the PRDM1/BLIMP1 gene in diffuse large B cell lymphoma', *The Journal of Experimental Medicine*, 203(2), pp. 311-317.

Pasqualucci, L., et al. (2011a) 'Inactivating mutations of acetyltransferase genes in B-cell lymphoma', *Nature*, 471(7337), pp. 189-195.

Pasqualucci, L., et al. (2011b) 'Analysis of the Coding Genome of Diffuse Large B-Cell Lymphoma', *Nature Genetics*, 43(9), pp. 830-837.

Péant, B., et al. (2011) 'IκB-Kinase-ε (IKKε/IKKi/IκBKε) expression and localization in prostate cancer tissues', *The Prostate*, 71(10), pp. 1131-1138.

Pedersen, I.M., et al. (2009) 'Onco-miR-155 targets SHIP1 to promote TNFα-dependent growth of B cell lymphomas', *EMBO Molecular Medicine*, 1(5), pp. 288-295.

Pedersen, L.M., et al. (2005) 'Serum levels of inflammatory cytokines at diagnosis correlate to the bcl-6 and CD10 defined germinal centre (GC) phenotype and bcl-2 expression in patients with diffuse large B-cell lymphoma', *British Journal of Haematology*, 128(6), pp. 813-819.

Pei, L., et al. (2012) 'Genome-wide DNA methylation analysis reveals novel epigenetic changes in chronic lymphocytic leukemia', *Epigenetics*, 7(6), pp. 567-578.

Pennica D, N.G., Hayflick JS, Seeburg PH, Derynck R, Palladino MA, Kohr WJ, Aggarwal BB, Goeddel DV. (1984) 'Human tumour necrosis factor: precursor structure, expression and homology to lymphotoxin', *Nature*, 312(5996), pp. 724-9.

Perkins, N.D. (2007) 'Integrating cell-signalling pathways with NF-[kappa]B and IKK function', *Nat Rev Mol Cell Biol*, 8(1), pp. 49-62.

Perkins, N.D. (2012) 'The diverse and complex roles of NF-κB subunits in cancer', *Nat Rev Cancer*, 12(2), pp. 121-132.

Perotti, V., et al. (2012) 'NFATc2 Is a Potential Therapeutic Target in Human Melanoma', *J Invest Dermatol*, 132(11), pp. 2652-2660.

Pfeifer, M., et al. (2013a) 'PTEN loss defines a PI3K/AKT pathway-dependent germinal center subtype of diffuse large B-cell lymphoma', *Proceedings of the National Academy of Sciences of the United States of America*, 110(30), pp. 12420-12425.

Pfeifer, M., et al. (2013b) 'PI3K/AKT addiction in subsets of diffuse large B-cell lymphoma', *Cell Cycle*, 12(21), pp. 3347-3348.

Pfreundschuh, M., et al. (2011) 'CHOP-like chemotherapy with or without rituximab in young patients with good-prognosis diffuse large-B-cell lymphoma: 6-year results of an open-label randomised study of the MabThera International Trial (MInT) Group', *The Lancet Oncology*, 12(11), pp. 1013-1022.

Pham, L.V., et al. (2010) 'An epigenetic chromatin remodeling role for NFATc1 in transcriptional regulation of growth and survival genes in diffuse large B-cell lymphomas', *Blood,* 116(19), pp. 3899-3906.

Pham, L.V., et al. (2005) 'Constitutive NF-κB and NFAT activation in aggressive B-cell lymphomas synergistically activates the CD154 gene and maintains lymphoma cell survival', *Blood,* 106(12), pp. 3940-3947.

Phan, R.T., et al. (2004) 'The BCL6 proto-oncogene suppresses p53 expression in germinal-centre B cells', *Nature*, 432(7017), pp. 635-639.

Pimentel-Muiños, F.X., et al. (1999) 'Regulated Commitment of TNF Receptor Signaling: A Molecular Switch for Death or Activation', *Immunity*, 11(6), pp. 783-793.

Podolin, P.L., et al. (2005) 'Attenuation of Murine Collagen-Induced Arthritis by a Novel, Potent, Selective Small Molecule Inhibitor of IκB Kinase 2, TPCA-1 (2-[(Aminocarbonyl)amino]-5-(4-fluorophenyl)-3-thiophenecarboxamide), Occurs via Reduction of Proinflammatory Cytokines and Antigen-Induced T Cell Proliferation', *Journal of Pharmacology and Experimental Therapeutics,* 312(1), pp. 373-381.

Prasad, A.M., et al. (2011) 'Silencing calcineurin A subunit reduces SERCA2 expression in cardiac myocytes', *American Journal of Physiology - Heart and Circulatory Physiology*, 300(1), pp. H173-H180.

Pulvino, M., et al. (2015) *Inhibition of COP9-signalosome (CSN) deneddylating activity and tumor growth of diffuse large B-cell lymphomas by doxycycline*.

Putney Jr, J.W., et al. (1993) 'The signal for capacitative calcium entry', *Cell*, 75(2), pp. 199-201.

Pyzocha, N., et al. (2014) 'RNA-Guided Genome Editing of Mammalian Cells', in Storici, F. (ed.) *Gene Correction*. Humana Press, pp. 269-277.

Qin, B., et al. (2010) 'Silencing of the IKKε gene by siRNA inhibits invasiveness and growth of breast cancer cells', *Breast Cancer Research : BCR*, 12(5), pp. R74-R74.

Qin, J.-J., et al. (2014) 'NFAT as cancer target: Mission possible?', *Biochimica et Biophysica Acta (BBA) - Reviews on Cancer*, 1846(2), pp. 297-311.

Qin, S.N., S. Voruganti, W. Wang and R. Zhang (2012) 'Natural Product MDM2 Inhibitors: Anticancer Activity and Mechanisms of Action ', *Current medicinal chemistry* 19(33), pp. 5705-5725.

Rabinovitz, I., et al. (1997) 'The Integrin α6β4 Functions in Carcinoma Cell Migration on Laminin-1 by Mediating the Formation and Stabilization of Actin-containing Motility Structures', *The Journal of Cell Biology*, 139(7), pp. 1873-1884.

Rajkumar, S.V. (2014) 'Multiple myeloma: 2014 Update on diagnosis, risk-stratification, and management', *American Journal of Hematology*, 89(10), pp. 998-1009.

Ranger, A.M., et al. (1998) 'The transcription factor NF-ATc is essential for cardiac valve formation', *Nature*, 392(6672), pp. 186-190.

Ranuncolo, S.M., et al. (2007) 'Bcl-6 mediates the germinal center B cell phenotype and lymphomagenesis through transcriptional repression of the DNA-damage sensor ATR', *Nat Immunol*, 8(7), pp. 705-714.

Rauert-Wunderlich, H., et al. (2013) 'The IKK Inhibitor Bay 11-7082 Induces Cell Death Independent from Inhibition of Activation of NFκB Transcription Factors', *PLoS ONE*, 8(3), p. e59292.

Rauert, H., et al. (2010) 'Membrane Tumor Necrosis Factor (TNF) Induces p100 Processing via TNF Receptor-2 (TNFR2)', *Journal of Biological Chemistry*, 285(10), pp. 7394-7404.

Rawlings, D.J., et al. (2012) 'Integration of B cell responses through Toll-like receptors and antigen receptors', *Nature reviews. Immunology*, 12(4), pp. 282-294.

Rencher, A.C. (2003) 'Principal Component Analysis', in *Methods of Multivariate Analysis*. John Wiley & Sons, Inc., pp. 380-407.

Rengarajan, J., et al. (2000) 'Sequential Involvement of NFAT and Egr Transcription Factors in FasL Regulation', *Immunity*, 12(3), pp. 293-300.

Rengarajan, J., et al. (2002) 'Interferon Regulatory Factor 4 (IRF4) Interacts with NFATc2 to Modulate Interleukin 4 Gene Expression', *The Journal of Experimental Medicine*, 195(8), pp. 1003-1012.

Rezzani, R. (2004) 'Cyclosporine A and adverse effects on organs: histochemical studies', *Progress in Histochemistry and Cytochemistry*, 39, pp. 85-128.

Richter, C., et al. (2012) 'The Tumor Necrosis Factor Receptor Stalk Regions Define Responsiveness to Soluble versus Membrane-Bound Ligand', *Molecular and Cellular Biology*, 32(13), pp. 2515-2529.

Rickert, R.C. (2013) 'New insights into pre-BCR and BCR signalling with relevance to B cell malignancies', *Nat Rev Immunol*, 13(8), pp. 578-591.

Rivoltini, L., et al. (2005) 'Escape strategies and reasons for failure in the interaction between tumour cells and the immune system: how can we tilt the balance towards immune-mediated cancer control?', *Expert Opinion on Biological Therapy*, 5(4), pp. 463-476.

Robbs, B.K., et al. (2008) 'Dual roles for NFAT transcription factor genes as oncogenes and tumor suppressors', *Molecular and cellular biology*, 28(23), pp. 7168-7181.
Robbs, B.K., et al. (2013) 'The transcription factor NFAT1 induces apoptosis through cooperation with Ras/Raf/MEK/ERK pathway and upregulation of TNF-α expression', *Biochimica et Biophysica Acta (BBA) - Molecular Cell Research*, 1833(8), pp. 2016-2028.
Roehrl, M.H.A., et al. (2004) 'Selective inhibition of calcineurin-NFAT signaling by blocking protein–protein interaction with small organic molecules', *Proceedings of the National Academy of Sciences of the United States of America*, 101(20), pp. 7554-7559.
Rosenwald, A., et al. (2002) 'The Use of Molecular Profiling to Predict Survival after Chemotherapy for Diffuse Large-B-Cell Lymphoma', *New England Journal of Medicine*, 346(25), pp. 1937-1947.
Rosenwald, A., et al. (2003) 'Molecular Diagnosis of Primary Mediastinal B Cell Lymphoma Identifies a Clinically Favorable Subgroup of Diffuse Large B Cell Lymphoma Related to Hodgkin Lymphoma', *The Journal of Experimental Medicine*, 198(6), pp. 851-862.
Rossi, D., et al. (2013) 'Genetic aberrations of signaling pathways in lymphomagenesis: Revelations from next generation sequencing studies', *Seminars in Cancer Biology*, 23(6, Part A), pp. 422-430.
Rossille, D., et al. (2014) 'High level of soluble programmed cell death ligand 1 in blood impacts overall survival in aggressive diffuse large B-Cell lymphoma: results from a French multicenter clinical trial', *Leukemia*, 28(12), pp. 2367-2375.
Rudolf, R., et al. (2014) 'Architecture and Expression of the Nfatc1 Gene in Lymphocytes', *Frontiers in Immunology*, 5, p. 21.
Rui, L., et al. (2011) 'Malignant pirates of the immune system', *Nat Immunol*, 12(10), pp. 933-940.
Ruuls, S.R., et al. (2001) 'Membrane-Bound TNF Supports Secondary Lymphoid Organ Structure but Is Subservient to Secreted TNF in Driving Autoimmune Inflammation', *Immunity*, 15(4), pp. 533-543.
Safford, M., et al. (2005) 'Egr-2 and Egr-3 are negative regulators of T cell activation', *Nat Immunol*, 6(5), pp. 472-480.
Saito, M., et al. (2009) 'BCL6 suppression of BCL2 via Miz1 and its disruption in diffuse large B cell lymphoma', *Proceedings of the National Academy of Sciences of the United States of America*, 106(27), pp. 11294-11299.

Sales, K.J., et al. (2009) 'Prostaglandin F2α-F-prostanoid receptor regulates CXCL8 expression in endometrial adenocarcinoma cells via the calcium–calcineurin–NFAT pathway', *Biochimica et Biophysica Acta (BBA) - Molecular Cell Research*, 1793(12), pp. 1917-1928.

Sander, J.D., et al. (2014) 'CRISPR-Cas systems for editing, regulating and targeting genomes', *Nat Biotech*, 32(4), pp. 347-355.

Sankar, S., et al. (2011) 'Promiscuous Partnerships in Ewing's Sarcoma', *Cancer genetics*, 204(7), pp. 351-365.

Saunders, B.M., et al. (2004) 'T cell-derived tumour necrosis factor is essential, but not sufficient, for protection against Mycobacterium tuberculosis infection', *Clinical and Experimental Immunology*, 137(2), pp. 279-287.

Sauter P, M.P. (1997) 'The B cell-specific coactivator OBF-1 (OCA-B, Bob-1) is inducible in T cells and its expression is dispensable for IL-2 gene induction.', *Immunobiology*, 198(1-3), pp. 207-16.

Savage, S.R., et al. (2015) 'RNA-Seq Reveals a Role for NFAT-Signaling in Human Retinal Microvascular Endothelial Cells Treated with TNFα', *PLoS ONE*, 10(1), p. e0116941.

Scamuffa, N., et al. (2008) 'Selective inhibition of proprotein convertases represses the metastatic potential of human colorectal tumor cells', *The Journal of Clinical Investigation*, 118(1), pp. 352-363.

Schmitz, R., et al. (2014) 'Oncogenic Mechanisms in Burkitt Lymphoma', *Cold Spring Harbor Perspectives in Medicine*, 4(2).

Schubart, D.B., et al. (1996) 'Gene structure and characterization of the murine homologue of the B cell-specific transcriptional coactivator OBF-1', *Nucleic Acids Research*, 24(10), pp. 1913-1920.

Schuetz, J.M., et al. (2012) 'BCL2 mutations in diffuse large B-cell lymphoma', *Leukemia*, 26(6), pp. 1383-1390.

Schulz, R.A., et al. (2004) 'Calcineurin signaling and NFAT activation in cardiovascular and skeletal muscle development', *Developmental Biology*, 266(1), pp. 1-16.

Scott, D.W., et al. (2015) 'Prognostic Significance of Diffuse Large B-Cell Lymphoma Cell of Origin Determined by Digital Gene Expression in Formalin-Fixed Paraffin-Embedded Tissue Biopsies', *Journal of Clinical Oncology*, 33(26), pp. 2848-2856.

Sehn, L.H., et al. (2007) 'The revised International Prognostic Index (R-IPI) is a better predictor of outcome than the standard IPI for patients with diffuse large B-cell lymphoma treated with R-CHOP', *Blood*, 109(5), pp. 1857-1861.

Sen, R., et al. (1986) 'Multiple nuclear factors interact with the immunoglobulin enhancer sequences', *Cell*, 46(5), pp. 705-716.

Sengupta, S., et al. (2014) 'TGF-β-Smad2 dependent activation of CDC 25A plays an important role in cell proliferation through NFAT activation in metastatic breast cancer cells', *Cellular Signalling*, 26(2), pp. 240-252.

Sengupta, S., et al. (2013) 'Cooperative involvement of NFAT and SnoN mediates transforming growth factor-β (TGF-β) induced EMT in metastatic breast cancer (MDA-MB 231) cells', *Clinical & Experimental Metastasis*, 30(8), pp. 1019-1031.

Serfling, E., et al. (2004) 'NFAT and NF-κB factors—the distant relatives', *The International Journal of Biochemistry & Cell Biology*, 36(7), pp. 1166-1170.

Serfling, E., et al. (2006a) 'NFATc1 autoregulation: a crucial step for cell-fate determination', *Trends in Immunology*, 27(10), pp. 461-469.

Serfling, E., et al. (2006b) 'NFAT transcription factors in control of peripheral T cell tolerance', *European Journal of Immunology*, 36(11), pp. 2837-2843.

Shaffer, A.L., et al. (2002a) 'Blimp-1 Orchestrates Plasma Cell Differentiation by Extinguishing the Mature B Cell Gene Expression Program', *Immunity*, 17(1), pp. 51-62.

Shaffer, A.L., et al. (2002b) 'Lymphoid Malignancies: the dark side of B-cell differentiation', *Nat Rev Immunol*, 2(12), pp. 920-933.

Shaffer, A.L., et al. (2012a) 'Pathogenesis of Human B Cell Lymphomas', *Annual Review of Immunology*, 30(1), pp. 565-610.

Shaffer, A.L., et al. (2012b) 'Pathogenesis of Human B Cell Lymphomas*', *Annual Review of Immunology*, 30(1), pp. 565-610.

Shaffer, A.L., et al. (2000) 'BCL-6 Represses Genes that Function in Lymphocyte Differentiation, Inflammation, and Cell Cycle Control', *Immunity*, 13(2), pp. 199-212.

Shapiro-Shelef, M., et al. (2003) 'Blimp-1 Is Required for the Formation of Immunoglobulin Secreting Plasma Cells and Pre-Plasma Memory B Cells', *Immunity*, 19(4), pp. 607-620.

Shaw, J., Utz, P. J., Durand, D. B., Toole, J. J., Emmel, E. A., & Crabtree, C. R. (1988) 'Identification of a putative regulator of early T cell activation genes', *Science* 241(4862), pp. 202-205.

Sherman, M.A., et al. (1999) 'NF-ATc Isoforms Are Differentially Expressed and Regulated in Murine T and Mast Cells', *The Journal of Immunology*, 162(5), pp. 2820-2828.

Shilatifard, A. (2012) 'The COMPASS Family of Histone H3K4 Methylases: Mechanisms of Regulation in Development and Disease Pathogenesis', *Annual review of biochemistry*, 81, pp. 65-95.

Shipp, M.A. (2007) 'Molecular Signatures Define New Rational Treatment Targets in Large B-Cell Lymphomas', *ASH Education Program Book*, 2007(1), pp. 265-269.

Shiratori, M., et al. (2010) 'P2X7 receptor activation induces CXCL2 production in microglia through NFAT and PKC/MAPK pathways', *Journal of Neurochemistry*, 114(3), pp. 810-819.

Shou, J., et al. (2015) 'Nuclear factor of activated T cells in cancer development and treatment', *Cancer Letters*, 361(2), pp. 174-184.

Shukla, U., et al. (2009) 'Tyrosine Phosphorylation of 3BP2 Regulates B Cell Receptor-mediated Activation of NFAT', *Journal of Biological Chemistry*, 284(49), pp. 33719-33728.

Sica, A., et al. (1997) 'Interaction of NF-κB and NFAT with the Interferon-γ Promoter', *Journal of Biological Chemistry*, 272(48), pp. 30412-30420.

Sieber, M.a.B., R (2009) 'Novel inhibitors of the calcineurin/NFATc hub - alternatives to CsA and FK506?', *Cell Communication and Signaling*, 7(25).

Singh, R.R., et al. (2010) 'Hedgehog signaling pathway is activated in diffuse large B-cell lymphoma and contributes to tumor cell survival and proliferation', *Leukemia*, 24(5), pp. 1025-1036.

Skerka, D.E., Zipfel PF. (1995) 'A regulatory element in the human interleukin 2 gene promoter is a binding site for the zinc finger proteins Sp1 and EGR-1', *J Biol Chem*, 270(38), pp. 22500-6.

Skobe, M., et al. (2001) 'Induction of tumor lymphangiogenesis by VEGF-C promotes breast cancer metastasis', *Nat Med*, 7(2), pp. 192-198.

Smith, C.A., et al. (1994) 'The TNF receptor superfamily of cellular and viral proteins: Activation, costimulation, and death', *Cell*, 76(6), pp. 959-962.

Song, M.S., et al. (2012) 'The functions and regulation of the PTEN tumour suppressor', *Nat Rev Mol Cell Biol*, 13(5), pp. 283-296.

Spender, L.C., et al. (2014) 'Developments in Burkitt's lymphoma: novel cooperations in oncogenic MYC signaling', *Cancer Management and Research*, 6, pp. 27-38.

Srinivasan, L., et al. (2009) 'PI3 Kinase Signals BCR-Dependent Mature B Cell Survival', *Cell*, 139(3), pp. 573-586.

Starr, R., et al. (1997) 'A family of cytokine-inducible inhibitors of signalling', *Nature*, 387(6636), pp. 917-921.

Staudt, L.M. (2010) 'Oncogenic activation of NF-kappaB', *Cold Spring Harbor perspectives in biology*, 2(6), p. a000109.

Steinhardt, J.J., et al. (2012) 'Promising Personalized Therapeutic Options for Diffuse Large B-cell Lymphoma Subtypes with Oncogene Addictions', *Clinical Cancer Research*, 18(17), pp. 4538-4548.

Strickson, S., et al. (2013) 'The anti-inflammatory drug BAY 11-7082 suppresses the MyD88-dependent signalling network by targeting the ubiquitin system', *Biochemical Journal*, 451(3), pp. 427-437.

Su, I.h., et al. (2003) 'Ezh2 controls B cell development through histone H3 methylation and Igh rearrangement', *Nat Immunol*, 4(2), pp. 124-131.

Szuhai, K., et al. (2009) 'The NFATc2 Gene Is Involved in a Novel Cloned Translocation in a Ewing Sarcoma Variant That Couples Its Function in Immunology to Oncology', *Clinical Cancer Research*, 15(7), pp. 2259-2268.

Takahashi, K., et al. (2015) 'CCL3 and CCL4 are biomarkers for B cell receptor pathway activation and prognostic serum markers in diffuse large B cell lymphoma', *British Journal of Haematology*, pp. n/a-n/a.

Tan, T.H., et al. (1992) 'κB Site-Dependent Activation of the Interleukin-2 Receptor α-Chain Gene Promoter by Human c-Rel', *Molecular and Cellular Biology*, 12(9), pp. 4067-4075.

Tang, P., et al. (1996) 'Human pro-Tumor Necrosis Factor Is a Homotrimer', *Biochemistry*, 35(25), pp. 8216-8225.

Taylor, P.C., et al. (2000) 'Reduction of chemokine levels and leukocyte traffic to joints by tumor necrosis factor α blockade in patients with rheumatoid arthritis', *Arthritis & Rheumatism*, 43(1), pp. 38-47.

Teimourian, S., et al. (2015) 'CARD15 gene overexpression reduces effect of etanercept, infliximab, and adalimumab on cytokine secretion from PMA activated U937 cells', *European Journal of Pharmacology*, 762, pp. 394-401.

Terui, Y., et al. (2004) 'Dual Role of Sumoylation in the Nuclear Localization and Transcriptional Activation of NFAT1', *Journal of Biological Chemistry*, 279(27), pp. 28257-28265.

Thiery, J.P. (2002) 'Epithelial-mesenchymal transitions in tumour progression', *Nat Rev Cancer*, 2(6), pp. 442-454.

Thome, M., et al. (2010) 'Antigen Receptor Signaling to NF-κB via CARMA1, BCL10, and MALT1', *Cold Spring Harbor Perspectives in Biology*, 2(9), p. a003004.

Tie, X., et al. (2013) 'NFAT1 Is Highly Expressed in, and Regulates the Invasion of, Glioblastoma Multiforme Cells', *PLoS ONE*, 8(6), p. e66008.

Tone, Y., et al. (2008) 'Smad3 and NFAT cooperate to induce Foxp3 expression through its enhancer', *Nat Immunol*, 9(2), pp. 194-202.

Tong G, S.D., Jahr CE. (1995) 'Synaptic desensitization of NMDA receptors by calcineurin

', *Science*, 10(267), pp. 1510-2.

Traenckner, E.B., et al. (1995) 'Phosphorylation of human I kappa B-alpha on serines 32 and 36 controls I kappa B-alpha proteolysis and NF-kappa B activation in response to diverse stimuli', *The EMBO Journal*, 14(12), pp. 2876-2883.

Tripathi, P., et al. (2013) 'Activation of NFAT signaling establishes a tumorigenic microenvironment through cell autonomous and non-cell autonomous mechanisms', *Oncogene*.

Tsujimoto Y, F.L., Yunis J, Nowell PC, Croce CM. (1984) 'Cloning of the chromosome breakpoint of neoplastic B cells with the t(14;18) chromosome translocation', *Science*, 226(4678), pp. 1097-9.

Ulrich, J.D., et al. (2012) 'Distinct Activation Properties of the Nuclear Factor of Activated T cells (NFAT) Isoforms NFATc3 and NFATc4 in Neurons', *The Journal of Biological Chemistry*, 287(45), pp. 37594-37609.

Unknown (1993) 'A Predictive Model for Aggressive Non-Hodgkin's Lymphoma', *New England Journal of Medicine*, 329(14), pp. 987-994.

Vafadari, R., et al. (2013) 'Tacrolimus Inhibits NF-κB Activation in Peripheral Human T Cells', *PLoS ONE*, 8(4), p. e60784.

Vallabhapurapu, S., et al. (2009) 'Regulation and Function of NF-κB Transcription Factors in the Immune System', *Annual Review of Immunology*, 27(1), pp. 693-733.

Van Herreweghe, F., et al. (2010) 'Tumor necrosis factor-mediated cell death: to break or to burst, that’s the question', *Cellular and Molecular Life Sciences*, 67(10), pp. 1567-1579.

Vázquez-Cedeira, M., et al. (2012) 'Human VRK2 (Vaccinia-related Kinase 2) Modulates Tumor Cell Invasion by Hyperactivation of NFAT1 and Expression of Cyclooxygenase-2', *The Journal of Biological Chemistry*, 287(51), pp. 42739-42750.

Velichutina, I., et al. (2010) *EZH2-mediated epigenetic silencing in germinal center B cells contributes to proliferation and lymphomagenesis*.

Vilimas, T., et al. (2007) 'Targeting the NF-[kappa]B signaling pathway in Notch1-induced T-cell leukemia', *Nat Med*, 13(1), pp. 70-77.

Vincent Feng-Sheng Shih, R.T., 1 Andrew Caldwell,1 and Alexander Hoffmann (2011) 'A single NFκB system for both canonical and non-canonical signaling', *Cell Res*, 21(1), pp. 86-102.

Vose, J.M. (2013) 'Mantle cell lymphoma: 2013 Update on diagnosis, risk-stratification, and clinical management', *American Journal of Hematology*, 88(12), pp. 1082-1088.

Wada, H., et al. (2002) 'Calcineurin-GATA-6 pathway is involved in smooth muscle–specific transcription', *The Journal of Cell Biology*, 156(6), pp. 983-991.

Wajant, H., et al. (2002) 'Tumor necrosis factor signaling', *Cell Death Differ*, 10(1), pp. 45-65.

Wang, J.-Y., et al. (2012) 'Involvement of store-operated calcium signaling in EGF-mediated COX-2 gene activation in cancer cells', *Cellular Signalling*, 24(1), pp. 162-169.

Wang, Q., et al. (2011) 'Nuclear factor of activated T cells (NFAT) signaling regulates PTEN expression and intestinal cell differentiation', *Molecular Biology of the Cell*, 22(3), pp. 412-420.

Wang, Y., et al. (2015) 'Targeting Bruton's tyrosine kinase with ibrutinib in B-cell malignancies', *Clinical Pharmacology & Therapeutics*, 97(5), pp. 455-468.

Werneck, M.F., et al. (2011) 'NFAT1 transcription factor is central in the regulation of tissue microenvironment for tumor metastasis', *Cancer Immunology, Immunotherapy*, 60(4), pp. 537-546.

Whiteside, S.T., et al. (1997) 'I kappa B epsilon, a novel member of the I kappa B family, controls RelA and cRel NF-kappa B activity', *The EMBO Journal*, 16(6), pp. 1413-1426.

Willis, T.G., et al. (2000) 'The role of immunoglobulin translocations in the pathogenesis of B-cell malignancies', *Blood*, 96(3), pp. 808-822.

Wilson, N.S., et al. (2009) 'Death receptor signal transducers: nodes of coordination in immune signaling networks', *Nat Immunol*, 10(4), pp. 348-355.

Winslow, M.M., et al. (2006) 'Calcineurin/NFAT Signaling in Osteoblasts Regulates Bone Mass', *Developmental Cell*, 10(6), pp. 771-782.

Wright, G., et al. (2003) 'A gene expression-based method to diagnose clinically distinct subgroups of diffuse large B cell lymphoma', *Proceedings of the National Academy of Sciences of the United States of America*, 100(17), pp. 9991-9996.

Wu, E.K., Chao W, Low WC. (2010) 'NFAT and AP1 are essential for the expression of a glioblastoma multiforme related IL-13Ra2 transcript', *Cell Oncology*, 32(5-6), pp. 313-29.

Wu, H., et al. (2001) 'Activation of MEF2 by muscle activity is mediated through a calcineurin-dependent pathway', *The EMBO Journal*, 20(22), pp. 6414-6423.

Wu, S., et al. (1993) 'Tumor Necrosis Factor α as an Autocrine and Paracrine Growth Factor for Ovarian Cancer: Monokine Induction of Tumor Cell Proliferation and Tumor Necrosis Factor α Expression', *Cancer Research*, 53(8), pp. 1939-1944.

www.dharmacon.com (2015).

www.ensembl.org (NFAT2) *Accessed 26/08/2015*. Available at: http://www.ensembl.org/Homo_sapiens/Gene/Summary?db=core;g=ENSG00000131196;r=18:79395856-79529325.

www.ensembl.org (NFAT3) *Accessed 26/08/2015*. Available at: http://www.ensembl.org/Homo_sapiens/Gene/Summary?db=core;g=ENSG00000100968;r=14:24365673-24379604.

Wyckoff, J., et al. (2004) 'A Paracrine Loop between Tumor Cells and Macrophages Is Required for Tumor Cell Migration in Mammary Tumors', *Cancer Research*, 64(19), pp. 7022-7029.

Wyszomierski, S.L., et al. (2005) 'A knotty turnabout?: Akt1 as a metastasis suppressor', *Cancer Cell*, 8(6), pp. 437-439.

Xaus, J., et al. (2000) *LPS induces apoptosis in macrophages mostly through the autocrine production of TNF-α.*

Xiao, C., et al. (2008) 'Lymphoproliferative disease and autoimmunity in mice with elevated miR-17−92 expression in lymphocytes', *Nature immunology*, 9(4), pp. 405-414.

Xie, X., et al. (2005) 'Systematic discovery of regulatory motifs in human promoters and 3[prime] UTRs by comparison of several mammals', *Nature*, 434(7031), pp. 338-345.

Xue, G.J., Zhang Q, Mavis C, Hernandez-Ilizaliturri FJ, Czuczman MS, Guo Y. (2015) 'Vorinostat, a histone deacetylase (HDAC) inhibitor, promotes cell cycle arrest and re-sensitizes rituximab- and chemo-resistant lymphoma cells to chemotherapy agents', *J Cancer Res Clin Oncol*, Epub ahead of print.

Xue, X., et al. (2015) 'Diffuse large B-cell lymphoma: sub-classification by massive parallel quantitative RT-PCR', *Lab Invest*, 95(1), pp. 113-120.

Yamada, Y., et al. (1997) 'Initiation of liver growth by tumor necrosis factor: Deficient liver regeneration in mice lacking type I tumor necrosis factor receptor', *Proceedings of the National Academy of Sciences of the United States of America*, 94(4), pp. 1441-1446.

Yang, Y., et al. (2012) 'Exploiting Synthetic Lethality for the Therapy of ABC Diffuse Large B Cell Lymphoma', *Cancer Cell*, 21(6), pp. 723-737.

Yaseen, N.R., et al. (1993) 'Comparative analysis of NFAT (nuclear factor of activated T cells) complex in human T and B lymphocytes', *Journal of Biological Chemistry*, 268(19), pp. 14285-14293.

Ye, B.H., et al. (1993) 'Alterations of a zinc finger-encoding gene, BCL-6, in diffuse large-cell lymphoma', *Science*, 262(5134), pp. 747-750.

Yiu, G.K., et al. (2006) 'NFAT Induces Breast Cancer Cell Invasion by Promoting the Induction of Cyclooxygenase-2', *Journal of Biological Chemistry*, 281(18), pp. 12210-12217.

Yoeli-Lerner, M., et al. (2009) 'Akt/Protein Kinase B and Glycogen Synthase Kinase-3β Signaling Pathway Regulates Cell Migration through the NFAT1 Transcription Factor', *Molecular Cancer Research*, 7(3), pp. 425-432.

Yoeli-Lerner, M., et al. (2005) 'Akt Blocks Breast Cancer Cell Motility and Invasion through the Transcription Factor NFAT', *Molecular Cell*, 20(4), pp. 539-550.

Young, R.M., et al. (2009) 'Mouse models of non-Hodgkin lymphoma reveal Syk as an important therapeutic target', *Blood*, 113(11), pp. 2508-2516.

Yu, H., et al. (2012) 'Selective Modulation of Nuclear Factor of Activated T-Cell Function in Restenosis by a Potent Bipartite Peptide Inhibitor', *Circulation Research*, 110(2), pp. 200-210.

Yuan, J., et al. (2015) 'Identification of Primary Mediastinal Large B-cell Lymphoma at Nonmediastinal Sites by Gene Expression Profiling', *The American Journal of Surgical Pathology*, Publish Ahead of Print.

Zanoni, I., et al. (2009) 'CD14 regulates the dendritic cell life cycle after LPS exposure through NFAT activation', *Nature*, 460(7252), pp. 264-268.

Zhang, B., et al. (2015) 'An Oncogenic Role for Alternative NF-κB Signaling in DLBCL Revealed upon Deregulated BCL6 Expression', *Cell Reports*, 11(5), pp. 715-726.

Zhang, J., et al. (2013a) 'Genetic heterogeneity of diffuse large B-cell lymphoma', *Proceedings of the National Academy of Sciences*, 110(4), pp. 1398-1403.

Zhang, L.-H., et al. (2013b) 'Lenalidomide efficacy in activated B-cell-like subtype diffuse large B-cell lymphoma is dependent upon IRF4 and cereblon expression', *British Journal of Haematology*, 160(4), pp. 487-502.

Zhang, L.N., Chen Z, Shao K, Zhou F, Zhang C, Mu X, Wan J, Li B, Feng X, Shi S, Xiong M, Cao K, Wang X, Huang C, He J. (2007) 'High expression of nuclear factor of activated T cells in Chinese primary non-small cell lung cancer tissues.', *Int J Biol Markers*, 22(3), pp. 221-5.

Zhao, B., et al. (2014) 'The NF-κB Genomic Landscape in Lymphoblastoid B cells', *Cell reports*, 8(5), pp. 1595-1606.

Zhao X, C.Z., Zhao S, He J. (2010) 'Expression and significance of COX-2 and its transcription factors NFAT3 and c-Jun in non-small cell lung cancer', *Zhongguo Fei Ai Za Zhi*, 13(11), pp. 1035-40.

Zheng, J., et al. (2011) 'Negative Cross Talk between NFAT1 and Stat5 Signaling in Breast Cancer', *Molecular Endocrinology*, 25(12), pp. 2054-2064.

Zhou, B., et al. (2002a) 'Regulation of the Murine Nfatc1 Gene by NFATc2', *Journal of Biological Chemistry*, 277(12), pp. 10704-10711.

Zhou, B., et al. (2005) 'Characterization of Nfatc1 regulation identifies an enhancer required for gene expression that is specific to pro-valve endocardial cells in the developing heart', *Development*, 132(5), pp. 1137-1146.

Zhou, X.-Y., et al. (2002b) 'Molecular Mechanisms Underlying Differential Contribution of CD28 Versus Non-CD28 Costimulatory Molecules to IL-2 Promoter Activation', *The Journal of Immunology*, 168(8), pp. 3847-3854.

Zhou, Z., et al. (2014) *An enhanced International Prognostic Index (NCCN-IPI) for patients with diffuse large B-cell lymphoma treated in the rituximab era*.

Zhu, J., et al. (1999) 'NF-AT activation requires suppression of Crm1-dependent export by calcineurin', *Nature*, 398(6724), pp. 256-260.

Zhu, J., et al. (1998) 'Intramolecular Masking of Nuclear Import Signal on NF-AT4 by Casein Kinase I and MEKK1', *Cell*, 93(5), pp. 851-861.

Zwilling, S., et al. (1997) 'Inducible Expression and Phosphorylation of Coactivator BOB.1/OBF.1 in T Cells', *Science*, 277(5323), pp. 221-225.